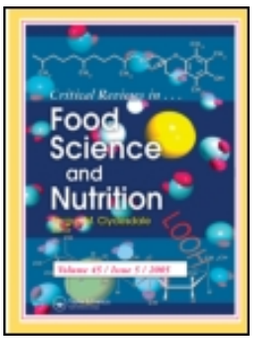

Critical Reviews in Food Science and Nutrition

ISSN: 1040-8398 (Print) 1549-7852 (Online) Journal homepage: http://www.tandfonline.com/loi/bfsn20

Beyond water activity: Recent advances based on an alternative approach to the assessment of food quality and safety

Louise Slade , Harry Levine & David S. Reid

To cite this article: Louise Slade , Harry Levine & David S. Reid (1991) Beyond water activity: Recent advances based on an alternative approach to the assessment of food quality and safety, Critical Reviews in Food Science and Nutrition, 30:2-3, 115-360, DOI: 10.1080/10408399109527543

To link to this article: https://doi.org/10.1080/10408399109527543

Published online: 29 Sep 2009.

Critical Reviews in Food Science and Nutrition, 30(2-3):115—360(1991)

Beyond Water Activity: Recent Advances Based on an Alternative Approach to the Assessment of Food Quality and Safety

Louise Slade and Harry Levine

Nabisco Brands, Inc., Fundamental Science Group, P.O. Box 1944, East Hanover, New Jersey 07936-1944.

Referee: **David S. Reid, Dept. of Food Science and Technology, Cruess Hall, University of California at Davis, Davis, California 95616.**

ABSTRACT: Water, the most abundant constituent of natural foods, is a ubiquitous plasticizer of most natural and fabricated food ingredients and products. Many of the new concepts and developments in modern food science and technology revolve around the role of water, and its manipulation, in food manufacturing, processing, and preservation. This article reviews the effects of water, as a near-universal solvent and plasticizer, on the behavior of polymeric (as well as oligomeric and monomeric) food materials and systems, with emphasis on the impact of water content (in terms of increasing system mobility and eventual water "availability") on food quality, safety, stability, and technological performance. This review describes a new perspective on moisture management, an old and established discipline now evolving to a theoretical basis of fundamental structure-property principles from the field of synthetic polymer science, including the innovative concepts of "water dynamics" and "glass dynamics". These integrated concepts focus on the non-equilibrium nature of all "real world" food products and processes, and stress the importance to successful moisture management of the maintenance of food systems in kinetically metastable, dynamically constrained glassy states rather than equilibrium thermodynamic phases. The understanding derived from this "food polymer science" approach to water relationships in foods has led to new insights and advances beyond the limited applicability of traditional concepts involving water activity. This article is neither a conventional nor comprehensive review of water activity, but rather a critical overview that presents and discusses current, usable information on moisture management theory, research, and practice applicable to food systems covering the broadest ranges of moisture content and processing/storage temperature conditions.

KEY WORDS: water activity, water relationships, moisture management, water as plasticizer, food polymer science, glass transition, water dynamics, glass dynamics

I. INTRODUCTION

Before 1950, many of the attributes of water-based food products were expressed in terms of water content, as was the ability of living cells to function optimally. In 1952, Scott[1] suggested that the (equilibrium thermodynamic) water activity (Aw), rather than water content, provided the true measure of physiological functioning and technological performance and quality. In recent years, more perceptive studies have shown that neither water content nor water activity can adequately account for the observed behavior of most moist, semi-moist, or almost-dry food systems.[2] Processes such as "water binding" and osmoregulation have been invoked in several empirical descriptions of food product stability or biological viability,[3] but none of these descriptions can be correlated with product safety or performance.[4-8]

In response to these shortcomings, a discussion conference, Water Activity: A Credible Measure of Technological Performance and Physiological Viability?, was convened at Girton

1040-8398/91/$.50

College, Cambridge, July 1 to 3, 1985, by the Industrial Physical Chemistry Group of the Faraday Division of the Royal Society of Chemistry, in association with the Food Chemistry Group (Industrial Division). Its main purpose was to clarify the significance and relevance of water activity as a measure of food product performance or the ability of living organisms to survive and function. A subsidiary objective was to arrive at recommendations for a more credible quality standard beyond water activity, still based on the properties of water. This conference was the genesis of this review.

The conference was divided into 4 half-day sessions on the basis of a "map of water regimes", defined by temperature and moisture content: very dilute systems near room temperature, steady-state systems at physiological temperatures, dry systems at and above room temperature, and concentrated systems over the broad range from subzero to elevated temperatures. The sessions emphasized the topics of the equilibrium thermodynamic basis of water activity, salting-in/salting-out phenomena, and specific molecular/ionic effects in dilute solutions near room temperature;[9,10] "compatible solutes" and osmoregulation in microbiological systems as complex dilute systems at physiological temperatures;[11] low-moisture food systems at room temperature and above, water vapor sorption, and sorption hysteresis as an indication of the inappropriate use of vapor pressure as a measure of water activity;[12,13] and intermediate-moisture, concentrated, and supersaturated glassy and rubbery food systems over a broad range of temperatures from subzero to over 200°C, water as plasticizer, and the mystique of "bound water".[14] In each session, an introductory critical review, by the speakers cited above,[9-14] was followed by a discussion among the participants (including industrial and academic scientists from the U.K., the Netherlands, France, Scotland, Switzerland, the U.S., Canada, and China; see Appendix) to develop a consensus of opinion. The final session was devoted to the drafting of a set of guidelines and recommendations for criteria of food quality and safety, more consistent with the current state of our knowledge of the physics and chemistry of aqueous systems.

The consensus of the meeting was that neither the equilibrium thermodynamic water activity nor its use as a parameter in water vapor sorption experiments should be used any longer as a criteria for performance and functioning of nonequilibrium food and biological systems in limited water.[2,15] Moreover, the concept of "bound water" is neither useful nor correct.[7,15] Discussion of alternative experimental approaches and interpretations for prediction of stability and biological behavior was based largely on the dynamically constrained behavior of polymers at different levels of plasticization. The consensus led to the adoption of a "water dynamics map" to describe the "map of water regimes" categorized by the speakers and to the recommendation of "water dynamics"[15,16] as a concept to serve as the next step in the evolution of criteria for food quality and safety.

This review describes the concept of water dynamics and its basis as a central element of a framework based on a "food polymer science" approach to the study of structure-property relationships in food products and processes.[8,14-39] The depth, breadth, and utility of this new research approach is contrasted with the limited scope and practical and technological shortcomings of the concept of water activity. In a critical rather than comprehensive fashion, this article reviews recent advances in the field of water relationships and moisture management in food systems during the decade of the 1980s, with emphasis on the period from the 1985 Faraday conference to the present. These advances have resulted in part from new interpretations and insights derived from the understanding provided by water dynamics and related elements of the food polymer science approach.

II. HISTORICAL BACKGROUND: SHORTCOMINGS OF THE TRADITIONAL APPROACH BASED ON THE CONCEPT OF Aw

It has been known for thousands of years that the quality and safety of naturally high-moisture foods are best preserved by storage at low moisture content and/or low temperature. Since the time of the Pharoahs, the shelf-lives of natural foods have been extended by removing water and

making foods dryer and/or by lowering the temperature and making foods colder. Ancient methods of food preservation were based on the generally correct assumption that the dryer and/or colder, the better, in terms of longer shelf-life. However, in modern times economic considerations regarding drying and refrigeration processes require us to ask the question: How dry is dry enough and how cold is cold enough to ensure optimum product quality and safety? Since the answers to these questions are not universal but rather specific to individual foods, we must be able to determine these answers, either empirically or, preferably, theoretically and predictively, based on fundamental physicochemical properties, which are both meaningful and measurable, of specific food materials.[40-42]

In recent decades, the concept of water activity advanced by Scott has become the traditional approach used universally to try to answer these questions. Because Aw (actually in terms of the relative vapor pressure of water in the headspace above a food) is an easily measured physicochemical property that can be empirically related to product shelf-life, Aw has become a strongly entrenched concept in the food science and technology literature. Despite this fact, the Aw concept is not universally useful or applicable, and an alternative, technologically practical approach is needed. A number of workers[2,16,43] have pointed out shortcomings and described serious problems that can arise when Aw is used as a predictor of food quality and safety. An alternative approach to the technological challenges of moisture management should emphasize three fundamental principles.[8,30] The first is that real food systems are never equilibrium systems, so that one must always deal with kinetics. Another is that there are interrelationships among the moisture content of a food sample, the time of an experiment or of a storage study, and the temperature, and that one can make manipulations or transformations among these three variables, so that one can predict shelf-life by interchanging the moisture and temperature parameters. Lastly, with respect to the question of just how cold and/or dry is good enough, one can establish reference conditions of temperature and moisture content to be measured for each solute or blend of solutes in an aqueous food system, so that one can begin to say, for example, that a particular freezer temperature is low enough, and closer to that temperature is better than farther above it for a given food material whose specific extent of maximal freeze-concentration in a realistic time frame (the process whereby the water-compatible solutes in a high-moisture food are maximally concentrated, due to the maximal phase separation of some portion of the total water in a food as *pure* ice, as the food is frozen by cooling to a sufficiently low subzero temperature[4]) can be measured quantitatively.[27,31-34,40-42]

The genesis of an alternative approach to moisture management based on these three principles dates back at least to 1966 and a seminal review by White and Cakebread[44] of glassy states in certain sugar-containing food products. They recognized (1) the importance of the glassy state, and of the glass transition temperature (Tg) and its location relative to the temperature of storage (either ambient or subzero), in a variety of aqueous food systems, including but not limited to boiled sugar candies, and (2) the critical role of water as a plasticizer of food glasses and the quantitative Tg-depressing effect of increasing content of plasticizing moisture, whereby Tg of a particular glass-forming solute-water mixture depends on the corresponding content of plasticizing water (Wg) in that glass at its Tg.[15] Tg and Wg represent the reference conditions of temperature and moisture content mentioned earlier.[16,30,40,41] White and Cakebread were apparently the first food scientists to allude to the broader implications of non-equilibrium glassy and rubbery states to the quality, safety, and storage stability of a wide range of glass-forming aqueous food systems. Evidently, outside a small community of candy technologists, the work of White and Cakebread, and its broader relevance to the field of moisture management and water relationships in foods, went largely unnoticed until the early 1980s. Since that time, other workers have helped to advance, with increasing momentum, concepts and approaches based on a similar recognition and ap-

plication of the principles underlying the importance of non-equilibrium glassy and rubbery states to food quality and safety.[4-8,14-43,45-66]

A. Intermediate Moisture Foods — Chemical, Physical, and Microbiological Stability

1. Intermediate Moisture Systems — Definitions

Most composite materials derived from naturally occurring molecules are subject to chemical, physical, and/or microbiological degradation and deterioration. As alluded to earlier, it was realized quite early on that such systems can be stabilized to some extent via the control of the moisture content. The role of water in processes that take place in semi-dry (or semi-moist) systems is complex: it can act as continuous phase (solvent, dispersion medium), as reactant (hydrolysis, protonation, etc.), and as plasticizer of biopolymer structures.

As already noted, in 1952 Scott[1] put forward the concept that it is the water activity, Aw, rather than the water content, that controls the various deterioration processes. (It should be clearly noted that the definition used by Scott was not actually the thermodynamic activity, but rather a steady-state relative vapor pressure.) This view has since been universally (and uncritically) adopted by the food industry and regulatory authorities,[67] and food products are labeled "intermediate moisture" when they are so formulated that their stabilities (physical, chemical, microbiological) depend on a critical value of Aw that must not be exceeded. The remainder of Section II.A reviews the factors that limit the utility of Aw as a measure of food quality and safety and as a predictive tool for the development of new "intermediate moisture foods" (IMFs).

2. Equilibrium Water Activity

Basic equilibrium thermodynamics teaches that the sign of the Fibbs free energy change, ΔG, determintes whether a given chemical reaction *can* proceed or not. Thus, chemical equilibrium is associated with the condition

$$\Delta G = 0 \text{ (at constant T and P)}$$

but the equilibrium is of a dynamic nature, i.e., the rates of the forward and backward reaction are equal. In an ideal aqueous system, the partial free energy (chemical potential) μ_i of any one component i is proportional to its mol fraction concentration x_i, which is itself proportional to its partial vapor pressure (Raoult's law). In a mixture where water is the only volatile component, its chemical potential is expressed in terms of the vapor pressure p by the equation

$$\mu_1 = \mu_1^\circ + RT \ln p \qquad (1)$$

where it is also assumed that the vapor above the system behaves as an ideal gas ($pV = RT$). For a real system, which deviates from Raoult's law and Henry's law, Equation 1 becomes increasingly approximate. Lewis and Randall[68] advanced the device of activity (Aw) to replace vapor pressure in Equation 1, such that Aw is proportional to p and becomes equal to p in the infinite dilution limit where the solution is ideal. This device makes it possible to retain simple, compact equations for the various thermodynamic properties even for nonideal systems. (The alternative would have been to add a series of correction terms.) Equation 1 is now rewritten in terms of Aw and contains a vapor pressure (p) term and an activity coefficient (f) term:

$$\begin{aligned} \mu_w &= \mu_w^\circ + RT \ln Aw \\ &= \mu_w^\circ + \underset{\text{ideal}}{RT \ln p} + \underset{\text{nonideal}}{RT \ln f} \end{aligned} \qquad (2)$$

The last term is a correction to allow for nonideal behavior in the system. In the limit of infinite dilution, $f = 1$ and

$$Aw = p/p^\circ \qquad (3)$$

where p° is the vapor pressure of pure *liquid* water under the same external conditions. Equation 3 is the expression usually found in the technical literature.

In many situations, other related quantities are used to express water activity, e.g., osmotic coefficients, water potential, relative humidity. Examples for ideal solutions (f = 1) are illustrated in Table 1.[9]

As described by Lilley,[9] reasons for departure from ideal behavior (shown in Figure 1)[9] include

1. Solute size (excluded volume).
2. Solvation effects; it is assumed that some solvent molecules, presumably those closest to the solute molecule, can be distinguished from the other solvent molecules by their interactions with the solute or their unique configurations — hence, the concept of "bound" water.
3. Intermolecular forces (between solute species); these might be modified as a result of specific solvation effects, see above.

Volume exclusion: for a binary aqueous solution

$$\ln Aw = 1 - [1/(x_w + Rx_s)] + \ln[x_w/(x_w + Rx_s)]$$

where x_i is the mol fraction of component i and R is the molar volume ratio solute:water. The effect on Aw is shown in Figure 2[9] for a 0.1 m solution; it can be significant.

Solvation: if a solute has a fixed hydration number h (water binding), then the effect on Aw is given by

$$Aw = (x_w - x_s h)/(x_w - x_s[h - 1])$$

The effect is shown in Figure 3[9] for 0.1 and 1.0 m solutions; note the marked dependence of Aw on h for high values of h.

Solute-solute interactions (association, aggregation, etc.): a simple example is given by the dimerization equilibrium

$$2S \Leftrightarrow S_2$$

In the limit where the association goes to completion and the dimerization constant becomes infinite, then

$$Aw = 2x_w/(2x_w + x_s)$$

This is illustrated in Figure 4.[9]

Cautionary note: for many aqueous systems, free energy-related functions such as Aw can be adequately fitted to one or more of the above

TABLE 1
Values of Some Properties, Related to Water Activity, of Ideal Aqueous Solutions at 25°C[9]

		Osmotic coefficients		Water potential	
Aw (= x_w)	m (mol kg^{-1})	g (ln Aw = g ln x_w)	ϕ (ln Aw = $-mM\phi$)	$-\Psi$ (Mpa) (ln Aw = $(\bar{v}_w/RT)\Psi$)	RH (Aw = RH/100)
0.9999	0.006	1	0.9999	0.0138	99.99
0.999	0.056	1	0.9995	0.138	99.9
0.99	0.561	1	0.994	1.38	99.0
0.90	6.17	1	0.948	14.5	90
0.80	13.8	1	0.898	30.7	80
0.70	23.8	1	0.832	40.1	70
0.60	37.0	1	0.766	70.3	60
0.50	55.5	1	0.693	95.4	50
0.40	83	1	0.613	126	40
0.30	130	1	0.514	165	30
0.20	222	1	0.402	221	20
0.10	500	1	0.256	317	10
0.01	5495	1	0.047	634	1

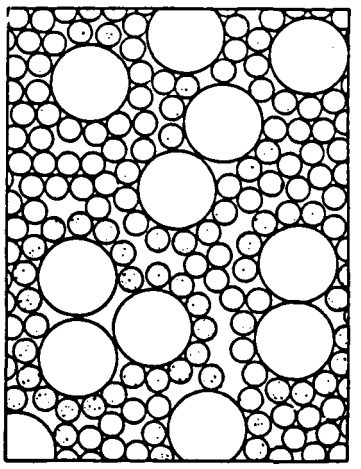

FIGURE 1. Schematic representation of a solution that would behave non-ideally, due to effects of volume exclusion, solvation, and solute-solute interactions. (Reproduced with permission from Reference 9.)

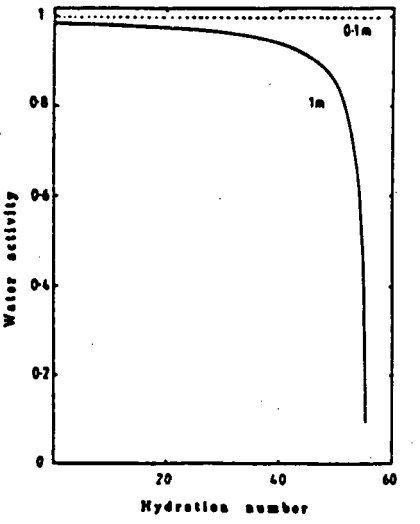

FIGURE 3. The effect of solute hydration number on the water activity of 0.1 and 1.0 molal solutions. (Reproduced with permission from Reference 9.)

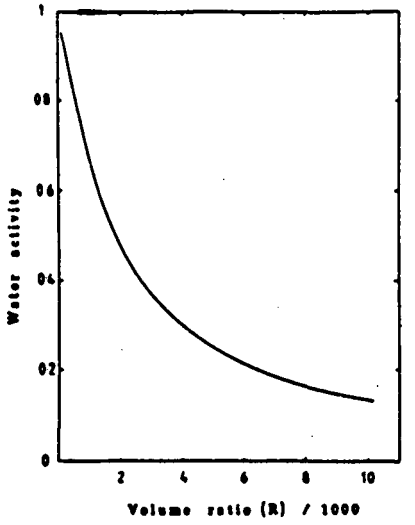

FIGURE 2. The effect of the molar volume ratio solute:water on the water activity of a non-ideal, binary aqueous solution. (Reproduced with permission from Reference 9.)

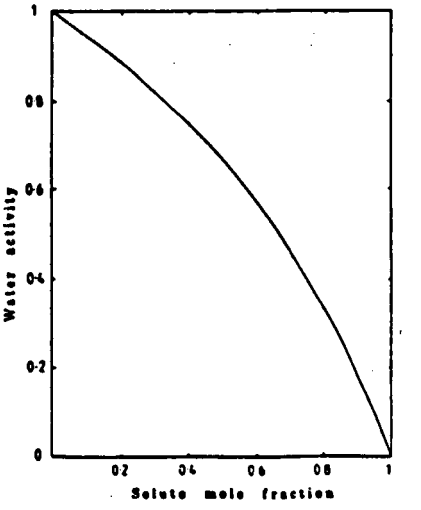

FIGURE 4. Variation of water activity with solute mole fraction. (Reproduced with permission from Reference 9.)

equations with only one parameter: R, h, or K (equilibrium constant). However, a good fit to the experimental data is not necessarily evidence of physical reality. A good test is the calculation of the effect of temperature on Aw and comparison with experiment. For instance, Aw of aqueous sugar solutions can usually be fitted by simple hydration equilibria of the type

$$S_{i-1} + H_2O \overset{K_{i-1}}{\Longleftrightarrow} S_i \quad i = 1,2,\ldots n$$

Assuming that all hydration sites i and all equilibrium constants K_{i-1} are equivalent, an average hydration number h can be calculated that depends only on Aw. Alternatively, Aw can be calculated by assigning a hydration number to

the sugar (usually equal to the number of −OH groups). At 25°C the glucose data can be fitted up to saturation by putting h = 6 and K = 0.789 and the sucrose data (h = 11 and K = 0.994) up to 6 *M*! The fallacy of the model becomes apparent when the temperature dependence of K is considered. In both cases the model predicts that the equilibrium is shifted to the right by an increase in temperature, which is contrary to chemical common sense.

All of the previous equations only apply to ideal mixtures, i.e., Aw has been expressed without the introduction of activity coefficients (i.e., Aw = p). It is, of course, most unlikely that any real food system behaves ideally in the thermodynamic sense, especially at high concentrations (low Aw). It is also most unlikely that Aw can be realistically expressed in terms of any one of the described effects only. Probably Aw and its change with composition depend on the resultant of the molecular features of the particular system and its deviations from the laws that govern ideal mixtures.

Another cautionary note: all of the previous thermodynamic arguments apply to equilibrium situations only, but most food systems are formulated and processed such that equilibrium is deliberately avoided, e.g., butter, ice cream, bread dough, mayonnaise. The same is true for most fabricated products, e.g., paper, metal alloys, ceramics, plastics.

3. Equilibrium or Kinetics?

Although thermodynamics predicts whether a physical or chemical process *can* occur, it does not predict whether such a process *will* occur within a measurable time period. For example, at 25°C, liquid water has a lower free energy than a mixture of gaseous oxygen and hydrogen, i.e., liquid water is the stable phase under such conditions, and the conversion of the gaseous mixture to liquid water should occur spontaneously. However, the gases do not react. They do so, explosively, when a small amount of manganese dioxide powder is added (catalyst). The system is thus seen to be under kinetic control, and its observed behavior is dictated by the reaction rate, although the reaction could not take place under any circumstances if the free energy condition was not satisfied.

A distinction therefore must be made between true equilibrium and a (kinetic) stationary state. In practice this can be done by subjecting a system to a perturbation, e.g., raising the temperature, followed by a return to the initial temperature. If the system returns to its previous state (viscosity, pH, turbidity, etc.), i.e., exhibits no hysteresis, it is in equilibrium. Only then can one be sure that vapor pressure is a measure of activity.[43] If it does not, but it exhibits hysteresis and settles to another time-independent state, then it was under kinetic control. Examples are provided by concentrated polymer solutions, such as those illustrated in Figure 5.[10]

It has been emphasized repeatedly in recent years that, where a system is under kinetic control, the term water activity is meaningless and should not be used.[2,15,16,30,43,69] The experimentally measured vapor pressure (or relative humidity, RH) in the headspace over a food product is actually an apparent, relative vapor pressure (RVP), which cannot then be related to Aw or any other equilibrium thermodynamic quantity. In practical situations, p/p° *may* still be a good measure of stability and safety, but this cannot be taken for granted, and extreme care must be taken to ensure that it is indeed the case. In practice, deviations from ideal behavior can be expected for Aw < 0.995, calling into question the validity of Equation 3, and the onset of nonequilibrium behavior can be expected at p/p° < 0.9, making the uncritical application of thermodynamics dangerous. In the realm of IMFs (0.65 < Aw < 0.95),[43] safety and stability therefore depend almost completely on kinetic factors and not on a true Aw.

A prime example of the confusion between equilibrium and kinetics is provided by Labuza's well-known "food stability map"[70] shown in Figure 6, in which relative deterioration rates (kinetics) are plotted against alleged water activity (thermodynamics). Such a practice is not to be recommended. While it has been suggested that this generalized diagram can be used to define safety limits for the spoilage of foods, van den Berg[43] has described such usage as a misapplication of the water activity concept. In any case, there is no formal cause/effect relationship

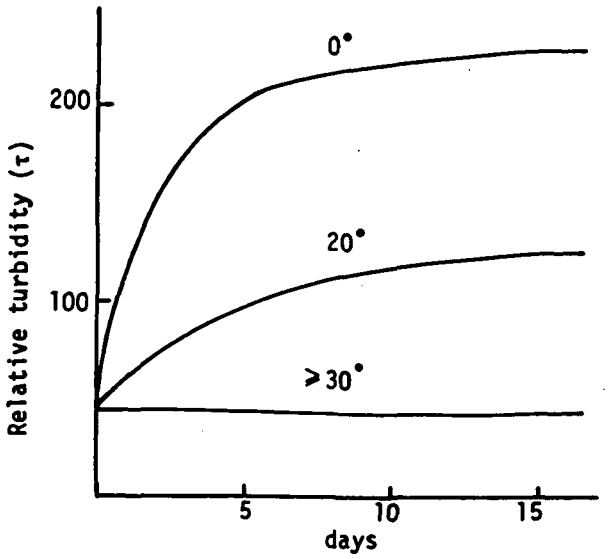

FIGURE 5. The increase in relative turbidity of an 8.5% aqueous solution of polyvinyl alcohol after rapid quenching from 90°C to the temperature indicated. (Reproduced with permission from Reference 10.)

between a reaction *rate* and Aw, which is an equilibrium thermodynamic function. In other words, y is *not* a function of x, as is implied. Note also that time dependence of a process has no place in equilibrium thermodynamics. No doubt some form of correlation can be described between a rate constant k and p/p°, but the generalized plot in Figure 6 is misleading,[43] and its misuse can be dangerous.[69] A comparison of maps drawn for different temperatures would probably show up its shortcomings, while a comparison of maps drawn for food systems composed of different solutes would most certainly do so.[2,15,16,30,43,69]

The map in Figure 6 can be useful generically, because it indicates qualitatively, for a given product, that at very low water content and measured RVP, lipid oxidation, and other free-radical reactions occur more rapidly than at somewhat higehr RVP, whereas in the limit of high RVP and moisture content, biological reactions occur with increasing rates. However, in order for Figure 6 to be universally applicable, the absolute values of RVP relevant to the quantitative spoilage behaviors of a product should be independent of the particular food system and its specific solutes composition. As is well known, this is emphatically not the case. For different food products composed of characteristic mixtures of different solutes, e.g., bread and pudding, at the same moisture content or the same measured RVP, the deterioration rate curves in Figure 6 would not be identical.

Van den Berg[43] has emphasized that the ef-

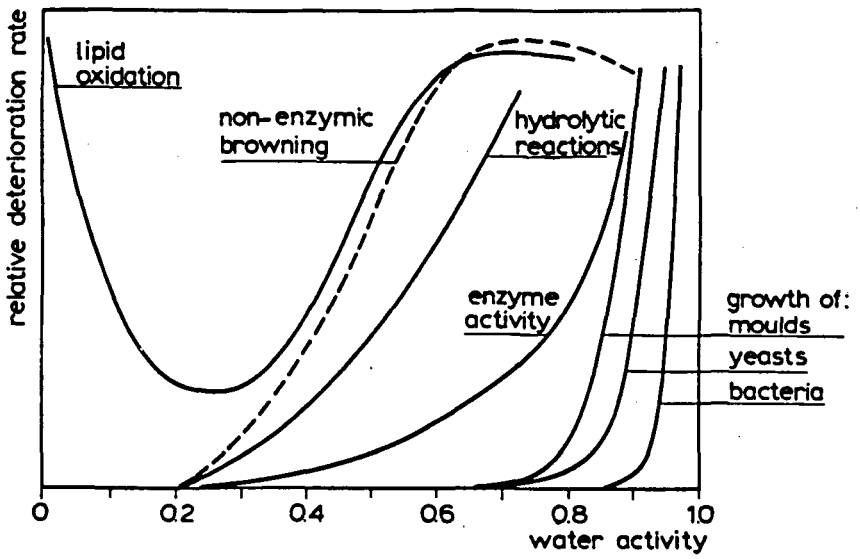

FIGURE 6. Generalized diagram of relative deterioration rates of food spoilage mechanisms as a function of water activity ("food stability map"). (Reproduced with permission from Reference 70.)

fect of water activity in foods depends on the composition of the solute(s). He has cited specific literature examples of both (a) different microbial reactions at identical Aw values adjusted with different solutes and (b) identical microbial reactions at different Aw values adjusted with different solutes. Other similar examples have been reported by Lang[71] and reviewed by Gould and Christian.[72] As a general rule, RVP increases with increasing solute molecular weight (MW), at the same solute concentration. Consequently, the effect of solute MW on microbiological stability is such that, at the same RVP, polymeric solutes produce more stable systems than do monomeric or oligomeric solutes.[16,71] Even though RVP is equal, the apparent "availability" of water is greater in the system containing the lower MW solute. Conversely, at the same moisture content, the lower MW solute system is more stable, apparently because its water "availability" is lower. Van den Berg[43] has concluded, in accord with Franks,[2] Gould,[11] and Gould and Christian,[72] that "apparently the microbial cell is not just a simple osmometer that stops working at a certain osmotic pressure." The term "water availability", although frequently used, is prone to misunderstanding, and its use should be discouraged, because it focuses unwarranted attention on the behavior of water in isolation. The actual basis for the concept of "water availability" concerns the nonequilibrium behavior, i.e., the kinetic nature, of a plasticizing diluent (e.g., a concentrated solute-water blend), in terms of its cooperative mobility and its mobilizing contribution to an included reporter (e.g., a microbial cell or amorphous food polymer in an aqueous sugar solution) compared with the corresponding plasticizing effectiveness of water alone. In a related vein, Mathlouthi et al.[73] have recently demonstrated that the mobilities of specific carbohydrate-water solutions (i.e., plasticizing solute-water diluents), rather than their Aw values, are the primary determinant of enzymatic activity (of lysozyme) and enzyme stability (of yeast alcohol dehydrogenase) in concentrated solutions of various small sugars and polyols at room temperature.

A more recent and graphic confirmation of these facts with respect to the rate of germination of mold spores has been reported by Slade and Levine.[14-16,30] Near room temperature, the initial germination of mold spores of *Aspergillus parasiticus* depends only on the availability of water, not on the presence of nutritents.[71] The experimental protocol, adapted from a microbiological assay used by Lang,[71] compared the inhibitory effects on conidia germination for a series of concentrated solutions of selected monomeric and polymeric glass-formers. The germination is essentially an all-or-nothing process, with the massive appearance of short hyphae surrounding the previously bare spores occurring within 1 d at 30°C in pure water or dilute solution (RVP $\simeq$ 1.0). As shown in Table 2,[16] the various glass-formers were assayed in pairs, deliberately matched as to the individual parameters of approximately equal RVP (at 30°C), solute concentration, MW, Tg′ and/or Wg′ (i.e., the particular Tg and Wg of the maximally freeze-concentrated solution[8,32,74]). Since true water activity is a colligative property of dilute solutions (i.e., it depends primarily on the number density of solute molecules),[2,43] solutes of equal MW, at the same concentration, should produce equal values of Aw. While this is generally true for dilute solutions, it is well known that concentrated solutions of, for example, different monosaccharide or disaccharide sugars, produce significantly different values of measured RVP at equal solute concentrations.[75,76] The relationship between experimental results for number of days required to germinate (as a relaxation time) and measured solution RVP was scrutinized. These results demonstrated conclusively that the observed rates of germination at 30°C showed no relationship with the measured RVPs. However, an approach based on mobility transformations to describe the kinetics of this mechanical relaxation process did facilitate interpretation of the germination data.[30] Rates of such a relaxation process reflect the kinetic nature of the plasticizing diluent (in this case, concentrated aqueous solutions), which depends on the cooperative translational mobility of the solute-water blend, rather than on "water availability" or "water activity" as reflected by measured apparent RVP. The results shown in Table 2 represented a graphic experimental demonstration of the failure of the Aw concept to account for the relative efficacy of different solute additives for microbial stabilization.

TABLE 2
Germination of Mold Spores of *Aspergillus Parasiticus* in Concentrated Solutions[16]

	Design parameters					Solution		Days required to germinate at 30°C
RVP[a] (30°C)	Tg′ (°K)	Wg′[b] (w% H_2O)	Tg (°K)	Tm (°K)	Tm/Tg	Conc. (w% H_2O)	Solute type	
Controls								
1.0						100	None	1
~1						99	Glucose (α-D)	1
~1						99	Fructose (β-D)	1
~1						99	PVP-40	1
~1						99	Glycerol	2
0.92	251.5	35	373	—		50	PVP-40	21
0.92	227.5	49.5	302	444.5	1.47	60	α-Methyl glucoside	1
0.83	231	49	373	397	1.06	50	Fructose	2
0.83	208	46	180	291	1.62	60	Glycerol	11
0.99	243.5	20	316	402	1.27	60	Maltose	2
0.97	241	36	325	465	1.43	60	Sucrose	4
0.95	250	31	349	406.5	1.16	50	Maltotriose	8
0.93	232	26	303	412.5	1.36	50	Mannose	4
0.95	250	31	349	406.5	1.16	50	Maltotriose	8
0.92	251.5	35	373	—		50	PVP-40	21
0.93	232	26	303	412.5	1.36	50	Mannose	4
0.87	231	49	373	397	1.06	54	Fructose	2
0.92	227.5	49.5	302	444.5	1.47	60	α-Methyl glucoside	1
0.87	231	49	373	397	1.06	54	Fructose	2
0.92	227.5	49.5	302	444.5	1.47	60	α-Methyl glucoside	1
0.70	231	49	373	397	1.06	30	Fructose	2
0.85	230	29	304	431	1.42	50	Glucose	6
0.83	231	49	373	397	1.06	50	Fructose	2
0.82	230.5	48	293	—		40	1/1 Fructose/ Glucose	5
0.98	247	36	339	—		50	PVP-10	11
0.98	231	49	373	397	1.06	60	Fructose	2
0.93	247	36	339	—		40	PVP-10	11
0.95	251.5	35	373	—		60	PVP-40	9
0.99	247	36	339	—		60	PVP-10	11
0.99	243.5	20	316	402	1.27	60	Maltose	2

[a] Relative vapor pressure measured after 7 d "equilibration" at 30°C.
[b] Wg′ expressed here in terms of w% water, for ease of comparison with solution concentration (also expressed in terms of w% water).

Despite the weight of such evidence, the misuse of Aw, a thermodynamic concept rigorously applicable only to dilute aqueous solutions at equilibrium, as a parameter to describe RVPs of concentrated aqueous systems of multiple, diverse solutes continues to be an everyday occurrence in the food industry. The real danger in this careless and oversimplified usage relates to government-defined and -imposed specifications for values of Aw (e.g., derived from Figure 6) required by law for microbiological safety and stability of IMF products for human consumption.[69] The potential for disaster inherent in naive compliance with such a rigid quantitative approach is frightening. The possibility that a community of food scientists could believe that specifying a maximum Aw value of 0.85 (or 0.75 or even 0.65) for a cheese cake filling can guarantee product safety, without any consideration of the nature of the mixture of water-compatible solids used to produce a particular Aw value, is both disheartening and potentially deadly.

Van den Berg[43] has remarked, with considerable understatement, that "it is not surprising therefore that in recent years, misconceptions have led to some difficulties in the preservation of intermediate moisture products." For example,[69] consider an intermediate-moisture pet food product that was originally formulated with a mixture of solutes (so-called "water binders") predominated by glucose and glycerol. This commercial product was empirically determined to be microbiologically safe and stable at an Aw of 0.92, which was thus incorporated as a product specification. Then, for the purpose of cost reduction, the glucose-glycerol combination was replaced by fructose and propylene glycol, but the Aw specification was not lowered in a corresponding and appropriate fashion,[30] but rather naively kept at 0.92. The financially disastrous result required a recall of millions of dollars worth of spoiled product. With knowledge of similar cases, van den Berg[43] concluded that "although Scott in his acclaimed papers was aware of the theoretical background of water activity, he did not distinguish clearly enough between product RVP and thermodynamic Aw." At least part of the subsequent blame for the current state of affairs must also rest with those who continue to make uncritical and indiscriminate use of Scott's work.

Take-home lesson: most physical and chemical processes that occur in intermediate moisture systems are under kinetic control (diffusion-limited), and product stability corresponds to a stationary state but not to equilibrium. Important practical implications of this statement are treated in later sections. Note: free radical-induced reactions may be an exception to the above rule. For now, suffice it to quote van den Berg's[43] conclusion regarding Figure 6: "it is more appropriate to make a clear distinction between the equilibrium nature of water activity and the kinetics of deterioration reactions . . . In practice, conclusions with regard to safe and economic specifications for dehydration and storage of a specific product should be drawn up only after careful consideration of the relevant water relations and conducting shelf-life studies . . . Because microorganisms respond differently to identical Aw levels set by different solutes, and because many foods are not in a state of equilibrium, as evidenced by hysteresis effects during humidification and drying, the use of water activity concepts cannot guarantee the accurate prediction of food shelf-life."

4. Water Activity and the Control of Microbiological Growth

As alluded to earlier, microbiological safety is the overriding consideration in food processing and storage. Products have to be seen to be safe for a period that extends beyond the stated shelf-life. Microbial and fungal growth must therefore be inhibited. Common techniques include sterilization (by heat or irradiation), pasteurization (extends shelf-life while maintaining quality), and moisture control. Like all other living organisms, microorganisms require water for their metabolism and growth. The cell is sensitive to osmotic pressure differences, as reflected in Aw. Conventional wisdom states that, for each cell type, there is a limiting Aw below which it cannot grow/metabolize. Usually the Aw values for optimal growth fall in the range (>0.99) where true equilibrium conditions exist, so that p/p° is probably a true description of Aw. This is no longer true for the limiting growth conditions (see Figure 7).[77] The absolute limit for microbial growth seems to be at RH = 60%, which is close to the value (55%) quoted for DNA denaturation. There is an upper growth limit for some organisms (e.g., halophilic bacteria, *Xeromyces*).

In their partly dehydrated states, cells stop growing and become metabolically inert. They sometimes survive in this state for long periods and may increase greatly in heat resistance, even by factors in excess of 1000-fold. They superficially resemble bacterial endospores, which are by far the most dormant and resistant forms of life on Earth.[72]

Many vegetative cells can respond to osmotic stress by the synthesis of cytoplasmic solutes (osmoregulation), i.e., they lower the internal "Aw", and this enables them to survive and grow. Osmoregulatory solutes include K^+, proline, betaines, glutamic acid, glucose, trehalose, sucrose, sorbitol, and glycerol.[72] They interfere minimally with the stabilities of intracellular enzymes at concentrations where most of the environmental solutes, especially NaCl, cause se-

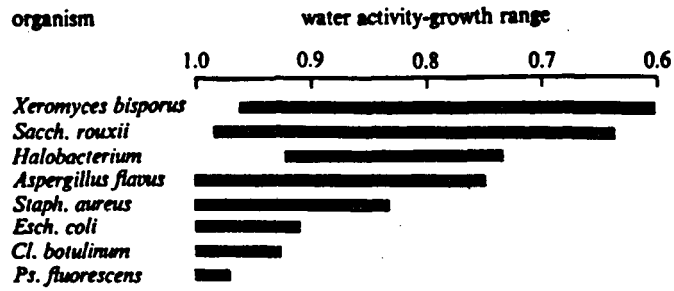

FIGURE 7. The water activity ranges for microbial growth of various microorganisms. (From Gould, G. W. and Measures, J. C., *Phil. Trans. R. Soc. London B.*, 278, 151, 1977. With permission.)

vere inhibition. They have high solubilities; they sometimes exist in concentrations >1 *M*. They have been termed "compatible solutes". Their synthesis requires energy and metabolic readjustments, as seen in the growth behavior of *B. subtilis* that has been subjected to a NaCl shock (see Figure 8).[77] Compatible solutes play a significant role in rendering overwintering insects resistant to freezing. The question is — why are they compatible?

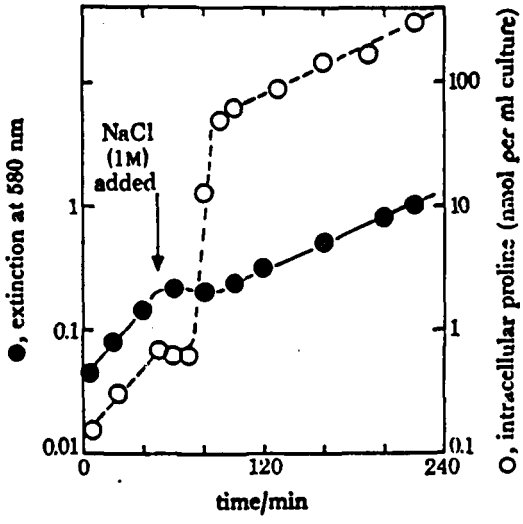

FIGURE 8. The growth behavior of *B. subtilis*, and its synthesis of proline, in response to a NaCl shock. (From Gould, G. W. and Measures, J. C., *Phil. Trans. R. Soc. London B.*, 278, 151, 1977. With permission.)

That Aw is not the only determinant of growth is demonstrated by culturing cells in different media at the same Aw. For example, as reviewed by van den Berg,[43] the limiting Aw values for some *Pseudomonas* species are 0.970 (in NaCl), 0.964 (in sucrose), and 0.945 (in glycerol). If a product was formulated to Aw = 0.970 with sucrose, it might not be safe. In any case, the measured RH is not necessarily related to Aw, i.e., what looks like osmotic equilibrium may be a steady state.

For any given solute, cell viability is usually correlated almost linearly with osmolality. The same holds for the effect of osmolality (Aw) on the stability of isolated enzymes, but notice, as shown in Figures 9[10] and 10,[10] the qualitatively different effects: sulfates stabilize most enzymes against heat denaturation, whereas CNS^-, NO_3^- or ClO_4^-, at the same measured Aw, destabilize enzymes almost to the same degree.

As mentioned earlier, there is no reason to believe that cells have evolved mechanisms capable of sensing Aw as such, i.e., they do not respond as simple osmometers.[11,72] Are there some other parameters that would form the basis of more rationally based criteria of cell activity as influenced by water and the aqueous environment? We do not know of any, but we can speculate that such criteria should include some factor related to environmental osmolality, but also[72]

1. Some measure of membrane permeability to the major solutes that are present
2. Some factor related to ionic vs. nonionic nature of the solutes (e.g., the salting-in vs. salting-out effect of salts, as illustrated in Figure 9, or nonelectrolytes, and the thermal stabilizing or destabilizing effect on en-

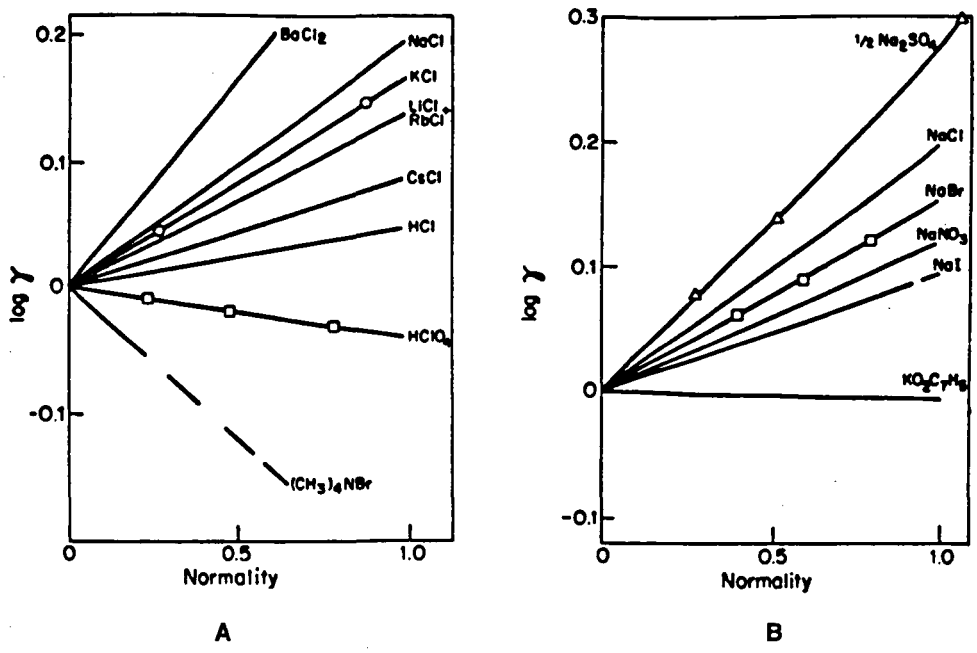

FIGURE 9. (A) Activity coefficients of ne benzene in aqueous chlorides, $HClO_4$ and $(CH_3)_4NBr$. (B) As in (A), but for Na^+-salts and K^+benzoate. (Reproduced with permission from Reference 10.)

zymes of nonionic hydroxy compounds, as shown in Figure 10)

3. Some factor related to the chemical (stereochemical) nature of the solutes (e.g., the marked differences in Aw between isomers at equal concentrations, as observed for ribose and xylose (see Figure 11))[10]
4. Some factor to take account of specific nutritional or toxic effects of the molecules that are present

So far, no synthesis of all these factors has been attempted.

Cautionary note — As described earlier, attempts to control the growth of food pathogens or other spoilage bacteria only by adjustment of RH can lead to disaster. Even chemically closely similar compounds (e.g., glucose and fructose) may have very different degrees of growth inhibition potential at the same measured RH, as they have likewise been shown by the results in Table 2 to have very different degrees of inhibition of mold spore germination.

Similar arguments apply to control by pH buffering. Isolated protein experiments show that the stability toward thermal denaturation is a function of pH, but the quantitative details of the function vary for different buffer systems. For example, denaturation temperature of ribonuclease at pH 2.1, I = 0.019:

Buffer	HCl–KCl	$H_2PO_4^-$–H_3PO_4	SO_4^{2-}–HSO_4^-
Temp. °C	29.9	32	43

The growth of cells in buffered systems may also depend on the nature of the buffer salts used. For instance, phosphates and acetates are used in the metabolism of *S. cerevisiae*, and do not act solely as pH controls. Citrate and phthalate ions are not metabolically active; they function as "normal" buffers. The growth behavior therefore depends not just on the pH but on the chemical nature of the buffer.

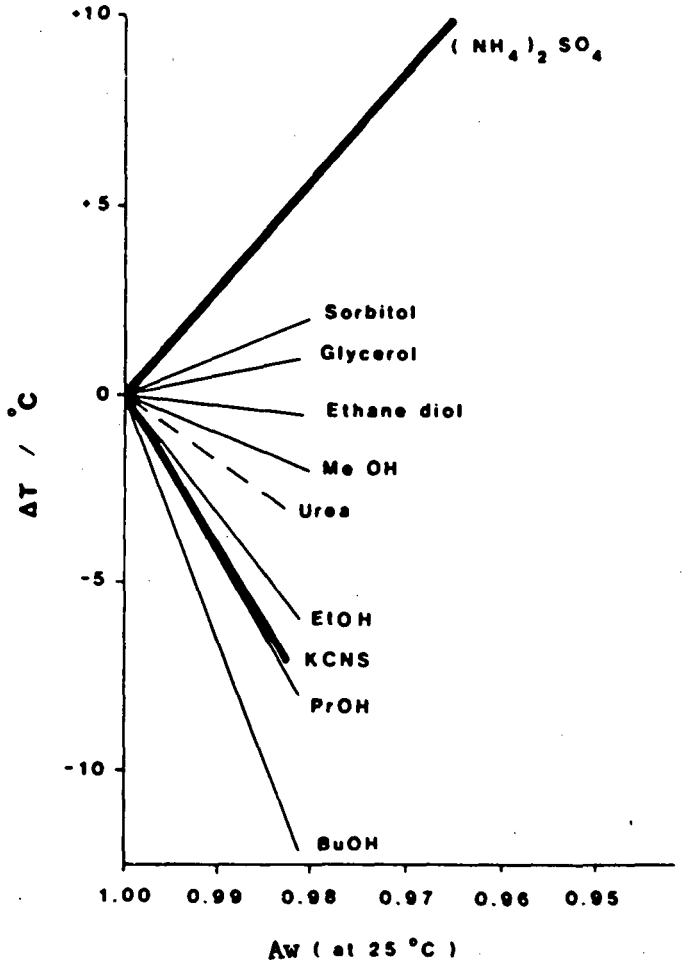

FIGURE 10. The effect of the osmolality (Aw) of various stabilizing or destabilizing solutes (mostly nonionic hydroxy compounds) on the thermal stability of ribonuclease enzyme at pH 7. (Reproduced with permission from Reference 10.)

Example: Growth of *S. aureus* at pH 5.4

	Generation time (h) at R.H. values:				
Acid	**0.99**	**0.95**	**0.93**	**0.91**	**0.89**
Citric	2.11	3.26	4.07	6.92	–
Phosphoric	0.84	1.36	3.85	–	–
HCl	0.49	1.66	2.36	7.83	–
Acetic	1.62	1.88	3.67	10.42	–

Conclusion: RH and pH are easy to measure, but they are only partially diagnostic of cell growth and metabolic rates.

5. Moisture Distribution in Heterogeneous Systems

All intermediate moisture systems are heterogeneous in chemical composition and/or physical structure. Most foods contain mixtures of proteins, carbohydrates, and lipids, each with a different affinity for water. Depending on such differences and also on diffusion rates within different substrates, water will become distributed non-uniformly in the product. This forms the basis of isopiestic vapor pressure measurements.

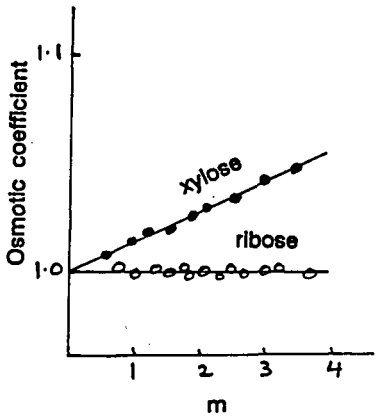

FIGURE 11. The marked difference in the variation of osmotic coefficient with solute molal concentration for the stereoisomers, ribose and xylose, at equal concentrations. (Reproduced with permission from Reference 10.)

It is commonly found that carbohydrates will dehydrate proteins, with the result that the carbohydrate component of a product may become susceptible to microbial growth, while the protein component is "safe".

Physical heterogeneity arises from the coexistence of several phases; commonly a crystalline phase can coexist with an amorphous solid phase (e.g., starch). In practice, the moisture content is calculated per gram solid. However, if the crystalline phase is anhydrous, the water is physically confined to the amorphous domains, and a more relevant estimate would be grams water per gram amorphous solid. When the crystalline phase is also hydrated (e.g., starch, gelatin), the moisture content may be non-uniformly distributed between the crystalline and amorphous domains, and separate estimates of grams water per gram crystalline solid and grams water per gram amorphous solid should be made. The ease of migration of water through a multiphase material depends on whether the amorphous component is in the glassy or rubbery (plastic) state and on the interfacial properties of the crystalline and amorphous domains. At $T < Tg$, diffusion-limited processes are inhibited during a realistic time period, so that water in the amorphous domains becomes essentially "unavailable" (i.e., immobilized) for typical deterioration reactions within practical food storage time periods.[8,14,16,43]

Physical heterogeneity and consequent unavailability of water can also arise from the existence of microscopic capillaries or pores in food systems such as biological tissues (with intact cell structure) and other porous materials (e.g., fabricated foods such as gels and emulsions). Pure water in capillaries of radius <1000 Å has a highly curved concave interface and consequently a lowered vapor pressure, depressed freezing point, and elevated boiling point relative to bulk water. The magnitude of the effect (on RVP, freezing point, and boiling point), which increases with decreasing capillary radius, can be calculated from Kelvin's equation.[78] Thus, in capillaries of 10 Å radius, even in the absence of dissolved solutes, water has a vapor pressure less than one third that of bulk water and a depressed freezing point of −15°C, so that such water can remain unfrozen indefinitely at freezer-storage temperatures above −15°C. In practice, water in capillaries <40 Å radius has been reported to be nonfreezing.[78]

No great reliance should be placed on moisture sorption isotherms, or on calculations based on such isotherms, for the following reasons. Both the Langmuir and BET equilibrium sorption theories are firmly based on a number of basic assumptions:[62,79]

1. The solid surface is inert and uniform; all sorption sites are equivalent.
2. The adsorbate does not penetrate the solid.
3. No interactions between sorbed molecules.
4. Sorption equilibrium is established such that the rates of adsorption and desorption are equal.
5. Only the first sorbed layer is affected by the solid substrate. Beyond that, multilayer sorption can be treated as condensation.

None of these assumptions holds good for food materials. The surfaces are not uniform; sorbed water molecules do interact, so that the probability of a site being occupied depends on whether neighboring sites are occupied; water penetrates and softens (plasticizes) the substrate,[15,25] thus affecting the nature of the surface (see Figure 12);[80] and equilibrium is *not* established,[15,26] as demonstrated by the inevitable sorption hysteresis[43,62] (see Figure 13).[43] Many workers have demonstrated that no sorption the-

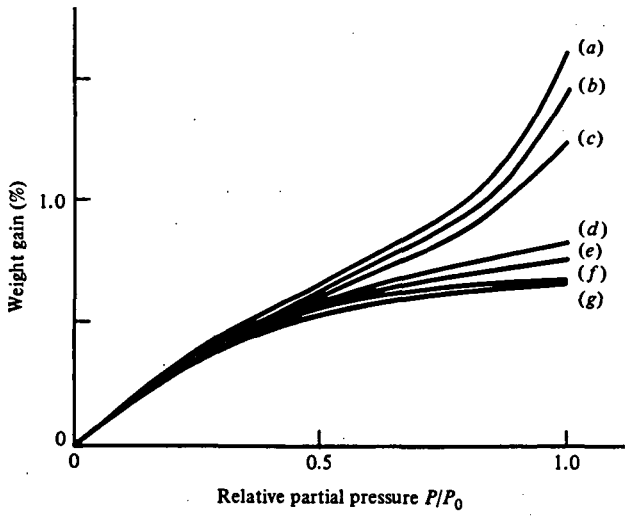

FIGURE 12. "Equilibrium" water vapor sorption isotherms of epoxy resin: (a) 25°C; (b) 35°C; (c) 75°C; (d) 100°C; (e) 125°C; (f) 150°C; (g) 175°C. (From Moy, P. and Karasz, F. E., *Water in Polymers*, Rowland, S. P., Ed., ACS Symp. Ser. 127, American Chemical Society, Washington, D.C., 1980, 505. With permission.)

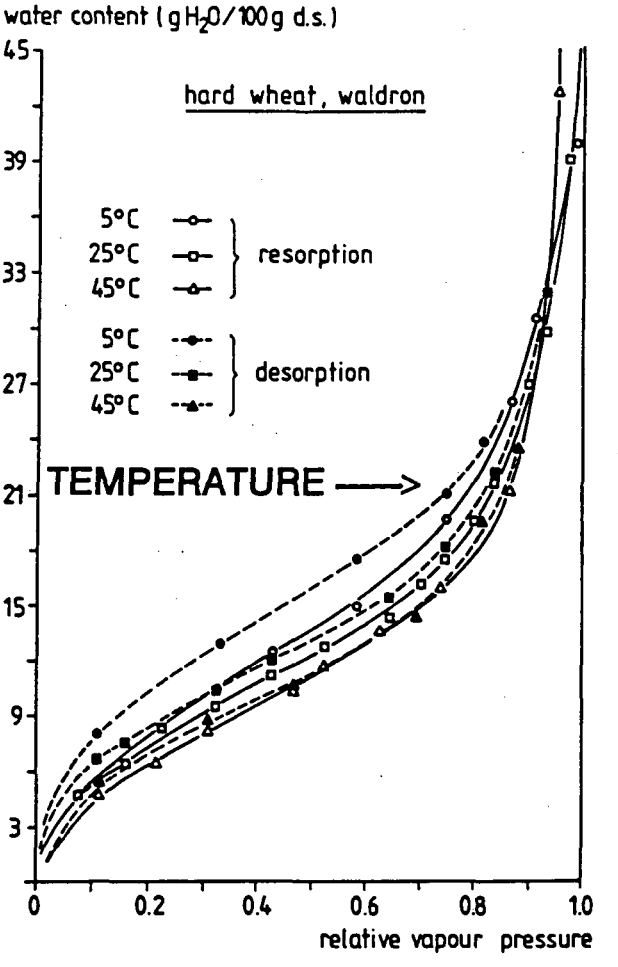

FIGURE 13. Hysteresis effect between desorption and resorption at three temperatures, as observed for milled hard wheat, type Waldron, origin U.S. (From van den Berg, C., *Concentration and Drying of Foods*, MacCarthy, D., Ed., Elsevier, London, 1986, 11. With permission.)

ory originally derived from equilibrium thermodynamics is capable of explaining this widely observed phenomenon of adsorption/desorption hysteresis which characterizes most "real world", non-equilibrium, sorbent-water systems. Despite this fact, the current literature still abounds with arguments over which is the best sorption theory (e.g., BET, GAB, etc.)[79] to apply to be *un*able to understand hysteresis.

The calculation of a notional monolayer coverage (e.g., BET) is meaningless under such conditions. As mentioned earlier, most free energy functions for aqueous solutions can be fitted by simple one- or two-parameter equations, but the assignment of physical meaning to the parameters is questionable. A correlation is no evidence for a cause/effect relationship. That is not to deny the practical usefulness of sorption isotherms; correlations may exist between isotherm shapes and shelf-lives. Thus, a particular isotherm may predict the storage life of tuna steaks and another the shelf-life of cheese crackers, but if the formulation of the cracker dough is altered, so will be the shape of the sorption isotherm. As a means of prediction from first principles, isotherms have very limited uses.

The fundamental problem with using moisture sorption isotherms to predict the shelf-lives of solid and semi-solid foods from their measured RVPs is that, due to the non-equilibrium nature of both aqueous food systems and sorption experiments,[14-16] the exact position and shape of an isotherm are sensitive to many factors, including[12,43]

1. Chemical composition, i.e., the specific combination of particular solutes and their MWs (e.g., sugars, polyols, polysaccharides, proteins) (see Figure 14)[81]
2. Temperature (see Figure 14), and its large effect on hysteresis (see Figure 13, where van den Berg[43] showed that (a) the extent

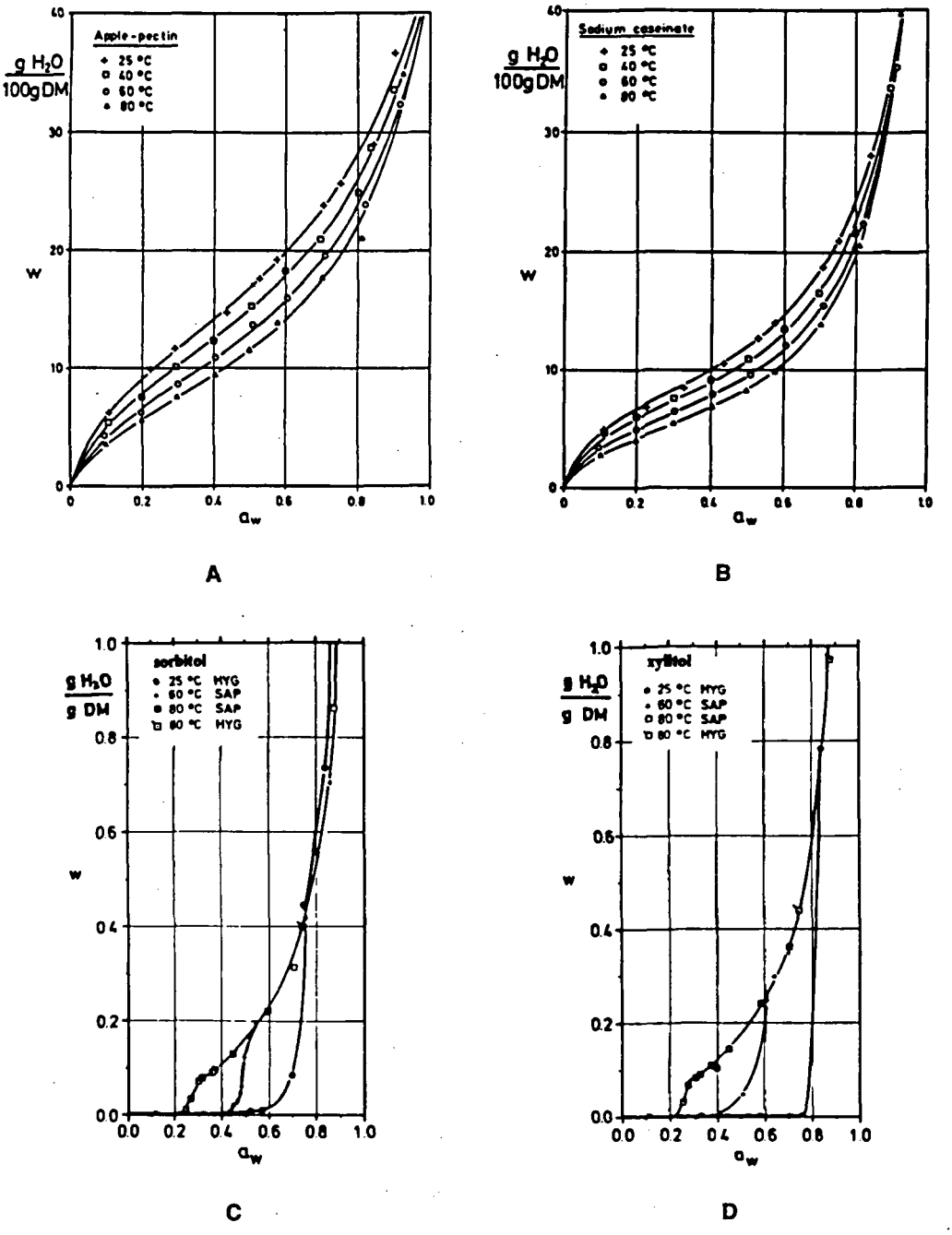

FIGURE 14. Sorption isotherms of (A) apple pectin and (B) sodium caseinate at 25, 40, 60, and 80°C. Adsorption isotherms of (C) sorbitol and (D) xylitol at 25, 60, and 80°C (HYG = Hygrostat; SAP = Sorption apparatus "rotasorp"). (From Weisser, H., *Properties of Water in Foods,* Simatos, D. and Multon, J. L., Eds., Martinus Nijhoff, Dordrecht, 1985, 95. With permission.)

of hysteresis between resorption and desorption isotherms measured at 5, 25, and 45°C for milled wheat increased with decreasing temperature, and (b) the effect of temperature was greater on the desorption isotherms than on the resorption isotherms)

3. Physical structure and state, i.e., amorphous or crystalline (see Figure 15A vs.

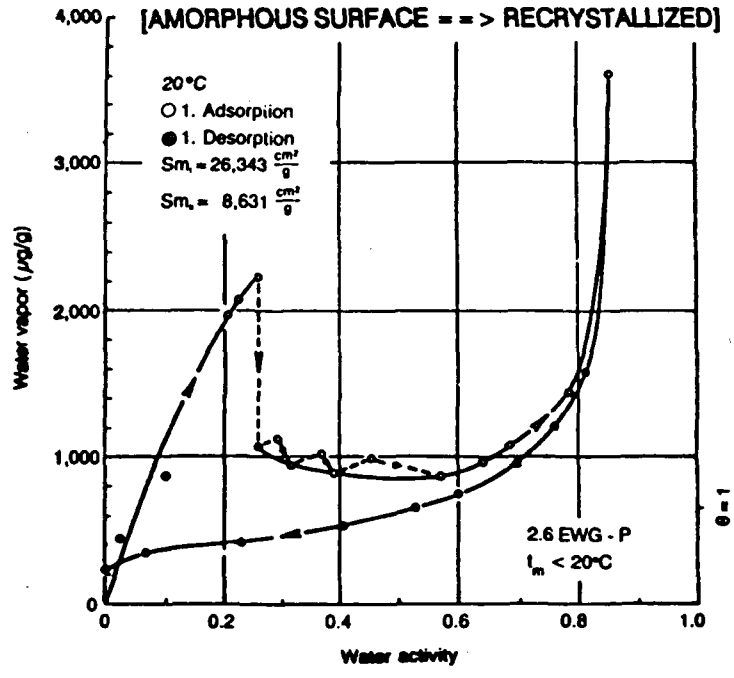

A

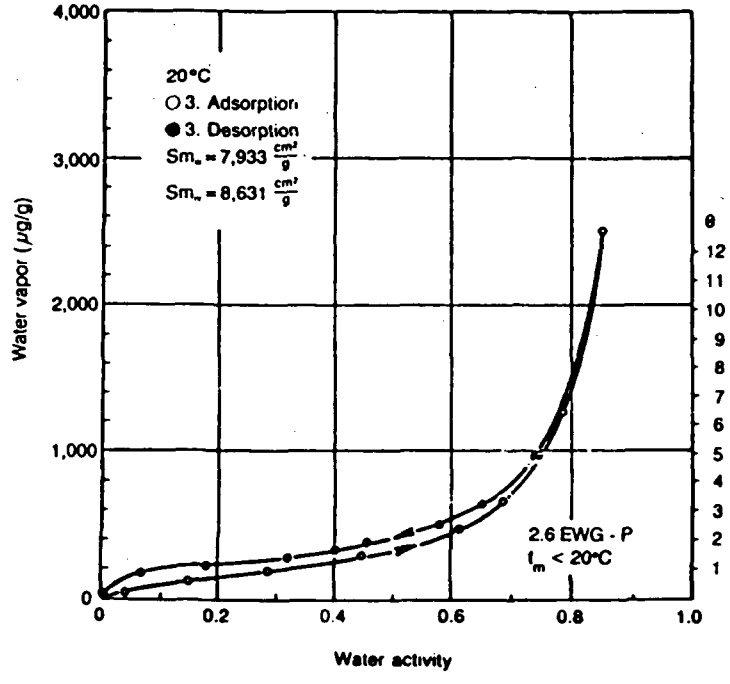

B

FIGURE 15. Sorption isotherms of (A) dry-milled sucrose and (B) crystalline sucrose, showing adsorption and desorption of water vapor. (From Niediek, E. A., *Food Technol.*, 42(11), 81, 1988. With permission.)

15B[82] for amorphous vs. crystalline sucrose), glassy or rubbery (see Figure 12, where the water-plasticized polymeric sorbent was still glassy up to 75°C, but had become rubbery by 100°C)[80]

4. Experimental history, i.e., previous desorption/resorption cycles (and resulting sample water content), and the hysteresis arising therefrom (see Figures 13 and 16A, where, in the latter, Bizot et al.[83] showed that, starting with fresh (wet) native potato starch, (a) there was a gradual closing of the hysteresis loop with repeated desorption/resorption cycles, and (b) the desorption curves were affected more than the resorption curves by the cycling history)
5. Sample history, i.e., origin and pretreatment (and resulting sample water content), and the hysteresis arising therefrom (see Figure 16B, where Bizot et al.[83] showed for a particular potato starch sample that (a) the extent of hysteresis depended on the pretreatment (native, dried vs. gelatinized, freeze-dried), and (b) the effect of pretreating the sample and thereby changing its microscopic structure was again greater on the desorption curve than on the resorption curve)
6. Isotherm measurement methodology

As a consequence of hysteresis, the RVP of a sample at a given moisture content differs between its adsorption and desorption isotherms. For equal RVP, there is greater apparent water "availability" (i.e., plasticizer mobility) in the system prepared by removing water, so the desorption system is less stable. Van den Berg[43] has pointed out that, in practice, factors 4 and 5 can have unknown and unpredictable effects on isotherms and their accuracy and reproducibility. For example, in Figure 16A, at a given moisture content, depending on whether the sample is being dried or remoistened and how many times it had occurred previously, there are six different choices of measured RVP or so-called "Aw" for this sample of native potato starch. Thus, van den Berg further cautions against using sorption isotherms measured by other workers when accurate isotherms are required, noting the wide scatter in literature values of isotherms for various food products, and emphasizes the limited value, except as a first estimate, of literature compilations of food isotherms.[43]

Examples from everyday experience serve to illustrate the consequences of sorption hysteresis due to sample history, as revealed in Figure 17. If we plot measured RVP in the headspace above the product vs. water content of the material (data from van den Berg)[43] for a series of common food systems that spans wide ranges of RVP and water content, the overall shape of the resulting curve resembles that of a typical sorption isotherm for a single food material. The most obvious departure from this overall behavior is the anomalous location of the data point for a raisin, which exhibits unexpectedly low RVP for such a moisture content. It is inferred that the anomalous behavior is due to desorption hysteresis, because the raisin is the only product in the series that is an IMF created by dehydration. It is interesting to note that the other two products that depart from the overall behavior exhibit the opposite anomaly. These two materials (French bread and Gouda cheese) are distinguished from others in the series by the fact that creation of these products, such that they have high quality, requires a deliberate thermosetting process.[25,26]

In the moisture management of IMF products, packaging is important. If dry air comes into contact with a product of high water content, then water evaporates from the surface. This sets up a concentration gradient, with the results that solutes migrate toward the interface together with the water. Also, solutes migrate away from the interface (which is a region of high concentration). The evaporation of water lowers the surface temperature of the solid, causing heat transfer between air and the solid, as well as inside the solid. If the air is not dry, then moisture might condense on the surface and migrate into the bulk, a well-known phenomenon. Lipid surface layers and membranes significantly retard such moisture redistribution processes.

Limited attempts have been made to map the sorption characteristics of lysozyme.[84] There is no reason why similar procedures cannot be applied more generally. The protein/enzyme complex was subjected to long-term desiccation at room temperature under vacuum. Water vapor

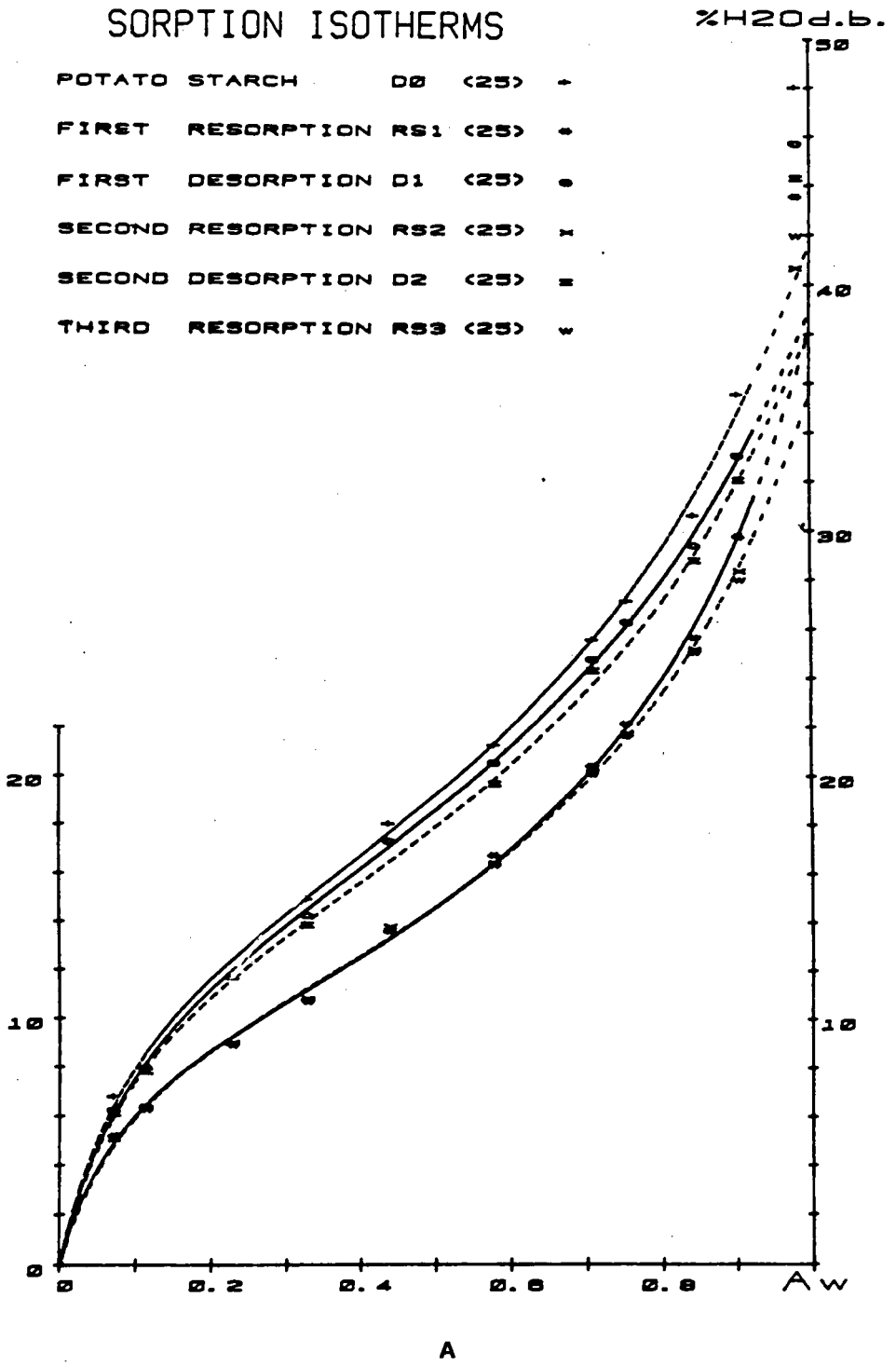

FIGURE 16. (A) Successive desorption-"resorption" cycles on fresh native potato starch (water content determination 1.5 h at 130°C; conditioning 8 d, reduced pressure, saturated salt solutions). (B) Comparison between sorption isotherms of potato starch: native (dotted lines) and 5% freeze-dried gel (full line). (From Bizot, H., Buleon, A., Mouhoud-Riou, N., and Multon, J. L., *Properties of Water in Foods,* Simatos, D. and Multon, J. L., Eds., Martinus Nijhoff, Dordrecht, 1985, 83. With permission.)

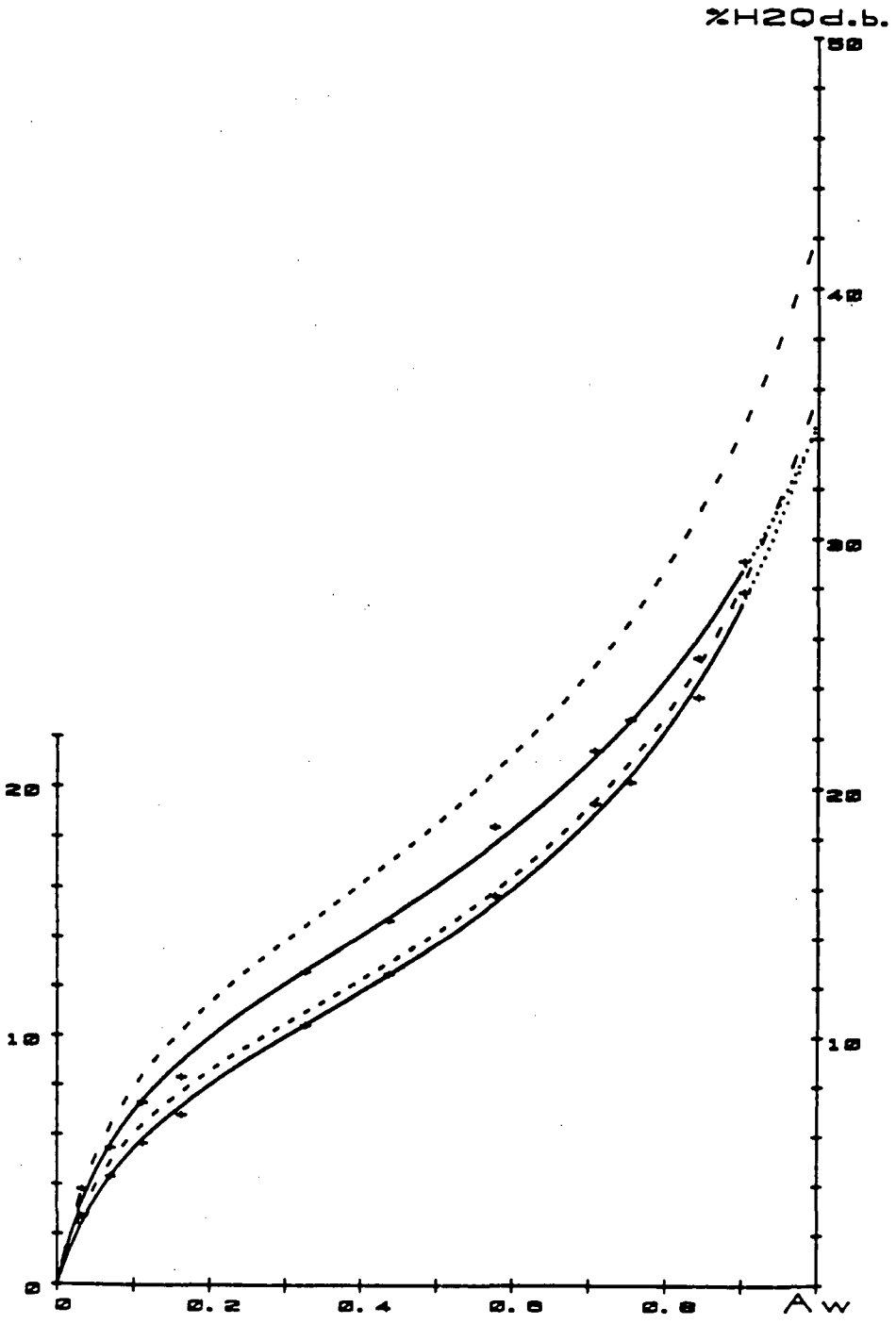

B

was then readmitted and the following properties were monitored:

1. Infrared amide bands (monitor peptide bonds)
2. Infrared COO^- bands (monitor acidic residues: glu, asp)
3. Infrared $-OD$ stretch (monitors perturbations of water molecules)

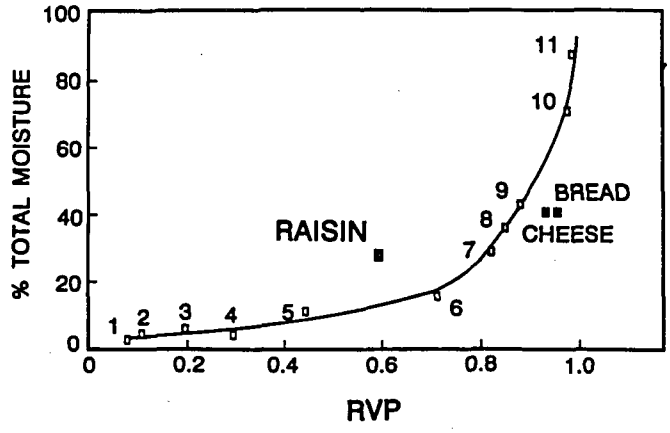

FIGURE 17. Plot of measured RVP at room temperature vs. water content for a series of common foods. Key to numbered data points: (1) crisp potato chips; (2) nonfat dry milk powder; (3) cookie; (4) boiled candy; (5) dry pasta; (6) wheat flour; (7) condensed milk; (8) marmalade; (9) sausage; (10) meat; (11) milk. (Data adapted from van den Berg, C., *Concentration and Drying of Foods*, MacCarthy, D., Ed., Elsevier Applied Science, London, 1986, 11.)

4. Specific heat (monitors internal degrees of freedom of macromolecule)
5. EPR (or NMR) rotational correlation time (estimate of freedom of rotational diffusion of macromolecule)
6. Enzyme activity

Changes and plateaus in the various properties as functions of moisture content indicate the order in which different atomic groupings become hydrated, as shown in the scheme in Figure 18.[85] Eventually enzyme activity is recovered (beginning at about 0.2 g water/g enzyme),[86] but full recovery only occurs at hydration levels of 9 grams water per gram enzyme. The moisture sorption isotherm for lysozyme is quite conventional in appearance[87] and does not (cannot) reveal any of the details shown in the scheme in Figure 18.

6. The Mythology of Bound Water

The food technology literature abounds in references to "bound" water (so do the literatures of other technological and biological disciplines). To be taken seriously, binding must be specified in terms of either position, energy, or lifetime. It must also be established that the binding is of an equilibrium type. The assignment of hydration numbers or hydration shells, obtained by fitting experimental data to a correlation equation, is not in itself proof of water binding, nor is the observation that a certain proportion of water in a complex amorphous material does not freeze within the time of the experiment. The notion that solid materials bind water (as manifested by measurements of so-called "water-binding capacity") can be of no help in the formulation of IMF products. The conclusive arguments debunking this popular myth and an alternative perspective based on the established role of water as a plasticizer of glass-forming materials are detailed in later sections.

III. AN ALTERNATIVE APPROACH TO MOISTURE MANAGEMENT IN FOOD SYSTEMS: THE FOOD POLYMER SCIENCE APPROACH

A. Key Elements of the Food Polymer Science Approach

Among a small but increasing number of food scientists, especially since 1980, there has been

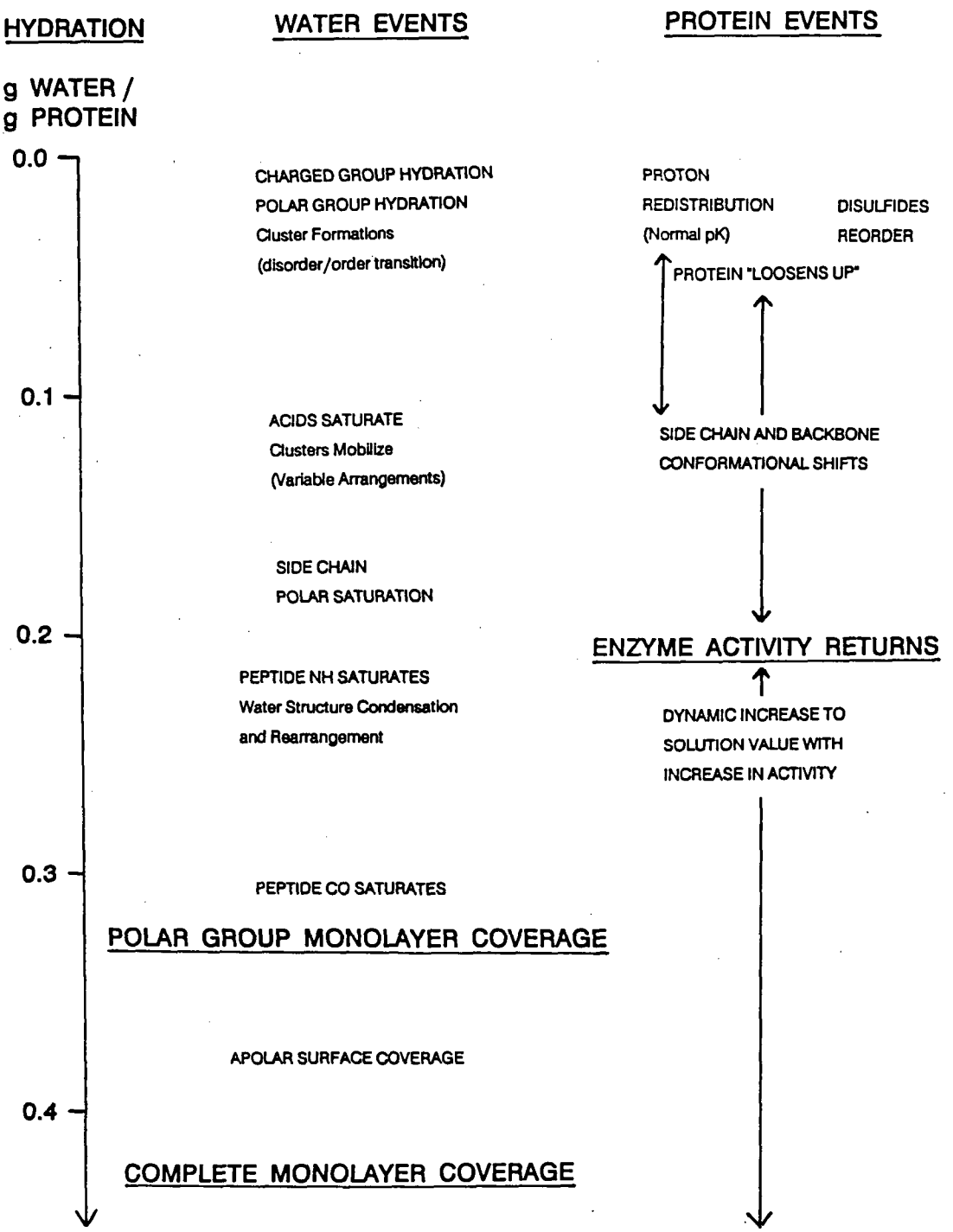

FIGURE 18. Scheme showing events postulated on sequential hydration of dry lysozyme. (From Franks, F., *Characterization of Proteins,* Franks, F., Ed., Humana Press, Clifton, NJ, 1988, 127. With permission.)

a growing awareness of the value of a polymer science approach to the study of food materials, products, and processes.[6-8,17-19,21,27,29-61,63-66,88-99] In this respect, food science has followed the compelling lead of the synthetic polymers field. As reviewed in detail in a number of recent publications,[15,16,20,22-26,28,34] the emerging research discipline of "food polymer science" empha-

sizes the fundamental and generic similarities between synthetic polymers and food molecules, and provides a new theoretical and experimental framework for the study of food systems that are kinetically constrained. On a theoretical basis of established structure-property relationships from the field of synthetic polymer science,[100-122] this innovative discipline has developed to unify structural aspects of foods, conceptualized as kinetically metastable, completely amorphous or partially crystalline, homologous polymer systems, with functional aspects, dependent upon mobility and conceptualized in terms of "water dynamics" and "glass dynamics".[15,16,20,22-26,28,34] These unified concepts have been used to explain and predict the functional properties of food materials during processing and product storage.[8,14,17-19,21,27,30-33,35-39] Key elements of this theoretical approach to investigations of food systems, with relevance to moisture management and water relationships, include recognition of[15,16,20,22-26,28,34-42]

1. The behavior of foods and food materials as classic polymer systems, and that the behavior is governed by dynamics rather than energetics
2. The importance of the characteristic temperature Tg, at which the glass-rubber transition occurs, as a physicochemical parameter that can determine processibility, product properties, quality, stability, and safety of food systems
3. The central role of water as a ubiquitous plasticizer of natural and fabricated amorphous food ingredients and products
4. The effect of water as a plasticizer on Tg and the resulting non-Arrhenius, diffusion-limited behavior of amorphous polymeric, oligomeric, and monomeric food materials in the rubbery liquid state at $T > Tg$
5. The significance of non-equilibrium glassy solid and rubbery liquid states (as opposed to equilibrium thermodynamic phases) in all "real world" food products and processes, and their effects on time-dependent structural and mechanical properties related to quality and storage stability.

In previous reports and reviews,[8,14-39] we have described how the recognition of these key elements of the food polymer science approach and their relevance to the behavior of a broad range of different types of foods (e.g., IMFs, low-moisture foods, frozen foods, starch-based foods, gelatin-, gluten-, and other protein-based foods) and corresponding aqueous model systems has increased markedly during this decade. We have illustrated the perspective afforded by using this conceptual framework and demonstrated the technological utility of this new approach to understand and explain complex behavior, design processes, and predict product quality, safety, and storage stability, based on fundamental structure-property relationships of food systems viewed as homologous families (i.e., monomers, oligomers, and high polymers) of partially crystalline glassy polymer systems plasticized by water. Referring to the food polymer science approach, John Blanshard (personal communication, 1987) has stated that "it is not often that a new concept casts fresh light across a whole area of research, but there is little doubt that the recognition of the importance of the transition from the glassy to the crystalline or rubbery state in food-stuffs, though well known in synthetic polymers, has opened up new and potentially very significant ways of thinking about food properties and stability." In a recent lecture on historical developments in industrial polysaccharides, James BeMiller has echoed Blanshard's words by remarking that a key point regarding the future of polysaccharide research and technology is "the potential, already partly realized, in applying ideas developed for synthetic polymers to polysaccharides; for example, the importance of the glassy state in many polysaccharide applications."[123]

In the rest of this article, we illustrate the theory and practice of food polymer science by highlighting selected aspects of experimental studies of both natural food materials and fabricated food ingredients and products, the results of which have been interpreted based on the theoretical physicochemical foundation provided by food polymer science. The studies have demonstrated the major opportunity offered by this food polymer science approach to expand not only our quantitative knowledge but also, of broader practical value, our qualitative understanding of moisture management and water re-

lationships in food products and processes well beyond the limited scope and shortcomings of the traditional Aw approach.

The technological importance of the glass transition in amorphous polymers and the characteristic temperature at which it occurs (Tg) is well known as a key aspect of synthetic polymer science.[107-109] Eisenberg[110] has stated that "the glass transition is perhaps the most important single parameter which one needs to know before one can decide on the application of the many non-crystalline (synthetic) polymers that are now available." Especially in the last several years, a growing number of food scientists have increasingly recognized the practical significance of the glass transition as a physicochemical event that can govern food processing, product properties, quality, safety, and stability.[4-8,12,14-66,74,82,88-99,124-126]

This recognition has gone hand-in-hand with an increasing awareness of the inherent non-equilibrium nature of all "real world" food products and processes, as exemplified by the category of IMFs, in which amorphous carbohydrates (polymeric and/or monomeric) and proteins are major functional components.[14,16] Other specific examples illustrative of food systems whose behavior is governed by dynamics far from equilibrium and of the practical problems of food science and technology posed by their non-equilibrium nature include graininess and iciness in ice cream, reduced survival of frozen enzymes and living cells, reduced activity and shelf-stability of freeze-dried proteins, lumping of dry powders, bloom on chocolate, recipe requirements for gelatin desserts, cooking of cereals and grains, expansion of bread during baking, collapse of cake during baking, cookie baking — effects of flour and sugar, and staling of baked products.[15] Thermal and thermomechanical analysis methods have been shown to be particularly well-suited to study such non-equilibrium systems, in order to define structure-activity relationships, e.g., of synthetic amorphous polymers, from measurements of their thermal and mechanical properties.[117] Differential scanning calorimetry (DSC) and dynamic mechanical analysis (DMA) have become established methods for characterizing the kinetic (i.e., time-dependent) transition from the glassy solid to the rubbery liquid state that occurs at Tg in completely amorphous and partially crystalline, synthetic and natural polymer systems,[127] including many food materials.[128] The focus of a polymer science approach to thermal analysis studies of structure-function relationships in food systems[8,14-39] emphasizes the insights gained by an appreciation of the fundamental similarities between synthetic amorphous polymers and glass-forming aqueous food materials with respect to their thermal, mechanical, and structural properties. Based on this approach, DSC results have been used to demonstrate that product quality and stability often depend on the maintenance of food systems in kinetically metastable, dynamically constrained, time-dependent glassy and/or rubbery states rather than equilibrium thermodynamic phases, and that these non-equilibrium physical states determine the time-dependent thermomechanical, rheological, and textural properties of food materials.[8,14-39]

Plasticization, and its modulating effect on the temperature location of the glass transition, is another key technological aspect of synthetic polymer science.[109] In that field, the classic definition of a plasticizer is "a material incorporated in a polymer to increase the polymer's workability, flexibility, or extensibility".[109] Characteristically, the Tg of an undiluted polymer is much higher than that of a typical low MW, glass-forming diluent. As the diluent concentration of a solution increases, Tg decreases monotonically, because the average MW of the homogeneous polymer-plasticizer mixture decreases, and its free volume increases.[107] A polymer science approach to the thermal analysis of food systems (both model and real) involves recognition of the critical role of water as an effective plasticizer of amorphous polymeric, oligomeric, and monomeric food materials.[4-8,14-66,74,88-94,98,124] Sears and Darby[109] have stated unequivocally that "water is the most ubiquitous plasticizer in our world." Karel[54] has noted that "water is the most important . . . plasticizer for hydrophilic food components." It has become well documented, in large part through DSC studies, that plasticization by water results in a depression of the Tg (and of the melt viscosity and elastic modulus) of completely amorphous and partially crystalline food ingredients, and that

this Tg depression may be advantageous or disadvantageous to product processing, functional properties, and storage stability. Recently, there has been expanding interest in the importance of the effect of water as a plasticizer of many different food materials and other biopolymers (see[15,25,26] and references therein), including starch, gluten,[99] starch hydrolysis products (SHPs),[59] low MW sugars[42,66,124] and polyhydric alcohols,[42,91] gelatin, collagen, elastin, lysozyme and other enzymes, and the semicrystalline cellulose and amorphous hemicelluloses and lignin components of wood.[129]

Atkins[90] has succinctly stated the important observation that "water acts as a plasticizer, dropping the Tg of most biological materials from about 200°C (for anhydrous polymers, e.g., starch, gluten, gelatin)[15] to about −10°C or so (under physiological conditions of water content), without which they would be glassy" (in their native, *in vivo* state). The latter Tg of about −10°C is in fact characteristic of high MW biopolymers at or above moisture contents near 30% corresponding to physiological conditions, as has been reported for many polymeric carbohydrates and proteins, including starch, gluten, gelatin,[15] hemicelluloses,[129] and elastin.[90] Elastin epitomizes a case where this subzero Tg is critical to healthy physiological function. Elastin exists as a completely amorphous, water-plasticized, covalently crosslinked (via disulfide bonds), network-forming polymer system whose viscoelastic properties have been likened to those of wheat gluten.[45,88] In its role as a major fibrous structural protein of skin, ligaments, and arteries, elastin exists *in vivo* as a rubbery liquid that demonstrates classic rubber-like elasticity[107] only as long as its Tg remains well below 0°C, due to a water content of 0.40 g/g protein. In contrast, in the pathologic state of arteriosclerosis ("hardening of the arteries"), elastin becomes a glassy solid at body temperature due to a decrease in water content to 0.17 g/g and a corresponding increase in Tg to 40°C (as shown by the so-called "glass curve" of Tg vs. moisture content in Figure 19A).[130,131] As with the case of lysozyme described earlier, the moisture sorption isotherm for dry elastin (see Figure 19B)[132] is also quite conventionally sigmoid-shaped in appearance and does not reveal the critical implications of the

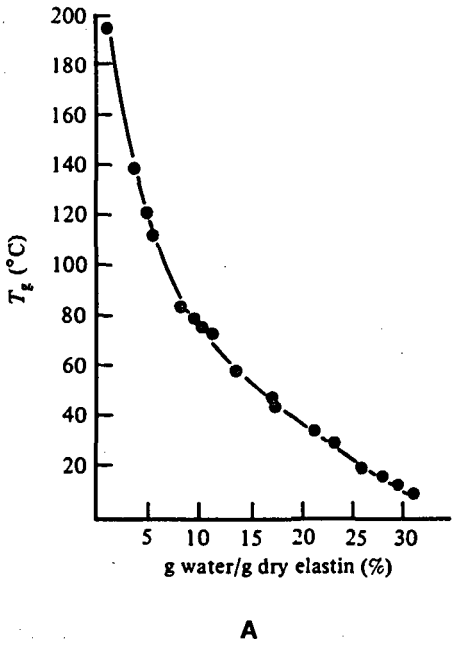

FIGURE 19. (A) Tg as a function of water content for elastin. (Reproduced with permission from Reference 130.) (B) Sorption isotherm for water in elastin at 25°C. (From Scandola, M., Ceccorulli, G., and Pizzoli, M., *Int. J. Biol. Macromol.*, 3, 147, 1981. With permission.)

structure-function relationship described earlier.

A unified conceptual approach to research on water relationships in food polymer systems, based on established principles translated from

synthetic polymer science, has enhanced our qualitative understanding of structure-function relationships in a wide variety of food ingredients and products.[8,14-39] Lillford et al.[45,97] have advocated a related "materials science approach" to studies of (1) the influence of water on the mechanical behavior of dough and batter before, during, and after baking, and (2) the mechanical properties of solid food foams as affected by "the plasticizing action of water". Similarly, in a recent review of structure-property relationships in starch, Zobel[61] has cited concepts used to characterize synthetic polymers and advocated this approach to provide increased understanding of the amorphous state and its role in determining physical properties of native and gelatinized starches. Others who have recently applied a synthetic polymers approach to characterize the glass transition, crystallization, melting, or annealing behavior of food polymers such as starch or gluten have included Blanshard,[47-49,88,94] Hoseney,[51-53,95,96] Ring,[59,92] Biliaderis,[46] and Fujio.[99] A central theme of our so-called "food polymer science" approach focuses on the effect of water as a plasticizer on the glass transition and resulting diffusion-limited behavior of water-soluble or water-miscible (collectively referred to as water-compatible) and water-sensitive amorphous materials or amorphous regions of partially crystalline materials.[15,25,26] Plasticization, on a molecular level, leads to increased intermolecular space or free volume, decreased local viscosity, and concomitant increased mobility.[107] Plasticization implies intimate mixing, such that a plasticizer is homogeneously blended in a polymer, or a polymer in a plasticizer. Note that a true solvent, capable of cooperative dissolution of the ordered crystalline state and having high thermodynamic compatibility and miscibility at all proportions, is always also a plasticizer, but a plasticizer is not always a solvent.[109] Water-compatible food polymers such as starch, gluten, and gelatin, for which water is an efficient plasticizer but not necessarily a good solvent, exhibit essentially the same physicochemical responses to plasticization by water as do many water-compatible synthetic polymers[111] and many readily soluble monomeric and oligomeric carbohydrates.[15] This fact demonstrates two underlying precepts of the food polymer science approach: (1) synthetic amorphous polymers and glass-forming aqueous food materials are fundamentally similar in behavior, and (2) food ingredients can be viewed generically as members of homologous families of completely amorphous or partially crystalline polymers, oligomers, and monomers, soluble in and/or plasticized by water. The series from glucose through malto-oligosaccharides to the amylose and amylopectin components of starch exemplifies such a homologous polymer family.

On a theoretical basis of established structure-property relationships for synthetic polymers, the functional properties of food materials during processing and product storage can be successfully explained and often predicted.[15,25,26] The discipline of food polymer science has developed to unify structural aspects of foods, conceptualized as completely amorphous or partially crystalline polymer systems (the latter typically based on the classic "fringed micelle" morphological model[100,103,113] shown in Figure 20),[24] with functional aspects, depending on mobility and conceptualized in terms of the integrated concepts of "water dynamics" and "glass dynamics". Through this unification, the appropriate kinetic description of the non-equilibrium thermomechanical behavior of food systems has been illustrated in the context of a "dynamics map", shown in Figure 21.[30] This map was derived from a generic solute-solvent state diagram,[74,133] in turn based originally on a more familiar equilibrium phase diagram of temperature vs. composition. The dynamics map, like the "supplemented state diagram",[133] is complicated by the attempt to represent aspects of both equilibrium and non-equilibrium thermodynamics in a single figure. The primary distinction at atmospheric pressure is that the equilibrium regions are completely described as shown in two dimensions of temperature and composition, with no time dependence, while the non-equilibrium regions emphatically require the third dimension of time, expressed as t/τ, where τ is a relaxation time. In this way, the time dependence of a dynamic process can be defined in terms of the relationship between the experimental time scale and the time frame of the relaxation process undergone by the system. The established principle of time-temperature superpositioning[134] has been extended to

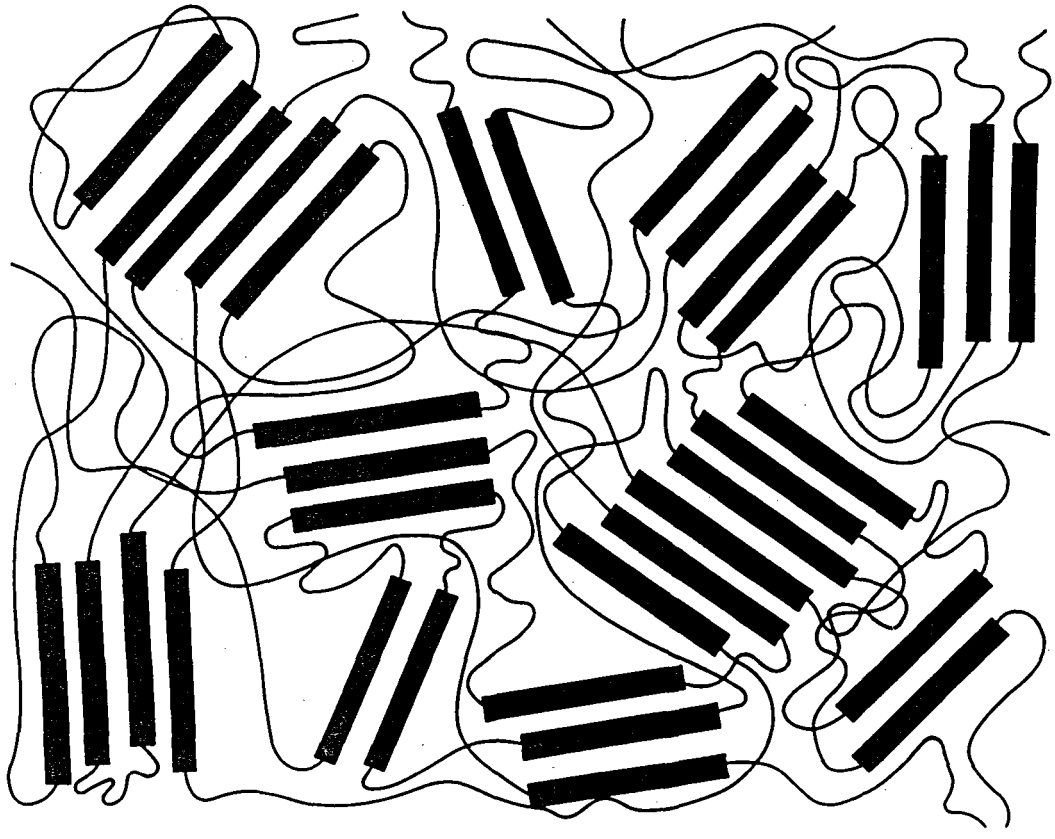

FIGURE 20. "Fringed micelle" model of the crystalline-amorphous structure of partially crystalline polymers. (From Slade, L. and Levine, H., *Advances in Meat Research,* Vol. 4, Collagen as a Food, Pearson, A. M., Dutson, T. R., and Bailey, A., Eds., AVI, Westport, 1987, 251. With permission.)

define "mobility transformations" in terms of the critical variables of time, temperature, and moisture content (with pressure as another variable of potential technological importance). The dynamics map has been used[30] to describe mobility transformations in water-compatible food polymer systems that exist in kinetically metastable glassy and rubbery states[15,25,26] always subject to conditionally beneficial or detrimental plasticization by water. For example, the kinetics of starch gelatinization have been explained in terms of mobility transformations by locating on the dynamics map the alternative pathways of complementary plasticization by heat and moisture.[22,23,26] The map domains of moisture content and temperature, traditionally described with only limited success using concepts such as Aw and "bound water" to interpret and explain sorption isotherms and sorption hysteresis, have been treated alternatively in terms of water dynamics.[15,16] As the name implies, water dynamics focuses on the mobility and eventual "availability" of the plasticizing diluent (be it water alone or an aqueous solution) and a theoretical approach to understanding how to control the mobility of the diluent in glass-forming food systems that would be inherently mobile, unstable, and reactive at temperatures above Tg and moisture contents above Wg. This concept has provided an innovative perspective on the moisture management and structural stabilization of IMF systems[16] and the cryostabilization of frozen, freezer-stored, and freeze-dried aqueous glass-forming food materials and products.[8,27,31-34,40-42]

Glass dynamics deals with the time- and temperature-dependence of relationships among composition, structure, thermomechanical properties, and functional behavior. As its name implies, glass dynamics focuses on (1) the glass-forming solids in an aqueous food system, (2)

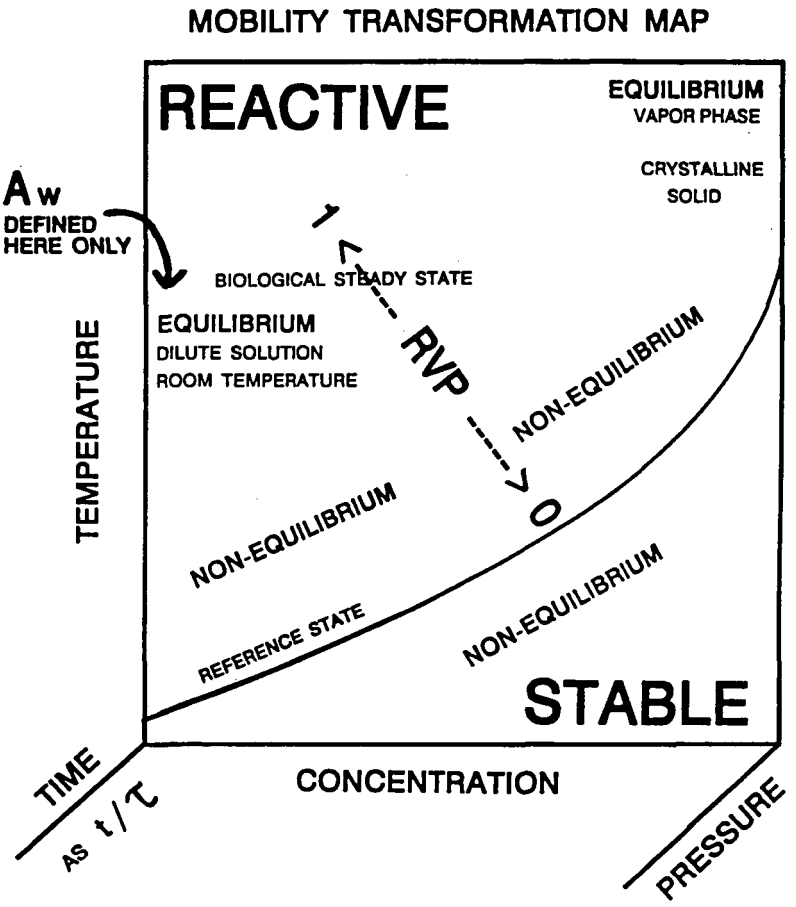

FIGURE 21. A four-dimensional "dynamics map", with axes of temperature, concentration, time, and pressure, which can be used to describe mobility transformations in non-equilibrium glassy and rubbery systems. (From Slade, L. and Levine, H., *Pure Appl. Chem.*, 60, 1841, 1988. With permission.)

the Tg of the resulting aqueous glass that can be produced by cooling to $T < Tg$, and (3) the effect of the glass transition and its Tg on processing and process control, via the relationships between Tg and the temperatures of the individual processing steps (which may be deliberately chosen to be first above and then below Tg). This concept emphasizes the operationally immobile, stable, and unreactive situation (actually one of kinetic metastability) that can obtain during product storage (of a practical duration) at temperatures below Tg and moisture contents below Wg. It has been used to describe a unifying concept for interpreting "collapse" phenomena, which govern, for example, the time-dependent caking of amorphous food powders during storage.[8,27] Collapse phenomena in completely amorphous or partially crystalline food systems[54,64,66,126,135-138] are diffusion-limited consequences of a material-specific structural and/or mechanical relaxation process.[8] The microscopic and macroscopic manifestations of these consequences occur in real time at a temperature about 20°C above that of an underlying molecular state transformation.[30,66] This transformation from kinetically metastable amorphous solid to unstable amorphous liquid occurs at Tg.[8] The critical effect of plasticization (leading to increased free volume and mobility in the dynamically constrained glass) by water on Tg is a key aspect of collapse and its mechanism.[27]

A general physicochemical mechanism for

collapse has been described,[8] based on occurrence of the material-specific structural transition at Tg, followed by viscous flow in the rubbery liquid state.[137] The mechanism was derived from Williams-Landel-Ferry (WLF) free volume theory for (synthetic) amorphous polymers.[101,107] It has been concluded that Tg is identical to the phenomenological transition temperatures observed for structural collapse (Tc) and recrystallization (Tr). The non-Arrhenius kinetics of collapse and/or recrystallization in the high viscosity (η) rubbery state are governed by the mobility of the water-plasticized polymer matrix.[8] These kinetics depend on the magnitude of $\Delta T = T - Tg$,[8,66] as defined by a temperature-dependent exponential relationship derived from WLF theory. Glass dynamics has proven a useful concept for elucidating the physicochemical mechanisms of structural/mechanical changes involved in various melting and (re)crystallization processes.[15] Such phenomena are observed in many partially crystalline food polymers and processing/storage situations, including, for example, the gelatinization and retrogradation of starches.[20] Glass dynamics has also been used to describe the viscoelastic behavior of amorphous polymeric network-forming proteins such as gluten and elastin.[25]

1. "Fringed Micelle" Structural Model

The "fringed micelle" model, shown in Figure 20, was originally developed to describe the morphology of partially crystalline synthetic polymers. It is particularly useful for conceptualizing a three-dimensional network composed of microcrystallites (with crystalline melting temperature, Tm) that crosslink amorphous regions (with glass transition temperature, Tg) of flexible-coil chain segments.[139] In pure homopolymers, for which Tg is always at a lower temperature than Tm,[106] the amorphous domains can exist in a glassy solid physical state at $T < Tg$ or in a rubbery liquid state at $Tg < T < Tm$.[15] The model is especially applicable to synthetic polymers that crystallize from an undercooled melt or concentrated solution to produce a metastable network of relatively low degree of crystallinity. Typically, such polymers contain small crystalline regions of only about 100 Å dimensions.[103] Thus, the model has also often been used to describe the partially crystalline structure of aqueous gels of biopolymers such as starch and gelatin,[17,18,61,65,103,139] in which the amorphous regions contain plasticizing water and the microcrystalline regions, which serve as physical junction zones, are crystalline hydrates. The model has also been used to conceptualize the partially crystalline morphology of frozen aqueous food polymer systems, in which case the ice crystals represent the "micelles" dispersed in a continuous amorphous matrix (the "fringe") of solute-unfrozen water (UFW).[15] An important feature of the model, as applied to high MW polymer systems such as starch (both native granular and gelatinized)[21] and gelatin, concerns the interconnections between crystalline and amorphous domains. A single long polymer chain can have helical (or other ordered) segments located within one or more microcrystallites that are covalently linked to flexible-coil segments in one or more amorphous regions.[139] Moreover, in the amorphous regions, chain segments may experience random intermolecular "entanglement couplings",[112] which are topological interactions rather than covalent or non-covalent chemical bonds.[140] Thus, in terms of their thermomechanical behavior in response to plasticization by water and/or heat, the crystalline and amorphous domains are neither independent of each other nor homogeneous.[106]

2. The Dynamics Map

The key to our new perspective on concentrated, water-plasticized food polymer systems relates to recognition of the fundamental importance of the dynamics map mentioned earlier. As shown in Figure 21, the major area of the map (i.e., the area surrounding the reference state in two dimensions and projecting into the third, time, dimension) represents a non-equilibrium situation corresponding to the temperature-composition region of most far-reaching technological consequence to aqueous food systems, including IMFs.[16] The critical feature in the use of this map is identification of the glass transition as the reference state, a conclusion[30] based on WLF

theory for glass-forming polymers. This line of demarcation (representing the glass curve of Tg vs. composition) serves as a basis for description of the non-equilibrium thermomechanical behavior of water-compatible polymeric materials in glassy and rubbery states, in response to changes in moisture content, temperature, and time.[15,30,40-42] Mobility is the transcendent principle underlying the definition of the glass transition as the appropriate reference state,[16] because mobility is the key to all transformations in time (or frequency), temperature, and composition between different relaxation states for a technologically practical system.[30] An interesting illustration of the practical relevance of mobility transformations to shelf-life problems in real food products is shown in Figure 22.[141] Marsh and Wagner[141] have described a "state of the art" computer model that can be used to predict the shelf-life of particular moisture-sensitive products, based on the moisture-barrier properties of a packaging material and the temperature/humidity conditions of a specific storage environment. As shown in Figure 22, shelf-life (i.e., time) increases with decreasing temperature and humidity conditions (e.g., Minneapolis in the winter) and decreases correspondingly with increasing temperature and humidity (e.g., Miami in the summer), such that shelf-life varies by a factor of 4 between the highest and lowest temperature/moisture combinations.

The interdependent concepts of water dynamics and glass dynamics embodied in the dynamics map have provided insights into the relevance of the glassy reference state to functional aspects of a variety of food systems.[15,30] For example, the kinetics of all constrained relaxation processes, such as translational and rotational diffusion, which are governed by the mobility of a water-plasticized polymer matrix in glass-forming systems, vary (from Arrhenius to WLF-type) between distinct temperature/structure domains, which are divided by this glass transition.[15,25,30] Thus, while familiar Arrhenius kinetics are ap-

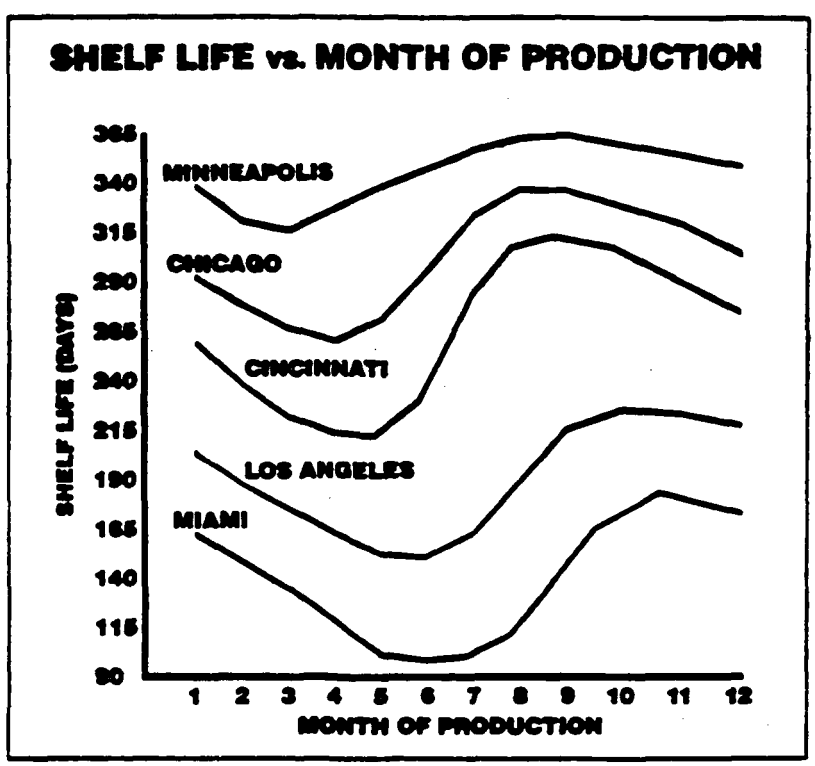

FIGURE 22. Plot of shelf life vs. month of production for a typical moisture-sensitive food product. (From Marsh, K. S. and Wagner, J., *Food Eng.*, 57(8), 58, 1985. With permission.)

plicable below Tg in the glassy solid state of very low mobility and very slow diffusion (the domain of glass dynamics, labeled STABLE in Figure 21), WLF kinetics[107] are applicable above Tg in the viscoelastic, rubbery liquid state of accelerating mobility and diffusion (the domain of water dynamics, labeled REACTIVE in Figure 21).[30] The WLF equation[101,107] defines the kinetics of molecular-level relaxation processes, which will occur in practical time frames only in the rubbery state above Tg, in terms of an exponential, but non-Arrhenius, function of ΔT above this boundary condition.[8,26,66] Of course, the highest mobility and most rapid diffusion occur in the region above a second set of reference lines, the equilibrium liquidus and solidus curves (shown and discussed later), which demark the upper boundary of the WLF region where Arrhenius kinetics again apply.[33] Within the WLF region, kinetics accelerate according to the WLF equation from the extremely steep temperature dependence of WLF kinetics just above Tg to the familiarly moderate temperature dependence of Arrhenius kinetics on approaching Tm.[30] The WLF equation describes the profound range of the kinetics between Tg and Tm, with correspondingly profound implications for process control, product quality, safety, and shelf-life. Sperling[114] has remarked that "for a generation of (synthetic) polymer scientists and rheologists, the WLF equation has provided a mainstay both in utility and theory." It should be noticed in Figure 21 that Aw would be correctly defined only in the region of the map corresponding to a dilute solution at equilibrium at room temperature. In contrast, the actual measured RVP of an IMF (non-equilibrium) system would approach zero in the limit of the glassy reference state at temperatures below Tg and moisture contents $<$ Wg, but would increase toward 1.0 with increasing temperature above Tg and increasing moisture content above Wg.

One particular location among the continuum of Tg values along the reference glass curve in Figure 21 results from the behavior of water as a crystallizing plasticizer and corresponds to an operationally invariant point (called Tg′) on a state diagram for any particular solute.[4-8,31-34,40-42,74] Tg′ represents the solute-specific subzero Tg of the maximally freeze-concentrated, amorphous solute/UFW matrix surrounding the ice crystals in a frozen solution. As illustrated in the idealized state diagram shown in Figure 23, the Tg′ point corresponds to, and is determined by, the point of intersection of the kinetically determined glass curve for homogeneous solute-water mixtures and the non-equilibrium extension of the equilibrium liquidus curve for the Tm of ice.[8,31-34] This solute-specific location defines the composition of the glass that contains the maximum practical amount of plasticizing moisture (called Wg′, expressed as g UFW/g solute or weight % (w%) water, or alternatively designated in terms of Cg′, expressed as w% solute)[8,15] and represents the transition from concentrated fluid to kinetically metastable, dynamically constrained solid which occurs on cooling to T $<$ Tg′.[16] In this homogeneous, freeze-concentrated solute-water glass, the water represented by Wg′ is not "bound" energetically but rather rendered unfreezable in a practical time frame due to the immobility imposed by the extremely high local viscosity of about 10^{12} Pa s at Tg′.[4-8,15,25,26,30-34,40-42] Marsh and Blanshard[94] have recently documented the technological importance of freeze-concentration and the practical implication of the description of water as a readily crystallizable plasticizer, characterized by a high value of Tm/Tg ratio $\simeq$ 2.[30,89] A theoretical calculation[94] of the Tg of a typically dilute (i.e., 50%) wheat starch gel fell well below the measured value of about -5 to -7°C for Tg′,[17,20] because the theoretical calculation based on free volume theory did not account for the formation of ice and freeze-concentration that occurs below about -3°C. Recognition of the practical limitation of water as a plasticizer of water-compatible solutes, due to the phase separation of ice, reconciled the difference between theoretical and measured values of Tg.[94] Moreover, the theoretical calculations supported the measured value of $\simeq$27% water[17,20] for Wg′, the maximum practical water content of an aqueous wheat starch glass. The calculated water content of the wheat starch glass with Tg of about -7°C is $\simeq$28%.[94]

Within a homologous polymer family (e.g., from the glucose monomer through maltose, maltotriose, and higher malto-oligosaccharides to the amylose and amylopectin high polymers of starch), Tg′ increases in a characteristic fashion

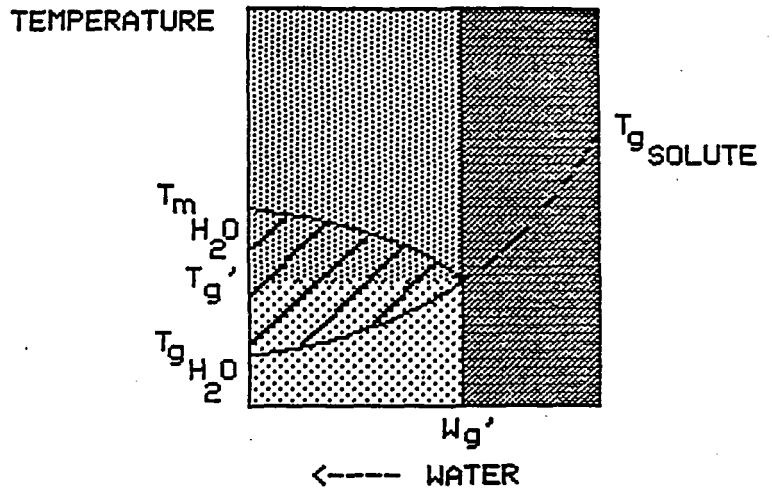

FIGURE 23. Idealized state diagram of temperature vs. w% water for an aqueous solution of a hypothetical, glass-forming, small carbohydrate (representing a model frozen food system), illustrating how the critical locations of Tg′ and Wg′ divide the diagram into three distinguishable structure-property domains.

with increasing solute MW.[8,27,31] This finding has been shown to be in full accord with the established and theoretically predictable variation of Tg with MW for homologous families of pure synthetic amorphous polymers,[107,113,114] described in the next section. The insights resulting from this finding have proven pivotal to the characterization of structure-function relationships in many different types of completely amorphous and partially crystalline food polymer systems.[8,14-39] It should be noted that Tg′ also corresponds to the subzero Tg mentioned by Atkins[90] as being characteristic of many water-plasticized, rubbery biopolymers *in vivo*.

3. The Effect of Molecular Weight on Tg

For pure synthetic polymers, in the absence of diluent, Tg is known to vary with MW in a characteristic and theoretically predictable fashion, which has a significant impact on resulting mechanical and rheological properties.[26,107] For a homologous series of amorphous linear polymers, Tg increases with increasing number-average MW ($\overline{M}n$), due to decreasing free volume contributed by chain ends, up to a plateau limit for the region of entanglement coupling in rubber-like viscoelastic random networks (typically at $\overline{M}n = 1.25 \times 10^3$ to 10^5 Da[112]), then levels off with further increases in $\overline{M}n$.[107,113] Below the entanglement $\overline{M}n$ limit, there is a theoretical linear relationship between increasing Tg and decreasing inverse $\overline{M}n$.[114] (For polymers with constant values of $\overline{M}n$, Tg increases with increasing weight-average MW ($\overline{M}w$), due to increasing local viscosity.[30] This contribution of local viscosity is reported to be especially important when comparing different MWs in the range of low MWs.[107])The difference in three-dimensional morphology and resultant mechanical and rheological properties between a collection of nonentangling, low MW polymer chains and a network of entangling, high MW, randomly coiled polymer chains can be imagined as analogous to the difference between masses of elbow macaroni and spaghetti.[26] For synthetic polymers, the $\overline{M}n$ at the boundary of the entanglement plateau often corresponds to about 600 backbone chain atoms.[114] Since there are typically about 20 to 50 backbone chain atoms in each polymer segmental unit involved in the cooperative translational motions at Tg,[102] entangling high polymers are those with at least about 12 to 30 segmental units per chain.[26] Figure 24[114] illustrates the characteristic dependence of Tg on $\overline{M}n$ (expressed in terms of the degree of polymerization, DP) for several homologous series of synthetic amorphous polymers. In this semi-log plot, the Tg values for each polymer reveal three distinguishable inter-

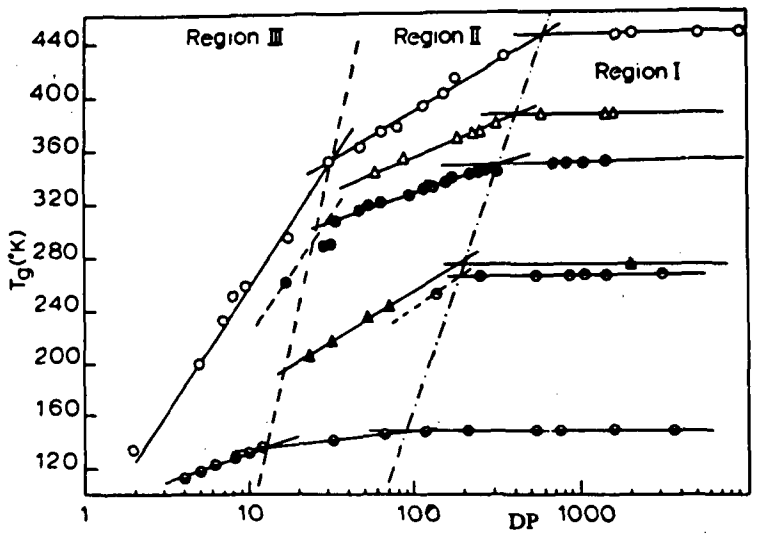

FIGURE 24. Plot of Tg as a function of log DP (degree of polymerization) (a measure of $\overline{Mn}$), for poly(alpha-methyl-styrene) (open circles); poly(methylmethacrylate) (open triangles); poly(vinyl chloride) (solid circles); isotactic polypropylene (solid triangles); atactic polypropylene (circles, top half solid); and poly(dimethylsiloxane) (circles, bottom half solid). (From Sperling, L. H., *Introduction to Physical Polymer Science*, Wiley-Interscience, New York, 1986. With permission.)

secting linear regions: (III) a steeply rising region for non-entangling small oligomers; (II) an intermediate region for non-entangling low polymers; and (I) the horizontal plateau region for entangling high polymers.[142] From extensive literature data for a variety of synthetic polymers, it has been concluded that this three-region behavior is a general feature of such Tg vs. log $\overline{Mn}$ plots, and demonstrated that the data in the non-entanglement regions II and III show the theoretically predicted linear relationship between Tg and inverse $\overline{Mn}$.[142]

4. Water Plasticization

Water acting as a plasticizer is well known to affect the Tg of completely amorphous polymers and both the Tg and Tm of partially crystalline polymers (see References 15, 25, 26 and references therein). Water is a "mobility enhancer", in that its low MW leads to a large increase in mobility, due to increased free volume and decreased local viscosity,[107] as moisture content is increased from that of a dry solute to a solution.[16,30] The direct plasticizing effect of increasing moisture content at constant temperature is equivalent to the effect of increasing temperature at constant moisture and leads to increased segmental mobility of chains in amorphous regions of glassy and partially crystalline polymers, allowing in turn a primary structural relaxation transition at decreased Tg.[108,109] State diagrams illustrating the extent of this Tg-depressing effect have been reported for a wide variety of synthetic and natural, water-compatible, glassy and partially crystalline polymers. In such diagrams[15,25,26] (e.g., see the one for elastin in Figure 19A), the smooth glass curve of Tg vs. composition shows the dramatic effect of water on Tg especially at low moisture contents (i.e., $\lesssim$10 weight % [w%] water). In this region, Tg generally decreases by about 5 to 10°C/w% water[15] (~12°C/w% for elastin), from the neighborhood of 200°C for the anhydrous polymer.[90] Another example is shown in Figure 25,[43] which depicts the amylopectin of freshly gelatinized starch as another typical water-compatible, completely amorphous polymer, which exhibits a Tg curve from about 125°C for pure anhydrous starch to about −135°C, the Tg of pure amorphous solid water,[143] passing through Tg′ at about −5°C (and Wg′ ≈ 27 w% water).[18]

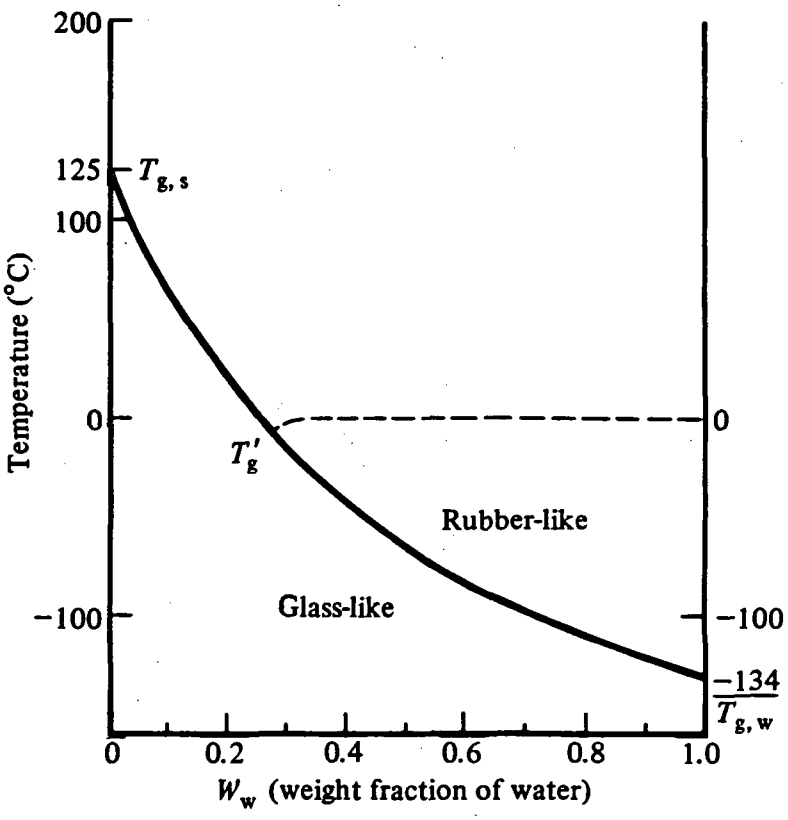

FIGURE 25. State diagram, showing the approximate Tg temperatures as a function of mass fraction, for a gelatinized starch-water system. (From van den Berg, C., *Concentration and Drying of Foods*, MacCarthy, D., Ed., Elsevier, London, 1986, 11. With permission.)

Figure 25 shows the Tg of starch decreasing by about 6°C/w% water for the first 10 w% moisture, in good agreement with another published glass curve for starch calculated from free volume theory.[49,94] Similarly, the glass curve for water-compatible, amorphous gluten[99] in Figure 26[51] shows a decrease in Tg from >160°C at ≤1 w% water to 15°C at 16 w% water, a depression of about 10°C/w% water in this moisture range. The plasticizing effect of water on gluten continues at higher moisture contents, until Tg falls to Tg′ ≃ −7.5°C and Wg reaches Wg′ ≃ 26 w% water ≃0.35 g UFW/g gluten.[25]

The plasticizing effect of water on the Tg of three other glass-forming food materials is illustrated and compared in the state diagrams shown in Figure 27.[91,129] Hemicellulose,[129] an amorphous component of wood, is another typical water-compatible biopolymer, with a dry Tg of about 200°C, which is dramatically depressed (by more than 15°C/w% water for the first 10% water) to a Tg around −10°C (i.e., Tg′) at about 30% moisture.[90] Hemicellulose, like starch, gluten, and elastin, exhibits the characteristic behavior common to all water-compatible, glass-forming solutes:[15] the practical limit to the extent of plasticization (i.e., depression of Tg by water) is determined by the phase separation of crystalline ice below 0°C, so that the minimum Tg achievable during slow cooling in a practical time frame is the solute-specific Tg′ (with the corresponding maximum content of plasticizing moisture, Wg′).[8,30-34] Accordingly, the glass curve shown for hemicellulose in Figure 27 is typical of the "practical glass curve for a water-compatible solute" that levels off at Tg′<0°C, rather than continuing along the monotonic descent of the "complete glass curve" to the Tg of water itself. In contrast to hemicellulose, lignin, the other major amorphous component of wood, typifies a high polymer that is only water-sensitive rather than water-compatible.[15] Its glass curve also starts at

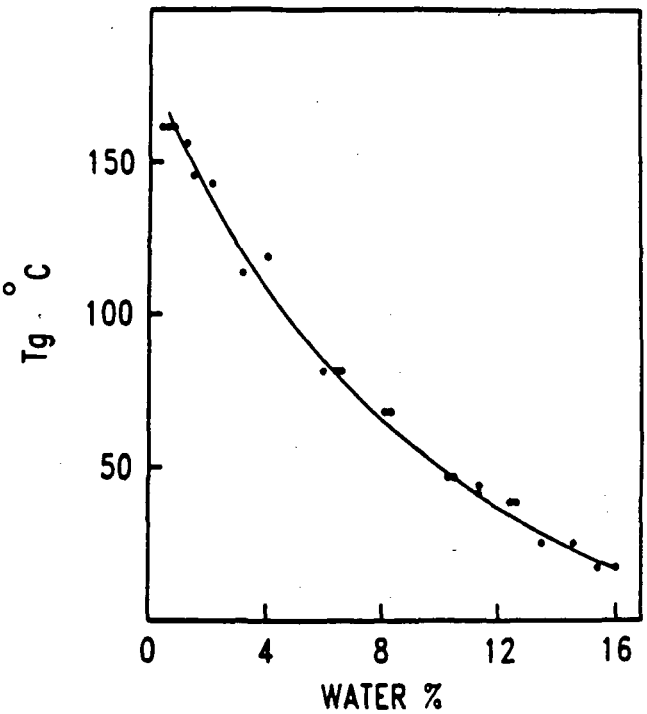

FIGURE 26. Change in Tg as a function of moisture for a hand-washed and lyophilized wheat gluten. (From Hoseney, R. C., Zeleznak, K., and Lai, C. S., *Cereal Chem.*, 63, 285, 1986. With permission.)

about 200°C for the dry solid and decreases by more than 10°C/w% water for the first 10% water. But the glass curve shown for lignin in Figure 27 is typical of the "practical glass curve for a water-sensitive solute"; it levels off at a lower moisture content and at a temperature well above 0°C. Lignin exhibits the characteristic behavior common to all water-sensitive, glass-forming solutes (e.g., synthetic high polymers that are relatively hydrophobic, such as polyethylene, poly[vinyl acetate], and nylons):[15] the practical limit to its extent of plasticization by water is determined by its much more limited water-solubility and thermodynamic compatibility, leading to the phase separation of liquid water (as clusters of water molecules) above 0°C, which would subsequently freeze on further cooling to 0°C.[15] Thus, the minimum Tg achievable during cooling of a lignin-water mixture is not Tg′, but some higher Tg>Tm of ice (about 50°C for lignin, as shown in Figure 27), because Tg cannot be depressed to Tg′ by clustered water in a separate (non-plasticizing) liquid phase.[15,30] In contrast to the two high MW biopolymers represented in Figure 27, sorbitol is a water-compatible, glass-forming, monomeric polyol. As shown in Figure 27, the glass curve for quench-cooled, completely amorphous sorbitol-water mixtures[91] begins at a much lower temperature (Tg = −2°C for anhydrous sorbitol),[28,91] because of the low MW of this solute, and shows an extent of plasticization of sorbitol at low moisture of about 3 to 4°C/w% water. The glass curve shown for sobitol in Figure 27 is the "complete glass curve" up to 50 w% water, as a result of quench-cooling to avoid phase separation of ice at water contents >Wg′, and would continue smoothly down to the Tg of pure amorphous water at about −135°C,[91] as do the "complete" glass curves of all water-compatible solutes, regardless of MW.[8,15,16] If these sorbitol-water mixtures had been cooled more slowly, so that ice formation and maximal freeze-concentration of the solute could have occurred during the experimental time frame, they would have been expected to manifest the "practical" glass curve for sorbitol, with

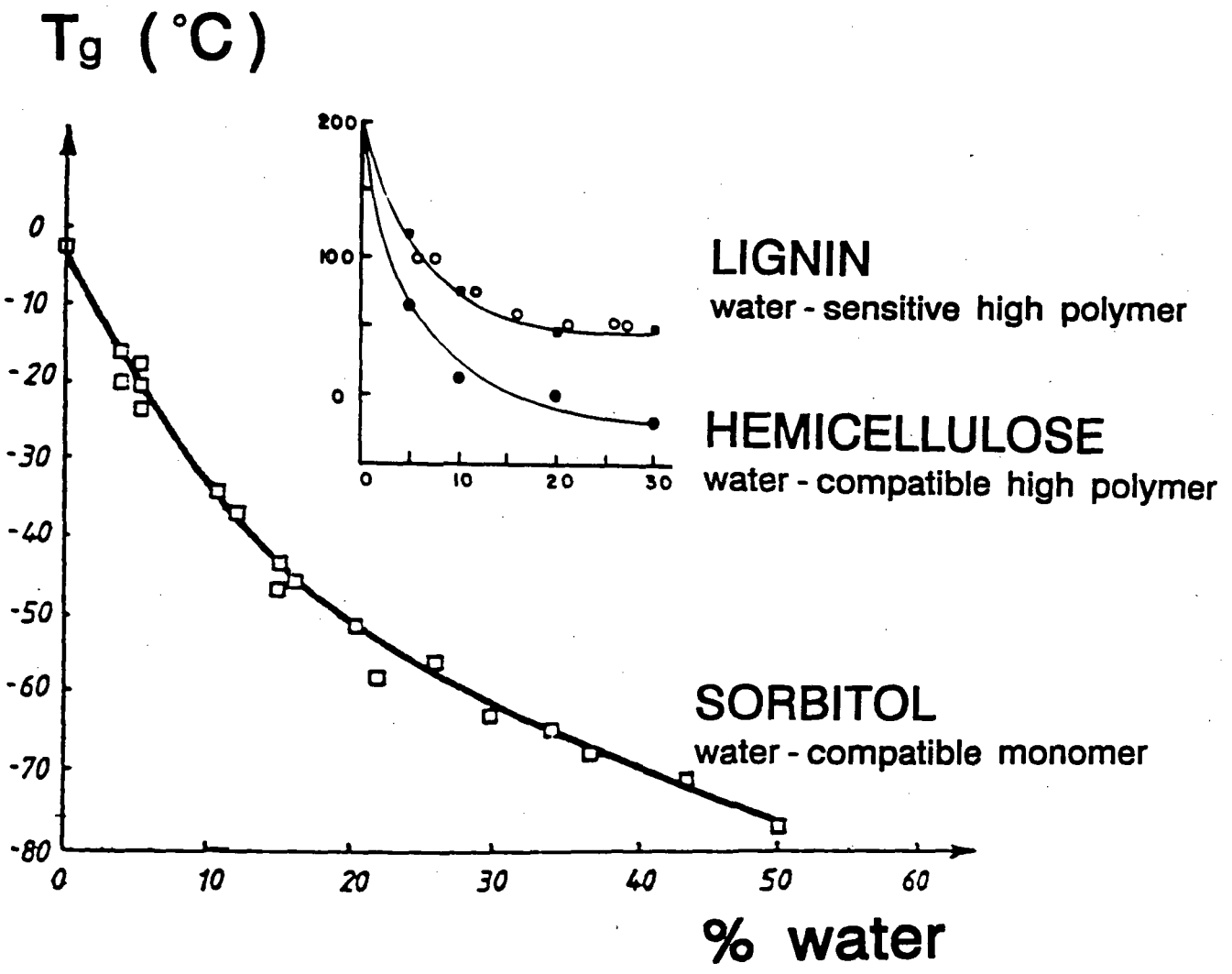

FIGURE 27. "Glass curves" of Tg as a function of weight percent water. The "complete" glass curve for sorbitol (adapted with permission from Reference 91) is shown up to 50 w% water. The "practical" glass curves for hemicellulose and lignin (adapted with permission from Reference 129) are shown up to 30 w% water.

invariant values of Tg = Tg′ ≃ −43.5°C and Wg = Wg′ ≃ 19 w% water ≃ 0.23 g UFW/g sorbitol.[27,33]

According to the prevailing view in the current synthetic polymer literature, the predominant contribution to the mechanism of plasticization of water-compatible glassy polymers by water at low moisture content derives from a free volume effect.[111,144,145] Free volume theory[107] provides the general concept that free volume is proportional to inverse $\overline{M}n$, so that the presence of a plasticizing diluent of low MW leads to increased free volume, allowing increased backbone chain segmental mobility. (Note that Sears and Darby[109] have stated that "free volume is considered thermodynamically as a solvent.") The increased mobility is manifested as a decreased Tg of the binary polymer-diluent glass.[94,109] For synthetic amorphous high polymers, it is well known that the ability of a diluent to depress Tg decreases with increasing diluent MW,[146] as predicted by free volume theory. These facts are illustrated in Figure 28,[107] which shows a series of glass curves for solutions of polystyrene with various compatible organic diluents that can be undercooled without crystallizing. These smooth curves illustrate the characteristic plasticizing effect of low MW, glass-forming diluents

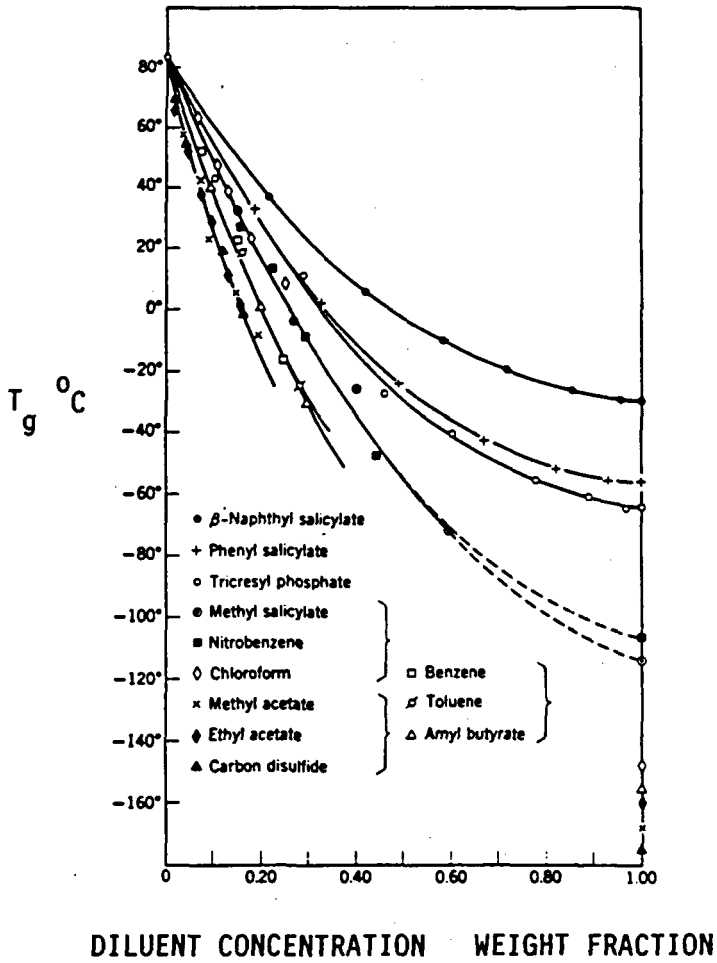

FIGURE 28. Glass transition temperatures of polystyrene solutions with various diluents of low molecular weight, plotted against weight fraction of diluent. (From Ferry, J. D., *Viscoelastic Properties of Polymers,* 3rd ed., John Wiley & Sons, New York, 1980. With permission.)

of low Tg on a typical polymer of higher Tg: Tg decreases monotonically with increasing concentration (weight fraction) of diluent, because the $\overline{M}w$ of the homogeneous polymer-plasticizer mixture decreases and its free volume increases.[114] Figure 28 also shows that, at a given weight fraction of diluent, Tg of the mixture increases with increasing MW of the diluent (generally over the entire set of diluents, but rigorously within a homologous series), because the Tg values of the neat diluents likewise generally increase with increasing MW and decreasing free volume.[114]

In contrast, the effect of synthetic polymer plasticization by a crystallizing diluent has been illustrated by Tg results for blends of poly(vinyl chloride) (PVC) with a terpolymeric organic plasticizer that is able to crystallize on undercooling, as shown in Figure 29.[147] In this interesting case of a polymer and plasticizer with more nearly equal MWs, while the diluent depresses the Tg of the polymer in the typical fashion, the polymer simultaneously depresses the crystallization temperature (Tcr) of the plasticizer. Thus, with increasing PVC concentration in the blend, Tcr of the plasticizer decreases as Tg of the blend increases. Upon cooling, crystallization of the plasticizer can no longer occur, within a realistic experimental time frame, in the region (on the state diagram in Figure 29) of temperature and

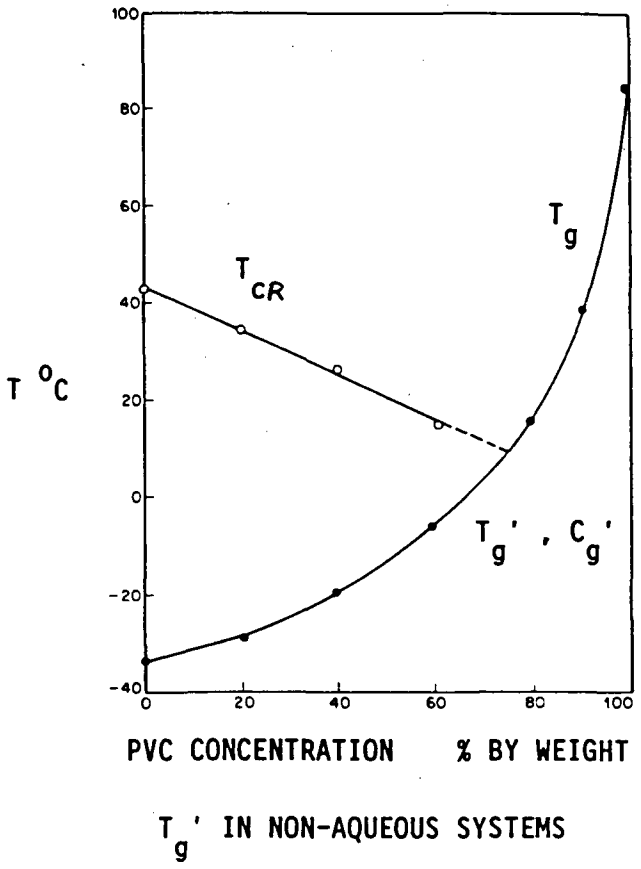

FIGURE 29. Crystallization and glass temperatures in terpolymeric plasticizer (TP)/polyvinyl chloride (PVC) blends as a function of PVC concentration. (From Bair, H. E., *Thermal Characterization of Polymeric Materials,* Turi, E. A., Ed., Academic Press, Orlando, 1981, 845. With permission.)

blend composition where the extrapolated crystallization curve intersects the glass curve at a particular point, which can be designated as Tg'.[30] Below a critical diluent concentration (i.e., the composition of the glass at Tg'), crystallization on cooling of the plasticizer, which would be readily crystallizable if pure, essentially ceases at an incomplete extent, due to the immobility imposed by the vitrification of the glass-forming plasticizer-polymer blend. Wunderlich[105] has described several other cases of the same type of behavior for binary mixtures of a synthetic amorphous polymer and its crystallizable monomer.[148] In each case, "the monomer liquidus curve was observed as usual. At its intersection with the Tg vs. concentration curve of the macromolecule, which shows a decreasing Tg with increasing amount of monomer (plasticization), the whole system becomes glassy without crystallization of the monomer. The polymer-rich side of the phase diagram remains thus a single-phase region throughout, while the monomer-rich samples change on cooling from a liquid solution to a two-phase system that consists of liquid solution and crystalline monomer at higher temperature, and changes at lower temperature to glassy solution and crystalline monomer."[105] The analogy between this behavior (as exemplified in Figure 29) of a non-aqueous high-polymer system, with its characteristic Tg' and corresponding composition Cg', and the general behavior of aqueous glass-forming systems of water-compatible solutes (discussed earlier and described with respect to the idealized state diagram in Figure 23) is important and fundamental to interpreting the non-equilibrium behavior of food polymer systems in the general context of the dynamics map and mobility transformations.[30]

Recent reports[111,144,145] have demonstrated that the effectiveness of water as a plasticizer of synthetic polymers[15] (by analogy with the effectiveness of typical low MW organic plasticizers, as shown in Figure 28) primarily reflects the low molar mass of water. These workers have discounted older concepts of specific interactions, such as disruptive water-polymer hydrogen bonding in polymer hydrogen-bonded networks, or plasticizing molecules becoming "firmly bound" to polar sites along a polymer chain, in explaining water's plasticizing ability. Although hydrogen bonding certainly affects solubility parameters and contributes to compatibility of polymer-water blends,[109] it has been convincingly shown that polymer flexibility does not depend on specific hydrogen bonding to backbone polar groups.[121] Rather, the relative size of the mobile segment of linear backbone,[114] and thus the relative $\overline{M}w$ of its blend with water, governs the magnitude of plasticization and so determines Tg.[121] To negate the older arguments for site-specific hydrogen bonding, NMR results have been cited that clearly indicate that water molecules in polymers with polar sites have a large degree of mobility.[144,145] As used in this context, mobility is defined in terms of translational and rotational degrees of freedom for molecular diffusion on a time scale of experimental measurements.[30] Franks[4-7,40-42,149,150] has advocated a similar view and presented similar evidence to try to dispel the popular[151] but outdated[57] myths about "bound" water and "water-binding capacity" in glass-forming food polymers or low MW materials. For example, as discussed later, proton NMR has been used to test the accessibility of water with reduced mobility in the crystalline regions of retrograded wheat starch gels.[152] Such gels are partially crystalline, with B-type hydrated crystalline regions in which water molecules constitute an integral structural part of the crystal unit cell.[153,154] NMR results have shown that all the water in such a starch gel can be freely exchanged with deuterium oxide.[152] Most recently, Ellis[111] has reported results of a comprehensive DSC study that show that several diverse synthetic "amorphous polyamides in pure and blended form exhibit a monotonic depression of Tg as a function of water content", and which "lend further credence to the simple and straightforward plasticizing action of water in polar polymers irrespective of their chemical and physical constitution." These results have helped to confirm the conclusions[15,25] that (1) the behavior of hydrophilic polymers with aqueous diluents is precisely the same as that of nonpolar synthetic polymers (e.g., polystyrene in Figure 28) with organic diluents, and (2) water-compatible food polymers such as starch, gelatin, elastin, and gluten, for which water is an efficient plasticizer but not necessarily a good solvent, exhibit the same physicochemical responses to plasticization as do many water-compatible synthetic polymers (e.g., poly[vinyl pyrrolidone] [PVP]).[15] A characteristic extent of plasticization at low moisture, typically in the range of about 5 to 10°C/w% water (as shown for starch in Figure 25 and gluten in Figure 26), but occasionally somewhat less than 5°C/w% (e.g., sorbitol in Figure 27) or as much as 20°C/w% (e.g., hemicellulose in Figure 27), has been shown to apply to a wide variety of water-compatible glassy and partially crystalline food monomers, oligomers, and high polymers.[15,25,26,66] As mentioned earlier, the excellent agreement between the measured value of Tg'[17,20] and the theoretical value recently calculated from free volume theory[49,94] for an aqueous wheat starch gel with $\gtrsim$27% moisture also lends further support to these conclusions.

In partially crystalline polymers, water plasticization occurs only in the amorphous regions.[62,145,155-157] In linear synthetic polymers with anhydrous crystalline regions and a relatively low capacity for water in the amorphous regions (e.g., nylons),[155] the % crystallinity affects Tg, such that increasing % crystallinity generally leads to increasing Tg.[145] This is due primarily to the stiffening or "antiplasticizing" effect of disperse microcrystalline crosslinks, which leads to decreased mobility of chain segments in the interconnected amorphous regions.[156] The same effect is produced by covalent crosslinks,[145] which, when produced by radiation, occur only in amorphous regions.[144] In polymers with anhydrous crystalline regions, only the amorphous regions are accessible to penetration and therefore plasticization by water.[144,145,157] Similar phenomena are observed in partially crystalline polymers with hydrated crystalline regions, such as gelatin and starch.[15,19,24] In native starches, hy-

drolysis by aqueous acid ("acid etching") or enzymes, at T < Tm, can occur initially only in amorphous regions.[153] Similarly, acid etching of retrograded starch progresses in amorphous regions, leading to increased relative crystallinity (or even increased absolute crystallinity, by crystal growth) of the residue.[153] Dehumidification of granular starch proceeds most readily from initially mobile amorphous regions, leading to non-uniform moisture distribution.[62] In partially gelatinized starches, dyeability by a pigment increases with increasing amorphous content.[158] It should be noted, however, that plasticization of the amorphous regions (e.g., the backbone segments and branch points of amylopectin molecules) of native granular starches by sorbed water is neither instantaneous nor simultaneous with the initial swelling caused by water uptake. It has recently been demonstrated by Aguerre et al.[159] that "the uptake of water takes place between the concentric layers" of the granule, leading to "interlamellar expansion of the starch granule structure." This sorbed water must subsequently diffuse from the interlamellar spaces to the amorphous regions of the granule before plasticization of the polymer molecules or chain segments in those amorphous regions can begin. The effective Tg that immediately precedes and thereby determines the temperature of gelatinization (Tgelat) in native starch depends on the extent and type (B vs. A vs. V polymorphs) of crystallinity in the granule (but not on amylose content) and on total moisture content and moisture distribution.[17-21] For normal and waxy (i.e., all amylopectin) starches, Tgelat increases with increasing % crystallinity,[160] an indirect effect due to the disproportionation of mobile short branches of amylopectin from amorphous regions to microcrystalline "micelles", thereby increasing the average MW and effective Tg of the residual amorphous constituents,[21] because these branches are unavailable to serve as "internal" plasticizers.[109] Two other related phenomena are observed as a result of the non-uniform moisture distribution in situations of overall low moisture content for polymers with hydrated crystalline regions:[15] (1) atypically high Tg/Tm (in K) ratios $\geqslant 0.80$ but, of course, <1.0,[89,105] in contrast to the characteristic range of 0.5 to 0.8 for many partially crystalline synthetic polymers,[102] and (2) a pronounced apparent depressing effect of water on Tm[93,161] as well as Tg, such that both Tg and Tm decrease with increasing moisture content.

To put this modern concept of water plasticization in a more familiar context of the older, more traditional literature on "bound" and "unfreezable" water and on water sorption by food polymers at low moisture (reviewed in detail elsewhere),[15,25] the earliest-sorbed water fraction is most strongly plasticizing, always said to be "unfreezable" in a practical time frame, and often referred to as "bound". The later-sorbed water fraction is said to be freezable, referred to as "free", "mobile", or "loosely bound", and is either weakly or non-plasticizing, depending on the degree of water compatibility of the specific polymer. As mentioned earlier, the degree of water compatibility relates to the ability of water to depress Tg to Tg′, and to the magnitude of Wg′.[15,16] Regardless of context, a key fact about the "freezability" of water relates to the homogeneous process for the prerequisite nucleation step of ice crystallization.[162] Even at temperatures as low as −40°C (the homogeneous nucleation temperature for ice in pure water),[4] a minimum on the order of 200 water molecules must associate within a domain of about 40 Å in order to form a critical nucleus that will grow spontaneously into an ice crystal.[4] Thus, within any food material at low moisture, clusters of water molecules of lower density than about 200 molecules/40 Å would certainly require temperatures below −40°C or heterogeneous catalysts for nucleation to occur.[33]

The solute-specific, invariant quantity of unfrozen water captured in the glass that forms at Tg′, defined as Wg′,[8] is traditionally referred to by many food scientists and technologists as one measure of "bound" water.[151] However, "bound" water, with respect to either frozen or room-temperature food systems, is a misnomer that has persisted for at least the last 30 years, despite constant debate[3,8,15,25,26,57,58,64] and evermore convincing arguments that the concepts of "bound" water, "water binding", and "water-binding capacity" of a solute are incorrect, inappropriate, and misleading rather than helpful.[4-7,40-42,149,150] The concept of "bound" water originated in large part from a fundamental misconception that discrete "free" and "bound"

physical states of water in food materials (or "free", "loosely bound", and "tightly bound" states) could provide a valid representation of water molecules in a solution at ambient temperature.[34] Actually, at $T > Tg'$, water molecules in a solution exist within a single physical state (i.e., liquid) characterized not by any kind of static geometry but rather by a dynamic continuum of degrees of hindered instantaneous mobility.[25] In this liquid solution state, individual water molecules are only transitorally hydrogen-bonded to individual polar sites on the solute.[149,150]

As explained recently,[8,30-34] the solute-specific value of Wg' is the maximum amount of water that can exist with that solute in a spatially homogeneous, compatible blend that, in the rubbery state, exhibits long-range cooperative relaxation behavior described by WLF kinetics, but not long-range lattice order. Further dilution beyond Wg' results in loss of cooperative mobility and onset of short-range fluid mechanics, described by Arrhenius kinetics. Thus, expression of Wg' as a water/solute number ratio (i.e., a "notional hydration number")[149] actually represents the technologically practical maximum limit for the amount of water that can act as a plasticizer of a particular solute,[6,15] rather than the amount of water that is "bound" to, or whose dynamics are governed by, that solute. Part of the reason for the persistence of the concept of "bound" water in such concentrated solute systems, despite convincing evidence of its invalidity, relates to a conclusion inadvisedly extrapolated from findings for very dilute solutions. The addition of a few isolated solute molecules to pure water already causes a profound effect on the self-diffusion properties in the solution. The hindered diffusion of water molecules instantaneously in the vicinity of individual solute molecules is construed as the effect of "viscous drag"; these less-mobile water molecules are visualized to be "pulled along" with the solute during flow. But it has been demonstrated repeatedly[149,150] than the less-mobile water molecules are freely exchangeable with all of the water in the solution, leading to the inescapable consensus view that the water is not bound to the solute. On the other hand, in describing dilute solutions, no one has ever suggested that the solute molecules are "bound" to water molecules. When the situation is reversed, adding a few water molecules to an anhydrous solute profoundly changes the viscoelastic properties of the solute via water plasticization, which increases the free volume and decreases the local viscosity.[34] Why then, in light of this evidence of a dramatic *increase* in the mobility of the solute, have many found it so easy to jump to the conclusion that these water molecules must be "bound" to solute molecules?

It is only recently becoming more widely acknowledged and accepted[15,25,33,50,57,58] that the so-called "bound" water corresponding to Wg' is not energetically bound in any equilibrium thermodynamic sense. Rather, it is simply kinetically retarded, due to the extremely high local viscosity ($\sim 10^{12}$ Pa s) of the metastable glass at Tg', and thus dynamically constrained from the translational and rotational diffusion required for ice crystal growth.[4-8,30-34,40-42] The crucial finding that water is not "strongly bound" to polar groups on hydrophilic polymers has been demonstrated in an especially convincing fashion by the meticulous low-temperature DSC and ambient-temperature sorption studies of Pouchly and Biros[163-166] on the thermodynamic interaction of water with (and plasticizing effect on) hydrophilic synthetic polymers in glassy and rubbery states. This conclusion regarding the true nature of "bound" water does not mean that there are not solute-water hydrogen bonds in the glass at Tg', only that such hydrogen bonds are the normal consequence of dissolution of a solute in water rather than the cause of the kinetic retardation that renders this water "unfreezable" in real time.[34] The stabilizing free energy of such solute-water hydrogen bonds is no greater than for water-water hydrogen bonds in ice.[150,163-166] Analogously, for model solutions of small sugars at room temperature, results of NMR and dielectric relaxation measurements have shown that "the residence time of a given water molecule at a solvation site (i.e., a hydroxyl group on a sugar) is extremely short, <1 ns."[149,150] Furthermore, such results, from studies of synthetic polymers[145] and polymeric carbohydrate and protein gels[58,152] alike, have demonstrated conclusively that water molecules said to be "bound" to polar groups on such polymeric solutes are in fact highly mobile (especially compared to the mobility of water in ice)[167] and able to exchange

freely and rapidly, likewise on a NMR time scale, with other (so-called "free" or "bulk") water molecules and deuterium oxide. Other studies have concluded that "bound" water has thermally labile hydrogen bonds,[163-166] shows cooperative molecular mobility,[168] has a heat capacity approximately equal to that of liquid water rather than ice,[131,164,168] and has some capability to dissolve salts.[169]

It has been concluded recently that "in the past, too much emphasis has been given to water activity and "water binding"."[57] In fact, the typical observation of two relaxation peaks (ascribed, following traditional dogma, to "free" and "bound" water) for all biological tissues and solutions that have been examined in dielectric experiments[170] is entirely consistent with, and exactly analogous to, the behavior of synthetic polymers with their non-aqueous, non-hydrogen bonding organic plasticizers.[109] The traditional point of view on the "structuring" effect of solutes on water (and its association with the concept of water activity), which helped give rise to the myth of "bound" water, is rightfully being replaced[57] by a new perspective and emphasis on the mobilizing effect of water acting as a plasticizer on solutes, which has led to a deeper qualitative understanding of structure-function relationships in aqueous food polymer systems.[8,14-39] For example, Labuza, who in the past has been a very well known proponent of the concept of "bound" water,[151] now writes, in the context of the "water binding capacity (WBC)" of dietary fiber, that "in fact, current opinion on bound water (if there is such a thing) is that it is very different from what the expression commonly means . . . Product development scientists should take the WBC values that currently are being bandied about with a grain of salt."[171]

5. Williams-Landel-Ferry Theory and WLF Kinetics

As alluded to earlier, the glass transition in amorphous systems is a temperature-, time- (or frequency-), and composition-dependent, material-specific change in physical state, from a glassy mechanical solid (capable of supporting its own weight against flow due to the force of gravity) to a rubbery viscous fluid (capable of flow in real time).[107] In terms of thermodynamics, the glass transition is operationally defined as a second-order transition[114] and denoted by (a) a change in slope of the volume expansion (which is a first-order derivative of the free energy), (b) a discontinuity in the thermal expansion coefficient, and (c) a discontinuity in the heat capacity (which is a second-order derivative of the free energy).[119]

The glass transition is also operationally defined, based on mechanical properties, in terms of a mechanical relaxation process such as viscosity. Figure 30[15] (adapted from Reference 4) shows that, as the temperature is lowered from that of the low η liquid state above Tm, where familiar Arrhenius kinetics apply, through a temperature range from Tm to Tg, a completely different, very non-Arrhenius, non-linear form of the kinetics, with an extraordinarily large temperature dependence,[172] becomes operative.[173] Then, at a temperature where mobility becomes limiting, a state transition occurs, typically manifested as a three orders-of-magnitude change in viscosity, modulus, or mechanical relaxation rate.[110,114] At this glass transition temperature, the viscosity of a liquid is $\simeq 10^{12}$ Pa s (10^{13} Poise), and the calorimetrically determined (e.g., by DSC) structural relaxation time for such a liquid is about 200 s.[172,174] A "mechanical" glass tran-

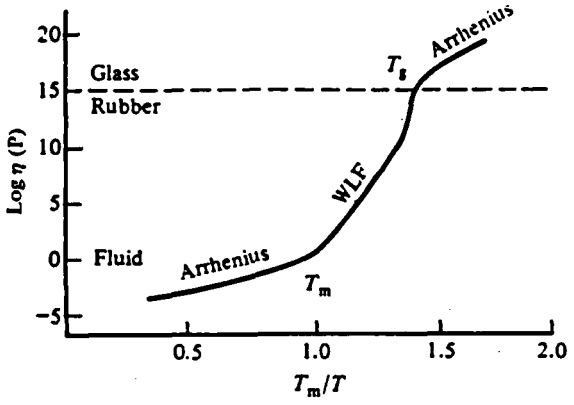

FIGURE 30. Viscosity as a function of reduced temperature (Tm/T) for glassy and partially crystalline polymers. (From Levine, H. and Slade, L., *Water Science Reviews*, Vol. 3, Franks, F., Ed., Cambridge University Press, Cambridge, 1988, 79. With permission.)

sition can be defined by combinations of temperature and deformation frequency for which sufficiently large numbers of mobile units (e.g., small molecules or backbone chain segments of a macromolecule) become cooperatively immobilized (in terms of large-scale rotational and translational motion) during a time comparable to the experimental period,[121,172,173,175] such that the material becomes a mechanical solid capable of supporting its own weight against flow. Arrhenius kinetics become operative once again in the glassy solid, but the rates of all diffusion-limited processes are much lower in this high η solid state than in the liquid state.[15] In fact, the difference in average relaxation times between the two Arrhenius regimes is typically more than 14 orders of magnitude.[30]

At temperatures above Tg, plasticization by water affects the viscoelastic, thermomechanical, electrical, guest/host diffusion, and gas permeability properties of completely amorphous and partially crystalline polymer systems to an extent mirrored in its effect on Tg.[15] In the rubbery range above Tg for completely amorphous polymers or between Tg and Tm for partially crystalline polymers (in either case, typically from Tg to about Tg + 100°C for well-behaved synthetic polymers),[30] the dependence of viscoelastic properties on temperature (i.e., the effect of increasing temperature on relative relaxation times) is successfully predicted[116] by the WLF equation, an empirical equation whose form was originally derived from the free volume interpretation of the glass transition.[101,107] The WLF equation can be written as[89,101]

$$\log_{10}\left(\frac{\eta}{\rho T}\Big/\frac{\eta g}{\rho g Tg}\right) = -\frac{C1(T-Tg)}{C2+(T-Tg)}$$

where η is the viscosity or other diffusion-limited relaxation process, ρ the density, and C1 and C2 are coefficients that describe the temperature dependence of the relaxation process at temperatures above the reference temperature, Tg. C1 is proportional to the inverse of the free volume of the system at Tg, while C2 is proportional to the ratio of free volume at Tg over the increase in free volume due to thermal expansion above Tg (i.e., ratio of free volume at Tg to the difference between the volumes of the rubbery liquid and glassy solid states, as a function of temperature above Tg).[107] C1 and C2 take on the values of "universal constants" (17.44 and 51.6, respectively, as extracted from experimental data on many synthetic amorphous polymers)[101] for well-behaved polymers.[30] The WLF equation describes the kinetic nature of the glass transition and has been shown to be applicable to any glass-forming polymer, oligomer, or monomer.[107] These particular values for the "universal constants" have also been shown to apply to molten glucose,[101] amorphous glucose-water mixtures,[176] amorphous sucrose and lactose powders at low moisture,[66] and concentrated solutions of mixed sugars,[89] as examples of relevance to foods.

The equation defines mobility in terms of the non-Arrhenius temperature dependence of the rate of any diffusion-limited relaxation process occurring at a temperature T compared to the rate of the relaxation at the reference temperature Tg, shown here in terms of log η related usefully to ΔT, where $\Delta T = T - Tg$. The WLF equation is valid in the temperature range of the rubbery or undercooled liquid state, where it is typically used to describe the time-/temperature-dependent behavior of polymers.[173] The equation is based on the assumptions that polymer free volume increases linearly with increasing temperature above Tg and that segmental or mobile unit viscosity, in turn, decreases rapidly with increasing free volume (as illustrated implicitly in Figure 30).[107] Thus, the greater the ΔT, the faster a system is able to move (due to increased free volume and decreased mobile unit viscosity), so the greater is the mobility, and the shorter is the relaxation time. In essence, the WLF equation and resulting master curve of log ($\eta/\eta g$) vs. $T - Tg$[89,101] represent a mobility transformation, described in terms of a time-temperature superposition.[30] Such WLF plots typically show a 5 orders-of-magnitude change in viscosity (or in the rates of other relaxation processes) over a 20°C interval near Tg,[6] which is characteristic of WLF behavior in the rubbery fluid range.[30] For example, as demonstrated by Soesanto and Williams,[89] the effects of temperature and concentration on the mobility of fluids above Tg can be combined to create a single master curve, which represents the WLF equation. The viscosity data shown in Figure 31[89] were obtained for highly concentrated (>90 w%)

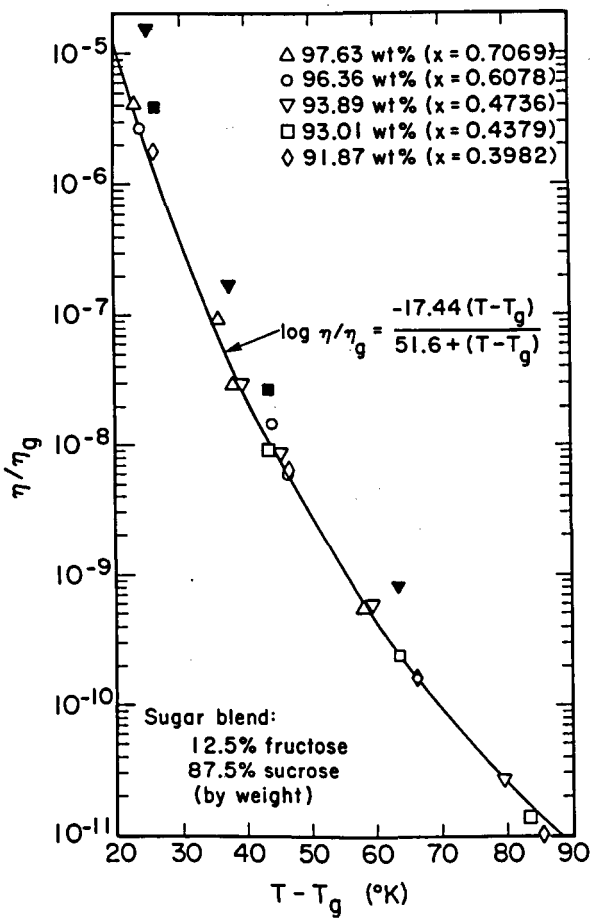

FIGURE 31. Temperature dependence of viscosity for aqueous solutions of a 12.5:87.5 (w/w) fructose:sucrose blend, illustrating the fit of the data to the curve of the WLF equation. (From Soesanto, T. and Williams, M. C., *J. Phys. Chem.*, 85, 3338, 1981.)

aqueous mixtures of fructose and sucrose. These results showed a five orders-of-magnitude change in the viscosity of concentrated sugar solutions, over a 20°C interval near Tg, a finding in excellent accord with the behavior predicted by the quantitative form of the WLF equation, with its "universally" applicable numerical values of the coefficients C1 = 17.44 and C2 = 51.6. These results constituted the first experimental demonstration that concentrated fructose and sucrose solutions obey the WLF equation quantitatively as well as synthetic high polymers. Similarly, it had been shown previously that a completely amorphous glucose melt, in the absence of diluent, has the same coeffients in the WLF equation, and thus also behaves like a typical well-behaved synthetic high polymer.[101,177]

In the context of the utility of the WLF equation, the underlying basis of the principle of time-temperature superpositioning is the equivalence between time (or frequency) and temperature as they affect the molecular relaxation processes that influence the viscoelastic behavior (i.e., the dual characteristics of viscous liquids and elastic solids) of polymeric materials and glass-forming small molecules.[107,134] This principle is illustrated in Figure 32,[26] which shows a master curve of the modulus as a function of temperature or frequency for a typical partially crystalline synthetic high polymer.[112] Figure 32 has been used to describe the viscoelastic behavior of such materials, as exemplified by a kinetically metastable gelatin gel in an undercooled liquid state, in the context of WLF theory.[178] At T > Tg, gelatin gels manifest a characteristic rubber-like elasticity,[179] due to the existence of a network of entangled, randomly coiled chains.[180] With increasing temperature, a gelatin gel traverses the five regions of viscoelastic behavior characteristic of synthetic, partially crystalline polymers,[180] as illustrated in Figure 32: (1) at T < Tg, vitrified glass; (2) at T = Tg, glass transition to leathery region, typically manifested as a three orders-of-magnitude decrease in modulus; (3,4) at Tg < T < Tm, rubbery plateau to rubbery flow; and (5) at T > Tm, viscous liquid flow. It is interesting to note that at Tg < T < Tm, a gelatin gel is freely permeable to the diffusion of dispersed dyes and molecules as large as hemoglobin;[25] only at T < Tg is such dye diffusion greatly inhibited.[181]

The WLF equation is not intended for use much below Tg (i.e., in the glassy solid state) or in the very low viscosity liquid state ($\eta < 10$ Pa s),[89] typically 100°C or more above Tg, where Arrhenius kinetics apply.[107,173,182] For partially crystalline polymers, the breadth of the temperature range of the rubbery domain of WLF behavior corresponds to the temperature interval between Tg and Tm,[104,107] as illustrated in Figure 30. Cheng[183] has noted that the size of this temperature interval between Tg and Tm may be as much as several hundred degrees for synthetic high polymers. An analysis of the variation of the size of this temperature interval with the Tm/Tg ratio of representational synthetic polymers and glass-forming, low MW carbohydrates has been reported recently.[30] This study compared

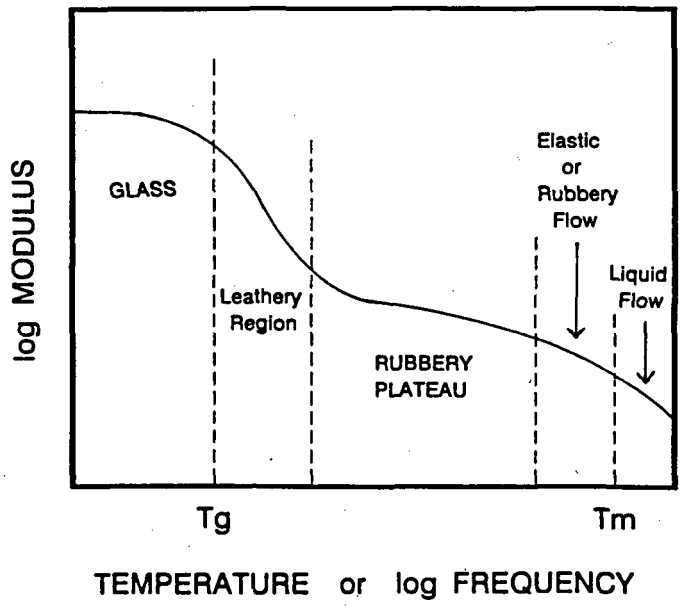

FIGURE 32. Master curve of the modulus as a function of temperature or frequency, illustrating the five regions of viscoelastic behavior characteristic of synthetic partially crystalline polymers. (From Levine, H. and Slade, L., *Dough Rheology and Baked Product Texture: Theory and Practice,* Faridi, H. and Faubion, J. M., Eds., Van Nostrand Reinhold/AVI, New York, 1989, 157. With permission.)

the WLF behavior of kinetically metastable carbohydrate-water systems to the corresponding knowledge base for synthetic high polymers. According to the conventional description, a typical well-behaved synthetic high polymer (e.g., a representational elastomer) would manifest its Tg around 200°K in the completely amorphous state, and its Tm around 300°K in the completely crystalline state,[105] so that the ratio of Tm for the pure crystalline material to Tg for the completely amorphous material is about 1.5 (or Tg/Tm about 0.67).[102] Such a polymer would also have a local viscosity of about 10^{12} Pa s and a free volume fraction of about 2.5% at Tg.[107] (This contribution of free volume to the discontinuity in heat capacity observed at Tg is illustrated in the plot of heat capacity vs. temperature for glassy, crystalline, and partially crystalline glassy materials, shown in Figure 33.) For this typical well-behaved polymer, WLF kinetics are considered to be operative in a temperature range about from Tg to 100°C above Tg.[101] It can be seen that this operational definition is related to the typical Tm/Tg ratio of 1.5, since in such a case the difference in temperature between Tg and Tm would be about 100°C. Figure 34A[30] illustrates the conventional description of the relaxation behavior of a typical well-behaved polymer (e.g., polyvinyl acetate[177,184]), which would obey the standard form of the WLF equation with the coefficients C1 = 17.44 and C2 = 51.6. In this plot of log a_T vs. ΔT, the relaxation rate progresses from WLF behavior very near Tg to Arrhenius behavior at about 100°C above Tg. Within this temperature range, where technological process control would be expected, relaxation rates for WLF behavior near Tg would change by a factor of 10 for every 3°C change in temperature. In contrast, for Arrhenius behavior with familiar $Q_{10} = 2$ kinetics above Tm, a factor of 10 change in relaxation rate would require a 33°C change in temperature.

Another class of amorphous polymers has been described[30] as typical but not well-behaved, in the sense that they are readily crystallizable.[102,105,107,118] Highly symmetrical polymers such as poly(vinylidene chloride) and poly(vinyl cyclohexane), which manifest crystalline melting

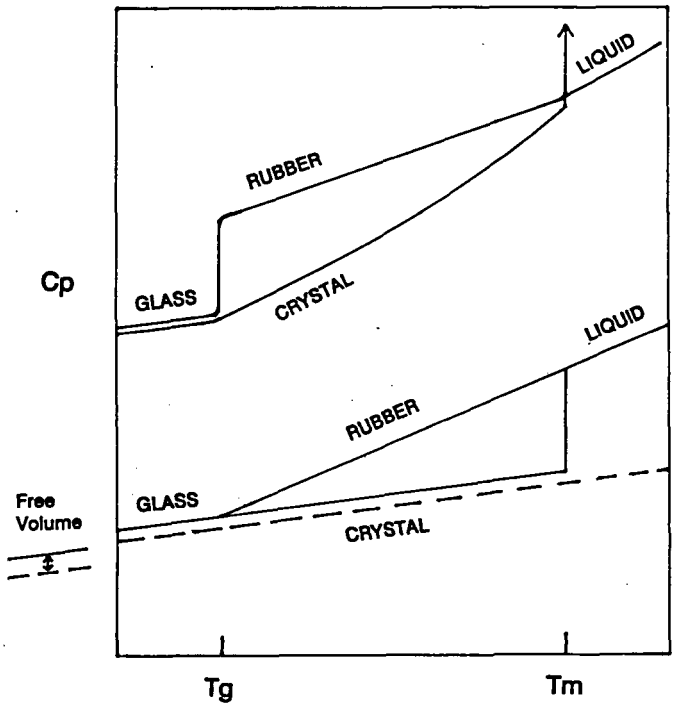

FIGURE 33. Plot of heat capacity as a function of temperature for glassy, crystalline, and partially crystalline glassy materials, illustrating the contribution of free volume to the discontinuity in heat capacity at Tg.

enthalpies of ≃170 J/g, fit this class. For such polymers, the ratio of Tm/Tg is frequently ⩾1.5, so the temperature range between Tg and Tm is ⩾100°C. Different WLF coefficients would be required to describe their relaxation profile, as illustrated by the plot in Figure 34B drawn for C1 = 20.4 and C2 = 154.8. For a representational case of Tg ≃ 200°K (with $\eta g \gtrsim 10^{12}$ Pa s, and free volume fraction ≃2.5%) and Tm/Tg ≃ 2 (Tg/Tm ≃ 0.5), Tm would be ≃400°K. Thus, there would be about a 200°C region in which relaxation rates would change from WLF behavior near Tg (in this case, by a factor of 10 for every 6°C) to Arrhenius behavior near Tm (by a factor of 10 for every 33°C). A notable example of a material with Tm/Tg ≃ 2 is water.[89]

A third class of polymers, often characterized by highly unsymmetrical structures, has been described[30] as atypical and poorly behaved, in that Tg is near Tm.[102,105] For such polymers, with Tm/Tg ≪ 1.5 (i.e., ≃1.25, or Tg/Tm ≃ 0.8), a quantitatively different form of the WLF equation would be required to describe their relaxation profile. In this case, as illustrated in Figure 34C, using C1 = 12.3 and C2 = 23.3, the intercept of log a_T was plotted as ≃ −3 for ΔT = 0 (i.e., at Tg), in contrast to Figures 34A and B, where log a_T was defined as 0 at Tg. For a representational polymer in this class, Tg ≃ 200°K (with $\eta g \ll 10^{12}$ Pa s, and free volume fraction ⩾2.5%) and Tm ≃ 250°K. Thus, the temperature range in which WLF kinetics would be operative is much smaller than usual. Relaxation rates would change from WLF behavior near Tg (in this case, by a factor of 10 for every 1°C) to Arrhenius behavior above Tm (by a factor of 10 for every 33°C) over a region of only about 50°C. The synthetic polymer cited as the classic example of this behavior, which has been attributed to anomalously large free volume at Tg, is bisphenol polycarbonate, with Tm/Tg ≃ 1.18.[102] This category of behavior has also been reported[15,28] to be exemplified by food materials such as native starch and gelatin (due to non-uniform distribution of moisture in amorphous and crystalline regions of these high polymers at low moisture) and the

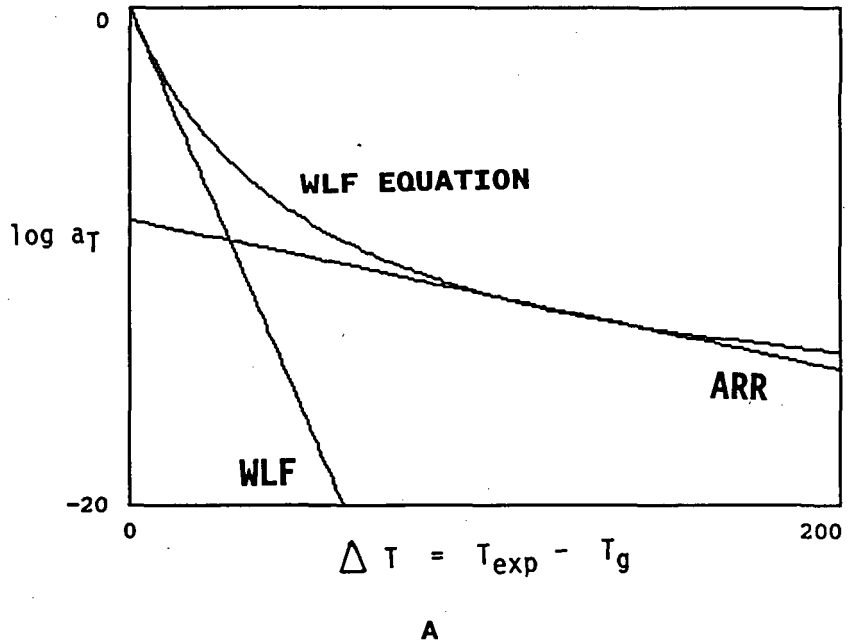

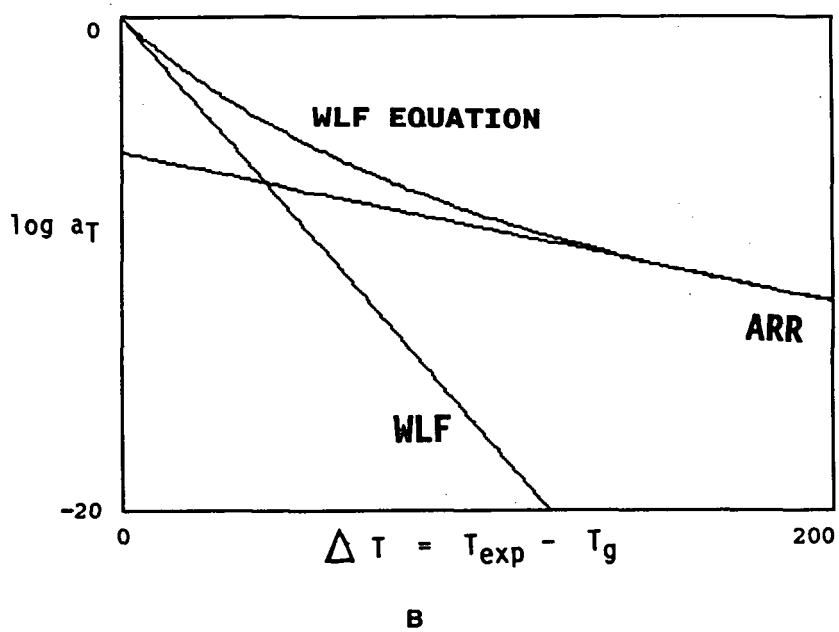

FIGURE 34. WLF plots of the time-temperature scaling parameter (WLF shift factor), a_T, as a function of the temperature differential above the reference state, Tg, with the limiting regions of low and high ΔT defined by the WLF and Arrhenius kinetic equations, respectively. The curves of the WLF equation (with coefficients C1 and C2 as noted) illustrate the temperature dependence of the relaxation rate behavior for hypothetical polymers with Tm/Tg ratios of: (A) 1.5 (C1 = 17.44, C2 = 51.6); (B) 2.0 (C1 = 20.4, C2 = 154.8); (C) 1.0 (C1 = 12.3, C2 = 23.3); (D) 2.0, 1.5, and 1.0. (From Slade, L. and Levine, H., *Pure Appl. Chem.*, 60, 1841, 1988. With permission.)

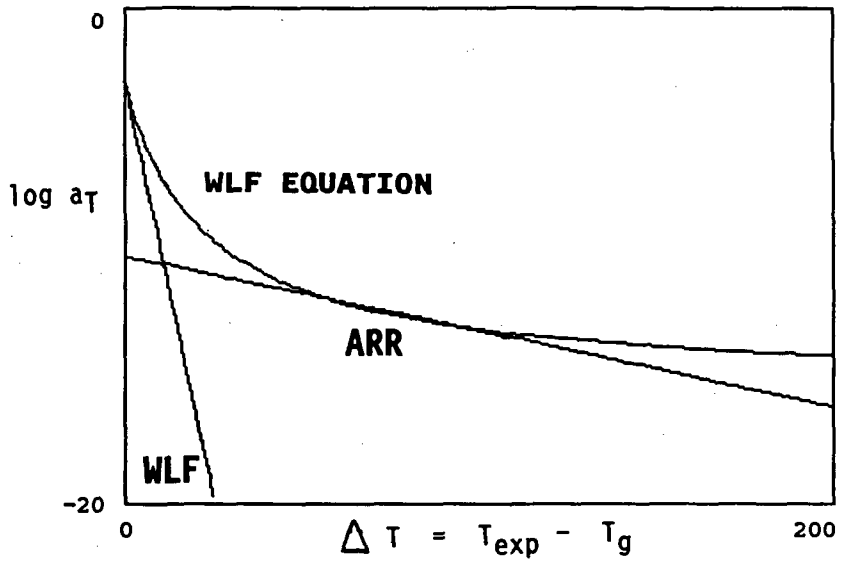

FIGURE 34C.

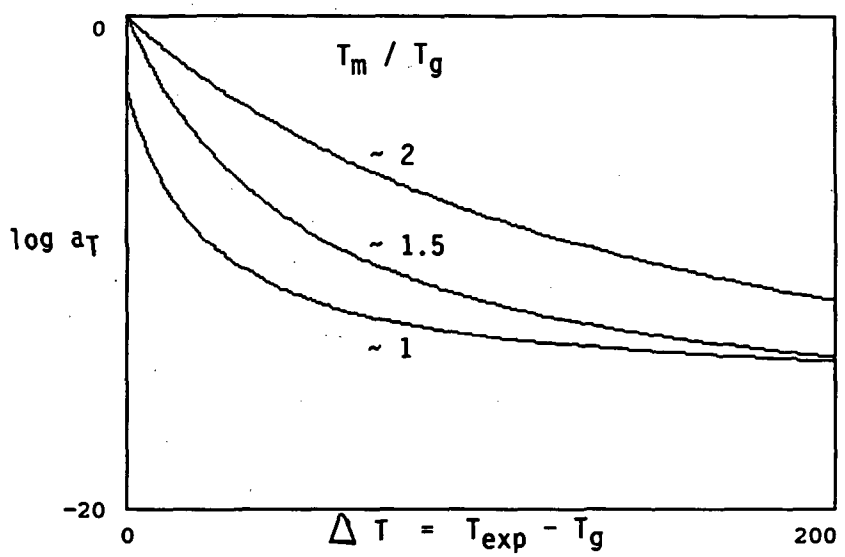

FIGURE 34D.

simple sugars fructose and galactose (due to anomalous translational free volume of these anhydrous monosaccharides).[30]

The three types of behavior exemplified in Figures 34A through C, in which the Tm/Tg ratio is either the typical value of 1.5, or much greater, or much less, have been compared in order to examine how the respective relaxation profiles change in the temperature interval between Tm and Tg for representational, diluent-free polymers with a common value of Tg.[30] As illustrated in Figure 34D, this analysis revealed the critical significance of the Tm/Tg ratio for any given polymer. For a common value of Tg, different values of Tm/Tg for different polymers (e.g., carbohydrates) can be used to compare relative mobilities at Tg and at $T \gg Tg$.[30] For different values of Tg, relative mobilities can be compared based on values of the difference, $Tm - Tg$, rather than the ratio, Tm/Tg.[30] In Figure 34D, the behavior of log a_T was compared for different values of Tm/Tg (i.e., about 2, 1.5, and the extreme

case of 1.0), to determine how mobility varies in the kinetically constrained regions of this mobility transformation map. At $T \gg Tg$, the overall free volume for different polymers may be similar,[107] yet individual free volume requirements for equivalent mobility may differ significantly, as reflected in the Tm/Tg ratio. The anisotropy in either rotational mobility (which depends primarily upon free volume)[107] or translational mobility (which depends primarily upon local viscosity, as well as free volume)[107] may be the key determinant of a particular polymer's relaxation behavior. The glass transition is a cooperative transition[106,172,173,183] resulting from local cooperative constraints on mobility, and Tg represents a thermomechanical property controlled by the local small molecule or segmental, rather than macroscopic, environment of a polymer. On cooling a viscous fluid of relatively symmetrical mobile units with relatively isotropic mobility, translational motions would be expected to be "locked in" at a higher temperature before rotational motions, because of the slower structural relaxations associated with the larger scale translational diffusion.[185,186] In this case, cooperative constraints of local viscosity and free volume on translational diffusion determine the temperature at which the glass transition is manifested, as a dramatic increase in relaxation times compared to the experimental time frame. However, in the case of motional anisotropy, molecular asymmetry has a much greater effect on rotational than translational diffusion, so that rotational motions could be "locked in" before translational motions as the temperature is lowered.[187,188] As illuminated by Figure 34D, a very small ratio of Tm/Tg (i.e., close to 1.0) is accounted for by an anomalously large free volume requirement for rotational diffusion.[102] When the free volume requirement is so large, a glass transition (i.e., vitrification of the rubbery fluid) on cooling can actually occur even when the local viscosity of the system is relatively low. Thus, instead of the typical "firmness" for a glass ($\simeq 10^{12}$ Pa s), such a glass (e.g., of bisphenol polycarbonate, or anhydrous fructose or galactose) may manifest a $\eta g \ll 10^{12}$ Pa s.[15,16,89,172] In such a glass, the time constant for translational diffusion may be anomalously small, indicative of high translational mobility. In contrast, in the glass of a typical well-behaved polymer, the time constant for translational diffusion would be greater than that for rotational diffusion, so that an increase in local viscosity would be concomitant with a decrease in free volume.[186] The above analysis has pointed out the critical significance of anomalous values of Tm/Tg ratio (for the dry solute) close to 1.0 on the mobility, resultant relaxation behavior, and consequent technological process control for non-equilibrium food polymer systems (in the *presence* of water) in their supra-glassy fluid state above Tg,[30] in terms of the WLF kinetics of various translational diffusion-limited, mechanical/structural relaxation processes, such as gelatinization, annealing, and recrystallization of starch.[21]

An interesting comparison has been made between the characteristic WLF ranges discussed above: (1a) about 100°C or more above Tg for many typical, completely amorphous, synthetic polymers, and (1b) from <50°C to 200°C or more between Tg and Tm for different categories of partially crystalline synthetic polymers, and (2) the relative breadth of the temperature range for the WLF region relevant to frozen aqueous food systems, i.e., the magnitude of the rubbery domain between Tg′ and the Tm of ice.[34] As illustrated conceptually in Figure 35,[34] the rubbery domains between Tg and Tm (represented by the solid vertical bars) for pure water (about 135°C) and pure solute (e.g., about 140°C for sucrose)[28] are similar in breadth to the 100 to 200°C span of the WLF region between Tg and Tm for many synthetic polymers.[30,104] In contrast, the breadth of the temperature range between Tg′ and Te (the melting temperature for the eutectic mixture of crystalline solute and ice) in Figure 35 is much smaller. For example, as reported for the specific case of a frozen sucrose solution,[33] the magnitude of the WLF rubbery domain between Te (−14°C)[133] and Tg′ (−32°C)[29] is only 18°C. The significant implications of this fact to the texture and freezer-storage stability of frozen food products[33,34] is discussed later.

Description of the time-/temperature-dependent behavior of food systems by the WLF equation requires selection of the appropriate reference Tg for any particular glass-forming material (of a given MW and extent of plasticization),[89,101,176] be it Tg for a low-moisture system or Tg′ for a frozen system.[8,27,66] For a typical,

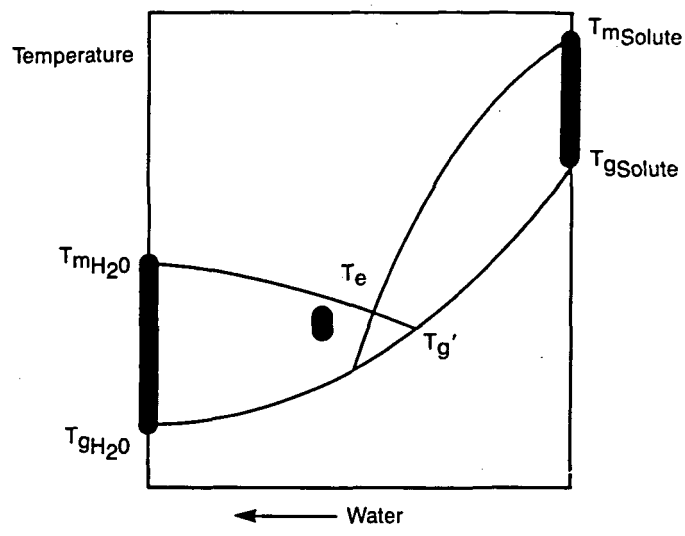

FIGURE 35. Idealized solute-water state diagram illustrating the relative magnitudes of $\Delta T = Tm - Tg$, the temperature range corresponding to the Williams-Landel-Ferry rubbery region, for pure solute, pure water, and the freeze-concentrated, amorphous solute-unfrozen water matrix which would exist at temperatures between the Tm of ice and Tg'. (From Levine, H. and Slade, L., *Thermal Analysis of Foods,* Ma, C.-Y. and Harwalker, V. R., Eds., Elsevier, London, 1990, 221. With permission.)

diluent-free polymer, Tg of the undercooled liquid is defined in terms of an iso-free volume state of limiting free volume[107] and also approximately as an iso-viscosity state somewhere in the range from 10^{10} to 10^{14} Pa s.[4,89,172,189] This iso-viscosity state refers to local, not macroscopic, viscosity. This fact constitutes a critical conceptual distinction,[30] as explained with respect to Figure 34D.

It is interesting to consider whether the WLF equation, which predicts the dependence of the viscoelastic properties of glass-forming polymers on temperature in terms of ΔT above Tg, could be transformed to an analogous empirical equation that predicts quantitatively the dependence of polymer properties on dilution by plasticizer in terms of ΔP (for plasticizer) away from the reference Tg of the undiluted glassy polymer. For example, one could examine the polystyrene plasticization data shown in Figure 28, and calculate the extent of depression of Tg as a function of diluent concentration for different plasticizers. If the experimental temperature is maintained constant, equivalent to the Tg of the undiluted polystyrene, then each extent of depression of Tg is equivalent to a ΔT. For the undiluted polymer, "ΔT above Tg" is achieved by raising the experimental temperature. For the diluted polymer, "ΔT above Tg" is achieved by keeping the experimental temperature constant and lowering the Tg of the system. One could plot these "ΔT" values, achieved by plasticization, in order to transform the graph of log a_T vs. ΔT in Figure 34A into a graph of log a_P vs. ΔP, by substituting the required amount of plasticizer for a given ΔT. Since the WLF equation for the effect of increased temperature on relative relaxation times is an empirical equation, it would be equally legitimate to obtain an equation for log a_P vs. ΔP.

The transformation from ΔT to ΔP would be strictly legitimate only for a system of a single monodisperse linear "polymer" (i.e., higher MW) and a single "plasticizer" (i.e., lower MW), and only if the free volume requirements for both translational and rotational mobility were the same for the "mobile segment" in the dry polymer, the diluted polymer system, and in the pure plasticizer. These conditions *might* be met in experiments in which the monomer, dimer, and low MW oligomers were used as the plasticizer series

for a particular linear polymer. Certainly, the conditions are not met when water is the plasticizer, not even for plasticization of small sugars, much less for starch (which is a mixture of branched and linear polymers with at least bimodal and broad MW distribution).

The most severe complication is that it would be essentially impossible in practice to verify experimentally the form of the WLF equation for log a_P vs. ΔP. Williams, Landel, and Ferry[101] were able to obtain sufficient data for so many polymers to be able to construct an empirical equation for log a_T vs. ΔT, because heat transfer is quite efficient in the solid state. It is experimentally feasible to raise the internal temperature of a sample with appropriate geometry from below Tg to well above Tg and expect that the temperature will be essentially uniform throughout the sample. Then a determination of viscosity, or self-diffusion coefficient for a reporter molecule, or other manifestation of mechanical relaxation will give usable data for construction of log a_T vs. ΔT above Tg. In contrast, mass transport is "infinitely" slow in the (glassy) solid state, and much slower in the leathery and rubbery states than can be accommodated in typical experimental time frames. Consequently, one would rarely be able to keep the experimental temperature constant and achieve ΔT values that represent uniform, steady-state moisture distribution for a sample at varying amounts of sample total moisture. For biological high polymers, the Tg of the undiluted polymer is usually so high as to cause degradation if this dry Tg is used as the experimental temperature. If one uses experimental temperatures below dry Tg and waits for plasticized Tg to drop to and below the experimental temperature, the experimental time scales will be unreasonable, and the instantaneous moisture gradients will allow incidental chemical and physical changes to occur in the system. For small sugars with lower dry Tg values, but that are readily crystallizable (a property usually related to a large temperature interval between Tm and Tg, such that the homogeneous nucleation temperature is well above Tg),[15] small extents of plasticization allow crystallization, and the bulk mechanical properties no longer reflect the effect of plasticizer on Tg. Possibly the best experimental system for direct construction of log a_P vs. ΔP (to allow comparison to the indirect method of transforming log a_T vs. ΔT, based on Tg vs. ΔP data) would be dry amorphous fructose glass plasticized by water. However, it is notoriously difficult to dry fructose syrups, and, in any event, the resulting equation could not be used to predict behavior for any other sugar.

Our feeling is that we must settle at present for a qualitative and indirect picture of log a_P vs. ΔP as a universal concept. For particular combinations of polymer and plasticizer, where the Tg vs. ΔP are known, one can substitute, for ΔT in the WLF equation, the plasticizer concentration that produces an extent of depression of dry Tg equivalent to ΔT.

WLF kinetics differ from Arrhenius kinetics in several important respects,[30,34] and we have emphasized the contrast because we believe that the qualitative differences are as influential as the quantitative differences in their impact on both experimental approach and technological significance.[39] A comparison between WLF and Arrhenius kinetics begins with the recognition that the temperature dependence of microscopic relaxation parameters (including the self-diffusion coefficient, viscosity, rotational and translational relaxation rates or times, and macroscopic processes that rely on them) changes monotonically from a steep dependence of log relaxation rate on temperature just above Tg to a shallow dependence above Tm, i.e., over a material-specific temperature range from Tg to far above Tg.[4,30,172,190] This realization manifests two underlying diagnostic characteristics that distinguish WLF from Arrhenius kinetics.[39] First, the coefficient of the temperature dependence (so-called "activation energy") is defined as a constant in the expression for Arrhenius kinetics, and a plot of log relaxation rate vs. 1/T is a straight line. But the coefficient itself is temperature dependent in the WLF expression; a plot of log relaxation rate vs. 1/T is characteristically curvilinear in the material-specific temperature range between Tg and Tm,[190] approaching linearity only below Tg or above Tm.[34] The absolute value of the derivative of log relaxation parameter vs. 1/T increases as Tg is approached from above, and decreases abruptly to an approximately constant value as the temperature falls below Tg, or decreases gently to an approximately constant value

as temperature is elevated above Tm and far above Tg, where the constant value corresponds to the Arrhenius coefficient (activation energy) that characterizes the particular system and relaxation process.[39] The shape of the derivative profile and the temperature range over which the derivative varies are material-specific properties: typically a range of $\gtrsim$100°C for materials with a ratio of Tm/Tg $\gtrsim$ 1.5, or a range of <100°C for materials with a ratio of Tm/Tg < 1.5.[30] Clearly, it is the fact that the derivative varies in a material-specific and temperature-dependent fashion, rather than the particular magnitude of the derivative, that constitutes the salient feature of WLF kinetics.[39] Second, there is no explicit reference temperature in the expression for Arrhenius kinetics, because in fact, the implicit reference temperature is taken generically to be 0 K, regardless of the distinctive thermomechanical properties of a system, and even though Arrhenius kinetics are applicable only below Tg and above Tm.[4,15,107] In contrast, the WLF expression benefits from an explicit material-specific reference temperature, which is the Tg of a component or compatible blend.[107] Therefore, it is critical to note that when the rate or time scale of a relaxation process can be shown to depend on a material-specific reference Tg, Arrhenius kinetics are not applicable to describe mobility transformations (time-temperature-moisture superpositions) for that process in the rubbery range from Tg to Tm, regardless of whether the average slope of the log k vs. 1/T curve can be empirically fitted by a $Q_{10}=n$ rule and regardless of the particular magnitude of n.[39] In summary, in the temperature and composition domain sufficiently above Tg, where equilibrium and steady-state thermodynamics apply, the coefficient of the temperature dependence of log relaxation rate is defined by Arrhenius kinetics to be a constant and is observed to approximate a relatively small constant value over a typical experimental range of about 20°C.[39] In the increasingly non-equilibrium domain of temperature and composition approaching Tg from above, the coefficient of the temperature dependence of log relaxation rate on 1/T is not a constant and increases evermore rapidly over a range of 20°C.[30] Typically, Arrhenius rates for aqueous systems above Tm might increase fourfold over a temperature range of 20°C,[39] while WLF rates near Tg would increase by 4 or 5 orders of magnitude.[6,30,34] As an example illustrating the significance of the difference between WLF and Arrhenius kinetics, Chan et al.[176] have noted that the dielectric relaxation behavior of amorphous glucose plasticized by water is "remarkably similar" to that of synthetic amorphous polymers in glassy and rubbery states. They showed that the rates of this mechanical relaxation process, which depends on rotational rather than translational mobility, follow the WLF equation for water-plasticized glucose mixtures in their rubbery state above Tg, but follow the Arrhenius equation for glucose-water glasses below Tg.[176] Also noteworthy is Angell's[191] pertinent observation that the temperature dependence of the transport and relaxation properties of undercooled liquid water is strikingly non-Arrhenius in the temperature range from Tm to the homogeneous nucleation temperature at −40°C (corresponding to a portion of the WLF rubbery domain shown in Figure 35). This non-Arrhenius temperature dependence also typifies the case for many other viscous liquid systems that undergo restructuring processes that require the "cooperative involvement of other molecular motions".[172,191] Included in these other viscous liquid systems that exhibit non-Arrhenius behavior are concentrated aqueous solutions at subzero temperatures,[190] according to a suggestion by Hofer et al.[189]

The impact of WLF behavior on the kinetics of diffusion-limited relaxation processes in water-plasticized, rubbery food polymer systems has been conceptually illustrated by the idealized curve shown in Figure 36.[34] Relative relaxation rates, calculated from the WLF equation with its universal numerical constants, demonstrate the non-linear logarithmic relationship: for ΔT = 0, 3, 7, 11, and 21°C, corresponding relative rates would be 1, 10, 10^2, 10^3, and 10^5, respectively. These rates illustrate the 5 orders-of-magnitude change, over a 20°C interval above Tg, typically shown by WLF plots, as mentioned earlier with respect to Figure 31. They are dramatically different from the rates defined by the familiar Q_{10} = 2 rule of Arrhenius kinetics for dilute solutions. As pointed out with respect to Figure 34A, for Arrhenius behavior above Tm, a factor of 10 change in relaxation rate would require a 33°C

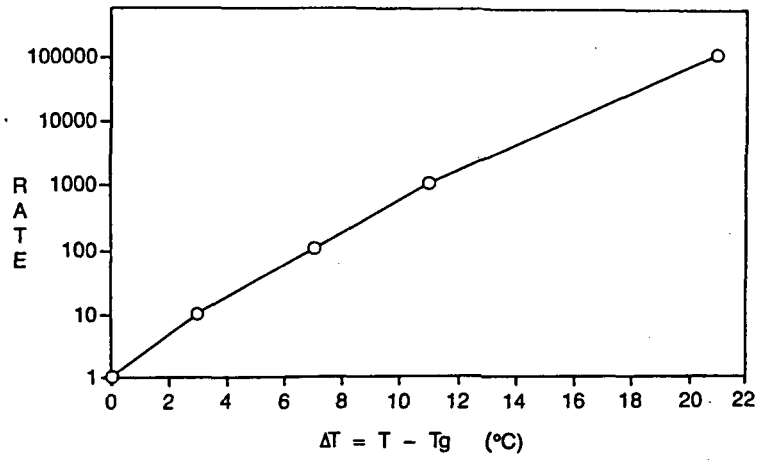

FIGURE 36. Variation of the rate of a diffusion-limited relaxation process against $\Delta T = T - Tg$, as defined by the Williams-Landel-Ferry equation with its "universal" numerical constants of C1 = 17.44 and C2 = 51.6. (From Levine, H. and Slade, L., *Thermal Analysis of Foods*, Ma, C.-Y., and Harwalker, V. R., Eds., Elsevier, London, 1990, 221. With permission.)

change in temperature, in comparison to a 3°C change for WLF behavior near Tg of a partially crystalline polymer of Tg/Tm = 0.67.[30]

Another general example of WLF-governed relaxation behavior concerns the kinetics of (re)crystallization.[15,25,26] (Re)crystallization is a diffusion-limited process[192] that, on a time scale of technological significance, can only occur within the WLF rubbery domain.[104] The propagation step in the recrystallization mechanism approaches a zero rate at T < Tg for an amorphous but crystallizable solute (either polymeric[104] or monomeric), initially quenched from the melt or liquid solution state to a kinetically metastable solid state. Due to immobility in the glass, migratory diffusion of either large main-chain segments or small molecules, required for crystal growth, would be inhibited over realistic times. However, the propagation rate increases exponentially with increasing ΔT above Tg (up to Tm),[94] due to the mobility allowed in the rubbery state. Thus, a recrystallization transition from unstable (i.e., undercooled) amorphous liquid to (partially) crystalline solid may occur at T > Tg,[44,55,193] with a rate defined by the WLF equation.[8] The facts that time-dependent recrystallization can only occur at temperatures above Tg and manifests kinetics defined by the WLF (rather than Arrhenius) equation[27] were recently confirmed in an experimental study of the recrystallization of amorphous, freeze-dried sugars (i.e., sucrose, lactose) by Roos and Karel.[66] Other specific examples of such a recrystallization process (i.e., a collapse phenomenon) include ice and solute (e.g., lactose in dairy products)[50] recrystallization in frozen aqueous systems at T > Tr ≡ Tg′.[8]

One of the most critical messages to be distilled at this point is that the structure-property relationships of water-compatible food polymer systems are dictated by a moisture-temperature-time superposition.[8,137,155] Referring to the idealized state diagram in Figure 23 (which reflects the "real world" cases illustrated in Figures 19A, 25, 26, and 27) as a conceptual mobility map (which represents an extension of the dynamics map in Figure 21), one sees that the Tg curve represents a boundary between non-equilibrium glassy and rubbery physical states in which various diffusion-limited processes (e.g., collapse phenomena involving mechanical and structural relaxations) either can (at T > Tg and W > Wg′, the high-moisture portion of the water dynamics domain corresponding to the upper-left part of Figure 23, or T > Tg and W < Wg′, the low-moisture portion of the water dynamics domain corresponding to the upper-right part of Figure 23) or cannot (at T < Tg, in the domain of glass dynamics corresponding to the bottom part of Figure 23) occur over realistic times.[8,15,40,41] The

WLF equation defines the kinetics of molecular-level relaxation processes, which will occur in practical time frames only in the rubbery state above Tg, in terms of an exponential, but non-Arrhenius, function of ΔT above this boundary condition.[8]

Further discussion of (1) Tg′ as the appropriate reference temperature for WLF kinetics in high-moisture food systems at temperatures above Tg′ and (2) Wg′ as the maximum *practical* amount of plasticizing water in such systems with water contents > Wg′ is detailed in a later Section IV.D.

6. Crystallization/Gelation Mechanism

A classic description of crystallization as a three-step mechanism has been widely used for partially crystalline synthetic polymers crystallized, from the melt or concentrated solution, by undercooling from T > Tm to Tg < T < Tm.[104,139] The mechanism is conceptually compatible with the "fringed micelle" model.[194] It involves the following sequential steps, which apply universally to all crystallizable substances, regardless of MW:[104] (1) nucleation (homogeneous) — formation of critical nuclei, (2) propagation — growth of crystals from nuclei by intermolecular association, and (3) maturation — crystal perfection (by annealing of metastable microcrystallites) and/or continued slow growth (via "Ostwald ripening"). Within this universal description, flexible macromolecules are distinguished from small molecules by the possibility of nucleation by intramolecular initiation of ordered (e.g., helical) chain segments and propagation by association of chain segments for the high polymers.[104]

The thermoreversible gelation, from concentrated solution, of a number of crystallizable synthetic homopolymers and copolymers has been reported to occur by this crystallization mechanism.[146,194-196] In contrast, a different gelation mechanism, not involving crystallization and concomitant thermoreversibility, pertains to polymers in solution that remain completely amorphous in the gel state.[25] Such high polymers are distinguished from oligomers by their capacity for intermolecular entanglement coupling, resulting in the formation of rubberlike viscoelastic random networks (called gels, in accord with Flory's[197] nomenclature for disordered three-dimensional networks formed by physical aggregation) above a critical polymer concentration.[107] It has been demonstrated for many synthetic linear high polymers that the mechanism of gelation from concentrated solution can be distinguished by a simple dilution test.[198] Gelation due to entanglement in a completely amorphous polymer-diluent network can be reversed by dilution, whereas a thermoreversible, partially crystalline, polymer-diluent network gel cannot be dispersed by dilution.[15] Examples of food polymers that can form such amorphous entanglement gels include gluten in unoriented wheat flour dough, sodium caseinate in imitation mozzarella cheese, and casein in real cheese.[25] As summarized by Mitchell,[140] "entanglement coupling is seen in most high MW polymer systems. Entanglements (in completely amorphous gels) behave as crosslinks with short lifetimes. They are believed to be topological in origin rather than involving chemical bonds." Importantly, hydrogen bonding need not be invoked to explain the viscoelastic behavior of completely amorphous gels formed from solutions of entangling polysaccharides or proteins.[25]

The gelation-via-crystallization process (described as a nucleation-limited growth process[195]) produces a metastable three-dimensional network[196] crosslinked by "fringed micellar"[194] or chain-folded lamellar[195] microcrystalline junction zones composed of intermolecularly associated helical chain segments.[146] Such partially crystalline gel networks may also contain random interchain entanglements in their amorphous regions.[195] The non-equilibrium nature of the process is manifested by "well-known aging phenomena"[194] (i.e., maturation),[15] attributed to time-dependent crystallization processes that occur subsequent to initial gelation. The thermoreversibility of such gels is explained in terms of a crystallization (on undercooling) ↔ melting (on heating to T > Tm) process.[195] Only recently has it been recognized that for synthetic polymer-organic diluent systems (e.g., polystyrene-toluene), such gels are not glasses[199] ("gelation is not the glass transition of highly plasticized polymer"[194]) but partially crystalline rubbers,[146]

in which the mobility of the diluent (in terms of rotational and translational motion) is not significantly restricted by the gel structure.[199] Similarly, for starch and gelatin gels, water as the diluent is highly mobile, and amounts > Wg′ freeze readily at subzero temperatures.[26] The temperature of gelation (Tgel) is above Tg,[199] in the rubbery fluid range up to about 100°C above Tg. Tgel is related to the flow relaxation temperature, Tfr, observed in flow relaxation of rigid amorphous entangled polymers[146] and to Tm observed in melts of partially crystalline polymers.[194] The basis for the MW-dependence of Tgel has been identified[146] as an iso-viscous state (which may include the existence of interchain entanglements) of $\eta gel/\eta g = 10^5/10^{12} = 1/10^7$, where ηg at Tg $\simeq 10^{12}$ Pa s.

The distinction among these transition temperatures becomes especially important for elucidating how the morphology and structure of food polymer systems relate to their thermal and mechanical behavior.[25] This distinction is a particularly important consideration when experimental methods involve very different time frames (e.g., mechanical measurements during compression tests or over prolonged storage; thermal analysis at scanning rates varying over 4 orders of magnitude; relaxation times from experiments at acoustic, microwave, or NMR frequencies)[200-204] and sample preparation histories (i.e., temperature, concentration, time).[25] In the case of morphologically homogeneous, molecular amorphous solids, Tg corresponds to the limiting relaxation temperature for mobile polymer backbone-chain segments. In the case of morphologically heterogeneous, supra-molecular networks, the effective network Tg corresponds to the Tfr transition above Tg for flow relaxation[146] of the network. For example, the ratio of Tfr/Tg varies with MW from 1.02 to 1.20 for polystyrene above its entanglement MW.[205] Tfr defines an iso-viscous state of 10^5 Pa s for entanglement networks (corresponding to Tgel for partially crystalline networks).[146] Tgel of a partially crystalline network would always be observed at or above Tfr (≡ network Tg) of an entanglement network; both transitions occur above Tg, with an analogous influence of MW and plasticizing water.[25] As an example, the effective network Tg responsible for mechanical firmness of freshly baked bread would be near room temperature for low extents of network formation, well above room temperature for mature networks, and equivalent to Tgel near 60°C for staled bread, even though the underlying Tg for segmental motion, responsible for the predominant second-order thermal transition, remains below 0°C at Tg′.[25]

Curiously, it has been well-established for a much longer time[195] that the same three-step polymer crystallization mechanism describes the gelation mechanism for the classic gelling system, gelatin-water.[105,139] The fact that the resulting partially crystalline gels[206] can be modeled by the "fringed micelle" structure is also widely recognized.[17,24,104,139] However, while the same facts are true with respect to the aqueous gelation of starch (i.e., retrogradation, a thermoreversible gelation-via-crystallization process that follows gelatinization and "pasting" of partially crystalline native granular starch-water mixtures),[207] and despite the established importance of gelatinization to the rheological properties of bread doughs during baking[208,209] and of retrogradation to the time-dependent texture of fresh-baked vs. aged breads,[210] recognition of starch (or pure amylose or amylopectin) retrogradation as a thermoreversible polymer crystallization process has been much more recent and less widespread.[45-47,61,63,65,92,211-221] Blanshard[49,94] has recently applied synthetic polymer crystallization theory to investigate the kinetics of starch recrystallization and thereby gain insight into the time-dependent textural changes (i.e., staling due to firming) occurring in baked products such as bread. Similarly, Zeleznak and Hoseney[95] have applied principles of polymer crystallization to the interpretation of results on annealing of retrograded starch during aging of bread stored at superambient temperatures. Many of the persuasive early insights in this area have resulted from the food polymer science approach to structure-property relationships in starch of Slade and her various co-workers.[17-23,26,30,35,46]

Slade et al.[17-23,26,30,35,46] have used DSC results to demonstrate that native granular starches, both normal and waxy, exhibit non-equilibrium melting,[105] annealing, and recrystallization behavior characteristic of a kinetically metastable, water-plasticized, partially crystalline polymer system with a small extent of crystal-

linity. This group has stressed the significance of the conclusion, in which others have concurred,[47-49,60,61,63,65,93,222-225] that gelatinization is a non-equilibrium polymer melting process. Gelatinization actually represents a continuum of relaxation processes (underlying a structural collapse)[207] that occurs (at T > Tg) during heating of starch in the presence of plasticizing water and in which crystallite melting is indirectly controlled by the dynamically constrained, continuous amorphous surroundings.[21] That is, melting of microcrystallites, which are hydrated clusters of amylopectin branches,[153,154] is controlled by prerequisite plasticization ("softening" above Tg) of flexibly coiled, possibly entangled chain segments in the interconnected amorphous regions of the native granule, for which the local structure is conceptualized according to the "fringed micelle" model.[20] Such non-equilibrium melting in metastable, partially crystalline polymer network systems, in which the crystalline and amorphous phases are neither independent of each other nor homogeneous, is an established concept for synthetic polymers.[105,183] In fact, Wunderlich[106] and Cheng[183] have both stressed the point that the melting of partially crystalline synthetic polymers is *never* an equilibrium process. Slade et al. have suggested,[17-23,26,35,46] and others have agreed,[60,65,221,224,225] that previous attempts (e.g., References 161, 226, 227) to use the Flory-Huggins thermodynamic treatment to interpret the effect of water content on the Tm observed during gelatinization of native starch have failed to provide a mechanistic model, because Flory-Huggins theory[100] only applies to melting of polymers in the presence of diluent under the conditions of the equilibrium portion of the solidus curve. In this context, it is interesting to note Cheng's[183] recent observation that multicomponent systems of solid polymers (especially those containing copolymers, such as a mixture of native normal starch [amylose + amylopectin] and water, where amylopectin can be considered a block copolymer[21,105]) "are even more beset by non-equilibrium problems (than are single-polymer systems). Only in the amorphous state above the glass transition can one expect (sluggish) equilibration."

An interesting and graphic illustration of the concept of non-equilibrium melting in partially crystalline synthetic polymer systems has been presented by Wunderlich[105] and is detailed here in generic terms to help the reader better understand the applicability of this concept to the gelatinization of native granular starch. Wunderlich described the case of a synthetic block copolymer produced from comonomers A and B. Monomer A was readily crystallizable and capable of producing a high MW, crystalline homopolymer of relatively low "equilibrium" Tm. In contrast, monomer B was not crystallizable and produced a completely amorphous, high MW homopolymer with a Tg much higher than the "equilibrium" Tm of homopolymer A. When a minor amount of A and a major amount of B were copolymerized to produce a linear block polymer (with runs of repeat A covalently backbone-bonded to runs of repeat B to yield a molecular structure of the type –BBBBB–AAAA–BBBBBBB–AAA–BBBBBB–), the resulting product could be made partially crystalline by crystallization from solution. Because the A and B domains were covalently linked, macroscopic phase separation upon crystallization of A was prevented, and microcrystalline "micelles" of A blocks remained dispersed in a three-dimensional amorphous network of B block "fringes". When the melting behavior of this block copolymer was analyzed by DSC, the melting transition of the crystalline A domains was observed at a temperature *above* the Tg of the amorphous B domains. The A domains were kinetically constrained against melting (by dissociation and concomitant volume expansion)[105] at their "equilibrium" Tm by the surrounding continuous glassy matrix of B. The A domains were only free to melt (at a non-equilibrium Tm $\gg$ "equilibrium" Tm) *after* the B domains transformed from glassy solid to rubbery liquid at their Tg. Another interesting example of similar non-equilibrium melting behavior is solution-crystallized poly(phenylene oxide).[228]

The fact that water plasticization occurs only in the amorphous regions of partially crystalline, water-compatible polymers is critical to the explanation of how these metastable amorphous regions control the non-equilibrium melting behavior of the crystalline regions. The concept of non-equilibrium melting established for synthetic partially crystalline polymers has been applied to

biopolymer systems such as native starch, in order to describe the mechanical relaxation process[17-23,26,30] that occurs as a consequence of a dynamic heat/moisture/time treatment.[229,230] The existence of contiguous microcrystalline and amorphous regions (e.g., in native starch, the crystallizable short branches and backbone segments with their branch points, respectively, of amylopectin molecules) covalently linked through individual polymer chains creates a "fringed micelle" network. Relative dehydration of the amorphous regions to an initial low overall moisture content leads to the kinetically stable condition in which the effective Tg is higher than the "equilibrium" Tm of the hydrated crystalline regions. Consequently, the effective Tm[21] is elevated and observed only after softening of the amorphous regions at Tg. Added water acts directly to plasticize the continuous glassy regions, leading to the kinetically metastable condition in which their effective Tg is depressed. Thus, the "fringe" becomes an unstable rubber at $T > Tg$, allowing sufficient mobility and swelling by thermal expansion and water uptake for the interconnected microcrystallites, embedded in the "fringed micelle" network, to melt (by dissociation, with concomitant volume expansion)[105] on heating to a less kinetically constrained Tm only slightly above the depressed Tg. For such a melting process, use of the Flory-Huggins thermodynamic treatment to interpret the effect of water content on Tm has no theoretical basis,[106,161,231] because, while water as a plasticizer does affect directly the Tg and indirectly the Tm of polymers such as starch, the effect on Tm is not the direct effect experienced in equilibrium melting (i.e., dissolution) along the solidus curve. In contrast to the case of native starch, in which initial "as is" moisture is limiting, in an excess-moisture situation such as a retrograded wheat starch gel with $\gtrsim$27 w% water (Wg′), in which the amorphous matrix would be fully plasticized and ambient temperature would be above Tg (i.e., $Tg' \simeq -5°C$), the fully hydrated and matured crystalline junctions would show the actual, lower (and closer to "equilibrium") Tm of $\simeq$60°C for retrograded B-type starch.[17-23,26] (Note the analogy between the above description of non-equilibrium melting in native granular starch and the case described previously of non-equilibrium melting in a synthetic, partially crystalline block copolymer. In this context, it is interesting that Wunderlich[105] defines branched polymers as a special case of copolymers, using the example of a synthetic polymer with crystallizable branches.)

Retrogradation has been described[17,18,20-23,26] as a non-equilibrium (i.e., time/temperature/moisture-dependent) polymer recrystallization process in completely amorphous (in the case of waxy starches) starch-water melts. In normal starches, retrogradation has been recently confirmed to involve both fast crystallization of amylose and slow recrystallization of amylopectin.[63,92,215,218-221] Amylopectin recrystallization has been described[17,18,20-23,26] as a nucleation-limited growth process that occurs, at $T > Tg$, in the mobile, viscoelastic, "fringed micelle" gel network plasticized by water, and which is thermally reversible at $T > Tm$. This description has also been confirmed recently, for both amylopectin[92,215] and amylose.[211-214,220] The aging effects typically observed in starch gels and baked bread have been attributed (as in synthetic polymer-organic diluent gels) to time-dependent crystallization processes (i.e., maturation), primarily involving amylopectin, which occur subsequent to initial gelation.[63,65,92,94,219,221,225] With respect to these effects, Slade[18] has reported that "analysis of results (of measurements of extent of recrystallization vs. time after gelatinization) by the classic Avrami equation may provide a convenient means to represent empirical data from retrogradation experiments,[63,94,183,219,232] but some published theoretical interpretations[233] have been misleading." Complications, due to the non-equilibrium nature of starch recrystallization via the three-step mechanism, limit the theoretical utility of the Avrami parameters, which were originally derived to describe crystallization under conditions far above the glass curve[26] and where details about nucleation events and constant linear growth rates were readily measurable.[104] Others have agreed with this conclusion[63,211] and pointed out that such an Avrami analysis allows no insight regarding crystal morphology[219] and provides no clear mechanistic information.[49,183] Furthermore, the Avrami theory gives no indication of the temperature dependence of the crystallization rate.[63,94]

It should be recalled that the same three-step crystallization mechanism also applies to low MW compounds,[4,104] such as concentrated aqueous solutions and melts of low MW carbohydrates,[16,30] and to recrystallization processes in frozen systems of water-compatible food materials.[15,27,32]

7. Polymer Crystallization Kinetics Theory

The classic theory of crystallization kinetics, applied to synthetic partially crystalline polymers,[104] is illustrated in Figure 37[26] (adapted from References 104, 139, 192). This theory has also been shown to describe the kinetics of starch retrogradation[17,18,20,49,94,95] and gelatin gelation.[17,24,139,195,234] Figure 37 shows the dependence of crystallization rate on temperature within the range $Tg < T < Tm$, and emphasizes the fact that gelation-via-crystallization can only occur in the rubbery (undercooled liquid) state, between the temperature limits defined by Tg and Tm.[15,94] These limits, for gels recrystallized from high MW gelatin solutions of concentrations up to about 65 w% gelatin (i.e., $W > Wg' \simeq 35$ w% water), are about $-12°C$ ($= Tg'$) and 37°C, respectively, while for B-type starch (or purified amylopectin) gels recrystallized from homogeneous and completely amorphous gelatinized sols or pastes containing $\gtrsim$27 w% water ($= Wg'$), they are about $-5°C$ ($= Tg'$) and 60°C, respectively.[17,18] In gelatinized potato starch:water mixtures (1:1 w/w), retrogradation has been demonstrated at single storage temperatures between 5 and 50°C.[235] In retrograding potato and wheat starch gels, low-temperature storage (at 5 and 4°C, respectively) results in recrystallization to lower-Tm, less symmetrically perfect polymorphs than those produced by storage at room temperature.[232,235] Conversely, a higher crystallization temperature generally favors formation of the higher-Tm, more stable A-type, rather than B-type, starch polymorph.[236,237] For amylopectins from waxy maize and other botanical sources, thermoreversible gelation-via-crystallization from concentrated (>10 w% solute) aqueous solution has been observed after long-term storage at 1 to 5°C.[92,216,218] In baked bread, low (4°C), intermediate (25°C), and high (40°C)-temperature storage results in starch recrystallization manifested by corresponding lower, intermediate, and higher-Tm staling endotherms.[95] In a 50% wheat starch gel, the extent of crystallization increases with decreasing storage temperature in the range 2 to 37°C (i.e., displays a negative temperature dependence), and the rate of recrystallization to the B-form is more rapid at 2 than at 37°C.[94] In contrast to the familiar Tm of about 60°C for thermoreversible B-type amylopectin gels with excess moisture stored at room temperature (and for stale bread),[20] the corresponding Tm for thermoreversible V-type amylose gels is well above 100°C,[35,92] owing in part to the much higher $\overline{DP}w$ of the amylose chain segments (i.e., $\overline{DP}w \simeq 50$ vs. $\simeq 15$ for amylopectin)[92] comprising the microcrystalline junction zones. Analogously, the familiar Tm well above 100°C for various V-type lipid-amylose crystalline complexes[35] is much higher than the corresponding Tm of about 70°C reported for a lipid-amylopectin crystalline complex.[20] These findings are fully consistent with the established relationship between increasing chain length (and MW) and increasing Tm within

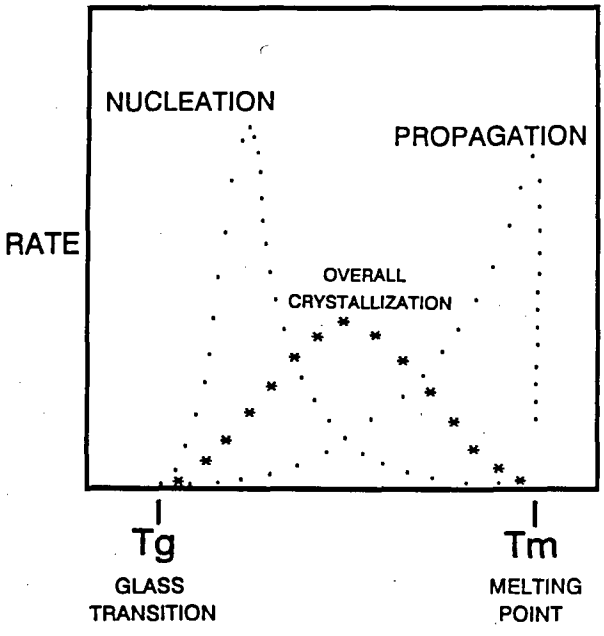

FIGURE 37. Crystallization kinetics of partially crystalline polymers, expressed in terms of crystallization rate as a function of temperature. (Reproduced with permission from Reference 26.)

homologous families of partially crystalline synthetic polymers.[105,113]

As illustrated by Figure 37 and the above results on the temperature dependence of starch recrystallization, the rate of crystallization would be practically negligible at $T < Tg$, because nucleation is a liquid-state phenomenon (i.e., in part, a transport process through a viscous medium)[49,94] that requires translational and orientational mobility, and such mobility is virtually disallowed (over realistic times) in a mechanical solid of $\eta \gtrsim 10^{12}$ Pa s.[4] The temperature of homogeneous nucleation (Th) can be estimated from the ratio of Th/Tm (K),[30] which is typically near 0.8 for partially crystalline synthetic polymers as well as small molecules, with a reported range of 0.78 to 0.85.[104,115] The rate of propagation goes essentially to zero below Tg, because propagation is a diffusion-limited process[192] for which practical rates also require the liquid state. At $T > Tm$, the rate of overall crystallization also goes to zero, because, intuitively, one realizes that crystals can neither nucleate nor propagate at any temperature at which they would be melted instantaneously.

Figure 37 illustrates the complex temperature dependence of the overall crystallization rate and of the rates of the separate mechanistic steps of nucleation and propagation. According to classic nucleation theory, the nucleation rate is zero at Tm and increases rapidly with decreasing temperature (and increasing extent of undercooling (Tm − T)) over a relatively narrow temperature interval, which for undiluted synthetic polymers begins at an undercooling of 30 to 100°C.[104] Within this temperature region, the nucleation rate shows a large negative temperature coefficient.[94,139] At still lower temperatures (and greater extents of undercooling), where nucleation relies on transport and depends on local viscosity, the nucleation rate decreases with decreasing temperature and increasing local viscosity, to a near-zero rate at Tg.[94,104] In contrast, the propagation rate increases rapidly with increasing temperature, from a near-zero rate at Tg, and shows a large positive temperature coefficient over nearly the entire rubbery range, until it drops precipitously to a zero rate at Tm.[94,104,139] The fact that the nucleation and propagation rates show temperature coefficients of opposite sign in the temperature region of intermediate undercooling has been explained[94] by pointing out that "when the temperature has been lowered sufficiently to allow the formation of (critical) nuclei (whose size decreases with decreasing temperature),[4,49] the (local) viscosity is already so high that it prevents growth of crystalline material."[192] The maturation rate for non-equilibrium crystallization processes, like the propagation rate, increases with increasing temperature, up to the maximum Tm of the most mature crystals.[15,18]

As shown by the symmetrical curve in Figure 37, the overall crystallization rate (i.e., the resultant rate of both the nucleation and propagation processes), at a single holding temperature, reaches a maximum at a temperature about midway between Tg and Tm, and approaches zero at Tg and Tm.[17,18,49,94,104,139] Identification of the location of the temperature of maximum crystallization rate has been described[104] in terms of a universal empirical relationship (based on two underlying concepts) for the crystallization kinetics of synthetic high polymers. The first concept identifies a model polymer (e.g., a readily crystallizable elastomer with Tg = 200 K and Tm = 400 K) as one for which the temperature dependence of polymer melt viscosity is described by WLF kinetics.[104] (The same concept has been shown to be applicable to describe the non-equilibrium thermomechanical relaxation behavior of "typical" and "atypical" food carbohydrates in aqueous glassy and rubbery states.)[30] The second concept empirically defines a reduced temperature, based on Tg and Tm for typical polymers, as (T − Tg + 50 K)/(Tm − Tg + 50 K).[104] (An analogous reduced temperature scale, based on Tg′ and Tm, has been shown to describe the rotational mobility [i.e., dielectric relaxation behavior] of concentrated aqueous sugar solutions in the supraglassy fluid state.)[30] For all synthetic high polymers analyzed, the temperature position of the maximum crystallization rate, on a universal master curve like the one shown in Figure 37, occurs at about 0.6 of the reduced temperature scale.[104] Low MW synthetic compounds have been fitted to a similar curve, but with a different position for the maximum crystallization rate, at about 0.8 of the reduced temperature scale.[104] Based on this empirical relationship for synthetic high polymers,

the calculated single holding temperature for maximum crystallization rate would be about 300 K for the model elastomer (in fact, exactly midway between Tg and Tm), −3°C for a gelatin gel with ≳35 w% water (a temperature made inaccessible without detriment to product quality due to unavoidable ice formation), 14°C for a typical B-type starch (or amylopectin) gel with ≳27 w% water, and 70°C for a V-type amylose gel (based on Tm = 153°C[92]).[26] It has been noted[26] that the calculated value of about 14°C for B-type starch is similar to (1) the empirically determined subambient temperature for the maximum rate of starch recrystallization and concomitant crumb firming during aging, reported in an excellent study of the kinetics of bread staling by Guilbot and Godon,[238] but not previously explained on the basis of the polymer crystallization kinetics theory described above, and (2) the temperature of about 5°C recently calculated from Lauritzen-Hoffman polymer crystallization kinetics theory by Marsh and Blanshard[94] for a 50% wheat starch gel. The fact that these subambient temperatures are much closer to the operative Tg (i.e., Tg′) than to Tm,[26] unlike the situation depicted by the symmetrical shape of the crystallization rate curve in Figure 37 that typifies the behavior of many synthetic polymers, clearly indicates that the crystallization process for B-type starch (or pure amylopectin) is strongly nucleation-limited.[18,20,94]

In contrast to the maximum crystallization rate achievable at a single temperature, Ferry[239] showed for gelatin that the rate of gelation can be further increased, while the phenomenon of steadily increasing gel maturation over extended storage time can be eliminated, by a two-step temperature-cycling gelation protocol that capitalizes on the crystallization kinetics defined in Figure 37. He showed that a short period for fast nucleation at 0°C (a temperature above Tg′ and near the peak of the nucleation rate curve), followed by another short period for fast crystal growth at a temperature just below Tm, produced a gelatin gel of maximum and unchanging gel strength in the shortest possible overall time. Recently, Slade has shown that a similar temperature-cycling protocol can be used to maximize the rate of starch recrystallization in freshly gelatinized starch-water mixtures with at least 27 w% water,[18,20] resulting in a patented process for the accelerated staling of starch-based food products.[36] Zeleznak and Hoseney[95] subsequently adopted this protocol in their study of the temperature dependence of bread staling.

IV. THE FOOD POLYMER SCIENCE DATA BANK AND ITS PHYSICOCHEMICAL FOUNDATION

As emphasized by the discussion in Section II, for pragmatical time scales and conditions (temperature, concentration, pressure), where "real-world" food systems are usually far from equilibrium, familiar treatments (e.g., water activity and moisture sorption isotherms) based on the equilibrium thermodynamics of very dilute solutions fail.[30] This is not too surprising, since limiting partial molar properties reflect the independent behavior of solute in the limit of infinite dilution where free volume is maximum at a given temperature, while Tg′-Wg′ properties reflect the cooperative behavior of plasticizer blends composed of concentrated solute-water mixtures at the limiting minimum value of free volume to observe relaxation within experimental time scales. As suggested by the information reviewed in Section III, successful treatments require a new approach to emphasize the kinetic description, relate time-temperature-concentration-pressure through underlying mobility transformations, and establish reference conditions of temperature and concentration (characteristic for each solute).[30] In this section covering the food polymer science data bank and its physicochemical foundation, it is demonstrated (and then corroborated in Section V) that small carbohydrate-water systems, with well-characterized structure and MW above and below the limit for entanglement coupling, provide a unique framework for the investigation of non-equilibrium behavior:[30] definition of conditions for its empirical demonstration, examination of materials properties that allow its description and control, identification of appropriate experimental approaches, and exploration of theoretical interpretations. This framework has been applied to the other major categories of food materials included in the data bank.

The food polymer science data bank has been established from measured thermal properties of hundreds of individual food materials, including (a) small carbohydrates — sugars, polyhydric alcohols, and glycoside derivatives; (b) carbohydrate oligomers and high polymers — starches and SHPs; (c) high MW, non-starch polysaccharides; (d) amino acids; (e) proteins; (f) organic acids; (g) biological tissues — fruits and vegetables; and (h) a wide variety of other food ingredients and products.[8,14-39] The data bank consists of the following reference parameters, measured for each individual solute by DSC (see methods described elsewhere):[8,27,28,34] (1) Tg′, the particular subzero Tg of the maximally freeze-concentrated glass that is formed on slow cooling of a 20 w% aqueous solution of the non-crystallizing solute to T < Tg′; (2) Wg′, the corresponding water content of the maximally freeze-concentrated glass that is formed on slow cooling of a 20 w% aqueous solution of the non-crystallizing solute to T < Tg′, representing the amount of water rendered "unfreezable" on a practical time scale (expressed as g UFW/g solute) by immobilization with the solute in this dynamically constrained, kinetically metastable amorphous solid of extremely high local viscosity; (3) Tm of the anhydrous crystalline solute; and (4) Tg of the completely amorphous, anhydrous solute, resulting from vitrification via quench-cooling after melting of the crystalline solute.

A. Monomeric, Oligomeric, and Polymeric Carbohydrates

The 84 small carbohydrates listed in Table 3[6-8,27-31,40-42] are polyhydroxy compounds (PHCs) of known, monodisperse (i.e., $\overline{M}w/\overline{M}n = 1$) MWs. These PHCs represent a comprehensive but non-homologous series of mono-, di-, and small oligosaccharides and their derivatives, including many common sugars, polyols, and glycosides, covering a MW range of 62 to 1153 Da. The 91 SHPs listed in Table 4[8,32,34] are monomeric, oligomeric, and high-polymeric carbohydrates, representing a homologous family of glucose polymers. These SHPs represent a spectrum of commercial products (including modified starches, dextrins, maltodextrins, corn syrup solids, and corn syrups), with polydisperse MWs (i.e., $\overline{M}w/\overline{M}n \gg 1$), covering a very broad range of dextrose equivalent (DE, where DE = 100/($\overline{M}n$/180.2)) values from 0.3 to 100.

1. Tg′ Database

Figure 38[8] shows typical low-temperature DSC thermograms for 20 w% solutions of (a) glucose and (b) a 10 DE maltodextrin (Star Dri 10). In each, the heat flow curve begins at the top (endothermic down), and the analog derivative trace (endothermic up and zeroed to the temperature axis) at the bottom. For both thermograms, instrumental amplification and sensitivity settings were identical, and sample weights comparable. It is evident that the direct analog derivative feature of the DSC (DuPont Model 990) greatly facilitates deconvolution of sequential thermal transitions, assignment of precise transition temperatures (to ±0.5°C for Tg′ values of duplicate samples), and thus overall interpretation of thermal behavior, especially for such frozen aqueous solutions exemplified by Figure 38A. We commented in 1986[8] on the surprising absence of previous reports of the use of derivative thermograms, in the many earlier DSC studies of such systems with water content >Wg′ (see Franks[4] for an extensive bibliography), to sort out the small endothermic and exothermic changes in heat flow that typically occur below 0°C. Most modern commercial DSC instruments provide a derivative feature, but its use for increased interpretative capability still appears to remain much neglected in the thermal analysis of foods in general, and frozen aqueous food systems in particular.[34,189]

Despite the handicap of such instrumental limitations in the past, the theoretical basis for the thermal properties of aqueous solutions at subzero temperatures has come to be increasingly understood.[4-6,74,133,240-242] As shown in Figure 38A, after rapid cooling (about 50°C/min) of the glucose solution from room temperature to < −80°C, slow heating (5°C/min) reveals a minor Tg at −61.5°C, followed by an exothermic devitrification (a crystallization of some of the previously UFW) at Td = −47.5°C, followed by another (major) Tg, namely, Tg′, at −43°C, and finally

TABLE 3
Tg′, Wg′, Dry Tg, Dry Tm, and Tm/Tg Ratio for Sugars and Polyols[27,28]

Polyhydroxy compound	MW	Tg′ °C	Wg′ (g UFW/g)	Dry Tg °C	Dry Tm °C	Tm/Tg °K
Ethylene glycol	62.1	−85	1.90			
Propylene glycol	76.1	−67.5	1.28			
1,3-Butanediol	90.1	−63.5	1.41			
Glycerol	92.1	−65	0.85	−93	18	1.62
Erythrose	120.1	−50	1.39			
Threose	120.1	−45.5				
Erythritol	122.1	−53.5	(Eutectic)			
Thyminose (deoxyribose)	134.1	−52	1.32			
Ribulose	150.1	−50				
Xylose	150.1	−48	0.45	9.5	153	1.51
Arabinose	150.1	−47.5	1.23			
Lyxose	150.1	−47.5		8	115	1.38
Ribose	150.1	−47	0.49	−10	87	1.37
Arabitol	152.1	−47	0.89			
Ribitol	152.1	−47	0.82			
Xylitol	152.1	−46.5	0.75	−18.5	94	1.44
Methyl riboside	164.2	−53	0.96			
Methyl xyloside	164.2	−49	1.01			
Quinovose (deoxyglucose)	164.2	−43.5	1.11			
Fucose (deoxygalactose)	164.2	−43	1.11			
Rhamnose (deoxymannose)	164.2	−43	0.90			
Talose	180.2	−44		11.5	140	1.45
Idose	180.2	−44				
Psicose	180.2	−44				
Altrose	180.2	−43.5		10.5	107	1.34
Glucose	180.2	−43	0.41	31	158	1.42
Gulose	180.2	−42.5				
Fructose	180.2	−42	0.96	100	124	1.06
Galactose	180.2	−41.5	0.77	110	170	1.16
Allose	180.2	−41.5	0.56			
Sorbose	180.2	−41	0.45			
Mannose	180.2	−41	0.35	30	139.5	1.36
Tagatose	180.2	−40.5	1.33			
Inositol	180.2	−35.5	0.30			
Mannitol	182.2	−40	(Eutectic)			
Galactitol	182.2	−39	(Eutectic)			
Sorbitol	182.2	−43.5	0.23	−2	111	1.42
2-*O*-methyl fructoside	194.2	−51.5	1.61			
β-1-*O*-methyl glucoside	194.2	−47	1.29			
3-*O*-methyl glucoside	194.2	−45.5	1.34			
6-*O*-methyl galactoside	194.2	−45.5	0.98			
α-1-*O*-methyl glucoside	194.2	−44.5	1.32			
1-*O*-methyl galactoside	194.2	−44.5	0.86			

TABLE 3 (continued)
Tg′, Wg′, Dry Tg, Dry Tm, and Tm/Tg Ratio for Sugars and Polyols[27,28]

Polyhydroxy compound	MW	Tg′ °C	Wg′ (g UFW/g)	Dry Tg °C	Dry Tm °C	Tm/Tg °K
1-*O*-methyl mannoside	194.2	−43.5	1.43			
1-*O*-ethyl glucoside	208.2	−46.5	1.35			
2-*O*-ethyl fructoside	208.2	−46.5	1.15			
1-*O*-ethyl galactoside	208.2	−45	1.26			
1-*O*-ethyl mannoside	208.2	−43.5	1.21			
Glucoheptose	210.2	−37.5				
Mannoheptulose	210.2	−36.5				
Glucoheptulose	210.2	−36.5	0.77			
Perseitol (mannoheptitol)	212.2	−32.5	(Eutectic)			
1-*O*-propyl glucoside	222.2	−43	1.22			
1-*O*-propyl galactoside	222.2	−42	1.05			
1-*O*-propyl mannoside	222.2	−40.5	0.95			
2,3,4,6-*O*-methyl glucoside	236.2	−45.5	1.41			
Isomaltulose (palatinose)	342.3	−35.5				
Nigerose	342.3	−35.5				
Cellobiulose	342.3	−32.5				
Isomaltose	342.3	−32.5	0.70			
Sucrose	342.3	−32	0.56	52	192	1.43
Gentiobiose	342.3	−31.5	0.26			
Laminaribiose	342.3	−31.5				
Turanose	342.3	−31	0.64	52	177	1.38
Mannobiose	342.3	−30.5	0.91	90	205	1.32
Melibiose	342.3	−30.5				
Lactulose	342.3	−30	0.72			
Maltose	342.3	−29.5	0.25	43	129	1.27
Maltulose	342.3	−29.5				
Trehalose	342.3	−29.5	0.20	79	203	1.35
Cellobiose	342.3	−29		77	249	1.49
Lactose	342.3	−28	0.69			
Maltitol	344.3	−34.5	0.59			—
Isomaltotriose	504.5	−30.5	0.50			
Panose	504.5	−28	0.59			
Raffinose	504.5	−26.5	0.70			
Maltotriose	504.5	−23.5	0.45	76	133.5	1.16
Nystose	666.6	−26.5		77	—	
Stachyose	666.6	−23.5	1.12			
Maltotetraose	666.6	−19.5	0.55	111.5	—	
Maltopentaose	828.9	−16.5	0.47	125	—	
α-Cyclodextrin	972.9	−9				
Maltohexaose	990.9	−14.5	0.50	134	—	
Maltoheptaose	1153.0	−13.5	0.27	138.5	—	

the melting of ice, beginning at T > Tg′ and ending at Tm. In Figure 38B, the maltodextrin solution thermogram shows only an obvious Tg′ at −10°C, followed by Tm. These assignments of characteristic transitions (i.e., the sequence Tg < Td < Tg′ < Tm) and temperatures have been

TABLE 4
Tg' Values for Commercial SHPs[8]

SHP	Manufacturer	Starch source	DE	Tg', °C	Gelling
AB 7436	Anheuser Busch	Waxy maize	0.5	−4	
AmioGum 23	Amaizo		1	−4	
47TT110	Staley	Potato	0.6	−4.5	
Paselli SA-2	AVEBE (1984)	Potato (Ap)	2	−4.5	Yes
Stadex 9	Staley	Dent corn	3.4	−4.5	Yes
Paselli SA-2	AVEBE (1987)	Potato	2	−5	
78NN128	Staley	Potato	0.6	−5	Yes
78NN122	Staley	Potato	2	−5	Yes
V-O Starch	National	Waxy maize		−5.5	Yes
N-Oil	National	Tapioca		−5.5	Yes
ARD 2326	Amaizo	Dent corn	0.4	−5.5	Yes
Paselli SA-2	AVEBE (1986)	Potato (Ap)	2	−5.5	Yes
Glucidex 2B	Roquette	Waxy maize	2	−5.5	
ARD 2308	Amaizo	Dent corn	0.3	−6	Yes
AB 7435	Anheuser Busch	Waxy/dent blend	0.5	−6	
Star Dri 1	Staley (1984)	Dent corn	1	−6	Yes
Crystal Gum	National	Tapioca	5	−6	Yes
Maltrin M050	GPC	Dent corn	6	−6	Yes
Star Dri 1	Staley (1986)	Waxy maize	1	−6.5	Yes
Paselli MD-6	AVEBE	Potato	6	−6.5	Yes
Dextrin 11	Staley	Tapioca	1	−7.5	Yes
MD-6-12	V-Labs		2.8	−7.5	
Capsul	National (1987)	Waxy maize	5	−7.5	
Stadex 27	Staley	Dent corn	10	−7.5	No
MD-6-40	V-Labs		0.7	−8	
Star Dri 5	Staley (1984)	Dent corn	5	−8	No
Star Dri 5	Staley (1986)	Waxy maize	5.5	−8	No
Paselli MD-10	AVEBE	Potato	10	−8	No
Paselli SA-6	AVEBE	Potato (Ap)	6	−8.5	No
α-Cyclodextrin	Pfanstiehl			−9	
Capsul	National (1982)	Waxy maize	5	−9	
Lodex Light V	Amaizo	Waxy maize	7	−9	
Paselli SA-10	AVEBE	Potato (Ap)	10	−9.5	No
Morrex 1910	CPC	Dent corn	10	−9.5	
Star Dri 10	Staley (1984)	Dent corn	10	−10	No
Maltrin M040	GPC	Dent corn	5	−10.5	
Frodex 5	Amaizo	Waxy maize	5	−11	
Star Dri 10	Staley (1986)	Waxy maize	10.5	−11	No
Lodex 10	Amaizo (1986)	Waxy maize	11	−11.5	No
Lodex Light X	Amaizo	Waxy maize	12	−11.5	
Morrex 1918	CPC	Waxy maize	10	−11.5	
Mira-Cap	Staley	Waxy maize		−11.5	
Maltrin M100	GPC	Dent corn	10	−11.5	No
Lodex 5	Amaizo	Waxy maize	7	−12	No
Maltrin M500	GPC	Dent corn	10	−12.5	
Lodex 10	Amaizo (1982)	Waxy maize	12	−12.5	No
Star Dri 15	Staley (1986)	Waxy maize	15.5	−12.5	No
MD-6	V-Labs			−12.5	
Maltrin M150	GPC	Dent corn	15	−13.5	No
Maltoheptaose	Sigma		15.6	−13.5	
MD-6-1	V-Labs		20.5	−13.5	
Star Dri 20	Staley (1986)	Waxy maize	21.5	−13.5	No

TABLE 4 (continued)
Tg′ Values for Commercial SHPs[8]

SHP	Manufacturer	Starch source	DE	Tg′, °C	Gelling
Maltodextrin Syrup	GPC	Dent corn	17.5	−14	No
Frodex 15	Amaizo	Waxy maize	18	−14	
Maltohexaose	Sigma		18.2	−14.5	
Frodex 10	Amaizo	Waxy maize	10	−15.5	
Lodex 15	Amaizo	Waxy maize	18	−15.5	No
Maltohexaose	V-Labs		18.2	−15.5	
Maltrin M200	GPC	Dent corn	20	−15.5	
Maltopentaose	Sigma		21.7	−16.5	
Staley 200	Staley (1987)	Corn	26	−17	
Maltrin M250	GPC (1987)	Dent corn	25	−17	
Maltrin M250	GPC (1982)	Dent corn	25	−17.5	
N-Lok	National	Blend		−17.5	
Staley 200	Staley	Corn	26	−19.5	
Maltotetraose	Sigma		27	−19.5	
Frodex 24	Amaizo (1987)	Waxy maize	28	−19.5	
Frodex 24	Amaizo (1982)	Waxy maize	28	−20.5	
Frodex 36	Amaizo	Waxy maize	36	−21.5	
DriSweet 36	Hubinger	Corn	36	−22	
Maltrin M365	GPC	Dent corn	36	−22.5	
Staley 300	Staley	Corn	35	−23.5	
Globe 1052	CPC	Corn	37	−23.5	
Maltotriose	V-Labs		35.7	−23.5	
Frodex 42	Amaizo (1982)	Waxy maize	42	−25.5	
Frodex 42	Amaizo (1987)	Waxy maize	42	−25.5	
Neto 7300	Staley (1987)	Corn	42	−25.5	
Staley 1300	Staley (1987)	Corn	43	−26	
Neto 7300	Staley (1982)	Corn	42	−26.5	
Globe 1132	CPC	Corn	43	−27.5	
Staley 1300	Staley (1982)	Corn	43	−27.5	
Neto 7350	Staley	Corn	50	−27.5	
Maltose	Sigma		52.6	−29.5	
Globe 1232	CPC	Corn	54.5	−30.5	
Staley 2300	Staley	Corn	54	−31	
Sweetose 4400	Staley	Corn	64	−33.5	
Sweetose 4300	Staley	Corn	64	−34	
Globe 1642	CPC	Corn	63	−35	
Globe 1632	CPC	Corn	64	−35	
Royal 2626	CPC	Corn	95	−42	
Glucose	Sigma	Corn	100	−43	

reconciled definitively with actual state diagrams previously reported for various solutes, including small sugars and water-soluble polymers.[4,32,33,242]

It has been demonstrated[8,33] that the thermogram for the glucose solution in Figure 38A represents a characteristic example, if somewhat trivial case,[30] of the unusual phenomenon of multiple values of Tg in glass-forming systems, which is a subject of increasing current interest in the cryotechnology field.[8,27,31-34,175,243-248] Due to incomplete phase separation[175,243-246] in an incompletely frozen aqueous solution, two distinguishable, dynamically constrained glasses, with local domains of sufficient dimension and cooperativity to allow ready detection, may coexist.[30,246] One is a "bulk" glass with the same spatial homogeneity and solute concentration as the original dilute solution and a corresponding low value of

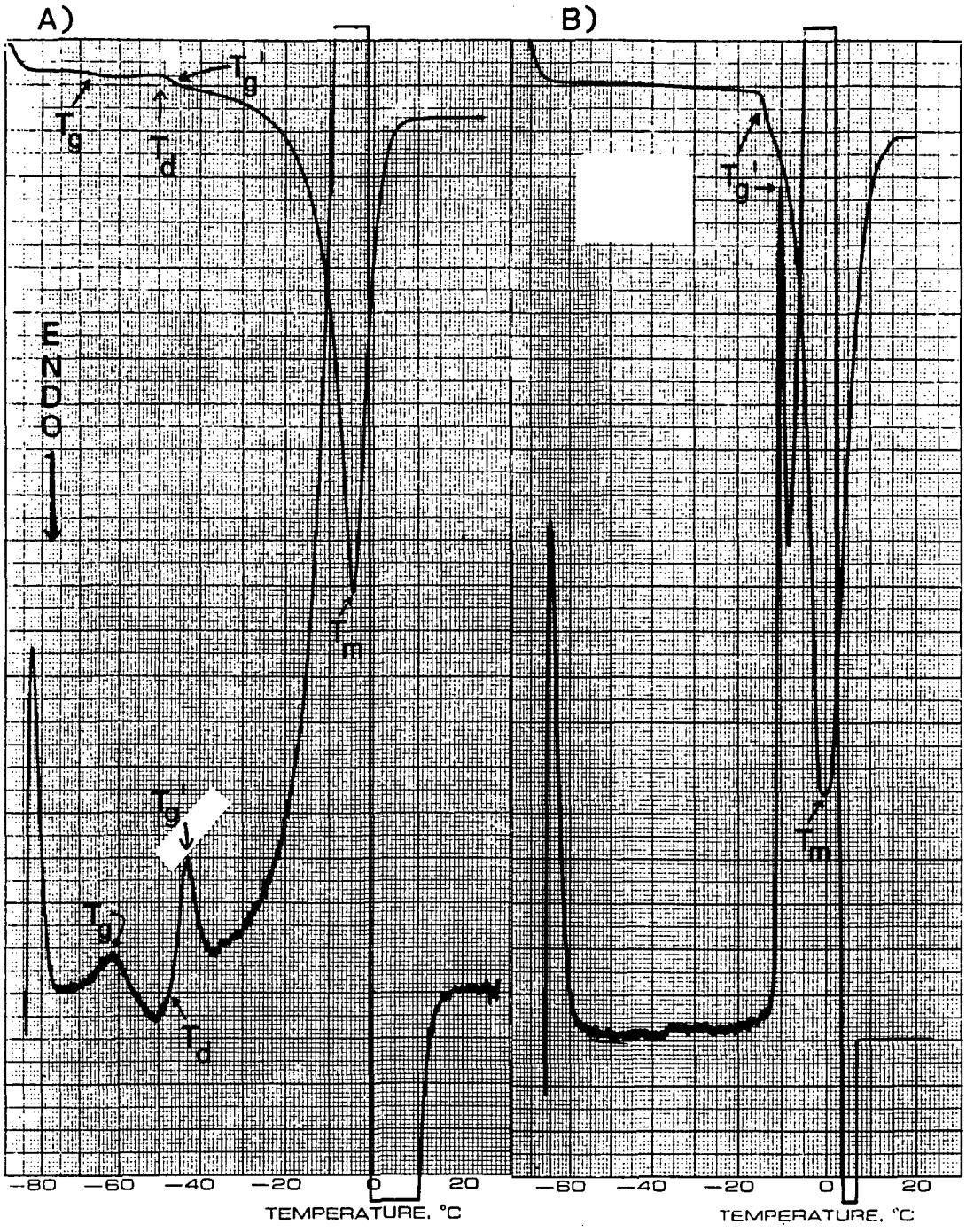

FIGURE 38. DuPont 990 DSC thermograms for 20 w% solutions of (a) glucose, and (b) Star Dri 10 (10 DE) maltodextrin. In each, the heat flow curve begins at the top (endothermic down), and the analog derivative trace (endothermic up and zeroed to the temperature axis) at the bottom. (From Levine, H. and Slade, L., *Carbohydr. Polym.*, 6, 213, 1986. With permission.)

Tg. The other, surrounding the ice crystals, is the freeze-concentrated glass with a higher value of Tg that is Tg′.[8,27,31-34] The lower limiting value of Tg for the dilute bulk glass is Tg of pure amorphous water itself, and the upper limiting value of Tg′ for the freeze-concentrated glass is Tm of pure crystalline water.[33] The observation of such a Tg + Tg′ doublet depends on sample

moisture content, cooling/heating history, and pressure history,[30,246] and represents an example of the difficulty that can be encountered in deconvoluting the non-equilibrium effects of sample history,[249,250] and the resulting potential for misinterpretation that can arise when experiments on frozen aqueous systems are not designed from a knowledge of the operative reference state.[243-245] It should be noted that other cases of multiple-Tg phenomena that have been reported are readily distinguishable from the Tg + Tg′ doublet behavior of incompletely frozen aqueous solutions. One type of general behavior (i.e., not restricted to low-temperature aqueous systems), representing another trivial case, involves simple molecular incompatibility in a two-component system, where, due to a lack of spatial homogeneity on a dimensional scale $\gtrsim$100 Å,[106] two separate glasses with different values of Tg may coexist. A non-trivial case of multiple values of Tg can result from a liquid-liquid phase separation (which can be pressure-induced or -facilitated in some instances,[247] but in others can occur at atmospheric pressure),[248] leading to spatial inhomogeneity in aqueous solutions of, for example, lithium chloride and tetraalkylammonium halides at low temperatures. Another non-trivial case can result from the formation of specific stoichiometric complexes in aqueous solutions of, for example, glycerol, DMSO, and lithium chloride[247] where each complex would exhibit its own discrete Tm (or eutectic melting temperature) and Tg′.

The idealized state diagram shown in Figure 39,[33] modified from MacKenzie and Rasmussen,[242] exemplifies those previously reported and reveals the various distinctive cooling/heating paths that can be followed by solutions of monomeric (glucose) vs. polymeric (maltodextrin) solutes. In the case of glucose, partial vitrification of the original solution can occur, as illustrated by Figure 38A, when the selected cooling rate is high relative to the rate of freezing out of ice.[5] Yet, in the case of maltodextrin, that same cooling rate would be low relative to the rate of freezing, and less vitrification is observed,[8] as shown in Figure 38B. This result is perhaps surprising, since relative rates of diffusion processes might have been expected to be more retarded in the maltodextrin solution of greater $\overline{M}w$ than in the glucose solution.[30,32] In fact, the relative rate of ice *growth* is greater in glucose solution than in maltodextrin solution.[32] However, in this example, the rate-limiting event that determines whether freezing or vitrification will predominate is the prerequisite nucleation step for the freezing process.[33] An empirical examination of available data[8,30-34] shows that efficient retardation of ice crystal growth is provided by solutes for which Tg′ of the freeze-concentrated glass is high, while enhanced potential for partial vitrification is provided by solutes for which the value of Wg′ is high, most typically concomitant with a low value of Tg′.[32] This empirical observation serves as the basis for two operational definitions of a "good" aqueous-glass former:[33,251] (1) a solute that enhances the vitrification of water as a solute-water glass over the energetically favored phase separation of ice, and (2) a solute that provides an aqueous glass with a high value of Wg′. As can be deduced from the relative sizes of the ice peaks for the samples of identical concentration and comparable weight in Figure 38A and 38B, Wg′ for the glucose-water glass is greater than Wg′ for this 10 DE maltodextrin-water glass,[8] so that glucose is a better aqueous-glass former than this maltodextrin by both criteria. The greater effect of glucose than 10 DE maltodextrin on ice nucleation cannot be attributed simply to a greater colligative depression of the homogeneous nucleation temperature by the smaller MW solute compared to the larger solute at the same w% concentration.[30,33] PVP, with $\overline{M}n$ more than 10 times greater than that of a 10 DE maltodextrin, is a good aqueous-glass former,[135] like glucose. Indeed, values of Wg′ for aqueous glasses of PVPs are greater than Wg′ of the aqueous glucose glass,[27] an anomaly inconsistent with the expected observation that the values of Tg′ for PVP glasses are greater than that of the glucose glass.[8] The location of Wg′ and Tg′ on the dynamics map for a particular solute determines the overall shape of the aqueous glass curve for that solute, such that higher values of either parameter result in a steeper rise in Tg with increase in w% solute at low solute concentrations.[16,30] The number of critical nuclei formed in a volume of solution at a given temperature within a given time interval depends both on the local viscosity of the solution and the temperature-dependence of the number

of water molecules required to constitute a critical nucleus through density fluctuations of pure water molecules.[5,40-42] Higher values of Wg′ suggest that lower nucleation temperatures would be required to create a critical nucleus, due to the smaller local dimensions available for unperturbed density fluctuations of pure water. Higher values of Wg′ or Tg′ suggest that the local viscosity of the solution would become limiting near temperatures that would effect nucleation of pure water. The value of Wg′ relates to both of the factors that determine the kinetics of ice nucleation in solution and, thus, to the ability of a solute to enhance partial vitrification at a selected cooling rate.[33]

However, as demonstrated by the DSC thermograms in Figure 38, in either general case, and regardless of initial cooling rate, rewarming from T < Tg′ forces the system through a solute-specific glass transition at Tg′.[8] As illustrated in the state diagram in Figure 39, the Tg′-Cg′ point represents a "universal crossroads" on this map, in that all cooling/heating paths eventually lead to this point.[33] As shown by one of the idealized paths in Figure 39, slow cooling of a stereotypical sugar solution from room temperature (point X) to a temperature corresponding to point Y can follow the path XVSUWY, which passes through the Tg′-Cg′ point, W. In the absence of undercooling (e.g., upon deliberate nucleation), freezing (ice formation) begins at point V (on the equilibrium liquidus curve, at a subzero temperature determined by the MW and concentration of the particular solute, via colligative freezing point depression) and ends at point W (on the non-equilibrium extension of the liquidus curve). Due to vitrification of the Tg′-Cg′ glass at point W, some of the water in the original solution (i.e., an amount defined as Wg′) is left unfrozen in the time frame of the experiment. This UFW is not "bound" to the solute nor "unfreezable" on thermodynamic grounds, but simply experiences retarded mobility in the Tg′-Cg′ glass. The extremely high local viscosity of this kinetically-metastable, dynamically constrained glass prevents diffusion of a sufficient number of water molecules to the surface of the ice lattice to allow measurement of its growth in real time.[4-8,40-42] As exemplified by the thermogram for the maltodextrin solution in Figure 38B, rewarming from point Y to point X can follow the reversible path YWUSVX, passing back through the Tg′-Cg′ point at W.[33]

In contrast to the slow-cooling path XVSUWY in Figure 39, quench-cooling can follow the direct path from point X to point Z, whereby vitrification can occur at T = Tg, the temperature corresponding to point A, *without* any freezing of ice or consequent change in the initial solution concentration.[242] However, unlike path XVSUWY, path XZ is not realistically reversible in the context of practical warming rates.[251] Upon slow, continuous rewarming from point Z to point X, the glass (of composition Cg-Wg rather than Cg′-Wg′) softens as the system passes through the Tg at point A, and then devitrifies at the Td at point D.[242] Devitrification leads to disproportionation, which results in the freezing of pure ice (point E) and revitrification via freeze-concentration of the non-ice matrix to Cg′ (point F) during *warming*.[242] Further warming above Td causes the glass (of composition Cg′-Wg′ rather than Cg-Wg) to pass through the Tg′-Cg′ point at W (where ice melting begins), after which the solution proceeds along the liquidus curve to point V (where ice melting ends at Tm), and then back to point X. The rewarming path ZADFWUSVX[33] is exemplified by the thermogram for the glucose solution in Figure 38A.

Mention can be made here about the possible consequences of an annealing treatment,[163,164,246,252,253] whereby the rewarming process just described is interrupted by an isothermal holding step carried out at different points along the path ZADFWUSV. As described for metastable, partially crystalline synthetic polymer systems,[104] annealing is a kinetic (i.e., time-dependent), transport-controlled process of crystal growth and/or perfection that occurs at Ta, a temperature above Tg but below Tm, typically = 0.75 to 0.88 Tm (K),[102] for "well-behaved" polymer systems[30] with characteristic Tg/Tm ratios of 0.5 to 0.8 (K).[102,105] In this metastable rubbery domain defined by WLF theory, within the temperature range between Tg and Tm, annealing is a diffusion-limited, non-equilibrium, structural relaxation process (another collapse phenomenon) for which the rate is governed by WLF, rather than Arrhenius, kinetics.[15,21] Specifically with respect to the behavior of frozen aqueous

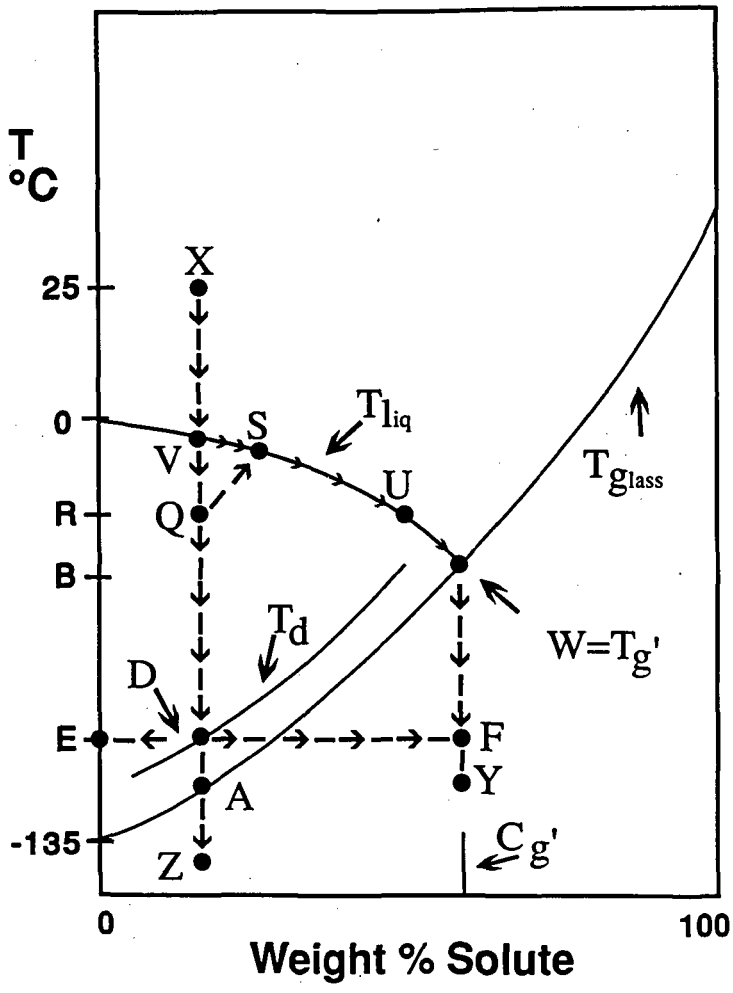

FIGURE 39. Idealized state diagram of temperature vs. weight percent solute for an aqueous solution of a hypothetical small carbohydrate (representing a model frozen food system), illustrating various cooling/heating paths and associated thermal transitions measurable by low-temperature differential scanning calorimetry (e.g., as shown by the thermograms in Figure 38). See text for explanation of symbols. (From Levine, H. and Slade, L., *Comments Agric. Food Chem.*, 1, 315, 1989. With permission.)

model solutions described by Figure 39, recognition of the time- and temperature-dependence of annealing is key to understanding the possible consequences potentially observable in a thermogram during rewarming after an annealing treatment performed at Ta < Tm of ice.[33] In all cases, the time required to achieve a measurable and comparable (in a reasonable and similar experimental time frame) extent of annealing is shortest at Ta just below Tm (greatest ΔT above Tg) and longest at Ta just above Tg (smallest ΔT).[21] For a solution initially quench-cooled from room temperature to T < Tg as described in Figure 39, the discussion[33] of the consequences of annealing can be complicated by the possible coexistence of two glasses with different glass transition temperatures (Tg and Tg'),[30] either or both of which could govern a subsequent annealing treatment. Annealing by an isothermal holding step at Tg < Ta < Td < Tg' < Tm would be predicted to occur quite slowly, because of the still very high local viscosity of the amorphous matrix at Ta just above Tg. Unless the experimental holding time were quite long, the

subsequent thermogram (during warming from T < Tg, after recooling from Ta) might well be indistinguishable in appearance from the one in Figure 38A. Moreover, if both the Tg and Tg′ glasses were present after initial quench-cooling, the slow annealing at Tg < Ta < Td < Tg′ just described would only occur locally, rather than spacially homogeneously throughout the frozen sample. In contrast, annealing by isothermal holding at Tg < Td < Tg′ < Ta < Tm would be a much faster and more spacially homogeneous process. After a sufficiently long experimental holding time for complete annealing, the subsequent thermogram (during warming from T < Tg of the original sample, after recooling from Ta > Tg′) would be predicted to show no detectable lower-temperature Tg or exothermic Td, only a Tg′ and Tm (i.e., have the qualitative appearance of Figure 38B). In the intermediate case of annealing by isothermal holding at Tg < Td < Ta < Tg′ < Tm, some of the consequences of partial annealing could be seen after a reasonable holding time at Ta just below Tg′. The subsequent thermogram (during warming from T < Tg, after recooling from Ta) might still show a remnant of the lower-temperature Tg, but an undetectably small Td, in addition to Tg′ and Tm. In fact, thermograms similar to that just described have been reported for solutions of sugars and other solutes[252,253] after an annealing treatment at Ta ≡ the so-called "antemelting" transition temperature (Tam, discussed later) just below Tg′. In the above discussion,[33] the different annealing times have been, of necessity, described only in relative qualitative terms, because experimental results of previously published studies are insufficient to allow quantitative generalizations. Quantitative times corresponding to the different annealing scenarios described above would have to be determined experimentally on a system-specific basis, i.e., for each particular solute, solute concentration, range of absolute temperatures, and cooling/warming rate protocol.[443]

The third cooling path illustrated in Figure 39, XQSUWY, is the one most relevant to the practical cooling and warming rates involved in commercial frozen food processes.[33] Cooling of a solution from point X can proceed beyond point V (on the liquidus curve) to point Q, because the system can undercool to some significant extent before heterogeneous nucleation occurs and freezing begins.[4] Upon freezing at point Q, disproportionation occurs, resulting in the formation of pure ice (point R) and freeze-concentration of the solution to point S.[4] The temperature at point S is above that at point Q due to the heat liberated by the freezing of ice.[4] The freeze-concentrated matrix at point S concentrates further to point U, because more ice forms as the temperature of the system relaxes to that at point U. Upon further cooling beyond point U, ice formation and freeze-concentration continue as the system proceeds along the liquidus curve to point W. Vitrification of the Tg′-Cg′ glass occurs at point W, and further cooling of this glass can continue to point Y without additional ice formation in real time. Rewarming of the kinetically metastable glass from point Y to point X follows the path YWUSVX, which passes through the Tg′-Cg′ point at W. The above descriptions of the various cooling/warming paths illustrated in Figure 39 demonstrate the critical fact that, regardless of cooling/warming rates (within practical limits), every aqueous system of initial concentration ≤Cg′, cooled to T ≤ Tg′, must pass through its own characteristic and operationally invariant Tg′-Cg′ point.[33] If, in commercial practice, a food product is not cooled to T ≤ Tg′ after freezing, but rather is maintained within the temperature range between points V and W, that system would track back and forth along the liquidus curve as Tf fluctuates during storage.

The technological significance of Tg′ to the storage stability of frozen food systems, implicit in the preceding description of Figure 39, is discussed in Section IV.C. Suffice it to say for now that Tg′ (of the freeze-concentrated solution), rather than Tg (of the original solution), is the *only* glass transition temperature relevant to freezer-storage stability at a given freezer temperature Tf,[33] because almost all "frozen" products contain at least some ice. Consistent with the description of the cooling path XVQSUWY, most commercial food-freezing processes, regardless of cooling rate, induce ice formation beginning at point Q (via heterogeneous nucleation after some extent of undercooling). Since the temperature at point Q (generally in the neighborhood of −20°C[40,41]) is well above that at point A, the lower Tg, that of the glass with the original

solute(s) concentration in a typical high-moisture product, is never attained and therefore has no practical relevance.[33] Once ice formation occurs in a frozen product, the predominant system-specific Tg′ becomes the one and only glass transition temperature that controls the product's behavior during freezer storage at any Tf below Tm and either above or below Tg′.[33]

In many earlier DSC studies,[125,133,252-255] performed without benefit of derivative thermograms, a pair of transitions (each said to be independent of initial concentration), called "antemelting" (am) and "incipient melting" (im), were reported in place of a single Tg′. Even though the underlying physicochemical nature of the antemelting transition has never been explained,[256] this interpretation is still advocated by some workers.[57,257] In fact, for many different solutes, reported values of Tam and Tim[241,258,259] bracket that of Tg′. This led to the alternative interpretation[8] that Tam and Tim actually represent the temperatures of onset and completion of the single thermal relaxation event (a glass transition) that must occur at Tg′, as defined by the state diagram in Figure 39. A similar lack of consensus among workers in this field persists with respect to the Tg < Td < Tg′ sequence of transitions (Figure 38A) that is universally characteristic of frozen solutions of non-crystallizing solutes rewarmed after cooling to T < Tg.[32] Instead, some have referred to "anomalous double glass transitions"[243-245] or "the phenomenon of vitreous polymorphs"[246] exhibited by aqueous solutions of, e.g., propylene glycol and glycerol. Far from anomalously, for each solute, the higher Tg of the doublet coincides with Tg′.[32] Similarly, Tr, corresponding to the onset temperature for opacity during warming of completely vitrified aqueous solutions, and known to be independent of initial concentration, is still a topic of current interest and discussion as to its origin,[260,261] but is not yet widely recognized as simply coinciding with Tg′ for low MW, non-crystallizing carbohydrate solutes[32] and non-crystallizing water-compatible polymers, e.g., PVP.[8]

In comparison to commercial SHPs, such as the 10 DE maltodextrin in Figure 38B, a starch itself has a Tg′ value of about −5°C,[17,18] as illustrated by the low-temperature DSC thermogram in Figure 40B.[21] A freshly gelatinized (but not hydrolyzed) sample of native granular wheat starch, at uniformly distributed 55 w% total moisture, showed a prominent and reversible glass transition for the fully plasticized, completely amorphous starch polymers at −5°C, immediately preceding the Tm of ice. This Tg is the Tg′ for gelatinized wheat starch in excess moisture, where the latter condition is defined by Wg′ ≃ 27 w% water (i.e., about 0.37 g UFW/g starch),[17,18] as illustrated by the state diagram in Figure 25. For the same instrumental sensitivity settings, Tg′ was not detectable in Figure 40A, because the cooperative, controlling majority of the amorphous regions of partially crystalline native starch prior to gelatinization show a much higher Tg indicative of a much lower local effective moisture content.[20]

For various PHC and SHP solutes listed in Tables 3 and 4, the experimentally measured Tg′ value falls between those reported for Tam and Tim,[241,259] and within a few degrees of values reported for Tr and Tc (see References 8 and 27 and references therein). Reid[262] has recently reported a Tg′ value for glycerol similar to ours. Also in apparent agreement with one of our measured Tg′ values, i.e., of −85°C for ethylene glycol, Hallbrucker and Mayer[263] have observed an endothermic peak at −86°C, following devitrification above Tg ≃ −128°C, in DSC rewarming scans of "hyperquenched" aqueous glasses of 47 and 50 w% ethylene glycol. They have noted the good correspondence between their peak at −86°C and the weak endothermic peak observed on rewarming slow-cooled ethylene glycol-water solution glasses in DTA experiments by Luyet and Rasmussen,[241,259] which these latter workers named the putative "antemelting" transition, purported to take place at the ice-solution interface.

In Table 3, Tg′ values for this non-homologous collection of low MW, monodisperse sugars, polyols, and glycosides range from −85°C for ethylene glycol (MW 62) to −13.5°C for maltoheptaose (MW 1153). These results, plotted in Figure 41,[27] showed a monotonic relationship between increasing Tg′ and MW, which yielded a fair linear correlation (r = −0.934) between Tg′ and 1/MW, as shown in the inset of Figure 41. The major source of scatter in this plot was the group of glycosides with chemically

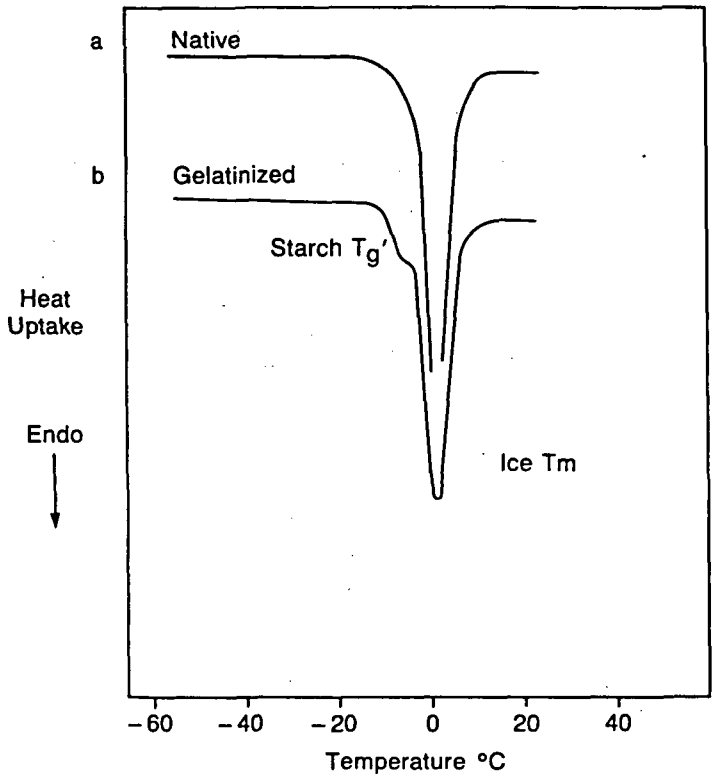

FIGURE 40. DuPont 990 DSC heat flow curves of wheat starch:water mixtures (45:55 w/w): (a) native granular; (b) immediate rescan after gelatinization of sample in (a), which reveals a prominent Tg' at −5°C, preceding the Tm of ice. (From Slade, L. and Levine, H., *Carbohydr. Polym.*, 8, 183, 1988. With permission.)

diverse substituent groups. In contrast, the corresponding results for glucose and malto-oligosaccharides of DP 2-7 (excerpted from Table 3 and shown in Figure 42[15]) demonstrated a better linear correlation, with r = −0.99 for a plot of Tg′ vs. 1/MW, shown in the inset of Figure 42. This linear dependence[106] of the Tg′ results for the malto-oligosaccharides in aqueous solution exemplified the theoretical glass-forming behavior (i.e., diluent-free Tg vs. 1/MW) characteristic of a homologous family of non-entangling, linear, monodisperse oligomers.[107,113] In contrast, for a polydisperse mixture of solutes, such as a commercial SHP,[264] the observed Tg′ actually represents a weight-average contribution from the solute.[6,30,40-42] Thus, an initial comparison of Tg′ results for the heterogeneous SHPs in Table 4 and monodisperse PHCs in Table 3 showed that glucose is representative of other monosaccharides, while maltoheptaose is comparable to 15 to 20 DE maltodextrins ($\overline{Mn} \simeq$ 900 to 1200).[31]

For the SHPs in Table 4, a homologous series of glucose oligomers and polymers, Tg′ values range from −43°C for glucose (the monomer itself, of DE = 100) to −4°C for a 0.5 DE maltodextrin. A plot of Tg′ vs. DE (shown in Figure 43[8,32,34]) revealed a linear correlation between increasing Tg′ and decreasing DE (r = −0.98) for all SHPs with manufacturer-specified DE values.[8] Since DE is inversely proportional to $\overline{DP}n$ and $\overline{M}n$ for SHPs,[264] these results demonstrated that Tg′ increases with increasing solute $\overline{M}n$ (from $\overline{M}n$ = 180 for glucose to 36000 for 0.5 DE maltodextrin).[8] Such a linear correlation between Tg and $1/\overline{M}n$ is the general rule for any homologous family of pure, glass-forming polymers.[113] The equation of the regression line is DE = −2.2(Tg′, °C) − 12.8, and the plot of Tg′ vs. DE in Figure 43 has proven useful as a calibration curve for interpolating DE values of new or "unknown" SHPs.[27]

Results for polymeric SHPs have demon-

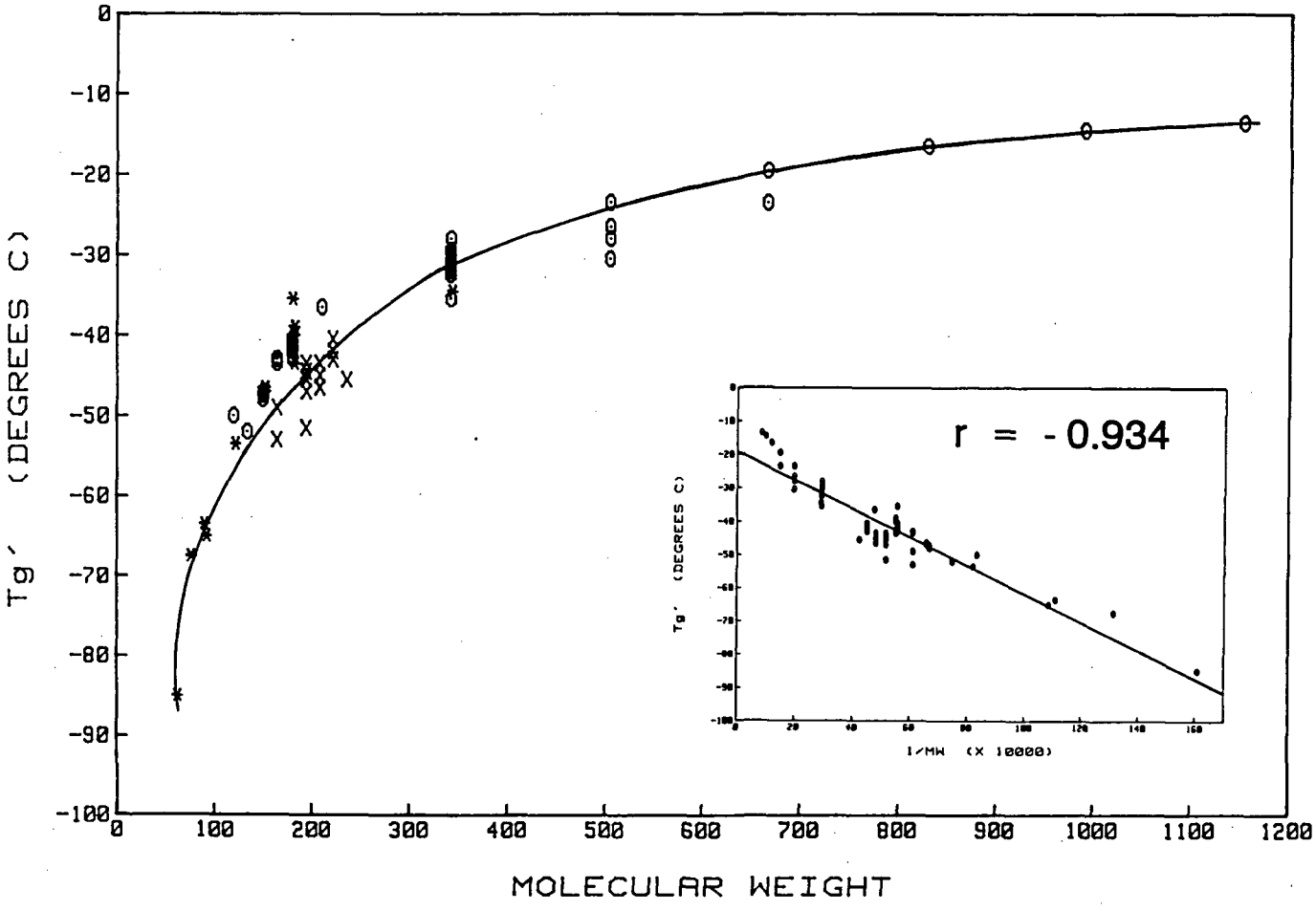

FIGURE 41. Variation of the glass transition temperature, Tg', for maximally frozen 20 w% solutions against MW for the sugars (o), glycosides (x), and polyols (*) in Table 3. (Inset: plot of Tg' vs. 1/MW ($\times 10^4$), illustrating the theoretically predicted linear dependence.) (From Levine, H. and Slade, L., *Food Structure — Its Creation and Evaluation*, Mitchell, J. R. and Blanshard, J. M. V., Eds., Butterworths, London, 1988, 149. With permission.)

strated that Tg′ depends rigorously on linear, weight-average DP ($\overline{DP}w$) for highly polydisperse solutes, so that linear polymer chains (e.g., amylose) give rise to a higher Tg′ than branched chains (e.g., amylopectin, with multiple chain ends[47]) of equal MW.[8,27] Due to the variable polydispersity and solids composition of commercial SHPs,[264,265] the range of Tg′ values for SHPs of the same specified DE can be quite broad. This behavior was shown by several pairs of SHPs in Table 4. For each pair, of the same DE and manufacturer, the hydrolysate from waxy starch (all amylopectin) had a lower Tg′ than the corresponding one from normal starch (containing amylose). This behavior was also exemplified by the Tg′ data for 13 10 DE maltodextrins in Table 4, for which Tg′ ranged from −7.5°C for a normal starch product to −15.5°C for a product derived from waxy starch, a ΔTg′ of 8°C. Such a ΔTg′ is greater than that between maltose (DP 2) and maltotriose (DP 3).[32] Further evidence was gleaned from Tg′ data for some glucose oligomers in Table 3. Comparisons of the significant Tg′ differences among maltose (1−>4-linked dimer), gentiobiose (1−>6-linked), and isomaltose (1−>6-linked), and among maltotriose (1−>4-linked trimer), panose (1−>4, 1−>6-linked), and isomaltotriose (1−>6, 1−>6-linked) have suggested that 1−>4-linked (linear amylose-like) glucose oligomers manifest greater "effective" linear chain lengths in solution (and, consequently, larger hydrodynamic volumes) than oligomers of the same MW that contain 1−>6 (branched amylopectin-like) links.[28] These re-

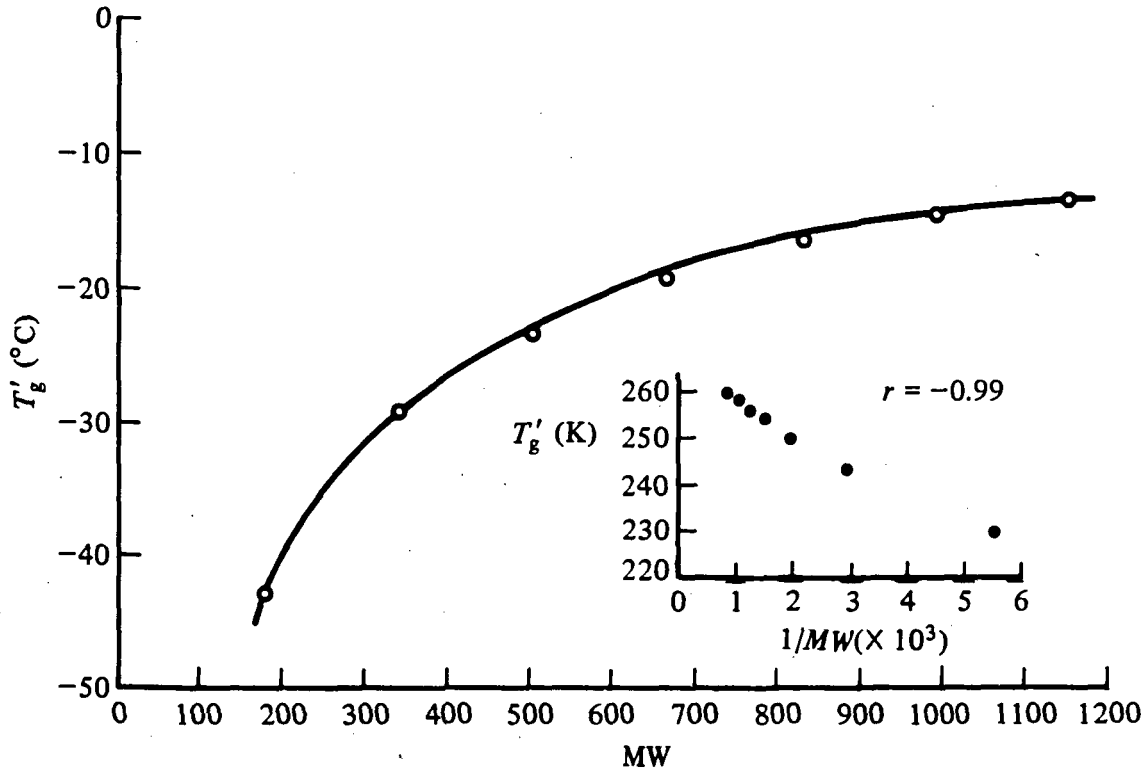

FIGURE 42. Variation of the glass transition temperature, Tg′, for maximally frozen 20 w% solutions against MW for the homologous series of malto-oligosaccharides from glucose through maltoheptaose in Table 3. (Inset: plot of Tg′ vs. 1/MW [× 1000] of solute, illustrating the theoretically predicted linear dependence.) (From Levine, H. and Slade, L., *Water Science Reviews,* Vol. 3, Franks, F., Ed., Cambridge University Press, Cambridge, 1988, 79. With permission.)

sults have also been used to illustrate the sensitivity of the Tg′ parameter to molecular configuration, in terms of linear chain length, as influenced by the nature of the glycosidic linkages in various non-homologous saccharide oligomers (not limited to glucose units) and the resultant effect on solution conformation.[31] Further evidence can be seen in Table 3, where, for sugars of equal MW (e.g., 164), ΔTg′ is as large as 10°C, a spread even larger than for the 10 DE maltodextrins.[32] Another interesting comparison is that between Tg′ values for the linear and cyclic α-(1−>4)-linked glucose hexamers, maltohexaose (−14.5°C) and α-cyclodextrin (−9°C). In this case, the higher Tg′ of the cyclic oligomer has led to a suggestion[15] that the ring of α-cyclodextrin apparently has a much larger hydrodynamic volume (due to its relative rigidity) than does the linear chain of maltohexaose, which is relatively flexible and apparently can assume a more compact conformation in aqueous solution.

The above comparisons have been discussed in the past to emphasize the subtleties of structure-property analyses of SHPs and PHCs by DSC.[34] The unavoidable conclusion, concerning the choice of a suitable carbohydrate ingredient for a specific product application, is that one SHP (or PHC) is not necessarily interchangeable with another of the same nominal DE (or MW). Characterization of fundamental structure-property relationships, in terms of Tg′, has been strongly advised before selection of such ingredients for fabricated foods.[8,27]

The Tg′ results for the commercial SHPs in Table 4 have demonstrated exactly the same characteristic Tg vs. $\overline{Mn}$ behavior as described earlier for synthetic amorphous polymers. Tg′ values for this series of SHPs (of polydisperse MWs, in the range from 180 for glucose to about 60,000 for a 360-DP polymer) have demonstrated their classic behavior as a homologous family of amorphous glucose oligomers and polymers.[8,27] The

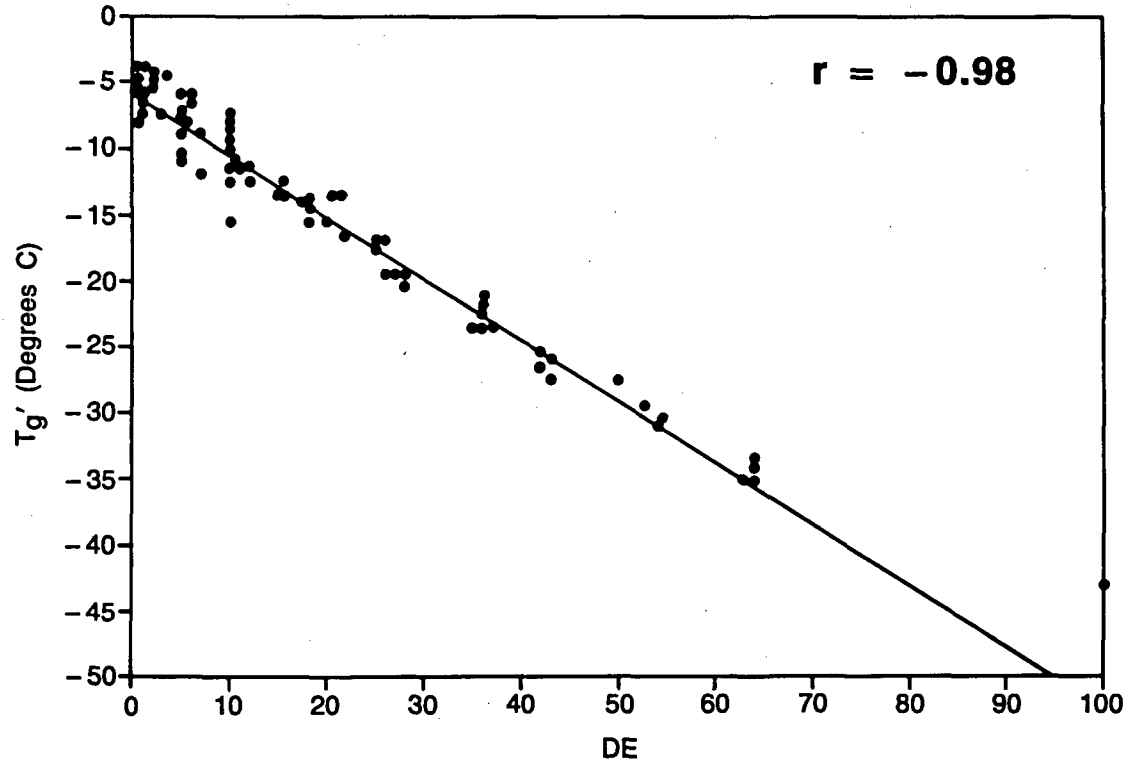

FIGURE 43. Variation of the glass transition temperature, Tg′, for maximally frozen 20 w% solutions against DE value for the commercial SHPs in Table 4. (Adapted from References 8, 32, and 34.)

plot of Tg′ vs. solute $\overline{M}n$ in Figure 44[8,32,34] clearly exhibits the same three-region behavior as shown in Figure 24:[26] (I) the plateau region indicative of the capability for entanglement coupling by high polymeric SHPs of DE $\leq$ 6 and Tg′ $\geq$ −8°C; (II) the intermediate region of non-entangling low polymeric SHPs of 6 < DE < 20; and (III) the steeply rising region of non-entangling, small SHP oligomers of DE > 20. The plot of Tg′ vs. $1/\overline{M}n$ in the inset of Figure 40, with a linear correlation coefficient r = −0.98, demonstrates the theoretically predicted linear relationship for all the SHPs in regions II and III, with DE values >6. The plateau region evident in Figure 44 has identified a lower limit of $\overline{M}n \simeq 3000$ ($\overline{DP}n \simeq 18$) for entanglement leading to viscoelastic network formation[100,197] by such polymeric SHPs in the freeze-concentrated glass formed at Tg′ and Cg′. This $\overline{M}n$ is within the typical range of 1250 to 19000 for minimum entanglement MWs of many pure synthetic amorphous linear high polymers.[112] The corresponding $\overline{DP}n$ of about 18 is within the range of 12 to 30 segmental units in an entangling high polymer chain, thus suggesting that the glucose repeat in the glucan-chain (with a total of 23 atoms/hexose ring) may represent the mobile backbone unit involved in cooperative solute motions at Tg′.[26] The entanglement capability has been suggested to correlate well with various functional attributes (see the labels on the plateau region in Figure 44) of low DE SHPs, including a predicted[8] and subsequently demonstrated[27] ability (see the right-hand column in Table 4) to form thermoreversible, partially crystalline gels from aqueous solution.[211,266-275] It has been suggested[15] that SHP gelation occurs by a mechanism involving crystallization-plus-entanglement in concentrated solutions undercooled to T < Tm, as described in Section III.A.6.

In contrast to the commercial SHPs, the series of quasi-homologous, monodisperse PHCs in Table 3, including the homologous set of maltooligosaccharides up to DP 7, has been found to manifest Tg′ values that fall below the Tg′ limit defined by SHPs for entanglement and the onset

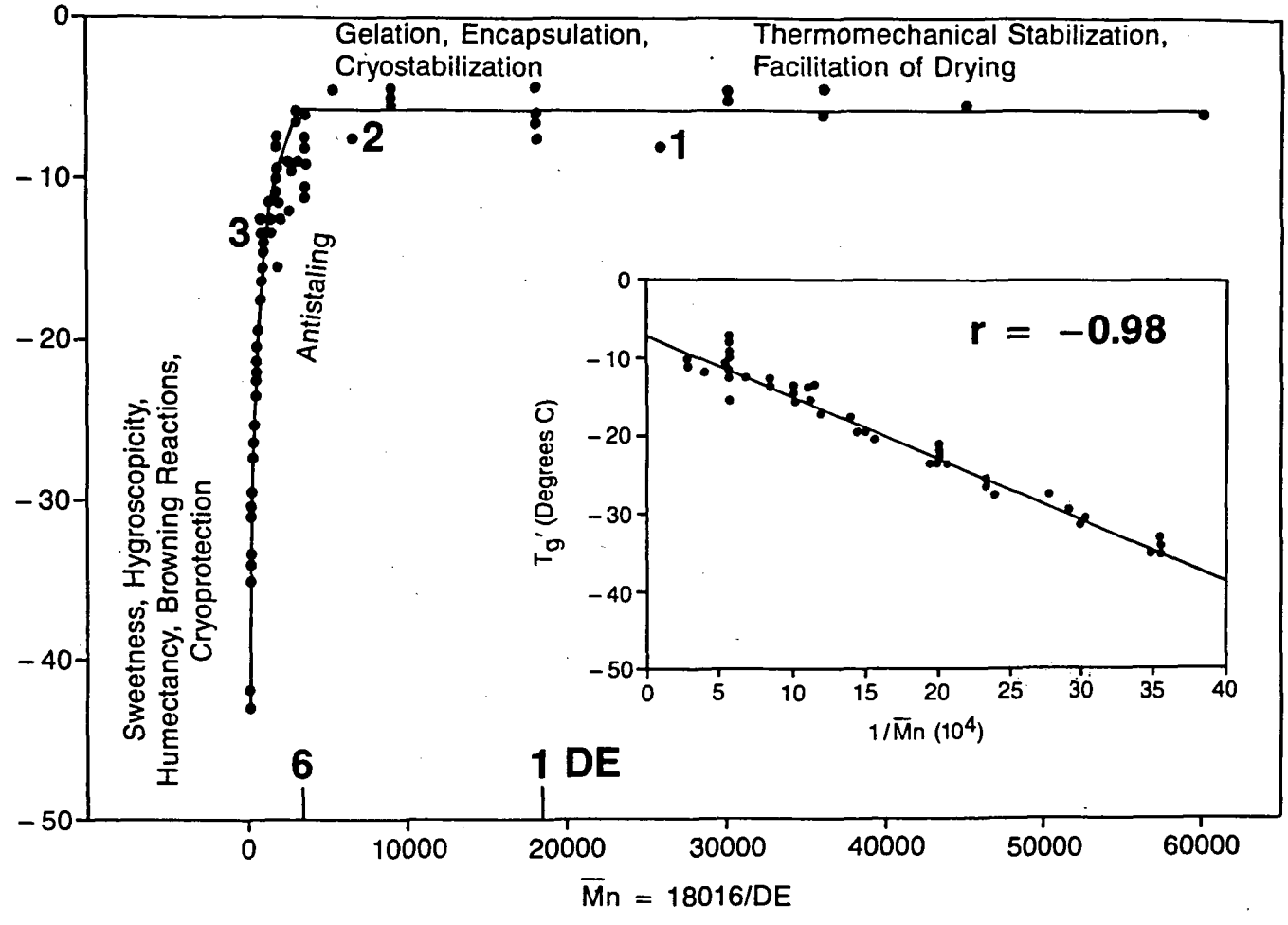

FIGURE 44. Variation of the glass transition temperature, Tg′, for maximally frozen 20 w% solutions against $\overline{M}n$ (expressed as a function of DE) for the commercial SHPs in Table 4. DE values are indicated by numbers marked above x-axis. Areas of specific functional attributes, corresponding to three regions of the diagram, are labeled. (Inset: plot of Tg′ vs. $1/\overline{M}n$ [× 10000] for SHPs with $\overline{M}n$ values below entanglement limit, illustrating the theoretically predicted linear dependence.) (From Levine, H. and Slade, L., *Carbohydr. Polym.*, 6, 213, 1986. With permission.)

of viscoelastic rheological properties and to be incapable of gelling from solution.[27,31] The plot of Tg′ vs. MW in Figure 41, drawn conventionally as a smooth curve through all the points,[113] can easily be visualized to represent two intersecting linear regions (III for MW <300 and II for 300 < MW <1200).[26] From the fair linearity of the Tg′ vs. 1/MW plot for all the data in the inset of Figure 41 (and from the better linearity of the corresponding plot for the series of maltooligosaccharides), it has been concluded that these diverse low MW sugars, polyols, and glycosides show no evidence of entanglement in the freeze-concentrated glass at Tg′. For these PHCs, none larger than a heptamer of MW 1153, the main plot in Figure 41 shows that region I, representing the entanglement plateau where Tg remains constant with increasing MW, has not been reached, in accord with the MW (and corresponding DP) range cited as the lower limit for polymer entanglement.

Tg′, as a physicochemically invariant but kinetically determined and structure-dependent thermal property of glass-forming solutions at subzero temperatures, has thus been used to interpret the thermomechanical behavior of carbohydrate-water systems in non-equilibrium glassy and rubbery states and to explain previously observed but poorly understood aspects of resulting functional behavior in various food ap-

plications.[8,27-34,40-42] It has been demonstrated that insights into structure-function relationships can be gleaned by treating Figure 44 as a predictive map, as indicated by the labeled regions of functional behavior for SHPs.[8,27] Some of the functional attributes of polymeric SHPs that fall on the entanglement plateau have been previously reported,[136] but not quantitatively explained from the theoretical basis of the entanglement capability revealed by DSC studies of Tg′.[8] For example, low DE maltodextrins and other high MW polymeric solutes are well known as drying aids for processes such as freeze-, spray-, and drum-drying.[137,138,254,276] Such polymeric stabilizers raise the observed Tc at a given moisture content, relative to the drying temperature, through their simultaneous effects of increasing the composite Tg′ and reducing the unfrozen water fraction (Wg′) of a system of low MW solids (with respect to freeze-drying)[40,41] or increasing the RVP (for all drying processes).[27] This stabilization of the glassy state facilitates drying without collapse or "melt-back".[28,40-42] By reducing the inherent hygroscopicity of a mixture of amorphous solids being dried, stabilizers such as proteins and polymeric carbohydrates can decrease the propensity of a system to collapse (from the rubbery state) due to plasticization by water.[15] These attributes are illustrated by recent findings on the freeze-drying behavior of beef extract with added dextrin[276] and of horseradish roots.[126] Figure 44 also suggested that maltodextrins to be used for encapsulation of volatile flavor and aroma compounds by freeze-drying (an application requiring superior barrier properties, i.e., relative impermeability to gases and vapors[55]) should be capable of entanglement and network formation ($Tg' \geq -8°C$). It had been reported[136-138] that effectiveness of encapsulation increases with increasing Tc, which increases with increasing $\overline{DP}n$ within a series of SHPs, but "a quantitative relationship between Tc and MW had not been established"[136] previously.

Figure 44 has been used as a guide to choose individual SHPs or mixtures of SHPs and PHCs that provide a particular target value of Tg′ in order to achieve desired complex functional behavior for specific food products.[8,27,31-34] Especially for applications involving such mixtures, data for the PHCs in Figure 41 have been used in combination with Figure 44,[37,38] since the leftmost portion of Figure 41 pertaining to low MW sugars and polyols corresponds to the sweetness/hygroscopicity/humectancy/browning/cryoprotection region of Figure 44. It was postulated that addition of a glass-forming sugar to an encapsulating maltodextrin would promote limited collapse and densification of the entangled network around an absorbed species, but would also decrease the ease of freeze-drying.[8] This postulate appeared consistent with reported results of improved encapsulation of volatiles in dense, amorphous matrices composed of a majority of maltodextrin (4 to 20 DE) plus a minority of mono- or disaccharide glass-former.[277,278]

2. Wg′ Database

As alluded to earlier, the thermograms in Figure 38 have also been used to illustrate some salient facts about Wg′.[8,27,30-34] Wg′ can be estimated from the measured area (enthalpy) under the ice-melting endotherm of the thermogram. By calibration with pure water, this measurement yields the weight of ice in a maximally frozen sample. The difference between the weight of ice and the known weight of total water in an initial solution is the weight of UFW in the glass at Tg′, per unit weight of solute. For a homologous series of 13 corn syrup solids (included among the SHPs listed in Table 4), a plot (not shown here) of Tg′ vs. the corresponding measured value of Wg′ demonstrated that Wg′ decreases with increasing Tg′, with $r = -0.91$.[8] For a larger, but less homologous, group of sugar syrup solids, another plot (not shown here) of Tg′ vs. Wg′ revealed the same trend of decreasing Tg′ (from $-19.5°C$ for a sample of 26 DE corn syrup solids to $-43°C$ for a high-fructose corn syrup (HFCS) 90) with increasing Wg′ (from 0.52 to 1.01 g UFW/g, respectively), with $r = -0.89$.[32] These results showed that as the solute $\overline{M}w$ increases, the fraction of total water unfrozen in the glass at Tg′ decreases and the extent of freeze-concentration increases. This fact is also illustrated by the thermograms in Figure 38. For comparable amounts of total water, the area under the ice-melting peak for the glucose solution is much smaller (i.e., Wg′ much larger) than that for the maltodextrin solution. Again in the context of the

idealized state diagram in Figure 39, these results, and many other experimental Wg′ (and Tg′) values for monomeric and polymeric carbohydrates, have been used to illustrate the general rule:[8,27,30-34] as $\overline{M}w$ of a solute (or mixture of homologous solutes) in an aqueous system increases, the Tg′-Cg′ point moves up the temperature axis toward 0°C and to the right along the composition axis toward 100 w% solute. As discussed in Section IV.C, the critical importance of this fact to the successful "cryostabilization" of frozen, freezer-stored, and freeze-dried foods has been described in the context of the functional behavior of food polymers vis-a-vis Tg′, especially with respect to the capability of inhibiting collapse processes in frozen and freeze-dried foods by formulating a fabricated product with polymeric "cryostabilizers" in order to elevate Tg′ relative to Tf.[8,27,30-34,40,41]

For the PHCs in Table 3, measured Wg′ values range from 1.90 g UFW/g for ethylene glycol to 0.20 to 0.30 g UFW/g for several sugars and polyols, including maltoheptaose. In contrast to the above-described results for a homologous set of glucose monomer and oligomer blends, the Tg′ vs. Wg′ results shown plotted in Figure 45[27] for the diverse PHCs yielded a r value of only −0.64. Thus, when Franks[6] noted that, among the (non-homologous) sugars and polyols most widely used as "water binders" in fabricated foods, "the amount of unfreezable water does not show a simple dependence on MW of the solute", he sounded a necessary caution. In fact, a plot of Wg′ vs. 1/MW for the substances in Table 3 showed an even poorer correlation, with r = 0.47.[27] The obvious conclusion was reached that the plot in Figure 45 could not be used as shown for predictive purposes, so the safest approach would be to rely on measured Wg′ values for each potential ingredient. However, the situation is not as nebulous as suggested by Figure 45. When some of the same data were replotted such that compounds were grouped by chemical class into specific homologous series (i.e., polyols, glucose-only solutes, and fructose- or galactose-containing saccharides), better linear correlations became evident.[15] These plots (shown in Figure 46[15]) illustrated the same linear dependence of Tg′ on the composition of the glass at Tg′ (i.e., as the amount of unfrozen, plasticizing water in the glass decreases, Tg′ increases) as did the data for the series of corn syrup solids. Still, Franks' suggestion[27] that future investigations of the non-equilibrium Tm and viscosity as functions of solute concentration, and the anomalous curvature of the liquidus as a function of solute structure, would be particularly worthwhile, for the most part continues to await experimentation, although Pegg and Arnaud have recently published "equilibrium" liquidus curves for glycerol and propylene glycol, compiled from experimentally measured freezing points for solute concentrations up to 60 w%.[279]

Because the effect of MW on Tg′ and Wg′ has been found to be such a critical aspect of the interpretive and predictive value of the food polymer science data bank,[8,14-39] this effect has been analyzed in detail.[30] As mentioned earlier, for pure synthetic polymers, in the absence of diluent, Tg varies with MW in the characteristic manner illustrated in Figure 24. For a homologous series of amorphous linear polymers, Tg increases with increasing MW, up to the limit of the entanglement plateau, then levels off with further increases in MW. The glass at Tg′ is not that of the pure, undiluted polymer, and so there is no theoretical basis for assuming that this Tg of the freeze-concentrated glass should depend on MW of the dry polymer. However, if the relative shapes of the polymer-diluent glass curves are similar within a polymer series, increases in MW lead to proportional increases in both Tg and Tg′.[30] Thus, as shown in Figures 41 and 44 for two extensive series of carbohydrates, the linear relationship between Tg and inverse MW of the solute does apply to the characteristic Tg′ of the solute-UFW glass. For the homologous series of commercial, polydisperse glucose oligomers and high polymers derived from starch, with $\overline{M}n$ values from 180 for glucose itself to about 60,000 for a 360 $\overline{DP}n$ polymer, Tg′ increased with decreasing inverse $\overline{M}n$ (with a linear correlation coefficient r = −0.98), up to a plateau limit for entanglement at $\overline{DP}n \simeq 18$ and $\overline{M}n \simeq 3000$. For the non-homologous series of small, monodisperse PHCs with known MWs in the range 62 to 1153, including many different sugars, polyols, and glycoside derivatives, Tg′

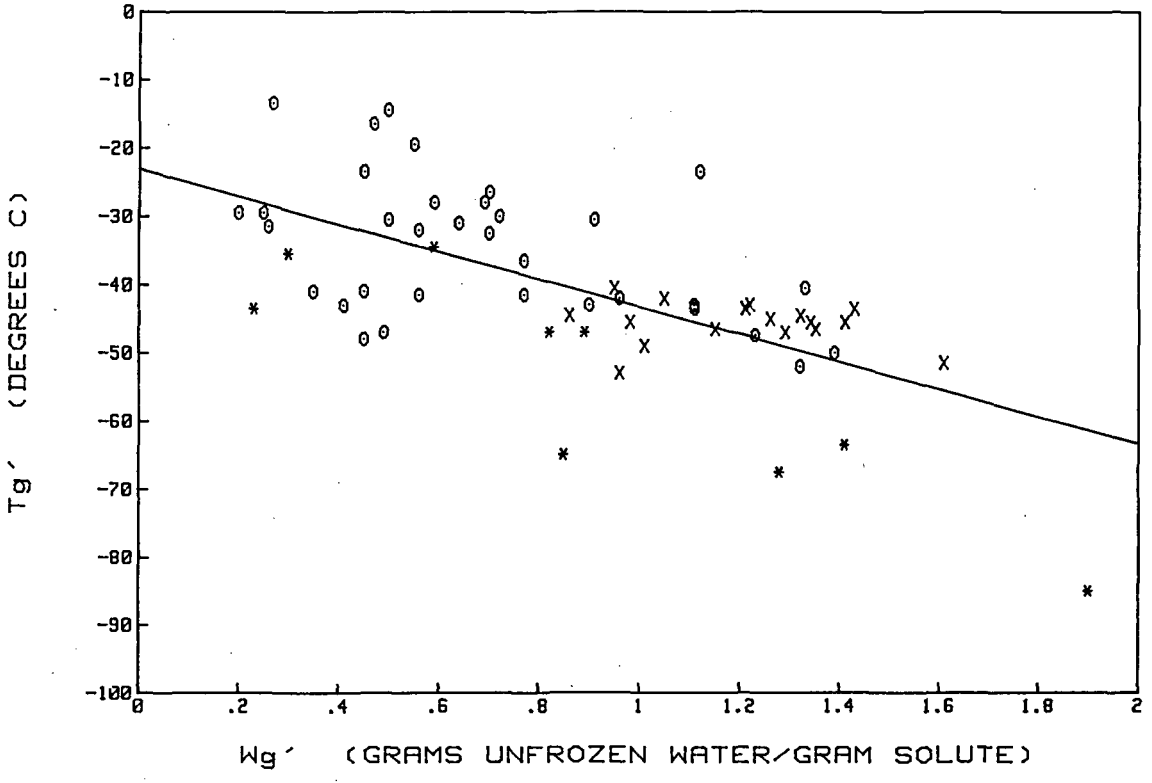

FIGURE 45. Variation of the glass transition temperature, Tg′, for maximally frozen 20 w% solutions against Wg′, the composition of the glass at Tg′, in g unfrozen water/g solute, for the sugars (o), glycosides (x), and polyols (⋆) in Table 3. (From Levine, H. and Slade, L., *Food Structure — Its Creation and Evaluation,* Mitchell, J. R. and Blanshard, J. M. V., Eds., Butterworths, London, 1988, 149. With permission.)

also increased linearly with decreasing inverse MW ($r = -0.934$), but the entanglement plateau was not reached.

For these small PHCs of known MW (see Table 3), the actual $\overline{M}w$ and $\overline{M}n$ of the homogeneous solute-water mixture in the glass at Tg′ were calculated from the corresponding Wg′ values in Table 2 (converted from g UFW/g solute to w% water).[30] The results were plotted as Tg′ vs. $1/\overline{M}n$ and Tg′ vs. $1/\overline{M}w$ in Figures 47A and 47B,[30] respectively. Figure 47A shows the poor linear correlation ($r = -0.71$) with $\overline{M}n$, which might be expected, because while Tg does vary with free volume of the solution, free volume is most effective as a determinant of Tg when it varies with $1/\overline{M}n$ of the *solute*, due to the effect of the number of its molecular chain ends.[107] In contrast, Figure 47B shows the much better linear correlation ($r = -0.95$) of Tg′ with $\overline{M}w$ of the aqueous PHC glass, a result that also supported a conclusion that Tg′ and Wg′ are not independent parameters of the mobility transformation.[30] Within the larger series of non-homologous PHCs in Table 3, the single homologous family of glucose and its linear malto-oligomers up to DP 7 showed (Figure 42 inset) an excellent linear correlation ($r = -0.99$) between Tg′ and inverse MW of the dry sugar. Again, the relationship between Tg′ and the actual $\overline{M}w$ and $\overline{M}n$ of the aqueous glass was examined by comparing plots of Tg′ vs. $1/\overline{M}n$ (Figure 47C) and Tg′ vs. $1/\overline{M}w$ (Figure 47D).[30] These results showed even more clearly than those in Figures 47A and B that there is no correlation between Tg′ and $\overline{M}n$ ($r = -0.20$), but a very good correlation ($r = -0.985$) between Tg′ and $\overline{M}w$.

The importance of this finding relates to the concept of the glass transition as an iso-relaxation state.[30,107] The molecular Tg is not related to *macroscopic* viscosity, and the origin of the temperature location of the molecular glass transition is not based on an iso-macroscopic viscosity state.[107]

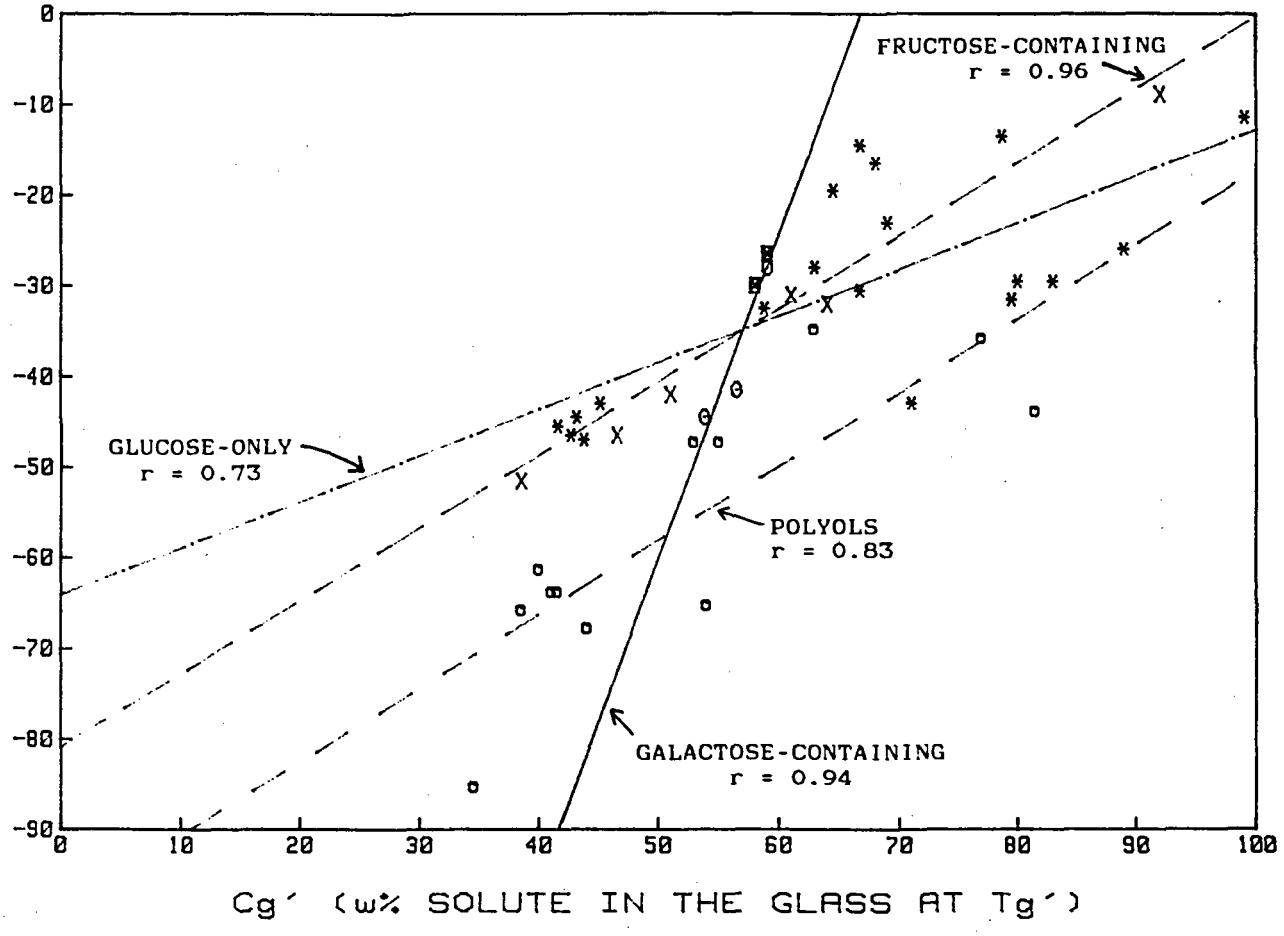

FIGURE 46. Variation of the glass transition temperature, Tg', for maximally frozen 20 w% solutions against Cg', the composition of the glass at Tg', in weight percent solute, for homologous series of polyhydric alcohols (o), glucose-only solutes (*), fructose- (x), and galactose-containing saccharides (O) in Table 3. (From Levine, H. and Slade, L., *Water Science Reviews*, Vol. 3, Franks, F., Ed., Cambridge University Press, Cambridge, 1988, 79. With permission.)

Moreover, the location of Tg is not based simply on either an iso-free volume or an iso-local viscosity state alone.[107] For MWs below the entanglement limit (e.g., ≃3000 for α-1 − >4 glucan oligomers), the temperature location of the molecular glass transition depends on the instantaneous average relaxation time compared to the experimental time frame. The operational relaxation time is an instantaneous property, because it depends on the instantaneous values of free volume and local viscosity. Free volume is associated with inverse $\overline{M}n$, rotational relaxation times, high average MWs, and low values of Tm/Tg ratio. Local viscosity is associated with $\overline{M}w$, translational relaxation times, low average MWs (e.g., small PHCs), and high values of Tm/Tg ratio.[30] (In contrast to the molecular glass transition, for MWs above the entanglement limit, the network Tg does involve macroscopic viscosity.[107]) The insight derived from these results led to the new suggestion[30] that different portions of the glass curve must be controlled by different parameters that determine molecular-level mobility, i.e., Tg is controlled by free volume (a function of inverse $\overline{M}n$) rather than local viscosity at higher values of average MW (i.e., higher solute concentrations in the glass, Cg), but by local viscosity (a function of $\overline{M}w$) rather than free volume at lower values of average MW (i.e., higher water concentrations in the glass, Wg).

The value of Tg' appears to reflect the hydrodynamic volume, in the glass, of the mobile "cluster entity"[89] represented by a solute molecule and its complement of unfrozen water mol-

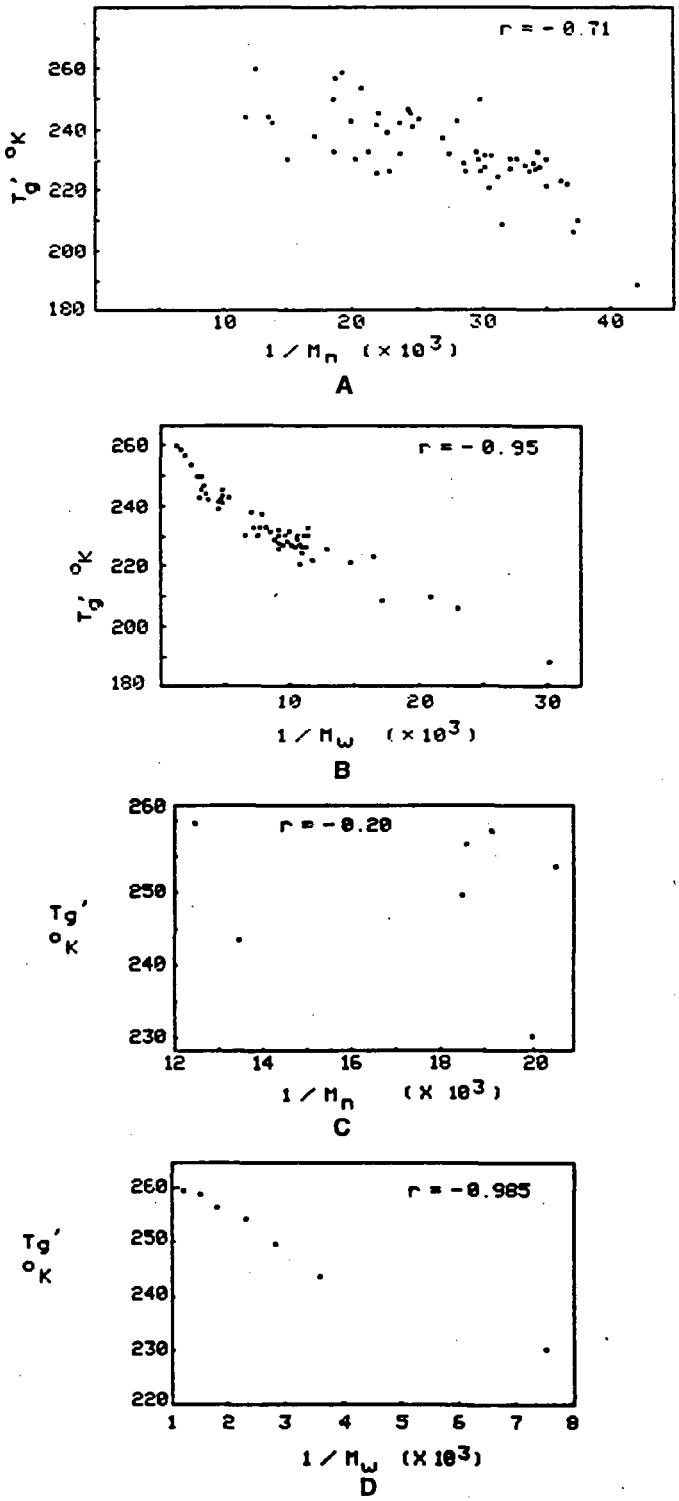

FIGURE 47. The variation of Tg′ with (A) inverse $\overline{Mn}$ and (B) inverse $\overline{Mw}$ calculated from Wg′ for the small carbohydrates listed in Table 3, and with (C) inverse Mn and (D) inverse Mw calculated from Wg′ for the homologous series of malto-oligosaccharides, from glucose through maltoheptaose, listed in Table 3. (From Slade, L. and Levine, H., *Pure Appl. Chem.*, 60, 1841, 1988. With permission.)

ecules, rather than a property of the isolated solute.[30] We have considered the question of whether it would be preferable to correlate Tg′ with partial molar volume (V°) rather than MW of dry solute,[31] since V°, like intrinsic viscosity, gives an indication of the effective solute size in solution. Just as free volume is related to inverse MW of monodisperse solutes (or inverse $\overline{M}n$ for polydisperse solutes) in the limit of zero dilution,[107] free volume should be related to inverse V° for comparison of conformational homologs of different MW in the limit of infinite dilution. But, of course, it is for comparison of different conformers of the same MW that we look for an advantage in the use of V° to replace MW. Unfortunately, while MW values are exact, an approach based on V° is not straightforward.[31]

Despite a relative wealth of V° data,[280] differences in the values for isomeric sugars are sufficiently small to discourage their use to interpret the influence of conformation on hydration[281] and may lie within the range of values reported by different research groups for a single sugar, in part due to differences in anomeric ratios.[282] If this complication is removed by comparison of methyl pyranosides, larger values of V° are observed for conformers with equatorial rather than axial OCH_3 substituents.[282] Similarly, for comparison of conformers at C4, contributions to apparent molar volumes are said to be greater for equatorial than for axial hydroxyls.[283] Yet, the general observation, for PHCs compared to their apolar structural analogs, is that hydroxyl groups are effectively invisible to limiting density measurements.[281,282] The greater contribution of certain equatorial hydroxyl groups to V° is attributed to greater spatial and orientational compatibility with the preexisting liquid water structure,[282] i.e., greater effective "specific hydration". Data for a few of the same sugars show that intrinsic viscosity increases with both contributions (MW and "specific hydration") to increasing V°.[284] We might expect, from this slim evidence, that both contributions to increased V° would also lead to increased Tg′.[31] However, there still remain the questions of temperature and concentration dependence of apparent molar volumes of PHCs.

Systematic extrapolation of V° data to subzero temperatures of interest for correlation with Tg′ is hindered by the paucity of data for mean limiting apparent molar expansibilities. Based on two relevant cases for which data are available,[282] such extrapolations would magnify differences in behavior predicted from measurements made near room temperature. The concentration dependence of apparent molar volumes is more questionable. As mentioned earlier, one of the most important, but often overlooked, aspects of the glass transition is its cooperative nature.[106] Upon slow cooling, the glass at Tg′, with solute-specific composition Wg′, represents the greatest dilution that retains this maximally cooperative behavior.[30] Cooperativity is maximum at the glass transition (where arrestation of large-scale molecular mobility occurs without change in structure), but decreases with increasing temperature or dilution above Tg (where retardation of mobility occurs and shows a WLF-type temperature dependence).[106,107] Of the two extremes, behavior in the limit of zero dilution is less remote from that of the cooperative system than is behavior in the limit of infinite dilution.[31] Apparent molar volumes of PHCs in aqueous solution have been shown to be characteristically (in contrast to apolar solutes) independent of concentration,[282] yet reported differences between apparent molar volumes for 3 and 10 w% solutions of a single sugar approach the greatest differences seen between equatorial vs. axial conformers at a single concentration.[283] There exists the possibility that a decrease in apparent molar volume upon extrapolation toward Tg′ and an increase upon extrapolation toward Cg′ might counterbalance.[31] Despite these issues, the subject is of sufficient interest to merit further exploration.

Wg′ results for the series of monomeric alkyl glycosides in Table 3 have been described[27,34] in terms of a possible relationship between the glycoside structure (e.g., position and size of the hydrophobic aglycone, which is absent in the parent sugar) and its function reflected by Wg′. Wg′ values for all methyl, ethyl, and propyl derivatives are much larger than those for the corresponding parent monosaccharides. However, Wg′ values appear consistently to be maximized for methyl or ethyl derivatives, and somewhat lower for the *n*-propyl derivatives. (In a related vein, Fahy et al.[251] have recently reported that methylation significantly enhances the glass-

forming tendency [i.e., potential for complete vitrification] of concentrated aqueous solutions of various polyols and other biological cryoprotectants.) It has been suggested that increasing hydrophobicity (of the aglycone) leads to both decreasing Wg′ and the demonstrated tendency toward increasing insolubility of propyl and larger glycosides in water.[27] The combined effects of several related mechanistic contributions almost obscure the underlying basis for this behavior. The predominant role of the methyl group provides the clue to the overall mechanism,[34] i.e., the phenomenon of "internal plasticization", by which the desired properties of depressed Tg and increased free volume and segmental mobility are achieved by incorporating them into the polymer itself, rather than by addition of exogenous plasticizer.[109] Internal plasticization to increase mobility of the polymer backbone can be achieved by branching. Additional free volume is provided by the motion of side chains, with greater contributions from chain ends associated with shorter side chains.[109] The traditional example of internal plasticization by side chains from synthetic polymer science, the poly(*n*-alkyl methacrylates),[109] mirrors the behavior of the alkyl glycosides of Table 3.[34] A monotonic depression of Tg is observed with increasing alkyl chain length, but the methyl group is most effective, and longer chains are progressively less effective. For the alkyl glycosides, internal plasticization is observed both directly, as depression of Tg′, and indirectly, as increase in Wg′. Although internal plasticization, by covalent attachment of the plasticizer to the polymer, serves to increase efficiency by retarding loss of plasticizer upon crystallization, long alkyl side chains eventually associate as seen for propyl side chains in the alkyl glycosides and for longer alkanes in high polymers.[105]

It has been demonstrated[34] that Wg′ values determined by the DSC method mentioned above are generally in good agreement with literature ranges for the so-called "water binding capacity (WBC)" values (determined by various methods other than DSC) of many different food ingredients, even though the spread of reported values for individual materials has often been considerable.[25,57] The latter fact is not surprising in view of experimental difficulties imposed by the kinetic constraints of the water-immobilization process and the wide variation in time frames (differing by orders of magnitude) for measurements of such relaxation processes.[167] Not surprising either is the consequent lack of reproducibility in, as well as frequent disagreement among, many types of "WBC" measurements,[34] including DSC. The dependence of the value of Wg′ on the specific time frame of the DSC measurement has been illustrated by a study of hydrated lysozyme glasses recently reported by Wolanczyk and Baust.[285] These workers have noted that the measured amount of unfrozen water decreases with increasing sub-ambient hold time (from 0 min to 24 h between cooling and subsequent rewarming) and decreasing sub-ambient hold temperature (from −50 to −150°C).

Ordinarily, one does not claim an accuracy of better than about 10% for DSC measurements of Wg′,[34] although some exceptionally precise studies have been reported.[163-166] Franks[149] has presented a comparison of experimental data from DSC, NMR, and dielectric relaxation measurements on concentrated solutions of several common small sugars, which summarizes the state of affairs. DSC results for unfrozen water at Tg′, expressed as a "notional hydration number" (explained earlier), were 3.7 for glucose and xylose, 3.5 for mannose, and 5.0 for maltose, with standard deviations of 12 to 20%. These "hydration numbers" were in surprisingly good agreement with NMR and dielectric relaxation results of 3.7 for glucose, 3.9 for mannose, and 5.0 for maltose. In comparison to the above DSC results, the Wg′ values shown in Table 3 correspond to calculated values of 4.1 for glucose, 3.7 for xylose, 3.5 for mannose, and 4.8 for maltose, in all cases within 11%[34] of the values reported by Franks.[149]

The method we advocate for determining Wg′,[8,27] i.e., from DSC measurements on a single maximally freeze-concentrated aqueous solution of 20 w% initial solute concentration, is not the only DSC method one can use to determine this technologically important quantity. Other workers[253,257,286,287] have recommended an "extrapolation method" for estimation of the limiting UFW content of a solute. In that method, a series of solutions covering a wide range of solute concentrations is analyzed, and the measured ice-melting peak areas (which decrease with

increasing solute concentration) are extrapolated to the solute concentration corresponding to zero peak area, i.e., the concentration that would allow no ice to form on slow cooling or rewarming, because all the water present in the solution would be "unfreezable" in the experimental time frame. In comparing results from the method we favor with those from the extrapolation method, and using sucrose as a common example, the following points are noteworthy. While we have reported a Cg′ value for sucrose of 64.1 w%,[27] as measured for a 20 w% sucrose solution (with a Tg′ of −32°C), Izzard et al.[287] have more recently reported Cg′ values for 2.6, 10.7, 20.2, 40.0, 60.1, and 65.8 w% (i.e., C > Ce) sucrose solutions of 35.1, 61.9, 63.9 (very close to our value), 71.7, 75.8, and 77.7 w% sucrose, respectively. Izzard et al.[287] have extrapolated their data to a limiting Cg′ value of ~80 w% sucrose (and a corresponding Tg′ value of ~−35°C), which they claim to be the *correct* Cg′ for sucrose, while they claim that our value (which is 20% different from theirs) "is clearly incorrect". After considering the discussion below, the reader will have to decide if there is such a thing as a "right" or "wrong" answer for Cg′, as Izzard et al.[287] claim.

Obviously, the extrapolation method is much more time-consuming than the one-solution, constant-concentration method, and this aspect represents a practical disadvantage. Moreover, the 20 w% solute concentration that we use in determining Wg′ (and Tg′) for PHCs has greater technological relevance to, for example, the total saccharides content in many frozen desserts and related products than do other much higher or much lower solute concentrations. In rationalizing its disadvantages, advocates of the extrapolation method have, as mentioned above, claimed it to be more accurate than alternative one-point measurements of Wg′.[257,287] However, it has been recently pointed out,[39] and illustrated with the particular case of the galactose-water system reported by Blond,[257] that the extrapolation method is *invalidated* in every case in which solute or hydrate crystallization during the DSC measurements (which would be favored by higher solute concentrations and might or might not be revealed by separate or multimodal melting peaks during warming) cannot be ruled out explicitly. In other words, whenever one cannot be certain that the so-called "ice-melting" peak represents only the melting of crystalline ice and not crystalline solute (i.e., eutectic melting) or crystalline hydrate, the potential accuracy of the extrapolation method is obviated.

The foundation for understanding the behavior of the galactose-water system, and others like it that are subject to solute or hydrate crystallization, has been provided by Forsyth and MacFarlane:[260] "The phase behaviour of a number of solutions of possible interest in cryopreservation as a function of solute concentration has been investigated by thermal analysis techniques with three regions being identifiable[288]

1. Solutions of low solute concentration (e.g., 20 w%, for most small PHCs) that supercool below their equilibrium melting temperature but eventually freeze on sufficient cooling
2. Intermediate concentration regions where the solution will vitrify (i.e., become glassy) on rapid cooling; however, on rewarming devitrification (i.e., crystallization) will take place at some temperature Td
3. High solute concentration where the sample becomes vitreous on cooling and does not easily crystallize ice on warming, but may crystallize a hydrate"

In this context of the distinctive behavior observed for the three regions of concentration identified by the investigations of Angell and coworkers,[260,288] the extrapolation method for the estimation of UFW content (by extrapolation to zero of the measured total heat of melting of unidentified species after cooling and rewarming of solutions with a wide range of initial concentrations, spanning the three behavioral regions) is *invalidated in principle* (regardless of whether the melting enthalpy of crystalline solute or hydrate can be deconvoluted from the overall heat of melting). For each of the three kinetically distinctive regions of concentration, pertinent cooling and heating rates would have to be used, corresponding to the critically different time scales of the relaxation behavior in the three concentration regimes. This is *not* routinely done by practitioners of the extrapolation

method.[253,257,286,287] In accordance with the concentration regimes defined by Angell and coworkers,[260,288] initial concentrations of galactose below 50 w% represent region (1), and their time scale for crystallization of ice would be shorter than the times involved in a typical experimental DSC procedure (e.g., cooling and heating at 10°C/min).[257] Initial concentrations of galactose between 50 and 65 w% fall in region (2), and their time scale for crystallization of ice would coincide with the typical experimental time scale. Initial concentrations above 65 w% fall in region (3), and their time scale for nucleation and crystallization of ice would be much *longer* than the typical experimental time scale. Even after depression of the operative solute concentration to <50 w%, due to previous crystallization of beta-galactose or monohydrate, the homogeneous ice nucleation curve would approach the galactose-water glass curve, and ice nucleation would be avoided (as is concluded from the experimental observation[257] that no ice melts during rewarming), as predicted by Angell et al.[288] In summary, solutions of region (1) analyzed at subzero temperatures approach equilibrium behavior sufficiently to be sometimes mistaken[257] for "equilibrium states". Solutions of region (2) are sufficiently far from equilibrium to be recognized as such.[257] Solutions of region (3) are so far from equilibrium[172] that their non-equilibrium status is not evident. Systems in this deceptive status, which appears to be a "steady state", because relaxation times greatly exceed typical experimental time scales,[172] are often mistaken for "equilibrium states". One consequence of the complexity of this situation and the kinetic constraints imposed on it is the obviation of the utility and validity of the extrapolation method of determining Wg′, especially when that method is routinely practiced using constant cooling and heating rates for DSC analysis of all solution concentrations.[253,257,286,287]

In contrast to the invalidity of the extrapolation method of determining Wg′, particularly with respect to crystallizable solutes such as galactose, glucose, and sucrose, ambiguity can be minimized through the use of the one-point method of determining Wg′ for the construction of glass curves.[32] By the selection of (1) solutes that avoid solute, eutectic, or hydrate crystallization; (2) an initial solute concentration in region (1) for characterization of aqueous glasses; and (3) diluent-free solute to characterize glasses with concentration greater than Cg′, reliable values of Wg′ and corresponding glass curves can be determined.[30,39] Poly(vinyl pyrrolidone) is justly popular as a model solute for aqueous-glass systems.[4,32,242] Selection of 20 w% solute as the standard initial solution concentration ensures reproducible freeze-concentration to the technologically relevant composition at Tg′-Cg′,[32] especially for solutes such as galactose, glucose, sucrose, and fructose, which would be much more prone to solute crystallization (e.g., eutectic formation) or hydrate crystallization from much more concentrated solutions.[4]

As another part of an experimental approach to understanding "water dynamics" in intermediate-moisture carbohydrate systems, the basis for a relationship between Wg′ and apparent RVP has been investigated.[15,16] RVP (rather than "Aw") is generally assumed to be an indicator of "free water" content in such intermediate-moisture systems at room temperature,[75,76] while Wg′ (rather than "WBC") is properly described as a measure of their unfrozen water content. Both parameters represent behavioral (functional) manifestations of the constrained mobility of water in aqueous carbohydrate glasses and supra-glassy fluids.[30] The study involved a quasi-homologous series of sugar syrup solids from commercial high-fructose corn, ordinary corn, sucrose, and invert syrups, all of which are commonly used ingredients in IMF products. This was the same series mentioned earlier, which showed a linear correlation ($r = -0.89$) between decreasing Tg′ and increasing Wg′. RVP was measured for a series of solutions with 67.2 w% solids content after 9 d "equilibration" at 30°C and plotted against Wg′ for maximally frozen 20 w% solutions of the same solids. The plot (shown in Figure 48[16]), with RVP values in the range 0.78 to 0.98 and Wg′ values in the range 0.52 to 1.01 g UFW/g solute (corresponding Tg′ values in the range −19.5 to −43°C), produced a linear correlation coefficient $r = -0.71$ for the relationship between decreasing content of UFW in the glass at Tg′ and increasing RVP in the corresponding supra-glassy solution some 50 to 70°C above the Tg′ reference state. The scatter

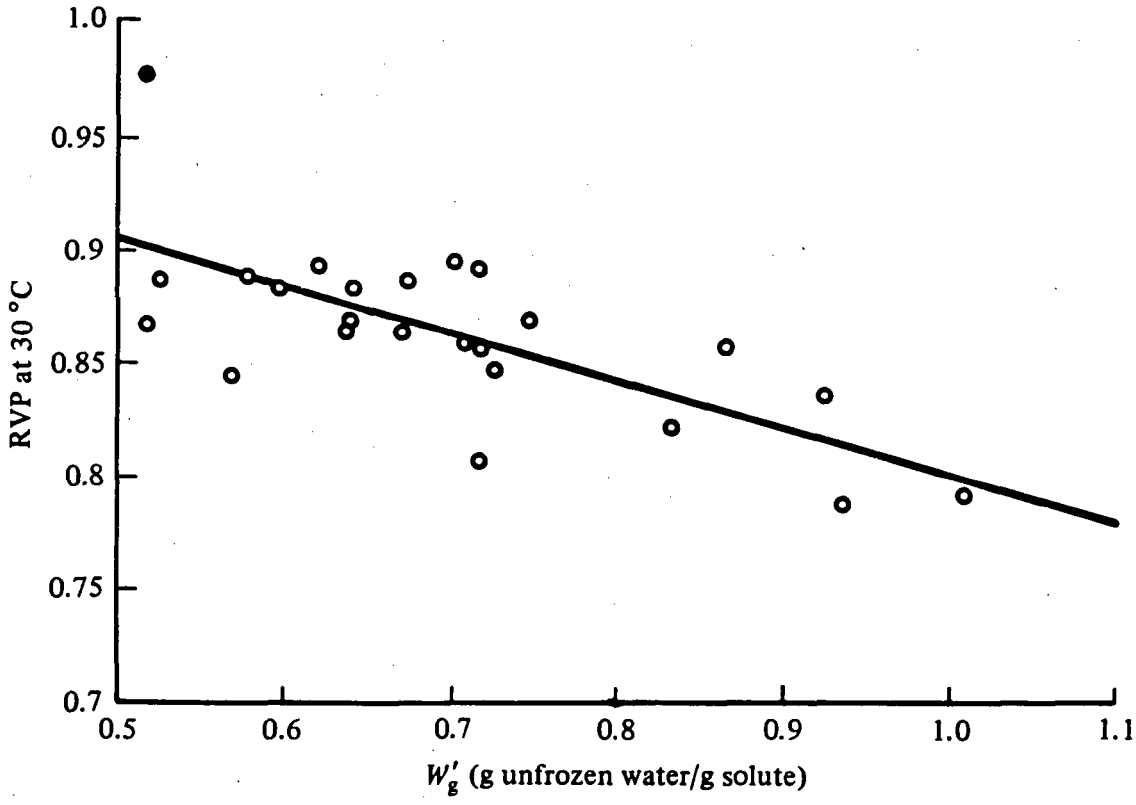

FIGURE 48. Variation of relative vapor pressure (measured for 67.2 w% solutions of various corn, sucrose, and invert syrup solids, after 9 d at 30°C) against Wg′, the composition of the glass at Tg′, in g unfrozen water/g solute, for maximally frozen 20 w% solutions of the same syrup solids. (From Slade, L. and Levine, H., *Food Structure — Its Creation and Evaluation,* Mitchell, J. R. and Blanshard, J. M. V., Eds., Butterworths, London, 1988, 115. With permission.)

in the data prohibited further insight into the question of water mobility in such systems. This was not unexpected, since many of the samples represented heterogeneous, polydisperse mixtures of polymeric carbohydrate solutes of unknown $\overline{M}w$ and MW distribution. While this study would be worth repeating with a homologous series of small monodisperse PHCs, the mold spore germination study described in Section II.A.3 was concluded to be a more definitive and revealing experimental approach to the issue of system mobility (especially at low moisture contents, i.e., W < 30 w% water, exemplifying a situation of W ≲ Wg for typical glass-forming PHCs) and eventual water "availability" (especially at high moisture contents, i.e., W ≳ 70 w% water, exemplifying a situation of W ≫ Wg, likewise for typical glass-forming PHCs).[30]

3. Dry Tg, Dry Tm, and Tm/Tg Ratio

As explained earlier, if the relative shapes of the polymer-diluent glass curves are similar within a polymer series, increases in MW (of the diluent-free polymer) lead to proportional increases in both Tg and Tg′.[30] This fact has been demonstrated recently by the aqueous glass curves for maltose, maltotriose, and maltohexaose published by Orford et al.,[59] coupled with the Tg′-Wg′ values for these oligosaccharides from Table 3, as illustrated in Figure 49. Prior to this confirmation, it had been assumed that a plot of Tg vs. MW for dry PHCs or SHPs would reflect the same fundamental behavior as that of Tg′ vs. solute MW shown in Figures 41, 42, and 44.[28] Earlier evidence supporting this assumption had been provided by To and Flink,[136] who reported

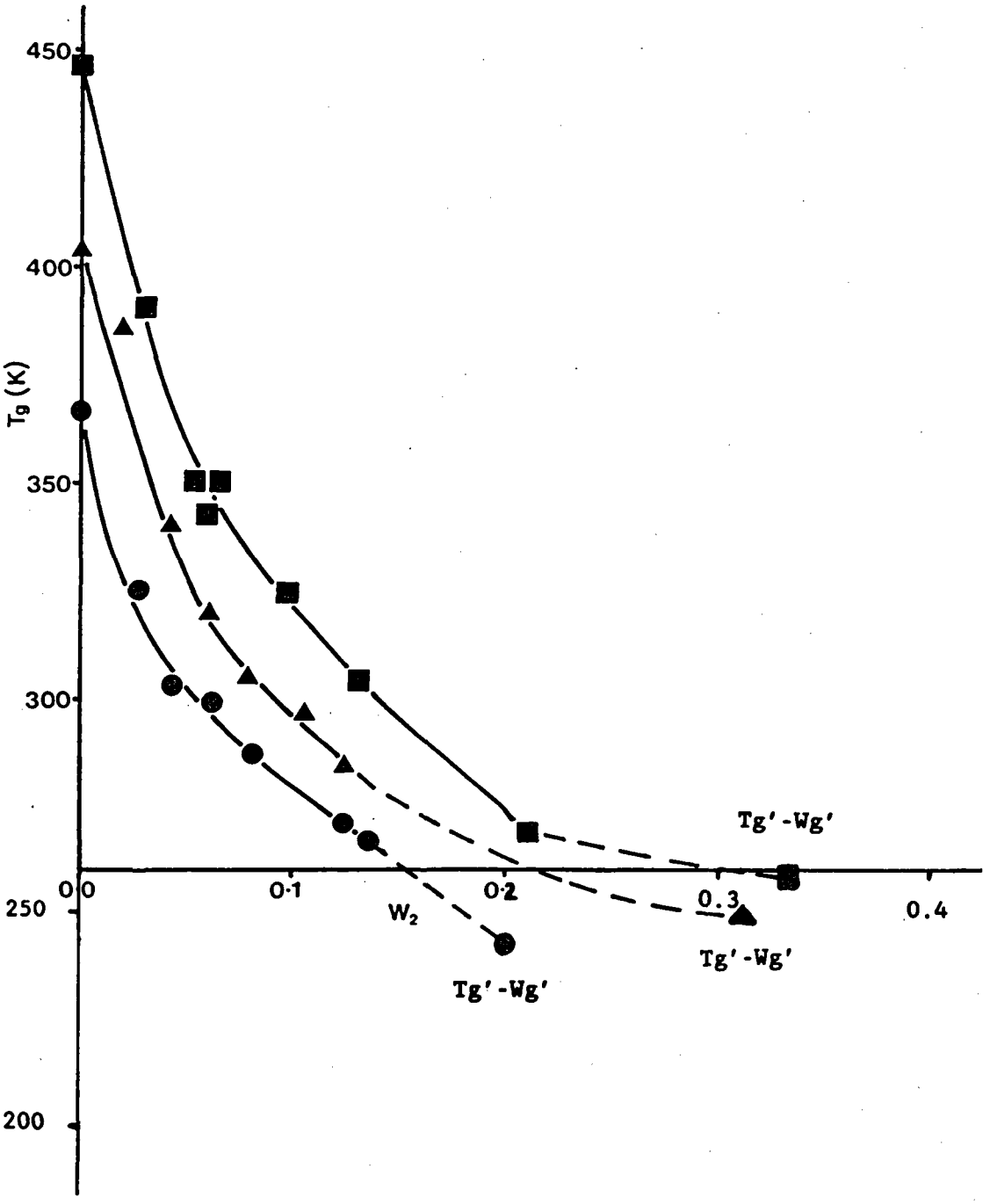

FIGURE 49. Graph of glass transition temperature (Tg) vs. mass fraction (w_2) of water for maltose (solid circles); maltotriose (solid triangles); and maltohexaose (solid squares). Reproduced, with permission, from Reference 59. The solid-line curves from Reference 59 are extrapolated (dashed lines) to the appropriate Tg′-Wg′ points (from Table 3) for these saccharides.

a plot of Tc vs. DP for a series of low-moisture, fractionated SHP oligomers of $2 \leq DP \leq 16$ (i.e., non-entangling),[8] similar in shape to the plot of Tg′ vs. MW for the non-entangling PHCs in Figure 41. It had been pointed out that Tc for low-moisture SHPs, which increases monotonically with increasing DP, represents a good quantitative approximation of dry Tg.[8] The basic as-

sumption was verified for the homologous series of glucose and its pure malto-oligomers of DP 2 to 7 in Table 3, as illustrated in Figure 50.[28] The plot of Tg vs. MW in Figure 50A showed that dry Tg increases monotonically with increasing MW of the monodisperse sugar, from Tg = 31°C for glucose (in good agreement with several other published values,[59,89,176] as shown in Table 5) to Tg = 138.5°C for maltoheptaose.[28] The plot in Figure 50A showed the same qualitative curvature (and absence of an entanglement plateau) as the corresponding Tg′ plot in Figure 42, and the plot of dry Tg vs. 1/MW in Figure 50B showed the same linearity and r value as the corresponding Tg′ plot in the inset of Figure 42. (The results shown in Figure 50A were subsequently corroborated by Orford et al.,[59] who recently reported a similar curve of dry Tg vs. DP for glucose and its malto-oligomers of DP 2 to 6.) Further verification of the assumption was demonstrated by a plot (shown in Figure 51[28]) of Tg vs. w% composition for a series of spray-dried, low-moisture powders (about 2 w% water) prepared from solution blends of commercial SHPs, Lodex 10 and Maltrin M365. This plot showed that Tg increases from 58°C for Maltrin M365 (36 DE, Tg′ = −22.5°C) to 121°C for Lodex 10 (11 DE, Tg′ = −11.5°C) for these SHPs at about 2 w% moisture. Here again, the characteristic monotonic increase of Tg with $\overline{M}w$ (≡ increasing composition as w% Lodex 10) and curvature expected and theoretically predicted for homologous (mixtures of) oligomers with $\overline{M}w$ values below the entanglement plateau limit were evident.

The glass curves (solid lines)[59] in Figure 49 for the three malto-oligosaccharides at low moistures (i.e., W < Wg′) are also noteworthy for their similarity to the glass curves shown earlier for starch (Figure 25), hemicellulose, sorbitol (Figure 27), elastin (Figure 19A), and gluten (Figure 26). At moisture contents ≤10 w%, maltose, maltotriose, and maltohexaose manifest extents of plasticization of about 9, 11, and 12.5°C/w% water, respectively,[59] values typical of many other water-compatible food oligomers and high polymers.[15,42,66] We have added the dashed portions to the solid lines in Figure 49 to show that the measured glass curves of Orford et al.[59] can be extrapolated, as expected, to the corresponding measured Tg′-Wg′ points (Table 3) on these state diagrams, at least in the cases of maltose and maltotriose. At moisture contents >Wg′, the Tg curves (for quench-cooled solute-water blends) would be expected to continue to extrapolate smoothly, but with more gradual curvature, to the Tg at about −135°C for pure amorphous solid water.

As mentioned earlier, beneath the generic approximation of $\eta g \simeq 10^{12}$ Pa s at Tg cited for many glass-forming synthetic polymers,[106,107] there are underlying distinguishing features, so that the glass transition is not rigorously a *universal* iso-viscosity state.[30,107] Were it so, in order for the glass transition to be both an iso-viscosity state and, as defined by the WLF equation, an iso-free volume state, all glass-forming liquids would have the same local viscosity at any given ΔT above Tg, to the extent that the WLF coefficients C1 and C2 are "universal" values.[107] The absolute viscosity of a glass at its Tg depends on the nature of the particular solute (e.g., its Tm/Tg ratio)[30] and plasticizer in question, and is thought to vary within the range 10^{10} to 10^{14} Pa s.[30,89,172,289] However, despite these qualifications, the concept that the glass curve of Tg vs. w% composition, for a particular solute-diluent system, reflects an iso-viscosity state for that system remains a valid and useful approximation.[189] Accordingly, all points along the glass curve (i.e., all compositionally dependent Tg values) for a given solute-diluent system represent glasses of approximately the same local viscosity at their Tg. Thus, for a particular glass-forming carbohydrate solute (of MW below the entanglement limit), the viscosity at Tg of the dry glass and at Tg′ of the maximally freeze-concentrated aqueous glass are approximately the same.[40-42] This point represents an important conceptualization related to food quality and safety. For example, for glucose and the malto-oligosaccharides through DP 7 shown in Figures 42 and 50, the corresponding glasses existing at the dry Tg and at Tg′-Wg′, although separated by temperature differentials of from 74°C for glucose to 152°C for maltoheptaose, have approximately the same viscosities. While this situation is also subject to qualification by the earlier-mentioned (1) fact that the temperature location of Tg is not based solely on either an iso-viscosity or iso-free volume state alone;[107] (2) suggestion that

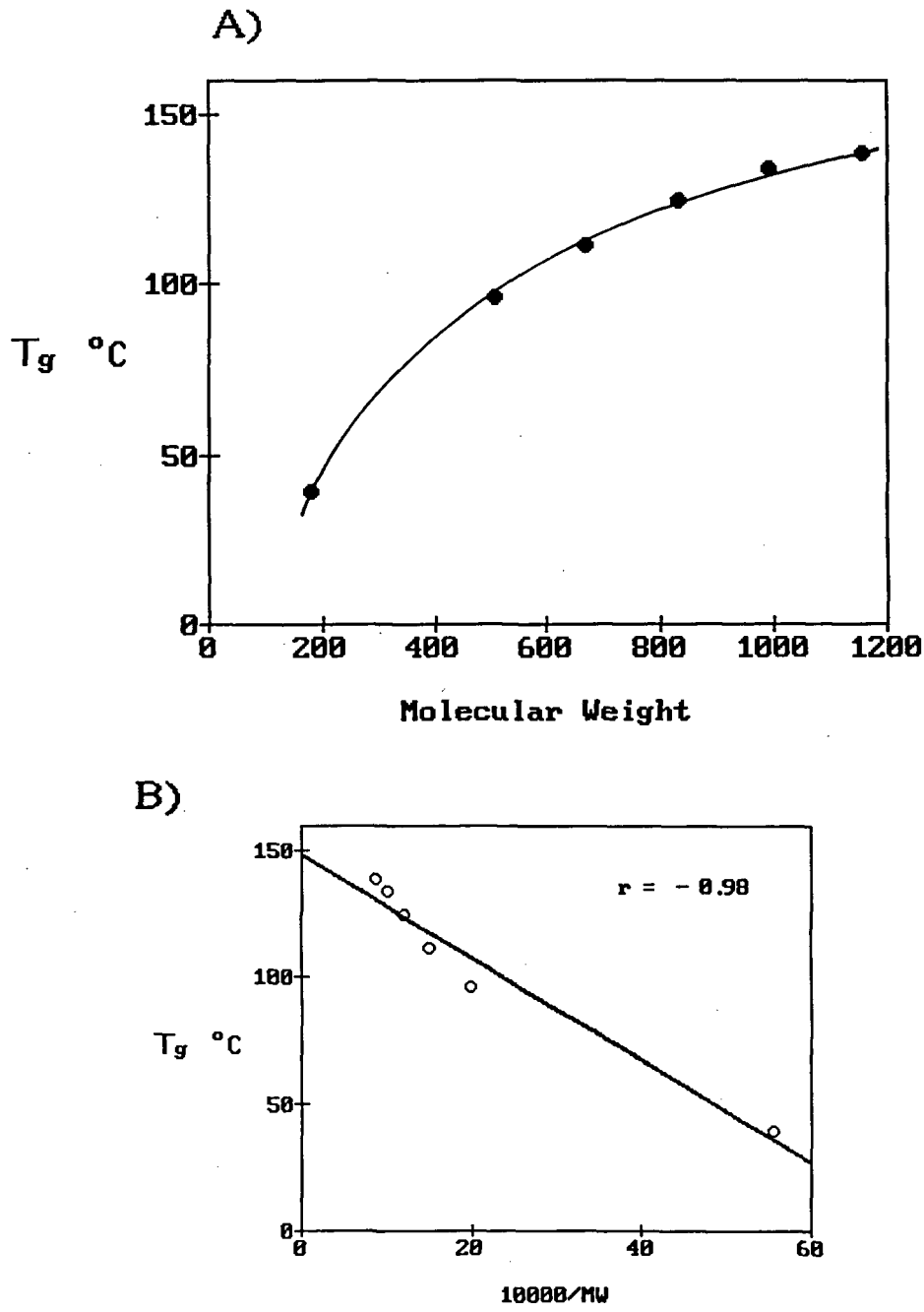

FIGURE 50. Variation of the glass transition temperature (Tg of dry powders) against (A) MW and (B) 10000/MW, for the homologous series of malto-oligosaccharides from glucose through maltoheptaose in Table 3. (From Levine, H. and Slade, L., *Water and Food Quality,* Hardman, T. M., Ed., Elsevier, London, 1989, 71. With permission.)

different portions of the glass curve are controlled by different mobility-determining parameters, i.e., free volume at lower moisture contents in the glass, but local viscosity at higher moisture contents in the glass;[30] and (3) realization that the best description of the glass transition is its definition as an iso-relaxation-time state,[30] the significance of the qualitative conceptual picture is not negated. The glass curve of approximately equivalent local viscosity still represents the

TABLE 5
Tg Values from DSC of Dry Sugars and Sugar Mixtures

Sugar	Tg, °K
Fructose	286,[a] 373[b] and 284[b]
Glucose	312,[a] 304,[b] 302,[c] 310,[d] 303,[e] 302[f]
Sucrose	330,[a] 325,[b] 340[c]
Fructose:glucose (1:1 w/w)	294,[a] 293[b]
Fructose:sucrose (1:7 w/w)	326,[a] 331[c]

[a] Value measured at 10°K/min heating rate.[124]
[b] Value measured at 10°K/min heating rate.[30]
[c] Value calculated or assumed, rather than measured.[89]
[d] Value measured at 10°K/min heating rate.[59]
[e] Value extrapolated to 0°K/min heating rate.[59]
[f] Value measured at 5°K/min heating rate.[176]

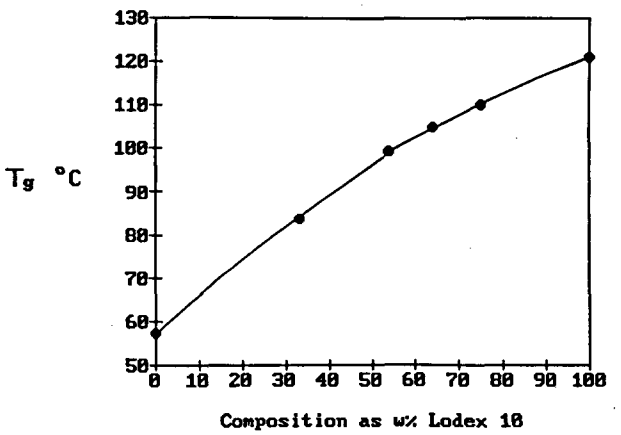

FIGURE 51. Variation of the glass transition temperature, Tg, against weight percent composition for spray-dried, low-moisture powders prepared from aqueous solution blends of Lodex 10 and Maltrin M365 SHPs. (From Levine, H. and Slade, L., *Water and Food Quality*, Hardman, T. M., Ed., Elsevier, London, 1989, 71. With permission.)

line of demarcation between long-term stability (at $\eta \geq \eta g$) and gradual deterioration (at $\eta < \eta g$),[8,40-42] whether one is talking about the shelf-life of a dry glucose candy glass (of Tg = 31°C) stored at ambient temperature or of a glucose-sweetened ice cream (of Tg′ = −43°C) stored in a freezer.

A compilation of measured values of dry Tg and dry Tm, and calculated Tm/Tg ratios, for various sugars and polyols is shown in Table 3.[28,30] Dry Tg values range from −93°C for glycerol (MW 92) to 138.5°C for maltoheptaose (MW 1153), and generally show the expected relationship of increasing Tg with increasing MW of the diluent-free PHC, but with several striking exceptions. Moreover, for a given MW, the spread of dry Tg values for different isomeric PHCs is large; in fact, many times larger than the corresponding spread of Tg′ values. For example: (1) among several pentoses and pentitols (MW ≃ 150), dry Tg values range from −18.5°C for xylitol to 9.5°C for xylose; (2) among several hexoses and hexitols (MW≃180), dry Tg values range from −2°C for sorbitol to 31°C for glucose (the anomalously high Tg values for anhydrous fructose and galactose are discussed in detail below); and (3) among several disaccharides (MW 342), dry Tg values range from 43°C for maltose to 90°C for mannobiose.

In Table 3, the calculated values of Tm/Tg (°K) ratio range from 1.62 to 1.06, with most values in the range 1.32 to 1.44. Of these sugars and polyols, fructose shows the most extremely anomalous Tm/Tg ratio of 1.06.[15,16] This value is much lower even than the lowest Tm/Tg ratio reported for a synthetic high polymer, i.e., 1.18 for bisphenol polycarbonate.[102] Levine and Slade[15] had reported previously that fructose's Tm/Tg ratio of 1.06 derives from the observation of *two* widely separated glass transition temperatures (see Table 5) in a quench-cooled, completely amorphous melt of pure crystalline β-D-fructose. The lower Tg appears at a lower temperature (11°C[30] or 13°C[124]) than the single values of Tg (around 30°C) of other common monosaccharides of the same MW, such as glucose and mannose. However, the much higher Tg is readily detectable at 100°C, a temperature only 24°C below the measured Tm of β-D-fructose. Another monosaccharide, galactose, shows analogous anomalous behavior, with a lower Tg similar to that of glucose and mannose, but a second, much higher Tg similar to the higher Tg of fructose.[28] The observed change in heat capacity at the higher Tg of fructose is smaller in magnitude than at the lower Tg, which may reflect either a smaller actual difference in heat capacity of the fructose population that vitrifies at the higher Tg than of the

second, structurally different fructose population that vitrifies at the lower Tg, or that the population of fructose molecules that vitrifies at the higher Tg of the conformationally heterogeneous melt is smaller, while the second population that vitrifies at the lower Tg is larger.[30] However, for reasons explained later, which are based on an interpretation of experimental results (including those in Table 2) involving several aspects of the anomalous behavior of fructose in non-equilibrium aqueous systems and processes, Slade and Levine have hypothesized that the higher Tg of dry fructose (and of galactose as well) is the critical one that defines the Tm/Tg ratio and controls the consequent mobility of plasticizing solute-water blends in their glassy and supra-glassy states.[15,16,30]

With respect to the unusual phenomenon of two values of Tg exhibited by quenched melts of fructose or galactose, Finegold et al.,[124] in their recent study of glass/rubber transitions and heat capacities of dry binary sugar blends, have reported similar anomalous behavior for the same two monosaccharides, and their contrast to well-behaved glucose and mannose. They have confirmed the existence of the higher-temperature "relaxation process" and that its amplitude (for fructose) is only 25% of that at the lower-temperature Tg.[124] While Finegold et al.[124] have remarked that "the actual physical origin of two distinct relaxation processes in an ostensibly one-component system is obscure", they have pointed out that both fructose and galactose are subject to complex mutarotation and have granted the possibility (suggested by Slade and Levine[30]) "that a quenched melt might exhibit microheterogeneity, with the appearance of two or more structural relaxations. This hypothesis is supported by the observation that annealing eventually removes the high-temperature relaxation process and increases the amplitude of the (low-temperature) relaxation."[124] Finegold et al. have also confirmed the earlier finding[15] that, in a two-component glass with another small sugar (in their case, sucrose or glucose[124]), the higher Tg of fructose is no longer detectable, as shown in Table 5 for a 1:1 (w/w) glucose:fructose glass (Tg = 20°C[30] or 21°C[124]) and a 1:7 (w:w) fructose:sucrose mixture.[89] This change in the thermomechanical behavior of fructose, to become more like glucose in the 1:1 mixture in the absence of diluent, is also manifested in the relative microbiological stability of concentrated solutions of glucose, fructose, and the 1:1 mixture, as will be discussed further with respect to Table 2.

In a possibly related vein discussed further below, it is interesting to note that Hallbrucker and Mayer[263] have also suggested the possibility of local microstructure in a heterogeneous molten fluid or glass of a one-component glass-forming system, in their discussion of the differences in thermal relaxation behavior between "hyperquenched" (i.e., cooling rate $>10^5$ °C/s) vs. slow-cooled glasses of aqueous or diluent-free PHC systems. They mentioned that the development of heterogeneous microstructure (i.e., local regions of different constitution and "activation energies") in a melt could contribute to the non-Arrhenius behavior of viscosity and flow processes in the temperature region above Tg. They have suggested "that hyperquenching produces a glass differing in local microstructure and (the temperature dependence of its) relaxation behavior from a slow-cooled glass," due to a corresponding difference in the temperature (relative to the Tg measured during subsequent rewarming) at which the molten fluid is immobilized to a glassy solid during cooling and thus at which the temperature dependence of relaxation processes switches from non-Arrhenius back to Arrhenius behavior.[263] Also pertinent to this line of discussion are recent remarks of Green and Angell,[290] who noted "that constant-composition samples (of molten glucose monohydrate) did yield variable Tg values depending on heat treatment. This reminds us that there is a structural variable for the solution (the anomer ratio), the time scale of which is much longer than the viscoelastic relaxation time and that may, therefore, be able to influence glass properties in new ways — all of which adds strength to Franks' recent call[281] (echoed by Slade and Levine[30]) for a renewed physicochemical interest in saccharide solutions."

Among a number of different cases of multiple values of Tg observed in amorphous and partially crystalline systems,[26,33] fructose may represent the interesting situation where two conformationally different populations of the same

chemical species manifest different free volume and local viscosity requirements for mobility.[30] Such a situation would arise if one of the conformational populations in a heterogeneous melt exhibited anisotropic rotational and translational mobilities, while the second population exhibited isotropic motion. For motional anisotropy, the free volume requirements for rotational mobility become much more stringent than those for translation,[187,188] and rotational relaxation would become limiting at a higher temperature than translational relaxation, as described with respect to Figure 34D for polymers with anomalously low values of Tm/Tg. For isotropic motion, the larger scale, slower translational relaxations become limiting at a higher temperature than rotational relaxations,[186,187] as described with respect to Figure 34D for polymers with typical and high values of Tm/Tg. For both anisotropic and isotropic motion, the temperature at which translational relaxations become limiting would be nearly the same. Thus, relaxation times for a conformational population with anisotropic motion would become limiting at a higher temperature, manifested as a higher Tg, than relaxation times for a second population with isotropic motion, manifested as a lower Tg.[30] A documented case, which might provide an explanation for the appearance of two conformationally different populations in a heterogeneous melt from a single crystalline conformation of a single chemical species, involves xylose, which has been shown to undergo rapid anomerization during melting.[291]

During the time between heating α-D-xylose to a temperature only slightly above Tm, to avoid decomposition, and quench-cooling the resulting melt to a glass in a conventional DSC experiment, a mixed population of anomers is able to form in the melt and be captured in the glass.[291] Thus, the initial crystal contains only the alpha anomer, while the final glass contains a simple anomeric mixture of α- and β-xylose,[124] and the particular conformer distribution in the glass depends on the experimental variables of temperature, pressure, and concentration. The fact that only a single value of Tg is observed for the xylose melt,[28,124] which is known to be conformationally heterogeneous, indicates either that all of the conformers are chemically and mechanically compatible so that a single glass vitrifies, or that all of the glasses that vitrify have the same free volume and local viscosity requirements for mobility and so the same value of Tg.[30] If other small PHCs, such as fructose and galactose, behave like xylose with respect to anomerization during the melting process, then depending on the specific Tm, the time the melt is held above Tm, and the quenching rate, they may also be capable of forming heterogeneous melts with conformationally different populations.[30] Then the fact that two values of Tg are observed would indicate that the two populations are not chemically and mechanically compatible and that they exhibit different free volume and local viscosity requirements for mobility. Finegold et al.[124] have reported another observation about the higher Tg of fructose that could support such speculation about the possibility of anomerization in a fructose melt. They noted that, after repeated heating and recooling of the initial fructose melt, the magnitude of the observed change in heat capacity at the higher Tg diminished and ultimately became undetectable, leaving only the lower Tg (representing the glass of the more stable anomer?[30]). This observation of changes in the sizes of the two populations upon repeated heating suggested that the difference in magnitude of the observed heat capacity for the two glasses after the initial fructose melt was due to different sizes of the two populations rather than different actual changes in heat capacities.[30]

There appear to be a number of analogies between aspects of (1) the double-glass-forming behavior of fructose and galactose and (2) the differences in thermal behavior, thermodynamic, and kinetic properties between ordinary slow-cooled vs. hyperquenched, diluent-free glasses of small PHCs such as ethylene glycol[263] and propylene glycol.[174] These analogies lead us to speculate about a common thread, as yet unidentified, in the two phenomena. Johari et al.[174] have suggested that "the temperature range over which the liquid-to-glass transition occurs on hyperquenching is wider than the range over which the transition occurs on normal cooling." In a corresponding fashion for each type of glass (and for glasses in general), "the temperature range of the glass transition is much less during the heating of a glass to liquid than it is during the cooling of a liquid to glass".[174] A hyperquenched

glass has a "fictive temperature" much higher than the normal Tg of a slow-cooled glass (of $\eta = 10^{12}$ Pa s) of the same material, i.e., hyperquenching immobilizes the liquid during quenching at higher temperatures than slow cooling.[174,263] Consequently, the kinetic and thermodynamic properties of a hyperquenched glass differ from those of a glass obtained by slow cooling.[174,263] For example, on subsequent rewarming, the Tg of a hyperquenched glass is observed at a higher temperature than the Tg of a corresponding slow-cooled glass.[174,263] (The Tg *observed* during heating [e.g., at 10°C/min] as a consequence of a particular previous sample history is a value of Tg somewhere below the fictive temperature [i.e., the fictively high Tg observed during fast cooling] and above the practical lower limiting Tg [i.e., the limiting value observed with ever slower cooling rates].[174]) As a consequence of higher fictive temperature, hyperquenching produces "a less dense glass (i.e., of lower viscosity) of a structure with a higher enthalpy and entropy, but with a much narrower distribution of structural relaxation times," the latter because the requirement for molecular cooperativity is gradually removed as the average intermolecular distance increases.[174] (It should be noted that the dependence of density on cooling rate is a general characteristic of glasses.[172]) As a consequence of lower density and viscosity in a hyperquenched glass at Tg, during rewarming of such a glass to temperatures above Tg, its constituent molecules exhibit greater rotational and translational mobility for diffusion-limited structural relaxation processes such as crystallization in the rubbery fluid.[263] For the same reasons, hyperquenched glasses show greater extents of structural collapse and resulting gradual viscous flow and concomitant densification (also referred to as sintering during heating) at temperatures 4 to 5°C above Tg than do slow-cooled glasses.[174] In contrast to the behavior of hyperquenched glasses at $T >$ Tg, during *sub*-Tg "aging" (referred to by Johari et al. as "annealing", but distinguished from the conventional definition of annealing at $Tg < Ta < Tm$[104]) of hyperquenched glasses, a spontaneous but slow structural relaxation, to a denser structure of lower fictive temperature and higher viscosity (more similar to the structure, viscosity, and fictive temperature of a slow-cooled glass), has been observed to begin at a temperature ≈0.73 Tg (K).[174] (By analogy, relative to the higher Tg of fructose at 100°C, the temperature at which such sub-Tg aging would begin would be 0°C.) It has been suggested that hyperquenched and slow-cooled samples of the same PHC glass-former, after sufficient aging at a temperature very close to Tg, would reach an identical structural state and show indistinguishable DSC scans.[174] However, "for the same temperature and time of (aging), spontaneous structural relaxation in hyperquenched glasses at $T < Tg$ is much slower than in ordinary glasses".[174]

We infer from the above comparison of the properties and behavior of hyperquenched vs. slow-cooled glasses of the polyols, ethylene glycol and propylene glycol, that the higher-Tg glass of fructose (and galactose) appears to manifest certain characteristics of a hyperquenched glass, while in contrast, the lower-Tg glass of fructose (and galactose) manifests the expected characteristics of a slow-cooled glass. The parallels, even though not all-inclusive, are provocative. But how and why a single cooling rate of 50°C/min, applied to a molten fluid of diluent-free fructose or galactose, could cause the formation of two distinct glasses, with properties analogous to those produced (in separate experiments) in polyol systems by two drastically different experimental cooling rates, are unknown and especially mystifying in light of the fact that our same experimental protocol has produced a single glass with a single Tg for every other small PHC that we have examined, including glucose, mannose, xylose, etc.[30] Likewise, in the studies of hyperquenched vs. slow-cooled polyol glasses, only a single Tg was observed in all cases upon rewarming of the glass following vitrification during cooling of the liquid, regardless of the cooling rate.[174,263] We can only speculate about the possibility of a different relationship between cooling rate and the kinetics of mutarotation for (what could be)[30] the two distinguishable populations of structural entities existing, at least initially, in a cooled melt of fructose or galactose.

The fundamental issue regarding the anomalous thermomechanical properties of fructose (vs. e.g., glucose) in foods[16,30] is still open to debate. As mentioned earlier, Slade and Levine[30] have stressed the evidently controlling influence of the

higher Tg of dry fructose, and resultant anomalously low Tm/Tg ratio, on the mobility-related kinetic behavior of fructose-water systems. In apparent contradiction, Finegold et al.[124] have suggested "that the low temperature relaxation is significant in determining the thermomechanical behavior of (this dry) sugar", both alone and in dry binary blends with other sugars. They have presented experimental glass curves (shown in Figure 52[124]) in which dry Tg was found to vary smoothly with composition for binary blends of fructose + glucose and fructose + sucrose, and which extrapolate smoothly to the lower Tg at 13°C for fructose. By analogy with the thermomechanical properties of synthetic high polymers, they have noted that, "in fructose-glucose blends, fructose takes on the role of plasticizer, since it depresses the Tg of glucose. An effect of MW on Tg can be seen (in Figure 52) from a comparison of sucrose with an equimolar mixture of glucose and fructose."[124] They have also pointed out that the lower dry Tg values of fructose and galactose would result in more typical Tm/Tg ratios around 1.4, more in line with the values for other well-behaved hexoses.[124] As discussed later, reconciliation of these two apparently divergent points of view is suggested to depend in part on the critical conceptual distinction between the non-equilibrium properties of diluent-free vs. water-containing glasses and rubbers. Because fructose is such a technologically important sugar, its glass-forming behavior in aqueous food systems and the thermomechanical ramifications thereof are a subject worthy and in need of further study by physical chemists.

The results for Tm/Tg ratio in Table 3 showed that fructose has the lowest value, based on selection of the higher Tg value as the one of overriding thermomechanical importance,[30] while galactose (along with maltotriose) has the next-lowest. Thus, this dry fructose glass would be predicted to have the highest requirement for free volume in the glass at (the higher) Tg, and conversely the lowest local viscosity ($\lesssim 10^{10}$ Pa s).[30]

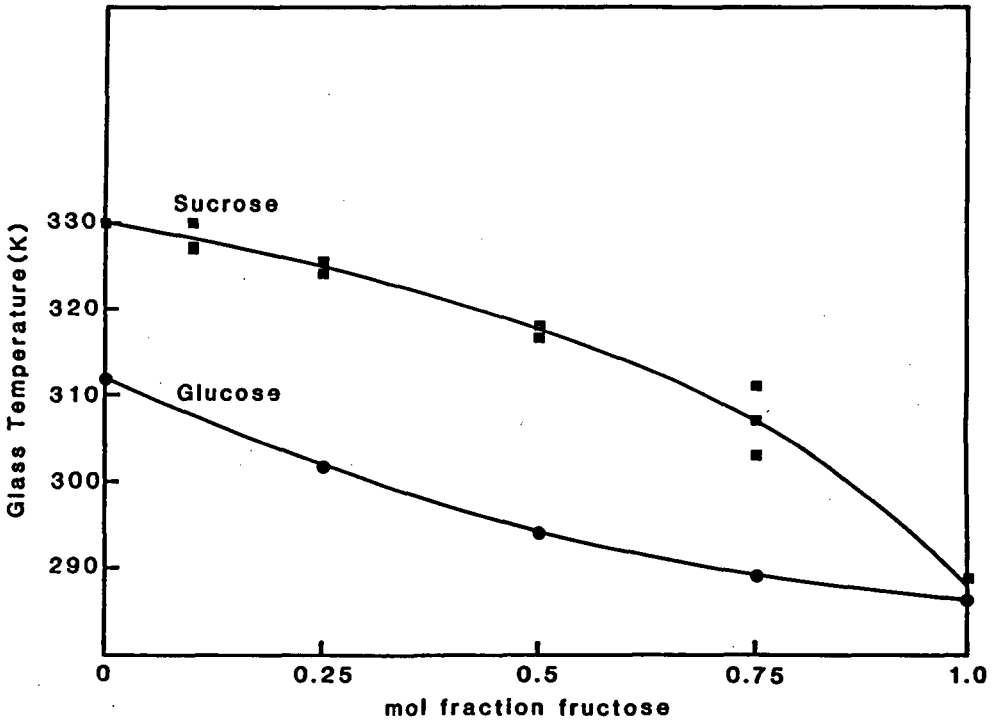

FIGURE 52. Glass/rubber transition temperature Tg vs. mol fraction of fructose for mixtures of fructose + glucose (circles) and fructose + sucrose (squares). The curve for the fructose-sucrose blends is a best-fit parabola. (From Finegold, L., Franks, F., and Hatley, R. H. M., *J. Chem. Soc. Faraday Trans. I.*, 85, 2945, 1989. With permission.)

Indeed, the Tg results of Finegold et al.[124] in Figure 52 can be interpreted as supporting this prediction. Because of its lower MW and concomitant higher free volume, fructose would be expected to take on the role of plasticizer and thus lower the Tg of sucrose in a dry binary blend. However, their finding[124] that fructose plasticizes glucose in a dry binary glass of these two monosaccharides (of the same MW) suggests that fructose manifests a higher free volume and lower local viscosity than glucose in the binary glass at its Tg. Such a situation would be consistent with a lower (rather than equal) Tm/Tg ratio for fructose in comparison to glucose. At the other end of the scale, glycerol, with the highest Tm/Tg ratio, would have the lowest requirement for free volume, but the highest viscosity ($\simeq 10^{14}$ Pa s) in its diluent-free glass at Tg. Consequently, at their respective values of Tg, a glycerol glass would be predicted to be significantly firmer (and thus less mobile and so more "stable" with respect to diffusion-limited relaxation processes) than a fructose glass.[30] This prediction awaits testing, with respect to both their diluent-free and Tg′-Wg′ glasses.

Experimental mobility transformation data for an extensive list of small carbohydrates, including most of the sugars, polyols, and glycoside derivatives in Table 3, are compiled in Table 6.[30] For each monodisperse PHC, Table 6 lists the measured Tg′ value for the maximally freeze-concentrated solute-UFW glass, which represents the reference state for the analysis that follows. This table also includes the corresponding Wg′ value (w% UFW), calculated $\overline{M}w$ and $\overline{M}n$ for the solute-water mixture in the glass at Tg′, the corresponding $\overline{M}w/\overline{M}n$ ratio, and the Tm/Tg ratios of some of the dry PHCs, from Table 3. The samples are ranked in Table 6 according to increasing value of $\overline{M}w$. Two other versions of this table, with samples ranked by increasing $\overline{M}n$ or increasing $\overline{M}w/\overline{M}n$ ratio, are not shown but will be alluded to, and so are left to the reader to construct.

If Table 6 had been ranked according to solute MW, all of the hexose monosaccharides would have appeared together, as they do in Table 3. But when such common sugars as fructose and glucose are ranked, not according to solute MW, but rather based on the Tg′-Wg′ reference state, they are widely separated on the list. The ranking according to increasing $\overline{M}n$ reflects decreasing requirement of free volume for mobility near Tg′ for PHCs with the same value of Tg′.[30] Thus, the free volume required for limiting mobility of fructose-water and captured in the fructose-water glass ($\overline{M}n = 33.3$) is much greater than that for glucose-water ($\overline{M}n = 49.8$). (Since the fructose-water glass at Tg′ has much greater free volume than the corresponding glucose-water glass, does the same relationship hold true for the corresponding dry glasses at Tg, as would be predicted from the much lower Tm/Tg ratio for fructose than for glucose?) It has been concluded that the composition and physicochemical properties of this glass at Tg′, which represents the crucial reference condition for technological applications involving any of the common functional properties of a small carbohydrate in water-containing food systems, cannot be predicted based on the MW of the dry solute.[30] The ranking according to increasing $\overline{M}w$ in Table 6 reflects increasing local viscosity in the glass at Tg′, for PHCs with the same values of Tg′ and $\overline{M}n$. Careful examination of the order of the PHCs in this table, compared to the different orders resulting from rankings by $\overline{M}n$ and $\overline{M}w/\overline{M}n$, has revealed that the order changes dramatically, depending on whether these small carbohydrates are ranked according to free volume, local viscosity, or the ratio of local viscosity/free volume.[30] Significantly, while ethylene glycol appears at the top of all three listings, trehalose appears at the bottom of the listing by $\overline{M}n$ (85.5), reflecting lowest free volume requirement for mobility near Tg′ compared to the other disaccharides in the list, while maltoheptaose appears at the bottom of Table 6 ($\overline{M}w = 911.7$), reflecting very high local viscosity of the glass at Tg′, but next to last (preceding maltohexaose) in the order of increasing $\overline{M}w/\overline{M}n$ ratio (11.39). So again, it has been concluded that one cannot predict, based on MW of the dry solute, even for the homologous series of glucose oligomers from the dimer to the heptamer, where such small carbohydrates would rank in terms of the free volume and local viscosity requirements for mobility near the solute-water glass at Tg′-Wg′.[30]

TABLE 6
Mobility Transformation Data for Small Carbohydrate Aqueous Glasses[30]

Polyhydroxy compound	MW	Tg' °K	Wg' w%	$\bar{M}w$	$\bar{M}n$	$\bar{M}w/\bar{M}n$	Tm/Tg
Ethylene glycol	62.1	188.0	65.5	33.2	23.8	1.39	
Propylene glycol	76.1	205.5	56.1	43.5	27.1	1.61	
1,3-Butanediol	90.1	209.5	58.5	47.9	26.9	1.78	
Glycerol	92.1	208.0	45.9	58.1	31.9	1.82	1.62
Erythrose	120.1	223.0	58.2	60.7	27.9	2.17	
Deoxyribose	134.1	221.0	56.9	68.0	28.7	2.37	
Arabinose	150.1	225.5	55.2	77.2	29.7	2.60	
2-*O*-methyl fructoside	194.2	221.5	61.7	85.5	27.6	3.10	
Deoxyglucose	164.2	229.5	52.6	87.3	31.1	2.80	
Deoxygalactose	164.2	230.0	52.6	87.3	31.1	2.80	
Tagatose	180.2	232.5	57.1	87.6	29.3	2.99	
Arabitol	152.1	226.0	47.1	89.0	33.7	2.64	
1-*O*-methyl mannoside	194.2	229.5	58.8	90.5	28.7	3.15	
Methyl xyloside	164.2	224.0	50.2	90.7	32.3	2.81	
Ribitol	152.1	226.0	45.1	91.7	34.9	2.63	
Methyl riboside	164.2	220.0	49.0	92.6	33.0	2.81	
3-*O*-methyl glucoside	194.2	227.5	57.3	93.3	29.4	3.17	
α-1-*O*-methyl glucoside	194.2	228.5	56.9	93.9	29.6	3.18	
Xylitol	152.1	226.5	42.9	94.6	36.3	2.61	1.44
β-1-*O*-methyl glucoside	194.2	226.0	56.3	94.9	29.8	3.18	
Deoxymannose	164.2	230.0	47.4	94.9	33.9	2.80	
1-*O*-ethyl glucoside	208.2	226.5	57.4	98.9	29.4	3.36	
Fructose	180.2	231.0	49.0	100.8	33.3	3.03	1.06
1-*O*-ethyl galactoside	208.2	228.0	55.8	102.2	30.2	3.38	
Glucose:Fructose 1:1	180.2	230.5	48.0	102.3	33.7	3.04	
1-*O*-ethyl mannoside	208.2	229.5	54.8	104.1	30.7	3.39	
2-*O*-ethyl fructoside	208.2	226.5	53.5	106.5	31.3	3.40	
Ribose	150.1	226.0	32.9	106.7	44.0	2.43	1.37
α-1-*O*-methyl glucoside	194.2	227.5	49.5	106.9	33.2	3.22	1.47
6-*O*-methyl galactoside	194.2	227.5	49.5	107.0	33.2	3.22	
2,3,4,6-*O*-methyl glucoside	236.2	227.5	58.5	108.5	29.2	3.72	
Xylose	150.1	225.0	31.0	109.1	45.8	2.38	1.51
Galactose	180.2	231.5	43.5	109.6	36.6	2.99	1.16
1-*O*-propyl glucoside	222.2	230.0	55.0	110.0	30.7	3.58	
1-*O*-methyl galactoside	194.2	228.5	46.2	112.7	35.1	3.21	
1-*O*-propyl galactoside	222.2	231.0	51.2	117.6	32.6	3.60	
Allose	180.2	231.5	35.9	122.0	42.6	2.87	
1-*O*-propyl mannoside	222.2	232.5	48.7	122.7	34.0	3.60	
Glucoheptulose	210.2	236.5	43.5	126.6	37.2	3.40	
Sorbose	180.2	232.0	31.0	129.9	47.5	2.74	
Glucose	180.2	230.0	29.1	133.0	49.8	2.67	1.42
Mannose	180.2	232.0	25.9	138.1	54.0	2.56	1.36
Inositol	180.2	237.5	23.1	142.8	58.5	2.44	
Sorbitol	182.2	229.5	18.7	151.5	67.3	2.25	1.42
Mannobiose	342.3	242.5	47.6	187.8	35.7	5.26	1.32
Lactulose	342.3	243.0	41.9	206.5	40.1	5.15	
Isomaltose	342.3	240.5	41.2	208.8	40.7	5.13	
Lactose	342.3	245.0	40.8	209.9	41.0	5.12	
Turanose	342.3	242.0	39.0	215.7	42.6	5.06	1.38
Maltitol	344.3	238.5	37.1	223.2	44.6	5.01	
Sucrose	342.3	241.0	35.9	225.9	45.8	4.93	1.43
Gentiobiose	342.3	241.5	20.6	275.4	72.6	3.80	
Maltose	342.3	243.5	20.0	277.4	74.4	3.73	1.27

TABLE 6 (continued)
Mobility Transformation Data for Small Carbohydrate Aqueous Glasses[30]

Polyhydroxy compound	MW	Tg′ °K	Wg′ w%	$\overline{M}w$	$\overline{M}n$	$\overline{M}w/\overline{M}n$	Tm/Tg
Trehalose	342.3	243.5	16.7	288.2	85.5	3.37	1.35
Raffinose	504.5	246.5	41.2	304.2	41.6	7.31	
Stachyose	666.6	249.5	52.8	323.9	33.3	9.74	
Panose	504.5	245.0	37.1	324.0	45.7	7.08	
Isomaltotriose	504.5	242.5	33.3	342.3	50.4	6.79	
Maltotriose	504.5	249.5	31.0	353.5	53.7	6.58	1.16
Maltotetraose	666.6	253.5	35.5	436.5	48.4	9.03	
Maltopentaose	828.9	256.5	32.0	569.6	53.8	10.59	
Maltohexaose	990.9	258.5	33.3	666.6	52.1	12.79	
Maltoheptaose	1153.0	259.5	21.3	911.7	80.0	11.39	

Note: The samples are ranked according to increasing values of $\overline{M}w$.

B. State Diagrams

State diagrams and their physicochemical basis represent a central element of the food polymer science data bank. Having already described several state diagrams for water-compatible polymeric, oligomeric, and monomeric food materials, in the context of the effect of water as a plasticizer, let us review further what has been gleaned from such state diagrams, viewed as mobility transformation maps for solute-water systems.

Figure 53[30] shows experimental data for the glass curves of the small PHCs, glucose, fructose, and sucrose, and a 40,000 MW PVP (PVP-40).[15] This mobility transformation map for these common sugars and PVP was constructed from measured values of (a) dry Tg and (b) Tg′ and Cg′, coupled with (c) Tg of pure amorphous solid water, (d) Tm of pure ice, and (e) the equilibrium[133] and non-equilibrium portions of the liquidus curve. Figure 53 demonstrates that the maximum practical (i.e., spacially homogeneous) dilution of each amorphous solute corresponds to a particular glass in each continuum of glassy compositions. As described earlier, alternative paths, such as drying by evaporation or freeze-concentration,[4,27] lead to the same operationally invariant w% composition (Cg′), with its characteristic Tg′.[30] The elevation of Tg, due to increased solute concentration, dramatically affects the shape of the non-equilibrium, very non-ideal portion of the liquidus curve. In other words, the extreme departure from the equilibrium liquidus curve for each of these solutes is related to the shape of the corresponding glass curve.[30] The locus of Tg′ on the transformation map depends on both the free volume and local viscosity, and therefore on the inverse $\overline{M}n$ and inverse $\overline{M}w$, respectively,[107] of the dynamically constrained, kinetically metastable solution.[30] Thus, it has been suggested that the anomalous shape of the extrapolated liquidus curve is a consequence of the system's approach to the immobile, glassy domain, rather than the cause of the particular location of the glass at Tg′.[30,33,34] The anomalous shape of the liquidus, which has been described elsewhere,[6] reflects the non-equilibrium melting behavior of the ice and the improbably low values of apparent RVP of the solution that result from the constrained approach to the glassy domain, which represents the limiting range of relaxation rates compared to the time frame of observation.[30] Equally anomalous values have been observed for the RVPs of aqueous supra-glassy solutions of PHCs at ambient temperature,[15,16] as described later with regard to Table 2. In both of these situations, the apparent RVPs are often inappropriately referred to as Aws, even though they are clearly non-equilibrium values, controlled by, rather than controlling, the long relaxation times of the solute-water system.[30]

It should be noticed that the three-point glass curves in Figure 53 are all characteristically smoothly and continuously curved over the entire

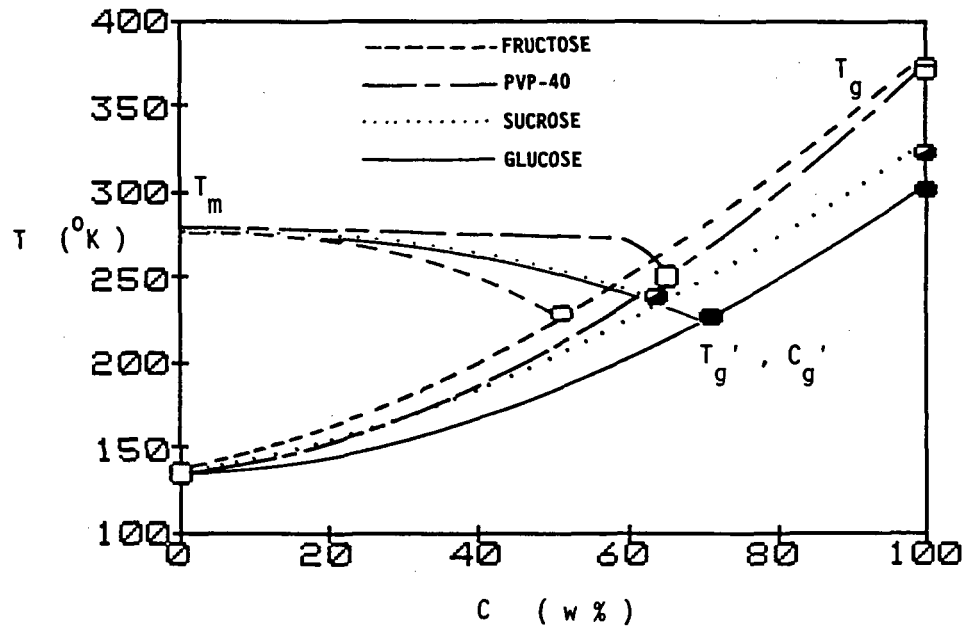

FIGURE 53. Solute-water state diagrams of temperature vs. concentration for fructose, glucose, sucrose, and PVP-40, which illustrate the effect of water plasticization on the experimentally measured glass curves, and the location of the invariant point of intersection of the glass curve and the non-equilibrium portion of the liquidus curve at Tg′ and Cg′, for each solute. (From Slade, L. and Levine, H., *Pure Appl. Chem.*, 60, 1841, 1988. With permission.)

range of solute-diluent w% compositions, as were the glass curves shown earlier in Figures 25, 28, and 29. Obviously, the shapes of these glass curves are determined by the particular locations of the Tg′-Cg′ and dry Tg points for each solute.[16] The glass curve for fructose-water is smoothly curved, only because it was drawn using the higher of the two dry Tg values (i.e., 100°C) for fructose.[15] If the lower dry Tg value of 11°C had been chosen instead, the resulting glass curve for fructose-water would not have been smooth. Rather, it would have a break (or cusp)[292] in it at Tg′-Cg′, such that the portion from Tg of water to Tg′-Cg′ would have a different curvature than the other portion from Tg′-Cg′ to the lower dry Tg. While unusually shaped glass curves, which exhibit a cusp in Tg as a function of composition (i.e., the Tg-composition variation is not monotonic), have been reported in the synthetic amorphous polymer literature for both miscible polymer-polymer and miscible polymer-diluent blends, such a cusp is generally manifested *only* when Tg is plotted vs. volume (rather than weight) fraction, and then *only* when one of the blend components is a high polymer with MW above the entanglement limit.[292] We know of only one report of such a cusp in a glass curve of Tg vs. w% composition (in that case, actually attributed to partial phase separation [i.e., immiscibility] in polymer-diluent mixtures),[293] but none of a cusp in any glass curve for a miscible solute-diluent blend (such as fructose-water) in which the solute MW is well below the entanglement limit. Other cases of maxima or minima in Tg-composition plots are ordinarily attributed to specific associations or complex formation occurring at stoichiometric compositions.[189] Thus, the smooth glass curve for fructose-water in Figure 53 represents supporting evidence for the choice of the higher dry Tg of fructose as the one which, in conjunction with the agreed location of Tg′ (and its corresponding Cg′-Wg′ composition),[6,7,14,27] determines the thermomechanical properties and thereby controls the mobility-related kinetic behavior of fructose-water systems in non-equilibrium glassy, rubbery, and supra-glassy states.[15,16,28,30]

It should be mentioned in passing that Hofer et al.[189] have recently reported an anomalous *depression* of the Tg of water (located at -135 ± 2°C) by the addition of quite small amounts of good aqueous-glass-forming solutes such as LiCl or ethylene glycol. Their Tg measurements of hyperquenched glasses of dilute binary aqueous solutions showed that the initial addition of ethylene glycol lowers the Tg of glassy water from -137°C to a minimum of -144°C for a solute concentration of <6.5 w% (*not* due to stoichiometric complex formation), after which Tg increases with increasing solute concentration (in the typical fashion for a solute of higher MW and diluent-free Tg than water), connecting with the glass curve for the "glass-forming composition region of concentrated solutions".[189] These new and surprising experimental results for Tg in the very low solute concentration region of the glass curve (previously inaccessible to complete vitrification at practical quench-cooling rates), even if substantiated by subsequent studies of other solutes by other investigators, have no bearing on the theoretical basis or experimental implications of the major portion of the solute-water glass curve, corresponding to the temperature-composition region of the dynamics map of greatest practical and technological relevance to food science.

We use weight fraction (w% concentration) for the abscissa of the dynamics map, rather than mole fraction as traditionally practiced for phase diagrams, for several reasons, of which the key supporting one was illustrated earlier by the results in Figure 47. As shown most definitively in Figures 47C and D, Tg′, the single most important point on a state diagram for any water-compatible solute, is determined by the $\overline{M}w$, rather than the $\overline{M}n$, of the solute-UFW composition in the maximally freeze-concentrated glass at Tg′-Wg′. Additional reasons include

1. To predict the composite Tg of compatible blends from the Tg values of individual components.[8] The Tg values of individual components already account for the occupied and free volume contributions to the limiting temperature for mechanical relaxations. Blending of components is then on a weight-fraction basis to determine the resulting local viscosity when volumes are added in different ratios.[30]
2. To allow the construction of state diagrams for materials with unknown MWs and linear DPs but known values of Tg.[15] Moreover, Tg and Wg are determined *not* by molecular volumes but by the volumes (sum of occupied + free) of mobile segments of polymer backbone or mobile units of the cooperative supra-glassy fluid, where the size of the mobile unit is roughly estimated from the total change in specific heat at Tg as a multiple of 11.3 J/K gmole of mobile unit.[106]
3. In a glass-forming mixture (e.g., a solute-plasticizer blend), before free volume becomes limiting, one can predict viscosity and mechanical relaxation times, based on the additivity of molar volumes. But once free volume becomes limiting (e.g., by increasing the solute concentration), cooperative motion of the supra-glassy fluid sets in, and τ is no longer predicted by molar volumes, but rather by the weight-average composition of the blend.[30] For two glass-forming mixtures of the same $\overline{M}n$ at the same temperature, the one with the larger $\overline{M}w$ will have greater η and greater τ.[107]

The latter reason why we plot mobility maps, such as those in Figure 53, in terms of weight fraction, rather than volume fraction, of solute is illustrated in Figures 54 through 56. In Figure 54, the plot of viscosity vs. w% solute data for sucrose and metrizamide[294] shows a comparison between a poor (metrizamide) and a good (sucrose) aqueous glass-former, both of which are hydrogen-bonding solutes. At a single temperature of 10°C, as the solute concentration of the poor glass-former increases, the average molar volume of the solution increases, and so the viscosity of the solution increases correspondingly, as predictable based on the additivity of molar volumes. But for the good aqueous glass-former, there is a concentration (between about 30 and 40 w% solute) above which the solution viscosity can no longer be predicted from the additivity of molar volumes, and above which one sees a dramatic influence of the limitation in free volume on the viscosity of such rubbery liquids.[30] This

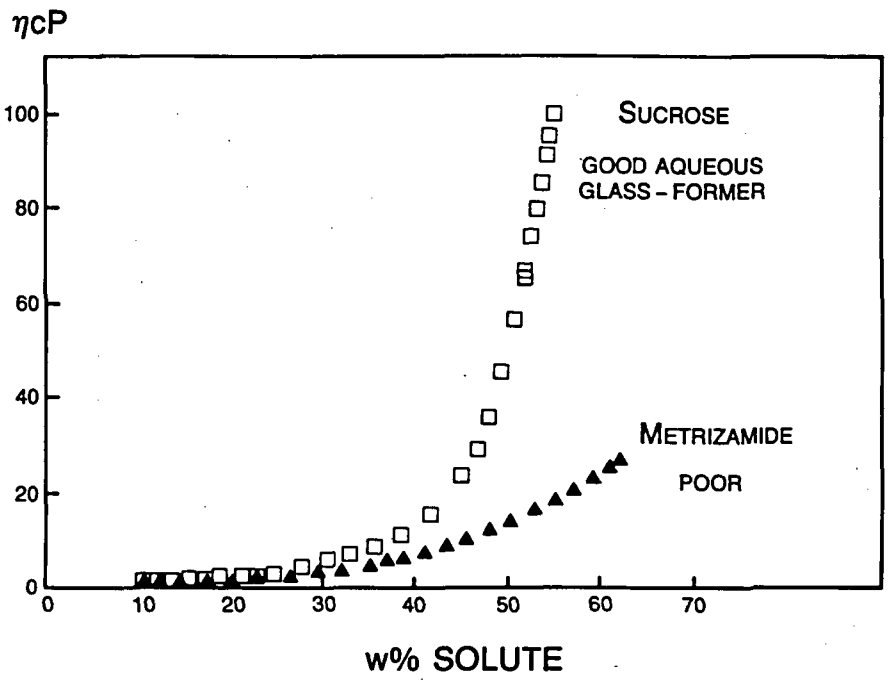

FIGURE 54. Plot of viscosity as a function of weight percent solute for aqueous solutions of two hydrogen-bonding solutes, sucrose and metrizamide, at 10°C. (From Cooper, T. G., *The Tools of Biochemistry,* Wiley-Interscience, New York, 1977. With permission.)

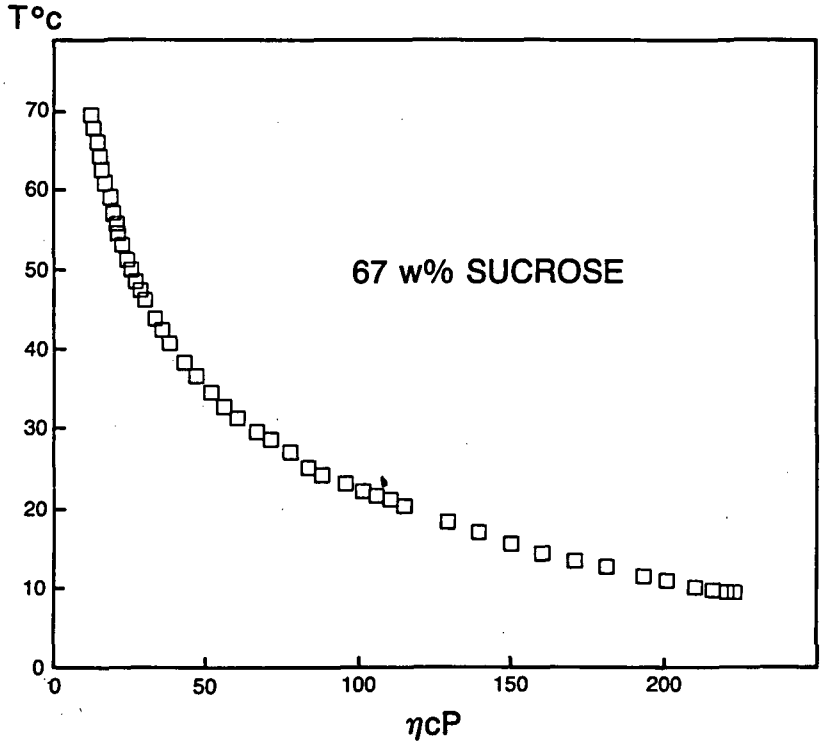

FIGURE 55. Plot of temperature vs. viscosity for a 67 wt% solution of sucrose in water. (Adapted from Parker, K. J., *Glucose Syrups and Related Carbohydrates,* Birch, G. G., Green, L. F., Coulson, C. B., Eds., Elsevier, Amsterdam, 1970, 58.)

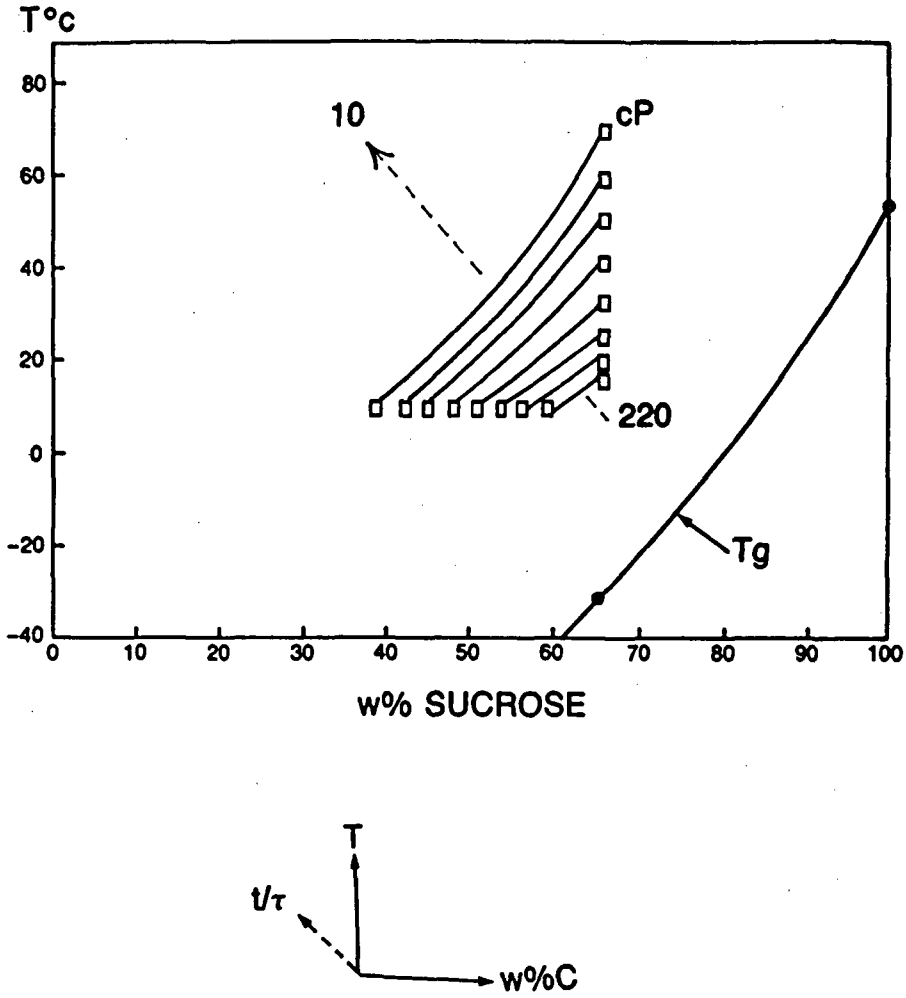

FIGURE 56. A two-dimensional mobility map for sucrose-water, plotted as temperature vs. weight percent sucrose, showing the relative locations of a series of iso-viscosity contours (constructed from the sucrose viscosity data in Figures 54 and 55) and a portion of the "complete" glass curve for sucrose-water.

behavior of the good glass-former reflects the cooperative nature of the glass transition.[106] While the experimental temperature of 10°C is well above the applicable Tg (i.e., Tg′ = −32°C) for such sucrose solutions, the limitations of free volume on mobility have been shown to be manifested even 100°C above the glass transition.[30,107] Thus, this cooperative behavior profoundly affects the observed time scales for mechanical relaxation processes such as viscosity in rubbery sucrose solutions. Figure 54 shows viscosity as a function of solute concentration for a single temperature. But we can also examine the effect of temperature on solution viscosity for a single sucrose concentration (67 w%),[295] as shown in Figure 55. As the temperature decreases from 70 to 10°C, viscosity increases dramatically. If we combine the sucrose data in Figures 54 and 55, by taking combinations of concentration and temperature that give the same solution viscosity, we can in fact build some iso-viscosity contours on the mobility map for sucrose, as shown in Figure 56. For example, combinations of 10°C and 38 w% sucrose and 70°C and 67 w% sucrose give exactly the same viscosity. Figure 56 demonstrates that relaxation times decrease dramatically with increasing ΔT or ΔW above the glass curve for sucrose-water solutions.[16] Thus, Figure 56 is actually a three-dimensional mobility map of content of water (acting as a

plasticizer), temperature (acting as a placticizer), and the experimental time scale (which for these viscosity experiments is constant) compared to the relaxation time (which decreases with decreasing w% solute concentration). This map, plotted as a function of weight fraction of solute, describes the time-dependence of the viscosity behavior of such rubbery or supra-glassy sucrose solutions.

Figure 57[30] illustrates the effects of a small PHC solute on the non-equilibrium thermodynamic properties of partially crystalline water, and focuses on glucose as an example of a typical, well-behaved, water-compatible polymer with a Tm/Tg ratio of 1.42. This dynamics map shows the effect of glucose addition on the Tg of water (in terms of measured values of Tg of the spacially homogeneous, aqueous glass), the Tm of phase-separated ice, and the Th of undercooled solutions.[4] Glucose elevates the Tg of water, through Tg′, up to the Tg of dry amorphous glucose, by its direct effect on the free volume and local viscosity of the resulting sugar-water solution.[107] At concentrations approaching infinite dilution, glucose affects the shape of the liquidus curve by colligative depression of the equilibrium Tm, and also depresses the non-equilibrium Th[296] of ice. However, at finite glucose concentrations in the range of technological importance, there is a non-colligative, very non-equilibrium effect of the solute on Tm, and a similarly anomalous effect on Th.[30] The changes in Tm and Th are empirically related by the ratio $\Delta Th/\Delta Tm \simeq 2$. Thus, at practicable concentrations of glucose, effective values of vapor pressure, osmotic pressure, Tm, Th, and crystal growth rate are all *instantaneous* values, determined by the effective relaxation time of the supra-glassy solution.[30] The dotted portion of the Th curve extrapolated below the Tg curve was included in Figure 57 to allude to the fact that, because this region of the dynamics map corresponds to a kinetically metastable domain in which homogeneous nucleation of ice is prohibited on a practical time scale,[288] such instantaneous values may persist for centuries (e.g., as demonstrated by the crystal growth rates of ice in undercooled PHC-UFW glass[7]). Indeed, the very enormity of the time-dependence beguiles with the appearance of equilibrium (e.g., as illustrated by the kinetics of water ad/absorption via diffusion in amorphous solids[297] or the water desorption "equilibration" of partially crystalline, rubbery substrates[83]).[30]

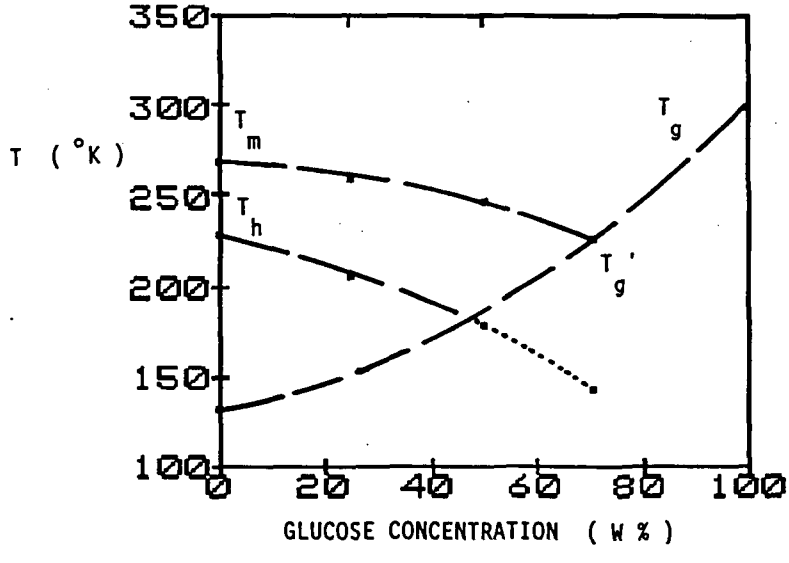

FIGURE 57. Glucose-water state diagram, which illustrates the relationship between the locations on this mobility transformation map of the curves for the glass transition temperature, Tg, the melting temperature, Tm, and the homogeneous nucleation temperature, Th. (From Slade, L. and Levine, H., *Pure Appl. Chem.*, 60, 1841, 1988. With permission.)

Figure 58[30] illustrates the effects of pressure, in the absence of solute, on the same non-equilibrium thermodynamic properties of partially crystalline water described in Figure 57, i.e., the Tg of pure amorphous solid water, the Tm of pure crystalline solid ice, and the Th of undercooled liquid water.[4,191] Increasing pressure elevates the Tg of numerous chemically and thermomechanically diverse polymers by about 20 ± 5°C per kbar (100 MPa).[107,120] The curve of predicted Tg values in Figure 58 was calculated on the basis of this same behavior for glassy water, which would show conventional volume expansion upon softening. Increasing pressure also depresses the Tm and Th of ice (the latter from −40°C at atmospheric pressure to a lower limit of −92°C at 2 kbar), an effect related to water's anomalous volume decrease upon melting.[4,191] The changes in Tm and Th produced by increasing pressure are empirically related by the ratio $\Delta Th/\Delta Tm \simeq 2$,[6] curiously analogous to the effect of solute cited above.[30] Thus, Figure 58 demonstrates that as Tg increases, both Tm and Th decrease anomalously.[30] It should be recalled that a 20°C change in Tg caused by a pressure change of 1 kbar would be comparable to a 5 orders-of-magnitude change in mechanical relaxation rates near Tg.[30]

The effects of a small PHC solute have been compared to the effects of pressure on the same non-equilibrium thermodynamic properties of partially crystalline water, by combining the results in Figures 57 and 58.[30] As illustrated in Figure 59,[30] the concentration and pressure scales were overlaid on this mobility transformation map so that one could compare the Tg of glucose-water glasses, the Tm of phase-separated ice in glucose solutions, and the Th of undercooled glucose solutions, all at atmospheric pressure, to the corresponding values of the predicted Tg of amorphous solid water alone, the Tm of pure crystalline ice, and the Th of undercooled liquid water, all up to 2 kbar. Figure 59 shows that glucose, representing a well-behaved molecular glass-former, at concentrations up to ≃25 w% in the glass, mimics high pressure in its effects on the thermomechanical behavior of water.[30] Both an increase in solute concentration and an increase in pressure result in an elevation of Tg and a concomitant depression of both the non-equilibrium Tm and Th (related by the same ratio $\Delta Th/\Delta Tm \simeq 2$).[30] By avoiding the eutectic be-

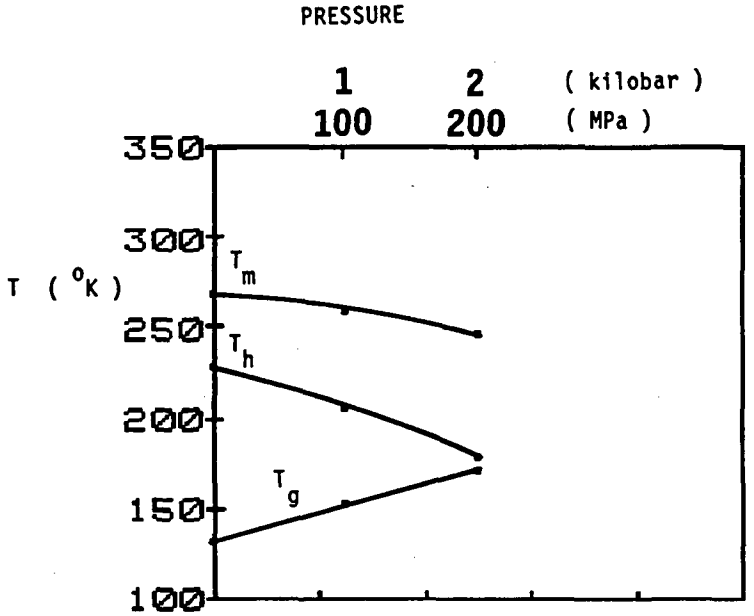

FIGURE 58. State diagram of temperature vs. pressure for pure water, which illustrates the effect of increasing pressure on the Tm, Th, and Tg curves. (From Slade, L. and Levine, H., *Pure Appl. Chem.*, 60, 1841, 1988. With permission.)

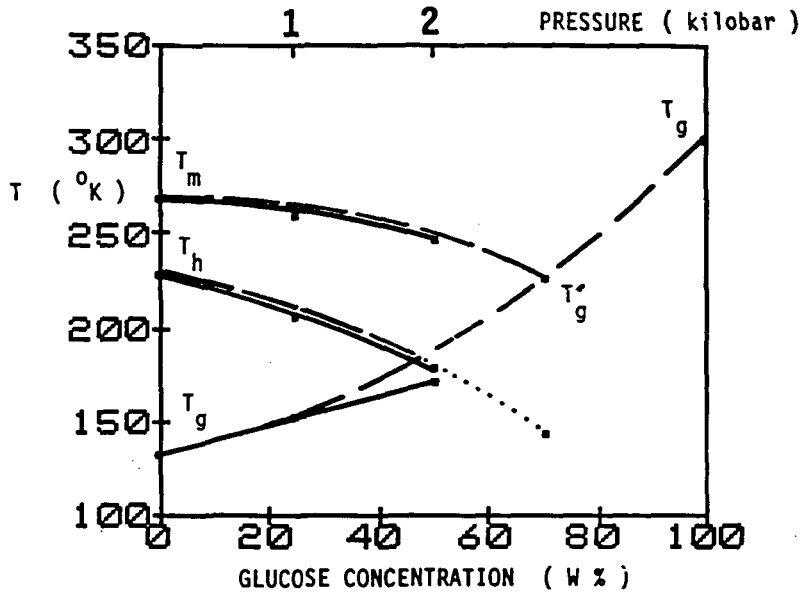

FIGURE 59. A superposition of the state diagrams in Figures 57 and 58, which illustrates the comparison between the effects of added glucose solute and increasing pressure on the non-equilibrium thermodynamic properties of water, in terms of its Tm, Th, and Tg. (From Slade, L. and Levine, H., *Pure Appl. Chem.*, 60, 1841, 1988. With permission.)

havior (i.e., ice I plus ice III) observed at pressures above 2 kbar for water alone[6,191] and instead allowing complete vitrification, higher solution concentrations of glucose (≳70 w%) have an even more drastic effect than pressure on the shapes of the non-equilibrium liquidus and Th curves.[30] So, while high pressure alone is not efficient for the prevention of ice formation, glucose solutions at high concentration,[241] or solutions of other even more ready aqueous-glass formers such as LiCl at much lower concentration (≃10 w%),[247,288] can be completely vitrified by cooling at atmospheric pressure. The additive effects of pressure and small PHC solute would allow complete vitrification at intermediate solution concentrations.[30] This has been demonstrated by Fahy et al.,[298] with respect to the concentration of a cryoprotectant solution required to achieve complete vitrification on cooling, in the context of vitrification as an approach to the cryopreservation of biological materials. They reported that, for concentrated solutions of a cryoprotectant such as propylene glycol, "high pressures lower Th and elevate Tg, thus shifting the point of intersection to a lower concentration of cryoprotectant".[298] Recent follow-up work by Forsyth and MacFarlane[299] has expanded the examination of the combined effects of solute concentration and pressure (up to 2 kbar) on Th and Tm of aqueous solutions of cryoprotectants such as propylene glycol. Their results showed that the Th-depressing effect of solute (e.g., 20 w% propylene glycol) at the highest pressures, over and above the Th-depressing effect of pressure in the absence of solute, is somewhat less than that predicted by the empirical ratio of $\Delta Th/\Delta Tm \simeq 2$, due to the relatively greater depressing effect of pressure on Tm than on Th of the solutions.[299]

It is worth pointing out that Figure 59 demonstrates that increased pressure serves as an "antiplasticizer", just as solute does, to elevate the Tg of water. However, the antiplasticizing effect of increased pressure is limited by the eutectic behavior of water (to form ice I plus ice III) above 2 kbar, whereas the antiplasticizing effect of solute is unlimited, if solute crystallization is avoided.

Taken together, the results in Figures 53 and 57 through 59 have been used to summarize the effects of water on thermomechanical behavior

of common sugars and the effects of pressure and common sugars on the non-equilibrium thermodynamics of partially crystalline water and aqueous solutions.[30] The aqueous glass curves in Figure 53 have been compared,[30] with emphasis on the recent finding of the striking difference in location on the mobility map of the curves for the two monosaccharides, fructose and glucose.[14] This comparison has shown that the glass curve for sucrose, at <50 w% solute, is located closer to that of fructose than glucose, but at >50 w% solute, sucrose is closer to glucose than fructose. In contrast, PVP-40, at <50 w% solute, is closer to glucose than fructose, but at >50 w% solute, PVP-40 is closer to fructose than glucose. As mentioned earlier, the insight derived from these results has led to the new suggestion that different portions of the glass curve must be controlled by different parameters that determine molecular-level mobility, i.e., Tg is controlled by free volume (a function of inverse $\overline{M}n$) rather than local viscosity at higher values of average MW (i.e., higher solute concentrations in the glass, Cg), but by local viscosity (a function of $\overline{M}w$) rather than free volume at lower values of average MW (i.e., higher water concentrations in the glass, Wg).[30]

The origin of the empirical ratio $\Delta Th/\Delta Tm \simeq 2$[4,6] had been previously obscured by the expectation that the liquidus curve must be colligatively controlled, while the Th curve is in part diffusion-controlled. The results in Figures 53 and 57 through 59 illustrated the parallel dynamic control over the non-equilibrium regions of both the liquidus and nucleation curves.[30] Figure 53 also points out that, at solute concentrations >20 w%, fructose and glucose (of equal MW) solutions have very different Tm, as well as Tg, profiles. So at these PHC concentrations (which are technologically the most important), the Tm curve is certainly not an equilibrium liquidus, but rather a non-equilibrium melting profile, which is affected by the underlying glass behavior.[30] Once again, the explanation for this behavior derives from the WLF kinetics governing the rubbery domain near Tg, where a 20°C temperature interval is equivalent to a range of 5 orders-of-magnitude in relaxation rates. Hence, within practical time frames, the immobility imposed by the glassy domain can have an all-or-nothing effect on homogeneous nucleation and crystal growth.[15,16,104,288]

As mentioned earlier, the effect on water of glucose concentrations up to 25 w% mimics the effect of pressure up to 100 MPa, and is nearly equivalent up to 50 w% glucose and 200 MPa pressure. However, while still higher pressure leads to nucleation of ice II or growth of ice III,[4] glucose concentrations >50 w% lead to continued elevation of Tg and so steadily increasing inhibition of all diffusion-limited processes, including nucleation and crystal growth of ice.[15,16] As a consequence, the lower limit of Th, to which pure water under high pressure can be undercooled without freezing, is −92°C.[4,191] In contrast, a glucose solution, of $C > Cg' \simeq 70$ w%, can be undercooled without limit, and complete vitrification will prevent ice formation in practical time frames.[241] In fact, Franks has calculated that the linear growth rate of ice, in an undercooled aqueous glass of typical viscosity of about 10^{13} Pa s at Tg, would be about 10,000 years per cm.[7] It should also be noted that, as a consequence of the differences between the map locations of the glass curves for fructose and glucose, the effect of fructose on the behavior of water is very different from the effect of pressure.[30] Even at concentrations as low as 20 w%, fructose causes a much greater elevation of the Tg of water and, concomitantly, a greater departure from the equilibrium liquidus curve.

As shown earlier by the results for PHCs in Figure 47, there is no correlation between Tg′ and $\overline{M}n$ of a given solute-UFW mixture, but a very good correlation between Tg′ and $\overline{M}w$. The significance of this finding has been related to the concept of the glass transition as an iso-relaxation state.[30,107] In order to explore the origin of this concept, the glass curves for the four solutes in Figure 53 were compared on the basis of a common value of Tg, and on the basis of a particular, distinctive Tg, as illustrated in Table 7.[30] For convenience, −32°C (the Tg′ of sucrose) was used as a common Tg, equivalent to drawing a horizontal line at Tg = −32°C so that it intersects the glass curves of Figure 53, as shown in Figure 60. The values of Tg′, as operationally invariant properties of the individual solutes, were used as a particular Tg. Then for each solute, the values of Wg or Wg′ corre-

TABLE 7
The Glass Transition as an Iso-Relaxation State. Relaxation Parameters are Compared on the Basis of a Common Value of Tg (−32°C) or Particular Values of Tg (Individual Values of Tg')[30]

	Based on common Tg = −32°C						Based on particular Tg = Tg'			
Solute	Mw	$\overline{M}n$	$\overline{M}w$	$\overline{M}w/\overline{M}n$	Tg − Tg' °C	Wg − Wg' %	$\overline{M}n'$	$\overline{M}w'$	$\overline{M}w'/\overline{M}n'$	% Δ
Fructose	180	36	107	3.01	10	−4	33	101	3.03	<1
PVP-40	40000	46	24407	529	−10	4	51	26006	506	~4
Sucrose	342	46	226	4.93	0	0	46	226	4.93	
Glucose	180	55	140	2.52	11	−4	50	133	2.67	~6

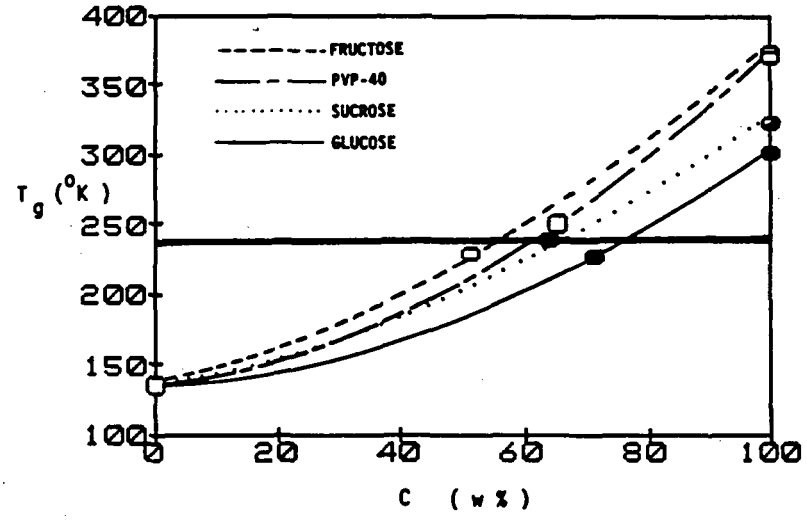

FIGURE 60. *The solute-water state diagrams of temperature vs. concentration for fructose, glucose, sucrose, and PVP-40 from Figure 53 (without the liquidus curves), which illustrate the effect of water plasticization on the experimentally measured glass curves, and the location of the invariant point of intersection of the glass curve and the non-equilibrium portion of the liquidus curve at Tg' and Cg', for each solute. The horizontal solid line at −32°C intersects the four glass curves at the Tg' of sucrose.*

sponding to the selected values of Tg were used to calculate $\overline{M}n$ and $\overline{M}w$, which govern the relative relaxation behavior. The results in Table 7 showed that, for the glasses that would exist at −32°C, those of sucrose and PVP-40 (solutes very different in MW) would have about the same free volume (as indicated by equivalent $\overline{M}n$ values), but very different local viscosities (as indicated by the corresponding $\overline{M}w$ values). As a general rule, when two polymeric glasses that have the same $\overline{M}n$ but different $\overline{M}w$ are compared at the same temperature in the absence of diluent, local viscosity increases with increasing polydispersity index, $\overline{M}w/\overline{M}n$.[107] Importantly, for polymer-plasticizer blends such as PHC-water solutions, both the Wg composition of the aqueous glass and MW of the dry solute contribute to the shape of the glass curve, the value of the ratio $\overline{M}w/\overline{M}n$, and the associated relaxation behavior.[30] Thus, the aqueous PVP-40 glass, with a much higher $\overline{M}w/\overline{M}n$ ratio, would have a higher local viscosity than the comparable sucrose glass. The results in Table 7 illustrated the point emphasized earlier that the absolute viscosity of the glass at its Tg depends on the nature of the solute and can vary within the range 10^{10} to 10^{14} Pa s. However, despite such a range of absolute viscosities at Tg, the respective ranges of relative relaxation rates that would result at T>Tg can all be described by a master curve based on the

WLF equation with appropriate respective values of the WLF coefficients.[107] The aqueous-glass formers in Table 7 were also compared at their individual Tg′ temperatures and characteristic Wg′ compositions.[30] These results showed, for example, that while the corresponding $\overline{M}n'$ values for PVP-40 and glucose are similar, indicative of similar free volumes, their $\overline{M}w'$ values are very different. Again, this indicated that the aqueous PVP-40 glass at its Tg′ has a much higher local viscosity, and so much longer relaxation times, than the aqueous glucose glass at its Tg′. This comparison shed light on the underlying mechanism for the greater microbiological stability provided by polymers and proteins than by small PHCs in concentrated solutions with equivalent RVPs, which has been observed empirically, and ascribed to a hypothetical ability of polymers to "bind" water more tightly (so-called "polymer water") than can small PHCs (so-called "solute water").[71] The actual mechanism plays an important role in the mold spore germination experiment mentioned earlier and discussed further later with respect to Table 2. Overall, the results in Table 7 demonstrated that the ratio of $\overline{M}w/\overline{M}n$ provides a better prediction of the shape of the glass curve as an iso-state, which requires a description of both the temperature and the moisture content at which relaxation times become limiting, than does MW or $\overline{M}n$ or $\overline{M}w$ alone.[30]

(Further comment on the concept of "polymer water" vs. "solute water" is in order. It has been suggested[30] that this distinction between solutes and polymers, and between their corresponding "states" [i.e., extents of mobility] of water, with respect to the water sorption behavior of such substrates, is artificial, meaningless, and misleading. This speculative concept of "polymer water" vs. "solute water", advocated by Steinberg and co-workers,[71] is completely untested and unproven to date. It has been suggested[15] that the actual basis for a proper distinction among different solid substrates, during non-equilibrium water sorption, lies in the structural state [i.e., completely crystalline, partially crystalline, or completely amorphous] of a given substrate at a given sorption temperature. The "acid test" would be to compare the water sorption behavior at 25°C of two water-compatible substrates, a completely amorphous, high MW polymer [e.g., water-sensitive polyvinyl acetate] and a completely amorphous, low MW solute [e.g., water-soluble maltose], of the same structural and physical [i.e., solid or liquid] states at low moisture contents. PVAc and maltose happen to have essentially the same Tg values of 39°C at 0 w% moisture and about 19°C at 4 w% moisture. Because amorphous maltose and PVAc share essentially the same Tg vs. w% water "glass curve" at these low moisture contents, they would be predicted to show indistinguishable sorption behavior, as solid or rubbery liquid substrates, in the 0 to 4 w% moisture range at 25°C.)

The Tg′-Cg′ point represents the end of ice formation in real time on cooling to $T < Tg'$, and conversely, the beginning of ice melting and concomitant melt-dilution (i.e., the opposite of freeze-concentration) of the solute in the aqueous rubber on heating to $T > Tg'$.[33] For very dilute solutions, the shape of the equilibrium liquidus curve is defined energetically, based on colligative freezing point depression by solute. At solute concentrations near and above the eutectic composition, melting of the metastable solution is described by a non-equilibrium extension of the equilibrium liquidus curve.[4,34] This has been illustrated by the actual state diagram for sucrose-water shown in Figure 61,[33] which was compiled from several sources, including Figure 53.[15,27-30,50,133,300] As mentioned above, the shape of the non-equilibrium extension of the liquidus curve is kinetically determined by the underlying glass curve,[34] as illustrated by the portion of the liquidus curve in Figure 61 between the points Te-Ce and Tg′-Cg′, where Ce is the composition of the eutectic mixture of pure crystalline ice plus pure crystalline solute.[33] Thus, for a typical solute that does not readily undergo eutectic crystallization on cooling (e.g., sucrose), Tg′ does not represent the incidental intersection of an independently existing equilibrium liquidus curve with the glass curve, but rather corresponds to the circumstantial intersection of the non-equilibrium extension of the liquidus curve and the underlying supersaturated glass curve that determined its shape.[30]

The state diagram for sucrose in Figure 61 has provided several noteworthy revelations concerning the relative locations of the glass, soli-

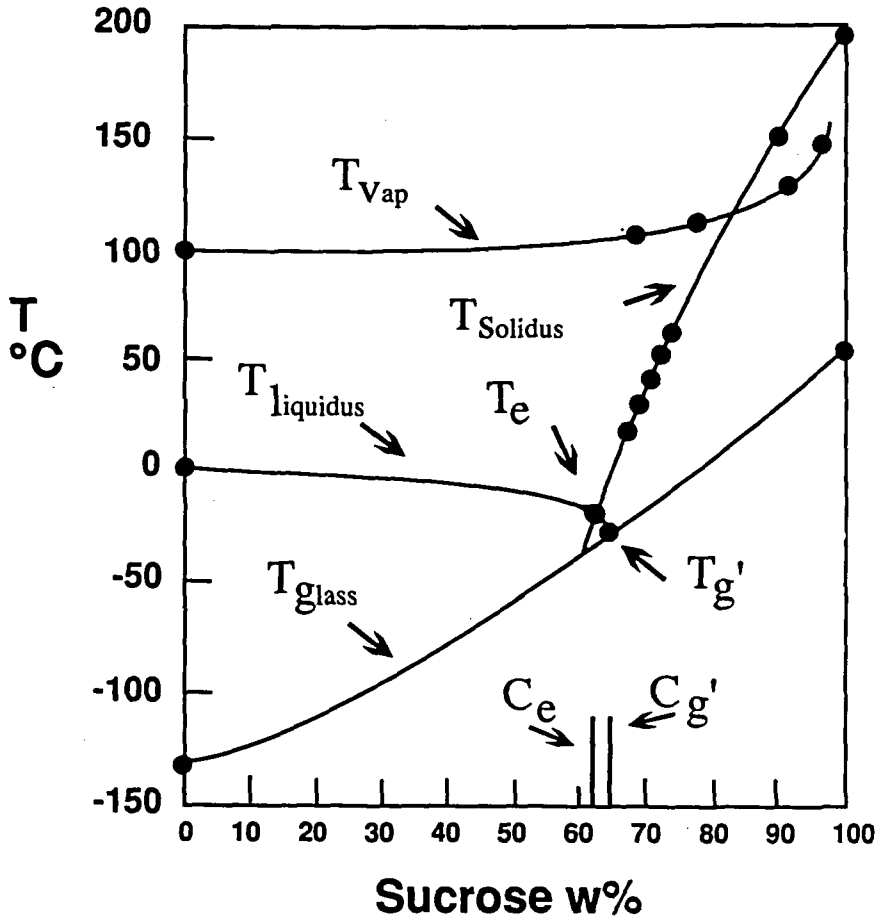

FIGURE 61. Solid-liquid state diagram for the sucrose-water system, illustrating the locations of the glass, solidus, and liquidus curves, and the points Tg′ and Te (eutectic melting temperature), corresponding, respectively, to the intersection of the liquidus (non-equilibrium extension) and glass curves and the intersection of the liquidus and solidus curves. The curve for the vaporization temperature of water as a function of sucrose concentration is also included. (From Levine, H. and Slade, L., *Comments Agric. Food Chem.*, 1, 315, 1989. With permission.)

dus, and liquidus curves.[33] Just as the liquidus curve describes the melting of crystalline solvent, in this case ice, the solidus curve describes the melting of crystalline solute. The melting process is called dilution when crystalline solvent melts in the presence of solution or dissolution when crystalline solute melts in the presence of its saturated solution. The solidus curve for the melting of crystalline sucrose decreases from Tm = 192°C for dry sucrose,[28,30] through several points for saturated sucrose solutions at different temperatures,[300] to Te = −14°C at Ce = 62.3 w% sucrose.[133] The glass curve decreases from Tg = 52°C for dry amorphous sucrose,[28,30,50] through Tg′ = −32°C at Cg′ = 64 w% sucrose,[29] to Tg = −135°C for pure amorphous solid water. The point Te-Ce is located at the intersection of the equilibrium solidus and equilibrium liquidus curves, while the point Tg′-Cg′ is located at the intersection of the non-equilibrium liquidus and glass curves. As mentioned earlier with respect to Figure 35, the temperature interval ΔT = Te-Tg′ between Te (as a particular value of Tm of ice) and Tg′ would correspond to an atypically small WLF rubbery domain of 18°C (relative to the typical Tm − Tg range of about 100°C for many diluent-free, synthetic amorphous polymers[30,107]) over which the microscopic viscosity of the sucrose-water solution would be estimated to decrease by about 13 orders of mag-

nitude from the characteristic ηg at Tg'.[30,89,107] (This value of $\Delta\eta$ was estimated as follows:[33] (1) at Tg'-Cg', $\eta g \simeq 10^{13}$ Pa s,[89] (2) at 20°C, $\eta \simeq 0.1$ Pa s for 62.3 w% sucrose,[300] and (3) at Te-Ce, $\eta e \simeq 1$ Pa s, based on an assumption of Arrhenius behavior between −14 and 20°C [i.e., at $T > Tm$, $Q_{10} = 2 \Rightarrow$ a factor of 10 change for a ΔT of 33°C].)[30] Consequently, the rates of deteriorative changes that depend on constrained diffusion in a frozen aqueous system of pure sucrose would be predicted correspondingly to *increase* by about 13 orders of magnitude vs. the rates at Tg',[33] with profound implications for the storage stability and kinetics of collapse processes in frozen food systems (e.g., ice cream and other frozen desserts and novelties) for which a freeze-concentrated sucrose solution could serve as a limiting model.[32,34] It has been noted that the 13 orders of magnitude predicted from the WLF equation[101] for the decrease in microscopic viscosity and concomitant increase in diffusion-limited relaxation rate over a rubbery domain with a temperature span from Tg' to Tg' + 18°C are based only on the effect of increasing temperature above the Tg' reference state, and not on any effect of dilution due to the melting of ice, which would begin on heating to $T > Tg'$, on the solute concentration in the rubbery fluid.[33] Such an effect of melt-dilution would obviously cause a further decrease in viscosity over and above the WLF-governed behavior. The resultant effect on diffusion-limited reaction rate (e.g., enzyme-substrate interactions)[8] would not be so obvious. The rate could increase *or* decrease, depending on whether or not the solute being diluted is a participant in the reaction.[33] The sucrose-water system shown in Figure 61 is remarkable with respect to the minimal effect of melt-dilution on heating from Tg' to Te. The sucrose concentration only decreases by 1.7 w%, from Cg' = 64 w% to Ce = 62.3 w%, over a temperature range of 18°C, due to the near-vertical path (compared to the path of colligative freezing point depression in the equilibrium portion) of the extremely non-equilibrium extension of the liquidus curve at $C > Ce$.[33] Despite this fact, the above discussion is not meant to negate the importance of melt-dilution (stressed by Simatos et al.[98]) as temperature is increased above Tg'. Analogous to experience in drier systems at $T > Tg'$ and $W < Wg'$,[28] either addition of water (ΔW) or increase in temperature (ΔT) above the glass curve accomplishes decreased relaxation times. However, water-rich systems differ from drier systems in that water is equivalently as effective as temperature as a plasticizer for drier systems at $C > Cg'$, but the practical limit of efficacy of water as a plasticizer is exceeded at $C < Cg'$.[26,30]

PVP is a completely water-miscible, non-crystallizable, synthetic, flexible-coil polymer that represents a much-studied model for amorphous polymeric food materials.[4] The state diagram for PVP-water (PVPs of $\overline{M}n = 10^4$, 4.4×10^4, and 7×10^5) in Figure 62,[15] compiled from several sources,[4,8,74,133,242,301] is the most complete one presently available for this polymer.[27] We include it here, because this figure exemplifies in a single diagram a number of the points illustrated by the other state diagrams described earlier. For example, as shown in Figure 62, PVP exhibits a smooth Tg curve from about 100°C for dry PVP-44 to −135°C for amorphous solid water. As with the various other water-compatible materials described earlier, the plasticizing effect of water on the Tg of PVP is most dramatic at low moisture contents, such that for PVP-44, Tg decreases by about 6°C/w% water for the first 10 w%. Figure 62 also illustrates that the phenomenological threshold temperatures for different collapse processes all correspond to the particular Tg' (or other Tg relevant to the situation in question), which is a function of the MW and concentration of the solute.[8,27] Thus, for PVP-44, $Tg' \simeq Tr \simeq Tc \simeq -21.5$°C and Cg' ≃ 65 w% PVP (Wg' ≃ 0.54 g UFW/g PVP),[4,8,133,242] while for PVP-700, $Tg \simeq Tc \simeq T$ sticky point ≃ 120°C at about 5 w% residual moisture.[27] The equivalent of Tr for ice or solute recrystallization, Tc for collapse, and the concentration-invariant Tg' for an ice-containing system has explained[8] why Tr and Tc are always observed to be concentration-independent for any initial solute concentration lower than Cg',[4,260] as illustrated in Figure 62. Figure 62 also illustrates the effect of increasing solute MW on dry Tg (which increases in the order PVP-10 < PVP-44 < PVP-700) and on Tg' and Cg'. As mentioned earlier, with increasing solute

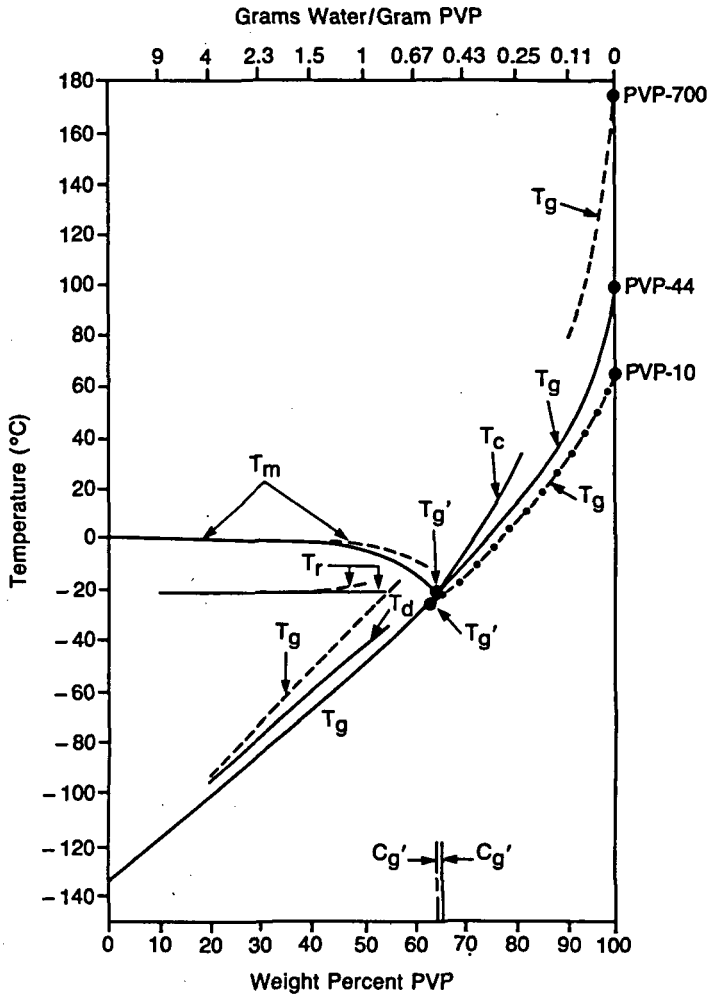

FIGURE 62. Solid-liquid state diagram for water-PVP, showing the following transitions: Tm, Tg, Tg', Td, Tr, Tc. (—— = PVP-44, - - - - - = PVP-700, -●-●-●-●-●-●-●-●- = PVP-10.) (From Levine, H. and Slade, L., *Water Science Reviews,* Vol. 3, Franks, F., Ed., Cambridge University Press, Cambridge, 1988, 79. With permission.)

MW, the Tg′-Cg′ point moves up the temperature axis toward 0°C and to the right along the composition axis toward 100 w% solute.[8]

C. Cryostabilization Technology

"Cryostabilization technology"[8,27,31-34] represents a new conceptual approach to a practical industrial technology for the stabilization during processing and storage of frozen, freezer-stored, and freeze-dried foods. This technology emerged from our food polymer science research approach and developed from a fundamental understanding of the critical physicochemical and thermomechanical structure-property relationships that underlie the behavior of water in all non-equilibrium food systems at subzero temperatures.[4,6] Cryostabilization provides a means of protecting products, stored for long periods at typical freezer temperatures (e.g., Tf = −18°C), from deleterious changes in texture (e.g., "grain growth" of ice, solute crystallization), structure (e.g., collapse, shrinkage), and chemical composition (e.g., enzymatic activity, oxidative reactions such as fat rancidity, flavor/color degradation). Such changes are exacerbated in many typical fabricated foods whose formulas are dominated by low MW carbohydrates. The key to this protection, and resulting improvement in product qual-

ity and storage stability, lies in controlling the structural state, by controlling the physicochemical and thermomechanical properties, of the freeze-concentrated amorphous matrix surrounding the ice crystals in a frozen system. As alluded to earlier, the importance of the glassy state of this maximally freeze-concentrated solute-UFW matrix and the special technological significance of its particular Tg, i.e., Tg′, relative to Tf, have been described and illustrated by solute-water state diagrams such as the idealized one in Figure 63.[32] Upon a foundation of pioneering studies of the low-temperature thermal properties of frozen aqueous model systems by Luyet, MacKenzie, Rasmussen,[133,135,240-242,254,259,302] and Franks,[4-7,74] an extensive cryostabilization technology data base of DSC results for carbohydrate and protein food ingredients has been built.[8,25-34] As reviewed earlier, DSC results for the characteristic Tg′ values of individual carbohydrate and protein solutes have demonstrated that Tg′ is a function of MW for both homologous and quasi-homologous families of water-compatible monomers, oligomers, and high polymers. Examples of how the selection and use of appropriate ingredients in a fabricated product have allowed the food technologist to manipulate the composite Tg′, and thus deliberately formulate to elevate Tg′ relative to Tf and so enhance product stability, have been described,[8,25-34] as reviewed below.

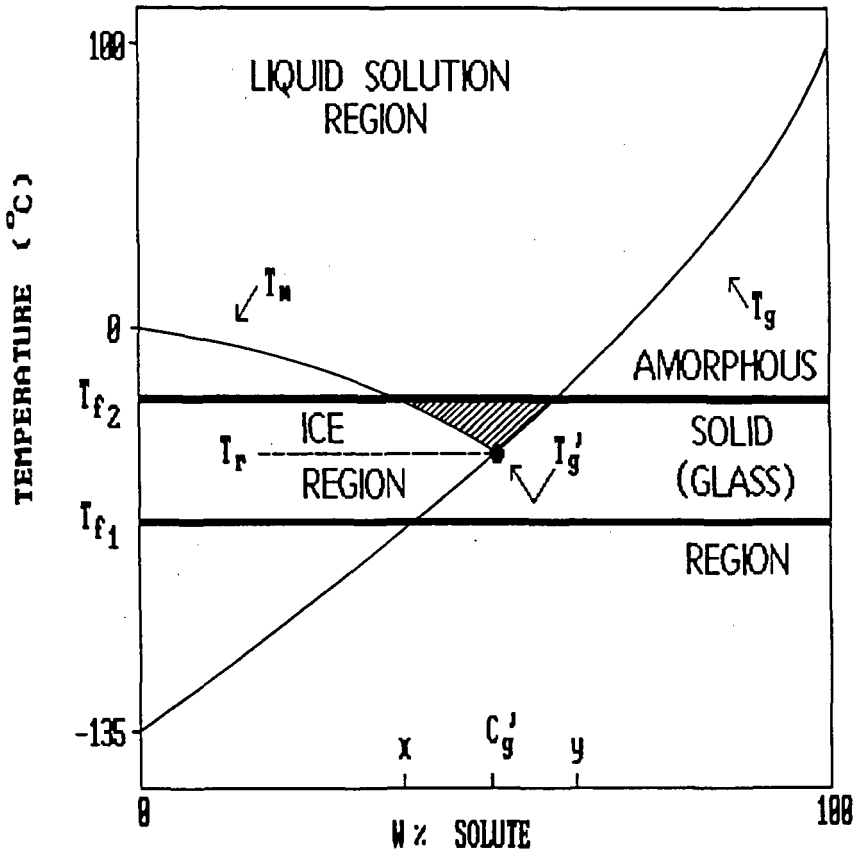

FIGURE 63. Idealized state diagram of temperature vs. w% solute for an aqueous solution of a hypothetical small carbohydrate (representing a model frozen food system), illustrating the critical relationship between Tg′ and freezer temperature (Tf), and the resulting impact on the physical state of the freeze-concentrated amorphous matrix. (From Levine, H. and Slade, L., *Cryo.-Lett.*, 9, 21, 1988. With permission.)

1. Historical Relationship between Cryotechnology and Collapse Phenomena

Much of our understanding of the thermal and thermomechanical properties of concentrated aqueous solutions has been derived from extensive studies of small glass-forming carbohydrates at subzero temperatures. These studies, which began over 50 years ago with the seminal work of Luyet,[302] have established that Tr, the microscopically observed temperature of irruptive ice recrystallization in such glass-forming systems of low MW sugars and polyols,[4,74,133,240-242,260,261] coincides with the solute-specific Tg′ measured by thermal or thermomechanical analysis.[6,8,27,29,31,40-42,50,262] It has also been recognized that ice recrystallization is but one of many possible manifestations (referred to as collapse phenomena) of the dynamically controlled behavior of aqueous glasses and rubbers, which exist at subzero temperatures in kinetically constrained, metastable states rather than equilibrium phases.[8,25-34] Generic use of the term "rubber" in this context describes all glass-forming liquids at $Tg < T < Tm$, including both molecular rubbers (viscous liquids) of low MW monomers and oligomers and viscoelastic network-forming rubbers of entangling high polymers.

As introduced earlier, a unifying concept for interpreting collapse phenomena, based on glass dynamics, has been described.[8,27] Collapse phenomena have been defined as macroscopic and microscopic relaxation processes. These translational and rotational diffusion-limited, material-specific, structural and/or mechanical relaxation processes occur far from equilibrium[33] and are therefore governed by the critical system variables of moisture content, temperature, and time.[303] Collapse processes occur at a characteristic collapse transition temperature, Tc,[4,64,66,135,136] which can coincide, on a comparable time scale (e.g., during storage), with an underlying Tg,[8] or can be manifested in real time (e.g., during processing) at a temperature about 20°C above Tg (i.e., at a relaxation rate 10^5 faster than at Tg).[30,33,66] At the relaxation temperature, moisture content is the critical determinant of collapse and its consequences,[138] through the plasticizing effect of water on Tg of the amorphous regions in both glassy and partially crystalline food polymer systems. Because the kinetics of collapse processes are governed by the free volume, local viscosity, and resultant mobility of the water-plasticized glass or rubber,[30] the effect of plasticization (leading to increased free volume and mobility in the dynamically constrained glass) by water on Tg is a key aspect of collapse and its mechanism.[8,27,28,66] In the rubbery liquid, rates of all translational and rotational diffusion-limited relaxation processes, including structural collapse and recrystallization, increase according to WLF kinetics with increasing ΔT above Tg.[8,30,66]

A generalized physicochemical mechanism for collapse, based on occurrence of the material-specific structural transition at Tg, followed by viscous flow in the rubbery liquid state,[137] has been derived from WLF theory and described as follows.[8,27] When the ambient temperature (during processing or storage) becomes greater than Tg, the free volume of the system increases, leading to increased cooperative mobility in the environment of polymer chain segments or small molecules in the amorphous regions of both glassy and partially crystalline systems. Consequently, the local viscosity of the dynamically constrained solid falls below the characteristic microscopic viscosity of about 10^{12} Pa s at Tg,[289] which permits viscous liquid flow.[137] In this rubbery state, translational diffusion can occur on a practical time scale, and diffusion-limited relaxations (which also frequently exhibit a prerequisite for nucleation) are free to proceed with rates defined by the WLF equation (i.e., rates that increase logarithmically in a non-linear fashion with increasing ΔT above Tg). The generalization of this mechanism is made possible by the fact that there are two paths by which the ambient temperature can become greater than Tg.[26] Heating (plasticization by heat) elevates the ambient temperature to above Tg for both diluent-free (bone-dry) and diluted (water-containing) systems. Increasing the moisture content (plasticization by water) depresses the Tg to below the ambient temperature for diluted systems only.

A comparison of literature values of subzero collapse transition temperatures for an extensive list of water-compatible monomers and polymers (shown in Table 8[27]) has established the

TABLE 8
Comparison of Tg′ Values and Literature Values for Other Subzero Collapse Transition Temperatures[27]

Substance	Tr, °C[a]	Tc, °C[b]	Tg′, °C
Ethylene glycol	−70[c,e], −81[f]		−85
Propylene glycol	−62[e]		−67.5
Glycerol	−58, −65[c,e]		−65
Ribose	−43		−47
Glucose	−41, −38	−40	−43
Fructose	−48	−48	−42
Sucrose	−32, −30.5	−32, −34[d]	−32
Maltose		−32	−29.5
Lactose		−32, −30[i]	−28
Raffinose	−27, −25.4	−26	−26.5
Inositol		−27	−35.5
Sorbitol		−45	−43.5
Glutamic acid, Na salt		−50	−46
Gelatin	−11	−8	
Gelatin (300 Bloom)			−9.5
Gelatin (250 Bloom)			−10.5
Gelatin (175 Bloom)			−11.5
Gelatin (50 Bloom)			−12.5
Bovine serum albumin	−5.3		−13
Dextran		−9	
Dextran (MW 9400)			−13.5
Soluble starch	−5, −6[c]		
Soluble potato starch			−3.5
Gelatinized wheat starch			−5
Hydroxyethyl starch	−21	−17[d]	−6.5
PVP	−22, −21, −14.5	−23, −21.6[d], −25[h]	
PVP (MW 35000)		−17[g]	
PVP (MW 10000)			−26
PVP (MW 40000)			−20.5
PVP (MW 44000)			−21.5
PEG	−65, −43	−13	
PEG (MW 200)			−65.5
PEG (MW 300)			−63.5
PEG (MW 400)			−61

[a] Recrystallization temperatures[4]
[b] Collapse temperatures during freeze-drying[4]
[c] Luyet[240]
[d] "Antemelting" temperatures[258]
[e] "Completion of opacity" temperatures[260]
[f] Recrystallization temperature[261]
[g] Pikal et al.[304]
[h] Pikal[305]
[i] Pikal and Shah[190]

fundamental identity of Tg′ with the minimum onset temperatures observed for various structural collapse and recrystallization processes,[8,27] for both model solutions and real systems of foods, as well as pharmaceuticals and biologicals.[4,40-42,190,262,304-306] The Tc and Tr values of frozen or vitrified samples, such as those in Table 8, are typically determined by cryomicroscopy,[135,304,305] thermal analysis,[307] or electrical resistance measurements,[258] on an experimental time scale similar to that for Tg′ by DSC.[190,262] A comprehensive list of collapse processes (shown in Table 9[8]), all of which are governed by Tg′ of frozen systems (or a higher Tg pertaining to low-moisture systems processed or stored at T > 0°C) and involve potentially detrimental plasticization by water, has been identified and elucidated.[8,15,25-28,31-34] Part B of Table 9 is included to emphasize how the Tg values relevant to both low- and high-temperature collapse processes are systematically related through the corresponding water contents, thus illustrating how this interpretation of collapse phenomena has been generalized to include both high-temperature/low-moisture and low-temperature/high-moisture food products and processes.[8,27,28] Table 9 contains extensive references from the food science and technology literature to specific examples of both low-temperature/high-moisture and high-temperature/low-moisture collapse processes. In all cases, a partially or completely amorphous system in the mechanical solid state at T < Tg and local viscosity $>\eta g$ would be stable against collapse, within the period of experimental measurements of Tg, Tc, and/or Tr.[8,66] Increased moisture content (and concomitant plasticization) would lead to decreased stability and shelf-life, at any particular storage temperature.[126,138] The various phenomenonological threshold temperatures for the diverse collapse processes listed in Table 9 all correspond to the particular Tg′ or other Tg relevant to the solute(s) system and its content of plasticizing water.[8,27]

The examination of the relationship between cryostabilization technology and collapse processes, and the interpretation of the latter within a conceptual context of glass dynamics, has resulted in a conclusion and explanation of the fundamental equivalence of Tg, Tc, and Tr, and their dependence on solute MW and concentration.[8,15] This new interpretive approach has provided a better qualitative understanding of empirical results previously observed but not explained on a basis of polymer structure-property principles.[136] While the similarity and apparent identity of measured Tc and Tr values for various frozen aqueous model systems (as illustrated in Table 8) had often been noted,[4,6,254] the conclusion regarding the fundamental equivalence of Tg, Tc, and Tr[8] represented a departure from the previous literature. For example, while To and Flink[136] had acknowledged that "the relationship between Tc and MW is identical to the equation for Tg of mixed polymers" and that "collapse and glass transition are (clearly) phenomenologically similar events," they differentiated between Tg and Tc by pointing out that "while glass transitions in polymeric materials are generally reversible, the collapse of freeze-dried matrices is irreversible". A molecular-level examination of this argument, which had been based on the observation of a macroscopic structural change, has shown it to be misleading.[27] At the molecular level, the glass transition for an amorphous thermoplastic aqueous food material is reversible, if the water content of the glass is always <Wg′. That is, a glass at Tg′-Wg′ can be repeatedly warmed and recooled (slowly) over a completely reversible T-W path between its solid and liquid states. The same is true for a completely amorphous (and non-crystallizable) freeze-dried material. Observation of irreversible collapse for a porous matrix does not negate the underlying reversibility between molecular states. Irreversible loss of porosity is simply a macroscopic, morphological consequence of viscous flow in the rubbery state at T > Tg, whereby a porous glass relaxes ("melts back") to a lower-viscosity fluid that is incapable of supporting its own weight against flow and thus becomes non-porous and more dense. As shown in Table 9, the same is true for shrinkage due to loss of entrapped leavening gases in frozen bread dough blanks or loss of overrun in ice cream products stored at Tf > Tg′.[25,32] Subsequent recooling to T < Tg yields a non-porous glass of the original composition, which can then be temperature-cycled with even macroscopic reversibility. The only irreversible aspect of this type of Tg-governed structural collapse is loss of porosity. However, as alluded to in Table 9, a dif-

TABLE 9
Collapse Processes Governed by Tg and Dependent on Plasticization by Water[8]

Processing and/or storage at T < 0°C	Ref.
Ice recrystallization ("grain growth") ≥ Tr	4, 6, 50, 74, 133, 255, 304, 308, 309
Lactose crystallization ("sandiness") in dairy products ≥ Tr	4, 44, 50, 137, 310
Enzymatic activity ≥ Tg′	8, 175, 311—315
Structural collapse, shrinkage, or puffing (of amorphous matrix surrounding ice crystals) during freeze drying (sublimation stage) ≅ "melt-back" ≥ Tc	4, 40, 44, 57, 125, 133, 136—138, 256, 258, 276, 303—305, 316
Structural collapse or shrinkage due to loss of entrapped gases during frozen storage ≥ Tg′	25, 32
Solute recrystallization during freeze drying (sublimation stage) ≥ Td	193, 317
Loss of encapsulated volatiles during freeze drying (sublimation stage) ≥ Tc	136—138
Reduced survival of cryopreserved embryos, due to cellular damage caused by diffusion of ionic components ≥ Tg′	262
Reduced viability of cryoprotected, frozen concentrated cheese-starter cultures ≥ Tg′	318
Reduced viability of cryoprotected, vitrified mammalian organs due to lethal effects of ice crystallization ≥ Td	251, 298, 319, 320
Staling due to starch retrogradation via recrystallization in breads and other high-moisture, lean baked products during freezer storage ≥ Tg′	26

Processing and/or storage at T > 0°C	Ref.
Cohesiveness, sticking, agglomeration, sintering, lumping, caking, and flow of amorphous powders ≥ Tc	44, 54, 66, 136—138, 289, 303, 321—328
Plating, coating, spreading, and adsorbing of, for example, coloring agents or other fine particles on the amorphous surfaces of granular particles ≥ Tg	329, 330
(Re)crystallization in amorphous powders ≥ Tc	44, 54, 55, 66, 136—138, 324
Recrystallization due to water vapor adsorption during storage of dry-milled sugars (i.e., grinding → amorphous particle surfaces) ≥ Tg	82
Structural collapse in freeze-dried products (after sublimation stage) ≥ Tc	54, 126, 136—138, 303
Loss of encapsulated volatiles in freeze-dried products (after sublimation stage) ≥ Tc	54, 136—138, 289, 331

TABLE 9 (continued)
Collapse Processes Governed by Tg and Dependent on Plasticization by Water[a]

Processing and/or storage at T < 0°C	Ref.
Oxidation of encapsulated lipids in freeze-dried products (after sublimation stage) ≥ Tc	54, 55, 136, 137
Enzymatic activity in amorphous solids ≥ Tg	86, 175, 332, 333
Maillard browning reactions in amorphous powders ≥ Tg	321
Sucrose inversion in acid-containing amorphous powders ≥ Tg	28
Stickiness in spray drying and drum drying ≥ T sticky point	54, 136—138, 289, 303, 317
Graining in boiled sweets ≥ Tg	44, 89, 137, 334-339
Sugar bloom in chocolate ≥ Tg	340, 341
Color uptake due to dye diffusion through wet fibers ≥ Tg	121
Gelatinization of native granular starches ≥ Tg	21, 207
Sugar-snap cookie spreading (so-called "setting") during baking ≥ Tg	25, 26
Structural collapse during baking of high-ratio cake batter formulated with unchlorinated wheat flour or with reconstituted flour containing waxy corn starch in place of wheat starch (due to lack of development of leached-amylose network Tg) ≥ Tg′	25, 26, 47
Recrystallization of amorphous sugars in ("dual texture") cookies at the end of baking vs. during storage ≥ Tg	26
"Melting" (i.e., flow) of bakery icings (mixed sugar glasses) due to moisture uptake during storage ≥ Tg	26
Staling due to starch retrogradation via recrystallization in breads and other high-moisture, lean baked products during storage ≥ Tg′	26

ferent scenario, potentially advantageous or disadvantageous to the processing and subsequent storage stability of particular materials, can pertain to the freeze-drying of a solute that is crystallizable during warming.[193,307] In such a case, the glass transition can be followed immediately by a second transition, solute devitrification, representing irreversible solute (re)crystallization and concomitant disproportionation in the mobile state of the undercooled rubbery fluid at T > Tg′.[31] The important distinction in this scenario is that only the solute (e.g., lactose[50]) crystallizes during warming to T ≥ Td ≥ Tg′ of the partially vitrified (i.e., ice-containing) solution, for which the operative Tc for the onset of collapse would be Tg′.[34] It is intended to be differentiated from the phenomenon of eutectic crystallization on cooling, such as for mannitol, in which case Tc = Te.[304,305]

This interpretation of the physicochemical basis of collapse has also provided insights to the empirical countermeasures traditionally employed to inhibit collapse processes.[27] In practice, collapse in all its different manifestations can be

prevented, and food product quality, safety, and stability maintained, by the following measures:[8] (1) storage at a temperature below or sufficiently near Tg;[44] (2) deliberate formulation to increase Tc (i.e., Tg) to a temperature above or sufficiently near the processing or storage temperature, by increasing the composite $\overline{M}w$ of the water-compatible solids in a product mixture, often accomplished by adding polymeric (cryo)stabilizers such as high MW SHPs or other polymeric carbohydrates, proteins, or cellulose and polysaccharide gums to formulations dominated by low MW solutes such as sugars and/or polyols;[44,66,136-138,289,303] and (3) in hygroscopic glassy solids and other low-moisture amorphous food systems especially prone to the detrimental effects of plasticization by water (including various forms of "candy" glasses),[44] (a) reduction of the residual moisture content to $\lesssim$3% during processing, (b) packaging in superior moisture-barrier film or foil to prevent moisture pickup during storage, and (c) avoidance of excessive temperature and humidity ($\gtrsim$20% RH) conditions during storage.[44,137] The successful practice of the principles of cryostabilization technology has often been shown to rely on the critical role of high-polymeric carbohydrates and proteins in preventing collapse (by raising the composite $\overline{M}w$ and resulting Tg′ of a frozen product relative to Tf) and to apply equally well to low-moisture foods, such as amorphous, freeze-dried powders.[8,15,25-28,31-34,40,41,66]

2. Physicochemical Basis

Collapse processes during freezer storage are promoted by the presence of high contents of small carbohydrates of characteristically low Tg′ and high Wg′ in the composition of many frozen foods (e.g., desserts).[8,27,31-34] The fundamental physicochemical basis of the cryostabilization of such products has been illustrated by the idealized state diagram (modeled after the one for fructose-water in Figure 53) shown in Figure 63, which has also been used to explain why Tg′ is the keystone of the conceptual framework of this technology.[31-34] As shown in Figure 63, the matrix surrounding the ice crystals in a maximally frozen solution is a supersaturated solution of all the solute in the fraction of water remaining unfrozen. This matrix exists as a glass of constant composition at any temperature below Tg′, but as a rubbery fluid of lower concentration at higher temperatures between Tg′ and the Tm of ice. If this amorphous matrix is maintained as a mechanical solid, as at Tf1 < Tg′ and local $\eta > \eta g$, then diffusion-limited processes that typically result in reduced quality and stability can be virtually prevented or, at least, greatly inhibited. This physical situation has been illustrated by scanning electron microscopy photographs[32] of frozen model solutions, which show small, discrete ice crystals embedded and immobilized in a continuous amorphous matrix of freeze-concentrated solute-UFW that exists as a glassy solid at T < Tg′. The situation has been described by analogy to an unyielding block of window glass with captured air bubbles.[32] In contrast, storage stability is reduced if a natural material is improperly stored at too high a temperature, or a fabricated product is improperly formulated, so that the matrix is allowed to exist as a rubbery fluid at Tf2 > Tg′ (see Figure 63), in and through which diffusion is free to occur. Thus, the Tg′ glass has been recognized as the manifestation of a kinetic barrier to any diffusion-limited process,[6,8] including further ice formation (within the experimental time frame), despite the continued presence of UFW at all temperatures below Tg′. (Analogously, Ellis[111] has remarked on the ability of a continuous glassy matrix of synthetic polyamide to act as a barrier to rapid moisture loss during DSC heating of a water-plasticized, partially crystalline glassy polyamide sample.) The delusive "high activation energy" of this kinetic barrier to relaxation processes has been identified as the extreme temperature dependence that governs changes in local viscosity and free volume (and, consequently, heat capacity,[106] as illustrated in Figure 33) just above Tg.[34] This perspective on the glass at Tg′-Cg′ as a mechanical barrier has provided a long-sought[256] theoretical explanation of how undercooled water can persist (over a realistic time period) in a solution in the presence of ice crystals.[32-34] Recognizing these facts, and relating them to the conceptual framework described by Figure 63, one can appreciate why the temperature of this glass transition is so important to aspects of frozen food

technology involving freezer-storage stability, freeze-concentration, and freeze-drying,[4,6,40-42,50] which are all subject to various recrystallization and collapse phenomena at $T > Tg'$.[8,27]

The optimum Tf for a natural material or optimum formula for a fabricated product is dictated by the Tg′ characteristic of a particular combination of solutes and UFW in the matrix composition of the glass at Tg′-Cg′.[8,27,31-34] Tg′ is governed in turn by the $\overline{M}w$ of this particular matrix combination in a complex food system.[6,8,30] Moreover, the dynamic behavior of rubbery frozen food products during storage above Tg′ is dramatically temperature-dependent, and the rates of diffusion-limited deterioration processes are quantitatively determined by the temperature difference $\Delta T = Tf - Tg'$ (in °C).[15,32] These rates have been shown to increase exponentially with increasing ΔT, in agreement with WLF, rather than Arrhenius, kinetics.[32-34] Results of a cryomicroscopy experiment (shown in Table 10[32]), in which the increase in ice crystal diameter was measured as a function of Tg′ for a series of model sugar/maltodextrin solutions (Tg′ range −9.5 to −31°C) after 4 weeks of storage in a −18°C home freezer, illustrated this dynamic behavior and the cryostabilizing (i.e., Tg′-elevating) effect of a high MW SHP.[8,27] When Tf was below Tg′ ($-18 < -9.5$°C), the ice crystal size remained nearly the same as for the initially frozen samples. When Tf was above Tg′, the increase in ice crystal size (i.e., decreasing stability) demonstrated a striking correlation with decreasing Tg′ (thus, increasing ΔT), and the temperature dependence was clearly greater than that expected for Arrhenius kinetics.

3. Food Cryostabilizers and Cryoprotectants

Tg′ and Wg′ results for a broad range of food ingredients have permitted the definition of a cryostabilization technology "spectrum" of low-temperature thermal behavior of frozen aqueous food systems, which is illustrated schematically by the hatched band in Figure 64.[32] Insights gained from this spectrum have led to the identification of "polymeric cryostabilizers" as a class of common water-compatible food ingredients, including low DE SHPs and proteins, with a characteristic combination of high Tg′ and low Wg′ values.[8,25] DSC investigations of polymeric cryostabilizers have provided an understanding of their stabilizing function, via their influence on the structural state of a complex amorphous matrix, as conceptualized in Figure 63. This function derives from their high MW, and the resulting elevating effect of such materials on the composition-dependent Tg′ (and corresponding depressing effect on Wg′) of a complex frozen system. Increased Tg′ leads to decreased ΔT (relative to Tf), which in turn results in decreased rates of change during storage, and so to increased stability of hard-frozen products. The efficacy of polymeric cryostabilizers in frozen products has also been explained in terms of the relative breadth of the temperature range for the relevant WLF region, i.e., the magnitude of the rubbery domain between Tg′ and the Tm of ice,[15,30] as described earlier with respect to the schematic state diagram in Figure 35 and the actual state diagram for sucrose in Figure 61, with its WLF domain between Te and Tg′ of

TABLE 10
Ice Crystal Size vs. Tg′ of Aqueous Carbohydrate Model Solutions[32]

Solution composition	Tg′, °C	Ice crystal diameter (μm)
10 w% 10 DE maltodextrin	−9.5	50
10 w% 10 DE maltodextrin + 20 w% sucrose	−21.5	150
10 w% 10 DE maltodextrin + 20 w% fructose	−31	300

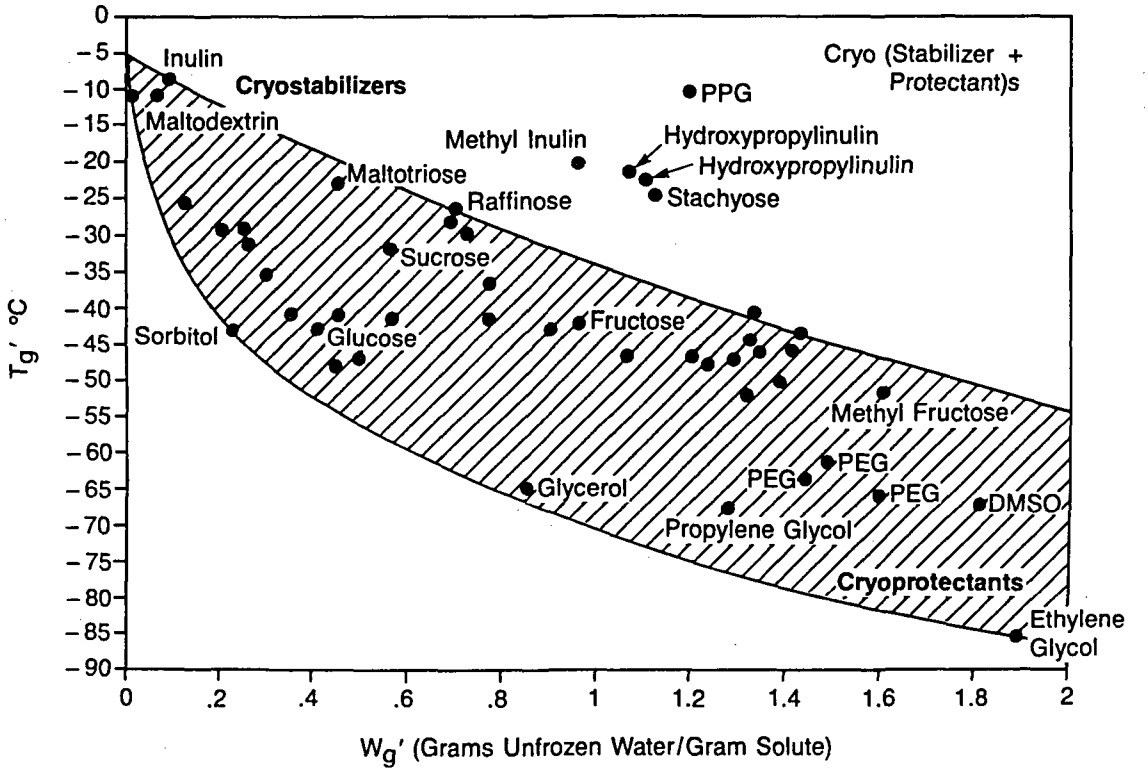

FIGURE 64. Variation of the glass transition temperature, Tg′, for maximally frozen 20 w% solutions against Wg′, the composition of the glass at Tg′, *in g unfrozen water/g* solute, for a series of water-compatible carbohydrates, including many compounds represented in Figures 41 and 44, illustrating the cryostabilization "spectrum" from monomeric cryoprotectants to polymeric cryostabilizers. (Solutes lying outside the hatched area of the "spectrum" [toward the *upper right corner*] exhibit properties of both cryoprotectants and cryostabilizers.) (From Levine, H. and Slade, L., *Cryo.-Lett.*, 9, 21, 1988. With permission.)

only 18°C. This ΔT (= Tm − Tg′) decreases with increasing solute MW, from >50°C for very low MW polyols and amino acids (with Tg′ < −50°C)[25,27] to <5°C for very low DE SHPs (with Tg′ > −5°C).[32] Thus, as this ΔT decreases, the magnitude of the corresponding temperature region of freezer-storage instability (between Tf and a lower Tg′) likewise decreases, so that even at higher freezer temperatures, the probability of acceptable product stability would be improved.[34] It has also been inferred from Figure 35 that the use of polymeric cryostabilizers provides another potential product benefit, in that it would only be necessary to traverse a much smaller temperature range in order to go from the hard-frozen (storage-stable) state of a glassy product at T < Tg′ to the soft texture of a partially melted product (of desirable eating quality) at T > Tm.[34] Again, the specific case of sucrose in Figure 61 illustrates this point explicitly. Over the temperature range of only 18°C from Tg′ to Te, the microscopic viscosity of the amorphous sucrose-water matrix would decrease dramatically from $\eta \gtrsim 10^{13}$ Pa s at T < Tg′ to $\eta \lesssim 1$ Pa s at T > Te.

In contrast to cryostabilizers, low MW solutes (e.g., sugars, polyols, glycosides, and amino acids)[25,27] with a characteristic combination of low Tg′ and high Wg′ values have been predicted and subsequently demonstrated to have utility as "monomeric cryoprotectants" in freezer-stored food products with desirably soft-frozen texture, but undesirably poor stability.[8,15,32-34] The poor stability results from low Tg′ and consequently relatively large ΔT of Tf above Tg′. The soft-frozen texture has a dual origin: high Wg′, the UFW in the reference glass, reflects the relatively low ice content of the system and large ΔT reflects the relatively large extent of softening of the non-ice portion of the system.[32] In contrast

to the use of cryoprotectants for soft-frozen texture of food products,[15] the medical use of cryoprotectants benefits only from the low ice content of cryopreserved specimens.[34,251,298]

For many of the low MW reducing sugars in Table 3, sweetness, hygroscopicity, humectancy, and browning reactions are salient functional properties.[8,264] A more specialized application involves the potential for cryoprotection of biological materials, for which the utility of various low MW, glass-forming sugars, polyols, and amino acids is well known.[4,5,243,260,261] Such cryoprotectants can be produced endogenously in complex biological systems or added as exogenous agents.[5] A recent illustration of the latter involved a straightforward example of cryoprotection by dilute PHCs in ice-containing solutions. As alluded to in Table 9, results of Chavarri et al.[318] showed that frozen concentrated cheese-starter cultures, stored for 2 months at $Tf < Tg'$ of a lactose or sucrose cryoprotectant solution, manifested higher viability and acid-producing activity than corresponding samples stored at $Tf > Tg'$.

In a different vein, complete vitrification has been mentioned as another possible approach to the prolonged cryopreservation of complex biological systems,[50] such as mammalian organs.[251,298,319,320] Consistent with this view, a comparison of Figure 41 with the functionality map of Figure 44 suggested that small sugars and glycosides, in sufficiently concentrated solution (i.e., $C > Cg'$, as illustrated in Figure 63), can be undercooled to a completely vitrified state, so that all the water would be immobilized in the solute-UFW glass.[27] Such vitrification, which can be easily achieved in the laboratory,[241] has been suggested as a natural, intracellular, cryoprotective mechanism in winter-hardened poplar trees,[342,343] and demonstrated as a potential means of cryoprotecting whole body organs and embryos.[251,298,319,320,344] The essence of this cryoprotective activity appears to be the prolonged avoidance (via kinetic metastability) of potentially lethal ice formation and solute crystallization in concentrated, undercooled solutions of PHCs with high Wg' values.[50] For several polyols typically used as exogenous cryoprotectants, a comparison of the concentration of infused cryoprotectant required to vitrify rabbit kidneys at atmospheric pressure[298] with the corresponding solute concentration, Cg', in the glass at Tg' has shown that, in each case, the minimum solute concentration required for complete organ vitrification was closely related to Cg'.[34]

This functionality of PHCs also appears to be related to food applications involving soft-, spoonable-, or pourable-from-the-freezer products.[15] An example is Rich's patented "Freeze-Flo" beverage concentrate formulated with high-fructose corn syrup.[345] Part of the underlying physicochemical basis of such products involves both colligative and non-equilibrium freezing point depression. This is illustrated by the idealized state diagram in Figure 63, which reveals a hatched liquid solution zone, bordered by the liquidus and glass curves and extending below Tf2, for w% solute concentrations between x and y, which bracket Cg'. However, contrary to first appearances, the functionality of specific PHC solutes in practical products depends more on the kinetically determined properties of Tg' and Wg' than on simple colligative depression of equilibrium freezing point.[31] This fact has been demonstrated by model-system experiments in which 60 w% solutions of fructose and mannose (3.3 *M*), methyl fructoside (3.1 *M*), ethyl fructoside, ethyl mannoside, and ethyl glucoside (2.9 *M*) remained pourable fluids (completely ice- and solute crystal-free) during more than 4 years of freezer storage at $-18°C$ (i.e., at a temperature substantially below their equilibrium freezing points),[15] at which point the experimental samples were left behind when the experimenters changed companies.

In the context of the above discussion of the aqueous-glass-forming properties of small PHCs, and their consequent functionality as endogenous or exogenous cryoprotectants in the cryopreservation (via complete vitrification) of biological systems, the remarkable properties of trehalose are worthy of special mention. This non-reducing disaccharide has attracted a great deal of recent interest (see[290] and references therein), due to its demonstrated role as the key endogenous biopreservation agent responsible for producing an "astounding propensity for drought survival" in certain plant seeds, spores, and lower animals capable of "passing, in dry times, into a state of suspended animation" (suggested to correspond

to a glassy solid state).[290] As reviewed by Green and Angell,[290] this "dehydroprotectant" effect has been shown to be related to the structural-functional stabilization of cell membranes and was previously hypothesized to involve the hydroxyl groups of trehalose. Note that, in contrast to the subzero temperature-low moisture (i.e., $W < Wg'$, but Wg' characteristically high) region of the dynamics map relevant to the functional behavior of typical endogenous biological cryoprotectants, the map region of ambient temperature-much lower moisture (i.e., $W \ll Wg'$, or $W < Wg'$, but Wg' uncharacteristically low [as is the case for trehalose, as shown in Table 3]) is the domain pertinent to the functional behavior in nature of trehalose as a dehydroprotectant. Trehalose has been shown to be significantly more effective in protecting cell membranes against dehydration and in inhibiting dehydration-induced fusion between liposomal membranes than many other "dehydroprotecting" small PHCs (all of which have higher Wg' values than trehalose), including various polyols and di- and monosaccharide sugars.[290] Importantly, however, Green and Angell[290] have noted that "there is no clear structural explanation for the relative efficiency (of trehalose over other small PHCs) except that it is *not* related to the number or position of hydroxyl groups available for hydrogen bonding."

Based on their analysis of the complete glass curves of trehalose, sucrose, maltose, glucose, and glycerol, Green and Angell have suggested that the superiority of trehalose as a dehydroprotectant is connected with the exceptional glass-forming characteristics of this dry solute and its low-moisture solutions.[290] They have reported that the dry Tg of trehalose (i.e., 79°C, if measured at the midpoint of the transition,[183] in agreement with our measured value shown in Table 3) is significantly higher than the corresponding dry Tg values of the other two disaccharides (of the same MW) and of glucose and glycerol (of lower MWs), and that the same order of Tg values applies to corresponding solute-water compositions over the entire measured glass curves for these PHCs.[290] While the descending order of Tg values for maltose (MW 342), glucose (MW 180), and glycerol (MW 92) can be accounted for (at least qualitatively) by the expected variation of dry Tg with solute MW,[28] the descending order of dry Tg values (see Table 3) for trehalose, sucrose, and maltose (disaccharides of equal MW) cannot be. Green and Angell have noted that "the order of Tg values is some function of the viscosity of an intracellular medium. The viscosity plays an important role in cell preservation by impeding crystallization during cooling and thereby permitting vitrification. It can also inhibit water loss by reducing diffusion rates to the free surface."[290] Green and Angell have remarked that "trehalose displays, as does glycerol, many of the characteristics of a (biological) cryoprotectant", but they have pointed out the absence of previous literature data for trehalose on the conditions of temperature and water content (a) "at which crystallization of ice or sugar is suppressed", and (b) at which "a principal cryoprotection feature, viz. the transition into the glass state, occurs."[290]

It can be deduced from Green and Angell's[290] Tg data for the anhydrous solutes and aqueous solutions that the portion of the glass curve for trehalose-water critical to dehydroprotection (i.e., at $Tg' < T <$ dry Tg and $W < Wg'$) is located well above the corresponding portions of the aqueous glass curves for the other PHCs, including the two other disaccharides. In support of their suggestion that trehalose-protected "anhydrobiotic organisms are actually in the vitreous state while in suspended animation", Green and Angell[290] have pointed out that, of the PHCs they analyzed, only in "the trehalose system at water contents less than approximately two water molecules per glucose ring (i.e., $W \lesssim Wg' \simeq 17$ w% water) are solutions in the glassy state at ambient conditions." In light of this illuminating finding, they have suggested that "formation of a glassy state would naturally account for the prevention of fusion of vesicles during dehydration as well as stopping solute leakage during rehydration, since fusion involves molecular diffusion which does not occur in the glassy state."[290] They have also noted that "the cryoprotectant role of trehalose is analogous to that of PVP. Trehalose would be a very effective non-penetrating agent preventing freezing of the extracellular fluid."[290] They have concluded that "it is apparent that the trehalose-water system whose passage into the glassy state arrests all long-range

molecular motion, suspending both life and decay processes, should be further investigated with respect to biopreservation."[290]

We echo the sentiment of their important conclusion, and suggest that it has broader relevance to the issue of the potential utility of trehalose as a preservative in foods. Coupling the findings of Green and Angell[290] with our own results, we suggest that the effectiveness of trehalose as a dehydroprotectant evidently involves its exceptional (for its MW) combination of high dry Tg and low Wg′. As shown by our data in Table 3, only one disaccharide (mannobiose) has a higher measured dry Tg than trehalose. And trehalose has the lowest measured Wg′ of *all* the PHCs listed in Table 3. Moreover, as pointed out earlier in Table 6, because it has the lowest Wg′, trehalose has the highest $\overline{M}n$ for the composition of the solute-UFW glass at Tg′, reflecting the lowest free volume requirement for mobility near Tg′. In the context of the spectrum of cryostabilizers and cryoprotectants illustrated in Figure 64, the anomalously low Wg′ and high dry Tg of trehalose correspond more closely (than do the Tg′ and Wg′ values of any other small PHC of comparable MW) to the characteristics diagnostic of a *polymeric* cryostabilizer. Thus, the unique aqueous-glass-forming characteristics and lipid bilayer membrane-protecting effects of trehalose strongly suggest its consideration as a stabilizer in a broad range of food applications involving water- and/or fat-based products (both natural and fabricated) that span the entire spectrum of water contents and processing/storage temperatures, including, for example (a) high-moisture, frozen, fat-containing (e.g., emulsified) products, and (b) intermediate-moisture or low-moisture, shelf-stored, fat-containing (e.g., emulsified) or fat-free products. The potential utility of trehalose (exogenous or endogenous) for the structural-functional stabilization of notoriously delicate plant cell membranes in certain fruits and vegetables (in fresh, refrigerated, frozen, freeze-dried or otherwise dehydrated forms) should be an obvious area of special focus.

Returning once more to the context of biological cryopreservation via glass formation, a final point is worthy of mention. As shown in Figure 64, certain solutes are unusual in their low-temperature thermal behavior, in that they exhibit the combined properties of both polymeric cryostabilizers (high Tg′) and monomeric cryoprotectants (high Wg′). For example, as illustrated in Figure 62, high-polymeric PVP has a typically high Tg′ of about −20°C, coupled with an unusually high Wg′ of about 0.54 g UFW/g (about the same Wg′ as sucrose). A recent study by Hirsh of the mechanism of biological cryoprotection of cells by extracellular polymeric cryoprotectants "showed that polymers which protect cells best have a Tg′ value of about −20°C (e.g., PVP); below −20°C, glass formation prevents the injurious osmotic stress that cells face during slow freezing by isolating cells from extracellular ice crystals, thus virtually eliminating cell water loss at lower temperatures".[346] Due to its high Wg′, as well as its high Tg′, PVP would be effective as an extracellular polymeric cryoprotectant by limiting the amount of extracellular ice formed, and thus reducing the osmotic stress on intracellular water, during slow freezing to $T < Tg'$.

The elucidation of the structure-property relationships of food cryostabilizers and cryoprotectants has revealed the underlying physicochemical basis of fundamental (and intuitive) correlations between the critical functional attributes of storage stability and texture of frozen foods.[32,34] As an essentially universal rule, for both complex products and model systems of single or multiple solutes, higher Tg′ and lower Wg′ values (due to higher $\overline{M}w$) have been shown to go hand-in-hand with, and be predictive of, harder-frozen texture and increased storage stability at a given Tf, while conversely, lower Tg′ and higher Wg′ values (due to lower $\overline{M}w$) go hand-in-hand with, and are predictive of, softer-frozen texture and decreased storage stability. These intrinsic correlations, which have been found to apply to various types of frozen foods,[25,37,38] have been recognized as underlying precepts of the cryostabilization technology spectrum, which derive from the effect of solute MW on Tg′ and Wg′.[32] A second contribution to textural hardness of products characterized by high Tg′ values derives from the elevated modulus of

the amorphous matrix and is directly related to the mechanical stabilization against diffusion-limited processes such as ice crystal growth.[34]

D. Ramifications of WLF Behavior in High-Moisture Food Systems at T > Tg'

In a further effort to clarify an area of possible confusion and contention, identified by the referee, we discuss in this section the following two interrelated issues: (1) Tg' as the appropriate reference temperature for WLF kinetics in high-moisture food systems at temperatures above Tg'; and (2) Wg' as the maximum *practical* amount of plasticizing water (but *not* to be defined as the mythical "bound water") in such systems with water contents >Wg'.

Let us consider first the case of an ice-containing, solute-water system located somewhere along the liquidus curve (i.e., at some Tm > Tg'), having originated at the Tg'-Wg' glass and undergone partial melting of ice during warming to the instant solute-unfrozen water composition (W > Wg') of the non-ice portion of the sample. For this particular case, with pre-existing ice, cooling at practical rates would return the system to the Tg'-Wg' glass. Still, one might ask why another Tg, lower than Tg' and corresponding to the glass with the same instant composition (W = Wg > Wg'), is not a more appropriate reference than Tg' for description of the behavior of this system according to WLF-type kinetics. As mentioned earlier, we consider this lower Tg to be an artificial, rather than pertinent, reference state for the ice-containing system under discussion, because the system would not have come from this lower Tg upon heating, nor would it return to this lower Tg upon cooling at practical rates.[33]

For this reason, we consider the Tg'-Wg' glass as *the* "practical reference state" for this particular ice-containing system at Tm > Tg' and W > Wg'. (An experimental validation of this point, with respect to the behavior of rubbery frozen food products during storage, is described later in Section V.D.3.) But what about a different case of (1) a system that is neither nucleated nor ice-containing, perhaps situated only just above the liquidus curve (i.e., at T[c] > Tm[c]), and (2) any desired, hypothetical cooling and warming rates, perhaps supplemented by any desired manipulation of pressure in the kilobar range? Then we may consider a solute-water solution instantaneously *captured* in an unstable, ice-free condition at some point along an imaginary vertical line between its Tm and Tg. The captivation might be accomplished by (a) extremely rapid cooling to T < Tg, followed by extremely rapid heating to Tg < T < Tm, or (b) cooling to Tm > T > Th > Tg, and prior to homogeneous nucleation upon further cooling to Tm > Th > T > Tg, or by cooling at 2 kbar pressure to Tg < T < Tm. This Tg below Tg' would then be a candidate for consideration as a WLF reference state, albeit not a practical one.

As discussed earlier in Section III.A.4, we make a critical distinction between water-compatible and water-sensitive solutes, with respect to the temperature-dependence of their *practical* (i.e., effective), solute-water glass curves. Because of the much more limited thermodynamic compatibility of water-sensitive solutes (e.g., nylons, PVAc, lignin) for solvating/plasticizing water, their practical glass curves are depressed much less by increasing water content and remain well above 0°C, no matter how much water is added to such a solute. The solubility parameter[113] of water is too high at room temperature to make water an effective plasticizer of nylon;[155] it decreases, and water becomes a more compatible plasticizer of nylon as temperature is increased above room temperature; it increases further, and water becomes incapable of plasticizing nylon as temperature is decreased. If water were added to nylon at a sufficiently high temperature and then quench-cooled at a sufficiently rapid rate, a lower Tg than the effective minimum value at about 6.5 w% water[155] could be demonstrated. However, the Tg of a water-sensitive solute is *never* capable of being depressed enough, such that, upon cooling at practical rates in the presence of excess water, it would reach a subzero Tg' (and corresponding Wg') that would be characteristic of, and specific for, each given solute-water system.[15] In contrast, the practical glass curve for a water-compatible solute can be depressed much more by increasing water content. Consequently, the Tg of a water-compatible solute is *always* capable of being depressed enough, such that,

upon cooling at practical rates in the presence of excess water, it reaches a subzero Tg′ (and corresponding Wg′) that is characteristic of, and specific for, each given solute-water system.[15] An important, related symptom of this greater extent of solute-water compatibility is that the solute-specific Tg′ is, by definition, equal to the corresponding solute-water Tm at Wg′, such that only the amount of water in excess of this Wg′ amount will be freezable (in a practical time frame) upon cooling at practical rates.[8] Thus, Wg′ represents the maximum *practical* amount of plasticizing water (≡ "unfreezable" water) for a given solute, and amounts of water in excess of Wg′ would not be additionally plasticizing under practical conditions.[8,15,30] (Note that we also distinguish, for this reason and based on grounds of what is practical [as already defined] and relevant to ice-containing, frozen aqueous systems, between the *practical* glass curve [which levels off at Tg′ for water contents ≥Wg′] and the *complete* glass curve [which decreases smoothly and continuously from the solute's dry Tg to the Tg of pure amorphous water at ~ −135°C] for a water-compatible solute, as illustrated in Figure 27.) Wg′ represents the maximum amount of water that can exist with all of the solute, under practical conditions *at any temperature* from T < Tvap to T = 0°K, in a homogeneous, single phase (liquid or metastable amorphous solid) capable of cooperative, molecular mobility (at T > Tg′).[30] In contrast, amounts of water in excess of Wg′ would exist in a separate, water-rich phase, as pure ice at T < Tm or as dilute solution at Tm < T < Tvap.[30] Thus, in the first case described above, the amount of water in the system that had arisen from the partial melting of ice would not be solute-plasticizing water (even though it would obviously be solute-diluting and viscosity-lowering water), and so would not alter the appropriateness of Tg′ as the Tg reference state for WLF-type kinetics.

In many critical aspects, the behavior of a water-compatible solute at a water content > Wg′ would be analogous to that of a synthetic high polymer in the presence of an excess amount (say, >30 w%, where Dg′ = 30 w%) of an organic plasticizing diluent (D) that can crystallize (as exemplified in Figure 29). For example, if one cooled the latter system at a sufficient rate, one *could* capture a metastable, homogeneous glass with a diluent content >30 w% and maintain this glassy state at temperatures below the Tg of the 70− w% polymer/30+ w% diluent mixture. However, if one then raised the temperature to T > Tg, under conditions such that some of the diluent could and would crystallize after devitrification, then Tg′ of the remaining 70 w% polymer/30 w% diluent mixture would become the appropriate reference Tg. If the excess amount of diluent (i.e., 30+ w% − Dg′), which had crystallized on warming, were permitted to melt on further warming to T > Tg′, this excess diluent would exist as a separate, diluent-rich phase, perturbed by the solute, but *not* plasticizing the solute.

We have suggested that, for water-compatible solutes at low moisture contents (0 < W < Wg′), the portion of the practical glass curve between Tg of the dry solute and Tg′ serves to define a continuum of real reference states (corresponding to a continuum of practical solute-water compositions) for WLF-type kinetics.[15,30] This suggestion has been recently validated by the results of an experimental study of the crystallization kinetics of amorphous sugars at low moisture contents by Roos and Karel.[66] In the region of the state diagram surrounding this portion of the glass curve, Tg is both defined *and* accessible on a 200-s time scale,[174] because no phase separation of water can occur, so the solute-water composition of the system remains constant and homogeneous.[30] In contrast, in the region of the state diagram (lower left quadrant) surrounding the portion of the glass curve between Tg′ and the Tg of water, Tg is still *defined* on a 200-s time scale, but is only accessible on a time scale many orders of magnitude smaller;[4] otherwise, water phase-separates as ice and the remainder of the system arrives at Tg′-Wg′.[33] Thus, in practice, Tg values in this region are neither real nor relevant to questions about the kinetics of diffusion-limited processes.[33,39] Unfortunately, it is in this same region of the state diagram, for higher-moisture situations (W ≥ Wg′) for the diluted solute, that our interpretation of the applicable form of the WLF equation and the appropriate reference state for its use has been questioned.[98] Based on (1) the explicit description, in Chapter 17 of Ferry's book,[107] of the

variation of the WLF coefficients (C1 and C2) with increasing diluent concentration, for plasticizers that are both (a) non-crystallizing, and (b) thermodynamically compatible over the entire temperature range of dilution, and (2) our analysis[30] of (a) the effect of temperature-dependent thermodynamic compatibility of the plasticizer, and (b) the effect of the variation of the magnitude of the WLF region (Tm − Tg) for crystallizing plasticizers on the WLF coefficients, we have suggested that the proper coefficients of the WLF equation must change with changing diluent concentration.[30] When the plasticizer is non-crystallizing and thermodynamically compatible over the entire temperature range, (1) the change in coefficients is continuous from 0 to 100% plasticizer, (2) the total diluent concentration defines the concentration of the plasticizer in the glassy solute-diluent blend, and (3) the Tg of the glassy solute-diluent blend is *the* reference temperature for the WLF equation with appropriate coefficients for that extent of dilution.[107] Most of the literature on the free volume description of WLF kinetics deals with either undiluted synthetic polymers or dilution by such well-behaved, non-crystallizing, thermodynamically compatible plasticizers.[107] In contrast, when the plasticizer becomes ever-less thermodynamically compatible with decreasing temperature, such as tricresyl phosphate with poly(vinyl chloride),[109] or in the extreme case, when the diluent, such as water, is capable of complete phase separation via crystallization, (1) the change in coefficients is only continuous from 0% diluent to the region of diluent concentration-temperature where incompatibility or phase separation is exhibited (namely, Wg′-Tg′ for water), (2) the total diluent concentration does *not* define the concentration of plasticizer in the glassy, plasticizer-plasticized solute blend, and (3) the minimum reference Tg is that of the glass with maximum *effective* plasticizer content. This complicated behavior, which is the rule for aqueous systems, has not been extensively described in the literature. In Chapters 11, 12, and 17 of his book,[107] Ferry provides the bare minimum of information that is required to deal with systems of small molecular weight, plasticizers of marginal compatibility, and crystallizing diluents. We have expanded his analysis by demonstrating that the Tm/Tg ratio or Tm − Tg for the diluent-free solute can be used to provide normalizing guidelines for the identification of appropriate WLF coefficients.[30]

Another salient feature of the behavior of water-compatible solutes, at water contents both above and below Wg′, which we believe emphasizes the singularity of the Tg′-Wg′ reference state/point, involves sorption isotherm data that we have treated in terms of iso-RVP contours for glassy, rubbery, and supra-glassy substrates (see Figure 65, described in detail later in Section V.A.2). RVP goes from zero for a glassy substrate at temperatures and moisture contents below its effective Tg to 1 for the corresponding liquid substrate at temperatures higher than those corresponding to its rubbery state (i.e., temperatures corresponding to its supra-glassy state). However, while at temperatures (T > Tg) and moisture contents (W > Wg) corresponding to the rubbery region, RVP increases significantly with increasing water content, and the iso-RVP contours (like iso-viscosity contours) essentially parallel the shape of the solute-water glass curve; at temperatures >Tg′ and water contents >Wg′, RVP approaches 1, and the iso-RVP contours become vertical, i.e., lose their temperature-dependence. We interpret this as evidence for the fact that the substrate would exist under these T-W conditions in a supra-glassy, liquid state well above the relevant reference state, Tg′-Wg′. Importantly, if sorption were to continue and, thus, the water content of the substrate were to continue to increase to higher and higher levels above Wg′ (a situation analogous in certain vital respects to that of the partially melted, frozen aqueous system described earlier), the resultant changes in RVP, caused by this additional amount of sorbed water, would become insignificant.

The focal point of our interpretations regarding Tg′ as the appropriate reference state for WLF-type kinetics in high-moisture systems of water-compatible solutes[32] concerns the singularity of the Tg′-Wg′ point for a given solute.[27] For example, were it not for this singularity, how else could one explain the frequently anomalous shape of the non-equilibrium extension of the equilibrium liquidus curve? We have suggested that the Tg′-Wg′ point is not one of *accidental* intersection of the liquidus and glass curves, but rather

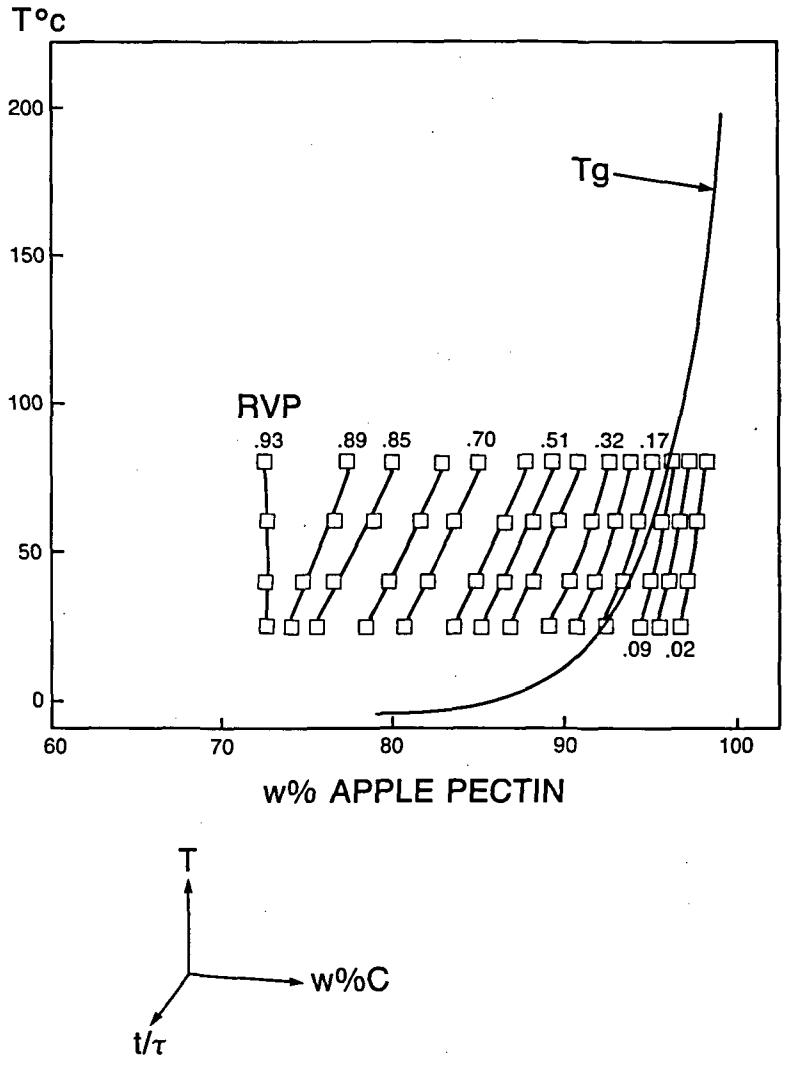

FIGURE 65. Ad/absorption isotherm data for apple pectin from Figure 14A transformed into a two-dimensional water/glass dynamics map of *temperature vs. weight percent solids, on which are compared the relative* locations of a series of iso-RVP contours and a schematic, "practical" glass curve for pectin-water, based on data for hemicellulose (from Reference 129).

the critical point to which the non-equilibrium portion of the liquidus curve *must* fall.[30] We have also noted that the shape of the liquidus curve is also determined indirectly and in part by the shape of the underlying homogeneous nucleation curve.[30] In the region around the Th curve, ice crystal formation (i.e., nucleation) in a dilute solution (W > Wg′) at a given T is influenced, in part, by the portion of the glass curve below the Th curve (i.e., by Tg values <Tg′). However, ice crystal growth (i.e., propagation) in that solution at a given T (and the kinetics thereof) is controlled by Tg′.[32] Once the homogeneous Tg′-Wg′ glass has been formed as a consequence of freezing, one would not expect that subsequent dilution of this glass (via partial ice melting at Tm > T > Tg′) would occur *uniformly* to produce a new supra-glassy, cooperative system.

Information in Chapters 11, 12, and 17 of Ferry's book,[107] on the effects of free volume and local viscosity in concentrated, plasticized polymers, has helped to provide a basis for under-

standing what determines the location of Tg′ (and corresponding Wg′) for a given solute. For synthetic high polymer-organic diluent systems, Ferry teaches that different factors/mechanisms are operative/predominant for different portions of the solute-diluent glass curve, i.e., free volume at low extents of solute dilution vs. local viscosity at lower solute concentrations (e.g., near Dg′). The simple WLF free volume theoretical approach based on the ΔT above Tg (described in Ferry's Chapter 11) is only applicable to the former case, i.e., low extents of solute dilution. However, our experimental results for frozen aqueous solutions of monodisperse PHCs have suggested that, in the maximally freeze-concentrated solute-UFW glass, Tg′ is *not* dependent on/determined by free volume, as evidenced by the lack of correlation between Tg′ and $1/\overline{M}n$ (of the solute-UFW glass), but rather is dependent on/determined by local viscosity, as evidenced by the excellent linear correlation between Tg′ and $1/\overline{M}w$ (Figure 47).[30] Thus, the simple WLF free volume treatment is evidently not applicable in a straightforward way to frozen food systems, and one must instead consider the solute-specific, maximum water content of the glass (Wg′ at Tg′) and base the treatment of kinetics on this singular Tg′-Wg′ reference state.

For the reasons described above, we have concluded that, for water-compatible solutes (monomeric, oligomeric, and polymeric, alike), at water contents ≥Wg′, Tg′ is the appropriate Tg corresponding to the reference state for WLF-type kinetics in the rubbery liquid region at T > Tg′,[32] and to the temperature boundary for Arrhenius kinetics in the glassy solid region at T < Tg′.[15] In contrast to some imaginary, artificial, or purely theoretical reference state, Tg′ is the *real, practical* reference state (and Tg′-Wg′ is the reference point on the state diagram) to which such a solute-water system goes upon cooling at rates such that ice formation occurs at some T < Tm but > Tg′, and from which it subsequently comes upon heating at rates such that the melting of pre-existing ice occurs in the temperature range between Tg′ and Tm.[33,39] This is what we mean by real and practical — cooling rates that permit ice formation, and warming rates that permit ice melting, in the rubbery region between Tg′ and Tm — and why our interpretations have been focused on this Tg′ reference state. It should be recognized that this interpretation goes beyond the WLF theory for diluent-free, synthetic high polymers described in Chapter 11 of Ferry's book,[107] and relies more on the material in Ferry's Chapter 17 on concentrated, plasticized polymers.

As described earlier in Section III.A.4, there is a growing appreciation of the fact that the existence of "bound water" is a myth. However, the preceding explanation of why Tg′ is a pivotal reference temperature for descriptions of WLF behavior depends on a supplementary appreciation of four underlying precepts: (1) rationale for selection of the particular state diagram used as a dynamics map; (2) definition of plasticizing water, in the context of the two primary requirements for an effective plasticizer; (3) identification of Wg′ as the maximum amount of plasticizing water in a practical operational time scale; and (4) reference to melt-dilution as the effect, at temperatures above Tg′, of amounts of water in excess of Wg′. As a result of an incomplete discussion of these points, possible philosophical riddles might appear to arise.[374]

If there is plasticizing water, and non-plasticizing, melt-diluting water, could not one equate plasticizing water with "bound water"? In what ways would plasticizing water be different from the mythical "bound water"? On the other hand, if all of the water is considered a uniform species, with no distinction between plasticizing water and melt-diluting water above Tg′, then the riddle reverts to the original question — is Tg′ the correct temperature to use as a reference for WLF kinetics above Tg′?

For considering the effects of changes in temperature or water content in the region of water content less than Wg′, there is, as alluded to earlier, a general consensus that the appropriate reference locations are the continuous set of pairs of solute-specific Tg-Wg values (such that Tg > Tg′, but Wg < Wg′) on a particular state diagram. This state diagram is a particular two-dimensional (temperature vs. water content, expressed as weight fraction or %) "snapshot" in time, which contains both equilibrium and non-equilibrium states and serves as a dynamics or mobility map.[30] The unique selection of this "snapshot", with its relevant set of Tg-Wg values, reflects the choice of 200 s by polymer scientists as the time scale for the conventional def-

inition of the glass transition.[174] In terms of a DSC experiment, the glass transition temperature is defined by convention as the midpoint of the temperature range (corresponding to a time interval of 200 s) from the onset to the completion of the relaxation that accounts for the increase in free volume that is manifested as a step-increase (discontinuity) in heat capacity (with a concomitant increase in expansion coefficient).[106] For example, at a heating rate of 10 K/min, the glass-to-rubber relaxation is observed as a step-increase in heat capacity over a temperature range of about 33 K; at a heating rate of 1 K/min, the midpoint of the transition is expected to occur about 3 K lower, with the temperature range decreased to about 3 K.[15] The curved line segment, containing the reference set of Tg-Wg values on the two-dimensional map, represents a single contour line from a three-dimensional surface, at a value of 200 s for the third (time) dimension. This 200-s time scale refers only to the convention used to specify a reference value of Tg; it should not be confused with the operational time scale that is relevant to the use of the dynamics map for the diagnosis of mobility. For practical application, the third dimension of the mobility map is expressed as a temporal ratio, rather than time itself.[30] This operational time scale is defined as the ratio of experimental time duration (or inverse experimental frequency) to the relaxation time of the relevant underlying process, at specified conditions of temperature and moisture content. A "practical operational time scale" is any time scale for which the quotient "experimental time scale/relaxation time of the relevant process in the glassy state" approaches a value sufficiently near zero as to be "practicably" zero.

As noted earlier in Section III.A.2, in all such discussions of the dynamics map, "mobility" refers specifically to cooperative segmental (or unit) motions, which are the underlying basis of all Tg-dependent relaxation behavior (also referred to as alpha relaxations),[15] with respect to the ratios of allowed (by the local environment, where "local" refers to dimensions greater than about 10 nm,[106] but smaller than bulk sample dimensions)/required (by the size and shape of the mobile unit) free volume, local viscosity, and time.[30] Thus, (1) inherent requirements of free volume, local viscosity, and time for cooperative rotational or translational motions and (2) method-related requirements of sufficient mobility for detection determine the observed relationship and location of the operational values of measured transition temperatures of polymer-plasticizer blends. In contrast, small-scale motions (also referred to as beta and gamma relaxations, such as non-cooperative vibrations and rotations[15]) are not kinetically constrained with the same non-Arrhenius temperature dependence as Tg-dependent relaxations[15] and, thus, are not diagnosed by the dynamics map. From a recent study of tracer diffusion at the glass transition, Ehlich and Sillescu[347] have suggested that the coupling of the diffusional motion of a tracer and the glass-to-rubber relaxation of a polymeric matrix "will increase with the size of the diffusant, which finally becomes a probe for monitoring the glass transition process."

The philosophical question relates to the region of water content greater than or equivalent to Wg′ and the designation of Tg′-Wg′ as the appropriate reference location on the dynamics map. As already noted, we have suggested that water contents greater than Wg′ are not effective to provide further plasticization at temperatures below Tg′, due to phase separation of ice, so that Tg′-Wg′ is the glass with the maximum content of plasticizing water in a practical time scale,[8,30] and water contents greater than Wg′ lead to melt-dilution at temperatures above Tg′.[33] Pure water, per se, exists in only two relevant circumstances: complete absence of solute, or occurrence of phase separation of ice in the presence of solute. Clearly, "plasticizing water" refers to the aqueous component of a water-solute blend in the non-ice portion of a sample and should not be confused with pure water as a separate entity.

Since there is a practical limit to the amount of plasticizing water, such that water content up to Wg′ is plasticizing, but water content greater than Wg′ is melt-diluting and non-plasticizing, the question might be raised as to how this newer description differs from the older and unacceptable description in terms of "bound" and "free" water. The question would require an answer to prevent the equivalence of "bound water" to plasticizing water and "free water" to melt-diluting water. The primary distinction between the two descriptions is that the use of "bound" and

"free" implies that there are two *types* of water, suggesting that they could be distinguished either chemically or energetically, a conclusion that is clearly contradicted by experimental observations.[149,150] In contrast, plasticizing and non-plasticizing refer to the temperature- and time-dependent operational conditions that result from different *amounts* of water, not different *types* of water. In short, "free" and "bound" unacceptably suggest two types of water that differ energetically, in contradiction to experimental observation. Plasticizing and non-plasticizing describe two regimes of operational conditions that have been observed experimentally, as discussed further later in Section V.A.2, in the context of Figure 65.

Moreover, the newer description is in accord with the fact that water, outside of an ice or other crystalline lattice, is considered a uniform species, with no existence of distinguishable types.[4] Then the question might arise as to why some amounts of water could be plasticizing, and other amounts (greater than Wg′) be non-plasticizing, if water is a uniform species. The answer here is based on an understanding that there are two necessary conditions for a diluent to act as an effective plasticizer: (1) thermodynamic compatibility over the entire temperature range between Tg of the pure solute and Tg of the pure diluent; and (2) the ability of the diluent to increase the free volume and decrease the local effective viscosity of the blend, compared to that of the solute alone at the same temperature. The first condition is typically determined as a solubility parameter (a measure of thermodynamic compatibility) for polymers.[113] Thermodynamic compatibility refers to both equilibrium thermodynamic compatibility (temperature-dependent, but time-independent) and non-equilibrium thermodynamic compatibility (time- and temperature-dependent). The most effective plasticizer would not require kinetic constraint to maintain a spatially homogeneous distribution of solute and diluent. The second condition requires that, in the context of translational mobility, the Tg of the diluent be less than the Tg of the solute, which is usually equivalent to the linear DP of the diluent being less than the linear DP of the solute. As a consequence, the free volume (required for translational motion) of the diluent alone > that of the compatible blend > that of the solute alone at the same experimental temperature. This understanding of the necessary conditions for effective plasticization also supports the nomination of Tg′-Wg′ as the practical reference state for systems with T > Tg′ and W > Wg′. For practical time scales, the time- and temperature-dependence of the thermodynamic compatibility of water with common food materials, such as PHCs, precludes its use as an effective plasticizer at T < Tg′. Only in shorter time scales compared to the effective relaxation time of the system (i.e., at small temperature intervals above Tg) would the family of Tg-Wg values at Wg > Wg′ and Tg < Tg′ be appropriate reference locations. Such an appropriate use of this part of the complete glass curve as a reference contour would be the explanation of the control of ice nucleation and initial growth of critical nuclei as a function of solute concentration or pressure, *before* maximum freeze concentration occurs.[30] In contrast, the sorption behavior mentioned earlier (to be described in the context of Figure 65) demands the use of Tg′-Wg′ as the primary reference location. In a typical experimental time scale, a dramatic dependence of the apparent RVP on the underlying glass curve is already observed as a strong temperature-dependence at constant moisture content for values of apparent RVP < 0.9. This condition exists at T > Tg′, when Wg′ > W > Wg. When W falls below Wg, the apparent RVP approaches zero, and the strong temperature-dependence at constant W is no longer observed. When W rises above Wg′, the apparent RVP approaches 1, and again the strong temperature-dependence at constant W is no longer observed.

E. Polysaccharides

The functionality of high MW polysaccharide gums as polymeric cryostabilizers in three-component model systems (polysaccharide:small sugar:water) has been demonstrated.[33] The Tg′ values shown in Table 11 (updated from Reference 33) illustrate the cryostabilizing contribution of several widely used saccharide high polymers (e.g., alginate, pectin, carageenan, xanthan, CMC, methocel) at the low concentrations rel-

TABLE 11
The Cryostabilizing Contribution of Polysaccharides to Tg′ of Three-Component Model Systems[33]

		Tg′ (°C)				
			Sucrose concentration			Fructose concentration
Polysaccharide	Concentration	Water	5 w%	10 w%	20 w%	20 w%
None			−31.5	−31.5	−32	−42
Na alginate	2%				−24.5	
(Kelcosol)	3%	?	−23.5			
(Manugel)	3%		−23			
(Kelgin HV)	3%		−23.5			
Ca Alginate	3%	?				
Pentosans	10%			−30.5		
(Wheat)	20%	?				
CMC (9H4XF)	2%				−29	−38
	3%		−25			
Methocel	1%	?			−28.5	−41
(A4M)	2%	?			−27.5	−39.5
(K100)	1%				−31	−40.5
(K100)	2%	?			−28	−40
(K100)	3%		−25			
Pectin	3%	?	−25		−25	−33.5
(low-methoxyl)						
i-Carageenan	1%				−31	−39
	2%	?			−27.5	−34
	3%		−28.5			
Xanthan gum						
(Keltrol F)	0.5%				−30.5	−39.5
	1%	?				
	2%				−24.5	−34
	3%	?	−25			
Inulin	1.65%	−7.5				
	2%				−30.5	−40.5
Gum arabic	5%		−22.5			
	10%	−13.5				
Dextran	5%	−13.5	−22.5			
(MW 9400)						
Pullulan	20%	−10				
Arabino-	20%	−17.5				
galactan						
Levan	20%	−19				
Polydextrose						
(A)	10%	−24.5			−29.5	−37.5
	20%	−24			−29	−35
	25%	−23.5			−28	−33.5
	30%	−24				
	40%	−24				

evant to practical usage levels in fabricated frozen products typically dominated by higher concentrations of low MW sugars. The three-component model system was developed as a diagnostic assay, because, as indicated by the question marks in the column headed "water" in Table 11, Tg′ values for many of the saccharide high polymers in water alone could not be determined directly by DSC. (An analogous three-component assay system had been developed to elucidate the cryostabilizing effect of wheat gluten proteins in a model system for frozen bread dough.[25,34]) By

extrapolation from measured Tg′ values for the highest MW SHPs (of <1 DE, Tg′ = −4°C)[8] and soluble potato starch (Tg′ = −3.5°C),[27] it was reasoned that, due to the very high MW of such water-soluble polysaccharides, the Tg′ transition would occur so close to 0°C that it would be buried under the predominating ice-melting endotherm and therefore not detectable. However, in the presence of a higher concentration (5 to 20 w%) of a small sugar (fructose or sucrose), the significant Tg′-elevating effect of a low concentration of polysaccharide, relative to the much lower Tg′ value of the corresponding sugar solution without added polysaccharide (the first line in Table 11), was clearly revealed. For many of the polysaccharides in Table 11, the diagnostic assay demonstrated that Tg′ increases significantly with increasing concentration of high polymer, relative to a constant concentration of small sugar. In other words, as previously reported[32] for three-component model systems containing polymeric SHPs and low MW sugars (reviewed below), Tg′ increases in a completely predictable way with increasing composite $\overline{M}w$ of a mixture of compatible solutes. It has been pointed out that the Tg′-elevating effect of pectin on sugar solutions is noteworthy in the context of its possible relevance to fruit-based food products, as inferred from measured Tg′ values for various fruit juices.[33]

It should be noted that, for some of the polysaccharides listed in Table 11, it was not necessary to *infer* their cryostabilizing functionality from Tg′ results for the diagnostic three-component assay system. In contrast to the gums already mentioned, polysaccharides such as gum arabic, dextran, pullulan, arabinogalactan, and levan, of higher water solubility and/or lower MW, showed Tg′ values (for solutions in water alone) in the range −10 to −19°C, comparable to Tg′ values for oligomeric and low-polymeric SHP cryostabilizers with DE values in the range 10 to 25. The samples of gum arabic and dextran illustrated very clearly the dependence of Tg′ on the weight-average composition of a compatible, multi-solute mixture.[8] In each case, the composite Tg′ of −22.5°C for a 1:1 w:w mixture of sucrose and polysaccharide was exactly midway between the Tg′ values for the individual solutes.

In the context of the cryostabilizing function of high MW polysaccharides in three-component aqueous solutions as model systems for frozen foods, an interesting illustration of what has been gleaned from an analysis of glass curves for such complex aqueous mixtures is shown in Figure 66.[15] In this artist's rendering of a three-dimensional state diagram for a hypothetical three-component system, both solutes (e.g., a polymer, 2, and its monomer, 1) are non-crystallizing, interacting (i.e., compatible), and plasticized by water, which is the crystallizing solvent, 3. The diagram revealed the postulated origin of a sigmoidal Tg′(c) curve, i.e., the Tg′ glass curve ABCDEF.[15] In fact, similar sigmoidal curves of Tc vs. w% concentration, for collapse during freeze-drying of analogous three-component aqueous systems, had previously been reported (Figure 5 in MacKenzie[135]), but "the basis for their non-linearity had not been determined".[135] Four series of model solutions at 10 w% total solids composed of mixtures with varying ratios of maltodextrins (0.5 to 15 DE) to fructose demonstrated an experimental verification of the postulated sigmoidal shape of Tg′(c) curves, as shown by the plots of Tg′ vs. w% maltodextrin in Figure 67.[32] It has been found that such sigmoidal glass curves represent the general behavior of compatible mixtures of both homologous and non-homologous polymeric (including Na caseinate protein) and low MW (including various sugars and acids) solutes.[32] In all such curves, the low- and high-Tg′ tie points were determined by the Tg′ values of the individual low and high MW solutes, respectively. Figure 67 illustrated (as did the results in Table 11 for gum arabic-sucrose and dextran-sucrose mixtures) that the composite Tg′ value characteristic of a given amorphous solute(s)-UFW composition is governed by the $\overline{M}w$ of the particular combination of compatible water-soluble solids in a complex frozen system. It has also been used to illustrate the principle of polymeric crystabilization: the stabilizing influence on the structural state of a complex amorphous matrix derives from the high MW of polymeric cryostabilizers and the resulting elevating effect on Tg′ of a food product.[8,32]

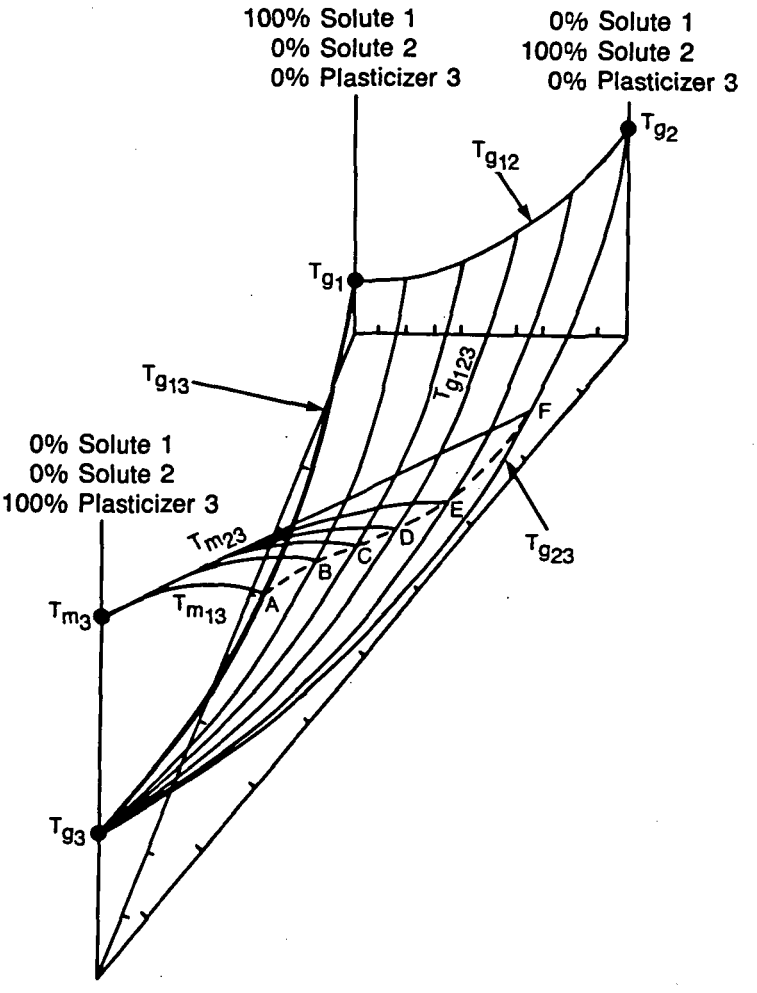

FIGURE 66. A schematic three-dimensional state diagram for a hypothetical 3-component aqueous system. The two solutes (e.g., polymer + monomer) are both non-crystallizing, interacting, and plasticized by water, which is the crystallizing solvent. The diagram illustrates the postulated origin of a sigmoidal curve of Tg′ vs. w% solute composition. (From Levine, H. and Slade, L., *Water Science Reviews,* Vol. 3, Franks, F., Ed., Cambridge University Press, Cambridge, 1988, 79. With permission.)

F. Proteins and Amino Acids

DSC results for Tg′ and Wg′ values of many proteins and amino acids are shown in Tables 12 and 13, respectively.[25] As noted earlier for many food carbohydrates, the Tg′ values for several of the gelatin samples in Table 12 are quite similar to values reported for Tr and Tc, as shown in Table 8. The Table 12 values of Tg′ of about −12°C and corresponding Wg′ of about 35 w% water for typical high-Bloom gelatin are also similar to values of Tg′ = −10°C and Wg′ = 30 w% water that have been extracted[25] from a state diagram for an industrially produced gelatin reported by Reutner et al.[360] The gelatins in Table 12 comprise a series of typical commercial products representing a homologous family of amorphous polymers, and, as such, demonstrated the expected behavior of increasing Tg′ (measured for 20 w% solutions) with increasing MW.[15] The fair linear correlation between increasing Tg′ and increasing "Bloom" value (i.e., gel strength), for a series from a non-gelling hydrolyzed gelatin to a 300 Bloom sample, has been noted previ-

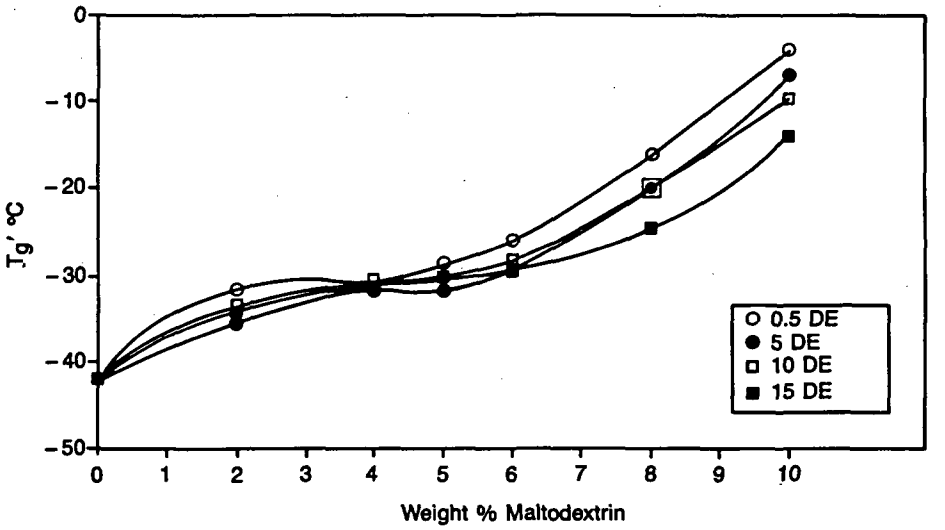

FIGURE 67. Variation of the glass transition temperature, Tg', for maximally frozen solutions against weight percent maltodextrin in 10 w% total solids solutions of maltodextrin + fructose, for four different low DE maltodextrins. (From Levine, H. and Slade, L., *Cryo.-Lett.*, 9, 21, 1988. With permission.)

ously, although it was recognized that Bloom value is not solely dependent on $\overline{M}w$.[24]

The proteins in Table 12 represent a collection of relatively high MW, water-compatible polymers. Their commensurately high Tg' values range from -5°C for wheat gluten to -16.5°C for hydrolyzed gelatin (MW = 20,000) and lysozyme (MW = 14,400), with most typically in the range from -10 to -15°C. This Tg' range corresponds to carbohydrate PHCs (e.g., malto-oligosaccharides) of DP $\gtrsim$ 6 and SHPs (e.g., maltodextrins) of DE 5 to 20. The correspondingly low Wg' values for the proteins generally fall in the range from 0.2 to 0.7 g UFW/g, with most typically in the range 0.3 to 0.5 g/g, in good agreement with previous DSC results.[357] This Wg' range is comparable to that for the linear malto-oligomers listed in Table 3. As illustrated in Table 12, this Wg' range also agrees well with the literature range of so-called "water-binding capacity" values (determined by various methods other than DSC) for many food proteins, even though the spread of reported values for individual proteins has often been considerable.[25,57]

Importantly, in the context of food product/process functionality, the proteins in Table 12 exhibit the low-temperature thermal properties characteristic of high-polymeric stabilizers against both low- and high-temperature collapse processes, referred to as food cryostabilizers. As shown in Table 12, the best protein cryostabilizers (with Tg' $\gtrsim -10$°C) are water-soluble, high-Bloom gelatin and water-compatible wheat gluten.[25] For the latter, the DSC results for Tg' and Wg' of a dozen different glutens have been reported to reflect the compositional variability of these commercial samples,[25] but most of the values fell in the ranges of -6.5 to -8.5°C and 0.3 to 0.4 g UFW/g typical of other high-polymeric protein and carbohydrate cryostabilizers. These physicochemical properties have been shown to underlie, in large part, the excellent functionality of vital wheat gluten (both endogenous and exogenous) as a stabilizer for frozen bread dough.[25]

In contrast to the protein polymers in Table 12, the water-soluble, non-crystallizing, monomeric amino acids in Table 13 exemplify the very low Tg' values (in the range from -40 to -60°C) and extremely high Wg' values (in the range from 1.0 to 2.0 g UFW/g) commensurate with their low MWs.[25] These Tg' and Wg' values are comparable to those of some of the lowest MW carbohydrates, such as polyols, monosaccharides smaller than hexoses, and glycosides. As dis-

TABLE 12
Tg′, Wg′, and/or "Water Binding Capacity (WBC)" Values for Proteins[25]

Solute	Tg′ °C	Wg′ (g UFW/g)	"WBC" (g water/g)	Ref.
Lysozyme (Sigma hen egg-white)	−16.5			25
Lysozyme		0.31		348
Lysozyme		0.33		349
Lysozyme			0.25—0.29	350
Lysozyme			0.20	351
Lysozyme			0.175	352
Lysozyme			0.13	86
Lysozyme		0.34		167
Ribonuclease			0.36—0.43	350
Cytochrome *c*			0.39	350
Chymotrypsinogen A			0.29	350
Chymotrypsinogen		0.34		167
Chymotrypsin		0.33		167
Elastin		0.3		168
Elastin		0.35		353, 354
Gelatin (hydrolyzed, MW = 20K)	−16.5	0.37		25
Gelatin (liquid, MW = 60K)	−13.5			25
Gelatin (50 Bloom)	−12.5			25
Gelatin (60 Bloom, calfskin)	−11	0.36		25
Gelatin (175 Bloom, pigskin)	−11.5	0.52		25
Gelatin (225 Bloom, calfskin)	−13.5	0.46		25
Gelatin (250 Bloom)	−10.5			25
Gelatin (300 Bloom, pigskin)	−9.5	0.66		25
Gelatin		0.36—0.58		355
Gelatin			0.29—0.35	350
Collagen (soluble)	−15	0.71		25
Collagen (native)		0.5		168
Collagen (native)		0.38		356
Collagen (native)		0.55		167
Tropocollagen		0.30		357
α-lactalbumin (Sigma)	−10.5	0.28		25
α-lactalbumin (Calbiochem)	−15.5			25
Bovine serum albumin	−13	0.44		25
Bovine serum albumin		0.33		348
Bovine serum albumin			0.49	358
Bovine serum albumin			0.32	350
Bovine serum albumin		0.40		167
Albumin (egg)		0.26—0.37		355
Albumin (egg)			0.30	350
Albumin (egg)		0.33		167
β-lactoglobulin			0.55	358
β-lactoglobulin			0.25—0.32	350
Globulins (egg)	−10.5	0.42		25
Hemoglobin			0.25—0.37	350
Hemoglobin (denatured)		0.42		167
Myoglobin			0.42	350
Myoglobin		0.42		167
Insulin			0.24	350
α-casein	−12.5	0.61		25
κ-casein		0.44		286
Casein			0.55	358
Casein		0.24—0.30		355
Sodium caseinate	−10	0.64		25

TABLE 12 (continued)
Tg', Wg', and/or "Water Binding Capacity (WBC)" Values for Proteins[25]

Solute	Tg' °C	Wg' (g UFW/g)	"WBC" (g water/g)	Ref.
Keratin		0.44		25
Zein		0.45		25
Whey		0.5		359
Whey		0.20—0.25		355
Gluten (Sigma - wheat)	−6.5	0.39		25
Gluten ("vital wheat gluten" commercial samples)	−5 to −10	0.07—0.41		25

TABLE 13
Tg' and Wg' Values for Amino Acids[25]

Solute	MW	pH (20 w%)	Tg' °C	Wg' (g UFW/g)	Remarks
Glycine	75.1	6.5	—	—	b,f
Glycine	75.1	9.1	−58	1.72	c
DL-Alanine	89.1	6.2	−50.5	—	b,f
DL-Alanine	89.1	2.0	−55.5	—	a,d
DL-Serine	105.1	10.1	−51.5	1.88	c
DL-Proline	115.1	7.2	—	—	a,b
DL-Valine	117.2	10.7	−50	—	a,c
DL-Norvaline	117.2	10.1	−54.5	—	a,c
DL-Threonine	119.1	6.0	−40.5	1.04	b
Hydroxy-L-proline	131.0	6.1	−53.5	—	b,f
DL-Leucine	131.2				e
DL-Norleucine	131.2	12.3	−54	—	a,c
DL-Isoleucine	131.2	0.5	−59.5	—	a,d,f
DL-Aspartic acid	133.1	9.9	−49.5	1.98	c
DL-Glutamic acid · H_2O	147.1	8.4	−48	1.59	c
DL-Methionine	149.2	0.8	−52	1.25	d
DL-Asparagine	150.1	10.1	−49.5	1.48	c
DL-Ethionine	163.2	1.1	−50.5	1.11	d
DL-Phenylalanine	165.2				e
DL-Citrulline	175.2	10.6	−50	1.98	c
DL-Tyrosine	181.2				e
DL-Lysine HCl	182.7	5.5	−47.5	1.21	b
DL-DOPA	197.2	0.6	−47	1.58	d
DL-Tryptophan	204.2				e
DL-Histidine HCl · H_2O	209.6	4.0	−44	—	b,f
DL-Histidine HCl · H_2O	209.6	1.3	−52	1.04	d
DL-Arginine HCl	210.7	6.1	−43.5	0.74	b
DL-Cystine	240.3				e

[a] Undergoes eutectic melting
[b] "As is" pH in water
[c] Solubilized with 1N NaOH
[d] Solubilized with 1N HCl
[e] Insoluble at 20 w%
[f] Undergoes solute crystallization

cussed earlier, these properties of amino acids, which characterize food cryoprotectants, translate to potential functionality in protein-based and other freezer-stored (but "soft-from-the-freezer") fabricated foods and as "moisture management" agents in "intermediate moisture" shelf-stable products.[16,25] As indicated by the remarks in Table 13 pertaining to aqueous solubility and pH sensitivity, the potential utility of amino acids in food systems would depend on usage levels and compatibility with product pH, in addition to dietary considerations.[25]

G. Tg′ Doublet Phenomena

As mentioned earlier, in order to refine the discriminative capability of DSC analysis to evaluate high-polymeric wheat gluten proteins for their cryostabilizing potential in frozen bread dough applications, a low-temperature DSC assay based on a three-component model system was developed.[25] The assay measured Tg′ of a hand-mixed sample of gluten/sucrose/water (100/10/100 parts by weight, prepared by addition of sucrose in solution to gluten powder), to examine the extent of depression by sucrose of Tg′ in the ternary glass, compared to the Tg′ of hydrated gluten in the simple binary glass. As described for the polysaccharide gums in Table 11, such a diagnostic assay, using sucrose or fructose to provide a ternary glass with a lower value of $\overline{M}w$, is useful in the characterization of high polymers with values of Tg′ near 0°C.[34] The Tg′ results shown in Table 14[25] for the gluten assay system have also been used to illustrate the non-trivial phenomenon of Tg′ doublets,[30] which has been observed in various model aqueous solutions and real frozen products composed of partially or completely incompatible blends of two or more water-compatible solids.[33,34] This phenomenon of two different Tg′ values detectable in the thermogram of a maximally frozen solution of two or more incompletely compatible solutes is distinguishable from the more trivial phenomenon, described earlier with respect to Figure 39, of a pair of glass transitions, Tg and Tg′, arising from the possible coexistence of two distinct glasses formed due to incomplete phase separation in an incompletely frozen solution of a single solute.[30]

As indicated by the results in Table 14, Tg′ for the freeze-concentrated, entangled-polymer glass occurred as a superimposed shoulder on the low-temperature side of the ice-melting endotherm. In the simplest case, when all of the added sucrose contributed to the ternary glass, depression of $\overline{M}w$ and Tg′ was dramatic and quantitative, allowing deconvolution of Tg′ from the Tm of ice, which was only colligatively depressed by more dilute sucrose upon melting. In the most complex cases for multicomponent systems, when only part of the added sucrose contributed to the major ternary glass, deconvolution was still possible, but the depression of Tg′ was only qualitative. Table 14 illustrates the effect of sucrose in ternary glasses of aqueous gluten samples. It is important to note that all of the test compositions in Table 14 contained excess water (i.e., water in excess of Wg′), which froze readily. Variation of the test system composition could have led to constraints in solubility and solute compatibility for different solute ratios and concentrations. The simplest case was exemplified by Henkel Pro-Vim. The ternary glass exhibited a single value of Tg′, depressed compared to the binary glass. For the same assay test system composition, gluten isolated from a high-protein varietal wheat flour (5409) exhibited the same, single value of Tg′. In contrast, a more complex case was exemplified by the same sample of isolated gluten when a higher concentration of sucrose was used in the assay, in that *two* values of Tg′ were observed. The expected further depression of Tg′ for the ternary glass was observed as a smaller transition, but the major transition occurred near Tg′ of sucrose itself (−32°C). For this same higher-sucrose composition in the test system, additional complexity was observed when another commercial gluten (IGP SG-80) was assayed. Again two values of Tg′ were observed, but the minor transition occurred near Tg′ of sucrose itself.

Based on other studies[30] of complex aqueous model systems, including mixtures of various proteins-sugars, polysaccharides-sugars, and many different multicomponent food ingredients and products, multiple Tg′ values have been attributed to the coexistence of two distinct aqueous glasses.[25,32-34] In a maximally frozen matrix, the presence of multiple aqueous glasses, having dif-

TABLE 14
Low Temperature Differential Scanning Calorimetry of Wheat Glutens — Tg′ Values for Gluten/Sucrose/Water Assay Test System Samples[25]

Gluten sample	Assay composition: Gluten	Maltodextrin	Sucrose	Water	Tg′ (°C)[a]
Henkel Pro-Vim	100	0	0	100	−5
Henkel Pro-Vim	100	0	10	100	−9
Gluten-5409 (1979)[b]	100	0	10	100	−9
Gluten-5409 (1979)[b]	100	0	100	133	−32.5 and −14
IGP SG-80 (lot 11/81)	100	0	0	100	−8.5
IGP SG-80 (lot 12/81)	100	0	0	100	−7.5
IGP SG-80 (lot 5/81)	100	0	100	133	−16.5 and −33
	0	100	100	133	−18
IGP SG-80 (lot 5/81)	100	100	50	133	−16.5 and −29.5
IGP SG-80 (lot 5/81)	100	33	0	89	−17.5 and −8
IGP SG-80 (lot 5/81)	100	100	0	100	−19.5 and −9
IGP SG-80 (lot 5/81)	100	300	0	267	−9
10 DE Maltodextrin[c]					−9.5
Solubles-5409 (1981)[c]					−22.5
Solubles-IGP SG-80 (lot 5/81)[c]					−29.5 and −37.5

[a] Tg′ of assay test system samples (gluten/water, gluten/sucrose/water, or gluten/10 DE maltodextrin/sucrose/water), with compositions as noted for individual samples. In each case, gluten ("as is" basis) was hand-mixed with the indicated total weight of water, sucrose syrup, or carbohydrate syrup.
[b] Hand-washed gluten from 1979 crop year of 5409 varietal flour.
[c] Tg′ of 20% aqueous solution.

ferent composition and heterogeneous spatial distribution (on a size scale of ≳100 Å),[106] results from partial disproportionation (i.e., partitioning) of non-homologous, molecularly incompatible solutes during freeze-concentration.[25] By convention, multiple values of Tg′ are listed in order of decreasing intensity of the transition (i.e., magnitude of the step-change in heat flow), such that the first Tg′ represents the major, and the second Tg′ the minor, glass.[25] Experience has shown that the Tg′ value of the predominant glassy phase largely determines the overall freezer-storage stability of a multicomponent food material.[32-34] In frozen bread dough, as in other complex, water-compatible food systems composed of mixtures of large and small proteins and carbohydrates (e.g., many dairy ingredients and products, typically dominated by large proteins and small sugars, as described elsewhere[33]), the higher-temperature Tg′ of a doublet corresponds to a glass with higher protein and polysaccharide concentration, while the lower Tg′ glass has a higher concentration of soluble sugars and amino acids.[25] (Hirsh et al.[343] have recently reported evidence [from DSC analysis] of similar, distinct protein- and sugar-enriched glassy domains resulting from liquid-liquid phase separations in frozen, multicomponent, aqueous model solutions containing proteins and sugars.) Saccharide or peptide oligomers of intermediate linear DP are critical to the specific partitioning behavior of lower oligomers and monomers. In model assay systems and in real food systems, these intermediate oligomers can be used to increase the compatibility of solutes in mixtures with an otherwise bimodal MW distribution.[25] Then the tendency to form two separate ternary glasses is diminished or prevented, and a single quaternary glass of intermediate Tg′ is observed. This increase in the underlying structural homogeneity at the molecular level is perceived macroscopically as an improvement in textural uniformity

(smoothness).[34] (A recent application of this concept of the "compatibilizing" effect of saccharide oligomers involved a patented dry mix for an instant cheesecake product, which relies on the addition of a maltodextrin ingredient [of 3 to 15 DE] to produce a cheesecake filling of excellent body and texture.[361])

In this context, the assay behavior of quaternary systems of gluten/10 DE maltodextrin/sucrose/water (shown in Table 14) was particularly informative.[25] The Tg′ of the simple binary glass of this 10 DE maltodextrin was −9.5°C, similar to Tg′ of a typical IGP gluten, −8.5 to −7.5°C.[25] However, addition of an equal weight of sucrose to IGP gluten led to a Tg′ doublet, representing both a more mobile gluten-enriched glass (Tg′ −16.5°C) and partition of a separate sucrose glass (Tg′ −33°C). In contrast, addition of an equal weight of sucrose to 10 DE maltodextrin led only to a more mobile carbohydrate glass, without partition of a separate sucrose glass, owing to the greater compatibility of maltodextrin and sucrose. Compared to the effect of addition of an equal weight of sucrose alone, the effect of addition of an equal weight of maltodextrin and partial removal of sucrose on Tg′ (−16.5°C) of the gluten-enriched glass was not detectable, but partition of maltodextrin into the separate sucrose-enriched glass was detected as a slight elevation of its Tg′ (−29.5°C). In order to interpret the effect of increasing maltodextrin concentration on gluten glass behavior in the absence of sucrose, it was necessary to examine the glass properties of the endogenous water-soluble components of the gluten, whose partition behavior was modulated by maltodextrin, as a compatible solute. Values of Tg′ for 20 w% aqueous solutions of freeze-dried water extracts from commercial gluten and varietal wheat flours ranged from −37.5°C for the lower Tg′ of a doublet to −22°C for the higher Tg′ or single Tg′ value.[25] The major constituents of the water-solubles are albumins, peptides, and nonstarch carbohydrates. Typical values of Tg′ for 20% solutions of isolated water-solubles are shown in Table 14. Addition of about 27 w% maltodextrin solution to gluten in the absence of sucrose, with a test system composition of gluten/maltodextrin/water (100/33/89), showed a reversal of the magnitudes of the doublet glasses. The major glass contained the endogenous water-solubles, with elevated Tg′ (−17.5°C) due to the presence of maltodextrin, and the minor glass was highly enriched in gluten proteins (Tg′ −8°C). Addition of increased concentration of maltodextrin solution (50 w%) to gluten, with simultaneous increase in maltodextrin/gluten ratio (100/100/100), enhanced partition of maltodextrin into the gluten phase, so that Tg′ of the minor glass was depressed by increased presence of maltodextrin, while Tg′ of the major glass was depressed by decreased presence of maltodextrin. Finally, addition of about the same concentration of maltodextrin solution (53 w%), with much greater ratio of maltodextrin to gluten (100/300/267), allowed total compatibility of the solutes, so a single glass was observed with Tg′ of −9°C.

H. Fruits and Vegetables

The data bank of measured Tg′ values for fruits and vegetables[33] has been used to reveal how insights to the behavior (i.e., quality, safety, and storage stability) of real, complex food products can be gleaned from analyses of the corresponding data bank for compositionally relevant, simple aqueous model solutions. In fact, the food polymer science approach has provided a technologically important predictive capability, exemplified with respect to the Tg′ values of various fruit juices, shown in Table 15.[33] This predictive capability is so powerful that Tg′ can often simply be calculated, rather than actually measured by DSC, for real food systems.[34] For

TABLE 15
Tg′ Values for Fruit Juices[33]

Fruit juice	Tg′ (°C)
Orange (various samples)	−37.5 ± 1.0
Strawberry	−41 and −32.5
Pineapple	−37.5
Pear	−40
Apple	−40.5
Prune	−41
White grape	−42.5
Lemon (various samples)	−43 ± 1.5

example, a composite weight-average Tg′ value of −37°C[34] has been calculated for orange juice (the water-soluble solids composition of which is predominated by an approximately 2:1:1 w% mixture of sucrose, fructose, and glucose) from the respective Tg′ values of −32, −42, and −43°C for the individual pure sugars sucrose, fructose, and glucose. As mentioned earlier with regard to Table 3, the Tg′ values for these common food sugars are characteristic of the ranges of Tg′ values for many different monosaccharides (−40.5 to −44°C) and disaccharides (−28 to −35.5°C). As shown in Table 15, actual measured Tg′ values for various samples of orange juice characteristically fall between −36.5 and −38.5°C, a temperature range that coincides with the operative Tc for freeze-drying of this relatively complex food product.[33] The measured Tg′ values for the other fruit juices listed in Table 15 likewise reflect, and are determined primarily by, the weight ratios of the predominant low MW sugars and acids (e.g., citric (Tg′ = −52.5°C), malic (Tg′ = −55.5°C)) present in each juice.[33] In comparison to the Tg′ values for orange and pineapple juice, the lower Tg′ values for the juices from pear, apple, prune, strawberry (for which the Tg′ doublet will be explained below), white grape, and lemon in Table 15 have been suggested to evidently reflect water-soluble solids compositions with higher monosaccharide/disaccharide ratios and/or higher contents of low MW acids (especially relevant to lemon juice).[33] As mentioned earlier, the potential effect of the presence of water-compatible, endogenous pectinaceous materials (debris from plant cell walls) on the Tg′ values of fruit juices also needs to be considered when interpreting the data in Table 15.

Table 16[33] shows Tg′ values (and some percent freezable water (FW) values) for a number of different varietal strawberries and other fresh fruits. The Tg′ values for the various fruits, all in the range between −32 and −42°C, are indicative of soluble solids compositions dominated by low MW sugars (i.e., mono- and disaccharides, mainly fructose, glucose, and sucrose).[33] For example, the composition of the sparkleberry strawberry (according to USDA Handbook #8) is 89.8% water and 7.8% soluble solids, with 6.2% sugars: 1.45% sucrose, 2.18% glucose, and 2.59% fructose. The observations of multiple Tg′ values and *different* Tg′ values for different locations within a single fruit have both been taken as indications of a non-uniform spatial distribution (e.g., a concentration gradient) of sugars (and/or other soluble solids such as pectins) within a fruit.[33] For example, in the blueberry, the minor Tg′ value of −32°C could be an indication of a much higher disaccharide (sucrose) content (and/or content of high MW pectin) in the skin than in the apparently monosaccharide-dominated meat of the fruit. The observation of different Tg′ values for many different varieties of a single fruit (strawberry) is suggestive of significant varietal differences in both the composition and spatial distribution of sugars (and/or other soluble solids).[33] Even within a single strawberry variety (i.e., Pajaro), two different lots of fruit showed different Tg′ values (and Tg′ singlet vs. doublet behavior). This finding suggested that both the composition and spatial distribution of sugars (and/or pectins) may also vary with the degree of maturity of a fruit.[33]

Due in part to a situation of Tg′ ≪ Tf = −18°C and high percent FW (about 75-90+ g ice/100 g frozen sample), most fruits, and especially delicate strawberries, show very poor textural stability during frozen storage.[33] For the many different strawberry varieties listed in Table 16, the predominant Tg′ value ranged from −33.5 to −41°C. While it is known that freeze-thaw stability (i.e., stability after freezing and immediate thawing, as distinguished from freezer-storage stability, which refers to stability after freezing, long-term storage, and thawing) varies greatly among strawberry varieties, the possibility of correlations between Tg′ and freeze-thaw stability and/or between percent FW and freeze-thaw stability has not been investigated. All of the varietal strawberries listed in Table 16 are claimed to show better freeze-thaw stability than the sparkleberry variety, which is the primary variety sold fresh in supermarkets in the U.S. The data in Table 16 showed that the predominant Tg′ value (all locations) of sparkleberry is lower than that of some of the other varieties, and its percent FW is significantly higher than that of most of the other varieties. However, among the specific varieties listed in Table 16, the possibility of a correlation among higher Tg′, lower

TABLE 16
Tg′ Values for Varietal Strawberries and Other Fresh Fruits[33]

Sample	Tg′ (°C)	% Freezable water
Strawberry		
Sparkleberry — center	−41	
Sparkleberry — edge	−39 and −33	
Sparkleberry — midway between	−38.5 and −33	93.0
Canoga —	−37	
Holiday —	−35.5	
Homeoye — midway	−40.5 and −34.5	
Pajaro (lot 1) — between	−33.5	79.9 ± 0.4
Pajaro (lot 2) — center	−34.5 and −39	80.3 ± 1.4
Douglas — and	−34 and −40	76.6 ± 0.8
Benton — edge	−40 and −33	78.9 ± 0.5
Selva —	−34.5 and −39.5	81.3 ± 0
Chandler —	−39.5 and −35	84.5 ± 10.9
Parker —	−41 and −34	80.3 ± 2.6
Blueberry		
Meat	−41	
Skin	−41 and −32	
Peach	−36.5	
Banana	−35	
Apple		
Red Delicious	−42	
Granny Smith	−41	

percent FW, and better freeze-thaw stability has also not been investigated. A critical fact about fruits in general, and delicate strawberries in particular, is that, even if a fruit is deep-frozen and stored at Tf < Tg′, freeze-thaw textural stability is often poor,[33] because of a loss of turgor pressure caused by cellular dehydration upon extracellular freezing and by physical damage to cell membranes due to irreversible loss of bilayer structure upon freeze-dehydration. A partial remedy to this situation has been demonstrated via Rich's "freeze-flo" process, whereby some protection against physical damage and maintenance of structural integrity is provided by infusion of strawberries with high-fructose corn syrup,[345] a food cryoprotectant with a Wg′ value of about 1.0 g UFW/g solute.[32] Fructose-infused strawberries contain minimal freezable water at Tf = −18°C,[33] and constitute an edible-from-the-freezer (i.e., soft but intact at Tf), but very sweet, food product.

Table 17[33,39] shows Tg′ values for some fresh or frozen vegetables. Generally, these Tg′ values are much higher than those for fruits in Table 16. This reflects the higher ratio of metabolic intermediates of biosynthesis of starch or other high MW polysaccharides/small sugars in the water-compatible solids compositions of most vegetables relative to most fruits.[33] However, as in fruits, the value of Tg′ varies with sample location in vegetables, indicative of a non-uniform spacial distribution of soluble solids. For example, in frozen broccoli and especially in cauliflower, the head has a much higher Tg′ value (indicative of high MW solids) than the stalk (Tg′ indicative of detectable amounts of smaller sugars). The Tg′ values around −25°C for the stalks of cauliflower and broccoli are similar to the Tg′ values for several other frozen vegetable products (e.g., peas, carrots, green beans), indicative of similar ratios of higher MW polysaccharides/small sugars in the water-compatible solids of these common vegetables. Interestingly, the Tg′ value of sweet corn (endosperm) was found to vary with

TABLE 17
Tg′ Values for Fresh and Frozen Vegetables[33]

Sample	Tg′ (°C)
Sweet corn	
Fresh-picked — endosperm	−14.5
Blanched	−9.5
Blanched and frozen	−9.5
Supermarket "fresh"	−8
Potato — fresh Russet Burbank	
Middle center	−12 and −16
Middle edge	−12
Root end	−11
Stem end	−12
Cauliflower — frozen	
Stalk	−25
Head	?
Celery — fresh	?
Pea — frozen	−25
Carrot — frozen	−25.5
Green bean — frozen	−27.5
Broccoli — frozen	
Stalk	−26.5
Head	−11.5
Spinach — frozen	−17
Tomato — fresh — meat	−41.5

the extent of processing and with the degree of "freshness" (i.e., age after harvesting at full maturity). It was deduced that Tg′ increases with increased processing or age post-harvest, in both instances because of a corresponding decrease in the ratio of sugars/starch intermediates or starch polymers in the endosperm.[33] It is known that this solids ratio decreases dramatically with age post-harvest due to enzymatic activity, and that this change is responsible for the corresponding decrease in perceived sweetness and eating quality (i.e., texture). It has been demonstrated, by high-temperature DSC analysis of matched samples of (fresh-picked, untreated) vs. (fresh-picked, blanched) sweet corn, that an industrial blanching process involving heat-moisture treatment produces a Tg′-elevating effect (and concomitant decrease in eating quality) analogous to that caused by aging post-harvest.[33] Blanching causes the native (i.e., *partially crystalline*) granular starch in the endosperm of fresh-picked corn to be completely gelatinized (i.e., rendered completely amorphous and devoid of granular integrity, a not-unexpected consequence of such a heat-moisture treatment[20]), thus increasing both the amount of amorphous starch (i.e., amylopectin) and its availability to be captured along with small sugars upon vitrification of the aqueous matrix at Tg′, and causing Tg′ to increase due to increased $\overline{M}w$ of the solutes in this glass.[33]

On the brighter side, the results in Table 17 showed that some vegetables naturally high in intermediates of starch biosynthesis (e.g., corn and potato) have Tg′ values > Tf = −18°C. This fact translates in technological practice to excellent freezer-storage stability (i.e., years) for such products.[33] The Tg′ of celery, apparently so close to 0°C as to be unmeasurable by DSC, evidently reflects a composition of only high MW polysaccharides (see Table 11) and water, with essentially no small sugars. In contrast to corn and potato, other vegetables (e.g., cauliflower, broccoli, peas, carrots, green beans), with higher ratios of sugars/starch intermediates (as reflected by Tg′ values < Tf = −18°C), exhibit much more limited freezer-storage stability.[33] The Tg′ value of tomato meat is remarkably low relative to those of other vegetables. Tomatoes appear to be analogous to strawberries in two possibly related respects.[33] Tomatoes manifest notoriously bad freeze-thaw textural stability and a soluble solids composition of the flesh (as reflected by Tg′) evidently dominated by monosaccharide sugars.

V. INTERPRETATIONS BASED ON THE FOOD POLYMER SCIENCE APPROACH: NEW THOUGHTS ABOUT OLD MOISTURE MANAGEMENT QUESTIONS

Up to this point, having begun with a discussion of the shortcomings and inappropriateness of the traditional Aw approach to studies of food quality and safety, we have reviewed (1) the basis for an alternative food polymer science approach founded on key structure-property relationships previously established for synthetic polymes, and (2) the resulting data bank for several categories of widely used food materials and the physicochemical principles underlying the non-equilibrium behavior of these materials in food products and processes. Now we review how this food polymer science approach, data

bank, and underlying physicochemical foundation have been used to provide new and revealing interpretations of a number of old problems and questions, related to moisture management and water relationships in food systems, to which the traditional Aw approach has been unable to provide solutions, explanations, or answers.

As emphasized in Section IV.A, small PHCs and their aqueous solutions offer a unique framework for the investigation of non-equilibrium behavior under conditions of importance to technological applications.[30] The small PHCs are monodisperse with known MW below the entanglement limit. They provide several homologous or nearly homologous series of oligomers. They exhibit an astonishing diversity of thermal and thermomechanical properties that can be studied within particular sub-groups: PHCs with the same MW, PHCs with different MW in a homologous series, single PHC with different conformations. It has been shown that use of the dynamics map as a new conceptual approach to the study of non-equilibrium thermomechanical behavior facilitates the selection of experimental conditions to allow each PHC to be examined at an equivalent distance of moisture (i.e., ΔW) and temperature (i.e., ΔT) from its respective reference glass curve.[30] For most effective use of the dynamics map as a mobility transformation map to elucidate the underlying basis of the differences in behavior of PHCs, it has been necessary to identify appropriate experimental approaches that are capable of separating the effects of translational and rotational mobility on different mechanical relaxation properties.[30] Since local viscosity is related to relaxations that are controlled by translational diffusion, it reflects the mobility of the molecular-level environment. Thus, the same relaxation rates and temperature dependence would be expected for results of, for example, small molecule diffusion, polymer frictional coefficient, and pulsed field gradient-spin echo NMR spectroscopy of PHC-water systems.[200-204]

In general, mechanical relaxations depend on both translational and rotational mobility. For a typical, well-behaved polymer, an increase in free volume would be expected to go hand-in-hand with a decrease in local viscosity. However, when either the rotational or translational relaxation time is the limiting aspect for a particular small PHC-water glass-forming system, the ranking of solutes, i.e., either by $\overline{M}n$ or $\overline{M}w$ (as in Table 6), would be expected to depend on the underlying mechanism of the specific mechanical relaxation.[30]

Experimental mechanical relaxation processes can be categorized in terms of their control by rotational or translational mobility.[30] For example, homogeneous nucleation depends on both translation and rotation, but can be completely controlled and limited by the rotational mobility.[4,104,115,296] The response to microwaves, in a microwave dielectric dispersion experiment,[200-202,204] is another rotational response. In contrast, the apparent, non-equilibrium RVP depends on translational mobility.[15,16] Other mechanical relaxation processes controlled by translational mobility include starch gelatinization,[20,21] mold spore germination,[15,16] crystal growth,[15,104] collapse phenomena,[8,27] and freeze-drying.[33,40,41] A conceptual experimental approach to the study of these various relaxation processes,[30] as they pertain to the non-equilibrium behavior of PHC-water and other aqueous food systems, are reviewed in the remainder of Section V.

The selection of a molecule to be used as a reporter to probe the local environment is a critical element of experiments to study mechanical relaxation processes. A very low concentration of reporter molecule (e.g., a dye) is required for translational and rotational diffusion experiments, in order to avoid concentration gradients and perturbation of the local relaxation due to plasticization by the reporter.[362] Water itself is *not* a good candidate for the role of reporter molecule to study the mobility of aqueous glasses, because water would then be both a functional part of the sample matrix and a reporter in many experiments.[30] For example, in a NMR investigation of the mobility of water in an amorphous polymer, the water concentration cannot be changed without significantly changing the system itself, because of the effect of water as a plasticizer.[25] Thus, a third molecule would be needed to act as the reporter. Later, we describe how high-polymeric starch has been used to fill this key role.[30] In this context of a discriminating experimental approach, it is worth reiterating that small-PHC aqueous glasses are uniquely excel-

lent model systems for the study of non-equilibrium relaxation processes.[30] For solute MWs below the entanglement MW of ≈3000 (glucose DP ≲ 18), such non-entangling polymers allow the study of the contributions of free volume and local viscosity (as the *measured* viscosity), without the ambiguity introduced by convolution with the bulk entanglement-network viscosity, which would be essentially the same for all polymers.[107] As shown earlier in Table 8, glass compositions can be measured quantitatively in terms of $\overline{M}n$ and $\overline{M}w$. Moreover, in contrast to aqueous glasses of ionic salts, complicating effects due to specific ion hydration and concentration-dependent pK can be avoided.[30]

A. Water Sorption Isotherms for Glassy and Rubbery Polymer Systems

Water sorption, and the beneficial or detrimental effects thereof, can play a critical role in many food processes and products. For example, with respect to doughs and baked goods,[26] absorption of liquid water by the amorphous polymeric carbohydrates and proteins in flours, leading to their kinetically controlled plasticization ("hydration") during dough mixing, is obviously a key element of dough formation and an important determinant of the rheological properties and mechanical behavior of doughs.[45,209,363] Non-equilibrium evaporative desorption of water vapor[58] is a crucial aspect of the baking process. Time- and temperature-dependent ad/desorption of water vapor during ambient storage is a potentially important aspect of the stability and shelf-life of baked products.[26] These examples simply help to emphasize the universal and indisputable fact that an understanding of the water sorption behavior of (1) individual ingredients or natural food materials prior to processing, (2) formulations of ingredients during processing, and (3) finished products after processing is a vital requirement of any assessment of food quality, safety, and stability.

1. Sorption Hysteresis, Sorption Kinetics, and Effect of Temperature on Sorption

It has been recently stated[364] that the reasons for the well-known irreversibility and hysteresis shown by water vapor sorption isotherms of biopolymers, including various food proteins and carbohydrates,[62,365,366] are not established. Bryan[364] has suggested that observed "irregularities reflect changes in the conformation and/or dynamic behavior of the biopolymer molecule." He has noted that "recent work on water-protein interactions[367,368] is compatible with the occurrence of small conformational changes and increased flexibility (perhaps a loosening of the protein structure) as more water is added to a protein" in the solid state. Lillford[58] has expressed a similar opinion, crediting (as others had previously[8]) the onset of enzymatic activity in low-moisture, amorphous lysozyme powders to plasticization by sorbed water, leading to sufficient segmental mobility for diffusion-limited enzyme-substrate interactions to occur. With respect to water-protein sorption hysteresis, Bryan[369] has suggested that hysteresis "could result from slow, incomplete conformational changes occurring upon addition of water" to proteins in the solid state, and its subsequent removal. These changes could result from incomplete "intermolecular phase annealing" or "phase changes", and the resulting hysteresis "might be related to the physical state and prior history of the sample".[369] Again, Lillford[58] has expressed similar sentiments, pointing out (again as others had previously[15]) that starch[62] and other hydrophilic polymers plasticized by water "are far from inert in the adsorption process", should not be modeled as "an immobile and unaffected substrate", manifest a "non-equilibrium desorption process responsible for hysteresis", and probably are "usually in a metastable kinetic state . . . where the interaction of polymers and water cannot be treated in terms of equilibrium thermodynamics". Bryan[369] has also noted the fact that

freeze-dried protein samples to be used as substrates in sorption experiments "might form an amorphous (solid) phase", a possibility overlooked by Lioutas et al.[351] in their discussion of the water sorption behavior of lysozyme.

In a recent review that included this subject,[15] an explanation (subsequently endorsed by Lillford,[58] Karel,[64] and Paakkonen and Roos[126]) for the sorption behavior described by Bryan[364,369] has been offered. Water vapor absorption in food systems can be treated as a diffusion-limited transport process involving structural relaxations in glassy and rubbery polymers. The kinetics of diffusion rates associated with adsorption leading to absorption[366] and with sorption-desorption hysteresis[365] depend, in part, on the ever-changing structural state of a polymer, relative to its Tg, and on the polymer's extent of plasticization by water.[15] For sorption by synthetic amorphous polymers at $T \ll Tg$, it has been suggested that classical Fickian diffusion of low MW plasticizing sorbate, which may appear to be time-independent[370] and to show Arrhenius-type temperature dependence, may actually be an indication of extremely slow and inconspicuous relaxation[172] in a kinetically metastable glassy polymer moving toward its equilibrium state.[371] In the temperature range near but below Tg to 5 to 10°C above Tg (the latter the so-called "leathery" region shown earlier in Figure 32), observations of anomalous, non-Fickian or viscoelastic,[372,373] time-dependent, cooperative diffusion have been suggested to indicate that the glassy state is relaxing more rapidly to the rubber,[371] or in other words, that the "polymer relaxation time matches the sorption time scale".[373] These sorption situations also reflect the fact that water plasticization of glassy polymers leads to increasing permeability of the substrate to gases and vapors, due to increasing segmental mobility of the polymer as Tg decreases relative to the constant sorption temperature, Ts.[15] In the rubbery state well above Tg, diffusion and relaxation rates increase sharply, as does polymer free volume (which is known to cause a dramatic increase in permeability to gases and vapors[55]). At the point where WLF-governed temperature dependence begins to approach Arrhenius temperature dependence,[168] Fickian diffusion behavior again applies.[156,371]

The dependence of non-equilibrium sorption behavior on Tg relative to Ts, described earlier, has been illustrated nicely by results of a study, shown in Figure 68,[297] of the kinetics of water uptake, as a function of environmental RVP at room temperature, in a low-moisture food material representative of other amorphous or partially crystalline substrates. The illustrated sorption behavior reflected both adsorption of water vapor and absorption of condensed liquid water via a diffusion-limited transport process (i.e., a mechanical relaxation process governed by the mobility of the substrate matrix). These sorption results of Duckworth were said to "reveal that the time which is required to reach equilibrium conditions needs special attention", and that "equilibration times of at least 14 d might be recommended".[297] It has been suggested[30] that

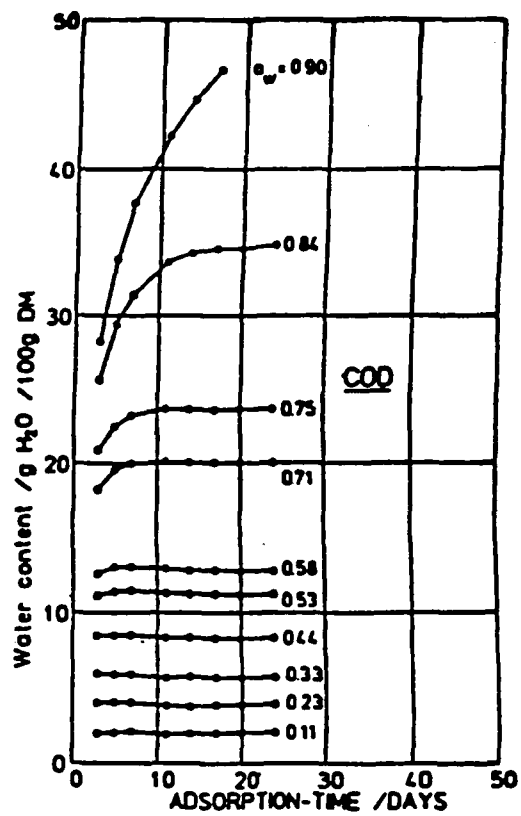

FIGURE 68. Water content as a function of adsorption time at different conditions of environmental RVP, illustrating the sorption kinetics of cod at 25°C. (From Wolf, W., Spiess, W. E. L., and Jung, G., *Properties of Water in Foods*, Simatos, D. and Multon, J. L., Eds., Martinus Nijhoff, Dordrecht, 1985, 661. With permission.)

the results in Figure 68 in fact demonstrated that times that are orders-of-magnitude greater than 14 d would be required to approach equilibrium conditions. In such sorption experiments, a low-moisture, amorphous food system may be in an extremely low mobility, "stationary" solid state so far from equilibrium[172] that it can be easily confused with equilibrium. Figure 68 showed that, even in 25 d, there was no change in water uptake when the environmental RH was 11%. The essentially immobile solid sample remained far from equilibrium in a low-moisture, negligibly plasticized "apparent steady state". In sharp contrast, in less than 25 d, there was a dramatic change in water uptake by the same substrate material when the RH was 90%. Under these conditions, the higher moisture sample was significantly plasticized and exhibited sufficient mobility to allow a more rapid approach toward a still-higher moisture and not-yet-achieved equilibrium condition. The fundamental trend of increasing sorption rate with increasing environmental RH evidenced by the results in Figure 68 has suggested a mechanistic correlation between increasing mobility and increasing rate of relaxation of the substrate-water system toward its unique final state of equilibrium.[30] This correlation reflects the sequential relationship between increasing water uptake, increasing plasticization, increasing free volume and decreasing local viscosity, which result in decreasing Tg. (Recall that the sequence of plasticization lagging behind water uptake and swelling was also suggested earlier in Section III.A.4 with respect to the sorption of water by native granular starches.[159]) Viewed in isolation on a practical time scale, the unchanging nature of the low-moisture substrate at low RH would prevent an observer from recognizing this non-equilibrium situation of extremely slow mechanical relaxation.[30]

From countless studies of so-called "equilibrium" water vapor sorption and sorption isotherms for completely amorphous or partially crystalline, water-compatible polymers, two general characteristics have become widely acknowledged.[15] One is that such experiments do not usually represent a true thermodynamic equilibrium situation, since the polymer substrate is changing structurally (and slowly, during sorption experiments that are often [and sometimes recognized to be][370,376] much too short) due to plasticization by sorbed water.[4,62,64,79,363,365,371,372] Secondly, since Tg decreases during sorption, such experiments are not even isothermal with respect to the ΔT-governed viscoelastic properties of the polymer, because ΔT ($= Ts - Tg$) changes dynamically over the sorption time course.[15,365,371] Consequently, both the extent of sorption and the mobility of sorbed molecules generally increase with increasing plasticization by water.[375,376]

As reviewed recently elsewhere,[15] the basic premises that underlie the interpretation of the water sorption characteristics of food polymer systems include the following: (1) the sorption properties of a "dry" polymer depend on its initial structural state and thermodynamic compatibility with water;[372] (2) in both completely amorphous and partially crystalline polymers, only the amorphous regions preferentially absorb water;[157,377] and (3) the shape of a particular sorption isotherm depends critically on the relationship between Ts and both the initial Tg of the "dry" polymer and Tg of the water-plasticized polymer during the sorption experiment.[378] Several interesting illustrations of these points have been described.[15] For example, for sorption experiments done at a series of temperatures that bracket Tg of the water-plasticized polymer, the classic sigmoidal shape of the isotherm, at $Ts < Tg$, flattens suddenly, at $Ts > Tg$, to one characteristic of solution sorption by a rubbery polymer. Such behavior was illustrated earlier for an epoxy resin in Figure 12.[80] This synthetic, water-sensitive polymer system manifests isotherms approaching linearity at high RVP for sorption temperatures above the water-plasticized Tg, which evidently lies between 75 and 100°C for this sample. It has been noted that the onset of the glass transition is indicated by a conspicuous change in a polymer's sorption behavior, which coincides with a dramatic change in the polymer's specific volume.[15] Thus, the temperature-percent moisture point (i.e., Tg) at which a plot of specific volume vs. temperature[15] characteristically changes slope is reflected in sorption isotherms (such as those in Figure 12) as the coincident temperature-percent moisture condition above which the sorption curve is a flat line characteristic of solution sorption by a rubbery

polymer, but below which the sigmoid sorption curve is characteristic of so-called "water clustering"[379] in a glassy polymer.[15]

In other instances of sorption at a series of temperatures, all well below the initial Tg of the "dry" polymer, the effect of increasing Ts on sorption behavior can be less pronounced than that evidenced in Figure 12. The result can be a set of typical sigmoid adsorption curves, such as shown in Figures 14A and B for pectin and caseinate,[81] two high MW biopolymers with dry Tg $\gg$ 100°C. In these cases, initial sorption, at any Ts, was by an immobile, glassy solid substrate. The effect of increasing plasticization of the substrate due to increasing Ts and increasing water uptake (thus, decreasing "wet" Tg) resulted in increasing system mobility, as both ΔT (i.e., Ts − Tg) and ΔW (i.e., Ws − Wg) increased with increasing moisture content. As shown in Figure 14 for these two amorphous food polymers, at a given moisture content, increased system mobility was reflected by increased RVP with increased Ts, but there was no sudden change in shape of the isotherms to that characteristic of liquid solution sorption at Ts > Tg.

Unlike the typical isotherms for amorphous high polymers in Figures 12, 13, 14A, and 14B, the adsorption isotherms for sorbitol and xylitol in Figures 14C and D[81] are not smooth sigmoidal curves. Moreover, at a given moisture content (e.g., 0.1 g water/g solid), these isotherms showed RVP decreasing with increasing Ts. These low MW, water-soluble polyols were initially crystalline solids, so the atypical shape of the isotherm at a given Ts reflected the amount of sorbed water needed to act as a solvent and dissolve the crystals. As the crystals began to dissolve, a supersaturated solution was formed. Thus, instead of the typical situation of increasing moisture content and increasing Ts acting together to plasticize an amorphous substrate and increase system mobility, these conditions acted together to dissolve more and more crystalline material and increase the amount of concentrated solution formed, thereby actually decreasing the mobility of the solute-solvent system. As shown in Figures 14C and D, this situation was manifested by RVP *decreasing* with increasing Ts, until enough water had been sorbed to dissolve all the crystalline solid. Beyond this point, increasing sorbed water and increasing Ts were acting to plasticize an amorphous substrate (i.e., a concentrated PHC syrup), so the isotherms (in Figure 14C) "crossed over" at higher moisture contents and showed the more typical sorption behavior of RVP increasing with increasing Ts. Thus, this unusual "crossover" behavior was revealed to be symptomatic of a change in structural state (and phase) of the water-soluble substrate with increasing water uptake, from crystalline solid (with RVP decreasing with increasing Ts) to amorphous liquid (with RVP increasing with increasing Ts).

The adsorption isotherms for amorphous glucose (dry Tg = 31°C) at 30 and 80°C, shown in Figure 69 (adapted from Loncin[75]), illustrate another interesting example of "crossover" behavior. However, in this case, the "crossover" behavior was opposite to that shown in Figure 14C, and so was revealed to be symptomatic of a change in structural state (and phase) of the substrate with increasing water uptake at 30°C, from amorphous liquid (with higher RVP at higher Ts) to crystalline solid (with lower RVP at higher Ts). Initially, one of these sorption experiments was conducted right at Tg of the amorphous substrate (i.e., assuming bone-dryness), while the other was performed at Ts 50°C above dry Tg. In each case, by a given low moisture content, the substrate was an amorphous rubbery fluid, so the isotherms showed the typical relationship of higher RVP at higher Ts. By the time amorphous glucose picked up about 9 w% water, its "wet" Tg was depressed to about 10°C, at which point the two sorption temperatures were 20 and 70°C above Tg. In the latter situation, the mobile glucose-water substrate evidently remained a very concentrated (but *not* supersaturated at 80°C) liquid solution as its moisture content and RVP continued to increase. (If glucose, under these temperature/moisture content conditions, had crystallized to the anhydrous crystalline solid form, the isotherm would have shown a discontinuity resulting from such a phase change,[64] as did the one for sucrose in Figure 15A.) However, in the former situation, the viscous fluid glucose-water substrate (which *was* a supersaturated solution at 30°C) became sufficiently mobile, due to plasticization by water, at about 20°C above Tg to permit some of the glucose to crystallize to the solid monohydrate (containing 10 w%

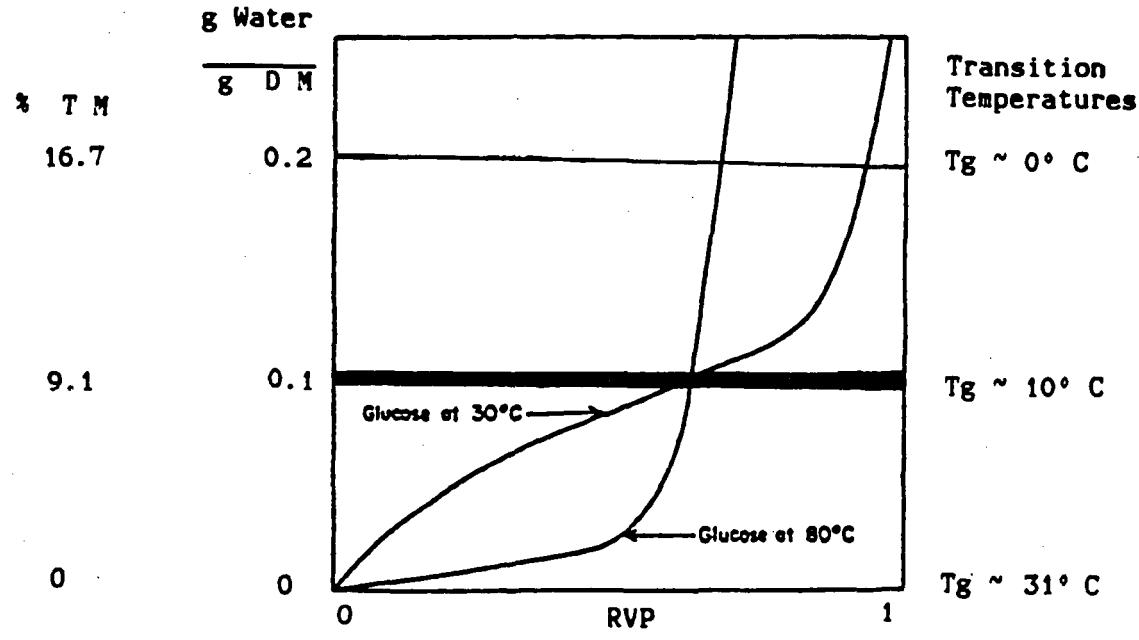

FIGURE 69. Adsorption isotherms of amorphous glucose at 30 and 80°C. (From Loncin, M., *Freeze Drying and Advanced Food Technology*, Goldlith, S. A., Rey, L., and Rothmayr, W. W., Eds., Academic Press, New York, 1975, 599. With permission.)

water, and thus not causing a discontinuity in the isotherm), while the rest remained in solution. As a consequence of this phase change during the sorption experiment at 30°C (but not at 80°C), the two isotherms "crossed over" and subsequently showed, at higher moisture contents, lower RVP at higher Ts.

For sorption at a single temperature, initially well below Tg of a "dry" polymer, but subsequently above the "wet" Tg, depressed due to water uptake and plasticization, an isotherm can show a sudden change in slope, due to the structural transition at Tg,[164,378,380] or even a discontinuity resulting from a change of phase. Similar dynamic behavior has been observed in cases where an amorphous but crystallizable substrate (e.g., low MW sugars such as sucrose[82,381] (as shown earlier in Figure 15A by the discontinuity in the adsorption isotherm), amylopectin in gelatinized starches,[62,382] or amorphous gelatin[24]), initially in the form of a low-moisture glass, recrystallizes from the rubbery state, after plasticization due to sorption of sufficient moisture, which allows the glass transition to occur, either deliberately during short-term sorption experiments or inadvertently during long-term product storage.[54,137] (Note, as alluded to above, that the adsorption isotherm for amorphous sucrose in Figure 15A showed a discontinuity, because sucrose recrystallized to an anhydrous crystalline solid form. In contrast, the adsorption isotherm for amorphous glucose at 30°C in Figure 69 showed no discontinuity, because glucose, in the rubbery fluid under those temperature/moisture conditions, would have recrystallized to the solid monohydrate.)

In other instances of single-temperature sorption by initially glassy polymers, an isotherm may not show a sudden, diagnostic change in slope at the effective "wet" Tg. Such behavior is illustrated for nylon 66 in Figure 70A[155] and for elastin in Figure 19B.[132] Starkweather's results for nylon[155] have demonstrated the important fact that, while RVP was, in typical fashion, *not* increasing linearly with increasing sample moisture content (Figure 70A) for this water-sensitive, synthetic polymer, RVP *was* linear with the effective "wet" Tg (identified as the so-called α-relaxation temperature, which decreased linearly with increasing RVP, as shown in Figure 70B), measured in terms of the mechanical loss modulus. The same linear relationship between

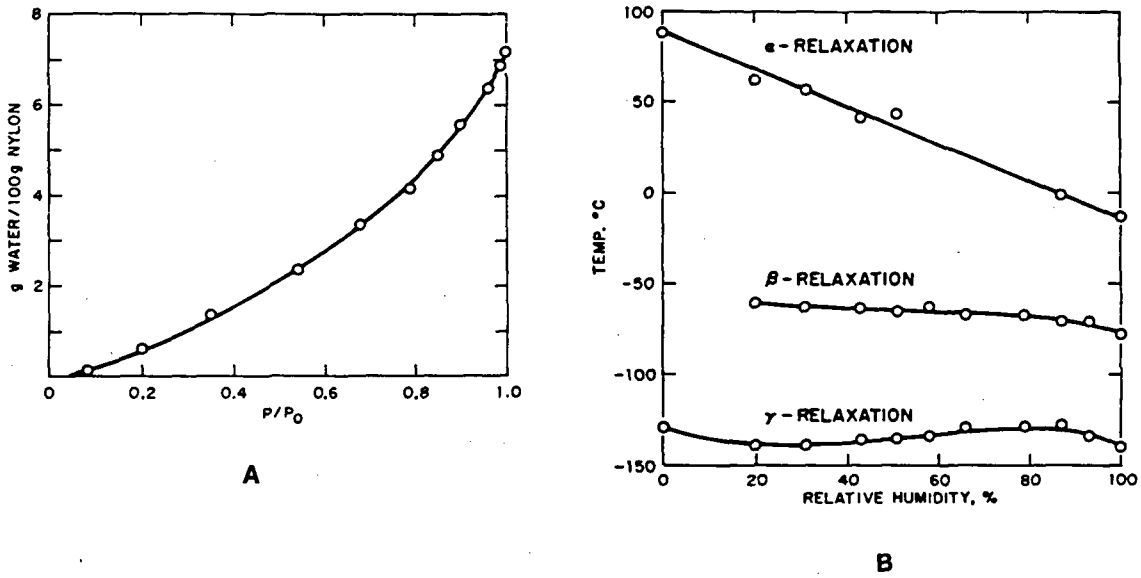

FIGURE 70. (A) Sorption isotherm for water in 66 nylon at 23°C. (B) Temperature of peaks in loss modulus vs. relative humidity. (From Starkweather, H. W., *Water in Polymers*, Rowland, S. P., Ed., ACS Symp. Ser. 127, American Chemical Society, Washington, D.C., 1980, 433. With permission.)

decreasing Tg and increasing RVP has also recently been reported for amorphous food materials by Roos and Karel, in their plots of Tg (measured by DSC) vs. so-called "water activity" for freeze-dried sugars[66] and freeze-dried strawberries.[125]

As mentioned in Section III.A, elastin is an amorphous, water-compatible, crosslinked, viscoelastic network-forming protein whose water sorption behavior has been studied extensively.[130-132,136,353,354,383] The fraction of sorbed water up to ≈0.35 g water/g dry elastin (= Wg′) is "unfreezable" and strongly plasticizing.[132,168,353,354] This water is said to represent a thermodynamically compatible solvent, so that such elastin-water mixtures are homogeneous, single-phase solutions.[130] The sigmoidally shaped sorption isotherm for dry elastin at 25°C shown in Figure 19B has been interpreted as showing "water clustering" and the start of cluster growth at water contents well below the thermodynamic compatibility limit of 0.35 g water/g.[132] (These so-called "water clusters" are imagined as long linear chains of hydrogen-bonded water molecules that form as a result of poor compatibility with relatively apolar polymers such as elastin and collagen.[168]) For example, after sorption at 70% RH to 0.16 g water/g and Tg ≃ 40°C, cluster size was said to begin to increase in still glassy elastin, while this increase was said to begin later in rubbery elastin, after sorption at 80% RH to 0.19 g water/g and Tg ≃ 25°C.[132] The second sorbed water fraction (0.35 to 0.60 g/g) is "freezable", less strongly plasticizing, and referred to as "loosely bound".[354] These sorption results have been interpreted in alternative ways. Some workers[136-138] have used the classic "BET monolayer" approach[80] to explain the sorption behavior of elastin. The calculated BET monolayer value of 7 w% water has been invoked[136] to account for the apparent fact that the Tg of elastin is depressed most strongly by the first 7 w% of sorbed water and then less strongly by the "BET-multilayered"[372] or Zimm-Lundberg "clustered"[379] sorbed water. In fact, as discussed earlier in this section and in Section II.A.5, no such sorption concepts (which are either meaningless, e.g., "BET monolayer", or misleading, e.g., "water clustering") need be invoked to understand the nonequilibrium sorption behavior of amorphous polymers such as elastin.[15]

At T > Tg of water-plasticized elastin, the crosslinked network manifests dynamic mechanical properties (which follow the WLF equation) characteristic of rubber-like elasticity, including a dramatic increase in extensibility, which, as

explained earlier, are critical to the physiological activity of this protein.[354] Elastin has been referred to as an especially mobile rubbery polymer.[132] The elastin-water system exhibits the classic symptoms of an amorphous polymer-plasticizer interaction.[130,131] From a comparison of the Tg curves for elastin (e.g., see Figure 19A) and collagen, Batzer and Kreibich[383] reported that the extent of plasticization is somewhat less for elastin, because elastin is more heavily crosslinked than collagen, but still within the typical range, at about 8°C/w% water, up to 24 w% water. The smooth glass curve for elastin in Figure 19A illustrates the dramatic plasticizing effect of sorbed water (initially, at Ts $\ll$ Tg) on such a water-compatible glassy polymer at low moisture. The first 7 w% moisture depresses the Tg of bone-dry elastin (about 200°C) by about 110°C, while the next 17 w% moisture depresses Tg by an additional 4°C/w% water. By the time dry elastin has sorbed about 24 w% water, its Tg has been depressed below room temperature, so that Ts $>$ Tg, and the kinetics that govern the diffusion-limited sorption by rubbery elastin have switched from Arrhenius to WLF (i.e., increases in diffusion rates have changed from about a doubling to about a factor of 10 for each 1 w% increase in water).[15] This fact, combined with recognition and quantitation of how ΔT changes during water sorption by elastin, can account for the shape of the Tg curve and the observation[132] of increased sorptive capacity by this especially mobile rubbery polymer.[15]

Sorption-desorption hysteresis has been called "the outstanding unexplained problem in sorption studies".[365] Many completely amorphous and partially crystalline polymers, both synthetic and natural, which swell slowly and irreversibly during water sorption, show marked hysteresis between their absorption and desorption isotherms.[64,366] In partially crystalline biopolymers (e.g., native starch), hysteresis increases with increasing percent crystallinity.[62] Buleon et al.[384] have attributed the sorption hysteresis observed in acid-hydrolyzed ("lintnerized") native starches to their metastable semicrystalline structure, by analogy to synthetic elastomers with crystalline domains, which "are more prone to develop hysteresis in association with internal stresses than other (completely amorphous) polymers, in which relaxation processes occur with ease".

Water-soluble polymers such as PVP have been reported to show hysteresis (for sorption at room temperature) at moisture contents $<$Wg', which corresponds to the "unfreezable" fraction of total sorbed water.[4] The PVP-water system at subzero temperatures has also been reported to show hysteresis in sorption behavior, as illustrated in Figure 71.[242] The sets of desorption and resorption isotherms measured at sample temperatures from -40 to 25°C, shown in Figure 71A and B, are those related to the freeze-drying process for PVP. These isotherms, like the ones in Figures 12, 13, 14A, and 14B, showed the expected variation of sorption behavior with temperature for amorphous polymers: i.e., at a given sample moisture content, sample RVP increases with increasing temperature. (The "crossover" behavior [in this case to RVP decreasing with increasing temperature] at the highest RVPs shown by the resorption isotherms in Figure 13 are discussed later, in comparison to the "crossover" behavior already described with respect to Figures 14C and 69.) They also showed, like the ones in Figures 13 and 16, the expected consequence of hysteresis: i.e., at a given sample moisture content and temperature, sample RVP is lower during desorption than during resorption. However, the set of desorption isotherms in Figure 71A showed an unexpected and unexplained discontinuity in behavior between -10 and 2°C. Below -10°C, 10°C jumps in temperature produced proportional changes in desorption behavior, but between -10 and 2°C (a similar jump of 12°C), a discontinuity was manifested. We suggest that this discontinuity arose as a consequence of the structural transition of the freeze-concentrated PVP-UFW matrix (i.e., the amorphous substrate undergoing desorption), which occurs at Tg' around -20°C (see Table 8). The discontinuity was not observed, on the time scale of the sorption experiment, until the temperature was increased to 2°C, because, as dictated by WLF kinetics and illustrated earlier in Figure 36, the mechanical/structural relaxation process underlying this sorption behavior by the rubbery fluid PVP-UFW substrate would not have occurred in real time, with a significant, experi-

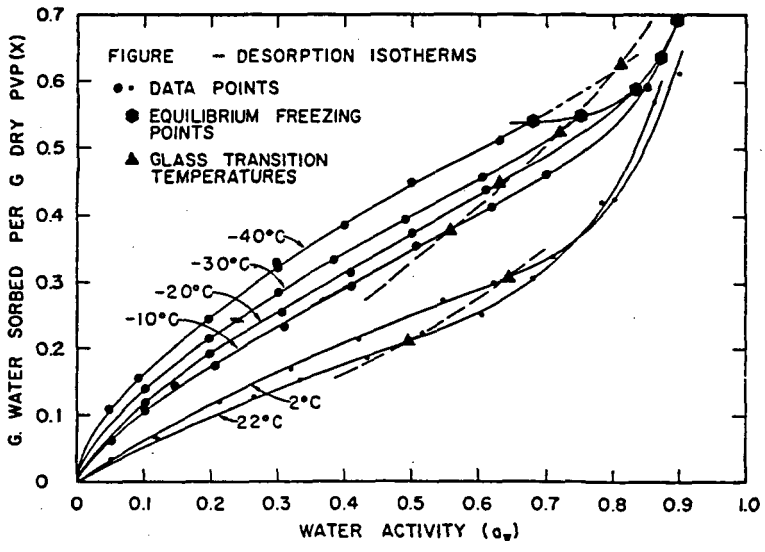

A

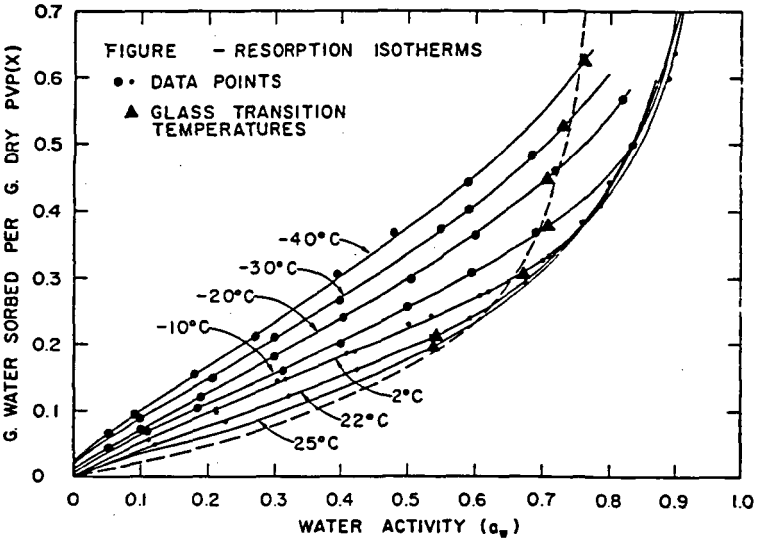

B

FIGURE 71. (A) Desorption isotherms and (B) resorption isotherms, measured over a temperature range of −40 to 25°C, for aqueous PVP samples (i.e., either frozen dilute solutions or freeze-dried powders). (From MacKenzie, A. P. and Rasmussen, P. H., *Water Structure at the Water-Polymer Interface,* Jellinek, H. H. G., Ed., Plenum Press, New York, 1972, 146. *With permission.*)

mentally observable rate (i.e., 10^5 higher than at Tg), until the temperature was increased to about 20°C above the reference Tg (i.e., Tg'). (Another similar example of the impact of WLF kinetics on the rate of a relaxation process observable in real time was shown earlier in Figure 69. At a sorption temperature [30°C] about 20°C above the instantaneous "wet" Tg of an amorphous glucose substrate plasticized by 9 w% water, the rubbery fluid glucose-water mixture was sufficiently mobile to allow glucose to crystallize to the monohydrate in the time frame of the sorption

experiment.) It should be noticed that the set of resorption isotherms in Figure 71B also showed a similar (albeit smaller) discontinuity, but it was manifested at a different temperature, i.e., between -10 and -20°C. We suggest that the reason for this difference in temperature is that the appropriate reference Tg underlying the discontinuity in the resorption behavior of already-freeze-dried, glassy solid PVP is not Tg′ but rather a higher-temperature Tg corresponding to an instantaneous condition of lower moisture (i.e., $Wg < Wg'$).

As illustrated by the PVP-water system described above, the extent of hysteresis (or other manifestations of anomalous sorption behavior) at a particular Ts depends on the rate of the swelling/deswelling relaxation process in an amorphous polymer substrate,[365,366,370,371,378] and thus has been suggested to depend on the instantaneous value of Tg (as governed by the instantaneous value of Wg[21]) and the corresponding magnitude of ΔT, during both the sorption and desorption experiments, in a manner consistent with WLF free volume theory.[15] Unfortunately, as has been noted frequently,[58,83] hysteresis cannot be explained by any thermodynamic treatment that applies only to, or any model originally derived for, reversible equilibrium states. Hysteresis is not an intrinsic feature of a sorbing polymer, but depends on the experimental conditions.[366] The often anomalous nature of sorption-desorption that has been associated with hysteresis, including non-Fickian diffusion behavior, is due to dynamic plasticization of a glassy or partially crystalline polymer by water during a sorption experiment.[62,371,372] It has been concluded that hysteresis characteristically results from a moisture-/temperature-/time-dependent, slow, non-equilibrium, swelling-related conformational change (involving a structural relaxation [as illustrated in Figure 71], and in some cases, even a subsequent phase change [as illustrated in Figure 15A]), which is facilitated by increasing free volume and segmental mobility in a polymer that is being plasticized dynamically during sorption.[58,64,83,126,366] For example, Buleon et al.[384] have suggested that the irreversible sorption behavior of lintnerized starches is due to a water-plasticized conformational change, leading to a "structural hysteresis" that develops in a temperature/moisture content domain corresponding to a partially rubbery, partially crystalline system. In such systems, true thermodynamic equilibration can take weeks, months, or even years to be achieved.[370,376]

Sorption hysteresis has also been observed in molten polymers well above their Tg, for example, in concentrated molten synthetic polymer-organic solvent solutions.[385] It had been argued[83] that such hysteresis cannot be simply explained by linking this behavior to non-equilibrium effects imposed by the properties of the glassy solid state. However, it has been recently demonstrated[30] that the correlated parameters of local viscosity and polymer Tm/Tg ratio do in fact critically influence the mobility of supra-glassy liquids (i.e., low-viscosity liquids well above their rubbery domain), such as molten polymers, even at temperatures 100°C or more above Tg. Figure 72[30] (adapted from Reference 107) revealed the critical importance of local viscosity even at 100°C above Tg, and disclosed the relationship between this local viscosity, the corresponding translational relaxation time, and polymer Tm/Tg ratio. The figure presents a ranking of values of log (translational friction coefficient) measured at $T = Tg + 100$°C, for a variety of synthetic polymers. The frictional coefficient was measured in two ways with equivalent results, as segmental mobility of the polymer backbone and as small-molecule diffusion of a reporter (probe) molecule at sufficiently low concentration that there was no measurable depression of Tg due to plasticization. Thus, the translational relaxation time, as reflected by the frictional coefficient or the translational diffusion coefficient, is related to the local viscosity surrounding polymer chain segments, rather than to an inherent structural/mechanical feature of the chain itself.[107] Decreasing translational relaxation time correlates with decreasing frictional coefficient, increasing diffusion coefficient, and decreasing local viscosity.

It has been generally thought that one can best compare and control the behavior of amorphous materials at temperatures at or near their Tg, and that in order to "freeze" events in time and thus magnify the behavioral differences between materials, one must do experiments at $T < Tg$, where relaxation rates are extremely slow. However, Figure 72 illustrated that when

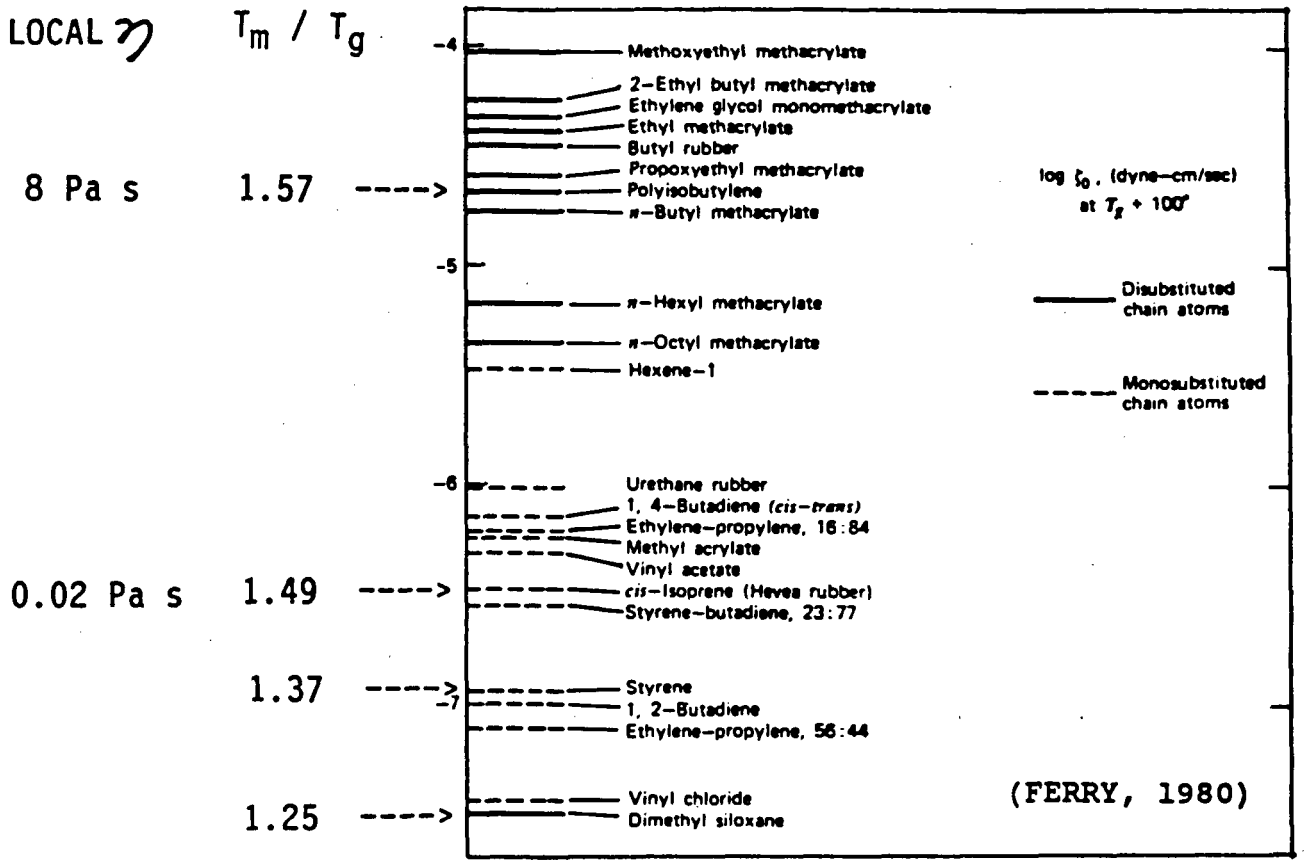

FIGURE 72. A ranking of synthetic polymers by their values of log (translational friction coefficient), measured at T = Tg + 100°C, and corresponding values of local viscosity at the same temperature, and Tm/Tg ratio. (The list of ranked polymers reproduced with permission from Reference 107.) (From Levine, H. and Slade, L., *Pure Appl. Chem.*, 60, 1841, 1988. With permission.)

polymers are studied even 100°C above their individual Tg values, there are orders-of-magnitude differences in the self-diffusion rate of the backbone-chain segments or the diffusion rate of small molecules that are similar to the monomer. For example, for poly(isobutylene) and Hevea rubber, at 100°C above their almost identical Tg, there is about a 100-fold difference in the translational diffusion rate of a small reporter molecule, with the Hevea rubber showing the lower local viscosity and lower frictional coefficient and allowing the faster diffusion rate. In the case of poly(dimethyl siloxane), whose low ranking on the list in Figure 72 had been considered quite anomalous,[107] there had been no previous explanation for why its frictional coefficient and local viscosity, 100°C above Tg, are so low compared, for example, to those of poly(isobutylene). However, addition of the Tm/Tg ratios,[30] calculated from reported data for Tm and Tg of these polymers,[107] to Figure 72 revealed a progressive decrease in this parameter with decreasing local viscosity and frictional coefficient, which in turn reflects an increase in mobility and translational diffusion rate, and a decrease in relaxation time. It was suggested[30] that the underlying basis for these behavioral correlations is that the least viscous, and thus most mobile materials, even 100°C above Tg, are those that have the lowest values of Tm/Tg ratio, while the most viscous, least mobile materials are those with the highest Tm/Tg ratios. This correlation in turn supported the earlier conclusion, from the analysis of Figure 34D, that for a common value of Tg (e.g., for the elastomers poly[isobutylene] and Hevea rubber), different values of Tm/Tg ratio for different polymers can be used to compare relative mobilities both at Tg and at T ⩾ Tg.[30] (This con-

clusion was also supported by the results of the mold spore germination experiment, analyzed as a mechanical relaxation process, mentioned earlier with respect to Table 2.) It was noted that a small difference in the values of Tm/Tg is manifested as a dramatic difference in local viscosity and translational diffusion. In the example described above, the values of Tm/Tg for Hevea rubber and poly(isobutylene) are 1.43 and 1.57, respectively, and the local viscosities at 100°C above Tg differ by nearly 2 orders of magnitude.

The importance of this correlation between local viscosity and Tm/Tg ratio has been related to the apparently pivotal influence of these two parameters on the mobility of supra-glassy liquids, such as molten polymers, even well above Tg.[30] This finding was coupled with the earlier explanation of how the relationship between ηg, Tm/Tg ratio, and mobility can be used to characterize the non-equilibrium behavior in the glassy solid state at Tg and in the rubbery fluid state above Tg, and also the size of the temperature domain corresponding to the WLF region.[30] It was mentioned with respect to Figure 34C that for an atypical, poorly behaved polymer with Tm/Tg = 1.25, the rubbery region of WLF behavior might only extend about 50°C above Tg. Thus, some of the polymers listed in Figure 72 (especially poly(dimethyl siloxane)), at 100°C above Tg, probably exist as low-viscosity liquids well above their rubbery domain. Yet, the influence of local viscosity and Tm/Tg ratio still carries over to their supra-glassy, non-equilibrium behavior. It has been suggested[30] that this point is crucial in countering the argument[83] mentioned earlier that sorption hysteresis observed in molten polymers well above their Tg cannot be simply explained by linking this behavior to non-equilibrium effects imposed by the properties of the glassy solid state. Analogous hysteresis between water vapor ad/absorption and liquid water desorption in native starch (shown earlier in Figure 16A) has been reported to result from desorption that remains non-equilibrated even after 2 years, vs. adsorption that achieves and remains in "well-defined equilibrium" states over the same period.[83] An alternative explanation for the observed hysteresis has been suggested,[30] whereby both limbs of the isotherm reflect the persistence of non-equilibrium states. The desorption limb represents the behavior of supra-glassy, partially crystalline starch drying slowly and irreversibly to a partially crystalline glassy state[20,21] different from the original native state. In contrast, the ad/absorption limb represents the behavior of partially crystalline glassy native starch undergoing an extremely slow, water-plasticized relaxation process,[62] which remains very far from equilibrium[172] even after 2 years, to a supra-glassy, partially crystalline state, i.e., a "pseudo steady state" easily mistaken for equilibrium. This same "pseudo steady state" behavior has been observed for the sorption of water vapor by cod,[297] as described earlier with respect to Figure 68.

It has been noted that the low values of local viscosity at T = Tg + 100°C shown in Figure 72 compare to a macroscopic viscosity of about 10^9 Pa s for an entanglement network, and even higher viscosities if the network is crosslinked.[107] This point and the above discussion of the implications of Figure 72 have underlined the importance of research on small PHC-water systems,[281] based on a polymer science approach.[30] Synthetic high polymers, as well as many high-polymeric food materials, often suffer from the handicaps of unknown, polydisperse MW and MW distribution, and MWs above their entanglement limit, in which case local viscosity is *not* equivalent to macroscopic viscosity. For such cases of MWs above the entanglement limit, a halving of MW results in a tenfold reduction in the macroscopic viscosity of the network.[107] (This behavior is illustrated, for a series of synthetic polymers, by the log-log plot of viscosity vs. MW in Figure 73.[107] In this plot, the entanglement MW limit, coinciding with the critical linear DP required for intermolecular network formation, corresponds to the point at which the slope changes abruptly.) In contrast, small PHCs have known, monodisperse values of MW, all below the entanglement limit, so that local viscosity *is* equivalent to macroscopic viscosity, and a halving of MW results only in a halving of local viscosity (as also illustrated in Figure 73 for synthetic polymers with MWs below their entanglement limits).[107] Such small PHCs offer a great variety and selection of glass-forming food materials for the study of water sorption and other aspects of non-equilibrium behavior.[30]

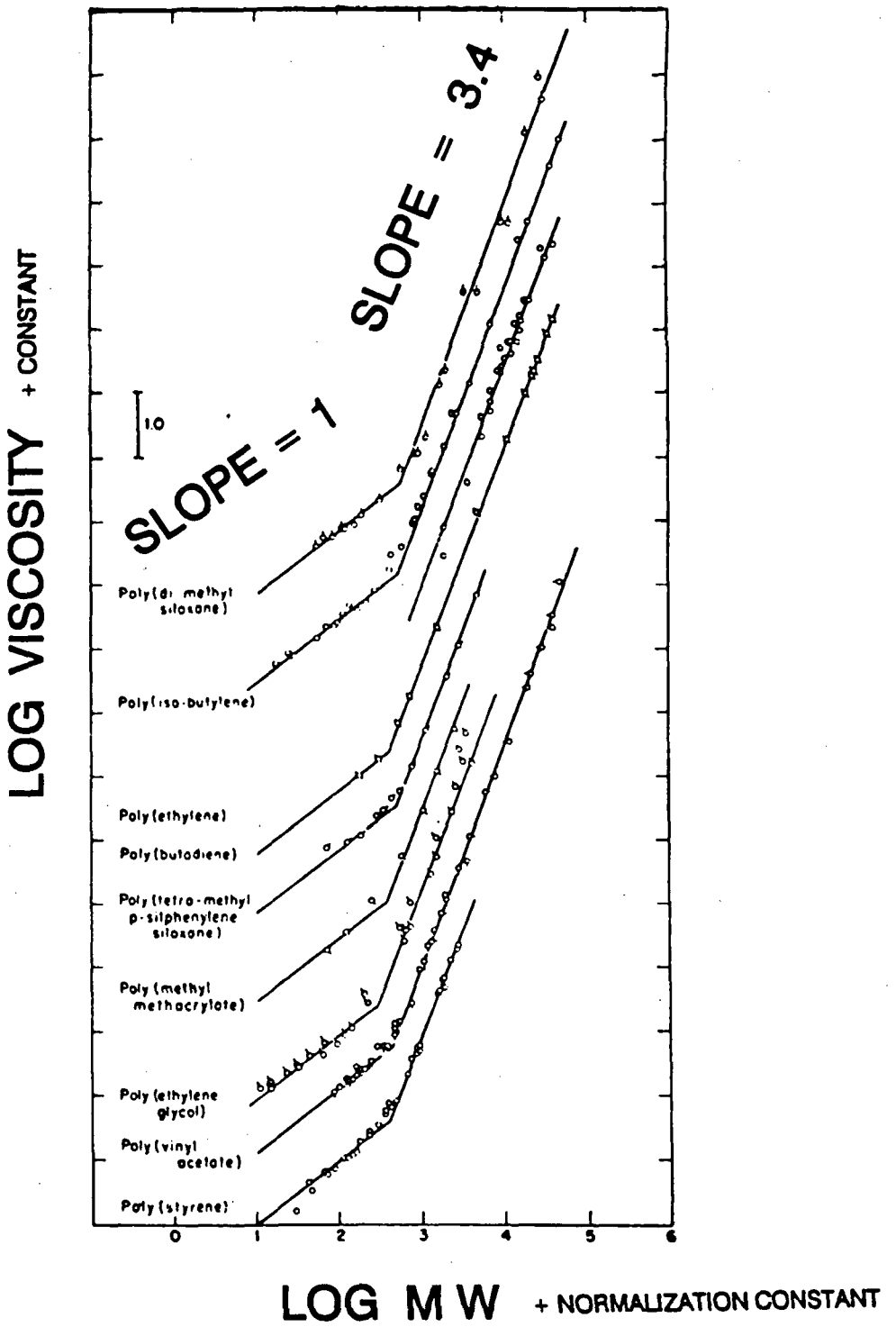

FIGURE 73. Plot of log viscosity + constant vs. log MW + normalization constant for a series of synthetic polymers, illustrating the generic behavior of polymers with MWs above and below the critical DP required for intermolecular entanglement and network formation. (From Ferry, J. D., *Viscoelastic Properties of Polymers,* 3rd ed., John Wiley & Sons, New York, 1980. With permission.)

A complete mechanistic understanding of the water sorption process for a water-plasticizable polymer, and the resulting predictive capability that this would provide, would require definition of the dependence of sorption behavior on the independent variables of moisture content, temperature, time (in other words, on a three-dimensional dynamics map, as described in the following section), and polymer MW (and dry Tg), and the dependent variable of the structural state of a water-plasticized polymer, in terms of its instantaneous Tg and ΔT, during sorption. It has been pointed out that, unfortunately, no single currently available sorption isotherm equation, model, or theory is capable of such a complete description.[15]

2. Sorption Isotherms Transformed into a Water/Glass Dynamics Map

Paakkonen and Roos[126] have recently illustrated the value of an experimental approach that combined measurements of water sorption isotherms and DSC measurements of Tg in an evaluation of the physical stability of freeze-dried horseradish roots. They concluded from their study that "sorption data and thermal behavior should be combined and used to determine the proper drying and storage conditions for such carbohydrate food materials".[126]

When DSC (or other thermal or mechanical analyses) instrumentation is not available, how can one "measure" glass curves for aqueous food systems? Illustrated below is a new experimental approach, whereby one can transform sorption isotherm data, based on RVP measurements as a function of temperature, into a water/glass dynamics map.

The first example of this approach utilizes the sorption data reported by Weisser[81] for apple pectin at temperatures of 25, 40, 60, and 80°C, shown in Figure 14A. As described earlier, the conventional data treatment illustrated the typical behavior of this amorphous substrate, i.e., at a given water content, the observed RVP increases with increasing temperature. But one can treat these temperature-moisture content data in a different way, as shown in Figure 65. One can take combinations of moisture content and temperature that give the same value of observed RVP, and replot these data (as a series of iso-RVP contours) in the two dimensions of temperature and w% solids, compared to the corresponding temperature-moisture content location of a hypothetical glass curve for pectin (Figure 65 actually utilizes the glass curve for hemicellulose in Figure 27). Figure 65 reveals that combinations of temperature and moisture content (increasing from bottom right to top left) that fall below the glass curve give observed RVPs approaching zero. As the combinations of temperature and moisture content rise above the glass curve, the observed RVP increases. In this region of the map above Tg′ but below Wg′ (corresponding to the contours for iso-RVPs of >0.17 to 0.89), the interaction of temperature- and moisture content-dependence with the time-dependence of the experiment increases, as evidenced by those iso-RVP contours that are increasingly slanted and more nearly parallel to the glass curve. (All of the experimental temperatures are well above Tg′, but the water contents corresponding to RVPs of 0.02 to 0.09 fall below both the effective Tg and the effective Wg.) Only for water content situations both above Tg′ and at or above Wg′ (which is estimated to be about 25 w% water, from the glass curve for hemicellulose in Figure 27) does one observe RVPs near 1.0 (i.e., the 0.93 RVP contour, which is not slanted).

The RVP data in Figure 65 were all obtained from water-uptake experiments that started out with essentially bone-dry pectin to which water was added. As noted earlier with respect to the ad/absorption isotherms for native starch in Figure 16A, results of such sorption experiments can be misleading, because the bone-dry glassy solid behaves like an inert substrate at time zero. So let us re-examine and compare the resorption/desorption data reported by van den Berg[43] for milled hard wheat at temperatures of 5, 25, and 45°C, shown in Figure 13. As discussed earlier, classic hysteresis was observed between the isotherms obtained by adding water to the bone-dry, partially crystalline glassy solid and by removing water from the wet substrate. In this second example of our new approach, we can once again take combinations of moisture content and temperature (for both dehumudification and humid-

ification experiments) that give equivalent observed RVPs, and replot these data (as a series of iso-RVP contours) in the two dimensions of temperature and w% solids, compared to the corresponding temperature-moisture content location of a hypothetical glass curve for wheat flour (Figure 74 actually utilizes a glass curve for the amylopectin component of native starch,[21,23,26] which is the major component of wheat flour). Like Figure 65, Figure 74 reveals that combinations of temperature and moisture content (whether from resorption or desorption) that fall below the glass curve give observed RVPs approaching zero, while combinations of temperature and moisture content above the glass curve, and particularly approaching and exceeding Wg' (≃27 w% water), give observed RVPs approaching 1.0. In Figure 74, it is especially interesting to note the relatively inert behavior of the water-uptake system, as evidenced by those iso-RVP contours (i.e., 0.17 to 0.71) for resorption that are closer to the glass curve and less slanted than are the corresponding desorption contours. In the resorption experiment that starts with a mechanical solid substrate, it appears that not as high a temperature nor as high a moisture content is needed to produce the same observed RVP, because at early sorption times, this glassy substrate is behaving like an inert system. This system (like those described earlier, i.e., native starch in Fig-

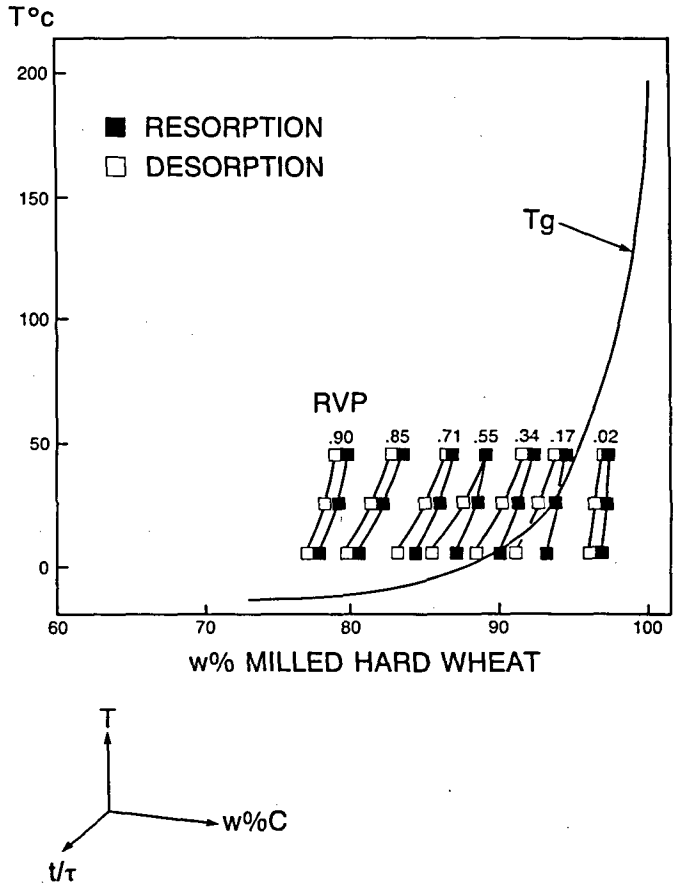

FIGURE 74. Resorption and desorption isotherm data for milled hard wheat from Figure 13 (data adapted from Reference 43) transformed into a two-dimensional water/glass dynamics map of temperature vs. weight percent solids, on which are compared the relative locations of two series of iso-RVP contours (for resorption and desorption) and a schematic, "practical" glass curve for wheat flour-water, based on data for starch and gluten.[18,25,43,49,51,94,99]

ure 16A and cod in Figure 68) is so far from equilibrium[172] that it is essentially inert at time zero. Eventually, as a result of increased temperature or increased moisture content, the system begins to be plasticized and reveal the limitation in diffusion that is so readily seen for the rubbery desorption system, during water removal from an already plasticized substrate above its glass curve. Thus, just because the resorption system looks like a steady-state system (in fact, it even begins to look like an equilibrium situation, because such long times are required before any changes in behavior are seen), one should not confuse this situation with that of true equilibrium. We suggest that what one is actually observing is a system so far from equilibrium that one cannot wait long enough (not experimentally feasible) to see that the system is not at equilibrium, much less wait long enough to measure true equilibrium RVPs.

Our treatment in Figure 74 of van den Berg's classic sorption data illustrates the salient point that water is an effective plasticizer of starch and other food polymers, but the mere *presence* of water does *not* attest that plasticization has occurred. Thus, when one reads the following quote from Hoseney,[386]

> "When starch is placed in water, the granule is freely penetrated by water, or for that matter, by most small molecules. The starch can hold about 30% of its dry weight as moisture. The granule swells slightly; its increase is generally considered to be about 5%. The volume change and water absorption are reversible, and heating the system to just below its gelatinization temperature will not bring about any other changes."

one must be careful not to equate rapid penetration (e.g., through pre-existing channels and voids) with rapid plasticization by water. In fact, plasticization at T < the initial Tg of a given substrate is slow, whereas plasticization occurs more rapidly at T > the initial Tg. This has been demonstrated most graphically by some remarkable swelling studies of PVC described by Sears and Darby.[109] It was found that several "common PVC plasticizers . . . would not swell an unplasticized PVC sheet at room temperature in two years' time . . . Yet, all of the plasticizers swelled the rigid PVC sheet at 76°C, the approximate Tg of the resin. When the same PVC was hot-compounded with a plasticizer, cooled, and then immersed in various other plasticizers, it would imbibe more plasticizer."

The above information and interpretations support the concept of *time as a plasticizer,* which depresses the Tg of a solute, just as water does. Water is extremely efficient as a plasticizer in the range where it is effective in practice, i.e., up to the level of Wg′ for a given water-compatible solute. In this range, 1 w% water can often depress Tg by 10 to 15°C; this extent of Tg depression is equivalent to that produced by a 3 orders-of-magnitude increase in time. Thus, in this range, water is more effective as a plasticizer than *log* time. However, when considered *in isolation,* there is no limit to plasticization of a solute by time. In contrast, when the operative time scale becomes short, water's ability to plasticize has a practical limit. For example, once ice forms in a solution during cooling to a given subzero temperature, this ice will not melt at this temperature, so this phase-separated water will not be able to diffuse back to plasticize the solute. Analogously, for a water-sensitive solute at its maximum extent of plasticization by water (e.g., lignin in Figure 27, with a resulting Tg > 0°C at W = Wg), once water in excess of Wg is removed by phase separation at this Tg above 0°C, this phase-separated water will also not be able to diffuse back to plasticize the solute upon further cooling.

For those readers who find three-dimensional representations of data more intuitive, understandable, and interpretable than two-dimensional ones, Figure 75 shows such three-dimensional representations of the two series of iso-RVP contours in Figure 74. Like Figure 74, Figures 75A and B show contours of equivalent RVP going from zero to 1.0, in the concentration range of water from zero to Wg′. Comparing the resorption and desorption experiments, we see a greater effect of temperature on resorption than on desorption, i.e., there is a greater temperature-dependence for the addition of water to the dry substrate below its Tg than for the removal of water from the wet substrate above its Tg. For a given moisture content, only at the higher sorption temperatures is the same RVP behavior approached during resorption as during desorption, i.e., the sorption behavior of the dry substrate is

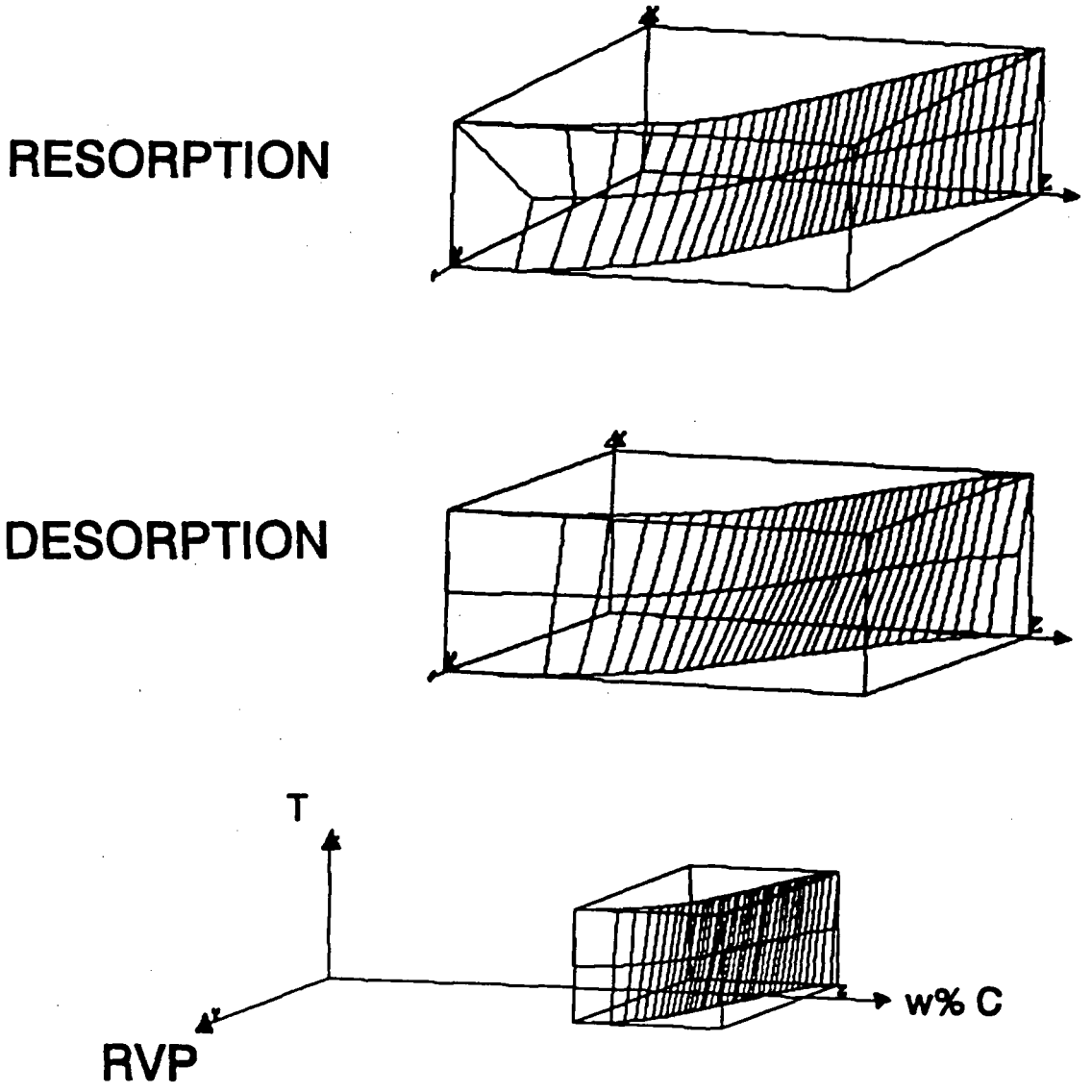

FIGURE 75. A three-dimensional representation of the two series of iso-RVP contours in Figure 74, for the resorption (A) and desorption (B) isotherm data for milled hard wheat from Figure 13. The location of the three-dimensional desorption data from part B on the three axes in part C illustrates the fact that the observed RVP goes from zero to one in a very small region of moisture content from 0% moisture to Wg'.

more sensitive to temperature. The most important feature of Figure 75 is revealed by the location of the three-dimensional desorption data from part B on the three axes in part C. Figure 75C illustrates the fact that the experimentally observed RVP goes from zero to 1.0 in a small region of moisture content from 0% moisture to Wg', i.e., a RVP of 1.0 is already reached by the time the moisture content reaches the Wg' of only about 27 w% water.

Despite the non-equilibrium nature of typical water sorption experiments, the measurement of such sorption data is a useful exercise, because without a DSC, one can, at least qualitatively, estimate the location of the glass curve on a two-dimensional mobility map of temperature and w% moisture, by the experimental approach illustrated in Figures 65 and 74. In fact, one could even estimate the shape of the glass curve, if one had a few more temperature points and a few more sorption time points to add to the sorption data in Figures 65 and 74.

With respect to this last conclusion, evidently such analogous temperature-time data have already been provided by Ferry, as shown in Figure 76.[107] Notice the *strikingly* similar appearance of the sorption data in Figures 65 and 74 and the data in Figure 76, for the storage compliance (a viscoelastic property related to creep in entangling high polymers) of a synthetic polymer in the transition zone between glasslike and rubberlike consistency, measured at 24 different temperatures and 12 different frequencies (≡ times). Notice how the orientations of the iso-RVP contours in Figures 65 and 74, i.e., from nearly vertical below the glass curve, to most slanted in the rubbery region above the glass curve, back to nearly vertical well above the glass curve, faithfully mimic the orientations of the storage compliance isotherms in Figure 76, for an entangling high polymer (with a measured Tg of −20°C,[107] corresponding to the conventional timescale of 200 s[172,174]) that, on the frequency scale of Figure 76, acts as a glassy solid at $T < -5$°C (for which compliance is low and little-changing with frequency), but as a supra-glassy liquid at $T > 120$°C (for which compliance is high and again little-changing with frequency).[107] Ferry has presented Figure 76 as a classic example of the fact that "it is in the transition zone between glasslike and rubberlike consistency that the dependence of viscoelastic functions on temperature is most spectacular, just as is the dependence on time or frequency."[107] The data in Figure 76 were actually used by Ferry in the original development of the WLF equation.[101]

The new data treatment illustrated in Figures 65 and 74 (which Ferry would characterize as a method of "viscoelastic corresponding states"[107]) also reinforces our recognition of two critical facts:

1. The relative partial pressure of water vapor in the gas phase of the sample headspace (colloquially referred to as "Aw") is certainly *not controlling* the mechanical relaxation rates and chemical reaction rates in the rubbery fluid phase or glassy solid phase of an aqueous sample matrix. Rather, the observed RVP is *controlled by* the temperature-moisture content location of the matrix relative to the location of its glass curve on the dynamics map.
2. Liquid water as a plasticizer, which increases the mobility of a multicomponent supra-glassy matrix, is the key to understanding relaxation rates in restricted water environments.

B. Microbiological Stability — Germination of Mold Spores

As introduced earlier by the results in Table 2,[14-16] a microbiological experiment demonstrated that the rates of germination of mold spores in different PHC solutions can be analyzed as a mechanical relaxation process that is governed by the translational mobility of water.[30] In turn, the local viscosity of individual supra-glassy PHC solutions at the experimental temperature, which was 50 to 95°C above their Tg′ reference states, appeared to control the relative mobility of water. Results of the experiment revealed that the mobility of water in PHC-water solutions can be better understood and explained in terms of mobility transformations based on Tg′, Wg′, and the Tm/Tg ratios of PHC solutes of equal MW, rather than in terms of the measured RVP of the solutions. These results further demonstrated the undeniable technological importance of Tg′, Wg′, and Tm/Tg ratio as critical physicochemical parameters for IMF systems.[30] These parameters enable us to extend our predictive capability beyond the limitations imposed by characterizing IMF systems only in terms of total moisture content and RVP. Moreover, as illustrated by the results described below, even such simple model aqueous food systems reveal the necessity of increased understanding of the underlying physicochemical principles that govern their behavior. For example, in comparison to fructose-only and glucose-only solutions, the results for the 1:1 fructose:glucose mixture in Table 2 revealed that the thermal behavior of this mixture in concentrated aqueous solution is controlled by fructose, whereas its mechanical behavior is controlled by glucose.

As shown in Table 2, for the matched pair of fructose and glucose solutions at equal solute concentration, MW, and Tg′, fructose produced a much less stable system in which the mold spores germinated much faster, even at slightly

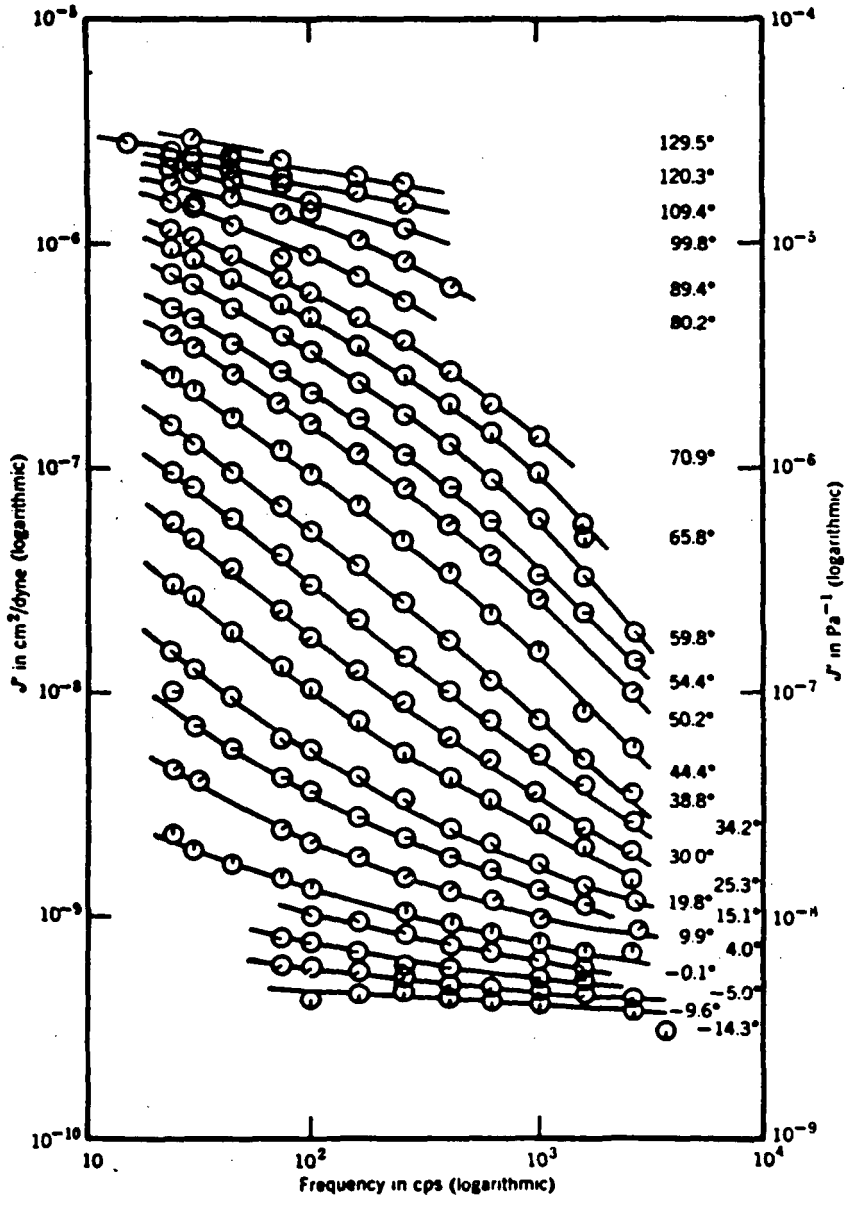

FIGURE 76. Storage compliance of poly(*n*-octyl methacrylate) in the transition zone between glasslike and rubberlike consistency, plotted logarithmically against frequency at 24 temperatures as indicated. (From Ferry, J. D., *Viscoelastic Properties of Polymers*, 3rd ed., John Wiley & Sons, New York, 1980. With permission.)

lower RVP. Likewise for the matched pairs of fructose vs. glycerol, maltose vs. sucrose, and mannose vs. fructose, the solute with the lower ratio of Tm/Tg allowed faster germination, regardless of RVP values. The Tm/Tg ratio is inversely related to the intrinsic mobility of a solute in its glassy reference state.[30] The temperature difference (ΔT) between the experimental temperature and Tg′, and the moisture difference (ΔW) between the water content of the solution and Wg′, account for the additional mobility of the experimental system above the reference state.[16] Thus, apparently due to the inherent mobility of a PHC in its glassy reference state and the lower local viscosity and so greater translational mobility in its supra-glassy solution, water

"availability" was greater for fructose (Tm/Tg = 1.06) than mannose (Tm/Tg = 1.36) than glucose (Tm/Tg = 1.42) than glycerol (Tm/Tg = 1.62), and greater for maltose (Tm/Tg = 1.27) than sucrose (Tm/Tg = 1.43).[30] Therefore, greater antimicrobial stabilization was observed for glycerol than glucose than mannose than fructose, and for sucrose than maltose. The extraordinary system mobility and eventual water "availability" of fructose samples were manifested by the same fast germination time observed for solutions of 40 to 70 w% fructose and corresponding RVPs of 0.98 to 0.70. Other noteworthy results in Table 2 involved the matched pairs of PVP-40 vs. methyl glucoside, maltotriose vs. mannose, and PVP-10 vs. fructose, for which Tg′ appeared to be the predominant functional determinant. In each case, the solute of higher MW and Tg′ manifested lower water "availability" in its supra-glassy solution (regardless of RVP values), and thus greater stabilization against germination.

Importantly, these experimental germination results were in accord with the unusual behavior often observed for fructose in non-equilibrium, IMF systems[75,76] and in solutions of similar RVP, in comparison to other more typical monomeric sugars like glucose and mannose, and polyols like glycerol. The microbiological data in Table 2 supported the conclusion[15,16] that the unusual behavior of fructose in aqueous systems is related to its anomalously low Tm/Tg ratio (calculated based on its second, higher dry Tg) and resulting low ηg at Tg, and the concomitant high mobility of its dry glass and supra-glassy solutions. An analysis of the results in Table 2, in the context of the description of the WLF behavior of polymers with different Tm/Tg ratios discussed earlier with respect to Figure 34, provided the following key insight.[30] A concentrated fructose solution at 30°C would be about 70°C above its Tg′ reference state. Such a supra-glassy fructose solution would exhibit anomalously low local viscosity at this temperature due to two factors related to the low Tm/Tg ratio of fructose. The magnitude of the WLF rubbery range is smaller for a lower Tm/Tg ratio, so that the fructose solution would exist as a liquid well *above* its WLF rubbery range. The local viscosity in the glassy reference state is lower for a lower Tm/Tg ratio, so that the viscosity of the fructose solution would be lower than could be accounted for by the temperature difference alone. In contrast, at the same experimental temperature and almost the same temperature difference above Tg′, supra-glassy solutions of glucose (Tm/Tg = 1.42) or mannose (Tm/Tg = 1.36), or even glycerol (Tm/Tg = 1.62), at a still greater temperature difference (95°C) above its Tg′, would exist as higher-viscosity fluids *within* their WLF rubbery ranges. Thus, like the lower-viscosity fructose-water reference glass at Tg, the fructose solution well above Tg would be a much more mobile system than the corresponding glucose, mannose, and glycerol solutions. Consequently, a mechanical relaxation process dependent on translational diffusion, as exemplified by the germination of mold spores, was able to occur more quickly in a fructose solution than in solutions of glucose, mannose, or glycerol of equal or higher RVP. It has been noted that the same apparent correlations among low local viscosity, fast translational diffusion, high translational mobility, short translational relaxation time, and low Tm/Tg ratio were suggested by the results in Table 2 for mold spore germination rates in small PHC-water systems at 50 to 95°C above Tg′ as were suggested also from the analysis of translational friction coefficients in Figure 72 for synthetic high polymers at 100°C above Tg.[30]

As mentioned earlier, the 1:1 fructose:glucose mixture in Table 2 received special attention, because of its importance in many technological applications, including IMFs, and because of its significant contribution to the theoretical interpretation of the non-equilibrium behavior of PHC-water systems.[30] The germination time for mold spores in a concentrated solution of this mixture was much more like that of a solution of glucose alone than fructose alone, which indicated that the mechanical relaxation behavior of the solution mixture is quite similar to that of a glucose solution with respect to *translational* mobility. A 20 w% solution of the mixture showed a Tg′ intermediate between the values for fructose and glucose, but a Wg′ almost identical to the value for fructose alone. As discussed earlier in the context of Figure 52, the glass curves of Figure 53 revealed that (1) the predominant conformer of fructose in its me-

chanically and spatially homogeneous vitrified aqueous solutions is the one responsible for the higher Tg value of dry fructose alone at 100°C, and (2) the anomalously large value of Wg′ for aqueous solutions of fructose alone results from the free volume requirement for rotational mobility of this "anisotropic" fructose conformer.[30] This important conclusion concerning the identity of the predominant fructose conformer in aqueous fructose glasses was demanded by the recognition, gained from the vast literature for plasticized synthetic polymers[107,109] and mentioned earlier, that the glass curve always exhibits a smooth monotonic decrease in Tg with increase in plasticizer content expressed as a weight fraction (because free volume in the plasticized blend is additive or cumulative, depending on the disparity in MW, on a weight fraction basis), with no local maxima unless stoichiometric complexes arise in particular composition ranges. Thus, the mechanical behavior of the solution of the 1:1 mixture of glucose with fructose is dominated by the free volume requirements of the "anisotropic" fructose conformer, with respect to *rotational* mobility. As mentioned earlier, the mechanically homogeneous dry glass obtained by melting a 1:1 mixture of β-D-fructose and α-D-glucose exhibited only one Tg at 20°C, exactly intermediate between the Tg of dry glucose alone at 31°C and the Tg of the second conformer of dry fructose at 11°C. It was suggested[30] and subsequently inferred from the results of Finegold et al.[124] that the predominant fructose conformer in the mixed dry glass is the second, glucose-like or "isotropic" conformer, with the lower of the two Tg values of fructose. The mold spore germination time for the solution mixture was determined by its constrained translational mobility. The constraint was much greater than for a solution of fructose alone and somewhat less than for a solution of glucose alone. This constrained translational mobility in the supra-glassy fluid was related to the single dry Tg of the mixture, which was much closer to that of glucose, with its higher value of Tm/Tg, than to that of the anomalous conformer of fructose, with its very low value of Tm/Tg. It was concluded[30] that the apparent RVP of a concentrated PHC solution does not control system mobility and eventual water "availability", but is simply another diagnostic manifestation, like the times required for spore germination, of the non-equilibrium translational relaxation behavior of the solution. It was suggested[30] that (1) the anomalous fructose conformer is the predominant species in aqueous fructose glasses and in aqueous glasses of the 1:1 mixture of fructose and glucose, (2) the anomalous fructose conformer is mechanically incompatible with the glucose-like fructose conformer in the dry melt of fructose alone, and (3) the glucose-like fructose conformer is the predominant species in the single dry glass of the 1:1 mixture. It was hoped that this speculative discussion,[30] which should have provided pregnant clues to one versed in the stereochemistry of small PHCs, might provoke appropriate experimentation with molecular modeling, NMR, and dielectric relaxation techniques to explore the effects of concentration, temperature, and pressure on the nature and kinetics of conformational changes during melting and vitrification of dry PHC systems and their aqueous solutions.

In the field of food technology, comparisons of the technological properties of the three most readily available sugars, fructose, glucose, and sucrose, are important and topical. Especially for applications involving the moisture management of IMFs, the choice between fructose and glucose to depress RVP and thus increase shelf-life is often controversial, confusing, and contradictory.[15,16] The situation has been summarized by the following paradoxical "truths".[75,76] In foods with limited total moisture, formulation on an equal weight basis with fructose rather than glucose typically results in a lower value of apparent RVP and greater storage stability, because the much greater solubility of fructose results in a greater effective concentration of fructose than glucose. However, if a product is formulated with glucose to achieve a certain RVP value that has been empirically demonstrated to provide stability with respect to a particular test microorganism (such as the IMF pet food product mentioned in Section II.A.3), then reformulation with fructose to the same RVP often produces a less stable product. This is so, because less fructose than glucose is required to achieve the same RVP, while, as illustrated by the mold spore germi-

nation results in Table 2, at the same RVP, fructose solutions are less stable than glucose solutions.

Since the colligative depression of the equilibrium water activity is the same for infinitely dilute solutions of fructose and glucose, the traditional approach to the fructose vs. glucose paradox has been to question why the observed RVP of a fructose solution of finite or high concentration is significantly lower than that of a glucose solution of equivalent concentration, as illustrated by the sorption isotherms in Figure 77A.[75] A further comparison of the glass curves in Figure 53 has led to the conclusion[30] that a concentrated fructose solution is anomalous, because its RVP is not depressed *enough* relative to that of glucose. In other words, one needs to ask the opposite question — why is the RVP for a fructose solution so *high*, for such a small vector above its glass curve? For the technologically practical case of a 50 w% solution at room temperature, the temperature differential (ΔT) or the water differential (ΔW) above the reference glass curve in Figure 53 is much smaller for fructose than for glucose.[30] One would therefore expect the translational mobility of water in the fructose solution so close to its glass curve to be more restricted (i.e., lower RVP) than it appears to be. It has been suggested[30] that the explanation lies in the anomalously large free volume requirement for rotational mobility in the supra-glassy fluid (as reflected in the very low value of Tm/Tg ratio), which results in anomalously low local viscosity. Thus, translational diffusion in the supra-glassy fructose solution is very rapid (relative to that in the solution of glucose, with its much higher Tm/Tg ratio), and the depression of its non-equilibrium RVP is less than expected.

Like the two monosaccharides, fructose and glucose, the two low MW polyols, propylene glycol and glycerol, are frequently employed as moisture management agents in IMFs. On what physicochemical basis can one best choose between these two polyols for IMF applications? As illustrated by the room temperature sorption isotherms in Figures 77A and B,[75] the relationship between the sorption behavior of propylene glycol and glycerol is analogous to that between fructose and glucose. The observed RVP of a propylene glycol solution of finite or high concentration is significantly lower than that of a glycerol solution of approximately the same concentration. We suggest that the basis for the difference in sorption behavior between the two polyols is also analogous to that for the two monosaccharides. As is the case between fructose and glucose, propylene glycol has a much lower Tm/Tg ratio (i.e., 214 K/169 K^{245} = 1.27) than does glycerol (1.62). As is also the case between fructose and glucose, propylene glycol has a higher value of Wg′ (56 w% water) than does glycerol (46 w% water), but their Tg′ values are very similar (−67.5 vs. −65°C). Thus, for solutions of propylene glycol and glycerol of equal solute concentration (and corresponding moisture content, W>Wg′) at 25°C, the ΔT above the Tg′ reference state is about the same for both polyols (i.e., 92.5 vs. 90°C), but the ΔW above the Wg′ reference state is lower for propylene glycol than for glycerol. As shown by the sorption isotherms in Figure 77, the relative positions of these RVP-moisture content profiles evidently also depend on Wg′, in addition to Tg′, such that, for equivalent ΔT above Tg′, RVP is directly related to ΔW above Wg′. Thus, for propylene glycol, as for fructose, lower ΔW is manifested as lower RVP, while for glycerol, as for glucose, higher ΔW is manifested as higher RVP, at the same total water content. We conclude that situations of anomalously low values of ΔW (e.g., propylene glycol and fructose) can arise when the ratio of Tm/Tg is anomalously low. It should be noted, however, that, as in the case of fructose vs. glucose with respect to mold spore germination in Table 2, a lower RVP at an equivalent solute concentration does *not* correlate with greater microbiological stability for propylene glycol vs. glycerol. In fact, as demonstrated by the germination results for fructose vs. glucose, at the same T, W, and ΔT above Tg′, lower Tm/Tg ratio and lower ΔW above Wg′ are predictive of *poorer* microbiological stability, despite lower RVP, for propylene glycol than for glycerol. This prediction is consistent with the empirical finding for the example of the IMF pet food product described in Section II.A.3. In that case, the original product, formulated with a "water binder" combination of glucose + glycerol, was determined to be microbiologically safe and stable at an empirical "Aw" specification of ≤0.92. When

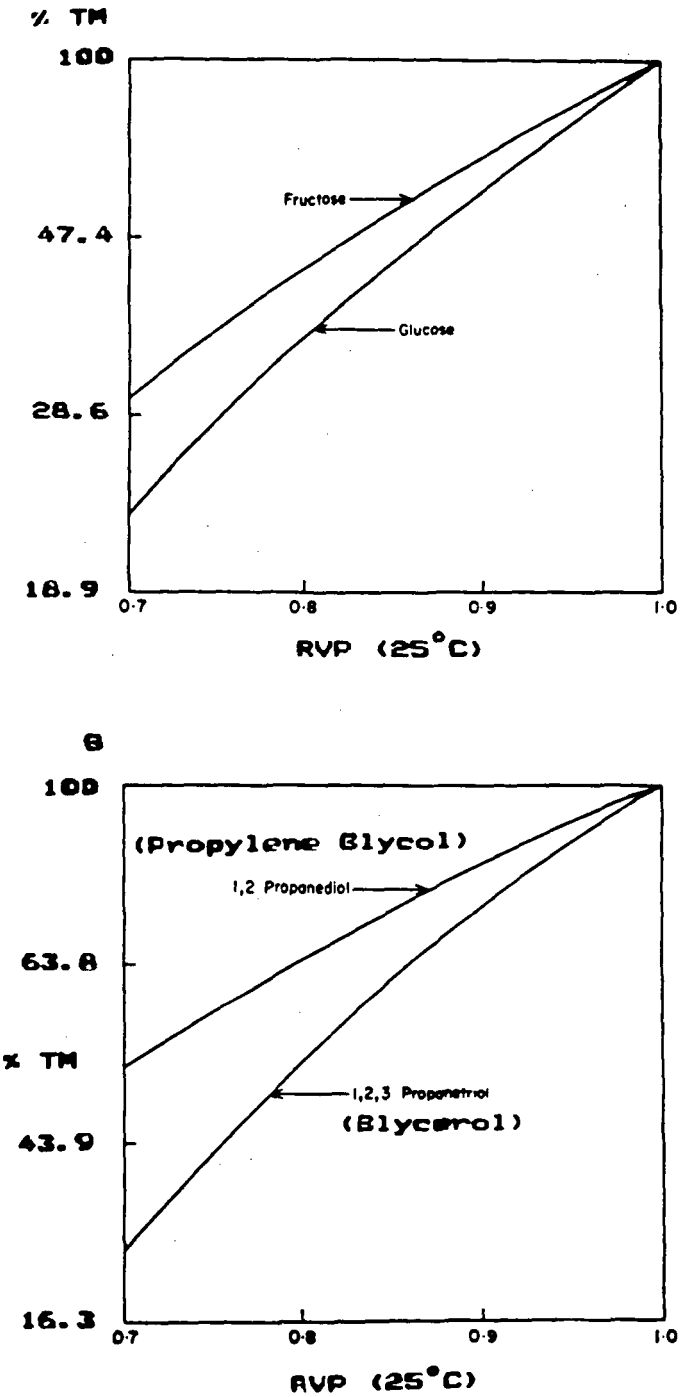

FIGURE 77. (A) Sorption isotherms for fructose and glucose at 25°C. (B) Sorption isotherms for propylene glycol and glycerol at 25°C. (From Loncin, M., *Freeze Drying and Advanced Food Technology*, Goldlith, S. A., Rey, L., and Rothmayr, W. W., Eds., Academic Press, New York, 1975, 599. With permission.)

the product was reformulated and the "safe" combination of glucose + glycerol was replaced by a fructose + propylene glycol combination to achieve the same "Aw" specification, the new product spoiled catastrophically.

C. Enzymatic Activity

1. Prevention of Enzymatic Activity in Amorphous Media at T < Tg

Enzyme-substrate interactions in amorphous aqueous media have been demonstrated to represent an example of a diffusion-limited chemical reaction that can be characterized as a collapse process governed by Tg and dependent on plasticization by water.[8] Such diffusion-limited enzymatic activity, which can only occur at T>Tg, is potentially important in many food applications that cover the entire spectrum of processing/storage temperatures and moisture contents, and is especially relevant to the issue of product shelf-life. For example, recent reports have documented (1) the significant reductions in quality and shelf-life that can be caused by residual enzymatic activity during frozen storage of cod fillets,[312] parsley,[311] cauliflower,[315] and green beans;[313] (2) the finding that the extent of product deterioration caused by enzymatic reactions increases with increasing freezer-storage temperature;[311,312] (3) the complementary finding that enzymatic reaction rates and the corresponding rates of quality loss increase with increasing Tf;[312] and (4) the unexplained finding[312] that the dependence of enzymatic reaction rates in cod fillets on Tf could not be predicted by the Arrhenius equation, as evidenced by non-linear Arrhenius plots. As described earlier in Table 9, examples exist which elegantly illustrate the fact that enzymatic activity is suppressed in low-moisture glassy solids at T < Tg,[54] and in frozen systems at T < Tg',[8] but commences in a rubbery fluid, at T>Tg or Tg'.[314] Examples of frozen vegetables that have recently been reported to show significant enzymatic activity and resultant quality loss during freezer storage (at a Tf above our measured value of Tg') include cauliflower[315] (at Tf (−20°C)>Tg' (−25°C)) and green beans[313] (at Tf (−23°C)>Tg' (−27.5°C)).[39]

Studies by Bone and Pethig[86,368] of the dynamics of lysozyme activity, involving the hydration of freeze-dried lysozyme powder at 20°C, showed that, at 20 w% water, lysozyme becomes sufficiently plasticized, so that measurable enzymatic activity commences. Their results were interpreted as follows.[8] A diffusion-limited enzyme-substrate interaction is essentially prohibited in a partially glassy solid at T < Tg, but sufficient water plasticization depresses the Tg of the lysozyme-containing medium to below 20°C, allowing the onset of enzymatic activity in a rubbery lysozyme solution at T>Tg, the threshold temperature for activity. This interpretation was consistent with results of related studies of "solid glassy lysozyme samples" by Poole and Finney,[332,333,367] who noted conformational changes in the protein as a consequence of hydration to the same 20 w% level, and were "tempted to suggest that this solvent-related effect is required before (enzymatic) activity is possible." Morozov et al.[87] studied the water desorption behavior and corresponding mechanical properties of amorphous lysozyme films at 25°C, and reported a sudden increase in modulus, attributed to an increase in the rigidity of lysozyme molecules (corresponding to a loss of enzymatic activity), at moisture contents <0.22 g water/g protein. Work by Morozov and Gevorkian[175] also revealed the critical requirement of low-temperature glass transitions for the physiological activity of lysozyme and other globular proteins plasticized by water.

Within a context of cryostabilization technology, such enzyme-substrate interactions in frozen food systems depend on the relationship between Tf and Tg' (as illustrated in Figure 63).[8] Tg', representing the threshold temperature for the onset of enzymatic activity in a frozen medium, depends in turn on the composition of a particular product, in terms of the average MW of the water-compatible solids. Rates of enzymatic reactions would be predicted to increase exponentially with the ΔT between Tf and Tg',[314] as dictated by WLF, rather than Arrhenius, kinetics.[32,39]

The prevention of enzymatic activity at T < Tg' has been demonstrated experimentally *in vitro* in a maximally frozen model system consisting of glucose oxidase, glucose, methyl red,

and bulk solutions of sucrose, a 10 DE maltodextrin, and their mixtures, which provided a range of samples with known values of Tg'.[8] The enzymatic oxidation of glucose produces an acid that causes a diagnostic color change from yellow to pink in the reaction mixture. Samples with a range of Tg' values from −9.5 to −32°C were stored at various temperatures: 25, 3, −15, and −23°C. All samples were fluid at the two higher temperatures, while all looked like colored blocks of ice at −15 and −23°C. However, only samples for which the storage temperature was above Tg' turned pink. Even after 2 months storage at −23°C, samples containing maltodextrin, with Tg' > −23°C, were still yellow. Frozen samples that turned pink, even at −23°C, contained a concentrated, substrate- and enzyme-enriched fluid surrounding the ice crystals, while in those that remained yellow, the non-ice matrix was a glassy solid. Significantly, enzymatic activity was prevented below Tg', but the enzyme itself was preserved (via cryostabilization with a low DE SHP) rather than inactivated during storage. When yellow samples were thawed, they quickly turned pink. As a necessary extension of this qualitative experiment, future studies of quantitative enzyme-substrate reaction rates, as a function of ΔT between Tf and Tg', in frozen model systems containing a variety of cryostabilizers and/or cryoprotectants would be quite informative.[33]

2. Unfolding of Native Globular Enzymes and Proteins at Subzero Temperatures

"Cold denaturation or inactivation" of native globular enzymes and proteins is a topic of much current interest in the protein literature.[5,387,388] The term is used to describe a cooperative, fully thermoreversible inactivation process, common to many enzymes and proteins in concentrated aqueous systems, involving disruption of the native structure by cooling, either due to a conformational transition involving dissociation of multiple peptide subunits or unfolding of a globular polypeptide chain.[5] Cold-induced unfolding has been conceptualized as an all-or-none, two-state, first-order phase transition from compact globule to disordered coil,[387,389] where the denatured, flexible-coil state has been modeled by PVP in aqueous solution at subzero temperatures.[390] Recently, direct experimental studies have been reported of cold inactivation in undercooled (or freezing-point depressed) solutions at subzero temperatures, involving subunit dissociation of lactate dehydrogenase,[391] and unfolding of chymotrypsinogen[392] and metmyoglobin.[389] In the chymotrypsinogen study, an emulsion droplet technique was employed to achieve substantial undercooling of aqueous solutions and maintain the inherent mobility of the liquid state, while in the work on lactate dehydrogenase, the same requirement of liquid state mobility was achieved through the use of a "cryosolvent" with significant colligative freezing point depression. Both experimental approaches permitted a cold-induced conformational transition to occur by a process entirely different from that of "freeze-denaturation" of proteins in freeze-concentrated solutions.[387,391] In the case of the cold-dissociated multisubunit enzyme, a low degree of enzymatic activity was retained.[391] Cold denaturation is similar in some but different in other thermodynamic aspects[387] to the more familiar high-temperature "thermal" or "heat denaturation" of native globular proteins,[5] a phase transition (analogous to crystal melting) typically analyzed by DSC measurements of concentrated solutions or hydrated crystals (as exemplified by the methodology of Sochava et al.[393]). However, while cold denaturation is not subject to the typical irreversibility caused by rapid aggregation immediately following unfolding that characterizes heat denaturation (and often leads to so-called "heat-set gelation") of many proteins in concentrated aqueous systems,[393] cold denaturation does manifest an unusual temperature hysteresis effect in the unfolding/refolding[392] and dissociation/reassociation processes.[391]

Reversible cold inactivation of proteins might have practical relevance[387] and offer potential benefit to commercial food processes such as blast-freezing of frozen products or freeze-drying of concentrated aqueous systems. In such processes, a significantly undercooled metastable liquid state might persist for a time long enough to allow cold inactivation to occur, although it has been suggested that such native/denatured transformations at subzero temperatures may be slow, kinetically governed changes.[388] Despite

this qualification, it has been stated that "low temperature denaturation could probably be used to enhance the storage stability of protein concentrates and may offer an attractive alternative to lyophilization".[391] These workers also noted that, "for practical applications, such as long-term storage, a reversible low-temperature inactivation, aided by cryosolvents, would appear to be a highly desirable process".[391] (This group has subsequently demonstrated the long-term stabilization, via substantial undercooling of solutions utilizing the emulsion droplet technique, of proteins subject to cold inactivation.[394]) In contrast, the significant undesirable consequences of irreversible freeze-denaturation of proteins (e.g., the syneresis due to protein denaturation in frozen meats) during ordinary frozen food processing are familiar. However, a potential remedy in certain cases of this type of damage could involve the use of low MW solutes (e.g., sugars and polyols), which are well known as stabilizers of native proteins against heat denaturation, and have been suggested (on the same physicochemical basis as used to explain the functional properties of food cryoprotectants[15]) to be capable of playing the same role against freeze denaturation.[5] Their protective effect, which has been attributed to their ability to "maintain the hydration shell of a protein under conditions of lowered water activity", has been noted to be "reflected in the application of sugars during industrial spray and freeze drying operations".[5]

D. Inhibition of Collapse Phenomena with Saccharide Polymers

1. Entanglement and Network Formation — Network Tg

There is a profound technological importance of MWs above the entanglement MW limit, as illustrated earlier for commercial SHPs (as a model for other homologous families of amorphous saccharide oligomers and polymers) by the structure-function relationships defined by the entanglement plateau in Figure 44.[8,27] Ferry[107] has described the generic behavior observed for all polymer systems with respect to the relationships between linear DP of the backbone chain, polymer concentration, and viscosity. MW is a relative measure of linear DP of the primary chain when the polymer has a uniform structure along its entire length. At any given concentration, there is a minimum DP required for entanglement and network formation. For very dilute solutions (such that the solution viscosity, measured as a relative flow rate, is similar to that of the solvent alone), high MW polymers are necessary to form gels or networks (characterized by very high macroscopic viscosity, measured as a relative firmness). For example, 1.5 w% gelatin solutions in water can form firm gel networks (which exhibit resistance to dehydration, due to mechanical resistance to shrinkage), through entanglement followed by crystallization of junction zones, if the linear DP is $\gtrsim$1000 (MW $\gtrsim 10^5$).[239] Similarly, 1.5 w% amylose solutions in water can form firm gel networks if the linear DP is about 3000 ($\overline{M}w \simeq 5 \times 10^5$).[211,273] At intermediate chain lengths, greater concentrations of chains are required for entanglement and network formation. In the case of SHPs, such as the low DE maltodextrins patented for partially crystalline, fat-mimetic gels,[266,267,272] concentrations must be increased to at least about 20 to 25 w% in water (i.e., typical of Cg′ of the freeze-concentrated glass at Tg′) as linear DP is decreased to approach 18 glucose units (MW $\simeq$ 3000).[15,27] In contrast, oligomers of hydrolyzed gelatin (peptones) or hydrolyzed starch (corn syrup solids or higher DE maltodextrins with MW $\lesssim$ 3000) are incapable of gel network formation via entanglement at any concentration.[15,24,27] However, recrystallization of such oligomers can occur due to concentration above the saturation limit or to a change of solvent. For carbohydrate polymers based on primary chains of α-1,4 glucans, the critical DP required for network formation via entanglement is $\gtrsim$18.

Network formation, especially in the absence of crystallization, depends on the ability of flexible chains to entangle.[107] (The contribution of crystallization to network formation and gelation, described earlier in Section III.A.6, is discussed further below in the specific context of saccharide polymers, with respect to the question — When is retrogradation synonymous with recrystallization and with gelation?) One convenient diagnostic test for entanglement relies on the fact,

previously illustrated in Figures 24 and 44, that the Tg values of a homologous family of polymers increase with increasing linear DP up to the chain length sufficient to allow entanglement. Entanglement networks consist of inter-node chains and network junction zones (nodes) that are transient topological constraints to chain motion. The probability of formation of (non-crystalline) junctions depends on chain length and concentration. The greater the number of junctions, the shorter the inter-node chain length (for a fixed parent chain length). Thus, there is a limiting length for any chain that exhibits translational freedom, and a limiting molecular Tg for that DP.

A second important diagnostic test for entanglement was illustrated earlier in Figure 73. For undiluted polymers or for polymer solutions studied at constant total concentration, a critical chain length can be demonstrated, above or below which the dependence of viscosity on MW changes dramatically.[107] Above the critical chain length, entanglement results in a drastic sensitivity of viscosity to chain length. In the absence of entanglement, chains shorter than the critical length show solution behavior with relative insensitivity of viscosity to chain length. The topological constraints of the (non-crystalline) entanglement network are not due to any particular chemical interactions (such as hydrogen bonds or dipolar or charge interactions) nor to any particular structural features. As demonstrated in Figure 73, entanglement is a generic behavior of polymers of sufficient chain length and can be seen equally in poly (ethylene glycol) and in nonpolar, structurally featureless polymers such as poly(isobutylene). The important lesson to be learned from Figure 73 was alluded to earlier. In the region of MW above the critical DP, the slope of log viscosity vs. log MW is 3.4. In this region, cutting molecules (e.g., SHPs) of DP 300 in half, to obtain the same total concentration of molecules with DP 150, would result in a dramatic tenfold reduction in viscosity. In contrast, in the absence of entanglement, the slope of log viscosity vs. log MW in the region below the critical DP is 1. In this region, cutting molecules of DP $\lesssim$ 18 in half would result in only a twofold reduction in viscosity.

In the context of starch retrogradation as a collapse process included in Table 9, retrogradation of gelatinized starch involves the recrystallization of both amylopectin and amylose.[61,63,65,215,219,221,395] It has been demonstrated for SHPs that the minimum linear chain length required for intermolecular entanglement upon concentration to Cg′ corresponds to $\overline{DP}n \simeq 18$ and $\overline{M}n \simeq 3000$.[8] Sufficiently long linear chain length ($\overline{DP}n \gtrsim 15$ to 20) has also been correlated with intermolecular network formation and thermoreversible gelation of SHPs[15,18,27,271,275] and amylopectin,[92] and with starch (re)crystallization.[92,215,218,221,396] It has been suggested that, in a partially crystalline starch, SHP, or amylopectin gel network, the existence of random interchain entanglements in amorphous regions and "fringed micelle" or chain-folded microcrystalline junction zones[271] each represents a manifestation of sufficiently long chain length.[8] This suggestion was supported by other work[211,215,273,397] that has shown that amylose gels, which are partially crystalline,[396] are formed by cooling solutions of entangled chains. For aqueous solutions of both high MW amylose[211,214,273] and amylopectin,[92,398] intermolecular entanglement and network formation have been evidenced by log-log plots of viscosity vs. concentration with a characteristic break in the curve (analogous to the break in the curves of log viscosity vs. log MW for the synthetic polymers shown earlier in Figure 73), such that the slope of the linear portion above the so-called "coil overlap" concentration is steeper than the slope of the other linear portion at lower concentrations. From such a plot, Miles et al.[211] have identified a critical minimum concentration ($\gtrsim$1.5 w% amylose) for entanglement of high-polymeric amylose ($\overline{M}w \simeq 5 \times 10^5$). These workers have stated that amylose gelation requires network formation, and this network formation requires entanglement, and they have concluded that "polymer entanglement is important in understanding the gelation of amylose".[211] A more recent study of aqueous amylose gelation by Gidley et al.,[212-214] using nearly monodisperse amyloses of DP 250-2800, has identified a somewhat lower critical gelling concentration of $\simeq$1.0 w%. This finding has been corroborated in a subsequent rheological study by Doublier and Choplin.[397] Gidley et al., while accepting the concept of intermolecular entan-

glement in "semi-dilute" amylose solutions advanced by Miles et al.,[211] have suggested that the lower gelling concentration of 1.0 w% results from the predominant contribution of crystalline junction zone formation to the gelation mechanism for amylose.[212-214]

The time-dependent gelation of amylose from dilute aqueous solution is generally agreed to occur in two stages: a relatively fast but finite stage due to viscoelastic network formation via entanglement (which is reversible by dilution but not thermoreversible); followed closely by a slower, but continually maturing, crystallization (in a chain-folded or extended-chain morphology) process (which is thermoreversible above 100°C).[92,211,215,217,220,221,273,397,399] In contrast, in partially crystalline, thermoreversible (below 100°C), aqueous amylopectin gels, viscoelastic network formation (which is relatively slow and time-dependent) is more closely related to the presence of microcrystalline junctions than to entanglements, although entanglement does occur.[92,218,221] Since most normal starches are 70 to 80% amylopectin,[400] their gelatinization and retrogradation processes are dominated by the nonequilibrium melting and recrystallization behavior of amylopectin,[17,18,20,63,65,219] although contributions due to amylose can be observed.[232,395,397] Generally, the early stages of starch retrogradation are dominated by chain-folded amylose (of DP from about 15 to about 50 and fold length about 100 Å[92,221,401]); the later stages by extended-chain amylopectin[94] outer branches (of DP about 12 to 16[92,402]).[18,20]

Experimental evidence, which supports these conclusions about the thermoreversible gelation mechanism for partially crystalline polymeric gels of starch, amylopectin, amylose, and SHPs, has come from DSC studies,[20] the favored technique for evaluating starch retrogradation.[207] Analysis of 25 w% SHP gels, set by overnight refrigeration, has revealed a small crystalline melting endotherm with Tm $\simeq$ 60°C,[15] similar to the characteristic melting transition of retrograded B-type wheat starch gels.[20] Similar DSC results have been reported for 20 w% amylopectin (from waxy maize) gels.[216,218] The small extent of crystallinity in SHP gels can be increased significantly by an alternative two-step temperature-cycling gelation protocol (12 h at 0°C, followed by 12 h at 40°C),[18,20] adapted from the one originally developed by Ferry[239] for gelatin gels, and subsequently applied by Slade et al.[36] to retrograded starch gels. In many fundamental respects, the thermoreversible gelation of aqueous solutions of polymeric SHPs, amylopectin, amylose, and gelatinized starch is analogous to the gelation-via-crystallization of synthetic homopolymer and copolymer-organic diluent systems, described earlier in Section III.A.6.[20] For the latter partially crystalline gels, the possibly simultaneous presence of random interchain entanglements in amorphous regions[146] and microcrystalline junction zones[195] has been reported. However, controversy exists[146,195] (as it also does for the case of amylose[211,212-214,397]) over which of the two conditions (if either alone) might be the necessary and sufficient one primarily responsible for the structure-viscoelastic property relationships of such polymeric systems. Part of this controversy could be resolved by the simple dilution test mentioned earlier,[198] which could also be applied to polysaccharide gels (e.g., amylose); entanglement gels can be dispersed by dilution at room temperature, microcrystalline gels cannot be when room temperature is <Tm.[15]

In the context of SHPs as inhibitors of collapse processes, it is worth mentioning that the literature on SHPs as anti-staling ingredients for starch-based foods (reviewed elsewhere[18,20]) includes a report by Krusi and Neukom[403] that (nonentangling) SHP oligomers of $\overline{DP}n$ 3 to 8 (i.e., within the intermediate region II of Figure 44) are effective in inhibiting, and *not* participating in, starch recrystallization.

An important consequence of entanglement and network formation is the effect on the Tg that determines all diffusion-limited structural and mechanical relaxation processes of the system. As shown schematically in Figure 78, while the molecular or segmental Tg remains constant above the entanglement MW limit, the *network* Tg, i.e., the macroscopic, controlling Tg of the supramolecular network (that would affect Instron measurements of the modulus for instance), continues to increase with increasing MW above the entanglement MW, because of the increased probability of crosslinks.[146,205] This fact has major structural and textural implications for food polymer systems, because such systems with

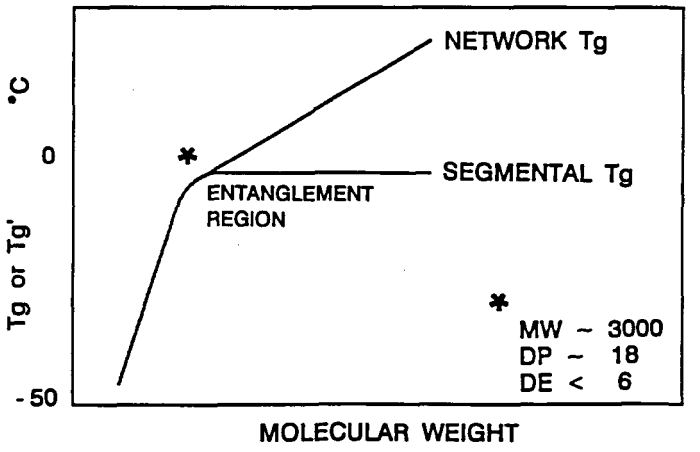

FIGURE 78. Schematic plot of Tg (or Tg') vs. molecular weight (modeled after the data plot for SHPs in Figure 44), which illustrates that, while the segmental Tg remains constant with increasing MW for MWs above the entanglement limit, the network Tg continues to increase monotonically with increasing MW above the entanglement MW limit.

MWs above the entanglement limit are capable of forming fibers, networks, and gels: i.e., macroscopic structures that can reinforce and support their own weight against gravity. An example mentioned earlier in Section III.A.6, but now noteworthy in a more fully developed context, is the gelatinized wheat starch-gluten matrix of baked bread. The effective network Tg responsible for mechanical firmness of freshly baked bread would be near room temperature for low extents of network formation (i.e., the contribution due to low extents of starch retrogradation), well above room temperature for mature networks (i.e., greater extents of retrogradation), and equivalent to Tgel near 60°C for staled bread (i.e., fully retrograded B-type wheat starch), even though the underlying Tg for segmental motion (of either starch or gluten at plasticizing moisture contents >Wg'), responsible for the predominant second-order thermal transition, remains below 0°C at Tg'.[25]

2. Saccharide Oligomers and Polymers as Moisture Management Agents

The relationship between the solute concentration and linear DP requirements for entanglement and network formation, and its resultant effect on Tg (molecular vs. network), also has important implications for moisture management by saccharide oligomers and polymers. As exemplified for the homologous family of amorphous glucose oligomers and polymers represented by the commercial SHPs in Figure 44, there are three distinguishable regimes of moisture management, which are analogous to the three regions of Tg vs. MW behavior shown in Figure 24 and mirrored in Figure 44. Aspects of moisture management relevant to these three regimes of functional behavior include hydration, freezing, drying, moisture migration, and biological stability. The first regime includes non-entangling solutes of linear DP < 3. For such small sugars at a given water concentration, this moisture management regime is characterized by low apparent (non-equilibrium) RVP, very large osmotic driving force to take up water, low local viscosity, and only a small barrier to local translational and rotational diffusion. The second regime, for non-entangling solutes of DP $\simeq 3$ to 17, is characterized by high apparent RVP, small osmotic driving force to take up water, high local viscosity, and a large barrier to local translational and rotational diffusion. The third regime, for entangling solutes of DP $\gg 17$, is characterized by very high apparent RVP, very large *local* osmotic driving force to swell, very low local vis-

cosity, and essentially no barrier to local translational and rotational diffusion. In this context, it is interesting to note that our finding of $\overline{DP}n \simeq 18$ for the minimum DP for entanglement and network formation by commercial SHPs, a result identified from the polymer characterization analysis represented by Figure 44, has been confirmed by a revealing finding recently reported by Radosta et al.[275] From their study of the water sorption behavior of maltodextrins, they concluded that "the transition between "polymer" and "oligomer" behavior under sorption conditions is located in the region of $\overline{DP}n$ values between 60 and 16. In this $\overline{DP}n$ region, the shifting from restricted swelling (by what Radosta et al. refer to as a "sorption gel") to solution under sorption conditions takes place."[275]

A conceptual representation of the three regimes of moisture management is shown in Figure 79. For a given temperature (e.g., room temperature) and time (e.g., a practical experimental time frame), T is well above Tg for concentrated solutions of regime I solutes, and such a system would be subject to viscous liquid flow due to gravity. In regime II at T > Tg, apparent RVP is not depressed as much as in regime I, because there are fewer solute molecules in solution. However, their higher linear DP results in higher local viscosity, which in turn results in a larger barrier to local diffusion and reduced viscous liquid flow due to gravity. In regime III (for a solute concentration high enough to allow entanglement), at network Tg > T > molecular Tg, there is elastic resistance to flow, and the gel is able to support its own weight against the force of gravity. In this regime, there is essentially no barrier to local diffusion, so a small molecule such as water or a dye molecule can diffuse freely in the gel network.[181] Hence, regime III manifests very high apparent RVP. Despite this, however, there is a very large *local* osmotic driving force to take up water, not only via hygroscopicity but via swelling, the latter due to the mechanical resistance of the entangled network to shrinkage. This mechanical resistance to shrinkage, which is analogous to hydraulic resistance to water removal, has an effect on the local chemical potential of the solvent, analogous to an addition to the osmotic pressure.[373] Thus, while there is a very large driving force to take up water via swelling in regime III, and a normal, classic osmotic driving force to take up water via hygroscopicity in regime I, there is a much lower driving force to take up water via classic osmotic pressure effects in regime II, because of the absence of a swelling force due to entanglement.

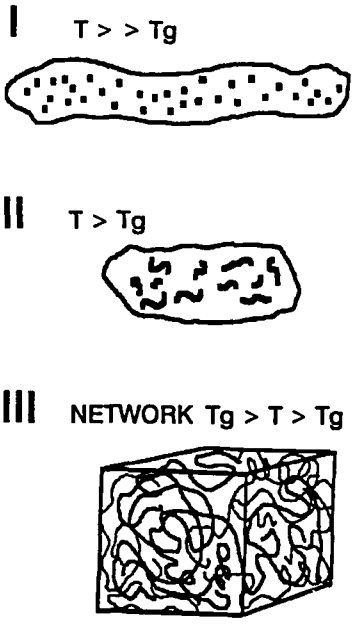

FIGURE 79. Conceptual representation of the three regimes of moisture management by a homologous family of saccharide polymers (e.g., the SHPs in Figure 44): (I) at T ≫ Tg of a concentrated solution of non-entangling saccharide oligomers of linear DP ≤ 3; (II) at T > Tg of a less-concentrated solution of non-entangling saccharide polymers of linear DP ≃ 3 to 17; (III) at network Tg > T > Tg of a dilute solution (but above the critical concentration for entanglement) of entangling saccharide high polymers of linear DP ≫ 17.

To illustrate the consequences of the three regimes of functional behavior of saccharide moisture management agents, one could use results from, for example, drying or freezing experiments. Drying and freezing are equivalent diffusion-limited processes in the sense that both involve removal of water via phase separation; in drying by increasing the temperature to produce water vapor and in freezing by decreasing the temperature to produce ice. Muhr and Blanshard[404] have measured the relative rates of linear ice front advancement at subzero temperatures in aqueous solutions of 35 w% sucrose with and without added polysaccharide "stabilizers". Their results showed conclusively that

the rates depend critically on the presence or absence of a gel network, even for exactly the same formulation. For the solution of sucrose alone at $T \gg Tg'$ (regime I), the relative rate of ice front advancement was 6.0. (It would have been essentially zero at $T < Tg'$.) At the same temperature, the rate was 4.1 in a sucrose solution containing 0.75 w% non-entangling (i.e., non-gelling) Na alginate (regime II), but only 1.0 in a sucrose solution containing 0.75 w% entangling (i.e., gelling) Ca alginate (regime III). Thus, when there was a hydraulic resistance to water removal, due to the resistance of the Ca alginate gel network to shrinkage, the rate of ice front advancement was dramatically reduced.

By analogy to other moisture management problems involving diffusion-limited processes (e.g., "Aw" control, textural stabilization), entangling, network-forming saccharide high polymers from regime III can be used as functional additives to retard moisture migration in baked goods, retain crispness of breakfast cereals, and reduce sogginess of pastries and pie crusts.

3. WLF Kinetics of Collapse Processes in Rubbery Frozen Products

For the cryostabilization of real frozen food products such as ice cream (with desirable smooth, creamy texture) against ice crystal growth over storage time (at $Tf > Tg'$), inclusion of polymeric cryostabilizers such as low DE maltodextrins elevates the composite Tg′ of a mix of soluble solids that is typically dominated by low MW sugars.[8,32] In practice, a retarded rate of migratory ice recrystallization ("grain growth" of pre-existing ice crystals)[240] at Tf and an increase in observed Tr result. Such behavior has been documented in several "soft-serve" ice cream patents.[37,38,405] In such products (and in a variety of other frozen foods and aqueous model systems), ice recrystallization has been shown to involve a diffusion-limited maturation process with a mechanism analogous to "Ostwald ripening", whereby larger crystals grow with time at the expense of smaller ones that eventually disappear.[50,255,308,309,406-408] The ripening rate at Tf is reduced (due to reduced ΔT above Tg′) by formulation with low DE maltodextrins of high Tg′.[8,32] Low DE maltodextrins have also been used to stabilize frozen dairy products against lactose crystallization during storage,[310] another collapse process (see Table 9) that can occur in a practical time frame at $Tf > Tg'$.

Ice recrystallization has been shown to exemplify a collapse process for which the kinetics fit the form of the WLF, but not the Arrhenius, equation.[15,32-34] As demonstrated by the Tg′ results for a series of commercial products in Table 18,[34] typical ice creams and related frozen foods have composite Tg′ values in the range −23 to −43°C,[15,32,50] representative of water-soluble solids compositions dominated by compatible blends of milk proteins and sugars with weight-average Tg′ values analogous to those of saccharide oligomers of DP 1-4.[8,34] As illustrated in Figure 63, such products exist as inherently *unstable* rubbery fluids with embedded ice and fat crystals under normal freezer storage at −18°C, and so WLF rather than Arrhenius kinetics are appropriate to describe their rates of ice crystal growth. Figure 80[34] contains two WLF plots of log (iciness score) vs. ΔT, one for a series of ice cream protocepts and the other for a set of frozen novelties, which verified the applicability of WLF kinetics to storage-stability data for such frozen desserts. Both plots show clearly that the rate of iciness development increased dramatically with increasing ΔT. Because the numerical values of the constants C1 and C2 in the WLF equation, appropriate for these two frozen products, were unknown and unassumable,[30] the two data sets were not fitted to a quantitative form of the WLF equation.[34] Instead, empirical curves were drawn through the data points in each plot. These curves (especially the one extrapolated to the origin in part B) are clearly similar in shape to the theoretical curve defined by the quantitative WLF equation, shown in Figure 36 as a plot of log relaxation rate vs. ΔT. In contrast, the straight dashed line drawn in part B represents the behavior expected for Arrhenius kinetics (i.e., $Q_{10} = 2$). Considering that iciness scores were measured by sensory evaluation, this unprecedented experimental demonstration of WLF behavior in frozen food systems was viewed as remarkable,[15,32] despite the obvious fact (discussed in subsequent papers[33,39,98]) that further studies, and more quantitative data, would be useful in con-

TABLE 18
Low-Temperature Differential Scanning Calorimetry Results for Commercial Ice Cream Products[34]

Sample	Description[a]	Tg′ (°C)	Tm (°C)	% Freezable water (g ice/100 g sample)
Dolly Madison	VIC	−31	−1	67.5
Sealtest	VIC	−31.5	−1.5	63.0
Breyer's	VIC	−32.5	−1	
Light 'n Lively	VIM	−29.5	−1	
Dolly Madison — "Less Sugar"	Sorbitol IC	−40	−1.5	64.0
Carvel	VSSIC	−30.5	−0.5	59.9
Rich's	VSSIC	−39	−4.5	47.5
Lipton	VSSIC	−41	−3	58.0
Landwide	VSSIC	−34	−4	43.0
Landwide	CSSIC	−37.5	−3.5	56.4
Dairy Queen	VSSIM	−30.5	−0.5	61.9
Dairy Queen	CSSIM	−30.5	−0.5	60.1
Crowley	VSSIC	−28.5	0	66.3
Crowley	VSSIM	−31.5	0	72.5
Crowley	CSSIC	−31	−0.5	59.0
Crowley	CSSIM	−30.5	0	69.9
Birds Eye — "Sheer Delight"	CSSM	−39	0	67.9
Pillsbury — "Spooners"	CSSM	−37	−4.5	
Pillsbury — "Spooners"	VSSM	−36.5	−4.5	
Pillsbury — "Spooners"	Strawberry SSM	−36.5	−4	
Dannon	Coffee Yogurt	−33.5	0	75.0
"Frozen Yogurt"	VSS	−27.5	0	60.3
General Foods — "Soft Swirl"	VSSIM	−31	−4	55.9
General Foods — "Soft Swirl"	CSSIM	−32	−3.5	56.2

[a] VIC = vanilla ice cream; VIM = vanilla ice milk; VSSIC = vanilla soft-serve ice cream; CSSIC = chocolate soft-serve ice cream; VSSIM = vanilla soft-serve ice milk; CSSIM = chocolate soft-serve ice milk; SSM = soft-serve mellorine.

firming the conclusion regarding the broad applicability of WLF kinetics to rubbery frozen food systems. (In this regard, it is pertinent to note two recent reports of non-linear Arrhenius plots of storage-stability data for frozen foods: (1) as mentioned earlier, for the dependence of enzymatic reaction rates in frozen cod fillets on Tf,[312] for freezer temperatures as high as −12°C, which is quite possibly above the Tg′ for cod,[39] and (2) for the effect of Tf on the kinetics of ice recrystallization in frozen beef muscle tissue,[309] for freezer temperatures as high as −5°C, again possibly above the Tg′ for beef.[39]) It has been pointed out that the WLF-type behavior (rather than Arrhenius-type Q_{10} = 2) of ice cream is apparently recognized, at least empirically, by the British frozen foods industry.[15] Ice cream packages in the U.K. carry the following shelf-life code: in a one-star home freezer (−10°C), storage life = 1 d; ★★ freezer (−18°C), 1 week; and ★★★ freezer

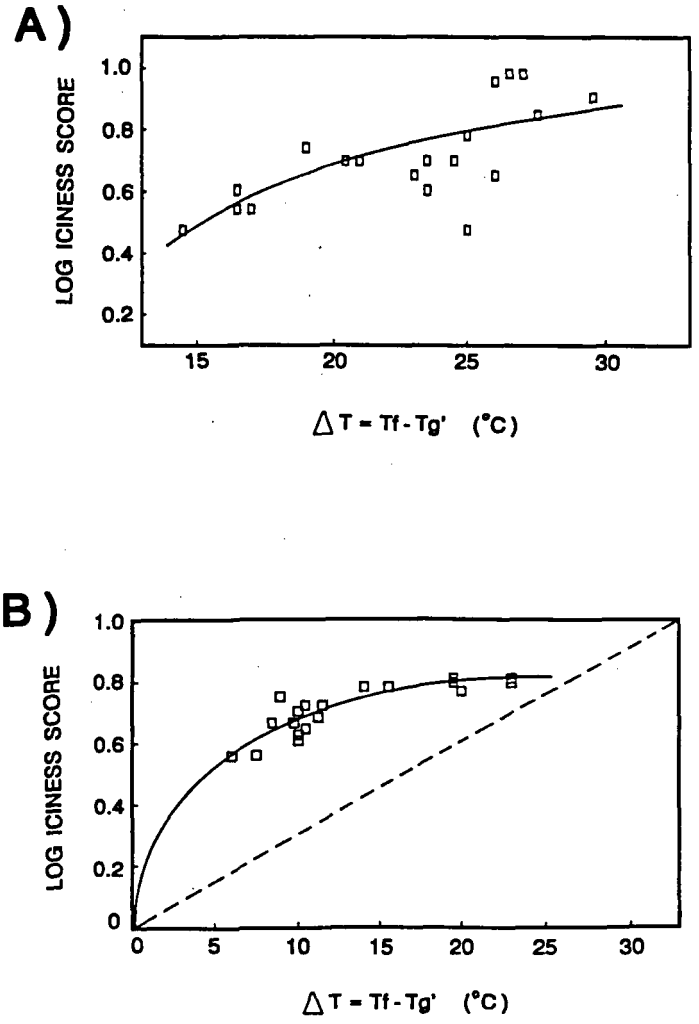

FIGURE 80. Williams-Landel-Ferry plots of log (iciness score) (determined organoleptically, on a 0 to 10 point scale) as a function of ΔT (= Tf − Tg'), for experimental (A) ice cream products and (B) frozen novelties, after 2 weeks of deliberately abusive (temperature-cycled) frozen storage in a so-called "Brazilian Ice Box". (The straight dashed line drawn in part B represents the behavior expected for Arrhenius kinetics.) (From Levine, H. and Slade, L., *Thermal Analysis of Foods,* Ma, C.-Y. and Harwalker, V. R., Eds., Elsevier, London, 1990, 221. With permission.)

(−23°C), 1 month. Such limited shelf-life, even at Tf = −23°C, testifies to the inherent instability of ice cream products with Tg' ≪ Tf.[34]

It should be noted that the kinetics of ice recrystallization (via "Ostwald ripening") as a maturation process in a frozen aqueous system with preexisting ice crystals are distinguishable, on the basis of the particular Tg that defines the lower limit of the operative temperature range, from the kinetics of the nucleation and growth processes of irruptive ice crystallization[240] in a completely vitrified solute-water system containing no preexisting ice crystals. As illustrated and discussed earlier with respect to Figure 39, the operative temperature range for ice recrystallization in a frozen system during a practical time frame is from Tg' of the freeze-concentrated solution to Tm of ice. In contrast, the operative temperature range for ice crystallization in a completely vitrified solute-water system is from Tg

of the original solution (with its initial solute concentration, e.g., point A in Figure 39) to Tm of ice. This is illustrated in Figure 81,[320] which shows Luyet's results for the temperature dependence of ice crystal nucleation and growth rates in a vitrified 50 w% aqueous solution of PVP. Notice the expected, but nonetheless striking, similarity in appearance between Figure 81 and the diagram of the crystallization kinetics for diluent-free partially crystalline synthetic polymers shown earlier in Figure 37. The Tg for the PVP solution represented in Figure 81, below which neither nucleation nor growth can occur on a realistic time scale but above which devitrification can occur, is evidently below −80°C. In comparison, the Tg′ for such a PVP solution (i.e., somewhere in the range −20 to −26°C, as shown in Table 8) is located 5 to 10°C below the temperature (i.e., about −15°C, which, either before or after ice was present in this system, would be within the operative WLF rubbery liquid range) at which Luyet's results showed a maximum ice crystal growth rate.

In practice, the technological utility of Tg′ and Wg′ results for sugars, polyols, and SHPs, in combination with corresponding relative sweetness data, has been demonstrated by successful formulation of ice cream products[37,38] with an optimum combination of stability and softness in a −18°C home freezer. With respect to these related issues of stability and softness of ice cream and similar frozen desserts, the DSC results in

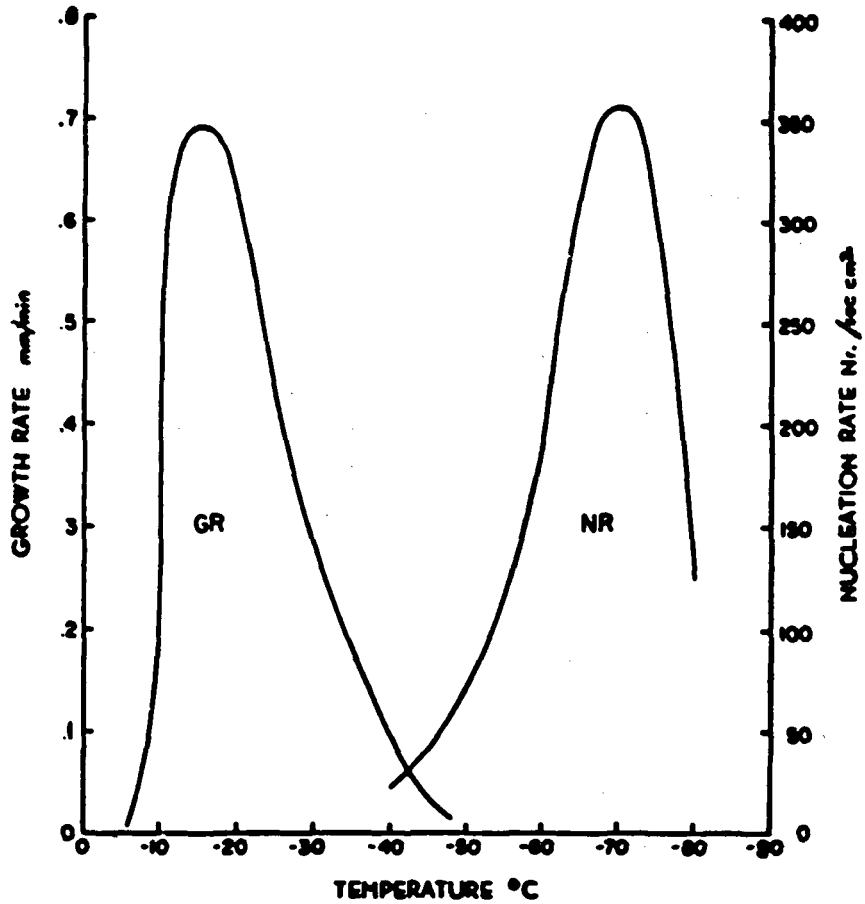

FIGURE 81. Temperature dependence of two-dimensional ice crystal radial growth rate and two-dimensional ice crystal nucleation rate in aqueous 50% w/w polyvinylpyrrolidone. (From Fahy, G. M., *Low Temperature Biotechnology: Emerging Applications and Engineering Contributions,* McGrath, J. J. and Diller, K. R., Eds., American Society Mechanical Engineering, in press. With permission.)

Table 18 have revealed some interesting and fundamental correlations.[34] As a general rule, higher values of Tg′ go hand-in-hand with higher values of Tm and percent freezable water (% FW, defined as maximum g ice/100 g sample), while lower Tg′ values go along with lower values of Tm and percent FW. (The rationale behind these internally consistent trends is easily explained based on state diagrams [analogous to Figure 39] constructed from DSC analyses for such complex systems.) For such products, increasing percent FW correlates intuitively with increasing hardness (due to more ice) at a given Tf. Since percent FW corresponds to an inverse measure of product Wg′, the correlation between increasing Tg′ and increasing percent FW is actually analogous to the overall trend of increasing Tg′ with decreasing Wg′ described earlier with respect to the cryostabilization technology spectrum in Figure 64. Thus, the fundamental and essentially universal correlations between the critical and related functional attributes of storage stability and texture for such products, which are directly reflected by their thermal properties of Tg′, Tm, and percent FW, are as follows:[34] at a given Tf, greater relative stability is coupled with harder-frozen texture, as determined by, and predictable from, higher values of Tg′ (thus smaller ΔT), Tm, and percent FW, while at the same Tf, poorer stability is coupled with softer-frozen texture of product variants with lower values of Tg′ (larger ΔT), Tm, and percent FW. As mentioned earlier, these intrinsic correlations of stability (high Tg′) with "hard-frozen" (low Wg′) and instability (low Tg′) with the "soft-frozen" (high Wg′) nature of products, which have been found to apply to many different types of frozen foods,[25,34] have been recognized as underlying precepts of cryostabilization technology,[32] as illustrated by the spectrum of cryostabilizers and cryoprotectants shown in Figure 64.

In the present context, another point emphasizes the distinction in functional behavior between non-entangling small carbohydrates and high-polymeric saccharides capable of intermolecular entanglement.[8] A freeze-concentrated glass at Tg′ of a SHP cryostabilizer (of DE ≤ 6) would contain entangled polymer chains, while in the glass at Tg′ of a low MW cryoprotectant, solute molecules could not be individually entangled.[8] (However, the possibility that small carbohydrates might form long-chain aggregates by hydrogen bonding or complex formation with alkaline salts should not be overlooked.) By analogy, various high MW polysaccharide gums, typically used at concentrations below 1 w% (whereby their impact on a product's composite MW and Tg′ would be small, as discussed earlier with respect to Table 11), are believed by some to be capable of improving freezer-storage stability of ice-containing fabricated foods, in some poorly understood way. In the absence of direct evidence of any effect on ice crystal size, and despite evidence that such "stabilizers" have no significant effect on ice nucleation or propagation rates,[50,404,409] or on rates of ice recrystallization at Tf>Tg′,[308] this stabilizing effect of gums has been attributed to viscosity enhancement.[407,410] It has been suggested[8] that such gums may owe their limited success not only to their ability to increase microscopic viscosity (a property shared by all glass-formers, regardless of MW, in the sense that ηg at Tg is independent of MW[30]), but to their capability to undergo intermolecular entanglement and increase macroscopic viscosity via network formation (thereby physically inhibiting translational diffusion-limited processes)[34,404] in the freeze-concentrated, amorphous matrix of a frozen food. Entanglement might provide an improved mouthfeel that masks the limited ability of gums to inhibit the growth of ice crystals.

E. Small Sugars at Low Moisture

1. Crystallization Kinetics

A conceptual description of the kinetically controlled relaxation process of sugar crystallization in aqueous systems at low moisture[15] has been illustrated by the schematic state diagrams in Figure 82.[30] These in turn were based on the idealized state diagram shown in Figure 83[23] for a plasticizer (component 3)-solute (component 2) system that exemplifies a typical sugar-water system. Notice the progression in the complexity of schematic state diagrams from (1) Figure 21 — glass curve only — neither the plasticizer nor the solute are crystallizable; to (2) Figure 23 — glass

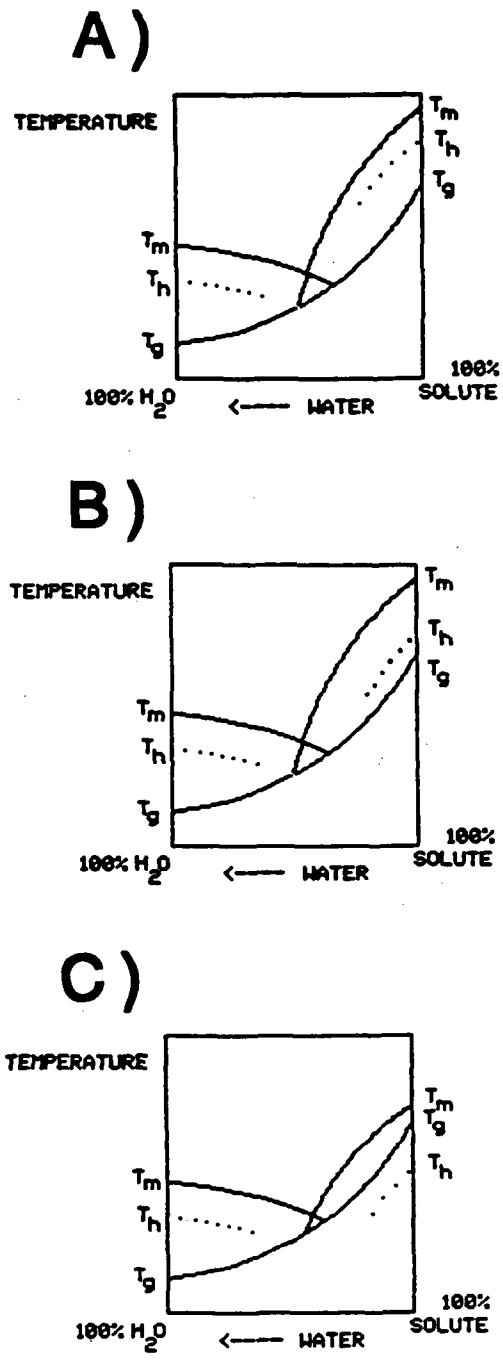

FIGURE 82. Schematic state diagrams for representational small PHC solutes with Tm/Tg ratios of (A) 1.5, (B) < 1.4, and (C) close to 1.0. The diagrams illustrate the locations of the solute-water Tm and Tg curves relative to the curve of estimated Th, and emphasize how the influence of the glass transition on the homogeneous nucleation of solute from undercooled concentrated solutions differs according to the location of Th within or outside the WLF region between Tm and Tg. (From Slade, L. and Levine, H., *Pure Appl. Chem.*, 60, 1841, 1988. With permission.)

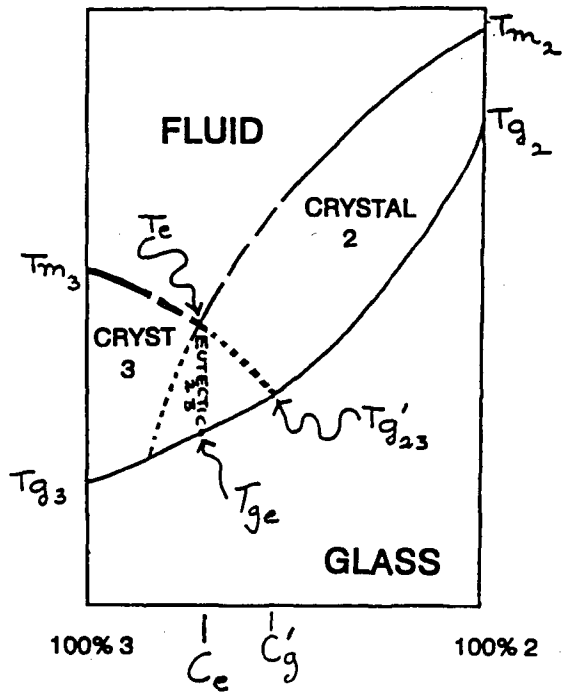

FIGURE 83. Idealized state diagram for a plasticizer (component 3)-solute (component 2) system in which both components are crystallizable. Diagram illustrates the locations of the glass, solidus, and liquidus curves. See text for definitions of symbols. (Reproduced with permission from Reference 23).

curve plus liquidus curve for the Tm of pure ice — the plasticizer is crystallizable but the solute is not; to (3) Figure 83 — glass curve plus liquidus curve plus solidus curve for the Tm of the solute — complete state diagram for a system in which both the plasticizer and the solute are crystallizable (e.g., sucrose in Figure 61). As shown by the solidus curve in Figure 83 for the melting or dissolution of solute as a function of solute-plasticizer blend composition, Tm decreases with increasing plasticizer content[66] from Tm2 for the pure dry solute to Te, the eutectic melting temperature, for the eutectic composition (Ce) of crystalline solute plus crystalline plasticizer. The solid-line portions of the liquidus and solidus curves in Figure 83 denote locations on this dynamics map, only far above the glass curve, which may be observed on a practical time scale to exist at equilibrium.[30] In contrast, the dashed-line portions of these curves (i.e., the solidus at compositions < Cg′ and the liquidus at compositions corresponding to the dashed-line por-

tion of the solidus) do not exist at equilibrium on a practical time scale and therefore contribute to the observed dependence of sample performance on processing rates, storage times, and previous sample history.[30] The critical area of the map in Figure 83, labeled "crystal 2", defines the metastable WLF rubbery region, bounded by the operative glass and solidus curves, within which solute crystallization can occur in undercooled solute-plasticizer blends.[23] By analogy to the metastable region ("cryst 3") in which water can crystallize and avoid its eutectic behavior, "crystal 2" is the region in which solute can crystallize or not, depending on the relationship of the temperature and moisture content to the underlying glass curve, and thereby avoid eutectic crystallization.[15,30,66] "Crystal 2" is the map domain relevant to the crystallization kinetics of small sugars in low-moisture food systems.[28,66]

As illustrated in Figure 83 and earlier in Figure 37, on a time scale of technological significance, crystallization can only occur within the kinetically metastable region of the dynamics map between Tm and Tg of a system.[15,104] In the process of crystallization for a polymer that is completely amorphous and unseeded, homogeneous nucleation in an undercooled melt is the first mechanistic stage, which must precede crystal growth. The necessary extent of undercooling in °K from Tm to Th, the homogeneous nucleation temperature, is a universal property of crystallizable materials. Just as Tg is related to Tm by the ratio Tm/Tg $\simeq$ 1.5, with a range of 1 to 2, for essentially all molecular glass-formers, including small molecules and high polymers, Th is related to Tm by the ratio Tm/Th $\simeq$ 1.25, with a narrow range of 1.17 to 1.28 for essentially all crystallizable substances, including metals, salts, small organic molecules, and high polymers.[104,115] Thus, in almost all known cases, Th > Tg.[28] For example, for the representational typical elastomer (Figure 34A) with Tg = 200°K and Tm = 300°K, the calculated Th value would be 240°K.

The relationship between Th, Tm, and Tg, for representational small PHCs in water, is illustrated in Figure 82,[30] which shows schematic state diagrams for three different situations that can govern homogeneous nucleation. The situations result from different values of the ratio Tm/Tg, which reflects the magnitude of the metastable WLF region in which crystallization can occur. In each case, Th was located according to the typical ratio of Tm to Th. These stylized state diagrams highlight the different ways in which Th and Tg can be related, depending on the Tm/Tg ratio for a particular PHC solute, and thus reveal how the relationship between Th and Tg determines and allows prediction of the stability against recrystallization of concentrated or supersaturated aqueous solutions of specific PHCs, such as small sugars.[15] In the first case (Figure 82A), for a PHC with a typical, higher Tm/Tg ratio of $\simeq$1.5, homogeneous nucleation of the solute would be very efficient, because Th lies well above Tg. Therefore, upon undercooling this concentrated PHC solution from T > Tm, homogeneous nucleation would occur at Th within the liquid zone, before vitrification could immobilize the system at Tg. Common examples of PHCs whose actual state diagrams resemble the one in Figure 82A, and which are known to crystallize readily from concentrated aqueous solution, include xylose (Tm/Tg = 1.51) and glucose (Tm/Tg = 1.42), and to a lesser extent, sucrose (Tm/Tg = 1.43).[15,28,66] The ratios Tm/Th and Tm/Tg reflect the relative distances Tm − Th and Tm − Tg on the dynamics map. The secondary influence of the magnitude of Wg′ for these PHCs on the relative mobility within the WLF region is reflected in the greater ease of homogeneous nucleation for glucose than sucrose, since the opposite behavior would be predicted on the basis of the ratio of Tm/Tg alone.[30] Both xylose and glucose exhibit simple mutarotation in aqueous solution, with their anomeric ratio depending on temperature and concentration.[281] Xylose also exhibits simple mutarotation in the diluent-free melt.[291] For both xylose and glucose, the anomers vitrify compatibly as a single glass. Sucrose, of course, does not exhibit mutarotation and vitrifies as a single glass.

In the second case (Figure 82B), for a PHC with an atypical, lower Tm/Tg ratio < 1.4, homogeneous nucleation would be retarded, because Th falls much closer to Tg, in the more viscous fluid region where transport properties can become a significant limiting factor on nucleation in non-equilibrium systems.[296] Ribose (Tm/Tg = 1.37) is an example of a PHC with

a state diagram resembling Figure 82B, whose nucleation would be so retarded.[30] Ribose exhibits complex mutarotation to six tautomeric and anomeric forms in aqueous solution,[281] which vitrify compatibly as a single aqueous glass. Further study is needed to determine if this existence of multiple conformers contributes to its crystallization inhibition. It is interesting that mannose (Tm/Tg = 1.36), which does not obey the "anomeric rule"[281] that water favors the species in tautomeric and anomeric equilibria with the largest number of equatorial –OH groups, has a Tm/Tg ratio more like ribose than like glucose, which does obey the rule.[30]

In the last case (Figure 82C), for a PHC with an anomalously low Tm/Tg ratio close to 1.0, homogeneous nucleation would be prevented on a practical time scale, because Th actually lies below Tg.[30,288] Thus, on undercooling a concentrated solution, vitrification would occur first, thereby immobilizing the system and preventing the possibility of solute nucleation at Th. Fructose (Tm/Tg = 1.06), which is well-known to be almost impossible to crystallize from aqueous solution without pre-seeding or precipitating with non-solvent, exemplifies the state diagram in Figure 82C and the nucleation inhibition behavior predicted from it.[15] Like ribose, fructose also exhibits complex mutarotation, with the composition of tautomers and their anomers depending on temperature and concentration.[281] Unlike ribose with its complex mutarotation, or xylose and glucose with their simple mutarotation, the conformers of fructose do not vitrify compatibly as a single glass, as discussed earlier with respect to the free volume requirements for mobility of fructose conformers. From the standpoint of mechanical relaxations, the compatibility of a solute with the structure of liquid water and the mutual compatibility of a mixture of solutes with water in aqueous glasses are highly cooperative properties, governed by the spatial and orientational requirements for isotropic or anisotropic mobility.[30] From the standpoint of energetics, little is known about cooperative effects that might differentiate between solute-solute or solute-water interactions, but differences in compatibility based on spatial and orientational requirements for labile intermolecular solute-solute and solute-water hydrogen bonds and maintenance of the time-averaged tetrahedral geometry of water are expected to be marginal.[281] Thus, in aqueous solutions and glasses of PHCs, the mutual compatibility of chemically heterogeneous solutes and water is likely to be governed by dynamics and mechanical requirements, rather than energetics.[30] Moreover, the marginal differences in energetics of solute-solute and solute-water interactions are reflected in the limiting partial molar volumes of PHCs, where differences between isomeric sugars are too small to interpret the effect of sugar stereochemistry on hydration[281] in very dilute solutions. It has been suggested that more can be learned about the effect of sugar stereochemistry on the solution behavior of PHCs in the region of the mobility transformation map where dynamics, rather than energetics, dominates.[30,31]

It should also be noted from the schematic mobility maps in Figure 82 that the homogeneous nucleation of ice from dilute solutions would not be prohibited during slow cooling, no matter what the Tm/Tg ratio of the PHC solute.[30] Because the Tm/Tg ratio of pure water is about 2.0, its Th lies well above its Tg of about 140°K.[89] The observed Th of pure water is about 233°K,[4] so that its ratio of Tm/Th is about 1.17, which falls at the low end of the reported range of values for essentially all crystallizable substances.[30] Thus, at least some of the water in a dilute PHC solution would freeze before it could vitrify, except under extremely fast cooling (e.g., "hyperquenching") conditions.[4]

2. Dynamics of Sucrose Glass-Formation and Recrystallization

Sucrose is arguably *the* most important single sugar for food manufacturing and also the sugar about which the most is known, as exemplified by the detailed state diagram for sucrose-water shown earlier in Figure 61. In many different food products and processes, the glass-forming vs. crystallizing behaviors of sucrose constitute critical functional attributes.[66] In the context of the kinetically controlled crystallization of sugars in low-moisture food systems, as described with reference to Figures 82 and 83, let us reexamine the state diagram for sucrose. And let us focus

attention on the region of this dynamics map encompassing the solidus and glass curves, wherein sucrose can crystallize or not, depending on the relationship of the temperature and moisture content to the underlying glass curve.

As shown in Figure 84, when some common food systems are positioned on this map, in terms of their operative temperatures and typical sucrose-water compositions, one quickly comes to appreciate the extreme complexity of the physicochemical aspects of such situations. For example, the locations of lean (i.e., low sugar/fat ratio) and rich (i.e., high sugar/fat ratio) cracker doughs in Figure 84 are sufficiently above the glass curve, so that it is relatively easy to dry these products (by raising T to above the vaporization curve) during baking. However, once these doughs are baked, the crackers fall in the box of final products (D) that spans the glass curve. Box D represents the range of possible products (in terms of sucrose-water composition and temperature), which is determined by initial sugar content, final moisture content, and distribution temperature(s) (e.g., F ≡ Miami in summer, E ≡ Minneapolis in winter). Typical high-sugar cookie (so-called "sugar-snap" cookie) doughs can be even more complex than cracker doughs, because, depending on not only how much flour, sugar, and water are added to the dough mixer, but also on how much crystalline sugar dissolves during dough mixing and lay time, the final dough before baking can be located either on one side (A) or the other side (B) of the solidus curve. Consequently, as the temperature rises during baking, either water evaporates first and then sugar dissolves (starting from A), or sugar dissolves

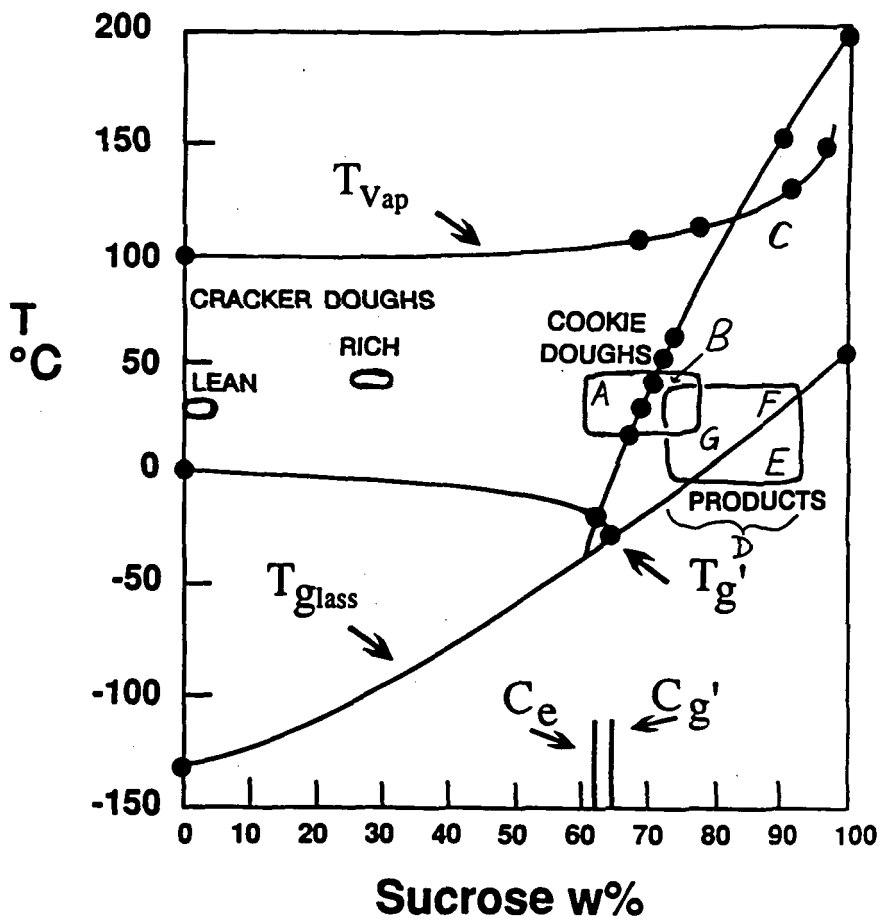

FIGURE 84. The sucrose-water state diagram from Figure 61, on which are indicated the locations (in terms of sucrose concentration and temperature) of lean and rich cracker doughs, rich cookie doughs, and final baked cookie and cracker products.

first and then water evaporates (starting from B). And if enough evaporation occurs during baking, the half-baked product can find itself in the metastable region (C) in which the sugar can recrystallize. Because of all these possible routes and scenarios, the DSC curves that one measures for such doughs, half-products, and final products can be exceedingly busy.

The most important point illustrated in Figure 84 is that all of the potential cracker and cookie products span the sucrose-water glass curve. Therefore, their storage stability against a variety of collapse processes (e.g., textural changes, flavor changes, oxidative rancidity) depends on the temperature and time (as well as the possibility of moisture-content changes) during distribution. By definition, high-quality products fall somewhere within box D. Classic sugar-snap cookies are composed of a continuous glassy sucrose-water matrix containing embedded ungelatinized starch granules, undeveloped gluten, and fat; typical crackers are composed of a continuous glassy network of (partially) gelatinized starch, (partially) developed gluten, amorphous sucrose, and fat.[26] Such products are deliberately formulated and processed to begin their shelf-lives in a kinetically metastable glassy solid state (E) commensurate with optimal initial quality (e.g., crisp texture) and storage stability. In contrast, finished products at F or G (i.e., an unstable rubbery liquid state) would have inferior (rubbery) texture and unacceptably short shelf-life. It is also critical to recognize that, in order to maintain the initial high quality of such cookie and cracker products during storage, one must control the distribution system/environment, so that the kinetically metastable glassy solid state is maintained and the potentially unstable rubbery liquid state is avoided.

F. Drying Processes

1. Mobility Map of a Generic Drying Rate Profile

When we examine drying as a moisture management problem and use the food polymer science approach to interpret results from analyses of conventional drying processes, increased understanding and insight result. Ease of drying can be viewed as a functional manifestation of mobility in a food system.

Food engineers and drying technologists ordinarily analyze drying processes in terms of a drying rate profile. The idealized drying rate profile of sample weight loss vs. time shown in Figure 85 is a typical profile of the time course of weight loss due to evaporation of sample volatiles, such as is used to explore ingredient influence on drying behavior and to evaluate the performance of drying equipment. At a selected drying temperature, residual sample weight is monitored as a function of time. For typical food ingredients and products, weight loss due to evolution and evaporation of volatiles is predominantly attributed to moisture loss.

Typical drying rate profiles,[411] e.g., Figure 85, have a characteristic sigmoid shape that can be described in terms of four distinct time periods during drying. Because heat transfer (thermal diffusivity) is much more efficient than mass transfer (effective diffusion coefficient of water), temperature gradients within the sample are considered to be near zero during the drying process.[412] The four periods of drying illustrated in Figure 85 are described as follows:

1. Sample temperature rises to a constant value, <100°C at atmospheric pressure, determined by the balance of applied heat and evaporative cooling.
2. Linear portion of the drying profile = the period of constant-rate drying before the sample experiences constrained moisture diffusion. The sample temperature and rate of moisture loss are constant. The slope of the drying rate profile in period 2 = a constant rate of drying, labeled rc.
3. Non-linear portion of the drying profile = the period of falling (decreasing) rate drying due to ever-increasing diffusion constraint. The sample temperature and rate of moisture loss are *not* constant. As the rate of moisture loss decreases but the application of heat remains constant, the temperature of the sample increases up to the temperature of the environment by the end of drying. The decrease in moisture content is partially balanced by the increase in sample temper-

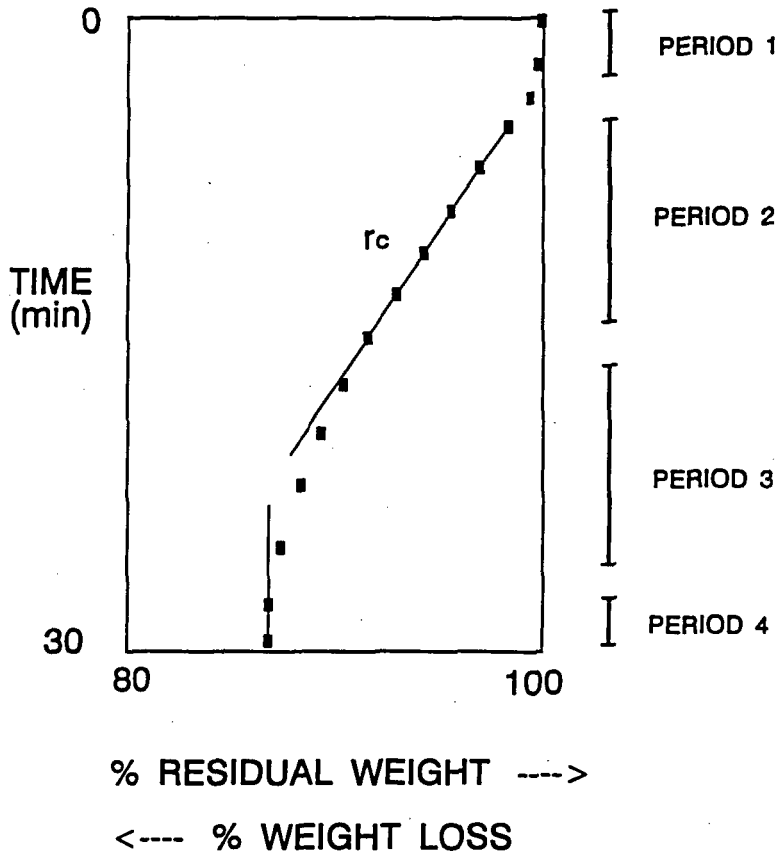

FIGURE 85. Idealized drying rate profile (sample weight loss vs. time) illustrating the time course of weight loss due to evaporation of sample moisture. The profile has a characteristic sigmoidal shape, which can be described in terms of four distinct time periods during drying.

ature, so that the estimation of the increasing constraint on diffusion is complicated. In the extreme of complete drying, the Tg of the sample approaches its dry Tg, which can be compared to the temperature of the environment.

4. End of the drying process, where the sample achieves a constant weight (in the absence of the production of water that was not present in the starting material, by Maillard browning reactions or combustion processes). The weight loss at the end of drying, as a percent of the original sample weight, represents the initial total moisture content of the sample, labeled mi.

If we convert Figure 85 into an even more generic drying rate profile, and emphasize drying periods 2 and 3, we obtain the schematic, two-dimensional mobility map of sample moisture content vs. time shown in Figure 86. Figure 86 suggests a critical moisture content that separates the period (2) of constant-rate drying, where the rate of water removal as a function of time is constant, from the period (3) of falling-rate drying, where the rate of water removal as a function of time decreases dramatically and is no longer constant. This critical point on the map occurs at particular characteristic moisture contents for different food systems. For example, for cooked white rice, the first part of a hot-air tunnel drying process from 70 w% down to about 30 w% moisture content is relatively easy to execute, while the part from about 30 w% to a final shelf-stable product at about 10 w% moisture is much more difficult (i.e., time- and energy-consuming). The characteristic moisture content, for rice and other starch-based foods, that separates the linear and

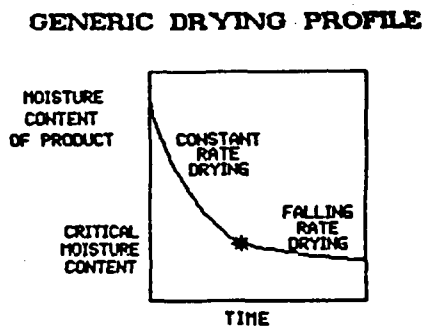

FIGURE 86. Generic representation of a drying rate profile plotted as a two-dimensional mobility map of sample moisture content vs. time. The critical moisture content that separates the constant-rate and falling-rate stages of drying at constant temperature is related to Wg′ of the sample.

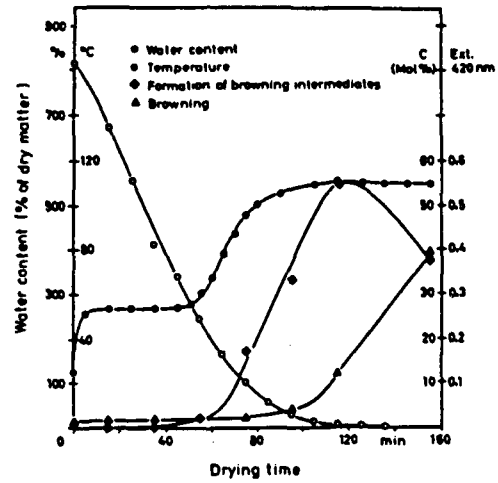

FIGURE 87. Plot of water content vs. drying time, describing the formation of browning intermediates and browning during air drying of carrot cubes (air temperature: 110°C). (From Nursten, H. E., *Concentration and Drying of Foods*, MacCarthy, D., Ed., Elsevier, London, 1986, 53. With permission.)

non-linear drying rate periods is about 27 to 30 w% water. This critical moisture content for drying of starch-based products is found to be related to Wg′. Thus, the solute-specific water content (UFW) that defines the maximally freeze-concentrated glass is also a reference point for functional behavior of the same system at higher temperatures and higher water contents. This reflects the fact that, as the sample moves (in terms of increasing temperature and decreasing moisture content) closer and closer to its glass curve as drying progresses from period 2 to period 3, its mobility decreases, resulting in increasing dynamic constraints on the diffusion-limited process of water removal.

One interesting example of the technological importance of the drying behavior described in Figures 85 and 86 involves Maillard browning reactions in dried foods, as reviewed by Nursten and illustrated in Figure 87.[411] Nursten has used the example of browning during air drying of carrot cubes to illustrate the interrelated effects of moisture content, temperature, and time on Maillard browning reactions,[411] effects that can be generalized to browning during processing and changes in browning during storage of other low-moisture food systems, such as baked goods. Figure 87 shows that the rates of development of browning reaction precursors and final browning products as a function of time depend on sample temperature and moisture content as determined by the progress of the drying (e.g., baking) process. Only when the moisture content becomes sufficiently low, once the temperature of the product is no longer being depressed by evaporative cooling, but rather is approaching the environmental temperature of the oven, do the browning reaction precursors start to build up. And the final browning products start to become apparent only *after* the maximum level of precursors is achieved, once the product reaches the maximum temperature and minimum moisture content at the effective end of the drying process. Thus, for example, if during baking, the process is stopped before the final minimum moisture content is achieved, only browning intermediates are produced, which form unstable browning reaction products. Consequently, fading can occur during subsequent shelf-storage of the baked product.

2. Improved Freeze-Drying: The Significance of Tg′ and the Glass Curve

Freeze-drying is an increasingly important commercial drying process for foods, pharmaceuticals, and biologicals.[40,41] However, despite its long history and widespread use, surprisingly little knowledge of its governing physicochemical principles is evidenced by the routine practice

of freeze-drying.[135] Franks[40,41] has recently noted that freeze-drying, as currently performed, relies on outmoded concepts, with little attention given to (and widespread ignorance prevailing about) the physicochemical changes that can take place in the substrate during freeze-concentration and subsequent drying. This is especially unfortunate in light of the fact that low-temperature processing and drying are more complex scientifically and technologically than spray-drying, solvent extraction, or ultrafiltration.[40,41] Franks[40,41] has also emphasized the fact that the physicochemical changes that take place in an aqueous mixture during freezing and subsequent drying can seldom, if ever, be predicted or modeled solely from a knowledge of the equilibrium phase behavior of the components of the mixture (even if such knowledge were available), because freeze-drying (like so many other food processes) is a non-equilibrium process that, when properly executed, is under kinetic control and involves dynamically constrained, metastable glassy states rather than equilibrium thermodynamic phases. Therefore, a good understanding of the glass-to-rubber transition is central to successful freezing and drying.[40,41,190,306]

As explained in the earlier discussion of Figure 39, Tg′ is the essence of cryostabilization technology. As described in Section IV.C, recent experimental studies[8,27,30-34] have demonstrated the significance of Tg′ in determining the behavior of frozen and freezer-stored foods, and have established that Tg′ is of fundamental technological importance to product quality and storage stability. Freeze-drying represents another aspect of frozen food technology that illustrates this point, as has been described in the context of the idealized state diagram in Figure 88.[33] The various cooling/heating paths illustrated in Figure 88 demonstrate the significance of Tg′ to freeze-drying without collapse or "melt-back",[33] as discussed earlier with respect to Table 9. For a model aqueous sugar solution cooled from room temperature (point A), freezing (as the first step in a typical freeze-drying process)[135] can follow the path ABQB′CD, or the alternative path ABPQB′CD, as described earlier for Figure 39. Either path to point D at $T < Tg'$ (where $Tg' \equiv$ the operative Tc for this high-moisture condition)[8] results in the solidification of the amorphous, freeze-concentrated solute-UFW matrix surrounding the ice crystals. The vacuum-drying stage of the process can be started, with the non-ice portion of the sample at point D, by allowing the sample temperature to rise in a controlled fashion. If the sample follows the dotted-line path from point D to point E, so that its temperature is maintained always below the solute-water glass curve as water is removed and its Tg ($\equiv$ the operative Tc for this progressively lower-moisture condition)[27] increases correspondingly, the glassy matrix would be able to support its own weight against flow under gravitational stress and so maintain its porosity (created by the sublimation of ice crystals) throughout the ice-sublimation and water-desorption stages of the drying process. At the end of the freeze-drying process, the porous glassy matrix at point E would be a (meta)stable solid at room temperature, because its Tg (which now represents the operative Tc for the low-moisture final product)[28] would remain above room temperature, in the absence of subsequent water uptake and plasticization. In contrast to the above scenario, freezing along the path ABQB′C in Figure 88 could be stopped at a temperature above point C (at $T > Tg' \equiv$ operative high-moisture Tc) before drying/heating begins, or, after freezing along the path ABQB′CD to point D, the sample could be inadvertently heated to $T > Tg$ ($\equiv$ operative Tc at lower moisture content $Wg < Wg'$) at point N, and held there[135] more than momentarily. In either of these cases, the amorphous solute-UFW matrix surrounding the ice crystals or their consequent voids would exist as a rubbery liquid capable of viscous flow. This situation could result in irreversible, macroscopic structural collapse and concomitant loss of porosity,[8,27] termed "melt-back".

For completeness, Figure 88 also illustrates several other alternative routes around the state diagram, i.e., schematic heating/drying paths (not involving freezing) followed by commercial drying processes other than freeze-drying, e.g., spray, drum, belt, oven tunnel, microwave, fluid bed, and extrusion drying. If the model sugar solution at point A follows the heating/drying/cooling path AFH′, the insufficiently dried sample at point H′ would be an unstable rubbery liquid at room temperature (at $T > Tg \equiv$ oper-

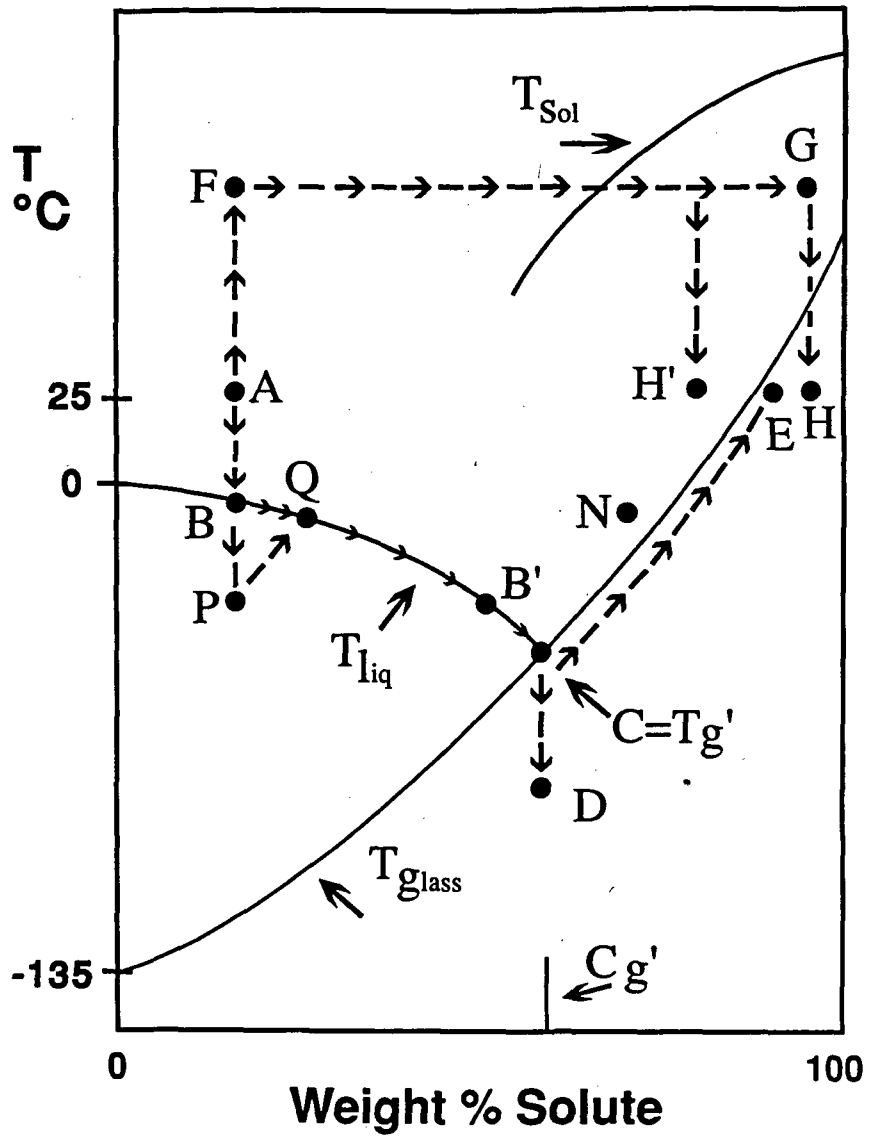

FIGURE 88. Idealized state diagram of temperature vs. weight percent solute for an aqueous solution of a hypothetical small carbohydrate (representing a model frozen food system), illustrating the cooling/heating paths associated with different freeze-drying protocols, relative to the locations of the glass, solidus, and liquidus curves, and demonstrating the technological significance of the Tg'-Cg' point to a freeze-drying process without collapse or "melt-back". See text for explanation of symbols. (From Levine, H. and Slade, L., *Comments Agric. Food Chem.*, 1, 315, 1989. With permission.)

ative Tc). It could be prone to solute recrystallization during storage at room temperature,[32] because of the location of point H′ within the metastable temperature region between the glass and solidus curves (as shown earlier in Figure 83).[15] In contrast, the heating/drying/cooling path AFGH would produce a sufficiently dried, (meta)stable glassy solid sample at point H (at room T < Tg ≡ operative Tc).[33]

As mentioned earlier in Section IV.C.1, collapse processes, such as "melt-back" during freeze-drying of aqueous solutions that do not undergo eutectic crystallization,[190,304-306] have been investigated and interpreted within a con-

ceptual context of "glass dynamics",[15,32] resulting in a conclusion regarding the fundamental equivalence of Tg, Tc, and Tr, and their dependence on solute $\overline{M}w$.[27] This new interpretive approach has provided a better qualitative and quantitative understanding of the equivalence of Tr for ice or solute recrystallization, Tc for collapse, and the concentration-invariant Tg′ for an ice-containing system, and has been used to explain why Tr and Tc are always observed to be concentration-independent for any initial solute concentration lower than Cg′,[4,260] as illustrated in Figure 88. This approach has also provided a technologically important predictive capability, exemplified with respect to freeze-drying.[33,34] Since Tg′ underlies and coincides with Tc and can be directly determined experimentally by DSC, Tc can be accurately predicted prior to the design of a freeze-drying process, rather than empirically determined by costly trial-and-error freeze-drying runs. In fact, this predictive capability is so powerful that Tg′ can often simply be calculated, rather than actually measured by DSC, for real food systems, as was described earlier in Section IV.G for orange and other fruit juices in Table 15.[33,34] Prior knowledge of Tg′ identifies the maximum allowable temperature for both initial product freezing and the primary stage of vacuum drying via sublimation of ice in the freeze-drying process.[34,40,41,190] Coupled with the Tg of the dry solute and the Tg of pure water, the Tg′-Cg′ point on the state diagram in Figure 88 defines a three-point glass curve. Knowledge of the location of this glass curve enables one to design a freeze-drying process with an optimum heating-rate profile, wherein the temperature-moisture-time protocol can be pre-programmed and controlled to maintain the temperature of the sample below its instantaneous Tg (determined by its instantaneous moisture content).[34] This ensures that the non-ice matrix remains a glassy mechanical solid capable of supporting its own weight against rubbery flow throughout the course of the ice-sublimation and desorption stages of the vacuum-drying process.[190,306] The latter stage, also referred to as secondary drying, is designed to remove residual plasticizer (moisture) from the glass and render the product stable at temperatures up to its dry Tg.[40,41,306] It is also critical to recall, as described earlier and emphasized recently by Franks,[40,41] that the composite Tg′ of a multicomponent product to be freeze-dried can be elevated (and should be, as much as is practical) and its composite Wg′ can be lowered (the lower, the better) by incorporation of polymeric cryostabilizers of high Tg′ and low Wg′.[8,27,28,32] Formulation with such high MW additives raises Tg′ (quantifiably and predictively), dry Tg, and thus the entire glass curve of a multicomponent, glass-forming blend, while shifting its composite unfrozen (but not "bound") water content to lower Wg′ values, thereby increasing the effectiveness (by lowering the probability of "melt-back") and efficiency (e.g., lower energy requirements, shorter secondary drying time) of the drying process and the subsequent shelf-stability of the freeze-dried product.[8,27,40,41]

Among a number of factors that should be known and taken into account in the production by freeze-drying of products of constant high quality and optimum stability, Franks has included the following, in summarizing his recent essay on the subject:[40]

1. Knowledge of Tg′ and Wg′ of the freeze-concentrate is essential.[190]
2. Knowledge of the Tg curve as a function of moisture content is essential for the proper control of secondary drying.[306]
3. For a stable, high-quality product, $W < Wg$ at ambient temperatures.

G. Cooking of Whole Cereal Grains Viewed as a Moisture Management Process

Cooking of whole cereal grains is a dynamic heat/moisture/time treatment that can be viewed as a moisture management process. The major effect of cooking of whole cereal grains is on the structure of native granular starch, because granular starch is the predominant component of the endosperm of cereal grains.[153,400] Thus, the process of complete cooking of whole cereal grains can be described in the context of a dynamics map of the amorphous regions of granular starch, as shown in Figure 89. The numbered locations (temperature-moisture content) on this schematic state diagram for starch correspond to different

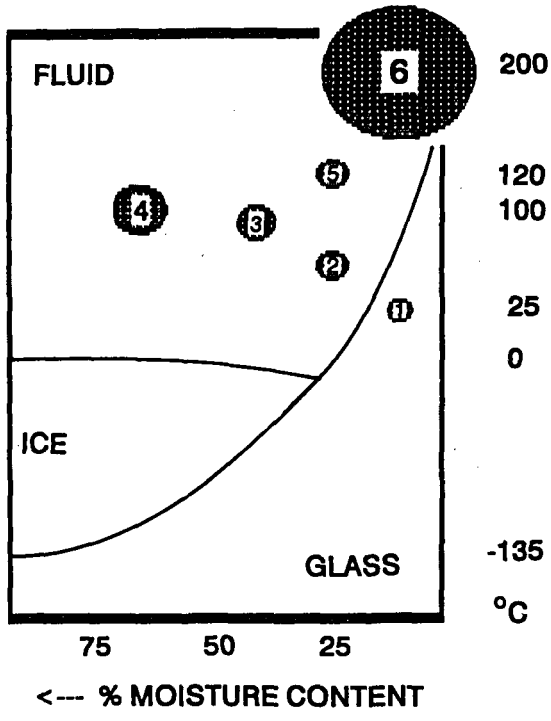

FIGURE 89. Dynamics map of the processing of whole cereal grains, conceptualized on a schematic state diagram for the amorphous regions of granular starch. The numbered locations (temperature-moisture content) on the map correspond to: (1) raw whole grain; (2) first-stage swelling; (3) beginning of second-stage swelling; (4) completion of second-stage swelling; (5) parboiling; (6) puffing or popping.

stages of various cooking processes for whole cereal grains, and the areas of these points signify the relative extents of volume expansion of the grain at each stage.

Complete cooking of whole cereal grains is a two-step process. For diagnostic purposes, the two steps can be accomplished independently. The first step, traditionally referred to as gelatinization,[207] involves initial hydration, and begins with the raw whole grain at 10 to 14 w% "as is" moisture content at room temperature (point 1 in Figure 89). This is the rate-determining step of cooking when comparing grains with different gelatinization temperatures (which is important for varietal rices and corns) or very different kernel weights due to size or density (which is important for varietal wheats). The minimum processing requirements for gelatinization are a temperature of at least about 60°C and a moisture content of at least about 27 w% on a *molecular level* within the grain (point 2 in Figure 89). This minimum temperature reflects the gelatinization temperature, which ranges from about 60°C for wheat and potato up to about 85°C for mutant corns.[413] Gelatinization is also called "first-stage swelling". Under controlled conditions to achieve 27 w% moisture content and gelatinization (e.g., pre-soak in excess water and then heat, or cook with water plus atmospheric steam), the volume expansion of the cereal kernel is almost insignificant (i.e., about 20% increase, as signified by point 2 in Figure 89). Gelatinization is a thermal process that can be monitored directly by DSC, for both whole grains[414,415] and isolated starches.[17-23] Gelatinization alone is sufficient to produce stabilized dried products that hydrate faster than the starting material, but is *not* sufficient to produce completely cooked and shreddable, flakable, or "instantized" half-products.

The second step of complete cooking of cereal grains, traditionally referred to as pasting,[207] involves major water uptake, swelling, softening, and loss of starch solids. Pasting is the rate-determining step of cooking when comparing grains with significant differences in composition of large linear polymers that are rigid at low moisture, have high swelling capacity, and soften upon swelling. The variation in amylose content among different varieties of cereal grains is most important for varietal rices and corns. The presence of bran (with a high pentosan content) and the variation in endosperm glutenins and pentosans among different varietal grains are important for varietal wheats. The minimum processing requirements for pasting are typically a temperature of at least about 85°C and a moisture content of at least about 45 w% on a *molecular level* within the grain (point 3 in Figure 89). "Typically" refers to grains with normal, rather than mutant, starch genotypes, i.e., with about 25% amylose and 75% amylopectin contents. Pasting is also called "second-stage swelling". Using controlled conditions to minimize the lag between heat transport and water transport and maximize the uniformity of water distribution at each water content (e.g., continued cooking with water plus atmospheric steam to about 45 w% moisture content, i.e., from point 2 to point 3 in Figure 89), expansion of the kernel is directly related to water

uptake. Pasting is a mechanical process that can be monitored directly by rheological methods,[413] but not by DSC.

Gelatinization *plus* pasting (to point 3 in Figure 89) are required to produce half-products that are optimally softened for shreddability and flakability, or dried quick-cooking/instantized products that hydrate *and* soften to ready-to-eat texture more rapidly than the starting material, so that overall cooking time is reduced during consumer preparation. (Tempering, as a shredding process step, appears to compensate for underpasting ("white spot" = uncooked kernel centers) by allowing time for uniform water distribution [which is most efficient near 85°C] and/or to compensate for overpasting [resulting in stickiness] by allowing retrogradation [which is most efficient below about 20°C]. Cooking only to the minimum requirements for pasting would minimize the requirement for tempering.)

In comparison to the above description, cooking of whole cereal grains is typically carried out as a continuous process, which masks the underlying two-step mechanism. The typical continuous cooking process used in the home or in commercial manufacturing depends on boiling water temperatures (e.g., atmospheric steam) and a great excess of cooking water (at or beyond the requirement for swelling to ready-to-eat softness). The overall cooking time is inversely related to the magnitude of the difference between the cooking temperature (about 100°C) and the gelatinization temperature (which is a glass transition temperature[17-23]). Because heat transfer is more efficient than mass transfer in the solid state, water uptake by the grain lags behind its increase in temperature and occurs from the outside to the center of the kernel. As a result, most of the kernel is above 27 w% moisture, when all of the kernel is at least 27 w%, in a typical continuous process with great excess water.

Parboiling is the best-known process to create stabilized half-products. The kernels with bran present are soaked at room temperature for a day or days to achieve an overall (but not necessarily uniform) moisture content above 27 w% (point 1 to point 2 in Figure 89) and then heated for 15 min at about 120°C in a pressurized steam (15 psi) chamber (point 2 to point 5 in Figure 89). The starch gelatinizes and recrystallizes *in situ* (without swelling of the kernel) to produce a kernel structure that is more stable to milling, hydrates more rapidly (because step 1 of cooking [i.e., point 1 to point 2] has already been achieved), but takes longer to soften to eating texture (because step 2 [point 2 to point 3] has not already occurred, and the new stable structure requires a greater extent of swelling to achieve the same softness) than does the starting material. When the parboiled grain at point 5 in Figure 89 is further cooked to point 3, the resulting product has a rubbery texture, reduced loss of starch solids, and reduced stickiness.

A variation on the parboiling process involves annealing (in place of gelatinization plus recrystallization) to perfect the native starch structure.[65] This is accomplished by atmospheric steam treatment of cereal kernels, grits, or flours at 30 w% moisture content and temperatures above 65°C but below 100°C. The so-called "steam-stabilized" half-product hydrates (step 1 in subsequent cooking by the consumer) faster than the starting material and softens to ready-to-eat texture (step 2 in cooking by the consumer) either faster (to be "quick-cooking") or slower (to be recipe-tolerant), depending on the process stabilization temperature.

Another variation, this on the conventional cooking process in excess water, involves the puffing or popping of whole grains to produce puffed wheat or rice, or popcorn.[416] In the puffing process, the temperature of the raw grain with "as is" 10 to 14 w% moisture (point 1 in Figure 89) is raised directly to about 185°C (point 6 in Figure 89) via gun-puffing, hot-air popping, hot-oil popping, or microwave popping. As the Tg and then the Tm of the partially crystalline native granular starch in the kernel endosperm are rapidly exceeded, there is a violent volatilization of the "as is" water, resulting in a dramatic expansion in volume to that characteristic of the puffed or popped grain.

Complete cooking to an end-point defined by ready-to-eat texture (i.e., from points 3 or 5, by continued cooking with water plus atmospheric steam, to the end of second-stage swelling at point 4 in Figure 89) typically requires water uptake to 70 w% moisture content or above with kernel expansion of 300% (i.e., 200% increase in volume) or even 400%. In contrast, complete

cooking to the minimum requirements for pasting (i.e., to point 3 in Figure 89), using controlled conditions of steam plus limited water, allows "instantization" with minimization of starch solids loss, stickiness, and drying requirements for quick-cooking consumer products or fouling of rollers in industrial shredding and flaking manufacturing operations.

The end-point for complete cooking in commercial processing of quick-cooking cereals (i.e., point 3 in Figure 89) is defined as the ability of the dried half-product to hydrate and soften to eating texture within a short target consumer preparation time. The standard assay for extent of cook is a "pour-off" test, applied to the cooked-and-dried half-product. One goal of current research is to replace such out-of-process assays by an in-process method using NMR (either pulsed or solid state) for the simultaneous determination of moisture content and its uniformity of distribution within the grain. A successful NMR method, to assess when the minimum requirements for pasting have been met (i.e., point 3 in Figure 89), would allow process optimization and enhanced product uniformity in commercial shredding, flaking, and instantization operations.

H. Starch Gelatinization and Retrogradation: Mechanical Relaxation Processes Affected by Mobility of Aqueous Sugar Solutions

Much has been learned about the structure-function relationships of starch in foods from analyses of the thermal and thermomechanical properties of starch in aqueous model systems and real products.[23] Just as the glass transition governs the practical temperature range for processing and commercial use of synthetic polymers, as well as the mechanical properties of both raw materials and products,[112,114] the same is true of the glass transition for starch, because of the dynamic influence of the glass transition on the events of annealing, gelatinization, pasting, and retrogradation.[17-23] Thermal analysis by DSC has revealed the critical role of water as a plasticizer for native, freshly gelatinized, and retrograded starches, and the importance of the glass transition as a physicochemical event that governs starch raw material properties, processibility, product quality, and storage stability.[15,26] The food polymer science approach has been used to study structure-property relationships of starches and sugars as water-compatible food polymers, which are treated as homologous systems of polymers, oligomers, and monomers with their plasticizers and solvents.[30] Recognition of the relevance of the key elements of the food polymer science approach to the behavior of starch-based food systems has provided a conceptual framework for understanding and explaining complex behavior, designing technologically useful processes, and predicting product quality and storage stability, based on fundamental structure-property relationships of starch viewed as a partially crystalline glassy polymer system.[15,26] The mechanical relaxation behavior of starch-water systems has been described in the context of a dynamics map of the critical variables of moisture content, temperature, and time.[23,26] Normal and waxy native granular starches have been found to exhibit non-equilibrium melting, annealing, and recrystallization behavior characteristic of kinetically metastable, partially crystalline polymer systems with a small extent of crystallinity.[17-23] Starch gelatinization and retrogradation in the presence of small sugars have been described as mechanical relaxation processes affected by the mobility of aqueous sugar solutions.[30] The retardation effect of concentrated sugar solutions on, for example, the Tg governing starch gelatinization, has been suggested to result from "antiplasticization" by sugar-water cosolvents, relative to the extent of plasticization by water alone.[20] Plasticization by sugar-water, of higher average MW than water alone, produces a smaller depression of starch Tg than does plasticization by water.[20] It has been shown that the non-Arrhenius kinetics of gelatinization, retrogradation, and annealing, defined by WLF relaxation transformations, depend on the magnitude of ΔT above the appropriate reference Tg.[21,26] It has also been demonstrated that the Tg observed during DSC analysis is often an effective Tg, resulting from instantaneous relative relaxation rates and non-uniform distribution of total sample moisture.[21]

1. DSC Analyses of Starch Gelatinization and Retrogradation — Insights Derived from the Dynamics Map

Despite the microscopic and macroscopic structural complexity of starch, many workers since 1980 have usefully discussed the physicochemical effect of water, acting as a plasticizer of the amorphous regions in the native granule, on the Tg of starch.[15-23,26,43,45-49,52,53,59,62,63,65,94,223] A number of these studies have involved DSC analyses that have convincingly demonstrated the non-equilibrium melting, annealing, and recrystallization behavior of native granular starch-water model systems — behavior that has been most clearly revealed by DSC results (e.g., Figure 90[20]) obtained for model systems with approximately equal weights of starch and added water.[15-23,26] Because the initial rate of plasticization in such model systems at room temperature is near zero, the added water remains predominantly outside the granules, and the native starch (e.g., wheat) with no pretreatment demonstrates a major glass transition and subsequent superimposed crystalline transition(s) in the temperature range from 50 to 90°C (as shown in Figure 90 curve a), which comprise the events of gelatinization (initial swelling) and pasting (second-stage swelling) of a starch granule.[19,20] The glass transition of the amorphous regions of amylopectin is observed at the leading edge of the first melting peak, between about 50 and 60°C.[17,18] This near superposition of the second-order glass transition followed by the first-order crystalline melting transition, due to the inhomogeneity of moisture contents within and outside the granules and to heating rate, has been revealed by the expected characteristic shift in heat capacity (diagnostic of a glass transition,[52,106] as illustrated earlier in Figure 33) shown by the extrapolated baselines in the DSC thermogram in Figure 90 curve a.[17-21] In fact, it has been demonstrated[26] that the magnitude of the baseline shift for the glass transition of amylopectin is equal in magnitude to the change in heat capacity that would be observed for an equal weight of completely amorphous pure polystyrene at its Tg. The important insight into starch thermal properties represented by the identification of this Tg for native wheat starch has been corroborated by subsequent DSC results for granular rice starches,[46,223] which likewise demonstrated that melting of microcrystallites is governed by the requirement for previous softening of the glassy regions of amylopectin, as described earlier in Section III.A.6.

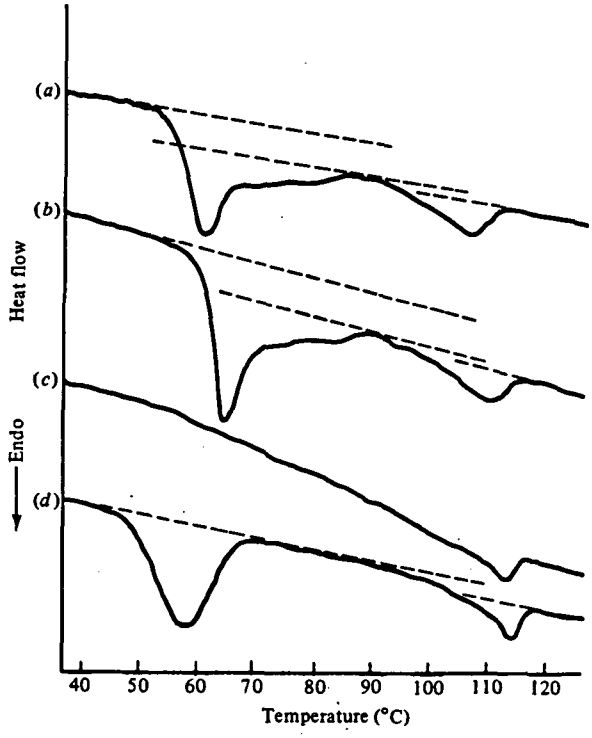

FIGURE 90. Perkin-Elmer DSC-2C heat flow curves of wheat starch:water mixtures (45:55 by weight): (a) native; (b) native, after 55 d at 25°C; (c) immediate rescan after gelatinization of sample in (a); (d) sample in (c), after 55 d at 25°C. Dashed lines represent extrapolated baselines. (From Slade, L. and Levine, H., *Industrial Polysaccharides — The Impact of Biotechnology and Advanced Methodologies,* Stivala, S. S., Crescenzi, V., and Dea, I. C. M., Eds., Gordon and Breach Science, New York, 1987, 387. With permission.)

When native wheat starch is allowed to anneal at 55 w% total sample moisture (initially 10 w% inside the granules and 100 w% outside) for 55 d at 25°C (Figure 90 curve b), the transition temperatures and extent of crystallinity increase. However, the characteristic baseline shift indicative of a preceding glass transition is still evident, demonstrating that melting of the microcrystallites is still governed by the requirement for previous softening of the glassy regions of amylopectin. Annealing is used in this context to describe a crystal growth/perfection process, in

a metastable, partially crystalline polymer system[104] such as native starch.[158] As mentioned earlier, annealing is ordinarily carried out at a temperature, Ta, in the rubbery range above Tg, typically at an optimal Ta = 0.75 − 0.88 Tm (K),[102] for polymers with Tg/Tm ratios of 0.5 to 0.8. In contrast, recrystallization is a process that occurs in a crystallizable but completely amorphous metastable polymer at Tg < Tr < Tm.[104]

After gelatinization during heating to 130°C, and quench-cooling to 25°C, an immediate rescan of wheat starch at 55 w% moisture (Figure 90 curve c) shows no transitions in the temperature range from 30 to 100°C. However, when this completely amorphous (i.e., no remaining amylopectin microcrystals) sample is allowed to recrystallize (at uniformly distributed 55 w% moisture) for 55 d at 25°C (Figure 90 curve d), it shows a major Tm at about 60°C (as a symmetrical endothermic peak, with essentially no baseline shift), which is not immediately preceded by a Tg. As described earlier, this Tm is well-known to characterize the melting transition observed in retrograded wheat starch gels with excess moisture (which are partially crystalline and contain hydrated B-type starch crystals) and in staled bread and other high-moisture wheat starch-based baked goods.[63,210,219,233]

Results of complementary low-temperature DSC analysis,[17,18,20,21] shown earlier in Figure 40, revealed why no Tg is observed in the sample of freshly gelatinized (thus completely amorphous amylopectin) wheat starch rescanned from room temperature to 130°C (Figure 90 curve c), or immediately before Tm in the sample of recrystallized starch (Figure 90 curve d). Native wheat starch, at 55 w% total sample moisture, shows only a Tm of ice at the instrumental sensitivity used for the thermogram (curve a) in Figure 40. In contrast, a gelatinized sample (curve b), at the same water content and instrumental sensitivity, shows a prominent (and reversible) glass transition of fully plasticized amorphous starch at about −5°C, preceding and superimposed on the ice melt. As mentioned earlier, this Tg is actually Tg′ for gelatinized (but not hydrolyzed) wheat starch in excess moisture, defined by Wg′ ≳ 27 w% water (i.e., ≃ 0.37 g UFW/g starch), as illustrated by the state diagram in Figure 25. For the same instrumental sensitivity settings, Tg′ is not detectable in Figure 40 curve a, because the cooperative, controlling majority of the amorphous regions of partially crystalline native starch prior to gelatinization show a much higher Tg indicative of a much lower local effective moisture content and the absence of contributions from short amylopectin branches that are sequestered in crystalline regions.[20,23]

A critical conclusion of these earlier studies[17-20] was that knowledge of total sample moisture alone cannot reveal the instantaneously operative extent of plasticization of amorphous regions of a starch granule. Amorphous regions of a native granule are only partially plasticized by excess water in a sample at room temperature, so that softening of the glassy matrix must occur (observed at about 50 to 60°C during heating at 10°C/min in the DSC) before microcrystallites can melt. (This situation of partial, and dynamically changing, plasticization at room temperature also explains why slow annealing is possible for the native starch sample shown in curve b of Figure 90.) After gelatinization, the homogeneously amorphous starch is fully and uniformly plasticized (by uniformly distributed water) at 55 w% moisture, and the metastable amorphous matrix exists at room temperature as a mobile, viscoelastic rubber in which diffusion-limited recrystallization, governed by WLF rather than Arrhenius kinetics, can proceed with rates proportional to ΔT ≃ 30°C above Tg. Another insight revealed by these DSC results concerns the dynamic effects on starch caused by the DSC measurement itself.[20] During a DSC heating scan, effective plasticizer (water) content increases dynamically from the initial 6 to 10 w% in a native sample before heating to the final 55 w% at the end of melting, and this kinetically constrained moisture uptake leads to dynamic swelling of starch granules above Tg, which is not reversible on cooling. The same behavior is manifested in volume expansion measurements on starch-water systems performed by ThermoMechanical Analysis (TMA).[19,46] The major contribution to the experimentally observed increase in volume above Tg is a typical polymer swelling process, characteristic of compatible polymer-diluent systems,[109] which is linear with the amount of water taken up. Thermal expansion of amorphous starch is also allowed above Tg, but it represents only

a minor contribution to the observed volume increase, i.e., about 0.1%/K for typical polymers.[107] Thus, the predominant mechanism, swelling, is indirectly related to the role of water as a plasticizer of starch, while the minor mechanism is directly related.

Once it had been established[17-20] that the thermal behavior of native wheat starch at 55 w% total moisture in the temperature range 50 to 100°C represents the superposition of a second-order glass transition followed by a first-order crystalline melting transition, it was shown (Figure 91[19]) that it is possible to accelerate plasticization of amorphous regions by water without melting crystalline regions. In Figure 91, waxy corn starch was used as a model system to study amylopectin in the absence of amylose. Like wheat starch, native waxy corn starch (curve a) exhibits nonequilibrium melting of a partially crystalline glassy polymer, with a requisite glass transition (signified by a baseline shift) preceding multiple crystalline transitions in the temperature range 50 to 100°C, when total sample moisture is 55 w%.

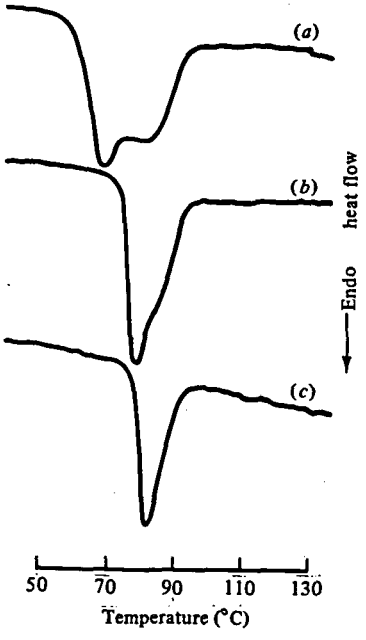

FIGURE 91. DuPont 1090 DSC heat flow curves of waxy maize starch:water mixtures (45:55 by weight): (a) native; (b) native, after 15 min at 70°C; (c) native, after 30 min at 70°C. (From Maurice, T. J., Slade, L., Page, C., and Sirett, R., *Properties of Water in Foods*, Simatos, D. and Multon, J. L., Eds., Martinus Nijhoff, Dordrecht, 1985, 211. With permission.)

When this sample is annealed for 15 min at 70°C (Figure 91 curve b), total excess heat uptake below the baseline is reduced by about 25% and the temperature range of the multiple transitions is shifted upward and becomes narrower, but the glass transition immediately before the crystalline melt is still evidenced by the characteristic baseline shift. A similar result had been seen, in Figure 90 curve b, for wheat starch annealed at 25°C for 55 d, and also previously reported for potato starch annealed at 50°C for 24 h.[396] (Note the apparently exponential dependence on ΔT, dictated by WLF kinetics, of rates for different annealing conditions.) Similar consequences of annealing by heat/moisture treatment have been observed during cooking of whole wheat grains.[232] In contrast, when native waxy corn starch is annealed for 30 min at 70°C (Figure 91 curve c), total excess heat uptake below the baseline is reduced by 50% and represents only the enthalpy of the first-order crystalline melting transition. This conclusion was confirmed by the symmetry of the endotherm and the absence of an obvious baseline shift associated with it. The baseline shift is not observed in the temperature range 40 to 130°C, because the glass transition preceding the crystal melt had been depressed to $Tg' < 0$°C, due to complete plasticization and concomitant relaxation of the amorphous regions by water.[17-19] Parallel analyses of percent crystallinity by X-ray diffraction[19] showed that a sample annealed as in Figure 91c manifests no significant loss in overall crystallinity by the starch in comparison to a control sample, despite the 50% reduction in total excess heat uptake below the baseline in Figure 91c vs. the control sample in Figure 91a. This crucial finding confirmed the conclusion that the portion of the total excess heat uptake below the baseline not representing the true enthalpy of the crystalline melting transition, i.e., the portion associated with the baseline shift shown in Figures 91a and b (but not in 91c), must be due to the glass transition that immediately precedes and is superimposed on the crystalline melt.[17-19]

The amorphous regions of a starch granule represent a continuous phase, and the covalently attached microcrystalline branches of amylopectin plus discrete amylose-lipid crystallites represent a discontinuous phase. For each polymer

class (distinguished by an arbitrarily small range of linear DP), water added outside the granule acts to depress Tg of the continuous amorphous regions, thus permitting sufficient mobility for the metastable crystallites to melt on heating to Tm above Tg.[17,18,20] The effect of changing the amount of added water on the thermal behavior of native rice starch can be seen in Figure 92.[19] At the "as is" 10 w% moisture content, with no added water (curve a), the glass transition of amylopectin occurs above 100°C and multiple crystalline melting transitions occur above 150°C. Similar profiles would be seen at increasing total sample moisture contents up to about 30 w% (i.e., Wg'), with the initial glass transition occurring at decreasing temperatures. At moisture contents higher than about 30 w% (Figure 92 curves b-f), the initial glass transition occurs at about the same temperature, and the subsequent cooperative events occur at lower and narrower temperature ranges as water content is increased.

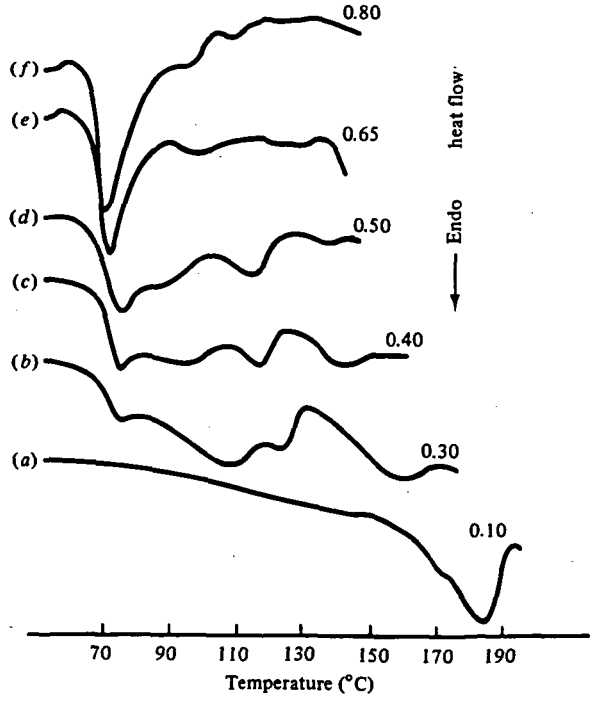

FIGURE 92. DuPont 1090 DSC heat flow curves of native rice starch at various water contents: (a) starch with "as is" moisture of 10 w%; (b through f) starch with moisture added to water weight fractions indicated. (From Maurice, T. J., Slade, L., Page, C., and Sirett, R., *Properties of Water in Foods*, Simatos, D. and Multon, J. L., Eds., Martinus Nijhoff, Dordrecht, 1985, 211. With permission.)

The moisture content that is sufficient to completely plasticize starch after gelatinization is about 27 w% (i.e., Wg').[17,18,158] However, unlike gelatin gels, which can be dried to different moistures so that water is uniformly distributed throughout the amorphous regions,[17,18,24] native starch starts out typically at 6 to 10 w% moisture, and the added water is outside the granule (and so initially non-plasticizing), prior to moisture uptake and swelling during DSC heating.[20]

The results and conclusions from Figure 92 have been confirmed by subsequent DSC results of Biliaderis et al.[46] on several other varietal rice starches. In addition to several composite thermograms similar in appearance to Figure 92, they have presented a graph of Tg vs. starch concentration (w%), for partially crystalline native starch-water mixtures, which starts at about 240°C for the dry sample, and decreases with increasing moisture to 68°C at about 30 w% total moisture ("as is" plus added). Beyond this moisture content (i.e., for further additions of (initially non-plasticizing) water outside the granules), and before gelatinization during DSC heating, the initial Tg appears to remain constant. (Colonna et al.[417] have presented an analogous plot of Tgelat [measured by thermal analysis] vs. water content for B-type potato starch [see Figure 93], which similarly shows Tgelat decreasing with increasing moisture content, from about 260°C at 0% water to about 66°C at about 37.5% water, and then leveling off at higher water contents.) The graph of the effect of water on the dynamically measured value of Tg for partially crystalline native rice starch reported by Biliaderis et al.[46] (and the one of Tgelat vs. water content for potato starch in Figure 93) should not be confused with the Tg curve in a state diagram for a homogeneous starch-water system, i.e., completely amorphous gelatinized starch-water, shown earlier in Figure 25. The latter illustrates the smooth glass curve that connects Tg of dry starch with Tg of amorphous water, and passes through Tg' (−5°C) and Wg' (27 w% water) for gelatinized starch.[17,18]

Zobel[61] has recently remarked that "glass transition is an expression familiar to the polymer chemist but still somewhat foreign to starch chemists" and that "while recognized as a factor in starch characterization, glass transition temperatures have been, and to a degree still are,

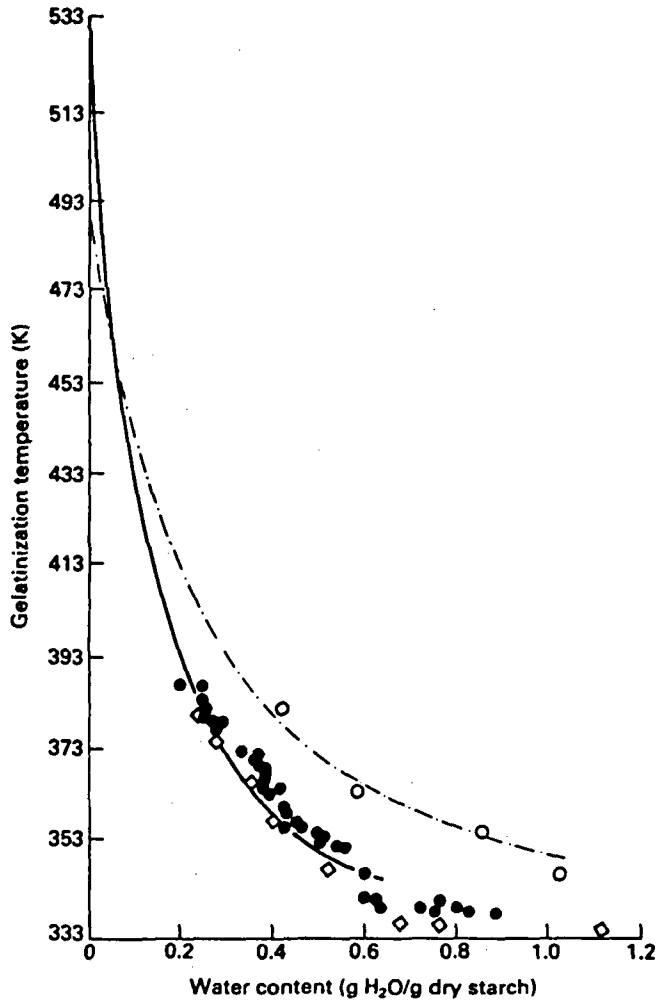

FIGURE 93. Changes in gelatinization temperatures as a function of hydration: —— potato starch (determined by differential thermal analysis (filled circles), DSC [diamonds]): - - - wheat starch (determined by birefringence [open circles]). (From Colonna, P., Buleon, A., and Mercier, C., *Starch: Properties and Potential,* Galliard, T., Ed., John Wiley & Sons, Chichester, 1987, 79. With permission.)

somewhat elusive." While the existence of a glass transition and measurable Tg in partially crystalline native granular starches has only recently become established by DSC studies reported by Slade and co-workers in the past 5 years,[17-23,35,46] and is therefore still in the process of becoming more widely recognized and accepted,[47-49,52,53,60,61,63,65,93,94,223,418] the temperature location of the glass transition associated with gelatinization of native starch has become a point of contention in the recent literature.[20,21,52,53]

Two recent reports[52,53] have explored the validity of the model in which the thermal behavior of native starch at 55 w% total moisture in the temperature range 50 to 100°C represents the superposition of a second-order glass transition followed by a first-order crystalline melting transition. Yost and Hoseney[52] have presented DSC results for gelatinization and annealing by heat/moisture treatment of wheat starch in water at 50 w% total sample moisture content. They have concluded that annealing occurs (in samples previously held for 24 h at room temperature) at

temperatures 3 to 8°C below the gelatinization Tm for wheat starch, but not at lower temperatures. These results do not contradict previous DSC results and conclusions[17-20] about the relative locations of Tg and Tm for gelatinization of starch, especially in light of existing knowledge about annealing of metastable, partially crystalline synthetic polymers.[102,104] As mentioned earlier, annealing occurs at $Tg < Ta < Tm$, typically at $Ta = 0.75\text{-}0.88\ Tm$ (°K), for polymers with Tg/Tm ratios of 0.5 to 0.8. In this metastable rubbery domain defined by WLF theory, annealing is another diffusion-limited, non-equilibrium process for which rate is governed by WLF, rather than Arrhenius, kinetics.[15,21,419] As demonstrated for various native granular starches in excess moisture situations,[17-20,48,52,158,419,420] the time required to achieve a measurable and comparable (in a reasonable and similar experimental time frame) extent of annealing is shortest at Ta just below Tm (greatest ΔT above Tg) and longest at Ta just above Tg (smallest ΔT). The minimum value of the Tg/Tm ratio for wheat starch (at a uniformly distributed excess moisture content $\gtrsim$27 w%) is about 0.80 (i.e., $Tg'/Tm = 268/333K$), and this ratio increases with decreasing moisture content to an anomalously high value >0.9.[21] This anomalous situation corresponds to conditions of the non-equilibrium gelatinization or annealing of native starch upon heating in the presence of water added to 50 w%. Consequently, the temperature range that encompasses the effective locations of Tg, Ta, and Tm for native starch heated with excess added water is quite narrow, a conclusion also suggested by the DSC results of Nakazawa et al.[419] Zeleznak and Hoseney[53] have investigated the Tg of both native and pregelatinized wheat starches as a function of moisture content, and concluded, in seeming conflict with the annealing results previously reported,[52] that their findings "contradicted the suggestion that Tg immediately precedes melting in starch." In both papers,[52,53] Hoseney and coworkers have based their argument, in large part, on the failure to observe a glass transition (in the form of a discontinuous change in heat capacity) in a rescan after gelatinization of native starch in excess added moisture in the DSC. Unfortunately, their DSC measurements were not extended below 0°C, and so the prominent Tg at $Tg' \simeq -5$°C for gelatinized starch, illustrated earlier in Figure 40, was not observed.

In an effort to resolve any questions raised by the conclusions of Yost and Hoseney[52] and Zeleznak and Hoseney,[53] a subsequent DSC study of representative A-type cereal starches[21] has verified and further quantified the temperature location of the effective glass transition that immediately precedes the non-equilibrium melting transition of amylopectin microcrystallites and thereby controls the melting process associated with gelatinization. For that study, native granular wheat and waxy corn starches were heated at 10°C/min in the presence of water added to about 55 w% total moisture to facilitate temporal resolution of the thermal events. This practice is consistent with the general rule of thumb that DSC experiments should be conducted with samples containing about 30 to 70 w% moisture for diagnostic evaluation of ingredient structure-function relationships for food materials.[23] The diagnostic information about potential ingredient functionality can be related to the real-world events that would be retarded by moisture contents below 30 w% or accelerated above 70 w%. Addition of water to less than about 30 w% moisture retards the thermomechanical events of gelatinization and pasting in time and temperature to such an extent that all of the thermal events occur cooperatively over a higher, narrower temperature range, due to excessive plasticization and mobilization by heat.[19,20] Addition of water to more than about 70 w% moisture accelerates all of the thermal events so that they occur cooperatively in a much lower, narrower temperature range, due to excessive plasticization and mobilization by water. Addition of an equal weight of water to starch having "as is" moisture content of 6 to 10 w% eases the preparation of samples for DSC analysis and allows separation in time and temperature of the successive, now non-cooperative, thermal events to provide diagnostic thermal profiles.[23] Such diagnostic profiles are required to isolate and demonstrate the contribution of free volume to heat capacity, observed as the characteristic step change in DSC baseline at Tg.[106] In the absence of such deconvolution of the thermal events, smaller and less reproducible changes in heat capacity are observed, due to the superposition of vibrational

and free volume contributions to heat capacity and endothermic and exothermic contributions to enthalpy for both amorphous and crystalline regions of the sample.[106] An exactly analogous behavior has been observed for the plasticization of synthetic high polymers by their compatible diluents.[109] Up to about 30 w% uniformly distributed diluent, the solute is incompletely plasticized by diluent alone, complete plasticization is achieved by a combination of diluent plus heat, and the microscopic behavior of the sample is dominated by the solute as modulated by the plasticizer in the blend. Between about 30 and 70 w% uniformly distributed plasticizer, complete plasticization can be achieved by diluent alone, and two distinguishable microscopic behaviors of the sample can be observed: solute modulated by plasticizing diluent and diluent modulated by solute. Above about 70 w% diluent, ambient temperature is typically far above the sample Tg, and a single microscopic behavior of the sample is again observed, that of the diluent modulated by the solute, exemplified in the extreme by the behavior of dilute solutions.[109] Of course, the behavior of solute modulated by plasticizer can be observed at diluent concentrations above 70 w%, but only at the macroscopic level, in the form of entanglement and partially crystalline networks and gels.[23] It should be noted that this description and the particular w% compositions of solute and diluent apply to the typical case of high MW food materials and synthetic polymers, for which Wg′ (or the organic equivalent) is about 30 w%.[25] For those materials with values of Wg′ very different from about 30 w%, appropriate ranges of diluent would be used to effect the same modulation of the Tg and mechanical behavior of the solute-diluent blend.[23]

The experimental DSC protocol used to study the A-type cereal starches[21] represents a novel and critically discriminative extension of procedures previously recommended[48] and used[52,60] to analyze starch gelatinization. Definitive DSC experiments, involving partial initial heating scans to intermediate temperatures in the range from 30 to 130°C, followed by quench-cooling and immediate complete rescans, have revealed the operational location of Tg for wheat starch (above 54°C and completed by 63°C) and waxy corn starch (above 63°C and completed by 71.5°C). Corresponding effective "end of melting" temperatures (Tm)[60,100,105,161,419] for the non-equilibrium melting transition of annealed amylopectin microcrystallites in normal wheat (about 92°C) and waxy corn (about 95°C) starches have also been identified. Results of this study have made it possible to achieve a deconvolution of the contributions of amylopectin and amylose to the non-equilibrium melting behavior of native granular starches,[21] through DSC analyses of normal wheat and waxy corn starches. These results have also been used to demonstrate the kinetically controlled relationship (based on the dynamics of plasticization by water) between the operative Ta, at which a non-equilibrium process of annealing can occur in native granular starches subjected to various heat/moisture/time treatments, and the effective Tg and Tm which are relevant to gelatinization and which bracket Ta,[48,102,104] thereby confirming that the location of Ta 3 to 8°C below Tm[52] is not inconsistent with a Tg immediately preceding melting.

The study has demonstrated that the effective Tg associated with gelatinization of native granular starch, most readily resolved as described above by heating in excess added moisture at nearly equal weights of starch and water, depends on the instantaneously operative conditions of moisture content, temperature, and time.[21] This finding has helped to eliminate any potential confusion over the absence of a single, "absolute" value of Tg for starch. Location of the effective Tg of gelatinization has illustrated the established fact[107,120,172,250] that the operational designation of a particular Tg value for any partially or completely amorphous material is only relevant to the instantaneously operative conditions of its measurement. This point has been depicted conceptually by the schematic state diagram for the amorphous regions of native granular cereal starch in Figure 94,[26] which has been used in the context of a dynamics map to describe the process of gelatinization. Figure 94 traces the route followed during a DSC experiment, in terms of the following path of temperature-moisture content loci: (1) initial heating of native starch (N), at "as is" moisture and blended with excess water, from room temperature, through the instantaneously operative Tg, into the rubbery region (whereupon the rates of moisture uptake and

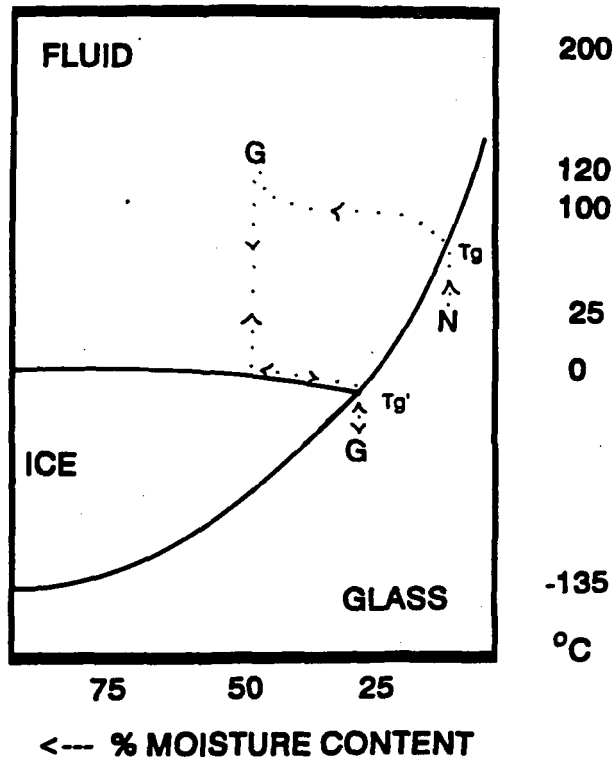

FIGURE 94. Schematic state diagram for the amorphous regions of granular starch, on which is traced the temperature-moisture content path followed during (1) initial heating, to T > the instantaneously operative Tg (and subsequent instantaneously operative Tm), to gelatinize (G) native (N) starch, (2) subsequent cooling, to T < the effective Tg (i.e., Tg′) of gelatinized starch, and (3) reheating to T > Tg′. (From Levine, H. and Slade, L., *Dough Rheology and Baked Product Texture: Theory and Practice,* Faridi, H. and Faubion, J. M., Eds., Van Nostrand Reinhold/AVI, New York, 1989, 157. With permission.)

swelling increase dramatically with increasing temperature[19,20,48]), through the instantaneously operative Tm (not shown, but located along the dotted line between Tg and 100°C), to G, representing the gelatinized sample with final uniform moisture content at the end of the first heating scan (130°C) (see Figure 90a); (2) cooling, to T < the effective Tg of the gelatinized sample (which has become Tg′), which is accompanied by freezing and freeze-concentration to W = Wg′; and (3) reheating, from T < Tg′, through Tg′ (whereupon ice melting and starch dilution begin), back up to G at the end of the second heating scan (see Figures 40b and 90c). The concept implicit in Figure 94 is that the glass transition represents a rate-limiting stage of a mechanical relaxation process, for which the spectrum of relaxation rates depends on the instantaneous magnitude of the free volume and/or local viscosity, which in turn depends on the relative values of experimental moisture content compared to the moisture content (Wg) of the operative glass, experimental temperature compared to the instantaneous Tg, and experimental time frame compared to the instantaneous relaxation rate.[30] Such a relaxation process, described by WLF theory, underlies various functional aspects of starch in food systems, such as gelatinization, crystallite melting, annealing, and recrystallization. The academic distinction between the kinetic control of gelatinization with this operational Tg as the reference temperature vs. the

energetic control through Tm might be dismissed as a semantic issue were it not for its overriding technological importance.[23] Control through Tm would dictate that the gelatinization temperature and mechanical behavior of a starch system during the events of gelatinization depend solely on the identity of the starch crystalline polymorph, without regard to the previous history of the sample. Practical experience related to aging of cereal grains prior to industrial processing, variations in the wet-milling process to isolate starches, and other heat/moisture treatments clearly confirm the role of sample history and the kinetic control of gelatinization through the path-determined operational location of the starch Tg.[22,23]

Conceptual descriptions of the kinetically controlled relaxation processes of annealing in native granular cereal starch and recrystallization in gelatinized cereal starch, analogous to the description of gelatinization according to the dynamics map in Figure 94, have been illustrated by the schematic state diagrams in Figures 95 and 96, respectively.[23] These in turn have been based on the idealized state diagram shown earlier in Figure 83 for a plasticizer (component 3)-solute (component 2) system in which both components are crystallizable, as exemplified by the starch-water system. Figure 95 traces the route followed during a DSC experiment, in terms of the following path of temperature-moisture content loci: initial heating of native granular A-type cereal starch (N), at "as is" moisture and blended with excess water, from room temperature, through the instantaneously operative Tg, into the rubbery region, through the instantaneously operative Tm for A-type microcrystalline regions (<100°C), to G, representing the gelatinized sample with final uniform moisture content at the end of the heating scan (130°C). Annealing in such a metastable, partially crystalline polymer system, subjected to such a heat/moisture treatment, can occur within the experimental time frame, during heating along the portion of the dotted path within the temperature range between the instantaneously operative Tg and Tm. If the initial DSC heating scan had been stopped somewhere between the effective Tg and Tm, or if the original starch-water mixture had been subjected to a heat/moisture/time treatment within the "crystal 2" domain in Figure 83 (as described earlier with respect to Figures 90b and 91b and c), the consequences of annealing would be manifested during subsequent DSC analysis. Crystal growth and/or perfection would be evidenced by a narrower melting endotherm (indicative of a more cooperative transition) of higher peak Tm and possibly higher enthalpy.[23]

The schematic state diagram in Figure 96 illustrates the process of recrystallization in gelatinized cereal starch. Figure 96 traces the route followed during a DSC experiment, in terms of the following path of temperature-moisture content loci: (1) initial heating, to T > the instantaneously operative Tg (and subsequent instantaneously operative Tm, not shown), to gelatinize (G) native (N) starch (as described in Figure 94 and illustrated by Figure 90a), (2) subsequent cooling to room temperature (i.e., to T > the effective Tg (i.e., Tg′) of gelatinized starch), in contrast to the cooling path of step 2 in Figure 94, (3) storage at room temperature to allow gelation and recrystallization of B-type microcrystalline regions, and (4) reheating from room temperature to T > the instantaneously operative Tm of B-type crystalline starch at >27 w% moisture, to melt the retrograded B-type starch gel (see Figure 90d).

The composite diagram of DSC heat flow curves for native wheat starch, shown in Figure 97,[21] has demonstrated conclusively that initial heating to at least 92°C is required (for a heating rate of 10°C/min, to a final sample moisture content of 50 w%) to complete the non-equilibrium melting process associated with gelatinization and pasting of this native granular starch. Partial initial scanning to temperatures ≥72°C but <92°C results in only partial melting, as evidenced in the rescans by a remnant of the melting profile, compared to the thermal profile of the complete melting process shown at the top of Figure 97. This remnant decreases in area with increasing maximum temperature (in the 72 to 92°C range) of the partial initial scan, but only disappears completely (yielding a featureless thermogram, as evidenced by a flat baseline, from 30 to 100°C) after initial heating to ≥92°C. From these preliminary DSC measurements, it was concluded that 92°C represents the effective Tm at the "*end* of melting" for native wheat starch heated at 10°C/min with 50 w% total moisture. The tem-

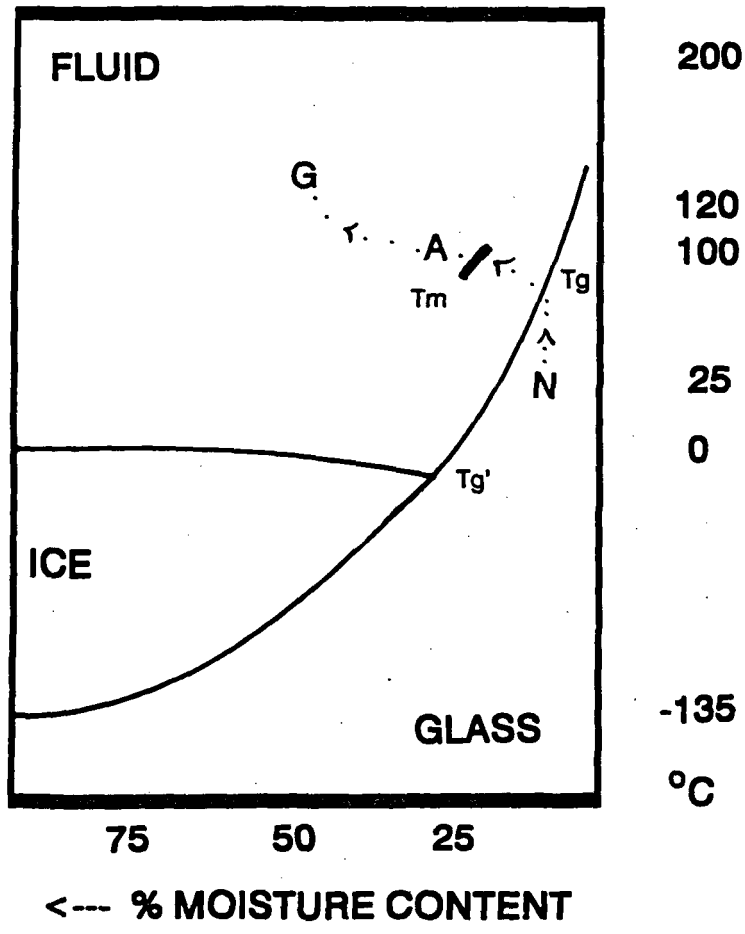

FIGURE 95. Schematic state diagram for the amorphous and A-type crystalline regions of granular cereal starch, on which is traced the temperature-moisture content path followed during heating, to T > the instantaneously operative Tg and subsequent instantaneously operative Tm, to gelatinize (G) native (N) starch. Annealing during initial heating can occur along the portion of the dotted path between the instantaneously operative Tg and Tm. (Reproduced with permission from Reference 23.)

perature at which melting begins was deduced from the DSC results shown in Figure 98,[21] which also reveal the temperature location of the effective glass transition that must precede the onset of this non-equilibrium melting process for wheat starch with water added to 55 w% total moisture. On the time scale of the DSC measurement, these two temperatures are essentially identical. Implicit in the results shown in Figure 97 is the fact that, at temperatures within the range from the effective Tg to the end-of-melting Tm, the extent of gelatinization is temperature-dependent. As mentioned earlier, this condition prohibits the application of Arrhenius kinetics to model the gelatinization process[65,222,224] and emphasizes the applicability of WLF kinetics.[17,18,20,21,30]

The composite diagram of DSC heat flow curves for native wheat starch with 55 w% water in Figure 98 shows the complete non-equilibrium melting process as an initial scan in curve A; the partial initial scans, with their end-of-scan temperatures indicated, as solid lines in parts B through K; and the complete rescans as dashed lines in parts B through L. For parts B through L, the TADS computer on the Perkin-Elmer DSC-2C was instructed to display simultaneously the initial and rescans and allowed to confirm that the same instrumental baseline response of heat

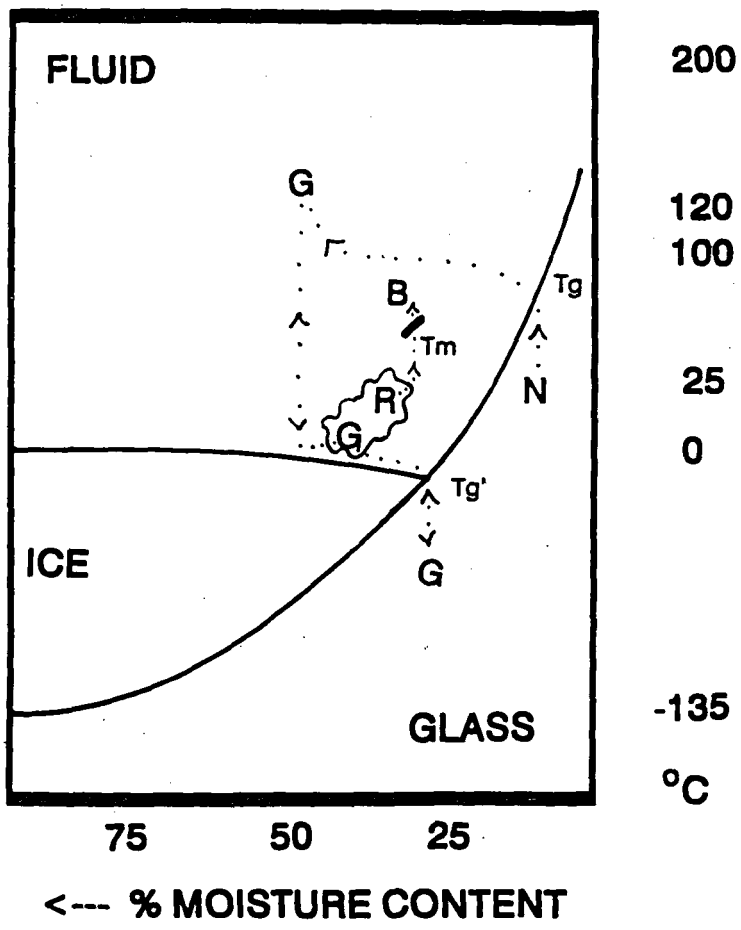

FIGURE 96. Schematic state diagram for the amorphous regions of granular starch, on which is traced the temperature-moisture content path followed during (1) initial heating, to T > the instantaneously operative Tg (and subsequent instantaneously operative Tm, not shown), to gelatinize (G) native (N) starch, (2) subsequent cooling to room temperature (i.e., to T > the effective Tg (i.e., Tg') of gelatinized starch), in contrast to the cooling path of step 2 in Figure 94, (3) storage at room temperature to allow gelation and recrystallization of B-type microcrystalline regions, and (4) reheating from room temperature to T > the instantaneously operative Tm of B-type crystalline starch at >27 w% moisture, to melt retrograded B-type starch gel. (Reproduced with permission from Reference 23.)

uptake (in mcal/s) at the instrumentally "equilibrated" starting temperature of 20°C occurred in both scans. This data processing step evidences successful experimental execution by the near-perfect superposition of the 20 to 50°C baseline portions of the initial scans and corresponding rescan segments in parts B, C, and D, and the 90 to 100°C baseline portions of the scans and rescans in parts J, K, and L. This step is critical to the identification of the effective Tg that governs gelatinization of commercially isolated native cereal starch in excess moisture during heating from room temperature to 100°C. The results in Figure 98 have been used to deduce the location of the effective Tg as the temperature by which there had occurred, in the initial scan, a characteristic and diagnostic baseline shift in heat capacity, during the time scale of the experimental measurement, for heating at 10°C/min. As an example, within the temperature range 30

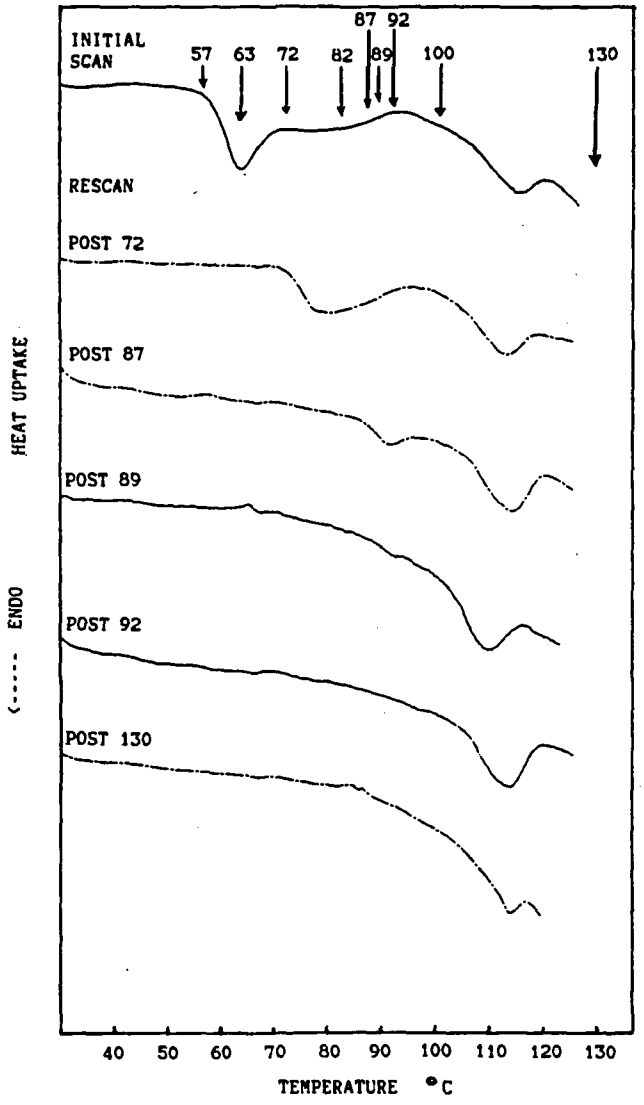

FIGURE 97. Perkin-Elmer DSC-2C heat flow curves of wheat starch:water mixtures (50:50 by weight): top — initial scan at 10°C/min for native starch; others — rescans at 10°C/min, immediately following partial initial scanning, at 10°C/min, from 20°C to maximum temperatures indicated and then immediate cooling, at nominal instrument rate of 320°C/min, to 20°C. (From Slade, L. and Levine, H., *Carbohydr. Polym.*, 8, 183, 1988. With permission.)

to 100°C in part L, comparison of the 30 to 60°C baseline portions of the initial scan and rescan demonstrates such a diagnostic difference in heat capacity, thereby documenting that a glass transition had occurred during the initial scan. Because of the previous occurrence of the change in heat capacity, the featureless (at $T < 100°C$) rescan is superimposed on the initial scan only after the latter returns to baseline after the end of the endothermic melting process at $Tm \simeq 92°C$. As expected, this effective end-of-melting Tm is the same as shown in Figure 97, since both 50 and 55 w% water represent conditions of large excess moisture for gelatinized starch. This effective end-of-melting Tm is also suggested by Figure 98I, for which the initial thermal profile,

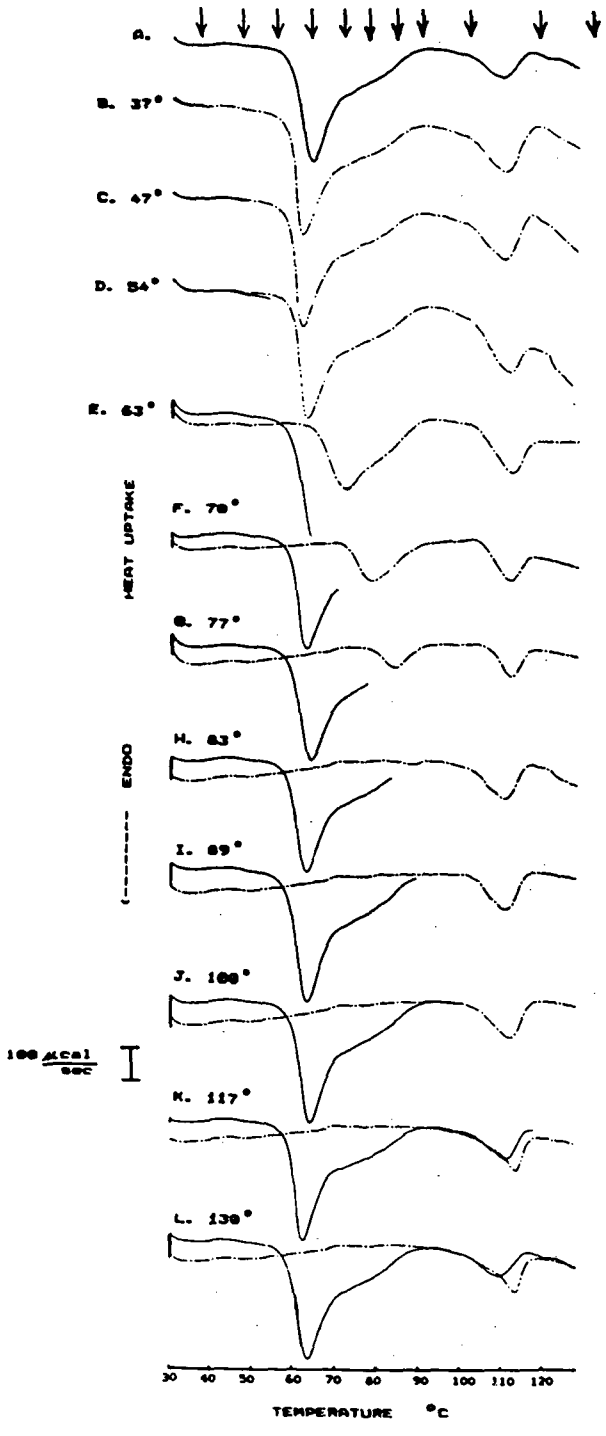

FIGURE 98. Perkin-Elmer DSC-2C heat flow curves of wheat starch:water mixtures (45:55 by weight): (A) initial scan at 10°C/min for native starch; (B through L) solid lines = partial initial scans for native starch, at 10°C/min, from 20°C to maximum temperatures indicated, dashed lines = rescans at 10°C/min, immediately following partial initial scanning and then immediate cooling, at nominal 320°C/min, to 20°C. (From Slade, L. and Levine, H., *Carbohydr. Polym.*, 8, 183, 1988. With permission.)

upon heating to 89°C, stops just short of a return to baseline. The reason for the apparent absence of a Tg in the rescan of part L was explained earlier by reference to Figure 40. After complete gelatinization upon heating to 130°C and 55 w% final moisture content, $Tg = Tg' = -5°C$.

The effective Tg preceding and controlling the non-equilibrium melting process associated with gelatinization is identified as that minimum, narrow temperature span in the initial scan, below which the change in heat capacity had not yet occurred (as reflected by superimposed baselines for scan and rescan), but at and above which it already had (as reflected by a displacement of baselines, at $T < Tg$, between scan and rescan). It can be seen in Figure 98 parts B, C, and D that the scans and corresponding rescan segments are essentially identical up to 54°C, and the heat capacity change had not yet occurred before the rescans, because initial heating to 37, 47, or 54°C had not yet reached the uniform requirements of time, temperature, and moisture for cooperative relaxation at Tg. In contrast, in parts E through K, the scan and rescan baselines, at $T < Tg$, are displaced, because initial heating to $T \geq 63°C$ had allowed the amorphous regions of the native granules to undergo a glass transition. By the convention described above, the effective "end of softening" Tg preceding crystallite melting is thus identified as >54 and ≤63°C, as illustrated in Figure 98E. This upper limit for Tg corresponds to the temperature at the "peak minimum" in the characteristic DSC thermal profile for wheat starch gelatinization shown in Figure 98A. As mentioned earlier, the narrow 55 to 63°C temperature span of the effective Tg occurs along the leading edge of the "gelatinization endotherm."[17,18] Figure 98E represents a temporal and thermal deconvolution of the melting transition of microcrystalline regions from the preceding glass transition of amorphous regions of water-plasticized starch. Nakazawa et al.[419] have alluded to a similar differentiation between the mobile amorphous regions and immobile crystalline regions with respect to the time frame of their DSC results for normal rice starches analyzed at 50 w% total moisture, but they have implausibly suggested that the elevated Tm observed in annealed starches is due to increased stability in the amorphous regions. Rather, for this case of starch

in excess moisture, annealing allows a relaxation in the amorphous regions from a more to a less (kinetically meta-) stable state, while the crystalline regions perfect from a less (meta-) stable state to a more stable state with higher Tm.[106] The rescan of Figure 98 part E exhibits the following features, compared to the typical appearance of curve A below 100°C; a more symmetrical melting endotherm with essentially no baseline shift, an onset temperature (essentially coincident with the initial effective Tg) of 63°C, a peak minimum of 70°C, and an effective end-of-melting Tm of 92°C. The essentially undetectable baseline shift in heat capacity associated with the crystalline melting transition at the instrumental settings that allow ready demonstration of the large change in heat capacity associated with the glass transition is expected, as explained by Wunderlich (Reference 106, Figures 13 and 16), due to the free volume contribution to heat capacity. The appearance of the thermal profile in the region of the glass transition is analogous in shape to an endothermic hysteresis peak, a common characteristic manifested by partially crystalline polymers.[106] An endothermic hysteresis peak is indicative of some jump, during the sample history, in temperature, plasticizer content, or pressure at a rate exceeding the relaxation rate of the appropriate process and is observed during subsequent DSC analysis as a "stress relief" via "enthalpic relaxation."[106] The apparent enthalpic relaxation of starch,[53] with a peak minimum at 63°C, is superimposed on the universal step-change in heat capacity. One can further imagine summing the glass and melting transitions, superimposed on one another in the temperature range 50 to 100°C, by adding together the scan and rescan in Figure 98 part E, thus reconstituting, with no discernible loss of total heat uptake below the baseline, the characteristic DSC thermal profile (curve A) for wheat starch gelatinization in excess water.

Figure 99[21] contains the analogous composite diagram of DSC heat flow curves for waxy corn starch with 55 w% total moisture. As in Figure 98, Figure 99 shows the complete non-equilibrium melting process as an initial scan in curve A; the partial initial scans, with their maximum temperatures indicated, as solid lines in parts B through G; and the complete rescans as dashed lines in parts B through H. In contrast to Figure 98, amylose-lipid melting transitions above 100°C are absent for this essentially amylose-free starch. Based on the same analysis and logic described for Figure 98, and equally successful superpo-

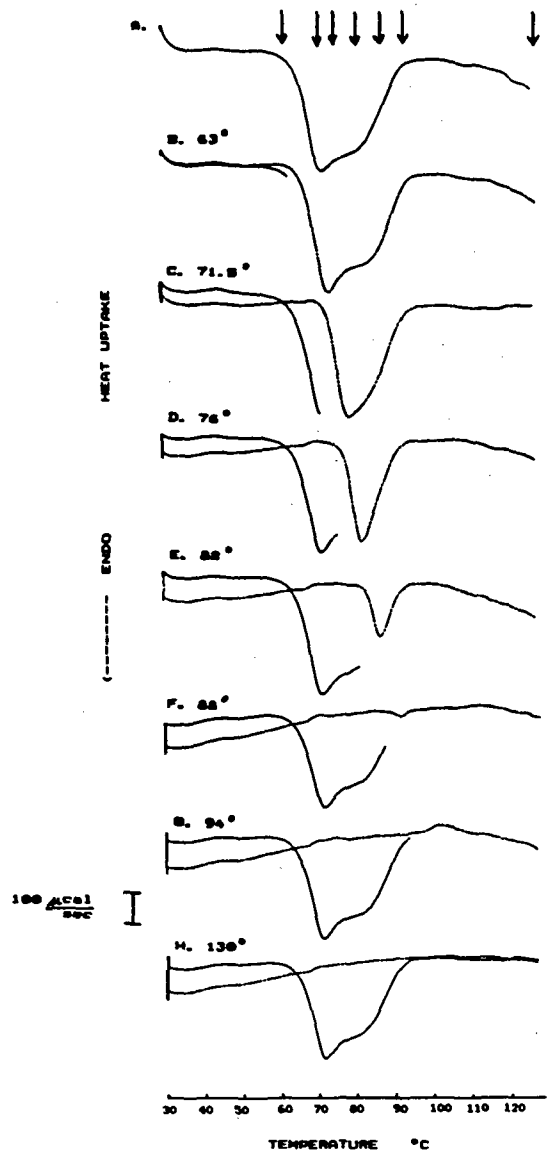

FIGURE 99. Perkin-Elmer DSC-2C heat flow curves of waxy corn starch:water mixtures (45:55 by weight): (A) initial scan at 10°C/min for native starch; (B through H) solid lines = partial initial scans for native starch, at 10°C/min, from 20°C to maximum temperatures indicated, dashed lines = rescans at 10°C/min, immediately following partial initial scanning and then immediate cooling, at nominal 320°C/min, to 20°C. (From Slade, L. and Levine, H., *Carbohydr. Polym.*, 8, 183, 1988. With permission.)

sition of the instrumental baseline response of initial and rescans (e.g., Figure 99 part B in the temperature range from 30 to 60°C and H from 95 to 130°C), the following results have been obtained from Figure 99. Parts C through H manifest displaced baselines, in the temperature range 30 to $\lesssim$ 65°C, for the initial and rescans, while part B shows superimposed baselines in the same temperature range. Accordingly, the effective end-of-softening Tg preceding crystallite melting is identified as >63 and ≤71.5°C from Figure 99C. As for wheat starch in Figure 98, this upper limit for Tg corresponds to the temperature at the "peak minimum" in the typical DSC thermogram for waxy corn starch gelatinization shown in Figure 99A. The narrow temperature span of this Tg occurs within the range 64 to 71.5°C, along the leading edge of the endotherm. Part H reveals an effective end-of-melting Tm ≃ 95°C, where the initial scan returns to baseline after gelatinization. This is corroborated in part G, where the thermal profile, upon initial heating to 94°C, stops just short of a return to baseline. As in Figure 98E, Figure 99C illustrates a separation of the melting transition of A-type microcrystallites from the glass transition that must precede it. However, in this case, the melting transition can be unambiguously assigned to the microcrystalline, clustered amylopectin branches, and the glass transition to the contiguous amorphous regions of water-plasticized amylopectin. The rescan of Figure 99C shows a nearly symmetrical melting endotherm with the following features: onset temperature of 71.5°C, coinciding with Tg; peak minimum of about 78°C; and end-of-melting Tm at 95°C. Waxy corn starch in Figure 99C, like normal wheat starch in Figure 98E, shows an undetectably small baseline shift from its leading to trailing end for the isolated melting transition associated with gelatinization in excess moisture. Thus, these DSC results demonstrate conclusively that the change in heat capacity, illustrated in Figures 98 and 99, is associated entirely with the glass transition that immediately precedes the crystalline melting endotherm. In contrast, Yost and Hoseney[52] have also observed such a change in heat capacity (between an initial partial heating scan, to a single intermediate temperature, and a complete rescan) for native wheat starch in 50 w% water, but because they did not observe a Tg (at the subzero Tg′) in the DSC rescan, Zeleznak and Hoseney[53] have suggested instead that it "merely indicates that the heat capacity of a starch-water suspension is lower than that of gelatinized starch." Figures 98E and 99C demonstrate the actual explanation for their observation.

Russell[60] has published DSC thermograms (showing initial complete heating scans and superimposed immediate complete rescans) for native wheat and waxy corn starches at 57 w% total moisture content that are very similar in appearance to Figure 98 (curves A and L) and Figure 99 (curves A and H), respectively. He also observed and recognized the characteristic change in heat capacity (ΔCp) as signifying a glass transition immediately preceding crystallite melting. However, because of the "very small ΔCp (about 0.1 J/°C g sample)" associated with this baseline shift, Russell's[60] concluding remarks stopped short of a wholehearted endorsement ("it is likely that a glass transition is associated with starch gelatinization") of the concept[17-21] by subsequently referring to "the putative glass transition". With respect to the magnitude of ΔCp for the glass transition exhibited in Figures 98 and 99, it has been demonstrated,[23] as mentioned earlier, that the magnitude of the baseline shift for the glass transition of amylopectin is equivalent in magnitude to the ΔCp that would be observed for a comparable weight of completely amorphous pure polystyrene at its Tg.

With the aim of deconvoluting the contributions of amylopectin and amylose to the nonequilibrium melting behavior of native granular wheat and waxy corn starches in 55 w% moisture, the effective values of Tg and end-of-melting Tm have been compared: for wheat starch, Tg ≃ 63°C and Tm ≃ 92°C, while for waxy corn starch, Tg ≃ 71.5°C and Tm ≃ 95°C. These effective end-of-melting Tm values, rather than the corresponding onset or peak values, have been chosen for comparison,[21] because they would represent melting of the largest and/or most perfected microcrystals,[100,105] and so would be most relevant to the comparison of Tg/Tm ratios.[60,161] For both starches, the Tm values are similar. In contrast, the effective Tg for wheat starch is significantly lower than the value for waxy corn starch. The values of the ratio of effective Tg/

end-of-melting Tm, relevant to gelatinization of these native granular starches in 55 w% water by DSC heating at 10°C/min, are 0.92 for wheat and 0.94 for waxy corn. For water-compatible polymers other than starch, such anomalously high Tg/Tm ratios >0.9 have been attributed to the influence of metastable supramolecular structure with non-uniform moisture distribution.[15,383]

The effective values of Tg identified as described earlier, which are associated with first-stage swelling of native granular starches heated in 55 w% water, do *not* represent the Tg of amorphous regions of native granules at about 10 w% total moisture. Recent evidence has suggested that the value for that operative Tg is >100°C for several different normal and waxy cereal grain starches.[19,46,53] Nor do they represent the Tg of completely amorphous gelatinized starch at 55 w% moisture, which is actually Tg′ of −5°C. The values of Tg reported are those manifested by the amorphous regions of native granules *during* the dynamic process of plasticization by heat (increasing at 10°C/min in the temperature range from 20 to 130°C) and moisture uptake (increasing in the range from 10 to 55 w%) and represent particular, intermediate values, within a continuum, which depend on the instantaneously operative temperature and content of plasticizing water.[21]

As discussed earlier, when the experimental history with respect to heating rate, temperature range, and total sample moisture content is the same, the thermal profiles of amylose-containing normal wheat starch in Figure 98 and essentially amylose-free waxy corn starch in Figure 99 do not differ qualitatively below 100°C. The major qualitative difference is the presence of a melting transition above 100°C for crystalline lipid-amylose complex in the initial scans of normal wheat starch (also seen in immediate rescans as a result of recrystallization from the self-seeded melt), and the absence of this transition in the thermal profiles for waxy corn starch. The qualitative similarity of the thermal behavior of normal and waxy starches below 100°C indicates that the thermal profiles represent non-equilibrium melting of microcrystals composed of hydrated clusters of amylopectin branches in both cases, with no significant contributions from amylose.[21] Thus, the quantitative differences between the values of the operative end-of-softening Tg and end-of-melting Tm for normal wheat vs. waxy corn starch should be explained on the basis of structure-property differences in their amylopectin components. Sample history (path dependence, such as jumps in moisture, temperature, or pressure) is often more important than inherent equilibrium thermodynamic properties, and as important as chemical structure for the explication of structure-property differences in non-equilibrium systems.[26,30] Moreover, the starch-water system is neither spatially nor molecularly homogeneous, and the greater anomaly in Tg/Tm ratio for waxy corn starch compared to normal wheat starch will also depend highly on contributions of sample history as well as the structural biochemistry of the starch.[21]

For a similar initial operative level of water plasticization in both the normal wheat and waxy corn starch systems, the quantitative differences seen for Tg, non-equilibrium Tm, and Tg/Tm ratio associated with gelatinization and pasting, can be explained by the previously mentioned fact that, for homologous amorphous polymers, Tg increases with increasing average MW.[21] Significantly lower average MW of the amorphous regions of the starch granule would allow a greater rate of water uptake and greater values for the instantaneous extent of water plasticization at each time point in the DSC experiment. The underlying basis for the difference in operative average MW of the amorphous regions of the native amylopectins was described earlier. Disproportionation of more mobile branches with lower linear DP to the microcrystalline domains leads to higher average MW in the residual amorphous regions, and, consequently, to higher effective values of Tg and kinetically constrained Tm.[20] For this reason, the relative extents of crystallinity, ranging from 15 to 45%, of native starches from various sources and with both A- and B-type diffraction patterns, are directly related to their gelatinization temperatures.[160,413,421] The "high amylose" starches that result from the amylose-extender mutation, and which give misleading blue value determinations of 60% amylose content,[422] are an apparent exception to this rule of thumb. But even in the case of this so-called high-amylose starch, it is the anomalous amylopectin, with its long, unclustered, non-crystalline branches, that

produces the dramatically elevated values of Tg and, indirectly, of Tm, in spite of the inherently low Tm of (isolated) B-type crystals.[21] (B-type crystals, isolated to remove kinetic constraints on melting due to amorphous surroundings, would melt at a lower temperature than isolated A-type crystals.[21]) Like the silo-aging process for rice and high-humidity drying process for potato,[421] the wet-milling process for corn provides an opportunity for annealing of starch[420] and concomitant elevation in extent of crystallinity, average MW of residual disproportionated amorphous regions of amylopectin, and gelatinization Tg.[21]

The study of the gelatinization process by Slade and Levine[21] has dealt exclusively with A-type cereal grain starches rather than B-type tuber and root starches, such as from potato. The same is true of earlier studies: (1) by Slade and coworkers,[17-20,46] (2) of Tg and annealing by Yost and Hoseney[52] and Zeleznak and Hoseney,[53] and (3) of annealing by Krueger et al.[420] and Nakazawa et al.[419] In addition to possible differences in extent of crystallinity due to process variations,[421] B-type native granular starches often have higher "as is" moisture contents in both the amorphous and crystalline regions than A-type starches (i.e., overall, but likewise heterogeneously distributed, moisture contents of about 18 to 20 w% for B-type vs. about 6 to 10 w% for A-type).[153,400] Thus, the initial instantaneously operative extent of plasticization of the continuous amorphous matrix, which subsequently governs the non-equilibrium melting of the disperse microcrystalline regions, can be significantly different for B- vs. A-type starches[20] and can contribute to the observed lower gelatinization temperature of potato starch.[421] However, the generic description of the gelatinization process for cereal starches[17,18] is still valid for potato starch. Less extensive drying subsequent to starch biosynthesis results in greater preexisting moisture content in the amorphous regions of commercial potato starch, greater free volume, and depressed effective Tg, and in the crystalline regions, depressed effective end-of-melting Tm.[23] The functional attributes and physical properties, including extent of crystallinity and X-ray diffraction pattern, of potato starch can be altered by deliberate drying[226,421] or heat/moisture treatment[158,421,423] to resemble those of cereal starches. As a consequence of preexisting plasticization by water, depressed initial Tg, greater initial mobility, and lower end-of-melting Tm, the entire heating profile of the gelatinization of native potato starch is sharper and narrower than for cereal-like treated potato starch at the same total moisture content of the sample (moisture content of starch plus added water) and is centered at a lower temperature.[21]

It cannot be overemphasized that the glass transition in starch, as in any other amorphous or partially crystalline material, represents a rate-limiting stage of a relaxation process,[107] for which the spectrum of relaxation rates depends on the instantaneous magnitude of the free volume and/or local viscosity, which in turn depends on the relative values of experimental moisture compared to Wg of the operative glass, experimental temperature compared to instantaneous Tg, and experimental time frame compared to the instantaneous relaxation time.[21] Thus, when DSC heating rates approach the operative relaxation rates for a measured process, a lower heating rate would result in observation of a lower Tg value. Angell[172] has described the heating-rate dependence of thermograms used to define Tg as "the most familiar feature of the glass transition." Theoretically, heating at 1°C rather than 10°C/min would result in a Tg lower by about 3°C, as calculated from the WLF equation for well-behaved polymers with Tg/Tm ratios near 0.67.[30] Tg differences of 3 to 5°C per order of magnitude are expected over broader ranges of experimental rates (or frequencies) for such well-behaved polymers, since the relaxation spectrum changes gradually from WLF to Arrhenius kinetics over a temperature interval of about 100°C above Tg.[30] Experimentally, this expectation has been confirmed in the case of polystyrene, for which the value of Tg is lower by 15°C when the heating rate is decreased from 1°C/s to 1°C/h, a factor of 3600.[106] DSC experiments with slow heating rates of less than 0.5°C/min, for very dilute aqueous potato starch suspensions of about 2% solids, have allowed a very small scale micro-reversibility, which has been misinterpreted as the ability to achieve and maintain equilibrium throughout the gelatinization process.[424] Loss of temporal resolution of the thermal events due to the greatly excess moisture content accounted for part of the

apparent micro-reversibility.[21] Actually, isothermal treatment of aqueous rice starch slurries with excess moisture (50% solids), for more than 100 h at various temperatures between 40 to 85°C (equivalent to infinitely slow heating rates), is not sufficient to approach an equilibrium state,[419] as expected, since the melting of partially crystalline systems is *never* an equilibrium process.[106]

The dynamic nature of the glass transition is also reflected in the non-equilibrium annealing process for native starches in the presence of moisture which is insufficient for massive second-stage swelling. For example, recent results for annealing (to measurable, but not necessarily equal, extents, for different granular starches) at different temperatures and times have included the following: (1) waxy corn at 55 w% moisture, 70°C for 10 min or 65°C for 30 min;[19] (2) wheat at 50 w% moisture, 72°C for 30 min or room temperature for 24 h;[52] (3) dent corn in excess added water, 60°C for 15 min, 55°C for 2 h, or 50°C for 48 h;[420] (4) normal and waxy rices at 50 w% moisture, at from 85°C for 5 min to 40°C for 140 h;[419] and (5) wheat at 55 w% moisture, 25°C for 55 d.[17,18] Comparison of these results demonstrates a mobility transformation with respect to time, temperature, and effectively plasticizing moisture content and has led to the conclusion that significant annealing at lower temperatures for longer times is controlled by a lower operative Tg (resulting from a longer experimental time frame) than the Tg that precedes crystallite melting by heat/moisture treatment in the DSC.[21] In other words, the operative Tg relevant to annealing at $Tg < Ta < Tm$ decreases with increasing holding time in excess added moisture at lower temperatures, due to the effect of dynamic plasticization. This situation can be visualized in the dynamics map in Figure 95. As the extent of plasticization increases (i.e., as Wg increases toward Wg′), the effective Tg decreases toward Tg′, and so the temperature range for annealing between the operative Tg and Tm broadens. Under conditions where the operative Tg has clearly fallen to Tg′ at −5°C (and Wg has increased to Wg′), significant annealing has also been observed in retrograded starch gels and baked bread aged at storage temperatures well above room temperature, and thus much closer to Tm than Tg.[95,425] The unifying explanation lies in the fact that the progressively resultant events of plasticization, mechanical relaxation above the glass transition, and functional manifestation (including starch gelatinization, crystallite melting, annealing, and recrystallization) are all dynamic, non-equilibrium processes, the kinetics of which are governed by WLF theory for glass-forming systems.[21]

2. Effect of Sugars on Starch Gelatinization

The description of the effect of water as a plasticizer on native starch, from the perspective of starch as a partially crystalline glassy polymer system, has been extended to the next level of complexity, i.e., three-component model systems of native starch, water, plus added sugars.[17,18,20] This extension is based on a recognition of gelatinization of granular starch in aqueous media as (1) a diffusion-limited, mechanical relaxation process with non-Arrhenius kinetics that depend on the mobility of the added plasticizer;[21,30] and (2) a non-equilibrium melting process (as a consequence of heat/moisture treatment), which becomes cooperative and occurs at a significant rate at a characteristic gelatinization temperature corresponding to the instantaneous Tg (i.e., Tgelat = Tg) of the water-plasticized amorphous regions of amylopectin.[21] Gelatinization in concentrated aqueous solutions of common small sugars begins at a higher Tgelat than in water alone; a retardation effect that has been suggested to result from "antiplasticization" (as defined for synthetic polymers[109]) by sugar-water cosolvents, relative to the extent of plasticization by water alone.[17,18,20] Sugar-water, of higher average MW than water alone, causes a smaller depression of starch Tg than does pure water. In fact, isothermal treatment of starch in sugar-water, at a temperature that would result in non-equilibrium melting of amylopectin in water alone, results instead in antiplasticization by annealing and crystallite perfection.[20]

It has been known empirically for decades that various sugars, including sucrose, fructose, and glucose, raise the temperature of gelatinization of starch in water and delay the increase in viscosity (pasting), and that this effect in-

creases with increasing sugar concentration.[48,65,230,413] This effect of sugars on the gelatinization and pasting behavior of native and modified starches is also well known to be important to the processing and properties of food products such as baked goods, in that the effect influences the extent of wheat starch gelatinization, its retardation, or even inhibition during baking of, e.g., high sugar cookie doughs and cake batters.[26,47,49] The elevating effect of sugars on Tgelat had been attributed in the past in part to a depression of "water activity" ("Aw") by sugars and in part to an unexplained interaction (called "sugar bridges" by Ghiasi et al.[426] and said to involve hydrogen bonding[427]) of sugars with the amorphous areas of starch granules. As illustrated in Figure 100,[427] Spies and Hoseney suggested that "Aw" affects Tgelat to some extent, such that Tgelat increases with decreasing "Aw" of various sugar solutions, yielding straight lines of different slope for mono-, di-, and trisaccharide sugars. However, these workers noted that the mechanism of this effect was not completely understood and that other factors were also important.[427] There had been no successful attempt to show how the two purported aspects ("Aw" and "sugar bridges") of the effect on Tgelat might be related, or to explain the mechanism of elevation of Tgelat, prior to the description of the antiplasticizing effect of sugar-water cosolvents.[17,18,20]

The effect of sucrose on Tgelat of wheat starch is illustrated in Figure 101.[20] For convenience, Tgelat is taken as the temperature at the peak of heat uptake, as measured by DSC (see Figure 101 inset). Figure 101 shows that as the weight of sucrose is increased in a ternary mixture with constant equal weight ratio of starch and water, Tgelat increases monotonically for samples up to a 1:1:1 mixture. The DSC heat flow curve of this 1:1:1 mixture (shown in the inset of Figure 101), in which 50 w% sucrose is the added fluid outside the granules, exhibits a glass transition (evidenced by a characteristic baseline shift, associated with the free volume contribution to Tg,[106] at the leading edge of the gelatinization endotherm) at an effective Tg > 30°C higher than that seen for a 1:0:1 mixture, when the added fluid is water alone. Immediately following and superimposed on the elevated glass transition is a relatively narrow crystalline melting transition, similar to that seen for native starch annealed

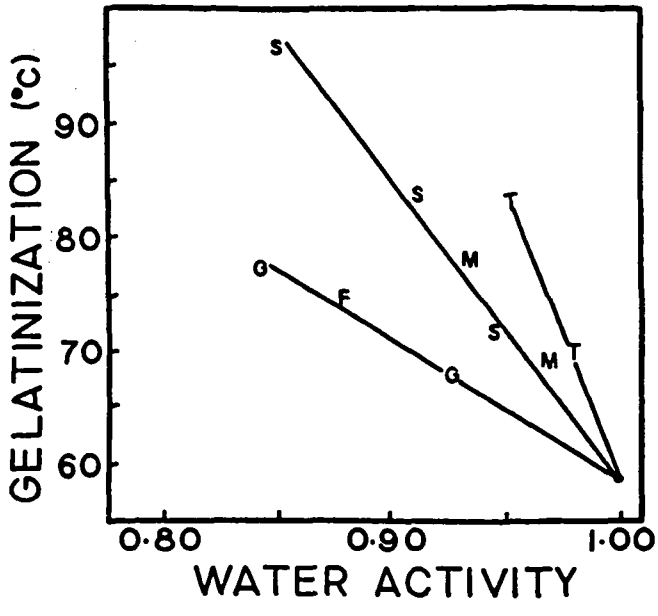

FIGURE 100. "Water activity" of sugar solutions vs. gelatinization temperature. F = fructose; G = glucose; M = maltose; S = sucrose; T = maltotriose. (From Spies, R. D. and Hoseney, R. C., *Cereal Chem.*, 59, 128, 1982. With permission.)

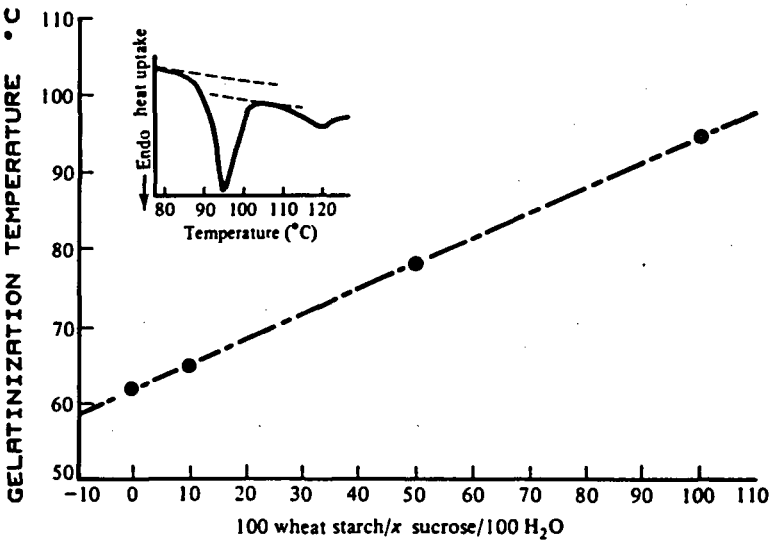

FIGURE 101. (A) Gelatinization temperature as a function of added sucrose content for three-component mixtures of native wheat starch:sucrose:water (100:×:100 parts by weight). Inset: DSC heat flow curve of 100:100:100 mixture. (From Slade, L. and Levine, H., *Industrial Polysaccharides — The Impact of Biotechnology and Advanced Methodologies*, Stivala, S. S., Crescenzi, V., and Dea, I. C. M., Eds., Gordon and Breach Science, New York, 1987, 387. With permission.)

under various time/temperature conditions (see Figure 91).[18,20]

The effect of sucrose on Tgelat has been explained, within predictions of the conceptual framework of starch as a partially crystalline glassy polymer, on the basis of WLF free volume theory.[20] If a sugar-water solution is viewed as a plasticizing cosolvent, it is evident that such a coplasticizer, of greater average MW than water alone, would be less effective in mobilizing and increasing the free volume of the amorphous fringes in the "fringed micelle" structure of a starch granule. Less effective plasticization would result directly in less depression of Tg, and thus indirectly in less depression of non-equilibrium Tm. In this sense, in comparing the efficiencies of aqueous solvents (including solutions of nonionic solutes such as sugars and polyols) as plasticizers of the glassy regions of native starch, water alone is the best plasticizer, and sugar-water cosolvents are actually *anti*plasticizers relative to water itself. By most effectively depressing the requisite Tg that initiates gelatinization, added water results in the lowest Tgelat. Increasing concentrations of a given sugar result in increasing antiplasticization and Tgelat vs. water alone.

Of course, increasing the concentration of a given sugar in an aqueous cosolvent also decreases "Aw" (actually RVP), but it has been established that the effective Tg of native starch in the presence of added water is independent of total sample moisture above about 30 w% total water content (i.e., $\gtrsim$Wg').[17-19] Moreover, according to WLF theory, it would be expected that the extent of antiplasticization would increase with increasing $\overline{M}w$ of the cosolvent, within a homologous series of cosolvent components, from monomer to dimer to oligomer to polymer. Yet, in such a case, the RVP of cosolvents at equal weight concentrations would generally increase with increasing cosolvent $\overline{M}w$. For example, for the homologous series glucose, maltose, maltotriose, 10 DE maltodextrin, RVPs of 50 w% solutions increase from 0.85 to 0.95 (for both maltose and maltotriose) to 0.99.[16]

Experimental results for the effect of this homologous series of cosolvents on Tgelat of starch have confirmed the prediction based on WLF theory, as illustrated in Figure 102,[18,20] and thus

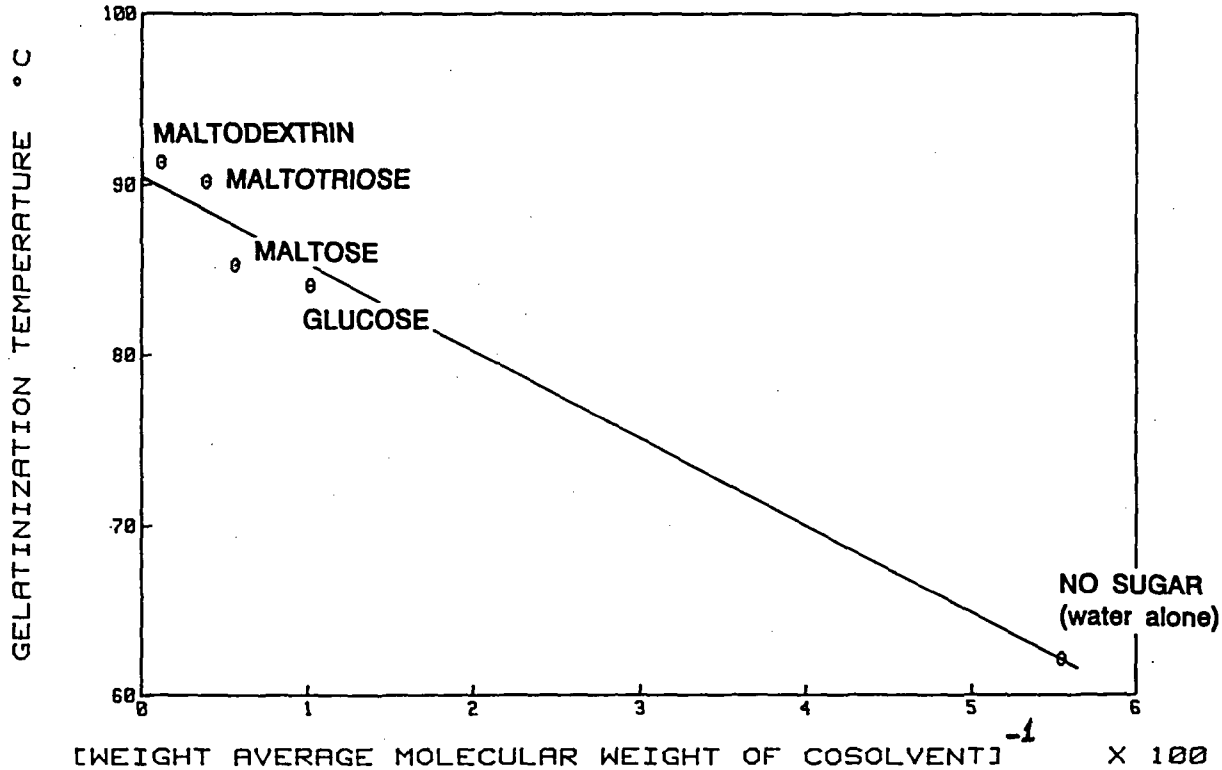

FIGURE 102. Gelatinization temperature, Tgelat, as a function of 100/$\overline{M}$w (of cosolvent, water + glucose polymer), for three-component mixtures of native wheat starch:glucose polymer:water (1:1:1 parts by weight) and two-component mixture of native wheat starch:water (1:2 parts by weight). (From Slade, L. and Levine, H., *Industrial Polysaccharides — The Impact of Biotechnology and Advanced Methodologies,* Stivala, S. S., Crescenzi, V., and Dea, I. C. M., Eds., Gordon and Breach Science, New York, 1987, 387. With permission.)

demonstrated that the underlying basis of this effect is not a depression of "Aw" by sugars. Figure 102 shows that as the $\overline{M}$w of the antiplasticizing cosolvent increases, free volume decreases, and the resultant Tg of the cosolvent increases. Consequently, the cosolvent becomes less efficient in depressing the effective Tg that initiates the gelatinization transitions in native starch, so Tgelat increases with increasing co solvent $\overline{M}$w, despite a corresponding increase in cosolvent RVP.[20]

A comparison of the degree of elevation of Tgelat of native wheat starch, for 1:1:1 sugar-water-starch mixtures of a larger and non-homologous series of sugars, has also been reported recently.[20] DSC results showed that Tgelat increases in the following order: water alone < galactose < xylose < fructose < mannose < glucose < maltose < lactose < maltotriose < 10 DE maltodextrin < sucrose. It has been suggested that the same structure-property relationships that act as determinants of coplasticizer mobility (as opposed to "Aw") in the water dynamics domain of the dynamics map[15,16] appear to influence the elevation of Tgelat. It has been concluded that no single parameter (e.g., Tg, Wg′, MW, or Tm/Tg ratio) can explain completely the mechanism of elevation of Tgelat by sugars, but a combination of these parameters that predicts the contributions of free volume and local viscosity provides useful clues to explain why the elevating effect on Tgelat is greater for sucrose than glucose than fructose.[20]

As pointed out earlier with respect to the effect of water content in binary starch-water systems, previous attempts to analyze the effect of sugar content in ternary starch-sugar-water systems on the observed Tm of starch by the Flory-Huggins equilibrium thermodynamics treatment of melting-point depression by diluents (e.g.,

Reference 161) have been recognized to be unjustified on a rigorous theoretical basis.[15,18,48] Aside from theoretical problems introduced by the facts that the interaction parameter "chi" is concentration-dependent and amylopectin microcrystallites are not a monodisperse system, Flory-Huggins theory is only appropriate to describe an equilibrium melting process. Regardless of the amount of water or sugar solution added to native starch, initial melting of a native granule remains a non-equilibrium process, in which melting of the microcrystallites is controlled by previous plasticization of the glassy regions via heat/moisture treatment to T > the effective Tg.[20]

As mentioned earlier, in general, mechanical relaxations depend on both translational and rotational mobility.[107] For a typical, well-behaved amorphous polymer-plasticizer system, an increase in free volume (which is related to rotational mobility) would be expected to go hand-in-hand with a decrease in local viscosity (which is related to translational mobility and reflects the molecular-level environment).[107] However, depending on the underlying mechanism of a specific mechanical relaxation, either the rotational or translational relaxation time can be the limiting aspect for a particular glass-forming system. The gelatinization of native granular starch in three-component starch-sugar-water model systems has been shown to be a mechanical relaxation process that appears to depend on both translational and rotational diffusion, but can be completely controlled and limited by the translational mobility of aqueous sugar solutions.[30]

Use of the dynamics map, in the form of the mobility transformation map in Figure 21, as a new conceptual approach to the study of non-equilibrium thermomechanical behavior of glass-forming food polymer systems, has facilitated the identification of a discriminating experimental approach and conditions that are capable of separating the effects of translational and rotational mobility on different mechanical relaxation properties, and thus elucidating the underlying basis of the differences in behavior of sugars during starch gelatinization.[30] The experimental approach developed to analyze the gelatinization process has utilized high-polymeric starch as a reporter molecule (probe) to study the relative translational mobilities of aqueous solutions of different sugars. Results of the study[30] have also demonstrated that investigation of the non-equilibrium relaxation behavior of different supra-glassy sugar-water solutions, in the context of the effect of their translational mobility on the diffusion-limited Tgelat of partially crystalline starch, is greatly enhanced by the simultaneous investigation of their rotational mobility, as measured by dielectric relaxation experiments.[200-204]

The response to microwaves in a microwave dielectric dispersion experiment is a rotational response.[202] The dielectric relaxation time, τ, for a sugar in aqueous solution is directly related to the rotational diffusion time. Maximum absorbance of electromagnetic radiation by pure water at room temperature occurs at a frequency of about 17 GHz in a microwave dielectric dispersion experiment. Microwave absorption maxima at lower frequencies result when free volume becomes limiting and relaxations occur at lower frequencies due to hindered rotation. For comparison, the commercial frequency used for domestic microwave ovens is 2.45 GHz. In the case of a dilute solution, when free volume is not limiting, the dielectric relaxation time is determined mainly by the intrinsic hydrodynamic volume of the solute.[200-202] As mentioned earlier, for each sugar solute in water at a given temperature, there is a limiting concentration below which the mobility shows a simple dependence on the average molar volume and above which the free volume limitation would begin to contribute to hindered rotation and increased local viscosity (which is equivalent to macroscopic solution viscosity only for solute MWs below the entanglement limit). At 20°C, this limiting concentration has been shown to be about 33 w% for sucrose and about 38 w% for glucose.[89] In other words, the hindered mobility characteristic of WLF behavior in the rubbery domain would be observed when $\Delta T \simeq 52$°C and $\Delta W \simeq 31$ w% above the Tg′-Wg′ reference state for a sucrose solution and when $\Delta T \simeq 63$°C and $\Delta W \simeq 33$ w% above the Tg′-Wg′ reference state for a glucose solution.[30]

Suggett and Clark[202] have assessed the rotational diffusion behavior of concentrated aqueous solutions (24.0 to 33.5 w% solute) of a series of sugars, including the pentoses ribose and xylose, the hexoses glucose and mannose,

and the disaccharides sucrose and maltose. They determined dielectric relaxation times from microwave dispersion measurements made over a frequency range from 100 KHz to 35 GHz at 5°C, where these supra-glassy sugar solutions would be expected to exhibit hindered rotation and the WLF behavior mentioned above. As mentioned earlier, the effect of the same sugars on starch gelatinization has been assessed from DSC measurements of Tgelat for native granular wheat starch suspensions in 50 w% aqueous sugar solutions.[20] The relative effects of the different sugar solutions on translational diffusion in the sugar-water-starch suspension have been estimated from these measurements of Tgelat, which reflect the relative deficit in depression of Tg of the amylopectin component of starch by sugar-water compared to water alone.[30] As revealed by the graph of Tgelat vs. dielectric relaxation time (in picoseconds) in Figure 103,[30] the effects of these sugars on starch gelatinization are highly linearly correlated (r = 0.97) with their rotational diffusion times in solution, as measured by dielectric relaxation. It is especially interesting to note that the surprising behavior of glucose and its dimer, maltose, which showed very similar rotational diffusion times, was reflected in exactly the same way by their very similar effect on Tgelat for the mechanical relaxation process reported by starch.

It has been suggested that the underlying explanation for this correlation is revealed by the graph in Figure 104,[30] which shows the fundamental relationship between the measured rotational diffusion times from the dielectric relaxation experiment[202] and the calculated relative mobilities of the supra-glassy sugar-water solutions. A mobility transformation map has been constructed for each sugar solution, and the relative mobility has been estimated from the relative distance between the experimental conditions and the reference glass curve, normalized with respect to the inherent mobility of the sugar. The inherent mobility of a sugar is related to the distance (in units of temperature) required by its dry glass to achieve the mobility of an Arrhenius liquid.[30] Thus, the relative mobility scale shown in Figure 104, calculated from the ratio of (T − Tg')/(Tm − Tg) for each sugar, has been defined in terms of the temperature difference between the experimental temperature T (5°C) and Tg' of the freeze-concentrated glass as the reference state, compared to the magnitude of the temperature difference in the WLF domain between Tm and Tg of the dry solute as a measure of inherent mobility. (As described earlier in Section III.A.7, there is a similarity between this relative mobility scale and the reduced temperature scale[104] that defines mobility in the temperature range from Tg to Tm with respect to the kinetics of polymer

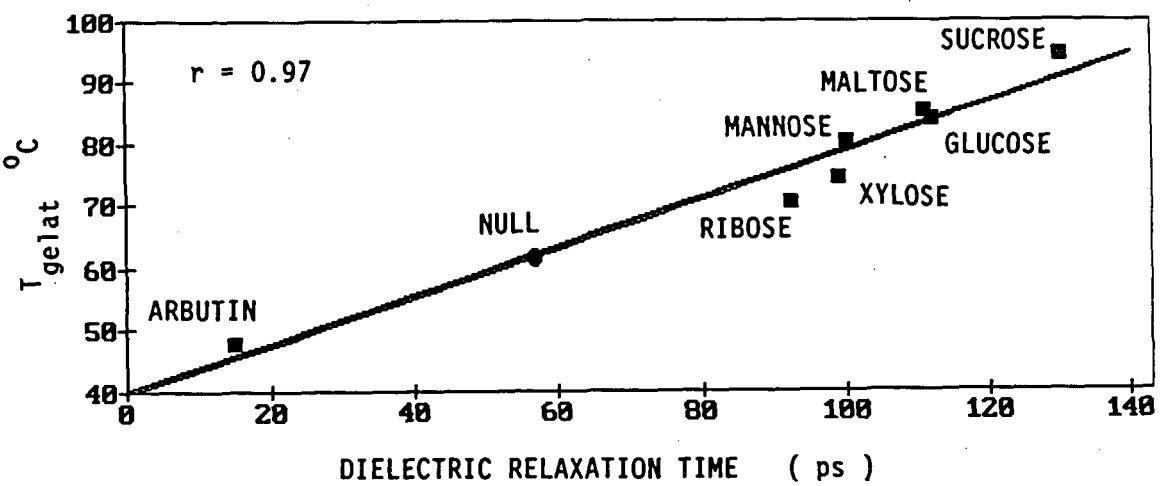

FIGURE 103. Variation of the gelatinization temperature of native wheat starch suspended in 50 w% aqueous sugar solutions with the corresponding dielectric relaxation time measured at 5°C for concentrated aqueous solutions of the same sugars. (From Slade, L. and Levine, H., *Pure Appl. Chem.*, 60, 1841, 1988. With permission.)

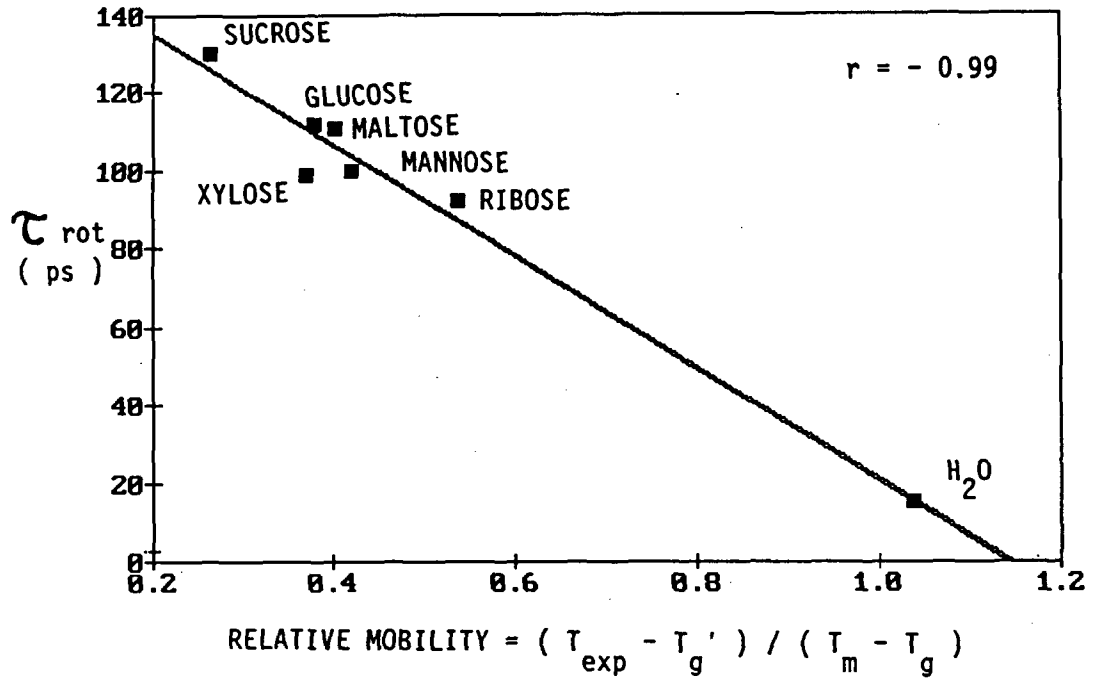

FIGURE 104. Variation of rotational diffusion time measured at Texp = 5°C for concentrated aqueous sugar solutions with the corresponding relative mobility parameter of aqueous solutions of the same sugars, calculated from the ratio of (Texp − Tg')/(Tm − Tg) for each sugar. (From Slade, L. and Levine, H., *Pure Appl. Chem.*, 60, 1841, 1988. With permission.)

crystallization, another mechanical relaxation process that depends on both translational and rotational mobility.[30]) Both dielectric relaxation times and translational diffusion coefficients of a broad range of glass-forming systems, including polyvinyl acetate and glucose, have been shown experimentally to follow the WLF equation near Tg.[177,362] The factor (Tm − Tg) has been chosen, in this case as a preferred alternative to the Tg/Tm ratio, for the comparison of mobilities, at T ⩾ Tg, of different sugars with different values of dry Tg.[30] Figure 104 illustrates the excellent linear correlation (r = 0.99) between the mobility, expressed in terms of WLF behavior, and the dielectric relaxation behavior of the aqueous sugar solutions in their non-equilibrium, supra-glassy states. As expected, in the absence of anomalous anisotropic requirements of free volume for mobility, both translational and rotational mobility depend correlatively on free volume, but translational motion becomes limiting at a higher temperature and determines Tg.[30] It should be noted that the calculated translational mobility for xylose is significantly lower than expected, based on its rotational relaxation time. The relatively low value of Tg/Tm for xylose accounts for the low calculated mobility,[30] which was previously confirmed experimentally by demonstrating the anomalous ability of xylose to retard the recrystallization of starch.[20]

3. Starch Retrogradation, the Kinetics of Staling, and the Effect of Sugars — Moisture Management Aspects of Staling

As introduced in Sections III.A.6 and 7 and discussed further in Section V.D.1, starch retrogradation exemplifies a polymer gelation-via-crystallization process, for which the kinetics have been described as illustrated in Figure 105.[23] This diagram has been specifically adapted for B-type starch, from the generic diagram for crystallizable synthetic polymers shown earlier in Figure 37. As noted in Section III.A.7, the overall crystallization rate curve in Figure 105 is not symmetrical like the one in Figure 37, but rather is

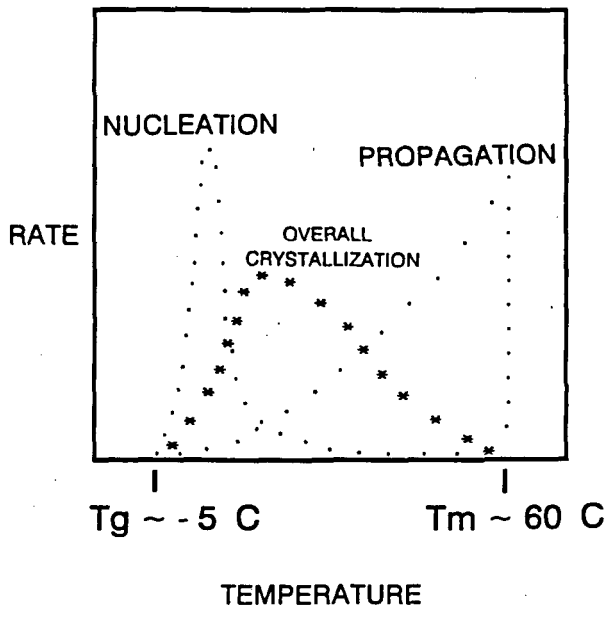

FIGURE 105. Crystallization kinetics of B-type starch as a partially crystalline polymer system, expressed in terms of crystallization rate as a function of temperature. (Reproduced with permission from Reference 23.)

skewed toward the Tg (i.e., $Tg' \simeq -5°C$) that limits the recrystallization process for gelatinized B-type starch or pure amylopectin. Thus, in agreement with previous experimental results[94,95,238] and theoretical calculations,[94] the maximum recrystallization rate at a single temperature occurs well below room temperature, in the 4 to 14°C range. This fact has been noted as a clear indication that the recrystallization process for B-type starch is strongly nucleation-limited.[18,20,94]

The rate and extent of staling in high moisture ($>Wg' \simeq 27$ w% water), lean (low sugar/fat ratio), wheat starch-based baked products (e.g., breads, rolls, and English muffins) are well-known to be correlated with the rate and extent of starch retrogradation during storage.[63,233,238] Retrogradation has been demonstrated to typify a non-equilibrium recrystallization process in a completely amorphous but crystallizable polymer system, which exists (around room temperature) in a kinetically metastable rubbery state and is sensitive to plasticization by water and heat.[18,20] The rate and extent of starch recrystallization are determined primarily by the mobility of the crystallizable outer branches of amylopectin.[18,20,92,94,219] In their retrogradation behavior, the baked crumb of wheat starch-based breads and experimental starch model systems (e.g., elastic amylopectin gels) are known to be analogous.[233] If adequate packaging prevents simple moisture loss, the predominant mechanism of staling in bread crumb or concentrated aqueous starch gels is the time-dependent recrystallization of amylopectin from the completely amorphous state of a freshly heated product to the partially crystalline state of a stale product,[18,20] with concomitant formation of network junction zones, redistribution of moisture (i.e., both microscopic and macroscopic migration),[65,428] and increased textural firmness.[63,219,233,429] (It is important to note the sharp distinction between this use of the word "staling" with respect to textural firming due to starch recrystallization in bread and another common use of the word "staling" to describe the loss of food product quality during storage. In *low* moisture, starch-based, baked or otherwise cooked [e.g., extruded or puffed] products [e.g., cookies, crackers, breakfast cereals] with initial moisture contents well below 27 w%, staling refers to the plasticization of the amorphous starch structure [initially in a glassy state at room temperature], due to moisture uptake/migration, with resulting progressive textural changes from crisp to firm/leathery to soggy.) The recrystallization of amylopectin depends strongly on sample history, since both initial heating during baking and subsequent aging during storage are non-equilibrium processes.[18,20,92] The local moisture content in the amorphous regions of a native granule determines the effective Tg that precedes melting of the crystalline regions (A-type in wheat) during gelatinization; complete melting of amylopectin crystallites during typical baking eliminates residual seed nuclei available for subsequent recrystallization.[18,20] The extents of swelling and release of protruding and extragranular polymer available for subsequent three-dimensional network formation by recrystallization depend on total moisture content during gelatinization and pasting.[215,413]

Immediately after baking, the amylopectin in the central crumb is completely amorphous, and the gelatinized starch network in white pan bread begins to recrystallize to a partially crystalline structure, upon cooling to room temper-

ature.[18,20] Concomitantly, freshly baked bread begins a process of mechanical firming (manifested by increasing modulus) and moisture redistribution,[65,428] which is perceived sensorily as a loss of "softness and moistness".[233] As described earlier, the early stages of these concurrent processes are dominated by amylose: formation of entanglement networks (followed closely by crystallization) by high MW amylose alone, and partially crystalline networks or chain-folded crystals by lower MW amylose-lipid complexes. Crystallization of amylose-lipid is favored over retrogradation.[20] The baking process is insufficient to melt the seeds of pre-existing amylose-lipid crystals, and homogeneous nucleation of new amylose-lipid crystals should occur somewhat above room temperature, while nucleation of retrograded amylose crystals in a high-moisture environment would be most rapid near $-5°C$ (i.e., Tg').[18,20]

The later stages of these concurrent processes, and the overall aging of bread, are dominated by recrystallization of amylopectin to a partially crystalline structure containing disperse B-type crystalline regions (see, for example, Reference 20 and references therein). As noted earlier, the B-type polymorph is a higher moisture crystalline hydrate than A-type starch.[152-154,400] Its recrystallization requires incorporation of water molecules into the crystal lattice,[154] which must occur while starch chain segments are becoming aligned. Thus, this recrystallization necessitates moisture migration within the crumb structure, whereby water (previously homogeneously distributed) must diffuse from the surrounding amorphous matrix and be incorporated as structural components in crystalline regions.[18,20] One manifestation of this moisture migration during amylopectin recrystallization is illustrated in Figure 106. This plot of percent freezable water (i.e., maximum grams of ice per 100 g sample, measured by DSC) vs. days after baking, for white pan bread samples hermetically sealed in DSC pans immediately after baking to prevent any changes in total sample moisture content during aging, demonstrates the progressive decrease in percent FW (from 21% on day 0 to 16% by day 11) with increasing extent of starch retrogradation that results from the migration of "freezable" water from the amorphous crumb matrix to the crystalline hydrate of recrystallized B-type wheat starch, wherein this crystalline hydrate water is structurally immobilized and thus rendered unfreezable. Since crystalline hydrate water

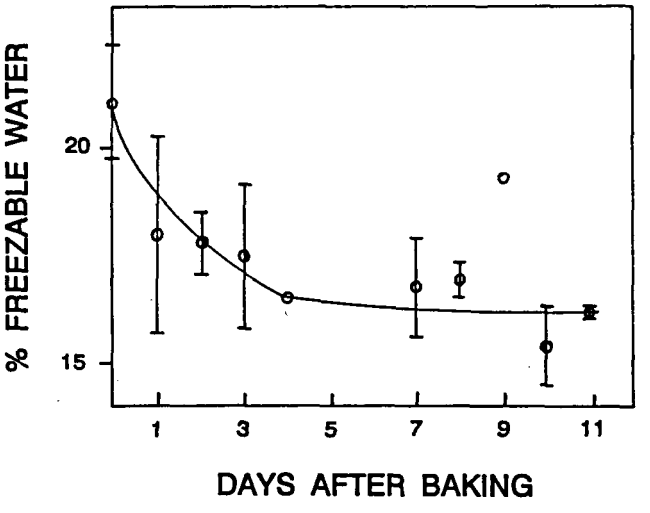

FIGURE 106. Plot of percent freezable water (measured by DSC) vs. days after baking for hermetically staled white pan bread, illustrating the decrease in percent FW with increasing extent of starch retrogradation that results from the migration of "freezable" water from the amorphous crumb matrix to the crystalline hydrate of recrystallized B-type wheat starch.

can plasticize neither amorphous regions of the starch network nor other networks (glutenin, pentosans) of the baked crumb matrix and cannot be perceived organoleptically,[20] the overall consequence of this phenomenon is a drier and firmer texture characteristic of stale bread.[65,233] An implicit requirement of starch recrystallization is availability of sufficient moisture, at least locally within the matrix, both for mobilizing long polymer chain segments (by plasticization) and being incorporated in B-type crystal lattices.[18,20,63,65,94,210,219,425] For the propagation step of crystallization, plasticization by heat may suffice for growth of A- or V-type crystals, but the negative temperature coefficient of the nucleation step limits the nucleation process to plasticization by water.[23] For gelatinized wheat starch, a moisture content ≳27 w% (Wg′) represents the minimum requirement for the nucleation process,[18,20] because Wg′ establishes sufficient ΔT above the reference Tg′ for mobility at typical staling temperatures and 27% is the water content of B-type crystals.[152-154,400] In fact, in low moisture baked goods, native starch granules in dough are not even gelatinized during baking.[47] Slade reported,[18] from DSC results for model wheat starch gels, that the percent recrystallization of completely amorphous (unseeded) amylopectin at room temperature increases monotonically with increasing percent total moisture in the range 27 to 50 w% (due to increasingly effective plasticization), then decreases with further increases in moisture up to 90 w% (apparently due to a dilution effect). These results were subsequently confirmed by Zeleznak and Hoseney, as shown in Figure 107[430] by their plot of the area of the DSC staling endotherm as a function of starch concentration during aging, for both model wheat starch gels and baked breads. Marsh and Blanshard[94] have recently reported that "no crystallization of (unseeded) starch-water systems that contain <15% water is predicted to occur when they are stored at temperatures <40°C. For gels containing 20% moisture, no crystallization should occur at storage temperatures below room temperature. Thus, as is found in practice, no crystallization of starch is predicted when low moisture-content systems are stored below room temperature."

Investigations to relate the concurrent processes of entanglement/network formation, B-type partially crystalline network formation, and moisture migration, in order to assign their roles in the overall process of bread aging and firming are complicated by the presence of many contributing polymer components with poorly characterized interactions, non-uniform local moisture, and multiple thermal/mechanical relaxation transitions.[20] Blanshard[47] has suggested that the textural changes observed at room temperature immediately after baking, before the onset of retrogradation, result from product cooling and transformation "through a continuum of rubbery states", to possibly a glassy state. At a typical moisture content of baked bread (>Wg′), the glassy state occurs at Tg′, ≃ −5°C, which corresponds to the limiting relaxation temperature for mobile polymer segments.[18,20,61] However, as mentioned earlier, in this case of a morphologically heterogeneous, supramolecular network (i.e., the crumb matrix containing networks of starch, gluten, and pentosans plasticized by water), the effective network Tg responsible for

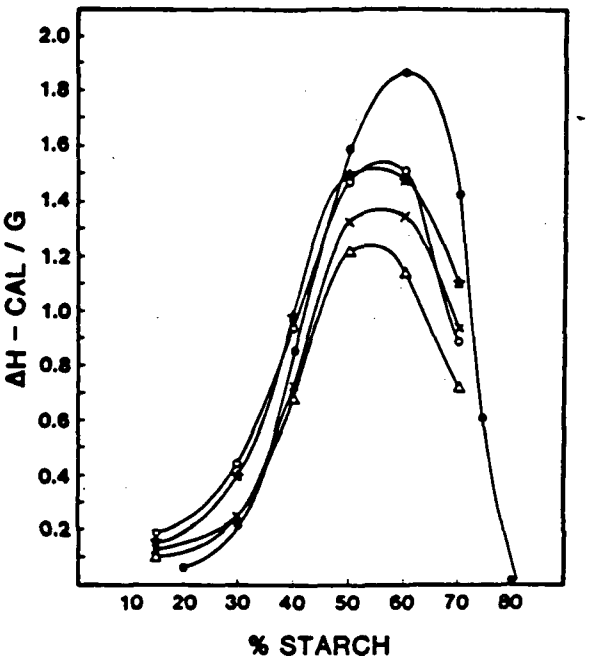

FIGURE 107. Effect of the moisture present during aging on the enthalpy (ΔH in calories per gram starch) of retrograded starch in starch gels (solid circles) and in bread baked with "antistaling" agents (i.e., various lipids). (From Zeleznak, K. J. and Hoseney, R. C., *Cereal Chem.*, 63, 407, 1986. With permission.)

mechanical firmness of freshly baked bread would be near room temperature for low extents of network formation, well above room temperature for mature networks, and equivalent to Tgel near 60°C for staled bread, even though the underlying Tg for segmental motion, responsible for the predominant second-order thermal transition, remains below 0°C at Tg′.[26] An additional complicating feature is introduced by the disproportionation of mobile short branches from water-plasticized amorphous regions upon retrogradation of amylopectin. The average DP of these outer branches[402] is well above the minimum chain length required for recrystallization[92,221,399] at the effective local concentration of clustered branches.[153] While 27 w% is the maximum moisture content of B-type crystals, it is the limiting moisture content (Wg′) for segmental relaxation of completely amorphous starch above Tg′, and higher moisture would be required to achieve the same segmental mobility in the absence of mobile amylopectin branches.[20] Because network Tg (Tfr) is higher than segmental Tg (Tg′), an even higher moisture content is required to maintain sufficient ΔT for mobility and softness in staled bread than in freshly baked bread.[23] Although currently available data are insufficient, it is likely that the use of NMR to investigate changes in water mobility during aging of bread and starch gels[152] will be especially complicated by these phenomena, so that it will be necessary to explore further the effects of initial moisture content, storage temperature, branching density, and branch length on the time course of the variation in relaxation times.[20,92,94] Moreover, NMR relaxation times for water do not reflect contributions from network Tg superimposed on contributions from segmental Tg.[23] It is likely that solid state NMR,[431] to examine the changing mobility of starch and crumb matrix networks directly, will provide a more complete understanding of the mechanism of firming during staling.

Retrogradation/staling has been studied extensively in bread crumb and model starch gels (e.g., wheat, potato, corn, pea) using DSC, mechanical compression tests, and X-ray crystallography to monitor formation and aging of the recrystallized starch network.[18,20,63,94,210,215,218,219,230,233,425,429,432] A quantitative DSC method has been developed and widely used to measure the rate and extent of starch (or pure amylopectin) recrystallization, as functions of additional ingredients, time, temperature, and moisture content during gelatinization and storage, in terms of increasing content of retrograded B-type crystalline starch (measured from the area of the characteristic melting endotherm at Tm ≃ 60°C associated with crystalline amylopectin).[17,18,63,95,215,218,225,232,235,396,429,430] (These studies have recognized that this so-called staling endotherm does not represent the melting of V-type crystalline retrograded amylose that may also be present.) Typical DSC results are illustrated in Figure 108[20] for two commercial bakery products: part A shows white pan bread, immediately after baking (completely amorphous = "fresh") and after 7 d storage at 25°C (extensively recrystallized amylopectin = "stale"); part B shows progressively increasing amylopectin recrystallization in English muffins after 1, 7, and 13 d ambient storage after baking.

As described earlier, sugars, acting as antiplasticizers relative to water alone, raise Tgelat and retard pasting of native starch. Sugars are also known to function as anti-staling ingredients in starch-based baked goods. For example, as mentioned earlier, glucose oligomers of DP 3-8 (i.e., non-entangling SHPs), used as anti-staling additives, have been reported to be effective in inhibiting, and not participating in, starch recrystallization.[403] It has been suggested[18,20] that these two effects are related as follows. Analogous to the inefficient depression of Tg and consequently Tm of partially crystalline native starch, and therefore Tgelat (relative to the plasticizing action of water alone), sugar solutions produce an elevated Tg of the continuous rubbery local environment of the resulting three-dimensional, completely amorphous, entangled starch gel matrix in a freshly baked product. When Wg′ of the sugar solution is similar to that of starch-water alone, as is the case for the homologous family of glucose oligomers, greater Tg of the local environment effects greater network Tg of the starch gel. This elevated Tg of the local environment and network Tg (relative to Tg of the corresponding network plasticized by water alone) controls subsequent recrystallization of B-type starch in

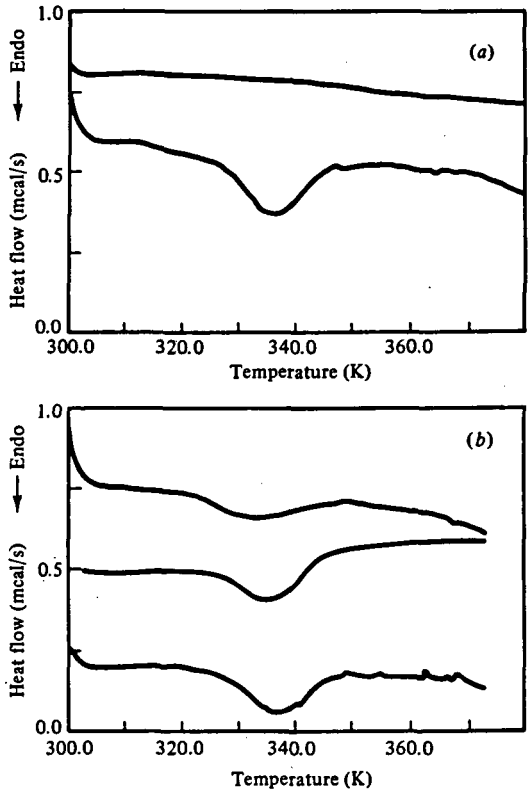

FIGURE 108. Perkin-Elmer DSC-2C heat flow curves illustrating the rate and extent of starch recrystallization in two types of commercial baked goods: (a) white bread, immediately after baking (upper curve) and after 1 week at room temperature (lower curve); (b) English muffins, on days 1 (upper curve), 7 (middle curve), and 13 (lower curve) after baking. (From Slade, L. and Levine, H., *Industrial Polysaccharides — The Impact of Biotechnology and Advanced Methodologies,* Stivala, S. S., Crescenzi, V., and Dea, I. C. M., Eds., Gordon and Breach Science, New York, 1987, 387. With permission.)

the undercooled rubbery gel, by controlling the rate of propagation at ΔT above Tg, according to WLF kinetics. For storage at T > network Tg, there is sufficient mobility for devitrification and subsequent formation of crystalline junction zones, resulting in a partially crystalline polymer system that constitutes the retrograded starch gel. Relative to typical storage at ambient temperature, a higher Tg of the local environment and of network Tg (due to addition of sugars with Wg′ similar to starch-water alone) translates to smaller values of ΔT and so a lower rate of propagation of starch recrystallization at the storage temperature. Thus do such sugars act to retard the rate and extent of starch staling during ambient storage. Moreover, WLF theory predicts that greater MW of a sugar would translate to greater antiplasticization by the sugar solution, and so a greater anti-staling effect.[18,20]

The situation is somewhat more complicated when Wg′ of the sugar solution is much greater than that of starch-water alone. Tg in the local environment of amylopectin branches is still elevated, relative to water alone, but greater network Tg may be compensated by increased plasticizing effectiveness of the sugar solution. A systematic study of anti-staling by a large and non-homologous series of common sugars has recently been reported.[20] DSC results have compared the degree of elevation of Tgelat of native wheat starch, described earlier, with the degree of inhibition of recrystallization of gelatinized starch, for the same series of sugars. Starch:sugar:water mixtures (1:1:1) were analyzed after complete gelatinization (i.e., heating to $T \gg$ Tgelat in each case, whatever the specific Tgelat) followed by 8 d of storage at 25°C, and the results have shown that the extent of recrystallization decreases in the order fructose > mannose > water alone > galactose > glucose > maltose > sucrose > maltotriose > xylose > lactose > malto-oligosaccharides (enzyme-hydrolyzed, DP > 3). For the glucose homologs within this sugar series, MW and resultant Tg are the apparent primary determinants of anti-staling activity. However, for the other sugars, it has been suggested, as it was with respect to their effect on gelatinization, that coplasticizer mobility (in this case during storage rather than during gelatinization), as determined by free volume and local viscosity and reflected by Wg′ and Tm/Tg ratio,[15] appears to play a key role in their anti-staling effect. It should be recognized that this suggestion does not contradict the statement by Paton[225] that "anti-staling agents do not operate (primarily) by a mechanism that alters moisture availability to the starch *during* the baking process, thus affecting retrogradation". In their inhibitory action on starch recrystallization, as in their elevating action on Tgelat, sucrose is more effective than glucose than fructose. The fact that fructose-water, relative to water alone, actually accelerates starch staling is a particularly salient finding,[20] since it supports the previous obser-

vation of anomalously large translational diffusion that promotes mold spore germination in fructose solutions, relative to glucose solutions.[30]

As alluded to earlier in the discussion of Figure 105, starch retrogradation can be viewed as a time/temperature/moisture-governed polymer crystallization process that can be manipulated.[18,20] This perspective has been illustrated as described below in the context of Figure 109,[23] wherein the numbered positions along the crystallization rate curve represent different process approaches, based on the crystallization kinetics of B-type starch, for either anti-staling or pro-staling of starch-based foods.

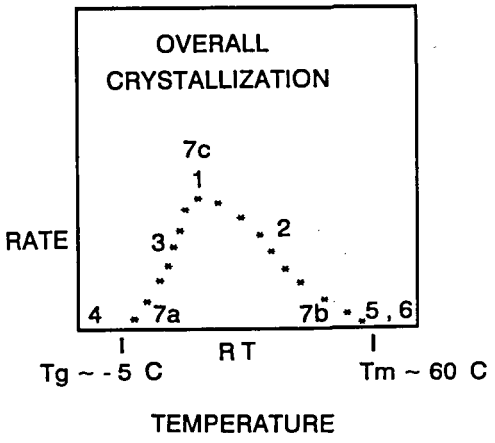

FIGURE 109. Crystallization kinetics of B-type starch, expressed in terms of overall crystallization rate as a function of temperature. Numbered positions on the diagram denote different process approaches which affect crystallization rate, as described in text. (Reproduced with permission from Reference 23.)

For partially crystalline synthetic[104] and food[24] polymers in general, and B-type amylopectin in particular,[18,20,94,215,232,238] for which the time and temperature of superheating above Tm of native amylopectin crystallites during baking is sufficient to eliminate self-seeding upon subsequent cooling,[20] the rate-limiting step in the crystallization process is nucleation (which is enhanced at lower temperatures) rather than propagation (which is enhanced at higher temperatures). The dominant role of nucleation in the process of thermoreversible gelation-via-crystallization for gelatinized starch (or pure amylopectin)-water systems (at $W > Wg' \simeq 27$ w%)[18,20] was emphasized by three earlier points: (1) the calculated temperature of about 14°C (position 1 in Figure 109) for the maximum crystallization rate of B-type hydrated starch crystals at a single temperature within the Tg-Tm range from −5 to 60°C,[26] rather than the expected (warm room) temperature about midway between Tg and Tm;[235] (2) the temperature of about 5°C for the maximum crystallization rate of a B-type, 50% wheat starch gel at a single storage temperature, calculated from experimental results obtained between 2 and 37°C;[94] and (3) the similarity of these calculated temperatures to the subambient temperature (in the range 0 to 10°C) observed to produce the maximum rate of starch recrystallization and concomitant crumb staling/firming during aging of white bread.[95,238] Nucleation control of starch recrystallization is also demonstrated by the DSC results in Figures 110 through 112.[18,20]

Typical results for the extent of starch staling

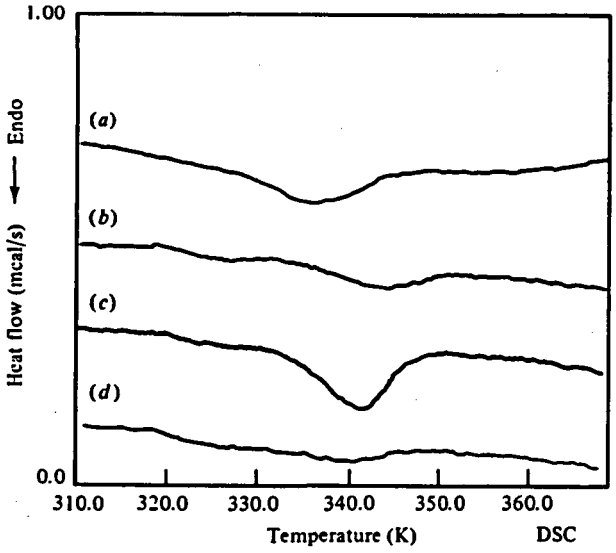

FIGURE 110. Perkin-Elmer DSC-2C heat flow curves of fresh-baked white bread crumb staled at different storage temperatures and times: (a) 25°C for 39 d; (b) 25°C for 42 h, then 40°C for 2.5 h; (c) 0°C for 42 h, then 40°C for 2.5 h; (d) −11°C for 42 h, then 40°C for 2.5 h. (From Slade, L. and Levine, H., *Industrial Polysaccharides — The Impact of Biotechnology and Advanced Methodologies,* Stivala, S. S., Crescenzi, V., and Dea, I. C. M., Eds., Gordon and Breach Science, New York, 1987, 387. With permission.)

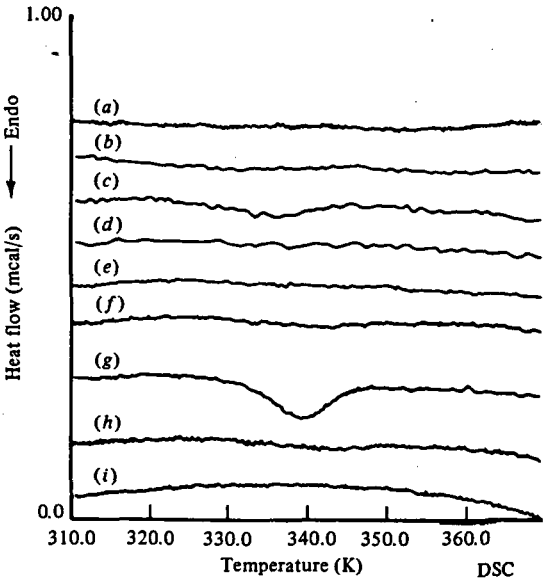

FIGURE 111. Perkin-Elmer DSC-2C heat flow curves of wheat starch:water 1:1 mixtures, stored under different temperature/time conditions immediately following gelatinization: (a) 40°C for 4.5 h; (b) 25°C for 3.5 h; (c) 4°C for 3 h; (d) −23°C for 2.5 h; (e) −196°C for 1 min, then −23°C for 2 h; (f) 25°C for 2 h, then 40°C for 5 h; (g) 4°C for 2 h, then 40°C for 6.5 h; (h) −23°C for 2 h, then 40°C for 6 h; (i) −196°C for 1 min, then −23°C for 2 h, then 40°C for 5.5 h. (From Slade, L. and Levine, H., *Industrial Polysaccharides — The Impact of Biotechnology and Advanced Methdologies,* Stivala, S. S., Crescenzi, V., and Dea, I. C. M., Eds., Gordon and Breach Science, New York, 1987, 387. With permission.)

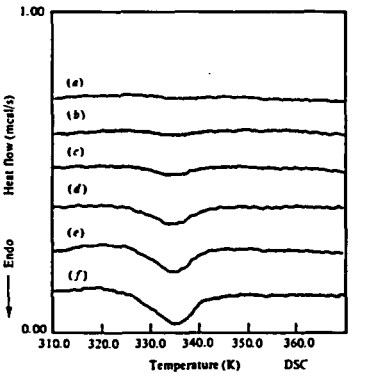

FIGURE 112. Perkin-Elmer DSC-2C heat flow curves of wheat starch:water 1:1 mixtures, nucleated for different times at 0°C, then propagated for 30 min at 40°C, immediately following gelatinization: (a) 10 min; (b) 30 min; (c) 60 min; (d) 180 min; (e) 240 min; (f) 300 min. (From Slade, L. and Levine, H., *Industrial Polysaccharides — The Impact of Biotechnology and Advanced Methodologies,* Stivala, S. S., Crescenzi, V., and Dea, I. C. M., Eds., Gordon and Breach Science, New York, 1987, 387. With permission.)

in freshly baked white bread crumb stored at 25°C for 39 d are shown in curve a of Figure 110. Curves b through d in Figure 110 illustrate how the rate and extent of staling can be influenced by separating the mechanistic steps of nucleation and propagation and maximizing the nucleation rate. Compared to nucleation and propagation at 25°C (curve a), faster propagation at 40°C produces significant staling (curve b) in much less time. Initial storage at −11°C (<Tg′) inhibits nucleation (except during cooling) and so produces less staling in an equivalent time (curves d vs. b). However, the greatest rate and extent of staling in the shortest time are achieved (curve c) by faster nucleation at 0°C (for long enough to allow extensive nucleation), followed by faster propagation at 40°C.[18] These results were recently confirmed in a subsequent study by Zeleznak and Hoseney.[95]

This DSC study[18,20] has also examined model wheat starch:water (1:1) mixtures exposed to different temperature/time storage protocols immediately following gelatinization, and represented an exploration of the optimum nucleation temperature to produce a maximum rate of recrystallization. As shown in Figure 111 curves a through c, for single-temperature storage conditions, the rate of nucleation and thus overall crystallization increases with decreasing temperature (i.e., 40 < 25 < 4°C, a finding in agreement with subsequent results of Zeleznak and Hoseney[95] and Marsh and Blanshard[94]), as long as the temperature is above Tg′. These results demonstrate the negative temperature coefficient expected for the nucleation rate in a typical polymer crystallization process.[94] Freezer storage at T < Tg′ inhibits nucleation (Figure 111 curves d and e), and so retards recrystallization, even when followed by propagation at 40°C. Zobel[61] has recently reached the same conclusion as Slade had from her experimental results.[18] Zobel has remarked that "knowledge about glass transitions appears to offer a way to control starch gel properties in food . . . applications" and that "in

the context of bread staling, a rational explanation of why freezing preserves bread from staling is that the bread is held below its Tg." It is important to note that, as represented by position 4 in Figure 109, starch recrystallization would be inhibited only *while* bread remains at a freezer temperature Tf < Tg', but not during cooling to Tf (when fast nucleation could occur) or after thawing (when propagation could occur in a previously nucleated matrix).[8,18,26] Once again, as for white bread crumb in Figure 110 curve c, starch gels first held at 4°C to promote rapid nucleation, then at 40°C to allow rapid propagation (Figure 111 curve g), show by far the greatest overall rate and extent of starch staling via amylopectin recrystallization. This finding of an optimum practical nucleation temperature of 4°C[18] to produce a maximum rate of recrystallization (also confirmed by Zeleznak and Hoseney[95]) is critically relevant to high moisture (i.e., starch gelatinized during baking) baked products with coatings, such as chocolate-covered cake donuts. When such a product is run through a refrigerated cooling tunnel (at 40°F) immediately after baking and coating, in order to rapidly solidify ("set") the coating, this process step can result in accelerated starch staling within the crumb matrix during subsequent ambient temperature storage, relative to the corresponding rate of staling in the same product not subjected to faster nucleation at subambient temperature via the cooling-tunnel treatment.[26]

Figure 112 shows DSC results for model wheat starch:water (1:1) mixtures, examined for the effect of increasing nucleation time at 0°C, immediately after gelatinization, and prior to 30 min of propagation at 40°C. It is apparent from the trend of steadily increasing endotherm areas in curves a through f that the extent of nucleation and overall crystallization increases monotonically with increasing time of nucleation. Moreover, amylopectin recrystallization is already measurable after only 1 h of total storage, and quite extensive after 5.5 h. The extraordinary rate and extent of recrystallization are evidenced by comparing the endotherm areas in Figure 112 with those in Figures 108, 110, and 111, all of which are plotted with 1.0 mcal/s full scale and for similar sample weights.

As mentioned earlier, these results[18] have been used to design a patented industrial process for the accelerated staling of bread (for stuffing) and other high moisture, lean, starch-based foods.[36] By a two-step temperature-cycling protocol involving, first, a several-hour holding period at 4°C (to maximize the nucleation rate) (position 7a in Figure 109), followed by a second several-hour holding period at 40°C (to maximize the propagation rate) (position 7b in Figure 109), a much greater overall extent of staling (indicated by position 7c in Figure 109) due to amylopectin recrystallization is achieved (vs. the same total time spent under constant ambient storage), which is equivalent to staling bread for several days at room temperature.[20]

Returning to Figure 109 for the last time, the remaining numbered positions represent anti-staling approaches that are either empirically well known or intuitively obvious, but not previously explained and understood on the basis of polymer crystallization kinetics theory.[23] Position 5 signifies the zero rate of staling achievable at T > Tm, for example, by holding bread or English muffins above about 60°C (at about 50% relative humidity to inhibit moisture loss) during the time between baking and arrival at the point-of-sale. Similarly, position 6 represents the familiar method of refreshening stale baked goods by microwave heating to 60 to 65°C in order to remelt B-type retrograded starch crystals. Position 2 denotes the classic empirical approach to retarding the rate of staling by storing products in a warm bread box at about 35°C. Lastly, position 3 indicates the slower rate of staling achievable, between the extremes of a maximum rate around 14°C and a near-zero rate below −5°C, *during* refrigerator storage near 5°C. In practice, the fast nucleation rate produced by slow cooling to refrigerator temperature, followed by the faster rate of propagation possible in an extensively preseeded matrix warmed slowly from refrigerator to room temperature by ambient thawing, may obviate the potential anti-staling benefit of refrigerator storage.[23]

4. Amylopectin-Lipid Crystalline Complex Formation at Low Moisture

It has long been known that amylose forms

a helical complex with lipids, which crystallizes readily from water as anhydrous crystals that give rise to V-type X-ray diffraction patterns.[61,401,433-438] The Tm of crystalline amylose-lipid complex is about 110°C (see Figure 90 for typical DSC thermograms) for endogenous lipids of cereals such as wheat, corn, and rice.[20,35,433,436,437,439,440] Amylose-lipid complex is more stable than the well-known amylose-iodine complex,[435] and linear chain-lipid crystals are more thermostable than linear chain-hydrate polymorphs (B-type, Tm ≃ 60°C, in retrograded amylose gels, or A-type, Tm ≃ 85°C, in low-moisture granular starches).[18,20,35,433,440] For a given MW of amylose, pure anhydrous amylose crystals are most thermostable of all, with Tm > 140°C.[35,92,219,221,433,440]

Depending on endogenous lipid content, the amylose (about 20 to 30%[400]) in a normal native starch granule may exist as a glassy or crystalline, hydrate or amylose-lipid complex.[20] Upon heating starch for DSC analysis at total sample moisture content ≳27 w%, preexisting crystalline amylose-lipid is seen as a melting endotherm at ≃110°C. Preexisting glassy amylose, in the presence of, but not necessarily precomplexed with, lipid, is evidenced by a crystallization exotherm near 95°C.[20] For starches with low endogenous lipid, addition of exogenous lipid results in a crystallization exotherm on the first heating, and a melting endotherm on the second heating.[35,433,438,440] Thus, amorphous amylose, rendered mobile and available via gelatinization and pasting during baking, may (1) complex with endogenous lipid and crystallize, (2) crystallize if previously complexed but restrained from crystallization, or (3) complex and crystallize with exogenous lipid, added as emulsifiers in dough conditioners or shortening.[23] In contrast, even when endogenous lipid content is high or exogenous lipid is added, DSC analysis of waxy starches (which contain essentially no amylose) in the conventional temperature range 20 to 130°C and moisture range >30 w% had not[437] until recently[20] revealed evidence of crystallization or melting of amylopectin-lipid complexes.

It is known that amylose can be precipitated with butanol, but typical amylopectin cannot; this is the basis for the traditional distinction between these two polymers.[401,437] The longest accessible linear chain segments in amylopectin are outer branches of DP ≃ 16 to 20.[402] These branches, which are responsible for the microcrystalline regions of amylopectin, are not long enough to form complexes with iodine or butanol[437] that are stable to dilution at room temperature. It had been assumed[437] until recently[20] that amylopectin branches are also too short to form stable complexes with lipids, and the absence of DSC transitions[437] had supported this assumption. The most stable complexes of linear amylose with iodine are formed by chains of DP > 40.[435] Despite the lack of previous evidence from DSC and other analytical methods for interactions between amylopectin and lipid, addition of stearoyl lipids (e.g., sodium stearoyl lactylate, SSL), is known to affect the texture and rheology of waxy corn starch samples.[437] Similarly, while amylopectin is believed to be capable of forming insoluble complexes (via its outer branches) with surfactants including monoglycerides such as glycerol monostearate, thereby implicating such monoglycerides in bread shortenings and emulsifiers with a possible role as an anti-staling agent, the nature of such amylopectin complexes remains obscure.[441] It was believed possible that amylopectin-lipid complexes do occur, but Tm of the crystals, if determined by the low MW of amylopectin branches, might be well below the DSC temperature range usually examined for starch-lipid complexes.[20]

Slade used native waxy maize starch, with only "as is" moisture (<10 w%), as the amylopectin source. A starch:SSL (10:1 w/w) mixture was heated at 120°C for 15 min (at 15 lb pressure), to assure comelting of the reactants. Starch alone, treated the same way, produces the featureless thermogram shown at the top of Figure 113,[20] while SSL alone melts at 45 to 50°C. The rationale for this experimental approach was that, in the presence of only enough moisture (<10 w%) to permit plasticization and melting of starch at high temperature, but not enough to allow the formation of amylopectin A- or B-type crystal hydrates, amylopectin-lipid crystalline complex formation would be possible and favored. The starch:SSL comelt was then nucleated at 4°C for 24 h, heated to 120°C at 10°C/min and recooled, then analyzed by DSC. The thermogram (bottom of Figure 113) shows a small crys-

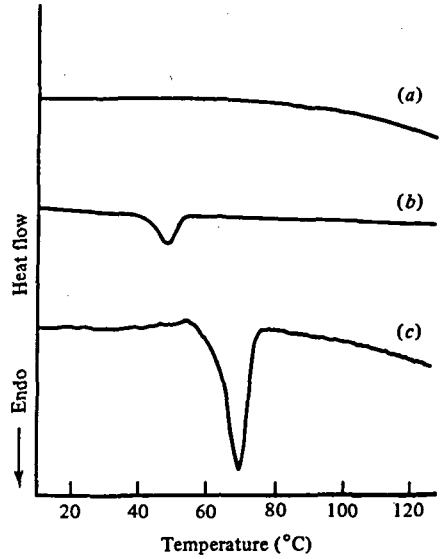

FIGURE 113. Perkin-Elmer DSC-2C heat flow curves of (a) waxy maize starch (<10 w% water), after heating at 120°C (15 lb pressure) for 15 min; (b) SSL alone, same heat treatment; and (c) 10:1 (w/w) waxy maize starch (<10 w% water):SSL, same heat treatment, followed by 24 h at 4°C, then heating to 120°C at 10°C/min and recooling, before rescanning. (From Slade, L. and Levine, H., *Industrial Polysaccharides — The Impact of Biotechnology and Advanced Methodologies,* Stivala, S. S., Crescenzi, V., and Dea, I. C. M., Eds., Gordon and Breach Science, New York, 1987, 387. With permission.)

tallization exotherm at 55°C, followed by a large and narrow melting endotherm at Tm ≃ 70°C. This has been presented[20] as the first DSC evidence of a crystalline amylopectin-lipid complex produced at low moisture. The low Tm, relative to that for amylose-lipid complex, has been suggested to indicate a lower MW complex, formed with the short, crystallizable outer branches of amylopectin.

As described above specifically with respect to the formation of starch-lipid crystalline complexes, and in general throughout Sections V.G and H, the processing and storage stability of starch-based foods are governed by the effective Tg and Tm that control starch structural transformations. This perspective has been illustrated recently by Colonna (personal communication, 1988), with specific regard to the physical modification of native granular starches, as shown in Figure 114. This diagram illustrates a conceptual representation of the temperature paths of various industrial processes used to produce physically modified starches. For each process, the heating/cooling treatment to which native granular starch is subjected is indicated in relation to the critical thermal transition temperatures, Tg and Tm, of partially crystalline starch. These transition temperatures define the physical and structural states of the starch before, during, and after processing: (a) partially crystalline glassy solid at T < Tg, i.e., the kinetically metastable starting material at room temperature; (b) partially crystalline rubbery liquid at Tg < T < Tm, during or after processing; and (c) completely amorphous liquid at T > Tm, during processing. After each illustrated process, the new structural form of the final physically modified starch product can be captured and stabilized by fast cooling to the glassy solid state at T < Tg. As illustrated by the discussion in Sections V.G and H, the conceptual representation exemplified in Figure 114 can be extended to describe the processing or storage of any starch-based food system.

VI. CONCLUSIONS AND FUTURE PROSPECTS

In the Foreword to the recent book entitled "Food Preservation by Moisture Control", Duckworth wrote:[442]

> "Those more immediately involved in practical aspects of methods of food preservation which depend for their effectiveness on control of the aqueous environment within a material must remain alive to the fact that newer research is currently leading to important changes in our understanding of the properties of water in foods, and that some previously widely-held views on the theoretical background to their activities are no longer tenable. At the same time, methods such as the measurement of relative water vapour pressure (Aw) which have long been used for characterising the state of water in foods and which continue to prove empirically highly useful, should still be exploited to their fullest advantage, yet with a greater appreciation of their theoretical limitations."

In the same book, Gould and Christian,[72] commenting on kinetic impediments to metabolism and microbial growth via high viscosity and glassy states, stated that "one would predict that high viscosity states would greatly interfere with, and glassy states prevent, the growth of micro-

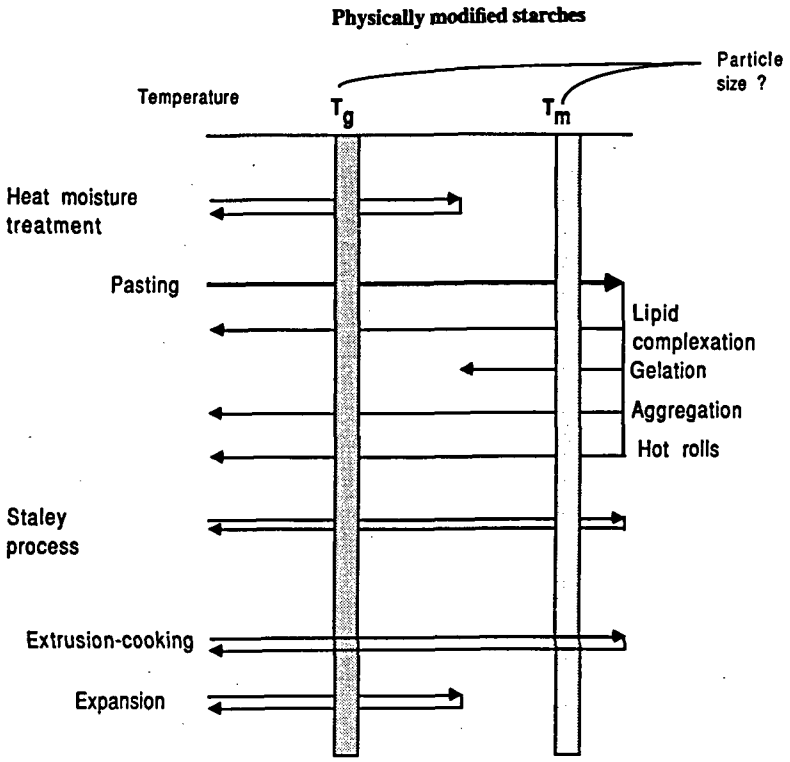

FIGURE 114. Conceptual representation of the temperature paths of various industrial processes used to produce physically modified starches. For each process, the heating/cooling treatment to which native granular starch is subjected is indicated in relation to the critical thermal transition temperatures, Tg and Tm, of partially crystalline starch. These transition temperatures define the physical and structural states of the starch: partially crystalline glassy solid at T < Tg; partially crystalline rubbery liquid at Tg < T < Tm; completely amorphous liquid at T > Tm. (From Colonna, P., personal communication, 1988. With permission.)

organisms in foods, for instance through the restriction of diffusion of nutrients to, and end-products away from (the microorganisms). This is clearly an area where much remains to be done in order to identify the potential for deliberate use of high viscosity states, and bearing in mind that conventional Aw determination will not define these metastable states." Regarding the dormancy-resistance mechanism of bacterial endospores, they noted that "it is the immobilisation and high viscosity in such systems that are the determinants of resistance rather than the water contents or water activities *per se*." Speaking about anhydrobiosis, they went on to say that "desiccation tolerance strategy may (involve) . . . the protection of cytoplasmic components by high concentrations of solutes that . . . may even reduce possibly deleterious chemical and enzymic reactions by promoting the formation of high viscosity or glassy states. It is therefore highly likely that the protective strategies will have relevance to the prevention of chemical, enzymic and microbiological deterioration reactions in stored foodstuffs, but in a way that is not necessarily predictable from the more conventional sorption isotherm/Aw-relationships that are widely used as predictor of stability." They concluded by pointing out that, because "the thermodynamic water activity is an equilibrium function and therefore takes no account of dynamic factors, . . . there is a danger that we may miss phenomena, and opportunities, that have a kinetic rather than equilibrium basis, such as those that may derive from better directed control of

viscosity/diffusivity in foods or from more soundly-based exploitation of metastable glassy states."

In this review, we have described a food polymer science approach to the study of structure-property relationships that ranges far beyond the limited applicability of the "water activity" approach to the assessment of food quality, safety, and stability. Investigations that compare, based on so-called "Aw" measurements, aqueous food systems composed of different water-compatible solutes are handicapped by "apples vs. oranges" comparisons devoid of predictive capability. In contrast, we have demonstrated that investigations based on measured thermomechanical properties, used to define the locations of the controlling glass, solidus, and liquidus curves on a dynamics map, allow predictive analyses of structure-function relationships in food products and processes. We have shown how the use of a water/glass dynamics map as a new conceptual approach to the study of non-equilibrium thermomechanical behavior facilitates the selection of experimental conditions to allow specific food systems to be examined at measurable distances of moisture content (i.e., ΔW) and temperature (i.e., ΔT) from their respective reference glass curves. We have discussed how the most effective use of the dynamics map, as a mobility transformation map to elucidate the underlying basis of differences in behavior of food materials, has necessitated the identification of appropriate experimental approaches that are capable of separating the effects of translational and rotational mobility on different mechanical relaxation properties. We have illustrated interpretations, based on the conceptual food polymer science approach to water relationships in foods, that have led to deeper qualitative understanding and new insights to moisture management aspects of sorption isotherms, microbiological stability, enzymatic activity, collapse phenomena, sugar crystallization, drying processes, cereal cooking processes, and starch gelatinization and retrogradation. In the following subsection, we summarize the generic experimental approach suggested for future investigations of water dynamics and glass dynamics to predict the quality, safety, and stability of foods.

A. Suggested Experimental Approach for Investigations of Water Dynamics and Glass Dynamics to Predict Quality, Safety, and Stability of Foods

As mentioned in the Introduction, the 1985 Faraday discussion conference on Water Activity at Girton College, Cambridge, generated (1) a set of guidelines (outlined below in updated form) for new criteria, based on current knowledge of the physical and chemical properties of aqueous systems, to assess the technological performance of food products and the physiological viability of biological systems, and (2) recommendations for a more credible quality standard to replace the current usage of "Aw".

Guidelines

I. Dilute Systems
   1. Probably are (i.e., *can* be) in chemical equilibrium. If so, then vapor pressure is a true indication of Aw.
   2. *In vivo* water stress is, by definition, equated with an osmotic imbalance.
   3. Although an osmotic contribution is evident, specific ion/molecule effects cannot be so interpreted.
   4. Where specific effects resemble salting in/out, then they probably arise from hydration interactions and *not* from a (statistical) osmotic lowering of the vapor pressure. The concept of a "compatible solute" is incompatible with Aw arguments.
   5. There are many instances of specific ion/molecule effects at constant Aw, e.g., enzyme activity, protein stability.

II. Intermediate Moisture Systems
   1. Characterized by non-equilibrium behavior.
   2. Aw is meaningless, and vapor pressure is *not* a measure of Aw.
   3. Systems are under kinetic control, i.e., rate of approach to equilibrium; usually, WLF kinetics apply, instead of Arrhenius kinetics. This is true even for living organisms under extremes of dehydration (caused by freezing, drought, or salt).

4. Factors that govern kinetics/mobility: T, composition expressed by $\overline{M}w$.
5. At constant concentration, a change in T changes mobility. At constant T, a change in concentration changes mobility.
6. Measurable variables: viscosity, diffusion, relaxation times. Tg(c) is diagnostic: defines $\eta \simeq 10^{12}$ Pa s locus. In the neighborhood of Tg, viscosity and diffusion coefficient change rapidly with temperature. Usually, Tm − Tg $\simeq$ 100°C (but *not* for fructose).
7. Must establish if *water* per se is required as a reactant or plasticizer, or whether any low MW species would suffice; for example, sugars can maintain proteins in their native states under conditions of extreme dehydration.
8. Water is the universal plasticizer; its low MW makes it effective as a "mobility enhancer".
9. Water is *not* bound. Aqueous mixtures are as homogeneous at T < Tg as they are at T > Tg. Unfrozen water is not unfreezable (provided that the right time scale is used [centuries]).
10. Estimation of shelf-life: determined by ΔT (T − Tg) and ΔW (W − Wg) (see below).

III. "Dry" Systems (operational definition), T ≪ Tg, Arrhenius kinetics

1. Conventional practice: water vapor sorption measurements and interpretation by means of isotherm models.
2. Sorption hysteresis implies non-equilibrium; Aw cannot be measured (see above).
3. Water is *not* an inert sorbate, and the substrate is *not* a uniform surface.
4. What is the significance of a measured isotherm, bearing in mind the assumptions of the sorption theory?
5. Calculated "monolayer" coverage values have no physical significance.
6. Shelf-life is determined by ΔT (see below); any correlation between a hypothetical monolayer coverage and shelf-life is due to the relative magnitude of ΔT at which the experiment is performed.

Based on these guidelines, the conference endorsed a recommendation of the dual concepts of water dynamics and glass dynamics, derived from the framework of the food polymer science approach, as the next step beyond "water activity" in the evolution of criteria for food quality, safety, and stability. An experimental approach was suggested for investigations of water/glass dynamics,[14,16] and this approach has undergone continued development and refinement since 1985. The current version is described below, in the context of the mobility map shown in Figure 115. This mobility map is conceptualized as a generic isogram for free volume and local viscosity. By analogy to an isotherm, an isogram is a representation of the measurement of some property under a constant condition, such that the resulting behavior of a system can be located on its mobility map, in terms of temperature and moisture content (always with time as the third dimension). Such a conceptual representation reminds us that an increase in temperature or moisture content, to a location above the domain between the solidus and glass curves, has an important effect on the mobility of the system, as reflected in various functional manifestations. ΔT and ΔW signify vectors of increasing mobility above the reference state defined by Tg and Wg. The mobility map in Figure 115, for a two-component glass-forming system of solute (e.g., a PHC) and solvent (water), both of which are crystallizable, demonstrates that the distance between Tm and Tg can vary dramatically, depending on the nature of the solute, as illustrated by the band of solute-water glass curves for specific PHC solutes with different values of dry Tg and consequent Tm/Tg ratios.

The experimental approach (based on WLF kinetics of partially crystalline polymer systems) suggested for investigations of (1) water dynamics to predict the quality and stability of intermediate moisture foods, and (2) glass dynamics to predict the quality and stability of low moisture foods, is as follows:

Measure Tg of anhydrous solute.

Measure Tg′ and Wg′ of freeze-concentrated glass.

Use literature value of −135°C for Tg of water.

Construct Tg(c) curve to define reference state for kinetic metastability ($\eta \simeq 10^{12}$ Pa s).

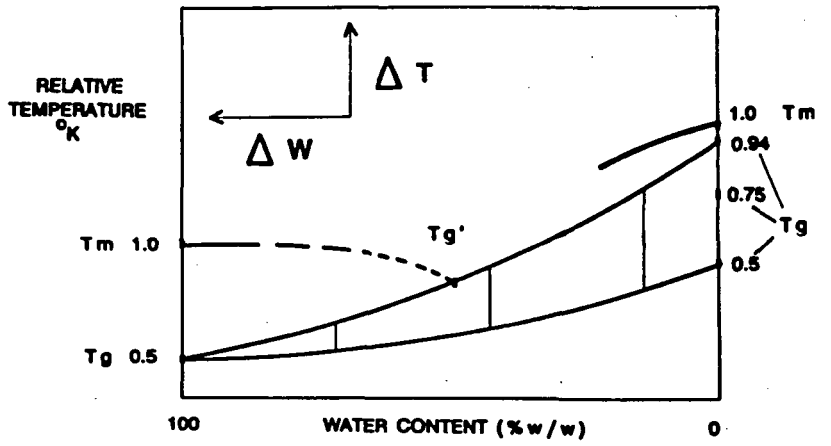

FIGURE 115. Mobility map as a generic isogram for free volume and local viscosity. Conceptualized in terms of a schematic state diagram of temperature vs. moisture content for a two-component glass-forming system of solute (e.g., a PHC) and solvent (water), both of which are crystallizable. The band of glass curves includes specific solutes with different values of dry Tg and consequent Tm/Tg ratios. ΔT and ΔW signify vectors of increasing mobility above the reference state defined by Tg and Wg.

Measure Tm/Tg to estimate departure from typical reference viscosity of $\eta \simeq 10^{12}$ Pa s. Then shelf-life depends on a combination of both ΔT and ΔW, where

$\Delta T = T - Tg$ for constant water content at $W < Wg'$
$\Delta W = W - Wg$ for any constant T at $W < Wg'$
$\Delta W = W - Wg$ for constant T at $W > Wg'$ and $T > Tg'$
$\Delta T = T - Tg'$ for $W > Wg'$
$\Delta W = W - Wg'$ for constant T at $W > Wg'$ and $T < Tg'$

For a convenient estimation of relative shelf-life, a composite vector can be constructed from the individual vectors for $\Delta T = T - Tg'$ and $\Delta W = W - Wg'$, as illustrated in Figure 115.
An alternative experimental approach (alluded to earlier, in the discussion of Figures 65 and 74), suggested when DSC instrumentation is not available, is as follows:

Document complete history of sample preparation.

Specify and control experimental conditions.

Measure non-equilibrium RH over broad range of temperature.

Measure non-equilibrium RH over several decades of time.

Measure total moisture content at one time point.

Measure sample weight gain/loss at every time point.

Calculate total moisture content at every time point.

Calculate total solids content (solute concentration) at every time point.

Calculate non-equilibrium RVP as non-equilibrium RH/100 at every time point.

Plot non-equilibrium RVP vs. total moisture for each temperature condition.

Construct two-dimensional mobility map of temperature vs. w% concentration, with iso-RVP contour lines as t/τ.

Construct three-dimensional mobility map of temperature vs. w% concentration vs. t/τ.

Recognize that the relative partial pressure of water vapor in the gas phase of the sample headspace (colloquially referred to as "Aw") is

certainly *not controlling* the mechanical relaxation rates and chemical reaction rates in the rubbery fluid phase or glassy solid phase of an aqueous sample matrix. Rather, the observed RVP is *controlled by* the temperature-moisture content location of the matrix relative to the location of its glass curve on the mobility map.

Recognize that liquid water as a plasticizer, which increases the mobility of a multicomponent supra-glassy matrix, is the key to understanding relaxation rates in restricted water environments.

As described in this review, the field of food science and technology has recently enjoyed a seemingly exponential growth of interest in glasses and glass transitions in foods and in the plasticizing effect of water on Tg. This spurt of interest stems from the growing realization of the importance of glassy and rubbery states to the quality, safety, and stability of foods. This state of affairs is evidenced by the fact that over 20% of the more than 400 references cited in this review were published in 1988, 1989, or 1990. In the decade of the 1990s, we expect to witness even greater growth and interest in this exciting subject area, because it offers so many challenging questions still to be answered, while promising so many opportunities for technological advancement.

GLOSSARY OF SYMBOLS AND ABBREVIATIONS

Å	Angstrom
ARR	Arrhenius
A-type	polymorphic crystalline form of starch
Ap	amylopectin
Aw	water activity
"Aw"	"water activity" (i.e., relative vapor pressure, p/p°)
a_T	WLF shift factor as a function of temperature
a_P	WLF shift factor as a function of plasticizer content
BET	Brunauer-Epstein-Teller
B-type	polymorphic crystalline form of starch
C	concentration
°C	degrees Centigrade
CMC	carboxymethyl cellulose
Ce	solute concentration at Te
Cg	solute concentration in an aqueous glass at its Tg
Cg′	solute concentration in an aqueous glass at its Tg′
Cp	heat capacity
ΔCp	change in heat capacity
C1, C2	coefficients in the WLF equation
cal	calorie
cm	centimeter
cP	centipoise
cps	cycles per second
D	diluent concentration
DE	dextrose equivalent
Dg	diluent concentration in a glass at its Tg
Dg′	diluent concentration in a glass at its Tg′
DM	dry matter
DMA	dynamic mechanical analysis
DMSO	dimethyl sulfoxide
DNA	deoxyribonucleic acid
DP	degree of polymerization
$\overline{DP}n$	number-average degree of polymerization
$\overline{DP}w$	weight-average degree of polymerization
DSC	differential scanning calorimetry
d	day
DTA	differential thermal analysis
d.b.	dry basis
d.s.	dry solids
EPR	electron paramagnetic resonance
e.g.,	for example
endo	endothermic
°F	degrees Farenheit
FW	freezable water
f	activity coefficient
G	Gibbs free energy
ΔG	change in Gibbs free energy
GAB	Guggenheim-Anderson-DeBoer
GHz	gigahertz
GR	growth rate

g	gram
H	enthalpy
ΔH	enthalpy change
HFCS	high fructose corn syrup
h	hydration number
h	hour
I	ionic strength
IMF	intermediate-moisture food
i.e.,	that is
J	Joule
J′	storage compliance
K	equilibrium dissociation constant
°K	degrees Kelvin
KHz	kilohertz
k	rate constant
kg	kilogram
kbar	1000 atmospheres pressure
$\log_{10}$	logarithm, base 10
ln	natural logarithm
M	molar concentration
MPa	megaPascal
MW	molecular weight
MWD	molecular weight distribution
$\overline{M}n$	number-average molecular weight
$\overline{M}w$	weight-average molecular weight
$\overline{M}n'$	number-average molecular weight of the solute-UFW glass at its Tg′
$\overline{M}w'$	weight-average molecular weight of the solute-UFW glass at its Tg′
$\overline{M}w/\overline{M}n$	polydispersity index
m	molal concentration
mcal	millicalorie
min	minute
mm	millimeter
N	normal concentration
NMR	nuclear magnetic resonance
NR	nucleation rate
n	number
nm	nanometer
ns	nanosecond
P	pressure
ΔP	plasticizer differential
Pa	Pascal
Pa s	Pascal second
PEG	poly(ethylene glycol)
PHC	polyhydroxy compound
PPG	poly(propylene glycol)
PVAc	poly(vinyl acetate)
PVC	poly(vinyl chloride)
PVP	poly(vinyl pyrrolidone)
p	vapor pressure
p°	vapor pressure of pure liquid water
pH	−log of the hydronium ion concentration in aqueous solution
pK	−log of the equilibrium dissociation constant
p/p°	relative vapor pressure
ps or psec	picosecond
Q_{10}	rate expression associated with Arrhenius kinetics
R	gas constant
R.H. or RH	relative humidity
% RH	percent relative humidity
RNase	ribonuclease
RT	room temperature
RVP	relative vapor pressure
r	linear correlation coefficient
S	solute
SHP	starch hydrolysis product
SSL	sodium stearoyl lactylate
s or sec	second
T	temperature
TADS	thermal analysis data station
% TM	percent total moisture
TMA	thermomechanical analysis
ΔT	temperature differential (e.g., T − Tg)
Ta	annealing temperature
Tam	"antemelting" transition temperature
Tc	collapse transition temperature
Tcr	crystallization temperature
Td	devitrification temperature
Te	eutectic melting temperature
Texp	experimental temperature
Tf	freezer temperature
Tfr	flow relaxation temperature
Tg	glass transition temperature
Tg′	subzero glass transition temperature of the amorphous solute/unfrozen water matrix surrounding the

	ice crystals in a maximally freeze-concentrated aqueous solution
Tg/Tm	ratio of Tg to Tm
Tgel	gelation temperature
Tgelat	gelatinization temperature
Th	homogeneous nucleation temperature
Th/Tm	ratio of Th to Tm
Tim	"incipient melting" temperature
Tliq	liquidus temperature
Tm	crystalline melting temperature
Tm/T	reduced temperature
Tm/Tg	ratio of Tm to Tg
Tm/Th	ratio of Tm to Th
Tr	recrystallization temperature
Ts	sorption temperature
Tsol	solidus temperature
Tsp	sticky point temperature
Tvap	vaporization temperature
t	time
UFW	unfrozen water
V	volume
V°	partial molar volume
V-type	polymorphic crystalline form of starch
vs.	versus
W	water content
ΔW	water content differential (e.g., W − Wg)
WBC	"water-binding capacity"
Wg	content of plasticizing water in an aqueous glass at its Tg
Wg′	content of plasticizing water in an aqueous glass at its Tg′
WLF	Williams-Landel-Ferry
Ws	water content at Ts
w	weight (or mass) fraction
w/w or w:w	composition of a mixture, expressed as a weight ratio
w% or wt%	weight percent concentration
w% C	weight percent concentration
x	mole fraction concentration
x_i	mole fraction concentration of component i
x_s	mole fraction concentration of solute
x_w	mole fraction concentration of water
η	viscosity
ηe	viscosity at Te
ηg	viscosity of a glass at its Tg
ηgel	viscosity at Tgel
ρ	density
μ	chemical potential
μ_i	chemical potential of component i
μ_w°	chemical potential of water
μcal	microcalorie
μm	micrometer
ρg	density of a glass at its Tg
ϕ	osmotic coefficient
Ψ	water potential
τ	relaxation time
τrot	rotational relaxation time
%	percent
=	equal to
≡	essentially identical to
~	about
≃	about equal to
>	greater than
<	less than
≥	greater than or equal to
≤	less than or equal to
≳	greater than about
≲	less than about
⩾	much greater than
⩽	much less than
/	per

ACKNOWLEDGMENTS

We thank F. Franks, C. van den Berg, T. H. Lilley, G. W. Gould, and K. Johnston, speakers at the 1985 Faraday Discussion Conference on Water Activity at Cambridge, for their important contributions to this review. We especially thank Professor Franks, whose lecture notes from a course on Moisture Management in Food Systems served as the basis for the material in Section II.A.

REFERENCES

1. **Scott, W. J.,** Water relations of food spoilage microorganisms, *Adv. Food Res.*, 7, 83, 1957.
2. **Franks, F.,** Water activity as a measure of biological viability and technological quality control, *Cereal Foods World*, 27, 403, 1982.
3. **Kuprianoff, J.,** Fundamental aspects of the dehydration of foodstuffs, in *Conference on Fundamental Aspects of the Dehydration of Foodstuffs*, Society of Chemical Industry, Aberdeen, 1958, 14.
4. **Franks, F.,** The properties of aqueous solutions at subzero temperatures, in *Water: A Comprehensive Treatise*, Vol. 7, Franks, F., Ed., Plenum Press, New York, 1982, 215.
5. **Franks, F.,** *Biophysics and Biochemistry at Low Temperatures*, Cambridge University Press, Cambridge, 1985.
6. **Franks, F.,** Complex aqueous systems at subzero temperatures, in *Properties of Water in Foods*, Simatos, D. and Multon, J. L., Eds., Martinus Nijhoff, Dordrecht, 1985, 497.
7. **Franks, F.,** Metastable water at subzero temperatures, *J. Microsc.*, 141, 243, 1986.
8. **Levine, H. and Slade, L.,** A polymer physicochemical approach to the study of commercial starch hydrolysis products (SHPs), *Carbohydr. Polym.*, 6, 213, 1986.
9. **Lilley, T. H.,** Water activity as a thermodynamic device; definitions and assumptions, presented at Faraday Division, Royal Society of Chemistry Discussion Conference — Water Activity: A Credible Measure of Technological Performance and Physiological Viability?, Cambridge, July 1-3, 1985, 1.
10. **Franks, F.,** Water activity and biochemistry — specific ionic and molecular effects, presented at Faraday Division, Royal Society of Chemistry Discussion Conference — Water Activity: A Credible Measure of Technological Performance and Physiological Viability?, Cambridge, July 1-3, 1985, 7.
11. **Gould, G. W.,** Complex dilute solutions. Osmoregulation: is the cell just a simple osmometer? The microbiological experience, presented at Faraday Division, Royal Society of Chemistry Discussion Conference, Water Activity: A Credible Measure of Technological Performance and Physiological Viability?, Cambridge, July 1-3, 1985, 11.
12. **van den Berg, C.,** On the significance of water activity in low moisture systems; water vapor sorption equilibrium and hysteresis; the starch/water system as a model, presented at Faraday Division, Royal Society of Chemistry Discussion Conference — Water Activity: A Credible Measure of Technological Performance and Physiological Viability?, Cambridge, July 1-3, 1985, 16.
13. **Johnston, K.,** Water-sorbent-solute relationships in dry food model systems, presented at Faraday Division, Royal Society of Chemistry Discussion Conference — Water Activity: A Credible Measure of Technological Performance and Physiological Viability?, Cambridge, July 1-3, 1985, 21.
14. **Slade, L. and Levine, H.,** Intermediate moisture systems; concentrated and supersaturated solutions; pastes and dispersions; water as plasticizer; the mystique of "bound" water; thermodynamics versus kinetics, presented at Faraday Division, Royal Society of Chemistry Discussion Conference — Water Activity: A Credible Measure of Technological Performance and Physiological Viability?, Cambridge, July 1-3, 1985, 24.
15. **Levine, H. and Slade, L.,** Water as a plasticizer: physico-chemical aspects of low-moisture polymeric systems, in *Water Science Reviews*, Vol. 3, Franks, F., Ed., Cambridge University Press, Cambridge, 1988, 79.
16. **Slade, L. and Levine, H.,** Structural stability of intermediate moisture foods — a new understanding?, in *Food Structure — Its Creation and Evaluation*, Mitchell, J. R. and Blanshard, J. M. V., Eds., Butterworths, London, 1988, 115.
17. **Slade, L. and Levine, H.,** Thermal analysis of starch and gelatin, in Proc. 13th NATAS Conf., McGhie, A. R., Ed., Philadelphia, 1984, 64.
18. **Slade, L.,** Starch properties in processed foods: staling of starch-based products, presented at AACC 69th Ann. Meet., Minneapolis, Sept. 30 to Oct. 4, 1984, Abstr. #112.
19. **Maurice, T. J., Slade, L., Page, C., and Sirett, R.,** Polysaccharide-water interactions — thermal behavior of rice starch, in *Properties of Water in Foods*, Simatos, D. and Multon, J. L., Eds., Martinus Nijhoff, Dordrecht, 1985, 211.
20. **Slade, L. and Levine, H.,** Recent advances in starch retrogradation, in *Industrial Polysaccharides — The Impact of Biotechnology and Advanced Methodologies*, Stivala, S. S., Crescenzi, V., and Dea, I. C. M., Eds., Gordon and Breach Science, New York, 1987, 387.
21. **Slade, L. and Levine, H.,** Non-equilibrium melting of native granular starch. I. Temperature location of the glass transition associated with gelatinization of A-type cereal starches, *Carbohydr. Polym.*, 8, 183, 1988.
22. **Slade, L. and Levine, H.,** A food polymer science approach to selected aspects of starch gelatinization and retrogradation, in *Frontiers in Carbohydrate Research-I: Food Applications*, Millane, R. P., BeMiller, J. N., and Chandrasekaran, R., Eds., Elsevier Applied Science, London, 1989, 215.
23. **Slade, L. and Levine, H.,** Thermal analysis of starch, in 1988 CRA Scientific Conf., Corn Refiners Assoc., Washington, D.C., 1988, 169.
24. **Slade, L. and Levine, H.,** Polymer-chemical properties of gelatin in foods, in *Advances in Meat Research, Vol. 4, Collagen as a Food*, Pearson, A. M., Dutson, T. R., and Bailey, A., Eds., AVI, Westport, 1987, 251.
25. **Slade, L., Levine, H., and Finley, J. W.,** Protein-

water interactions: water as a plasticizer of gluten and other protein polymers, in *Protein Quality and the Effects of Processing*, Phillips, D. and Finley, J. W., Eds., Marcel Dekker, New York, 1989, 9.
26. **Levine, H. and Slade, L.,** Influences of the glassy and rubbery states on the thermal, mechanical, and structural properties of doughs and baked products, in *Dough Rheology and Baked Product Texture: Theory and Practice*, Faridi, H. and Faubion, J. M., Eds., Van Nostrand Reinhold/AVI, New York, 1989, 157.
27. **Levine, H. and Slade, L.,** Collapse phenomena — a unifying concept for interpreting the behavior of low-moisture foods, in *Food Structure — Its Creation and Evaluation*, Mitchell, J. R. and Blanshard, J. M. V., Eds., Butterworths, London, 1988, 149.
28. **Levine, H. and Slade, L.,** Interpreting the behavior of low-moisture foods, in *Water and Food Quality*, Hardman, T. M., Ed., Elsevier Science, London, 1989, 71.
29. **Schenz, T. W., Rosolen, M. A., Levine, H., and Slade, L.,** DMA of frozen aqueous solutions, in Proc. 13th NATAS Conf., A. R. McGhie, Ed., Philadelphia, 1984, 57.
30. **Slade, L. and Levine, H.,** Non-equilibrium behavior of small carbohydrate-water systems, *Pure Appl. Chem.*, 60, 1841, 1988.
31. **Levine, H. and Slade, L.,** Thermomechanical properties of small carbohydrate-water glasses and "rubbers": kinetically metastable systems at subzero temperatures, *J. Chem. Soc. Faraday Trans. I*, 84, 2619, 1988.
32. **Levine, H. and Slade, L.,** Principles of cryostabilization technology from structure/property relationships of water-soluble food carbohydrates — a review, *Cryo.-Lett.*, 9, 21, 1988.
33. **Levine, H. and Slade, L.,** A food polymer science approach to the practice of cryostabilization technology, *Comments Agric. Food Chem.*, 1, 315, 1989.
34. **Levine, H. and Slade, L.,** Cryostabilization technology: thermoanalytical evaluation of food ingredients and systems, in *Thermal Analysis of Foods*, Ma, C.-Y. and Harwalkar, V. R., Eds., Elsevier Applied Science, London, 1990, 221.
35. **Biliaderis, C. G., Page, C. M., Slade, L., and Sirett, R. R.,** Thermal behavior of amylose-lipid complexes, *Carbohydr. Polym.*, 5, 367, 1985.
36. **Slade, L., Altomare, R., Oltzik, R., and Medcalf, D. G.,** Accelerated Staling of Starch-Based Food Products, U.S. Patent 4,657,770, 1987.
37. **Cole, B. A., Levine, H. I., McGuire, M. T., Nelson, K. J., and Slade, L.,** Soft, Frozen Dessert Formulation, U.S. Patent 4,374,154, 1983.
38. **Cole, B. A., Levine, H. I., McGuire, M. T., Nelson, K. J., and Slade, L.,** Soft, Frozen Dessert Formulation, U.S. Patent 4,452,824, 1984.
39. **Levine, H. and Slade, L.,** Response to the letter by Simatos, Blond, and Le Meste on the relation between glass transition and stability of a frozen product, *Cryo.-Lett.*, 10, 347, 1989.
40. **Franks, F.,** Improved freeze-drying: an analysis of the basic scientific principles, *Process Biochem.*, 24(1), R3, 1989.
41. **Franks, F.,** Freeze drying: from empiricism to predictability, *Cryo.-Lett.*, 11, 93, 1990.
42. **Franks, F. and Grigera, J. R.,** Solution properties of low molecular weight polyhydroxy compounds, in Water Science Reviews, Vol. 5, *The Molecules of Life*, F. Franks, Ed., Cambridge University Press, Cambridge, 1990, 187.
43. **van den Berg, C.,** Water activity, in *Concentration and Drying of Foods*, MacCarthy, D., Ed., Elsevier Applied Science, London, 1986, 11.
44. **White, G. W. and Cakebread, S. H.,** The glassy state in certain sugar-containing food products, *J. Food Technol.*, 1, 73, 1966.
45. **Ablett, S., Attenburrow, G. E., and Lillford, P. J.,** The significance of water in the baking process, in *Chemistry and Physics of Baking*, Blanshard, J. M. V., Frazier, P. J., Galliard, T., Eds., Royal Society of Chemistry, London, 1986, 30.
46. **Biliaderis, C. G., Page, C. M., Maurice, T. J., and Juliano, B. O.,** Thermal characterization of rice starches: a polymeric approach to phase transitions of granular starch, *J. Agric. Food Chem.*, 34, 6, 1986.
47. **Blanshard, J. M. V.,** The significance of the structure and function of the starch granule in baked products, in *Chemistry and Physics of Baking*, Blanshard, J. M. V., Frazier, P. J., and Galliard, T., Eds., Royal Society of Chemistry, London, 1986, 1.
48. **Blanshard, J. M. V.,** Starch granule structure and function: physicochemical approach, in *Starch: Properties and Potential*, Galliard, T., Ed., John Wiley & Sons, New York, 1987, 16.
49. **Blanshard, J. M. V.,** Elements of cereal product structure, in *Food Structure — Its Creation and Evaluation*, Blanshard, J. M. V. and Mitchell, J. R., Eds., Butterworths, London, 1988, 313.
50. **Blanshard, J. M. V. and Franks, F.,** Ice crystallization and its control in frozen food systems, in *Food Structure and Behaviour*, Blanshard, J. M. V. and Lillford, P., Eds., Academic Press, London, 1987, 51.
51. **Hoseney, R. C., Zeleznak, K., and Lai, C. S.,** Wheat gluten: a glassy polymer, *Cereal Chem.*, 63, 285, 1986.
52. **Yost, D. A. and Hoseney, R. C.,** Annealing and glass transition of starch, *Starke*, 38, 289, 1986.
53. **Zeleznak, K. J. and Hoseney, R. C.,** The glass transition in starch, *Cereal Chem.*, 64, 121, 1987.
54. **Karel, M.,** Effects of water activity and water content on mobility of food components, and their effects on phase transitions in food systems, in *Properties of Water in Foods*, Simatos, D. and Multon, J. L., Eds., Martinus Nijhoff, Dordrecht, 1985, 153.

55. **Karel, M.,** Control of lipid oxidation in dried foods, in *Concentration and Drying of Foods,* MacCarthy, D., Ed., Elsevier Applied Science, London, 1986, 37.
56. **Karel, M. and Langer, R.,** Controlled release of food additives, in *Flavor Encapsulation,* ACS Symp. Ser. 370, Risch, S. J. and Reineccius, G. A., Eds., American Chemical Society, Washington, D.C., 1988, 177.
57. **Simatos, D. and Karel, M.,** Characterizing condition of water in foods: physico-chemical aspects, in *Food Preservation by Moisture Control,* Seow, C. C., Ed., Elsevier Applied Science, London, 1988, 1.
58. **Lillford, P. J.,** The polymer/water relationship — its importance for food structure, in *Food Structure — Its Creation and Evaluation,* Blanshard, J. M. V. and Mitchell, J. R., Eds., Butterworths, London, 1988, 75.
59. **Orford, P. D., Parker, R., Ring, S. G., and Smith, A. C.,** The effect of water as a diluent on the glass transition behavior of malto-oligosaccharides, amylose and amylopectin, *Int. J. Biol. Macromol.,* 11, 91, 1989.
60. **Russell, P. L.,** Gelatinization of starches of different amylose/amylopectin content — DSC study, *J. Cereal Sci.,* 6, 133, 1987.
61. **Zobel, H. F.,** Starch crystal transformations and their industrial importance, *Starke,* 40, 1, 1988.
62. **van den Berg, C.,** Vapour Sorption Equilibria and Other Water-Starch Interactions: A Physicochemical Approach, Doctoral thesis, Agricultural University, Wageningen, 1981.
63. **Russell, P. L. and Oliver, G.,** The effect of pH and NaCl content on starch gel ageing, a study by DSC and rheology, *J. Cereal Sci.,* 10, 123, 1989.
64. **Karel, M.,** Role of water activity, in *Food Properties and Computer-Aided Engineering of Food Processing Systems,* Singh, R. P. and Medina, A. G., Eds., Kluwer, Dordrecht, 1989, 135.
65. **Lund, D. B.,** Starch gelatinization, in *Food Properties and Computer-Aided Engineering of Food Processing Systems,* Singh, R. P. and Medina, A. G., Eds., Kluwer, Dordrecht, 1989, 299.
66. **Roos, Y. and Karel, M.,** Plasticizing effect of water on thermal behavior and crystallization of amorphous food models, *J. Food Sci.,* 56, 38, 1991.
67. **Labuza, T. P. and Contreras-Medellin, R.,** Prediction of moisture protection requirements for foods, *Cereal Foods World,* 26, 335, 1981.
68. **Lewis, G. N. and Randall, M.,** *Thermodynamics,* 2nd ed., McGraw-Hill, New York, 1961.
69. **Levine, H.,** The value of a qualitative, conceptual approach to scientific understanding, *Cryo.-Lett.,* 9, 140, 1988.
70. **Labuza, T. P.,** Properties of water as related to the keeping quality of foods, in Proceedings 3rd International Conference Food Science and Technology, SOS 70, Institute Food Technologists, Washington, DC, 1970, 618.
71. **Lang, K. W.,** Physical, Chemical and Microbiological Characterization of Polymer and Solute Bound Water, Doctoral thesis, University of Illinois, 1981.
72. **Gould, G. W. and Christian, J. H. B.,** Characterization of the state of water in foods — biological aspects, in *Food Preservation by Moisture Control,* Seow, C. C., Ed., Elsevier Applied Science, London, 1988, 43.
73. **Mathlouthi, M., Larreta-Garde, V., Xu, Z. F., and Thomas, D.,** Solute-solvent and water activity of small carbohydrates: application to the study of enzyme stability in aqueous sugar solutions, *J. Carbohydr. Chem.,* 8, 233, 1989.
74. **Franks, F., Asquith, M. H., Hammond, C. C., Skaer, H. B., and Echlin, P.,** Polymeric cryoprotectants in the preservation of biological ultrastructure. I, *J. Microsc.,* 110, 223, 1977.
75. **Loncin, M.,** Basic principles of moisture equilibria, in *Freeze Drying and Advanced Food Technology,* Goldlith, S. A., Rey, L., and Rothmayr, W. W., Eds., Academic Press, New York, 1975, 599.
76. **Chirife, J., Favetto, G., and Fontan, C.,** The water activity of fructose solutions in the intermediate moisture range, *Lebensm.-Wiss. u.-Technol.,* 15, 159, 1982.
77. **Gould, G. W. and Measures, J. C.,** Water relations in single cells, *Phil. Trans. R. Soc. London B.,* 278, 151, 1977.
78. **Deodhar, S. and Luner, P.,** Measurement of bound (nonfreezing) water by DSC, in *Water in Polymers,* Rowland, S. P., Ed., ACS Symp. Ser. 127, American Chemical Society, Washington, DC, 1980, 273.
79. **van den Berg, C. and Bruin, S.,** Water activity and its estimation in food systems: theoretical aspects, in *Water Activity: Influences on Food Quality,* Rockland, L. B. and Stewart, G. F., Eds., Academic Press, New York, 1981, 1.
80. **Moy, P. and Karasz, F. E.,** The interactions of water with epoxy resins, in *Water in Polymers,* Rowland, S. P., Ed., ACS Symp. Ser. 127, American Chemical Society, Washington, DC, 1980, 505.
81. **Weisser, H.,** Influence of temperature on sorption equilibria, in *Properties of Water in Foods,* Simatos, D. and Multon, J. L., Eds., Martinus Nijhoff, Dordrecht, 1985, 95.
82. **Niediek, E. A.,** Effect of processing on the physical state and aroma sorption properties of carbohydrates, *Food Technol.,* 42(11), 81, 1988.
83. **Bizot, H., Buleon, A., Mouhoud-Riou, N., and Multon, J. L.,** Water vapor sorption hysteresis in potato starch, in *Properties of Water in Foods,* Simatos, D. and Multon, J. L., Eds., Martinus Nijhoff, Dordrecht, 1985, 83.
84. **Rupley, J. A., Gratton, E., and Careri, G.,** *Trends Biochem. Sci.,* p. 18, 1983.
85. **Franks, F.,** Protein hydration, in *Characterization of Proteins,* Franks, F., Ed., Humana Press, Clifton, NJ, 1988, 127.
86. **Bone, S. and Pethig, R.,** Dielectric studies of the

binding of water to lysozyme, *J. Mol. Biol.*, 157, 571, 1982.
87. **Morozov, V. N., Morozova, T. Y., Kachalova, G. S., and Myachin, E. T.,** Interpretation of water desorption isotherms of lysozyme, *Int. J. Biol. Macromol.*, 10, 329, 1988.
88. **Edwards, S. F., Lillford, P. J., and Blanshard, J. M. V.,** Gels and networks in practice and theory, in *Food Structure and Behaviour*, Blanshard, J. M. V. and Lillford, P., Eds., Academic Press, London, 1987, 1.
89. **Soesanto, T. and Williams, M. C.,** Volumetric interpretation of viscosity for concentrated and dilute sugar solutions, *J. Phys. Chem.*, 85, 3338, 1981.
90. **Atkins, A. G.,** Basic principles of mechanical failure in biological systems, in *Food Structure and Behaviour*, Blanshard, J. M. V. and Lillford, P., Eds., Academic Press, London, 1987, 149.
91. **Quinquenet, S., Grabielle-Madelmont, C., Ollivon, M., and Serpelloni, M.,** Influence of water on pure sorbitol polymorphism, *J. Chem. Soc., Faraday Trans. I*, 84, 2609, 1988.
92. **Ring, S. G., Colonna, P., l'Anson, K. J., Kalichevsky, M. T., Miles, M. J., Morris, V. J., and Orford, P. D.,** Gelation and crystallization of amylopectin, *Carbohydr. Res.*, 162, 277, 1987.
93. **Zobel, H. F., Young, S. N., and Rocca, L. A.,** Starch gelatinization: an X-ray diffraction study, *Cereal Chem.*, 65, 443, 1988.
94. **Marsh, R. D. L. and Blanshard, J. M. V.,** The application of polymer crystal growth theory to the kinetics of formation of the B-amylose polymorph in a 50% wheat starch gel, *Carbohydr. Polym.*, 9, 301, 1988.
95. **Zeleznak, K. J. and Hoseney, R. C.,** Characterization of starch from bread aged at different temperatures, *Starke*, 39, 231, 1987.
96. **Doescher, L. C., Hoseney, R. C., and Milliken, G. A.,** Mechanism for cookie dough setting, *Cereal Chem.*, 64, 158, 1987.
97. **Attenburrow, G. E., Goodband, R. M., Taylor, L. J., and Lillford, P. J.,** Structure, mechanics, and texture of a food sponge, *J. Cereal Sci.*, 9, 61, 1989.
98. **Simatos, D., Blond, G., and Le Meste, M.,** Relation between glass transition and stability of a frozen product, *Cryo.-Lett.*, 10, 77, 1989.
99. **Fujio, Y. and Lim, J. K.,** Correlation between the glass-transition point and color change of heat-treated gluten, *Cereal Chem.*, 66, 268, 1989.
100. **Flory, P. J.,** *Principles of Polymer Chemistry*, Cornell University Press, Ithaca, 1953.
101. **Williams, M. L., Landel, R. F., and Ferry, J. D.,** Temperature dependence of relaxation mechanisms in amorphous polymers and other glass-forming liquids, *J. Am. Chem. Soc.*, 77, 3701, 1955.
102. **Brydson, J. A.,** The glass transition, melting point and structure, in *Polymer Science*, Jenkins, A. D., Ed., North-Holland, Amsterdam, 1972, 194.
103. **Wunderlich, B.,** *Macromolecular Physics, Vol. 1, Crystal Structure, Morphology, Defects*, Academic Press, New York, 1973.
104. **Wunderlich, B.,** *Macromolecular Physics, Vol. 2, Crystal Nucleation, Growth, Annealing*, Academic Press, New York, 1976.
105. **Wunderlich, B.,** *Macromolecular Physics, Vol. 3, Crystal Melting*, Academic Press, New York, 1980.
106. **Wunderlich, B.,** The basis of thermal analysis, in *Thermal Characterization of Polymeric Materials*, Turi, E. A., Ed., Academic Press, Orlando, 1981, 91.
107. **Ferry, J. D.,** *Viscoelastic Properties of Polymers*, 3rd ed., John Wiley & Sons, New York, 1980.
108. **Rowland, S. P.,** *Water in Polymers*, ACS Symp. Ser. 127, American Chemical Society, Washington, DC, 1980.
109. **Sears, J. K. and Darby, J. R.,** The Technology of Plasticizers, Wiley-Interscience, New York, 1982.
110. **Eisenberg, A.,** The glassy state and the glass transition, in *Physical Properties of Polymers*, Mark, J. E., Eisenberg, A., Graessley, W. W., Mandelkern, L., and Koenig, J. L., Eds., American Chemical Society, Washington, DC, 1984, 55.
111. **Ellis, T. S.,** Moisture-induced plasticization of amorphous polyamides and their blends, *J. Appl. Polym. Sci.*, 36, 451, 1988.
112. **Graessley, W. W.,** Viscoelasticity and flow in polymer melts and concentrated solutions, in *Physical Properties of Polymers*, Mark, J. E., Eisenberg, A., Graessley, W. W., Mandelkern, L., and Koenig, J. L., Eds., American Chemical Society, Washington, DC, 1984, 97.
113. **Billmeyer, F. W.,** *Textbook of Polymer Science*, 3rd ed., Wiley-Interscience, New York, 1984.
114. **Sperling, L. H.,** *Introduction to Physical Polymer Science*, Wiley-Interscience, New York, 1986.
115. **Walton, A. G.,** Nucleation in liquids and solutions, in *Nucleation*, Zettlemoyer, A. C., Ed., Marcel Dekker, New York, 1969, 225.
116. **Cowie, J. M. G.,** *Polymers: Chemistry and Physics of Modern Materials*, Intertext, New York, 1973.
117. **Turi, E. A.,** *Thermal Characterization of Polymeric Materials*, Academic Press, Orlando, 1981.
118. **Haward, R. N.,** *The Physics of Glassy Polymers*, Applied Science, London, 1973.
119. **Kauzmann, W.,** Nature of the glassy state and behavior of liquids at low temperatures, *Chem. Rev.*, 43, 219, 1948.
120. **Petrie, S. E. B.,** The problem of thermodynamic equilibrium in glassy polymers, in *Polymeric Materials: Relationships Between Structure and Mechanical Behavior*, Baer, E. and Radcliffe, S. V., Eds., American Society Metals, Metals Park, Ohio, 1975, 55.
121. **Buchanan, D. R. and Walters, J. P.,** Glass-transition temperatures of polyamide textile fibers. I. Effect of water, *Textile Res. J.*, 47, 398, 1977.
122. **Sharples, A.,** Crystallinity, in *Polymer Science*, Jen-

kins, A. D., Ed., North-Holland, Amsterdam, 1972, 251.
123. **BeMiller, J. N.,** as reported by M. A. Hill, *Carbohydr. Polym.*, 10, 64, 1989.
124. **Finegold, L., Franks, F., and Hatley, R. H. M.,** Glass/rubber transitions and heat capacities of binary sugar blends, *J. Chem. Soc. Faraday Trans. I*, 85, 2945, 1989.
125. **Roos, Y.,** Effect of moisture on the thermal behavior of strawberries studied using DSC, *J. Food Sci.*, 52, 146, 1987.
126. **Paakkonen, K. and Roos, Y. H.,** Effects of drying conditions on water sorption and phase transitions of freeze-dried horseradish roots, *J. Food Sci.*, 55, 206, 1990.
127. **Fuzek, J. F.,** Glass transition temperature of wet fibers: its measurement and significance, in *Water in Polymers*, Rowland, S. P., Ed., ACS Symp. Ser. 127, American Chemical Society, Washington, DC, 1980, 515.
128. **Ma, C. Y. and Harwalkar, V. R.,** *Thermal Analysis of Foods*, Elsevier Applied Science, London, 1990.
129. **Kelley, S. S., Rials, T. G., and Glasser, W. G.,** Relaxation behavior of the amorphous components of wood, *J. Materials Sci.*, 22, 617, 1987.
130. **Kakivaya, S. R. and Hoeve, C. A. J.,** The glass transition of elastin, *Proc. Natl. Acad. Sci. U.S.A.*, 72, 3505, 1975.
131. **Hoeve, C. A. J. and Hoeve, M. B. J. A.,** The glass point of elastin as a function of diluent concentration, *Organ. Coat. Plast. Chem.*, 39, 441, 1978.
132. **Scandola, M., Ceccorulli, G., and Pizzoli, M.,** Water clusters in elastin, *Int. J. Biol. Macromol.*, 3, 147, 1981.
133. **MacKenzie, A. P.,** Non-equilibrium freezing behavior of aqueous systems, *Phil. Trans. R. Soc. London B*, 278, 167, 1977.
134. **Sichina, W. J.,** Predicting mechanical performance and lifetime of polymeric materials, *Am. Lab.*, 20(1), 42, 1988.
135. **MacKenzie, A. P.,** Collapse during freeze drying — qualitative and quantitative aspects, in *Freeze Drying and Advanced Food Technology*, Goldlith, S. A., Rey, L., and Rothmayr, W. W., Eds., Academic Press, New York, 1975, 277.
136. **To, E. C. and Flink, J. M.,** "Collapse", a structural transition in freeze dried carbohydrates. I, II, III, *J. Food Technol.*, 13, 551, 1978.
137. **Flink, J. M.,** Structure and structure transitions in dried carbohydrate materials, in *Physical Properties of Foods*, Peleg, M. and Bagley, E. B., Eds., AVI, Westport, 1983, 473.
138. **Karel, M. and Flink, J. M.,** Some recent developments in food dehydration research, in *Advances in Drying*, Mujumdar, A. S., Ed., Vol. 2, Hemisphere, Washington, 1983, 103.
139. **Jolley, J. E.,** The microstructure of photographic gelatin binders, *Photog. Sci. Eng.*, 14, 169, 1970.
140. **Mitchell, J. R.,** The rheology of gels, *J. Text. Stud.*, 11, 315, 1980.
141. **Marsh, K. S. and Wagner, J.,** Predict Shelf Life, *Food Eng.*, 57(8), 58, 1985.
142. **Shalaby, S. W.,** Thermoplastic Polymers, in *Thermal Characterization of Polymeric Materials*, Turi, E. A., Ed., Academic Press, Orlando, 1981, 235.
143. **Mayer, E.,** Hyperquenching of water and dilute aqueous solutions into their glassy states: an approach to cryofixation, *Cryo.-Lett.*, 9, 66, 1988.
144. **Ellis, T. S., Jin, X., and Karasz, F. E.,** The water induced plasticization behavior of semi-crystalline polyamides, *Polym. Prep.*, 25(2), 197, 1984.
145. **Jin, X., Ellis, T. S., and Karasz, F. E.,** The effect of crystallinity and crosslinking on the depression of the glass transition temperature in nylon 6 by water, *J. Polym. Sci.: Polym. Phys. Edn.*, 22, 1701, 1984.
146. **Boyer, R. F., Baer, E., and Hiltner, A.,** Concerning gelation effects in atactic polystyrene solutions, *Macromolecules*, 18, 427, 1985.
147. **Bair, H. E.,** Thermal analysis of additives in polymers, in *Thermal Characterization of Polymeric Materials*, Turi, E. A., Ed., Academic Press, Orlando, 1981, 845.
148. **Hardy, G., Cser, F., and Takacs, E.,** Investigation of the binary system of a crystalline monomer and its polymer, *J. Polym. Sci.:* Symp. No. 42, 663, 1973.
149. **Franks, F.,** Solute-water interactions: do polyhydroxy compounds alter the properties of water?, *Cryobiology*, 20, 335, 1983.
150. **Franks, F.,** Bound water: fact and fiction, *Cryo.-Lett.*, 4, 73, 1983.
151. **Labuza, T. P.,** Water binding of humectants, in *Properties of Water in Foods*, Simatos, D. and Multon, J. L., Eds., Martinus Nijhoff, Dordrecht, 1985, 421.
152. **Wynne-Jones, S. and Blanshard, J. M. V.,** Hydration studies of wheat starch, amylopectin, amylose gels and bread by proton magnetic resonance, *Carbohydr. Polym.*, 6, 289, 1986.
153. **French, D.,** Organization of starch granules, in *Starch: Chemistry and Technology*, Whistler, R. L., BeMiller, J. N., and Paschall, E. F., Eds., 2nd ed., Academic Press, Orlando, 1984, 183.
154. **Imberty, A. and Perez, S.,** A revisit to the three-dimensional structure of B-type starch, *Biopolymers*, 27, 1205, 1988.
155. **Starkweather, H. W.,** Water in nylon, in *Water in Polymers*, Rowland, S. P., Ed., ACS Symp. Ser. 127, American Chemical Society, Washington, DC, 1980, 433.
156. **Gaeta, S., Apicella, A., and Hopfenberg, H. B.,** Kinetics and equilibria associated with the absorption and desorption of water and lithium chloride in an ethylene-vinyl alcohol copolymer, *J. Membrane Sci.*, 12, 195, 1982.
157. **Murthy, N. S., Stamm, M., Sibilia, J. P., and**

Krimm, S., Structural changes accompanying hydration in nylon 6, *Macromolecules,* 22, 1261, 1989.
158. **Kuge, T. and Kitamura, S.,** Annealing of starch granules — warm water treatment and heat-moisture treatment, *J. Jpn. Soc. Starch Sci.,* 32, 65, 1985.
159. **Aguerre, R. J., Suarez, C., and Viollaz, P. E.,** Swelling and pore structure in starchy materials, *J. Food Engn.,* 9, 71, 1989.
160. **Juliano, B. O.,** Properties of rice starch in relation to varietal differences in processing characteristics of rice grain, *J. Jpn. Soc. Starch Sci.,* 29, 305, 1982.
161. **Lelievre, J.,** Theory of gelatinization in a starch-water-solute system, *Polymer,* 17, 854, 1976.
162. **Franks, F.,** Nucleation: a maligned and misunderstood concept, *Cryo.-Lett.,* 8, 53, 1987.
163. **Biros, J., Madan, R. L., and Pouchly, J.,** Heat capacity of water-swollen polymers above and below 0°C, *Collect. Czech. Chem. Commun.,* 44, 3566, 1979.
164. **Pouchly, J., Biros, J., and Benes, S.,** Heat capacities of water-swollen hydrophilic polymers above and below 0°C, *Makromol. Chem.,* 180, 745, 1979.
165. **Pouchly, J., Benes, S., Masa, Z., and Biros, J.,** Sorption of water in hydrophilic polymers, *Makromol. Chem.,* 183, 1565, 1982.
166. **Pouchly, J. and Biros, J.,** Comments on the interpretation of thermodynamic data on swollen hydrogels, *Polym. Bull.,* 19, 513, 1988.
167. **Derbyshire, W.,** Dynamics of water in heterogeneous systems with emphasis on subzero temperatures, in *Water: A Comprehensive Treatise,* Franks, F., Ed., Vol. 7, Plenum Press, New York, 1982, 339.
168. **Hoeve, C. A. J.,** The structure of water in polymers, in *Water in Polymers,* Rowland, S. P., Ed., ACS Symp. Ser. 127, American Chemical Society, Washington, DC, 1980, 135.
169. **Burghoff, H. G. and Pusch, W.,** Thermodynamic state of water in cellulose acetate membranes, *Polym. Eng. Sci.,* 20, 305, 1980.
170. **Mashimo, S., Kuwabara, S., Yagihara, S., and Higasi, K.,** Dielectric relaxation time and structure of bound water in biological materials, *J. Phys. Chem.,* 91, 6337, 1987.
171. **Labuza, T. P.,** Fiber's water binding capacity, *Cereal Foods World,* 34, 566, 1989.
172. **Angell, C. A.,** Perspective on the glass transition, *J. Phys. Chem. Solids,* 49, 863, 1988.
173. **Roberts, G. E. and White, E. F. T.,** Relaxation processes in amorphous polymers, in *The Physics of Glassy Polymers,* Haward, R. N., Ed., Applied Science, London, 1973, 153.
174. **Johari, G. P., Hallbrucker, A., and Mayer, E.,** Thermal behavior of several hyperquenched organic glasses, *J. Phys. Chem.,* 93, 2648, 1989.
175. **Morozov, V. N. and Gevorkian, S. G.,** Low-temperature glass transition in proteins, *Biopolymers,* 24, 1785, 1985.
176. **Chan, R. K., Pathmanathan, K., and Johari, G. P.,** Dielectric relaxations in the liquid and glassy states of glucose and its water mixtures, *J. Phys. Chem.,* 90, 6358, 1986.
177. **Matsuoka, S., Williams, G., Johnson, G. E., Anderson, E. W., and Furukawa, T.,** Phenomenological relationship between dielectric relaxation and thermodynamic recovery processes near the glass transition, *Macromolecules,* 18, 2652, 1985.
178. **Borchard, W., Bremer, W., and Keese, A.,** State diagram of the water-gelatin system, *Colloid Polym. Sci.,* 258, 516, 1980.
179. **Tomka, I., Bohonek, J., Spuhler, A., and Ribeaud, M.,** Structure and formation of the gelatin gel, *J. Photogr. Sci.,* 23, 97, 1975.
180. **Yannas, I. V.,** Collagen and gelatin in the solid state, *J. Macromol. Sci.-Revs. Macromol. Chem.,* C7, 49, 1972.
181. **Wesson, J. A., Takezoe, H., Yu, H., and Chen, S. P.,** Dye diffusion in swollen gels by forced Rayleigh scattering, *J. Appl. Phys.,* 53, 6513, 1982.
182. **Robertson, R. E.,** Segmental mobility in the equilibrium liquid below the glass transition, *Macromolecules,* 18, 953, 1985.
183. **Cheng, S. Z. D.,** Thermal characterization of macromolecules, *J. Appl. Polym. Sci.: Appl. Polym. Symp.,* 43, 315, 1989.
184. **Johnson, G. E., Bair, H. E., Matsuoka, S., Anderson, E. W., and Scott, J. E.,** Water sorption and its effects on a polymer's dielectric behavior, in *Water in Polymers,* Rowland, S. P., Ed., ACS Symp. Ser. 127, American Chemical Society, Washington, DC, 1980, 451.
185. **Franks, F.,** Biophysics and biochemistry of low temperatures and freezing, in *Effects of Low Temperatures on Biological Membranes,* Morris, G. J. and Clarke, A., Eds., Academic Press, London, 1981, 3.
186. **Bengtzelius, U. and Sjolander, A.,** Glass transitions in hard sphere and Lennard-Jones fluids, in *Conference on Dynamic Aspects of Structural Change in Liquids and Glasses,* New York Academy of Sciences, New York, Dec. 1-3, 1986, Abstr. #16.
187. **Cantor, C. R. and Schimmel, P. R.,** *Biophysical Chemistry. I. The Conformation of Biological Macromolecules,* W. H. Freeman, San Francisco, 1980.
188. **Van Holde, K. E.,** *Physical Biochemistry,* Prentice-Hall, Englewood Cliffs, New Jersey, 1971.
189. **Hofer, K., Hallbrucker, A., Mayer, E., and Johari, G. P.,** Vitrified dilute aqueous solutions. III. Plasticization of water's H-bonded network and the glass transition temperature's minimum, *J. Phys. Chem.,* 93, 4674, 1989.
190. **Pikal, M. J. and Shah, S.,** The collapse temperature in freeze drying: dependence on measurement methodology and rate of water removal from the glassy phase, *Int. J. Pharm.,* 62, 165, 1990.
191. **Angell, C. A.,** Supercooled water, *Ann. Rev. Phys. Chem.,* 34, 593, 1983.
192. **Baro, M. D., Clavaguera, N., Bordas, S.,**

Clavaguera-Mora, M. T., and Casa-Vazquez, J., Evaluation of crystallization kinetics by DTA, *J. Thermal Anal.*, 11, 271, 1977.
193. **Phillips, A. J., Yarwood, R. J., and Collett, J. H.,** Thermal analysis of freeze-dried products, *Anal. Proceed.*, 23, 394, 1986.
194. **Hiltner, A. and Baer, E.,** Reversible gelation of macromolecular systems, *Polym. Prep.*, 27(1), 207, 1986.
195. **Domszy, R. C., Alamo, R., Edwards, C. O., and Mandelkern, L.,** Thermoreversible gelation and crystallization of homopolymers and copolymers, *Macromolecules*, 19, 310, 1986.
196. **Mandelkern, L.,** Thermoreversible gelation and crystallization from solution, *Polym. Prep.*, 27(1), 206, 1986.
197. **Flory, P. J.,** Introductory lecture — gels and gelling processes, *Faraday Disc. Chem. Soc.*, 57, 7, 1974.
198. **Burchard, W.,** Entanglement and reversible gelation for polymers of different architectures, *Prog. Colloid Polym. Sci.*, 78, 63, 1988.
199. **Blum, F. D. and Nagara, B.,** Solvent mobility in gels of atactic polystyrene, *Polym. Prep.*, 27(1), 211, 1986.
200. **Tait, M. J., Suggett, A., Franks, F., Ablett, S., and Quickenden, P. A.,** Hydration of monosaccharides: study by dielectric and NMR, *J. Solution Chem.*, 1, 131, 1972.
201. **Franks, F., Reid, D. S., and Suggett, A.,** Conformation and hydration of sugars and related compounds in dilute aqueous solution, *J. Solution Chem.*, 2, 99, 1973.
202. **Suggett, A. and Clark, A. H.,** Molecular motion and interactions in aqueous carbohydrate solutions. I. Dielectric relaxation studies, *J. Solution Chem.*, 5, 1, 1976.
203. **Suggett, A., Ablett, S., and Lillford, P. J.,** Molecular motion and interactions in aqueous carbohydrate solutions. II. NMR studies, *J. Solution Chem.*, 5, 17, 1976.
204. **Suggett, A.,** Molecular motion and interactions in aqueous carbohydrate solutions. III. A combined NMR and dielectric relaxation strategy, *J. Solution Chem.*, 5, 33, 1976.
205. **Keinath, S. E. and Boyer, R. F.,** Thermomechanical analysis of Tg and T > Tg transitions in polystyrene, *J. Appl. Polym. Sci.*, 26, 2077, 1981.
206. **Marshall, A. S. and Petrie, S. E. B.,** Thermal transitions in gelatin and aqueous gelatin solutions, *J. Photogr. Sci.*, 28, 128, 1980.
207. **Atwell, W. A., Hood, L. F., Lineback, D. R., Varriano-Marston, E., and Zobel, H. F.,** Terminology and methodology associated with basic starch phenomena, *Cereal Foods World*, 33, 306, 1988.
208. **Bloksma, A. H.,** Rheological aspects of structural changes during baking, in *Chemistry and Physics of Baking*, Blanshard, J. M. V., Frazier, P. J., and Galliard, T., Eds., Royal Society of Chemistry, London, 1986, 170.
209. **Bloksma, A. H. and Bushuk, W.,** Rheology and chemistry of dough, in *Wheat Science and Technology*, 3rd ed., Pomeranz, Y., Ed., Vol. II, American Association of Cereal Chemists, St. Paul, Minn., 1988, 131.
210. **Hoseney, R. C.,** Component interaction during heating and storage of baked products, in *Chemistry and Physics of Baking*, Blanshard, J. M. V., Frazier, P. J., and Galliard, T., Eds., Royal Society of Chemistry, London, 1986, 216.
211. **Miles, M. J., Morris, V. J., and Ring, S. G.,** Gelation of amylose, *Carbohydr. Res.*, 135, 257, 1985.
212. **Gidley, M. J. and Bulpin, P. V.,** Aggregation of amylose in aqueous systems: the effect of chain length on phase behavior and aggregation kinetics, *Macromolecules*, 22, 341, 1989.
213. **Clark, A. H., Gidley, M. J., Richardson, R. K., and Ross-Murphy, S. B.,** Rheological studies of aqueous amylose gels: the effect of chain length and concentration on gel modulus, *Macromolecules*, 22, 346, 1989.
214. **Gidley, M. J.,** Molecular mechanisms underlying amylose aggregation and gelation, *Macromolecules*, 22, 351, 1989.
215. **Miles, M. J., Morris, V. J., Orford, P. D., and Ring, S. G.,** Roles of amylose and amylopectin in gelation and retrogradation of starch, *Carbohydr. Res.*, 135, 271, 1985.
216. **Ring, S. G.,** Observations on crystallization of amylopectin from aqueous solution, *Int. J. Biol. Macromol.*, 7, 253, 1985.
217. **Ring, S. G.,** Studies on starch gelation, *Starke*, 37, 80, 1985.
218. **Ring, S. G. and Orford, P. D.,** Recent observations on retrogradation of amylopectin, in *Gums and Stabilizers for the Food Industry 3*, Phillips, G. O., Wedlock, D. J., and Williams, P. A., Eds., Elsevier Applied Science, London, 1986, 159.
219. **Russell, P. L.,** Aging of gels from starches of different amylose/amylopectin content studied by DSC, *J. Cereal Sci.*, 6, 147, 1987.
220. **l'Anson, K. J., Miles, M. J., Morris, V. J., Ring, S. G., and Nave, C.,** Study of amylose gelation using synchrotron X-ray source, *Carbohydr. Polym.*, 8, 45, 1988.
221. **Mestres, C., Colonna, P., and Buleon, A.,** Gelation and crystallization of maize starch after pasting, drum-drying, or extrusion cooking, *J. Cereal Sci.*, 7, 123, 1988.
222. **Reid, D. S. and Charoenrein, S.,** DSC studies of starch-water interaction in gelatinization process, in *Proceedings 14th NATAS Conference*, NATAS, San Francisco, 1985, 335.
223. **Chungcharoen, A. and Lund, D. B.,** Influence of solutes and water on rice starch gelatinization, *Cereal Chem.*, 64, 240, 1987.
224. **Burros, B. C., Young, L. A., and Carroad, P. A.,** Kinetics of corn meal gelatinization at high temper-

ature and low moisture, *J. Food Sci.*, 52, 1372, 1987.
225. **Paton, D.,** DSC of oat starch pastes, *Cereal Chem.*, 64, 394, 1987.
226. **Donovan, J. W.,** Phase transitions of the starch-water system, *Biopolymers*, 18, 263, 1979.
227. **Biliaderis, C. G., Maurice, T. J., and Vose, J. R.,** Starch gelatinization phenomena studied by DSC, *J. Food Sci.*, 45, 1669, 1980.
228. **Cheng, S. Z. D. and Wunderlich, B.,** Glass transition and melting behavior of poly(oxy-2,6-dimethyl-1,4-phenylene), *Macromolecules*, 20, 1630, 1987.
229. **Blanshard, J. M. V.,** Physicochemical aspects of starch gelatinization, in *Polysaccharides in Food*, Blanshard, J. M. V. and Mitchell, J. R., Eds., Butterworths, London, 1979, 139.
230. **Lund, D. B.,** Influence of time, temperature, moisture, ingredients, and processing conditions on starch gelatinization, *Crit. Rev. Food Sci. Nutr.*, 20, 249, 1984.
231. **Alfonso, G. C. and Russell, T. P.,** Kinetics of crystallization in semicrystalline/amorphous polymer mixtures, *Macromolecules*, 19, 1143, 1986.
232. **Jankowski, T. and Rha, C. K.,** Retrogradation of starch in cooked wheat, *Starke*, 38, 6, 1986.
233. **Kulp, K. and Ponte, J. G.,** Staling of white pan bread: fundamental causes, *Crit. Rev. Food Sci. Nutr.*, 15, 1, 1981.
234. **Flory, P. J. and Weaver, E. S.,** Phase transitions in collagen and gelatin systems, *J. Am. Chem. Soc.*, 82, 4518, 1960.
235. **Nakazawa, F., Noguchi, S., Takahashi, J., and Takada, M.,** Retrogradation of gelatinized potato starch studied by DSC, *Agric. Biol. Chem.*, 49, 953, 1985.
236. **Gidley, M. J.,** Factors affecting crystalline type of native starches and model materials, *Carbohydr. Res.*, 161, 301, 1987.
237. **Gidley, M. J. and Bulpin, P. V.,** Crystallization of maltaoses as models of the crystalline forms of starch, *Carbohydr. Res.*, 161, 291, 1987.
238. **Guilbot, A. and Godon, B.,** Le pain rassis, *Cah. Nut. Diet.*, 19, 171, 1984.
239. **Ferry, J. D.,** Mechanical properties of substances of high molecular weight, *J. Am. Chem. Soc.*, 70, 2244, 1948.
240. **Luyet, B.,** On various phase transitions occurring in aqueous solutions at low temperatures, *Ann. NY Acad. Sci.*, 85, 549, 1960.
241. **Rasmussen, D. and Luyet, B.,** Complementary study of some non-equilibrium phase transitions in frozen solutions of glycerol, ethylene glycol, glucose and sucrose, *Biodynamica*, 10, 319, 1969.
242. **MacKenzie, A. P. and Rasmussen, D. H.,** Interactions in the water-PVP system at low temperatures, in *Water Structure at the Water-Polymer Interface*, Jellinek, H. H. G., Ed., Plenum Press, New York, 1972, 146.
243. **Vassoille, R., El Hachadi, A., and Vigier, G.,** Study by internal friction measurements of vitreous transition in aqueous propylene glycol solutions, *Cryo.-Lett.*, 7, 305, 1986.
244. **MacFarlane, D. R.,** Anomalous glass transitions in aqueous propylene glycol solutions, *Cryo.-Lett.*, 6, 313, 1985.
245. **Boutron, P. and Kaufmann, A.,** Stability of the amorphous state in the water-propylene glycol system, *Cryobiology*, 16, 557, 1979.
246. **Bohon, R. L. and Conway, W. T.,** DTA studies on the glycerol-water system, *Thermochim. Acta*, 4, 321, 1972.
247. **Kanno, H.,** Double glass transitions in aqueous lithium chloride solutions vitrified at high pressures, *J. Phys. Chem.*, 91, 1967, 1987.
248. **Kanno, H., Shimada, K., and Katoh, T.,** A glass formation study of aqueous tetraalkylammonium halide solutions, *J. Phys. Chem.*, 93, 4981, 1989.
249. **Vrentas, J. S. and Hou, A. C.,** History dependence of diffusion coefficients for glassy polymer-penetrant systems, *J. Appl. Polym. Sci.*, 36, 1933, 1988.
250. **Aras, L. and Richardson, M. J.,** The glass transition behavior and thermodynamic properties of amorphous polystyrene, *Polymer*, 30, 2246, 1989.
251. **Fahy, G. M., Levy, D. I., and Ali, S. E.,** Some emerging principles underlying the physical properties, biological actions, and utility of vitrification solutions, *Cryobiology*, 24, 196, 1987.
252. **Simatos, D., Faure, M., Bonjour, E., and Couach, M.,** DTA and DSC in the study of water in foods, in *Water Relations of Foods*, Duckworth, R. B., Ed., Academic Press, New York, 1975, 193.
253. **Simatos, D., Faure, M., Bonjour, E., and Couach, M.,** Physical state of water at low temperatures in plasma — DTA and DSC, *Cryobiology*, 12, 202, 1975.
254. **MacKenzie, A. P.,** Modeling the ultra-rapid freezing of cells and tissues, in *Microprobe Analysis of Biological Systems*, Hutchinson, T. E. and Somlyo, A. P., Eds., Academic Press, New York, 1981, 397.
255. **Maltini, E.,** Studies on the physical changes in frozen aqueous solutions by DSC and microscopic observations, *I.I.F.-I.I.R.-Karlsruhe*, 1, 1, 1977.
256. **Guegov, Y.,** Phase transitions of water in products of plant origin at low temperatures, *Adv. Food Res.*, 27, 297, 1981.
257. **Blond, G.,** Water-galactose system: supplemented state diagram and unfrozen water, *Cryo.-Lett.*, 10, 299, 1989.
258. Virtis SRC Sublimators Manual, Virtis Co., Inc., Gardiner, New York, 1983.
259. **Luyet, B. and Rasmussen, D.,** Study by differential thermal analysis of the temperatures of instability of rapidly cooled solutions of glycerol, ethylene glycol, sucrose, and glucose, *Biodynamica*, 10, 167, 1968.
260. **Forsyth, M. and MacFarlane, D. R.,** Recrystallization revisited, *Cryo.-Lett.*, 7, 367, 1986.
261. **Thom, F. and Matthes, G.,** Ice formation in binary

aqueous solutions of ethylene glycol, *Cryo.-Lett.*, 7, 311, 1986.
262. **Reid, D. S.,** Correlation of the phase behavior of DMSO/NaCl/water and glycerol/NaCl/water as determined by DSC with their observed behavior on a cryomicroscope, *Cryo.-Lett.*, 6, 181, 1985.
263. **Hallbrucker, A. and Mayer, E.,** Vitrified dilute aqueous solutions. II. Thermal behavior of hyperquenched NaCl-H_2O and ethylene glycol-H_2O glasses, *J. Phys. Chem.*, 92, 2007, 1988.
264. **Dziedzic, S. Z. and Kearsley, M. W.,** Physicochemical properties of glucose syrups, in *Glucose Syrups: Science and Technology*, Dziedzic, S. Z. and Kearsley, M. W., Eds., Elsevier Applied Science, London, 1984, 137.
265. **Brooks, J. R. and Griffin, V. K.,** Saccharide analysis of corn syrup solids and maltodextrins using HPLC, *Cereal Chem.*, 64, 253, 1987.
266. **Richter, M., Schierbaum, F., Augustat, S., and Knoch, K. D.,** Method of Producing Starch Hydrolysis Products for Use as Food Additives, U.S. Patent 3,962,465, 1976.
267. **Richter, M., Schierbaum, F., Augustat, S., and Knoch, K. D.,** Method of Producing Starch Hydrolysis Products for Use as Food Additives, U.S. Patent 3,986,890, 1976.
268. **Braudo, E. E., Belavtseva, E. M., Titova, E. F., Plashchina, I. G., Krylov, V. L., Tolstoguzov, V. B., Schierbaum, F. R., and Richter, M.,** Struktur und eigenschaften von maltodextrin-hydrogelen, *Starke*, 31, 188, 1979.
269. **Braudo, E. E., Plashchina, I. G., and Tolstoguzov, V. B.,** Structural characterisation of thermoreversible anionic polysaccharide gels by their elastoviscous properties, *Carbohydr. Polym.*, 4, 23, 1984.
270. **Bulpin, P. V., Cutler, A. N., and Dea, I. C. M.,** Thermally reversible gels from low DE maltodextrins, in *Gums and Stabilizers for the Food Industry 2*, Phillips, G. O., Wedlock, D. J., and Williams, P. A., Eds., Pergamon Press, Oxford, 1984, 475.
271. **Reuther, F., Damaschun, G., Gernat, C., Schierbaum, F., Kettlitz, B., Radosta, S., and Nothnagel, A.,** Molecular gelation mechanism of maltodextrins investigated by wide-angle X-ray scattering, *Coll. Polym. Sci.*, 262, 643, 1984.
272. **Lenchin, J. M., Trubiano, P. C., and Hoffman, S.,** Converted Starches for Use as a Fat- or Oil-Replacement in Foodstuffs, U.S. Patent 4,510,166, 1985.
273. **Ellis, H. S. and Ring, S. G.,** A study of some factors influencing amylose gelation, *Carbohydr. Polym.*, 5, 201, 1985.
274. **German, M. L., Blumenfeld, A. L., Yuryev, V. P., and Tolstoguzov, V. B.,** An NMR study of structure formation in maltodextrin systems, *Carbohydr. Polym.*, 11, 139, 1989.
275. **Radosta, S., Schierbaum, F., Reuther, F., and Anger, H.,** Polymer-water interaction of maltodextrins. I. Water vapor sorption and desorption of maltodextrin powders, *Starke*, 41, 395, 1989.
276. **Nagashima, N. and Suzuki, E.,** The behavior of water in foods during freezing and thawing, in *Properties of Water in Foods*, Simatos, D. and Multon, J. L., Eds., Martinus Nijhoff, Dordrecht, 1985, 555.
277. **Saleeb, F. Z. and Pickup, J. G.,** Fixing Volatiles in an Amorphous Substrate and Products Therefrom, U.S. Patent 4,532,145, 1985.
278. **Saleeb, F. Z. and Pickup, J. G.,** Fixation of Volatiles in Extruded Glass Substrates, U.S. Patent 4,820,534, 1989.
279. **Pegg, D. E. and Arnaud, F. G.,** Equations for obtaining melting points in the quaternary system propane-1,2-diol/glycerol/sodium chloride/water, *Cryo.-Lett.*, 9, 404, 1988.
280. **Cesaro, A.,** *Thermodynamic Data for Biochemistry and Biotechnology*, Hinz, H. J., Ed., Springer-Verlag, Heidelberg, 1986, 177.
281. **Franks, F.,** Physical chemistry of small carbohydrates — equilibrium solution properties, *Pure Appl. Chem.*, 59, 1189, 1987.
282. **Franks, F., Ravenhill, J. R., and Reid, D. S.,** Thermodynamic studies of dilute aqueous solutions of cyclic ethers and simple carbohydrates, *J. Solution Chem.*, 1, 3, 1972.
283. **Birch, G. G. and Shamil, S.,** Structure, sweetness and solution properties of small carbohydrates, *J. Chem. Soc., Faraday Trans. I*, 84, 2635, 1988.
284. **Mathlouthi, M. and Seuvre, A. M.,** Solution properties and sweet taste of small carbohydrates, *J. Chem. Soc., Faraday Trans. I*, 84, 2641, 1988.
285. **Wolanczyk, J. P. and Baust, J. G.,** The influence of hold temperature on the phenomenon of "time depency" in hydrated lysozyme glasses, *Cryo.-Lett.*, 10, 215, 1989.
286. **Ruegg, M., Luscher, M., and Blanc, B.,** Hydration of caseins as determined by DSC and sorption measurements, *J. Dairy Sci.*, 57, 387, 1974.
287. **Izzard, M. J., Ablett, S., and Lillford, P. J.,** A calorimetric study of the glass transition occurring in sucrose solutions, presented at Food Polymers, Gels and Colloids, University of East Anglia, Norwich, UK, March 28-30, 1990.
288. **Angell, C. A., Sare, E. J., Donnella, J., and MacFarlane, D. R.,** Homogeneous nucleation and glass transition temperatures in solutions of Li salts in deuterium oxide and water. Doubly unstable glass regions, *J. Phys. Chem.*, 85, 1461, 1981.
289. **Downton, G. E., Flores-Luna, J. L., and King, C. J.,** Mechanism of stickiness in hygroscopic, amorphous powders, *Indust. Eng. Chem. Fund.*, 21, 447, 1982.
290. **Green, J. L. and Angell, C. A.,** Phase relations and vitrification in saccharide-water solutions and the trehalose anomaly, *J. Phys. Chem.*, 93, 2880, 1989.
291. **Shafizadeh, F., McGinnis, G. D., Susott, R. A., and Tatton, H. W.,** Thermal reactions of alpha-D-xylopyranose and beta-D-xylopyranosides, *J. Organ. Chem.*, 36, 2813, 1971.
292. **Aubin, M. and Prud'homme, R. E.,** Analysis of

the glass transition temperature of miscible polymer blends, *Macromolecules*, 21, 2945, 1988.
293. **Fried, J. R., Lai, S. Y., Kleiner, L. W., and Wheeler, M. E.,** Experimental assessment of the thermodynamic theory of the compositional variation of Tg: PVC systems, *J. Appl. Polym. Sci.*, 27, 2869, 1982.
294. **Cooper, T. G.,** *The Tools of Biochemistry*, Wiley-Interscience, New York, 1977.
295. **Parker, K. J.,** The role of sucrose syrups in food manufacture, in *Glucose Syrups and Related Carbohydrates*, Birch, G. G., Green, L. F., and Coulson, C. B., Eds., Elsevier, Amsterdam, 1970, 58.
296. **Leubner, I. H.,** Crystal nucleation under diffusion-controlled conditions, *J. Phys. Chem.*, 91, 6069, 1987.
297. **Wolf, W., Spiess, W. E. L., and Jung, G.,** Standardization of isotherm measurements, in *Properties of Water in Foods*, Simatos, D. and Multon, J. L., Eds., Martinus Nijhoff, Dordrecht, 1985, 661.
298. **Fahy, G. M., MacFarlane, D. R., Angell, C. A., and Meryman, H. T.,** Vitrification as an approach to cryopreservation, *Cryobiology*, 21, 407, 1984.
299. **Forsyth, M. and MacFarlane, D. R.,** Homogeneous nucleation at high pressures in some aqueous solutions of cryoprotectant interest, *Cryo.-Lett.*, 10, 139, 1989.
300. **Nicol, W. M.,** Sucrose and food technology, in *Sugar: Science and Technology*, Birch, G. G. and Parker, K. J., Eds., Applied Science, London, 1979, 211.
301. **Olson, D. R. and Webb, K. K.,** The effect of humidity on the glass transition temperature, *Organ. Coat. Plast. Chem.*, 39, 518, 1978.
302. **Luyet, B. J.,** The devitrification temperatures of solutions of a carbohydrate series, *J. Phys. Chem.*, 43, 881, 1939.
303. **Tsourouflis, S., Flink, J. M., and Karel, M.,** Loss of structure in freeze-dried carbohydrate solutions, *J. Sci. Food Agric.*, 27, 509, 1976.
304. **Pikal, M. J., Shah, S., Senior, D., and Lang, J. E.,** Physical chemistry of freeze-drying, *J. Pharm. Sci.*, 72, 635, 1983.
305. **Pikal, M. J.,** Use of laboratory data in freeze-drying process design, *J. Parent. Sci. Technol.*, 39, 115, 1985.
306. **Pikal, M. J., Shah, S., Roy, M. L., and Putman, R.,** The secondary drying stage of freeze drying: drying kinetics as a function of temperature and chamber pressure, *Int. J. Pharm.*, 60, 203, 1990.
307. **Gatlin, L. and Deluca, P. P.,** Study of phase transitions in frozen antibiotic solutions by DSC, *J. Parent. Drug Assoc.*, 34, 398, 1980.
308. **Reid, D. S., Alviar, M. S. B., and Lim, M. H.,** The rates of change of ice crystal size in model systems stored at different temperatures relevant to the storage of frozen food, in *Development in Refrigeration, Refrigeration for Development*, Proceedings 17th Int. Congress Refrigeration, Vol. C, Biology and Food Science, Austrian Assoc. of Refrigeration and Air Conditioning, IIR, 1987, 397.
309. **Martino, M. N. and Zaritzky, N. E.,** Ice crystal size modifications during frozen beef storage, *J. Food Sci.*, 53, 1631, 1988.
310. **Kahn, M. L. and Lynch, R. J.,** Freezer Stable Whipped Ice Cream and Milk Shake Food Products, U.S. Patent 4,552,773, 1985.
311. **Duden, R. and Scholz, A.,** Enzymatic decomposition of phospholipids in frozen parsley, *Z. Ernahrungswiss.*, 21, 266, 1982.
312. **LeBlanc, E. L., LeBlanc, R. J., and Blum, I. E.,** Prediction of quality of frozen cod fillets, *J. Food Sci.*, 53, 328, 1988.
313. **Lee, C. Y., Smith, N. L., and Hawbecker, D. E.,** Enzyme activity and quality of frozen green beans as affected by blanching and storage, *J. Food Qual.*, 11, 279, 1988.
314. **Fennema, O.,** Activity of enzymes in partially frozen aqueous systems, in *Water Relations of Foods*, Duckworth, R. B., Ed., Academic Press, New York, 1975, 397.
315. **Baardseth, P. and Naesset, E.,** The effect of lipid-degrading enzyme activities on quality of blanched and unblanched frozen stored cauliflower estimated by sensory and instrumental analysis, *Food Chem.*, 32, 39, 1989.
316. **Maltini, E.,** Thermophysical properties of frozen juice related to freeze drying problems, *Ann. Ist. Sper. Valor. Tech. Prod. Agric.*, 5, 65, 1974.
317. **Wallack, D. A. and King, C. J.,** Sticking and agglomeration of hygroscopic, amorphous carbohydrate and food powders, *Biotechnol. Prog.*, 4, 31, 1988.
318. **Chavarri, F. J., DePaz, M., and Nunez, M.,** Cryoprotective agents for frozen concentrated cheese starter cultures, *Biotechnol. Lett.*, 10, 11, 1988.
319. **Fahy, G. M.,** Vitrification: a new approach to organ cryopreservation, in *Transplantation: Approaches to Graft Rejection*, Meryman, H. T., Ed., Alan R. Liss, New York, 1986, 305.
320. **Fahy, G. M.,** Vitrification, in *Low Temperature Biotechnology: Emerging Applications and Engineering Contributions*, McGrath, J. J. and Diller, K. R., Eds., American Society Mechanical Engineering, in press.
321. **Ogawa, H. and Imamura, Y.,** Stabilized Solid Compositions, U.S. Patent 4,547,377, 1985.
322. **Fukuoka, E., Kimura, S., Yamazaki, M., and Tanaka, T.,** Cohesion of particulate solids. VI, *Chem. Pharmaceut. Bull.*, 31, 221, 1983.
323. **Miller, D. H. and Mutka, J. R.,** Process for Forming Solid Juice Composition and Product of the Process, U.S. Patent 4,499,112, 1985.
324. **Moreyra, R. and Peleg, M.,** Effect of equilibrium water activity on the bulk properties of selected food powders, *J. Food Sci.*, 46, 1918, 1981.
325. **Passy, N. and Mannheim, C. H.,** Flow properties and water sorption of food powders. II, *Lebensm.-Wiss. u.-Technol.*, 15, 222, 1982.
326. **Peleg, M. and Mannheim, C. H.,** The mechanism of caking of powdered onion, *J. Food Process. Preserv.*, 1, 3, 1977.

327. **Rosenzweig, N. and Narkis, M.,** Sintering rheology of amorphous polymers, *Polym. Eng. Sci.*, 21, 1167, 1981.
328. **Tardos, G., Mazzone, D., and Pfeffer, R.,** Measurement of surface viscosities using a dilatometer, *Can. J. Chem. Eng.*, 62, 884, 1984.
329. **Barbosa-Canovas, G. V., Rufner, R., and Peleg, M.,** Microstructure of selected binary food powder mixtures, *J. Food Sci.*, 50, 473, 1985.
330. **Wuhrmann, J. J., Venries, B., and Buri, R.,** Process for Preparing a Colored Powdered Edible Composition, U.S. Patent 3,920,854, 1975.
331. **Szejtli, J. and Tardy, M.,** Honey Powder Preserving its Natural Aroma Components, U.S. Patent 4,529,608, 1985.
332. **Poole, P. L. and Finney, J. L.,** Sequential hydration of a dry globular protein, *Biopolymers*, 22, 255, 1983.
333. **Poole, P. L. and Finney, J. L.,** Sequential hydration of dry proteins, *Biopolymers*, 23, 1647, 1984.
334. **Cakebread, S. H.,** Factors affecting the shelf life of high boilings, *Manufact. Confect.*, 49(8), 41, 1969.
335. **Gueriviere, J. F.,** Recent developments in extrusion cooking of foods, *Indust. Aliment. Agric.*, 93, 587, 1976.
336. **Herrington, T. M. and Branfield, A. C.,** Physicochemical studies on sugar glasses, *J. Food Technol.*, 19, 409, 1984.
337. **Lees, R.,** Quality control in the production of hard and soft sugar confectionery, *Confect. Prod.*, Feb., 50, 1982.
338. **McNulty, P. B. and Flynn, D. G.,** Force-deformation and texture profile behavior of aqueous sugar glasses, *J. Text. Stud.*, 8, 417, 1977.
339. **Vink, W. and Deptula, R. W.,** High Fructose Hard Candy, U.S. Patent 4,311,722, 1982.
340. **Chevalley, J., Rostagno, W., and Egli, R. H.,** A study of the physical properties of chocolate. V, *Rev. Int. Chocolat*, 25, 3, 1970.
341. **Niediek, E. A. and Barbernics, L.,** Amorphisierung von Zucker Durch das Feinwalzen von Schokoladenmassen, *Gordian*, 80, 267, 1981.
342. **Hirsh, A. G., Williams, R. J., and Meryman, H. T.,** Novel method of natural cryoprotection, *Plant Physiol.*, 79, 41, 1985.
343. **Hirsh, A., Bent, T., and Erbe, E.,** Localization and characterization of intracellular liquid-liquid phase separations in deeply frozen Populus using electron microscopy, DMA, and DSC, *Thermochim. Acta*, in press.
344. **Rall, W. F. and Fahy, G. M.,** Ice-free cryopreservation of mouse embryos by vitrification, *Nature*, 313, 573, 1985.
345. **Kahn, M. L. and Eapen, K. E.,** Intermediate-Moisture Frozen Foods, U.S. Patent 4,332,824, 1982.
346. **Takahashi, T., Hirsh, A., Erbe, E., and Williams, R. J.,** Mechanisms of cryoprotection by extracellular polymeric solutes, *Biophys. J.*, 54, 509, 1988.
347. **Ehlich, D. and Sillescu, H.,** Tracer diffusion at the glass transition, *Macromolecules*, 23, 1600, 1990.
348. **Gekko, K. and Satake, I.,** DSC of unfreezable water in water-protein-polyol systems, *Agric. Biol. Chem.*, 45, 2209, 1981.
349. **Hays, D. L. and Fennema, O.,** Methodology for determining unfreezable water in protein suspensions by low-temperature NMR, *Arch. Biochem. Biophys.*, 213, 1, 1982.
350. **Fullerton, G. D., Potter, J. L., and Dornbluth, N. C.,** NMR relaxation of protons in tissues and other macromolecular water solutions, *Mag. Res. Imag.*, 1, 209, 1982.
351. **Lioutas, T. S., Baianu, I. C., and Steinberg, M. P.,** O-17 and deuterium NMR studies of lysozyme hydration, *Arch. Biochem. Biophys.*, 247, 68, 1986.
352. **Blake, C. C. F., Pulford, W. C. A., and Artymiuk, P. J.,** X-ray studies of water in crystals of lysozyme, *J. Mol. Biol.*, 167, 693, 1983.
353. **Scandola, M. and Pezzin, G.,** Density of elastin-water system, in *Water in Polymers*, Rowland, S. P., Ed., ACS Symp. Ser. 127, American Chemical Society, Washington, D.C., 1980, 225.
354. **Gosline, J. M. and French, C. J.,** Dynamic mechanical properties of elastin, *Biopolymers*, 18, 2091, 1979.
355. **Duckworth, R. B.,** DTA of frozen food systems. I. Determination of unfreezable water, *J. Food Technol.*, 6, 317, 1971.
356. **Sasaki, N., Shiwa, S., Yagihara, S., and Hikichi, K.,** X-ray diffraction studies on the structure of hydrated collagen, *Biopolymers*, 22, 2539, 1983.
357. **Wright, D. J.,** Thermoanalytical methods in food research, *Crit. Rev. Appl. Chem.*, 5, 1, 1984.
358. **Berlin, E., Kliman, P. G., and Pallansch, M. J.,** Changes in state of water in proteinaceous systems, *J. Colloid Interface Sci.*, 34, 488, 1970.
359. **Berlin, E., Kliman, P. G., Anderson, B. A., and Pallansch, M. J.,** Water binding in whey protein concentrates, *J. Dairy Sci.*, 56, 984, 1973.
360. **Reutner, P., Luft, B., and Borchard, W.,** Compound formation and glassy solidification in the system gelatin-water, *Colloid Polym. Sci.*, 263, 519, 1985.
361. **Wilson, M. N. and Steensen, W. L.,** Sugar-Free Cheesecake Filling and Dry Mix for Preparation Thereof, U.S. Patent 4,594,255, 1986.
362. **Huang, W. J., Frick, T. S., Landry, M. R., Lee, J. A., Lodge, T. P., and Tirrell, M.,** Tracer diffusion measurement in polymer solutions near the glass transition by forced Rayleigh scattering, *AIChE J.*, 33, 573, 1987.
363. **Riganakos, K. A., Demertzis, P. G., and Kontominas, M. G.,** Gas chromatographic study of water sorption by wheat flour, *J. Cereal Sci.*, 9, 261, 1989.
364. **Bryan, W. P.,** Thermodynamics of water-biopolymer interactions: irreversible sorption by two uniform sorbent phases, *Biopolymers*, 26, 387, 1987.

365. **Watt, I. C.,** Adsorption-desorption hysteresis in polymers, *J. Macromol. Sci.-Chem.*, A14, 245, 1980.
366. **D'Arcy, R. L. and Watt, I. C.,** Water vapor sorption isotherms on macromolecular substrates, in *Water Activity: Influences on Food Quality,* Rockland, L. B. and Stewart, G. F., Eds., Academic Press, New York, 1981, 111.
367. **Finney, J. L. and Poole, P. L.,** Protein hydration and enzyme activity: role of hydration-induced conformation and dynamic changes in activity of lysozyme, *Comments Mol. Cell. Biophys.*, 2, 129, 1984.
368. **Bone, S. and Pethig, R.,** Dielectric studies of protein hydration and hydration-induced flexibility, *J. Mol. Biol.*, 181, 323, 1985.
369. **Bryan, W. P.,** Thermodynamic models for water-protein sorption hysteresis, *Biopolymers,* in press.
370. **Berens, A. and Hopfenberg, H. B.,** Induction and measurement of glassy state relaxations by vapor sorption methods, *Stud. Phys. Theoret. Chem.*, 10, 77, 1980.
371. **Neogi, P.,** Anomalous diffusion of vapors through solid polymers, *Am. Inst. Chem. Eng. J.*, 29, 829, 1983.
372. **Roussis, P. P.,** Diffusion of water vapor in cellulose acetate. I-II, *Polymer,* 22, 768, 1058, 1981.
373. **Durning, C. J. and Tabor, M.,** Mutual diffusion in concentrated polymer solutions under small driving force, *Macromolecules,* 19, 2220, 1986.
374. **Reid, D.,** personal communication, 1990.
375. **Hopfenberg, H. B., Apicella, A., and Saleeby, D. E.,** Factors affecting water sorption in and solute release from EVA copolymers, *J. Membr. Sci.*, 8, 273, 1981.
376. **Apicella, A. and Hopfenberg, H. B.,** Water-swelling behavior of EVA copolymer, *J. Appl. Polym. Sci.*, 27, 1139, 1982.
377. **Starkweather, H. W. and Barkley, J. R.,** Effect of water on secondary dielectric relaxations in nylon 66, *J. Polym. Sci.:Polym. Phys. Ed.*, 19, 1211, 1981.
378. **Pace, R. J. and Datyner, A.,** Temperature dependence of Langmuir sorption capacity factor in glassy polymers, *J. Polym. Sci.: Poly. Phys. Ed.*, 19, 1657, 1981.
379. **Brown, G. L.,** Clustering of water in polymers, in *Water in Polymers,* Rowland, S. P., Ed., ACS Symp. Ser. 127, American Chemical Society, Washington, D.C., 1980, 441.
380. **Iglesias, H. A., Chirife, J., and Boquet, R.,** Prediction of water sorption isotherms of food models from sorption of components, *J. Food Sci.*, 45, 450, 1980.
381. **Chinachoti, P. and Steinberg, M. P.,** Moisture hysteresis due to amorphous sucrose in sucrose-starch mixtures, *J. Food Sci.*, 51, 453, 1986.
382. **Chinachoti, P. and Steinberg, M. P.,** Interaction of solutes with raw starch during desorption as shown by water retention, *J. Food Sci.*, 51, 997, 1986.
383. **Batzer, H. and Kreibich, U.,** Influence of water on thermal transitions in natural polymers and synthetic polyamides, *Polym. Bull.*, 5, 585, 1981.
384. **Buleon, A., Bizot, H., Delage, M. M., and Pontoire, B.,** Comparison of X-ray diffraction and sorption properties of hydrolyzed starches, *Carbohydr. Polym.*, 7, 461, 1987.
385. **Bonner, D. C. and Prausnitz, J. M.,** Thermodynamic properties of some concentrated polymer solutions, *J. Polym. Sci.: Polym. Phys. Ed.*, 12, 51, 1974.
386. **Hoseney, R. C.,** *Principles of Cereal Science and Technology,* American Association of Cereal Chemists, St. Paul, MN, 1986.
387. **Franks, F., Hatley, R. H. M., and Friedman, H. L.,** Thermodynamics of protein stability: cold destabilization as a general phenomenon, *Biophys. Chem.*, 31, 307, 1988.
388. **Franks, F.,** Protein stability and function at low temperatures, *Cryo.-Lett.*, 8, 108, 1987.
389. **Privalov, P. L., Griko, Y. V., Venyaminov, S. Y., and Kutyshenko, V. P.,** Cold denaturation of myoglobin, *J. Mol. Biol.*, 190, 487, 1986.
390. **Wakabayashi, T. and Franks, F.,** Heat capacities of aqueous PVP solutions at subzero temperatures, *Cryo.-Lett.*, 7, 361, 1986.
391. **Hatley, R. H. M. and Franks, F.,** Denaturation of lactate dehydrogenase at subzero temperatures, *Cryo.-Lett.*, 7, 226, 1986.
392. **Franks, F. and Hatley, R. H. M.,** Low temperature unfolding of chymotrypsinogen, *Cryo.-Lett.*, 6, 171, 1985.
393. **Sochava, I. V., Belopolskaya, T. V., and Smirnova, O. I.,** DSC study of reversible and irreversible thermal denaturation of concentrated globular protein solutions, *Biophys. Chem.*, 22, 323, 1985.
394. **Hatley, R. H. M., Franks, F., and Mathias, S. F.,** Stabilization of labile biochemicals by undercooling, *Process Biochem.*, 22, 169, 1987.
395. **Matsukura, U., Matsunaga, A., and Kainuma, K.,** Contribution of amylose to starch retrogradation, *J. Jpn. Soc. Starch Sci.*, 30, 106, 1983.
396. **Welsh, E. J., Bailey, J., Chandarana, R., and Norris, W. E.,** Physical characterization of interchain association in starch systems, *Prog. Fd. Nutr. Sci.*, 6, 45, 1982.
397. **Doublier, J. L. and Choplin, L.,** A rheological description of amylose gelation, *Carbohydr. Res.*, 193, 215, 1989.
398. **Steeneken, P. A. M.,** Rheological properties of aqueous suspensions of swollen starch granules, *Carbohydr. Polym.*, 11, 23, 1989.
399. **Gidley, M. J., Bulpin, P. V., and Kay, S.,** Effect of chain length on amylose retrogradation, in *Gums and Stabilizers for the Food Industry,* 3, Phillips, G. O., Wedlock, D. J., Williams, P. A., Eds., Elsevier Applied Science, London, 1986, 167.
400. **Whistler, R. L. and Daniel, J. R.,** Molecular structure of starch, in *Starch: Chemistry and Technology,*

2nd ed., Whistler, R. L., BeMiller, J. N., and Paschall, E. F., Eds., Academic Press, Orlando, 1984, 153.
401. **Buleon, A., Duprat, F., Booy, F. P., and Chanzy, H.,** Single crystals of amylose with a low degree of polymerization, *Carbohydr. Polym.*, 4, 161, 1984.
402. **Hizukuri, S.,** Polymodal distribution of chain lengths of amylopectins and its significance, *Carbohydr. Res.*, 147, 342, 1986.
403. **Krusi, H. and Neukom, H.,** Untersuchungen uber die Retrogradation der Starke in Konzentrierten Weizenstarkegelen, *Starke*, 36, 300, 1984.
404. **Muhr, A. H. and Blanshard, J. M. V.,** Effect of polysaccharide stabilizers on the rate of growth of ice, *J. Food Technol.*, 21, 683, 1986.
405. **Holbrook, J. L. and Hanover, L. M.,** Fructose-Containing Frozen Dessert Products, U.S. Patent 4,376,791, 1983.
406. **Bevilacqua, A. E. and Zaritzky, N. E.,** Ice recrystallization in frozen beef, *J. Food Sci.*, 47, 1410, 1982.
407. **Harper, E. K. and Shoemaker, C. F.,** Effect of locust bean gum and selected sweetening agents on ice recrystallization rates, *J. Food Sci.*, 48, 1801, 1983.
408. **Franks, F., Darlington, J., Schenz, T., Mathias, S. F., Slade, L., and Levine, H.,** Antifreeze activity of Antarctic fish glycoprotein and a synthetic polymer, *Nature*, 325, 146, 1987.
409. **Muhr, A. H., Blanshard, J. M. V., and Sheard, S. J.,** Effects of polysaccharide stabilizers on the nucleation of ice, *J. Food Technol.*, 21, 587, 1986.
410. **Keeney, P. G. and Kroger, M.,** Frozen dairy products, in *Fundamentals of Dairy Chemistry*, 2nd ed., Webb, B. H., Ed., AVI, Westport, 1974, 890.
411. **Nursten, H. E.,** Maillard browning reactions in dried foods, in *Concentration and Drying of Foods*, MacCarthy, D., Ed., Elsevier Applied Science, London, 1986, 53.
412. **Bakker-Artema, F. W.,** Heat and mass transfer aspects and modeling of dryers — a critical evaluation, in *Concentration and Drying of Foods*, MacCarthy, D., Ed., Elsevier Applied Science, London, 1986, 165.
413. **Zobel, H. F.,** Gelatinization of starch and mechanical properties of starch pastes, in *Starch: Chemistry and Technology*, 2nd ed., Whistler, R. L., BeMiller, J. N., and Paschall, E. F., Eds., Academic Press, Orlando, 1984, 285.
414. **Jankowski, T. and Rha, C. K.,** DSC study of wheat grain cooking process, *Starke*, 38, 45, 1986.
415. **Normand, F. L. and Marshall, W. E.,** DSC of whole grain milled rice and milled rice flour, *Cereal Chem.*, 66, 317, 1989.
416. **Hoseney, R. C., Zeleznak, K., and Abdelrahman, A.,** Mechanism of popcorn popping, *J. Cereal Sci.*, 1, 43, 1983.
417. **Colonna, P., Buleon, A., and Mercier, C.,** Physically modified starches, in *Starch: Properties and Potential*, Galliard, T., Ed., John Wiley & Sons, Chichester, 1987, 79.
418. **Shi, Y. C. and Seib, P.,** Properties of wheat starch compared to normal maize starch, in *Wheat is Unique*, Pomeranz, Y., Ed., Am. Assoc. Cereal Chem., St. Paul, MN, 1989, 215.
419. **Nakazawa, F., Noguchi, S., Takahashi, J., and Takada, M.,** Thermal equilibrium state of starch-water mixture studied by DSC, *Agric. Biol. Chem.*, 48, 2647, 1984.
420. **Krueger, B. R., Knutson, C. A., Inglett, G. E., and Walker, C. E.,** DSC study on effect of annealing on gelatinization behavior of corn starch, *J. Food Sci.*, 52, 715, 1987.
421. **Snyder, E. M.,** Industrial microscopy of starches, in *Starch: Chemistry and Technology*, 2nd ed., Whistler, R. L., BeMiller, J. N., Paschall, E. F., Eds., Academic Press, Orlando, 1984, 661.
422. **Shannon, J. C. and Garwood, D. L.,** Genetics and physiology of starch development, in *Starch: Chemistry and Technology*, 2nd ed., Whistler, R. L., BeMiller, J. N., and Paschall, E. F., Eds., Academic Press, Orlando, 1984, 25.
423. **Donovan, J. W., Lorenz, K., and Kulp, K.,** DSC of heat-moisture treated wheat and potato starches, *Cereal Chem.*, 60, 381, 1983.
424. **Shiotsubo, T. and Takahashi, K.,** Changes in enthalpy and heat capacity associated with gelatinization of potato starch, evaluated by isothermal calorimetry, *Carbohydr. Res.*, 158, 1, 1986.
425. **Longton, J. and LeGrys, G. A.,** DSC studies on crystallinity of aging wheat starch gels, *Starke*, 33, 410, 1981.
426. **Ghiasi, K., Hoseney, R. C., and Varriano-Marston, E.,** Effects of flour components and dough ingredients on starch gelatinization, *Cereal Chem.*, 60, 58, 1983.
427. **Spies, R. D. and Hoseney, R. C.,** Effect of sugars on starch gelatinization, *Cereal Chem.*, 59, 128, 1982.
428. **Czuchajowska, Z. and Pomeranz, Y.,** DSC, water activity, and moisture contents in crumb center and near-crust zones of bread during storage, *Cereal Chem.*, 66, 305, 1989.
429. **Russell, P. L.,** Kinetic study of bread staling by DSC, *Starke*, 35, 277, 1983.
430. **Zeleznak, K. J. and Hoseney, R. C.,** Role of water in retrogradation of wheat starch gels and bread crumb, *Cereal Chem.*, 63, 407, 1986.
431. **Schaefer, J., Garbow, J. R., Stejskal, E. O., and Lefelar, J. A.,** Plasticization of poly(butyral-co-vinyl alcohol), *Macromolecules*, 20, 1271, 1987.
432. **Eliasson, A. C.,** Retrogradation of starch as measured by DSC, in *New Approaches to Research on Cereal Carbohydrates*, Hill, R. D. and Munck, L., Eds., Elsevier, Amsterdam, 1985, 93.
433. **Biliaderis, C. G. and Galloway, G.,** Crystallization behavior of amylose-V complexes: structure-property relationships, *Carbohydr. Res.*, 189, 31, 1989.

434. **Jane, J. L. and Robyt, J.,** Structure studies of amylose-V complexes and retrograded amylose, *Carbohydr. Res.*, 132, 105, 1984.
435. **Yamamoto, M., Harada, S., Sano, T., Yasunaga, T., and Tatsumoto, N.,** Kinetic studies of complex formation in amylose-SDS-iodine ternary system, *Biopolymers*, 23, 2083, 1984.
436. **Kowblansky, M.,** Calorimetric investigation of inclusion complexes of amylose with long-chain aliphatic compounds, *Macromolecules*, 18, 1776, 1985.
437. **Evans, I. D.,** Investigation of starch/surfactant interactions using viscosimetry and DSC, *Starke*, 38, 227, 1986.
438. **Galloway, G. I., Biliaderis, C. G., and Stanley, D. W.,** Properties and structure of amylose-glycerol monostearate complexes formed in solution or on extrusion of wheat flour, *J. Food Sci.*, 54, 950, 1989.
439. **Eliasson, A. C.,** On the effects of surface active agents on the gelatinization of starch — a calorimetric investigation, *Carbohydr. Polym.*, 6, 463, 1986.
440. **Biliaderis, C. G., Page, C. M., and Maurice, T. J.,** Non-equilibrium melting of amylose-V complexes, *Carbohydr. Polym.*, 6, 269, 1986.
441. **Batres, L. V. and White, P. J.,** Interaction of amylopectin with monoglycerides in model systems, *J. Am. Oil Chem. Soc.*, 63, 1537, 1986.
442. **Duckworth, R. B.,** Foreword, in *Food Preservation by Moisture Control*, Seow, C. C., Ed., Elsevier Applied Science, London, 1988, ix.
443. **Simatos, D.,** personal communication, 1988.

APPENDIX

List of Participants at Faraday Discussion Conference, July 1-3, 1985

Arnold, Dr. B. J.	Mars UK
van den Berg, Dr. C.	Agricultural University Wageningen
Bizot, Dr. H.	INRA Nantes
Blanshard, Prof. J. M. V.	University of Nottingham
Corbet, Dr. Sarah A.	Cambridge University
Duckworth, Dr. R. B.	University of Strathclyde
Evans, Dr. E. W.	FRIR UK
Franks, Dr. Felix	Cambridge University & Pafra
Gal, Dr. Stefan	HACO Switzerland
Gedney, Miss S. E.	University of Nottingham
Gervais, Dr. Patrick	ENSBANA Dijon
Gordon, Miss Kay	United Biscuits UK
Gould, Dr. G. W.	Unilever UK
Grant, Mr. A. J.	University of Sheffield
Hanson, Dr. Steven W.	Humberside College
Holland, Mr. W. H.	Lyons Bakery UK
Johnston, Dr. Kenneth	Farley Health Products UK
Kent, Dr. Michael	Torry Research Station UK
Kinderlerer, Mrs. J. L.	Sheffield City Polytechnic
LeMeste, Dr. Martine	ENSBANA Dijon
Leslie, Miss Tracy	University of Sheffield
Lilley, Dr. T. H.	University of Sheffield
Marquis, Dr. Robert W.	University of Rochester USA
Morley, Mr. M. J.	Food Research Institute — Bristol
Morley, Dr. Robert G.	Delphi Consultant Services Inc. USA
Myers, Dr. Chester	General Foods Cobourg
Okojie, Dr. N. F.	British Sugar UK
Parker, Dr. Stephen B.	Unilever UK
Paynter, Dr. O.	Lyons Bakery UK
Poole, Dr. P. L.	University of London
Ratcliffe, Mr. G. C.	Pillsbury UK

Russell, Dr. Peter L.	FMBRA Chorleywood
Slade, Dr. Louise	General Foods Tarrytown
Tsvetkov, Dr. Tsvetan D.	Bulgaria
Vinnicombe, Ms. Debra Helen	Imperial College London
Walstra, Dr. P. Walstra	Agricultural University Wageningen
Webster, Mr. Stephen	University of Nottingham
Wilkes, Mr. M. S.	United Biscuits UK
Wolanczyk, Dr. Jan	University of London
Zhen Zhang, Dr. Ji	University of London